SPECTRAL ANALYSIS OF WAVE FORCES FOR THE DESIGN OF ROLLING GATES OF THE LOCK OF AMSTERDAM

Henry Tuin[1], Hessel Voortman[1], Tom Wijdenes[1], Wim van der Stelt[2], David van Goolen[2], Pieter van Lierop[2], Leon Lous[3], Wim Kortlever[4]

1: Arcadis Europe[1]
2: IV Infra, Papendrecht, The Netherlands
3: OpenIJ, Haarlem, The Netherlands
4: Rijkswaterstaat, The Netherlands

Key Words: inland navigation, locks, Linear wave theory, wave spectrum, wave forces

1. INTRODUCTION

In the Dutch city of IJmuiden, a new ship lock is currently under construction. With a lock chamber of 500 m long and 70 m wide, it will be the largest lock in the world. The latest generation of seagoing vessels will be able to access the harbour of Amsterdam using this lock. The lock closes with rolling gates constructed in steel. The driving mechanism (equipment to close or open the gate) of the lock gates needs to generate a driving force to overcome external and internal hydraulic forces. Wave forces acting on the gate have a major contribution to the total forces on the gate. The lock of IJmuiden will be available for navigation up to the hydraulic conditions corresponding a 10-year return period storm. When the wave field exceeds the 10-year return period (H_{m0}=1,5m, T_{m-10}=4s), the lock will be closed for navigation. For the 10-year period storm, a maximum period of the gate mission (opening or closing the gate) has been set.

Figure 1: Artist impression of the lock (ZUS, 2016)

Waves push the gate onto its supports. To open or close the gate, the driving mechanism should overcome the friction forces in the supports generated by waves, the longitudinal wave forces generated by the waves, and 'other loads' like density differences, translatory waves, etc. (Voortman, et al., 2017). The driving mechanism must have sufficient driving force to reduce the probability and the period of delay of the gate mission. Choosing a driving mechanism with too little driving force would result in unacceptable delay for navigation. Choosing a driving mechanism with a very large driving force would be unnecessary expensive.

[1] Henry.tuin@arcadis.com

Normally the wave force is calculated using either the formula of Goda (Goda, 2010), or the linear wave theory for a single wave height and wave period. However, the wave spectrum loading the gate consists of two peaks:

- Long waves (swell; <0,14 Hz
- Wind waves (>0,14 Hz)

Due to the large depth of the lock of 20 meters, long waves penetrate down to the toe of the gate, generating a large force at the gate. This force cannot accurately be calculated using general wave theories:

- When using a formula based on only one wave height and one wave period, the force during gate mission is constant. To calculate the duration of delay of a gate mission a wave force time series must be generated.
- The wave spectrum is required for deriving the force spectrum and elaborating the probability density function of the wave force and to express the probability of delay.
- The method of Goda appears to overestimate the total wave force due to the linear schematization of the wave pressure between still water level and the toe of the gate. The calculated force will result in a very large required capacity, of the driving mechanism resulting in high costs.
- Linear wave theory only using the significant wave height and wave period gives an underestimation of the wave force. This results in insufficient driving force and too much delay.

To include the effect of long waves, and to be able to calculate the wave force time series and gate mission delay, a spectral design approach based on the linear wave theory is applied (Holthuijsen, 2007). A response function is derived for the full gate mission (opening or closing of the gate) and for the full range of occurring wave frequencies (0Hz up to 1Hz) to calculate the wave force in each gate support. During gate mission the gate acts as a cantilever beam, this results in a combined absolute reaction force in the supports larger than the total incoming wave force. To calculate the total friction force during gate mission, the reaction force is multiplied with a friction coefficient. The cantilever effect is included in the final response function as the total friction force. The total friction force, delay and probability of exceedance of the delay duration is derived by the following steps:

1. Application of the linear wave theory for the lock gate
2. The conversion of the wave spectrum to wave force spectrum describing the transverse wave loads. (Figure 2; force number 1).
3. The conversion of the wave spectrum to a wave force spectrum describing the longitudinal wave loads. (Figure 2; force number 2)
4. The conversion of the transverse wave force spectrum in a longitudinal friction force spectrum. (Figure 2; force number 3)
5. The transformation of the total wave force spectrum to required driving forces and delays.

Remark: The results of the analysis are visualised in graphs. Because of the confidential status of the design of the lock gate, the axis representing variance densities, wave forces, and delays are not numbered.

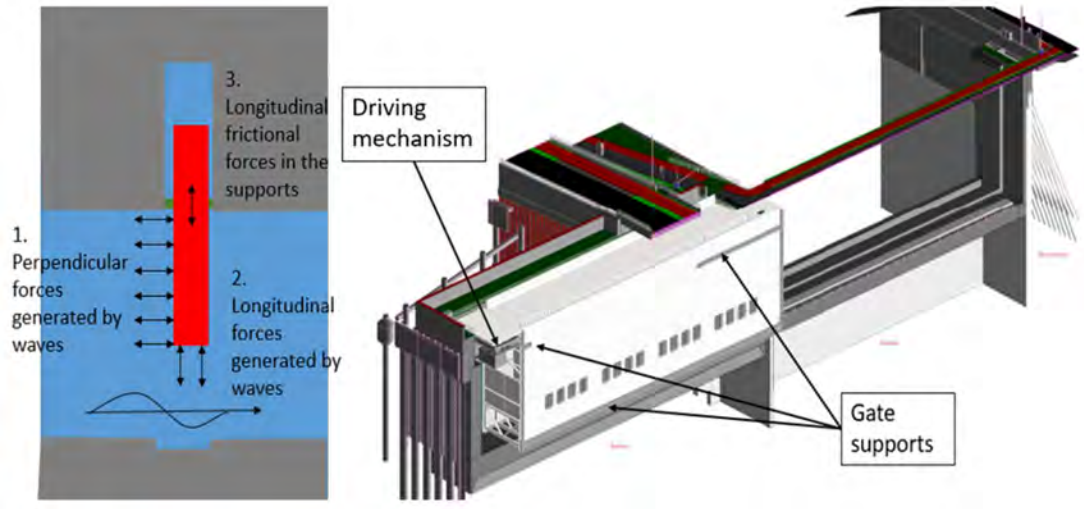

Figure 2: Overview of wave forces on the gate

2. METHDOLOGY – LINEAR WAVE THEORY

A wave spectrum of the incoming wave field which covers the wave energy directing towards the gate is the starting point of the analysis. The wave spectrum is shown in Figure 3 by the dashed line. The wave spectrum has two peak frequencies:

- A minor peak at 0.1 Hz corresponding to long waves penetrating the harbor from sea
- A major peak at 0.2 Hz corresponding to wind waves mainly generated in the harbor basin.

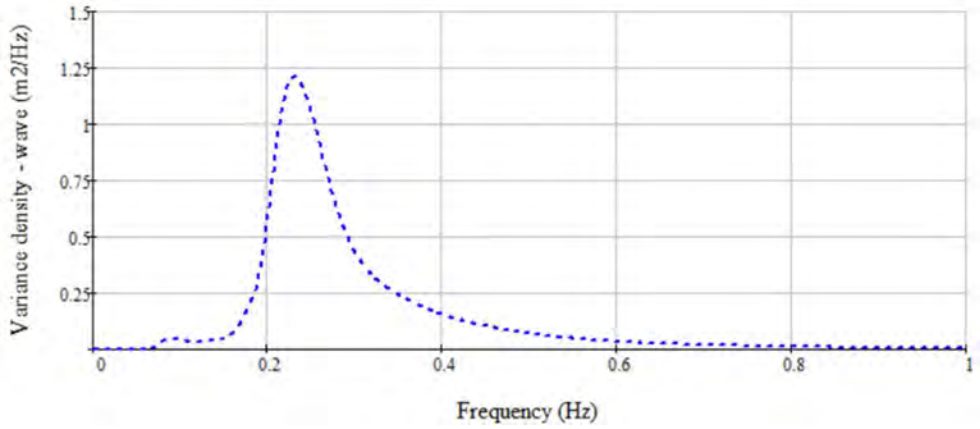

Figure 3: Wave spectrum

The wave spectrum is transferred into a wave force spectrum by using a transfer-function (Holthuijsen, 2007). The wave force spectrum is derived by multiplying the wave spectrum $S_{\eta\eta}(f)$ by the square of the response function $R_{F\eta}(f)$ *(1)*. We assume/know beforehand that the eigen-period of the gate itself is much shorter than the period of the waves. Therefore, dynamic amplification of the loads can be safely ignored.

$$S_{FF}(f) = R_{F\eta}^2(f) S_{\eta\eta}(f) \qquad (1)$$

In which:

$S_{FF}(f)$	=	Variance density of the wave force field (kN^2/Hz)
$S_{\eta\eta}(f)$	=	Variance density of the wave field (m^2/Hz)
$R_{F\eta}(f)$	=	Response function (kN/m)

3. SPECTRUM OF TRANSVERSE WAVE FORCES

The methodology given in chapter 2 is applied to find the spectrum of the transverse wave force. The transverse wave load is shown as force 'number 1' in Figure 2.

Response function below still water level

The wave pressure is the largest at still water level (SWL) and decreases with depth as presented in the left pressure figure of Figure 4. The rate of decline is related to the depth and frequency. The total transverse wave force is calculated by integrating the wave pressure over the height and multiplying the pressure by the width of the gate. The response function below SWL is derived by dividing *(2)* with the amplitude. Reflection is included in the equation by means of variable *r* (Ministerie van Verkeer en Waterstaat, 2000).

$$F_{sub}(f) = (1 + r)\, \rho_w\, g\, a\, B_{eff} \int_{h_{gate\_low}}^{h_w} \frac{\cosh(k(f)\,(\eta - h_{gate\_low}))}{\cosh(k(f)\,(h_w - h_{gate\_low}))} d\eta \qquad (2)$$

In which:

f	=	frequency	B_{eff}	=	Width of gate subjected to waves
r	=	reflection			
ρ_w	=	density water	k	=	wave number
g	=	gravitation constant	h_w	=	still water level
a	=	wave amplitude	h_{gate_low}	=	bottom of gate

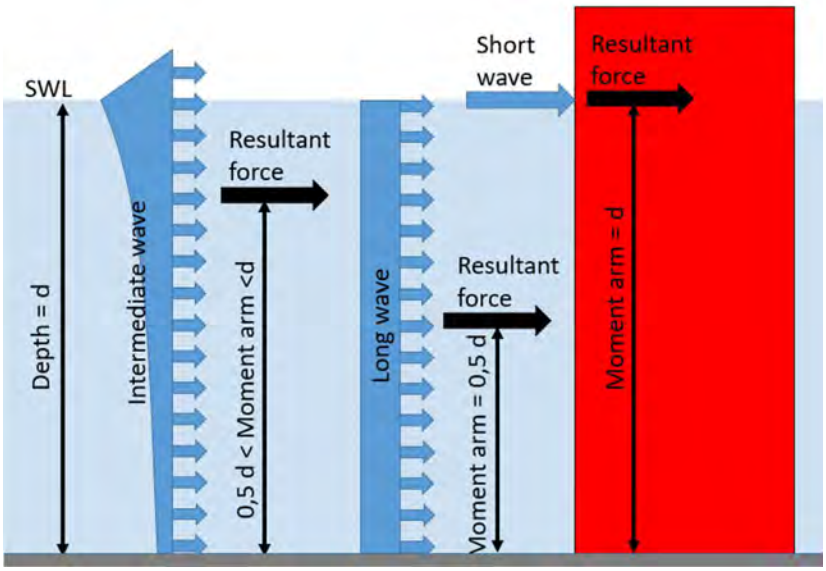

Figure 4: Wave forces acting on lock gate

Response function above still water level

The response above SWL is assumed to be of triangular shape which is illustrated in the left pressure figure in Figure 4. The wave pressure above SWL is a quadratic function of the wave amplitude. This expression cannot directly be used for the derivation of the response function, since a spectral approach requires response to be linear in the wave amplitude. We linearize the function by replacing the variable height of the pressure figure by a constant reference amplitude (a_{ref}) which is given in *(3)*. The response function is given in equation *(4)*.

$$F_{top} = (1+r)\frac{1}{2}\,\rho_w\, g\, a^2 \rightarrow linearization \rightarrow F_{f\eta_{top}} = (1+r)\frac{1}{2}\,\rho_w\, g\, a_{ref}\, a \qquad (3)$$

$$R_{f\eta_{top}} = \frac{F_{f\eta_{top}}}{a(f)} = (1+r)\frac{1}{2}\,\rho_w\, g\, a_{ref} \qquad (4)$$

In which:

a_{ref} = $\frac{1.5H_{m0}}{2}$

Response function of combined wave forces.

The total response is derived by combining the response of a wave below and above SWL. The response functions of each load signal must be added first before calculating the wave force variance density as given in equation *(5)*.

$$S_{FF}(f) = (R_{f\eta_{sub}}(f) + R_{f\eta_{top}})^2\, S_{\eta\eta}(f) \qquad (5)$$

Response functions below and above SWL are given in Figure 5. The relative contribution of low frequency waves is considerably larger than for high frequency waves. This can be explained by the longer waves penetrating deeper into the water column and thus loading the gate over a larger height as visualized in Figure 4. For an increasing frequency, the response is declining due to the larger decline of wave pressure. This results in a factor of 3,5 between the response of a 0.1 Hz wave compared to a 0.2 Hz wave. The contribution of the wave force below SWL dominates the response. A small error made by linearization for the wave above SWL can be accepted.

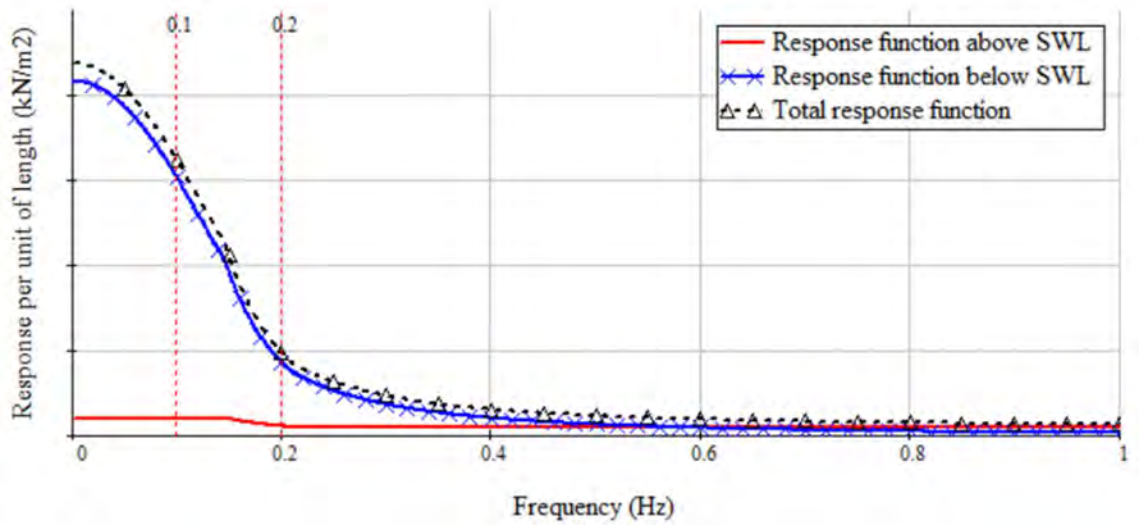

Figure 5: Response functions above and below still water (SWL)

Crest length effect

Low frequency waves are generally long crested; as the frequency increases and the waves becomes shorter the waves become short crested. This principle is illustrated in Figure 6.

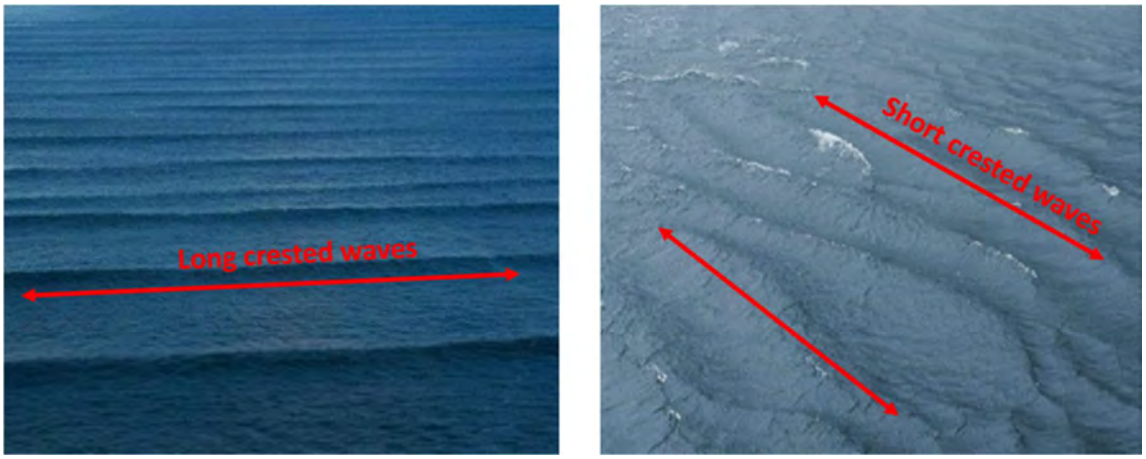

Figure 6: Low frequency waves (left) high frequency waves (right)

Waves with a crest length equal or larger than the available length of the gate in the lock chamber will exert an equal load over the whole length of the gate. Higher frequency waves have a shorter crest length than the available length of the gate in the lock chamber. Therefore, only a fraction of the gate is loaded by shorter waves. This crest length effect imposes a reduction of the total load.

To include this effect a crest length factor is applied (Ministerie van Verkeer en Waterstaat, 2000). When the gate starts to move from the recess into the lock chamber, a fraction of the gate is subjected to wave loads. In this case, the crest length of short waves is equal or larger than the available length of the gate and the reduction factor is equal to 1 (no reduction). When the gates move further into the lock chamber, the crest width of the short waves is smaller than the available gate length and the reduction factor is smaller than 1 with a minimum of 0.7 as presented in Figure 7.

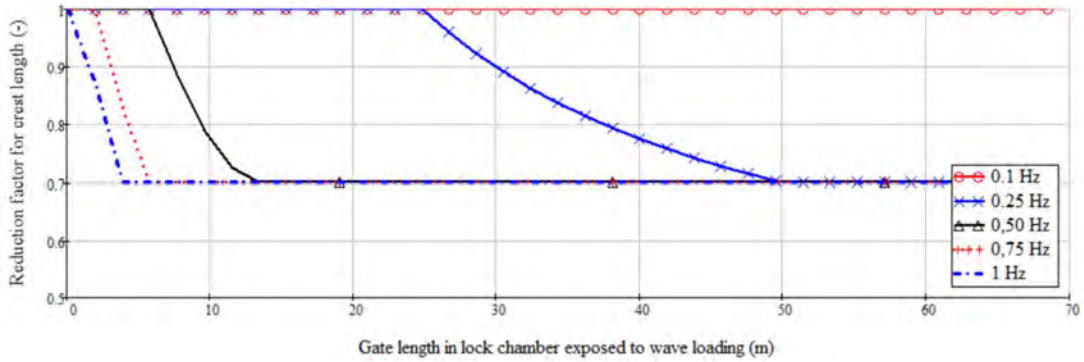

Figure 7: Crest width reduction factor

Due to this effect, the wave force variance density *per running meter* is larger for a gate exposed to waves over a small length than for a gate loaded by waves over the full length. This can be seen in the variance densities given in Figure 8. So, the total wave force is dependent upon the projected length of the gate in the lock chamber and therefore of the timing of the wave load within the gate mission.

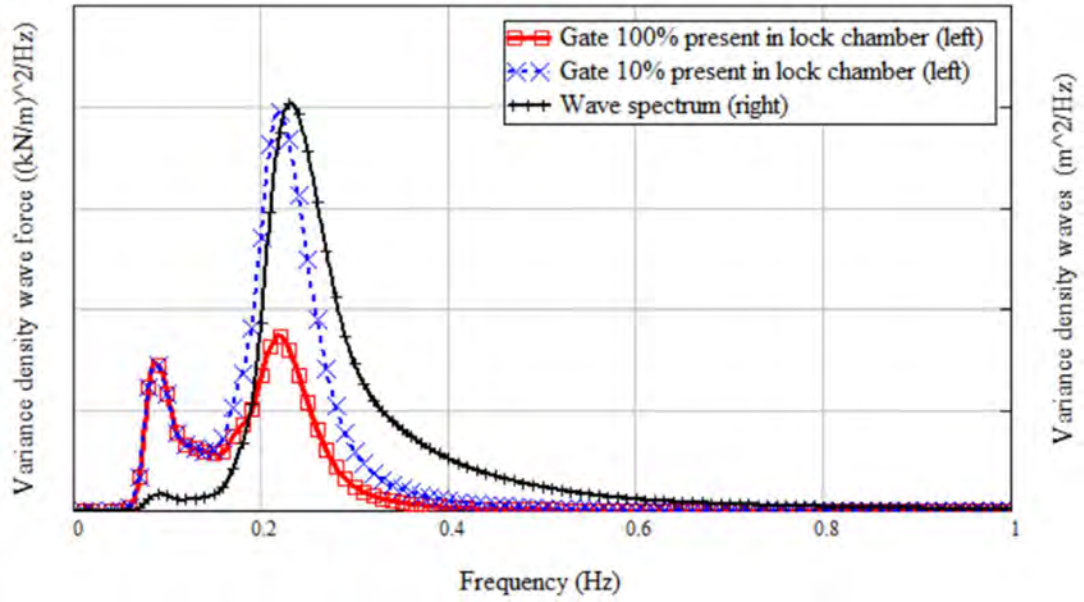

Figure 8: Spectrum of transversal wave force per meter running length

For a gate fully exposed to waves (red line Figure 8). The relative contribution per running meter of the wave force variance density for low frequencies is considerably larger than for the higher frequencies. This can be explained by the longer waves penetrating/reaching deeper into the water column and thus loading the gate over a larger height. A minor contribution of low frequency waves (2% of the wave energy) causes a major contribution to the total wave force (approximately 20% of the total wave force).

4. SPECTRUM OF LONGITUDINAL WAVE FORCES

When the gate is (partially) open, a wave can propagate into the lock chamber. The wave propagates in between the end of the gate and the concrete structure of the lock as indicated in Figure 2. Due to the large cross-sectional area of the gate, a force is generated by the waves traveling by. A wave peak will push the gate into its recess, a trough pulls the gate into the lock chamber. The magnitude of the force strongly depends on the wave length. Waves with a wave length equal or longer than to 2 times the thickness of the gate will push the gate over the full width into the recess. In this case, the peak of the wave is present from side to side of the gate. This is shown in the left figure of Figure 9. As waves

become shorter, the gate is simultaneously loaded by multiple peaks and troughs. The net force pushing the gate into its recess will become zero if the wave length fits exactly a discrete number of times in the gate thickness. For short wave lengths not exactly fitting, the wave force will be small because the peaks counteract the troughs.

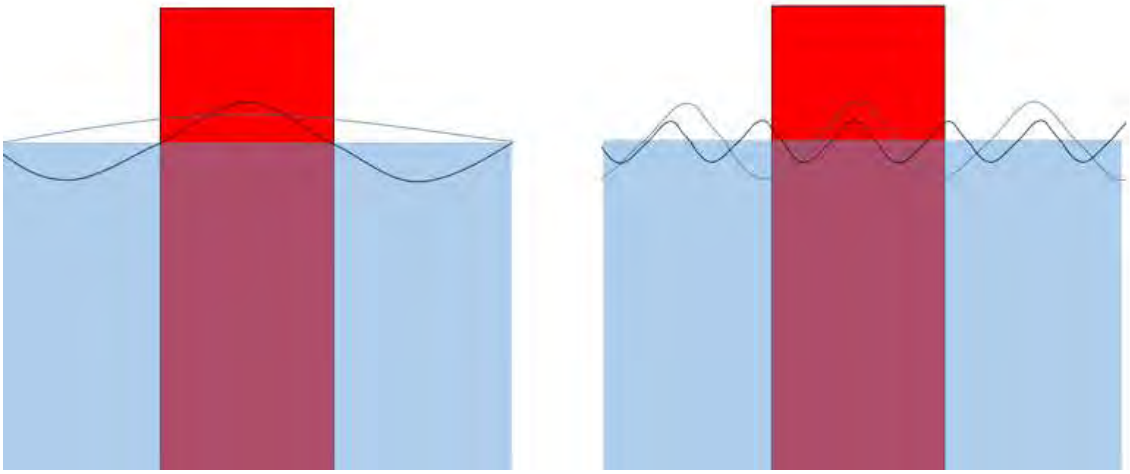

Figure 9: Waves at the end of the gate. Left: gate loaded by long waves, right: gate loaded by short waves.

To find the wave force, the wave pressure is integrated over the width and the height of the gate. The force below SWL is given in *(6)*. The largest forces are generated for waves which have a wave peak in the middle of the gate as illustrated in Figure 9. Therefore, the angular velocity is multiplied by a period shift Δt in *(6)* and *(7)*.

$$F_{sub} = \rho_w \, g \, a \int_{-\frac{B_{gate}}{2}}^{\frac{B_{gate}}{2}} \int_{h_{gate\_low}}^{h_w} \frac{\cosh(k\,(\eta - h_{gate\_low}))}{\cosh(k\,(h_w - h_{gate\_low}))} \sin(\omega\,\Delta t - k\,x)\;\mathrm{d}\eta\,\mathrm{d}x \qquad (6)$$

The force above still water level is based on *(7)*. Only the wave force above still water level is relevant for obtaining a conservative force, the negative wave force of the wave throughs is filtered out by setting the pressure to 0. The force above SWL is calculated using *(7)*. The response and the spectra of wave forces are given in Figure 10 and Figure 11. Due to the presence of multiple peaks and troughs, the force is negligible after 0.4 Hz. Long waves, which penetrate deep into the water column show the largest response for reasons explained earlier.

$$F_{top} = \frac{1}{2}\,\rho_w \, g \, a \, a_{ref} \int_{-\frac{B_{gate}}{2}}^{\frac{B_{gate}}{2}} \begin{matrix} \sin(\omega\,\Delta t - k\,x)\;\; if\;\; \sin(\omega\,\Delta t - k\,x) > 0\,m \\ 0m\;\; otherwise \end{matrix} \mathrm{d}x \qquad (7)$$

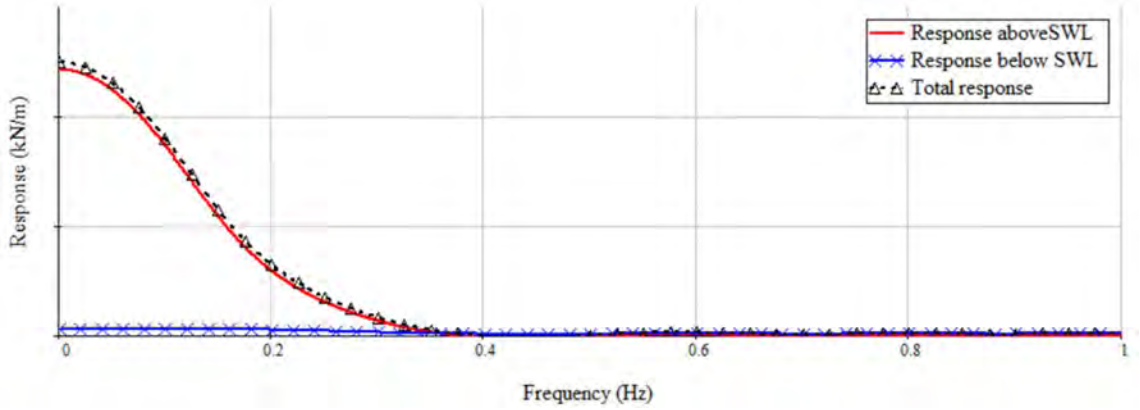

Figure 10: Response functions above and below still water (SWL)

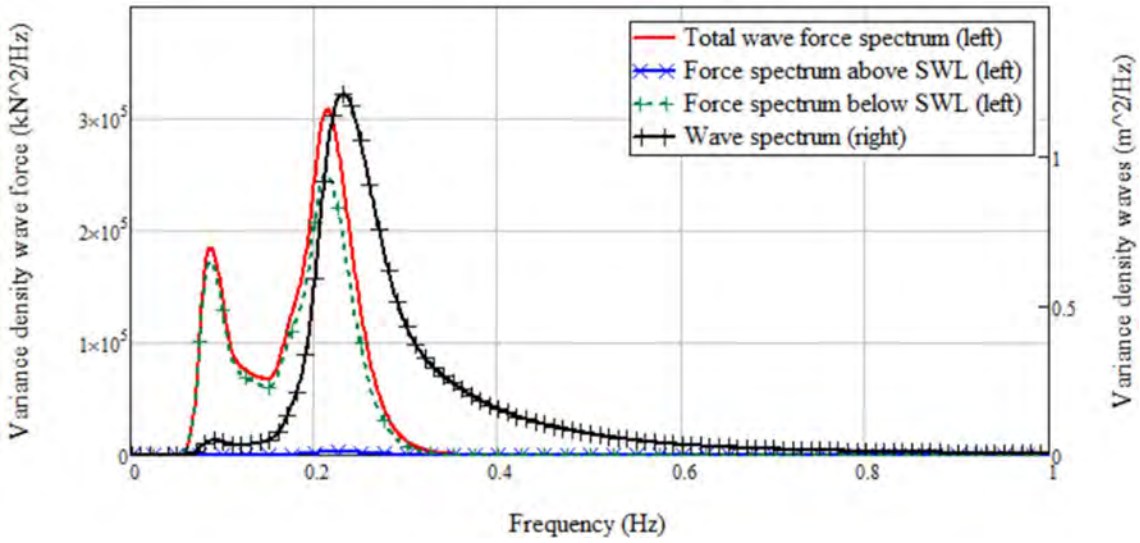

Figure 11: Longitudinal wave force variance density on gate

5. CONVERSION FROM TRANSVERSAL WAVE FORCE SPECTRUM TO LONGITUDINAL WAVE FORCE SPECTRUM

During gate mission, the gate is pushed or pulled by waves onto its supports. The driving mechanism needs to pull the gate along the supports. Between gates and supports, friction forces are generated which are always directed opposite to the gate motion. To calculate the total longitudinal force, the transversal wave force addressed in chapter 3 needs to be transformed into a longitudinal frictional wave force. The friction force is calculated by the multiplication of the transverse force by a friction factor as shown in the left section of Figure 12 for a simply supported beam. However, the gate is supported in three points (Figure 13, support A, B and C) resulting in a less simple mechanical scheme. When the gate is loaded by a wave with a resultant force located above the rotational axis shown in Figure 12, the gate acts as a cantilever beam. For a cantilever beam, the forces in one support counteracts the forces in another support as shown in the right section of Figure 12. The summed absolute values of the forces in the supports is larger than the total wave force, because the friction force depends on the absolute value of the support forces and not on their direction. With the equilibrium of the wave force ensured, the fiction force is equal to the absolute wave force (*F*) multiplied by an amplification-factor (*Fac*) for the structural behaviour of the system, multiplied by the friction factor (ϑ).

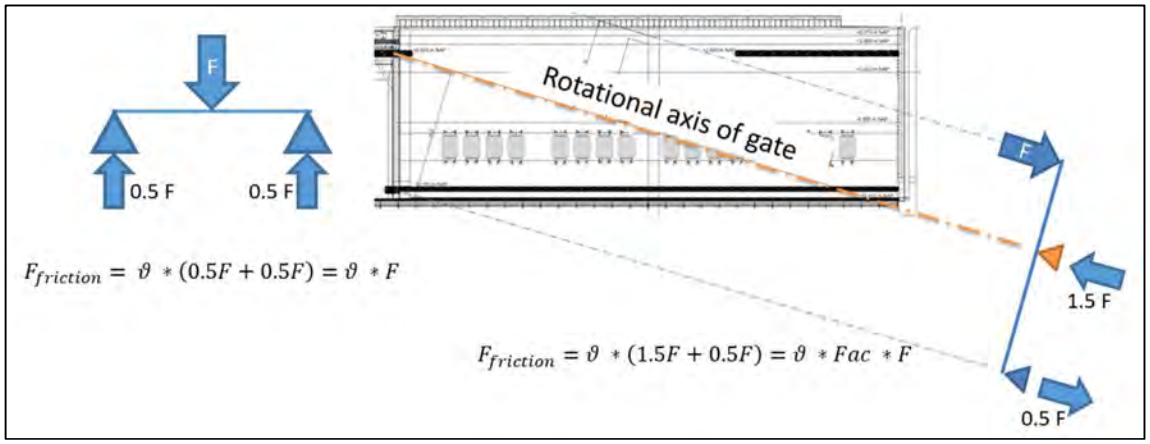

Figure 12: Mechanical behavior of a simple supported beam and the lock gate

The transversal wave forces are divided over three supports which are named A, B and C, Figure 13. Two supports (A and C) will cope with the direct wave force. Waves loading the gate above the rotational axis (dashed line in Figure 12 and Figure 13) will turn the gate over. A force will be generated in support B (B) to prevent the gate from turning over. The friction force is present in each support, irrespectively the sign of the force (positive for A and C negative for B).

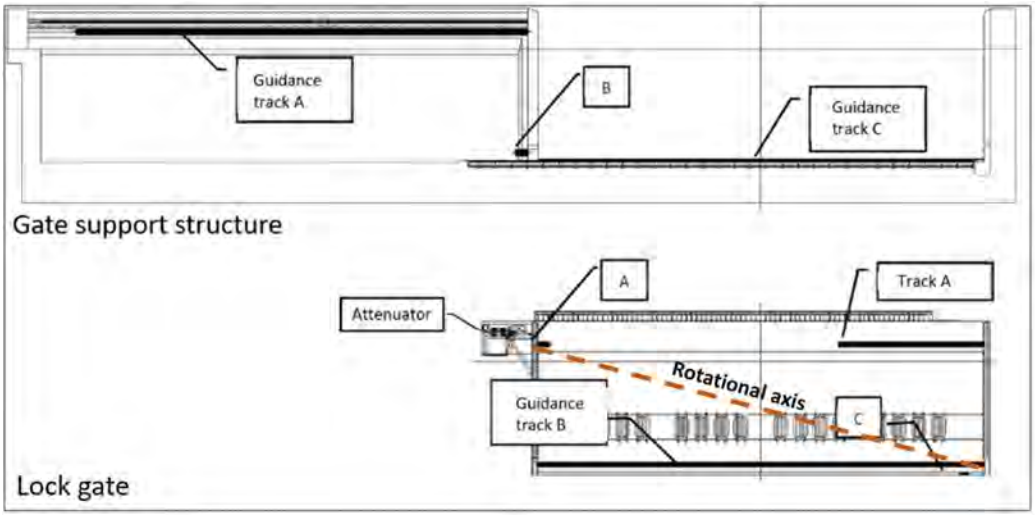

Figure 13: Gate schematization and location of supports

Derivation of response functions for each support

The transverse wave load is distributed over the supports. The magnitude of the force in each support depends on:

- Wave frequency
- The position of the gate.
    - During opening/closing of the gate the orientation of the rotational axis will change resulting in a different division of forces over the supports.

To calculate the force distribution over the supports, the distance relative to the bottom of the resultant wave force for a variable frequency is derived by dividing the wave tilting moment response function by the wave force response function. The tilting moment is calculated for every frequency, because the shape of the pressure distribution varies as a function of frequency as indicated in Figure 4. The moment response function is derived by multiplying the force response function by the moment arm. This results in the moment arm function given in *(8)* and Figure 14.

$$A_{moment}(f) = \frac{R_{M\eta}(f)}{R_{f\eta}(f)} \quad (8)$$

In which:

A_{moment} = Moment arm; distance between resultant force and bottom of gate (m)
$R_{M\eta}$ = Tilting moment response function
$R_{F\eta}$ = Wave force response function

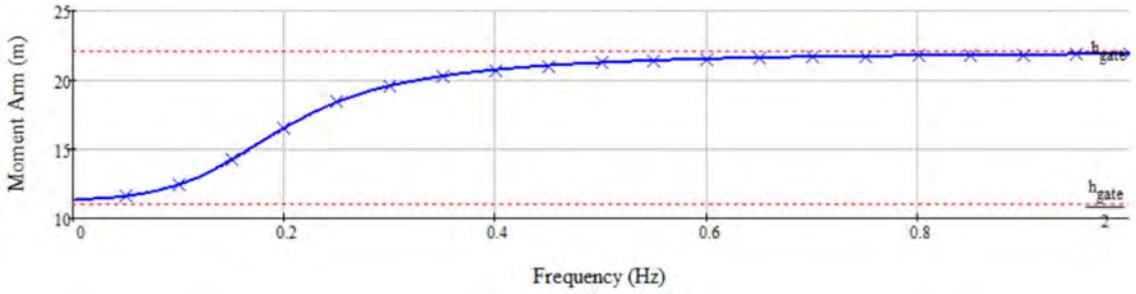

Figure 14: Moment arm as function of wave frequency

By knowing the moment arm and the wave force for each frequency and the orientation of the rotational axis for each position of the gate, the distribution of the wave force over the supports is derived by solving:

- the horizontal equilibrium of forces,
- the moment equilibrium over the x-axis
- and the moment equilibrium over the y-axis.

The result is given in Figure 15. The distribution of wave force over the supports is quantified as a factor between the total incoming wave and the reactional force in each support. The relative sum of the factors must always be equal to -1 to make equilibrium with the total incoming wave (set equal to +1). The absolute sum of the factors is always equal or higher than 1 due to the cantilever effect of a wave loading the gate above the rotational axis.

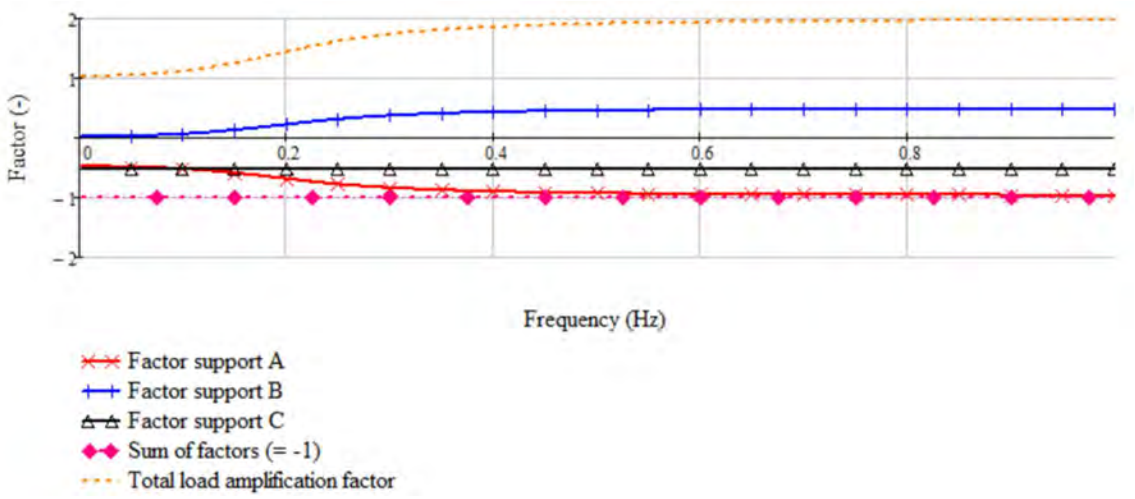

Figure 15: Relative factors for the division of the incoming wave force over the supports A, B and C

For infinitely long waves, the gate is loaded directly on the rotational axis. The reaction forces are equally distributed over support A and C and the extra compensating force in B is zero as shown in Figure 15. When the waves become shorter for an increasing frequency, the resultant force will be located above the rotational axis generating an extra compensating force in support B up to a maximum of 0.5 times the incoming wave force. To compensate this extra force in B, support A will experience an extra force with a maximum of 0.5 times the incoming wave force. In short: the

amplification of the load which corresponds to the absolute sum of the factors in each support is 1 for infinitely long waves and increases to a maximum of 2 for shorter waves.

The response function of each support is calculated by multiplying the response function of the incoming transversal wave by a friction factor (ϑ) and the function of the unitless amplification factor (*Fac*) given in Figure 15 for each support. The spectra of the friction force for each support is given in Figure 16.

$$R_{support} = \vartheta \, Fac \, (R_{f\eta_{sub}} + R_{f\eta_{top}}) \qquad (9)$$

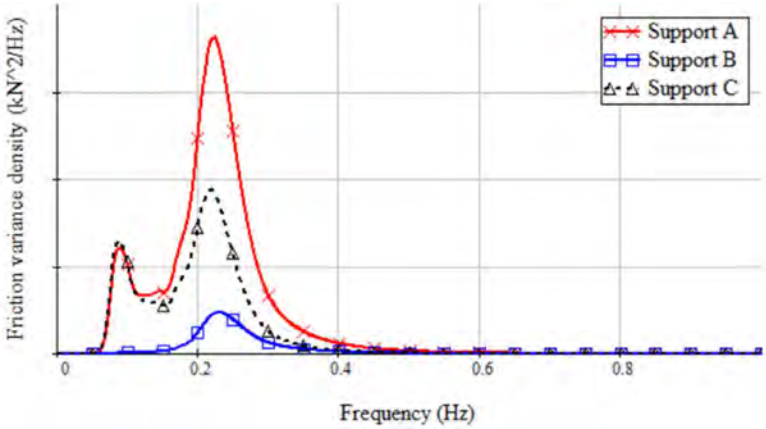

Figure 16: Variance densities of friction forces in supports, gate exposed over full width to waves.

Total longitudinal wave force spectrum

To derive the spectrum for the total longitudinal force, the spectrum of friction forces is combined with spectrum of longitudinal wave forces derived in chapter 4. The total longitudinal wave force spectrum is found by the square of the summation of the response functions as given in *(10)*.

$$S_{FF\ driving\ mechanism}(f) = (\, R_{suppprt\ A} + R_{support\ B} + R_{support\ C} + R_{longitudinal})^2 \, S_{\eta\eta}(f) \qquad (10)$$

In which:

$S_{FF\ driving\ mechanism}(f)$	=	Variance density required for driving mechanism (kN²/Hz)
$R_{support\ A}$	=	Response function support A
$R_{support\ B}$	=	Response function support B
$R_{support\ C}$	=	Response function support C
$R_{longitudinal}$	=	Longitudinal response function
$S_{\eta\eta}(f)$	=	Wave spectrum

The driving mechanism should have sufficient driving force to guarantee a sufficient low probability of delay of a gate mission for the spectrum of total wave forces given in Figure 17

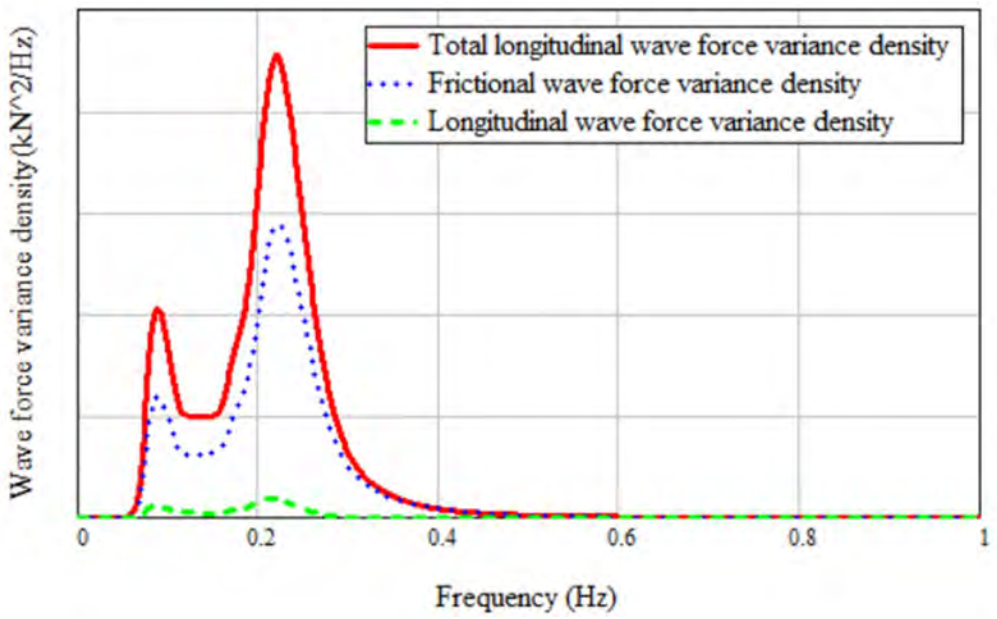

Figure 17: Total longitudinal wave force variance density, gate exposed over full width to waves.

6. CONVERSION FROM FORCE SPECTRUM TO DESIGN LOADS

The gate moves through a random wave field corresponding to the wave spectrum. A maximum force during the motion of the gate cannot be defined due to the randomness of the waves. Therefore, a probability distribution of the total longitudinal wave force is made based on the wave force spectrum (Figure 17). Using the probability distribution and the period between up-crossings a design choice is made for the required driving force of the driving mechanism.

Exceedance of the driving force by a wave does not immediately result in significant delay. The gate will not come to a standstill, but will only loose speed for a brief period since the mass of the gate prevents it from stopping immediately. To quantify the delay of a gate mission, a wave force time series is derived. The probability of delay and the period of delay is calculated by modelling numerous gate missions using the wave force time series.

In this chapter, the derivation of the wave force statistics, the wave force time series and the calculation of delay are described in three sections.

Wave force statistics

A first estimate of the required force of the driving mechanism is obtained by calculating the probability distribution. For the design of a general hydraulic structure, a significant wave height multiplied with a factor would have been applied. For example, quay walls or (smaller) hydraulic structures are designed using the significant wave height (probability of exceedance of 13%) multiplied by a factor 1.8 or 2.25. An exceedance of the installed capacity will only result in delay which is of minor importance for smaller hydraulic structures However, large delays are not allowed for the lock of Amsterdam. Therefore, more insight in the probability of exceedance and the number of exceedances during gate missions is required.

Following (Holthuijsen, 2007) a Rayleigh distribution is assumed for the wave forces. However, that choice is based on theoretical arguments and the validity is not fully ensured. Therefore, statistics have also been derived based on a peaks-over-threshold method using the wave force time series (see next section) and compared to the Rayleigh distribution using m_0 of the wave force spectrum spectrum. The found distribution closely resembles the Rayleigh distribution, so the latter was used in the remainder of the study. The result is given in Figure 18. Using this graph, a first estimation of the

required force can be evaluated based on a 'risk classification' corresponding to the significant wave force times a factor.

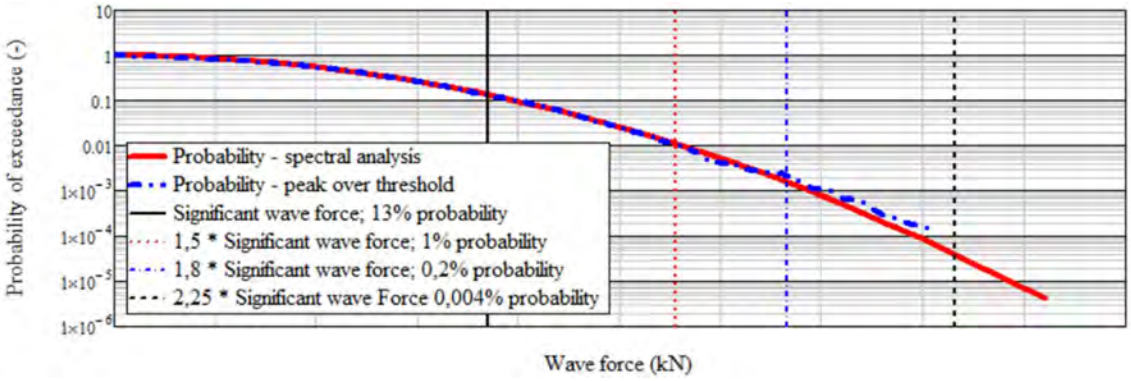

Figure 18: Probability of exceedance of wave forces

The duration of a gate mission is in the order of four minutes. The expected duration between exceedances of critical load levels for a single gate mission is therefore important, as it is related to the number of exceedances we can expect within a single mission.

To evaluate the number of exceedances of a certain wave force during gate mission the average time interval between successive up-crossings of a force is evaluated. The total number of up-crossings during a gate mission is found by dividing the time interval required for a gate mission by the average time interval between successive up-crossings. The average time interval between successive up-crossings is illustrated in Figure 19. The time interval is calculated using *(11)* (Holthuijsen, 2007). The periods between wave force up-crossings for a given wave force (η_{force}) are found by deriving the zeroth order and second order moments of the wave force variance density. The number of up-crossings during a gate mission is derived by dividing the period of the gate mission by the average time interval between up-crossings as given in *(12)*.

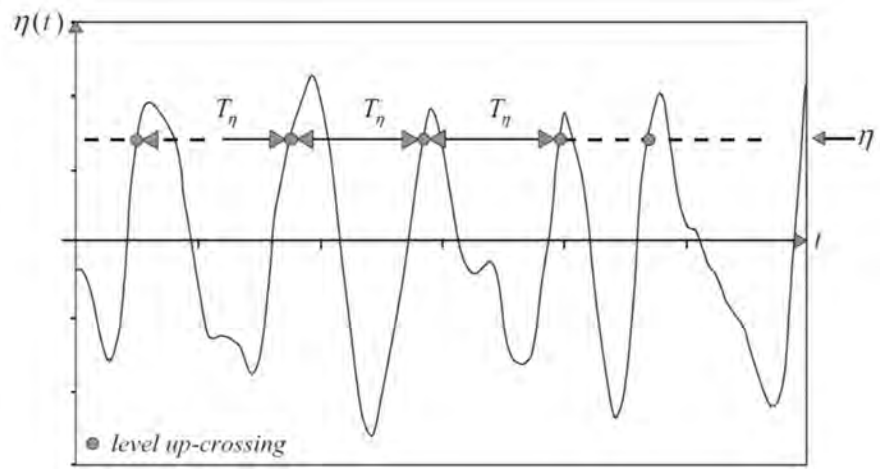

Figure 19: The up-crossings of the sea-surface elevation through level η and the corresponding time intervals T_η in a (statistically) stationary wave record (Holthuijsen, 2007)

$$\bar{T}_\eta(\eta_{force}) = \frac{\sqrt{m_0/m_2}}{e^{\left(-\eta_{force}^2/2m_0\right)}} \qquad (11)$$

$$nr_{up-crossings}(\eta_{force}) = \frac{T_{motion}}{\bar{T}_\eta(\eta_{force})} \qquad (12)$$

In which:

$\bar{T}_\eta(\eta)$ = Average time interval between successive up-crossings through level η

η_{force} = Level of up-crossing; wave force
m_0 = Zeroth order moment of the total force variance density
m_2 = Second-order moment of the total force variance density
T_{motion} = Required period to open or close the gate
$nr_{up-crossings}(\eta)$ = Number of up-crossings through level η during gate motion

The number of up-crossings during a gate mission for a variable force η_{force} is given in Figure 20. The significant wave force will on average be exceeded for 10 times during one mission. Therefore, the required installed driving force must be larger than the significant wave force. A force equal to 1.5 times the significant wave force will on average be exceeded once during a mission. To avoid frequent delay, the installed force of the driving mechanism should be larger than this force. Wave forces higher than 1.8 times the significant wave force will on average be exceeded one time per ten gate missions. So, expected delays during gate mission will be sufficient low by installing a higher driving force than 1.8 times the significant wave force. The expected quantity of delay cannot be evaluated using Figure 20. Therefore, the time series of the total longitudinal wave force derived and are further evaluated below.

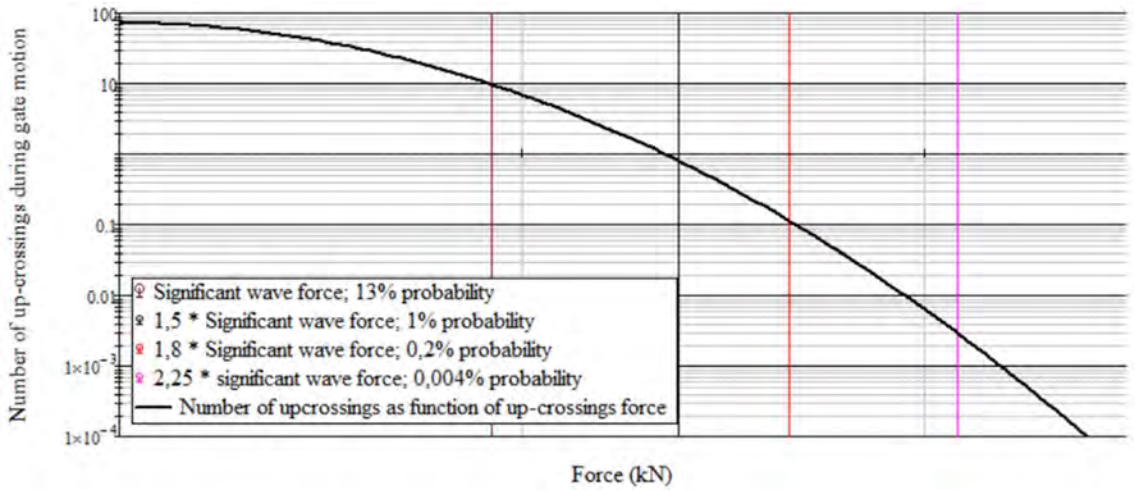

Figure 20: Number of up-crossings through level η during gate motion

Wave force time series and expected delays

The total delay of a gate mission depends on the statistics of the wave forces acting on the gate (the severity of storms) and the delay occurring within a single storm. To estimate the expected delay, we switch to an analysis in the time-domain. Using the variance density, a wave force time series is derived (Holthuijsen, 2007). The time series is derived by:

- Drawing a random phase from a uniform distributed probability distribution.
- Calculating the amplitudes from 0Hz till 1Hz with a step size of Δf using the wave force variance density given in Figure 17.
- Combining the calculated wave force amplitudes with the random phases.

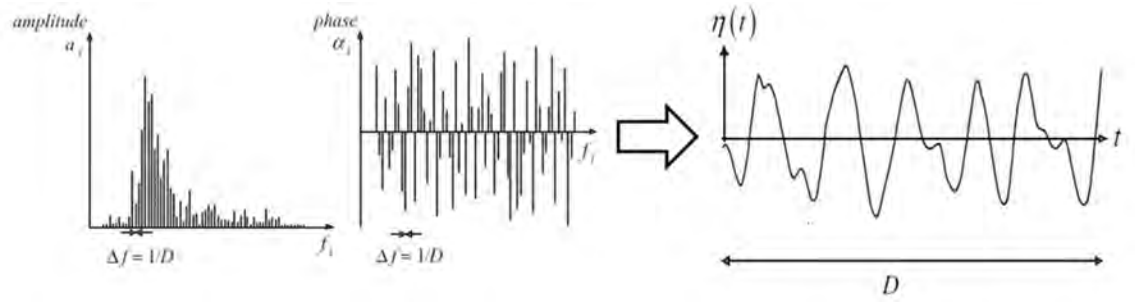

Figure 21: Generation of a time series (Based on (Holthuijsen, 2007))

As stated in Figure 2, the gate is loaded by a transversal and longitudinal force generating friction. The transversal force is pushing the gate onto the supports for a wave peak and pulling the gate onto the supports for a wave trough. Hence, for a wave peak or trough a positive transversal load is generated. To calculate the total longitudinal load on the driving mechanism, the absolute value of the frictional forces generated by the transversal force is used.

For longitudinal forces, a wave peak pushes the gate into the southern recess of the lock. This generates a positive force when the gate is opening and has a velocity towards the recess by itself. When the gate is closing and moving into the lock chamber a wave peak generates a negative force because the gate motion is opposite to the direction of the wave force. The opposite holds for a wave trough.

For the calculation of the wave force time series the absolute value of the frictional forces is combined with the relative value of the longitudinal load. The resulting wave force time series is given in Figure 22. Most of the times, the wave force is positive. For a fraction of the time the wave force is negative which means that the negative longitudinal load due to a wave through at the edge of the gate is larger than the friction force load. This time series is used for the calculation of delay.

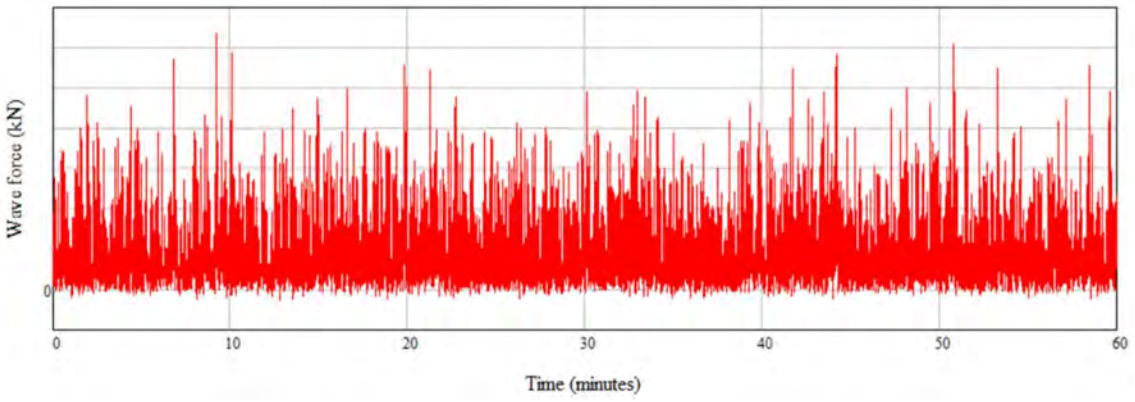

Figure 22: Wave force time series (10-year return period)

Calculation of delay

The total force to be overcome by the driving mechanism consists of the wave forces and “other loads” like density differences, translatory waves, etc (Voortman, et al., 2017). When the total load exceeds the installed driving force, the net available force for the gate mission becomes negative. According to the second law of Newton (F=m*a) the gate will slow down.

To evaluate the probability of delay, a wave force time series has been made corresponding to a storm of 10 hours. The wave force has been added up by the ‘other loads’ (Voortman, et al., 2017). In this time series, the gate is continuously being opened and closed to calculate the delay. In total 131 gate missions have been simulated of which a couple of gate missions have been shown in Figure 23. The total delay for each gate mission is calculated and transformed into a cumulative probability function which is shown in Figure 24.

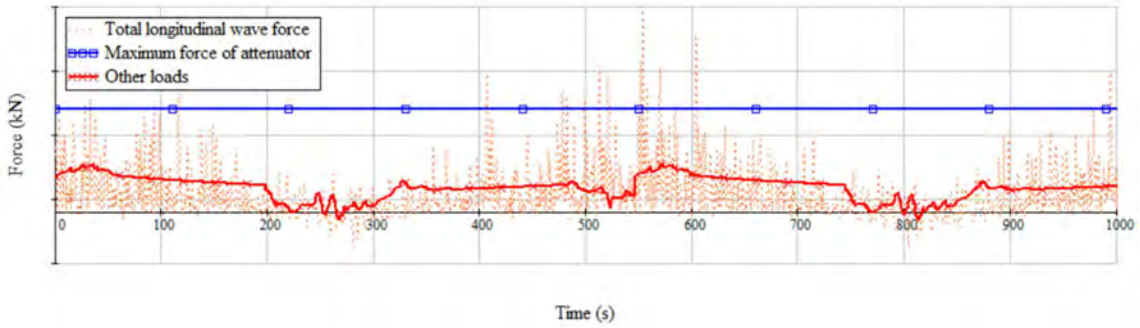

Figure 23: Total forces (red) and installed driving force (blue)

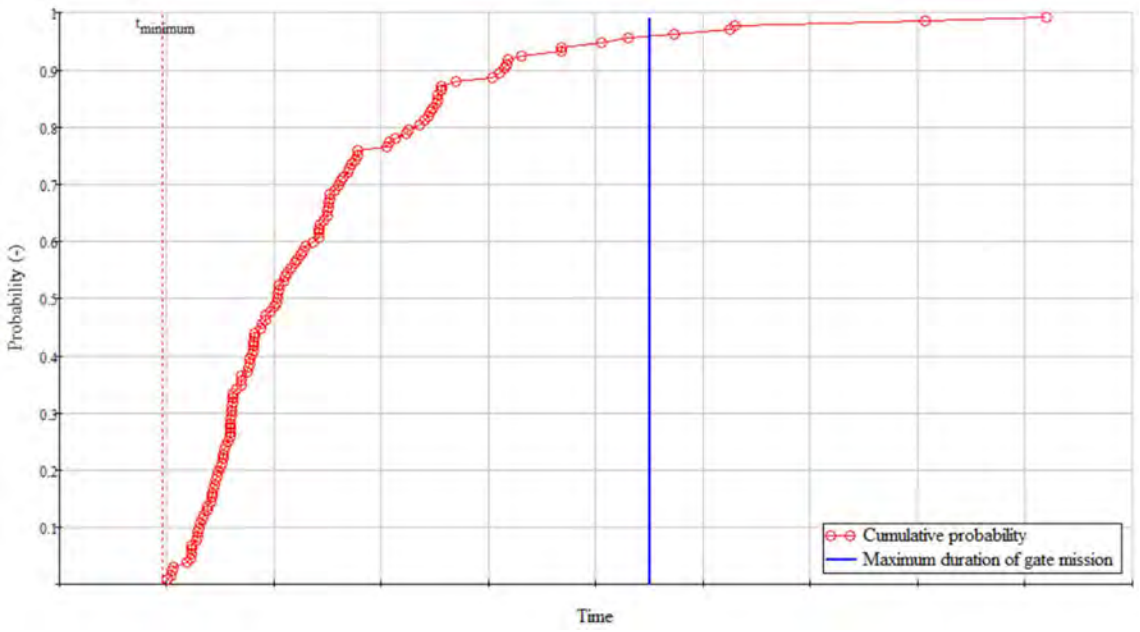

Figure 24: Probability of delay during a 1/10 per year storm

The required maximum duration for the gate mission is indicated by the blue line in Figure 24. The probability of exceedance of the set duration is 5% which is sufficient low. So, based on the estimated required driving force using the wave force up-crossings (Figure 20) a sufficiently low probability of exceedance is obtained for the duration of a gate mission.

CONCLUSION

The use of the linear wave theory gives more insight compared to other theories for a robust design and analysis of the driving mechanism of a lock gate.

Using the linear wave theory, representative forces are derived which are indirectly loading the driving mechanism. The spectral model showed that a double peaked wave spectrum with a minor contribution of low frequency waves resulted in a double peaked spectrum of longitudinal forces with a significant peak at low frequencies. Based on this model, the representative forces on the driving mechanism are well-derived. 1,5% of wave energy below 0,14Hz results in 17% of the total wave force. A small amount of wave energy gives a major contribution to the total wave force which would not be calculated when using only one wave height and wave period using either Goda's method or the linear wave theory. The proposed methodology gives an optimal evaluation of the loads on the driving mechanism for normal wave conditions up to a wave field with a return period of 10 years (H_{m0}=1,5m, T_{m-10}=4s).

The longitudinal wave force spectrum gives detailed information for the evaluation of the driving force of the driving mechanism. By evaluating the number of up-crossings during a gate mission a good first estimate for the driving force is derived. The driving force is verified using time series of the wave force. A model is developed in which the delay of a gate mission for a random wave force field could be derived. The probability of exceedance of the required period of a gate mission for a 10-year return period storm given the driving force evaluated using the up-crossings would only be 5% which is acceptable low. This analysis cannot be done when using a theory based on only one wave height and wave period, like is practice for the theory of Goda.

The results have been incorporated in the design of the gates and the driving mechanism. The gates and driving are currently being constructed. The lock is expected to be fully operational by the end of 2019.

REFERENCES

Goda, Y., 2010. *Random seas and design of maritime structures.* 3rd edition ed. s.l.:World scientific.

Holthuijsen, L., 2007. *Waves in Oceanic and Coastal Waters.* Cambridge: Cambridge University Press.

Ministerie van Verkeer en Waterstaat, 2000. *Ontwerp van Schutsluizen - Design of schiplocks.* s.l.:Ministerie van Verkeer en Waterstaat.

Voortman, H. et al., 2017. *Hydraulic loads on a large lock gate.* Liverpool, ICE Conference - Coastal Marine Structures and Breakwaters 2017.

ZUS, 2016. *Sealock IJmuiden.* Rotterdam: ZUS - Zones Urbaines Sensibles.

UNDERSTANDING RISK-DRIVING FACTORS, THEIR INDICATORS AND RESULTING DECISION CRITERIA: THE INTERDISCIPLINARY APPROACH IN GERMANY

by

A. Panenka[1], J. Sorgatz[2] and J. Kasper[3]

ABSTRACT

This paper presents an interdisciplinary research programme in context with the reliability of transport infrastructures. The programme initiated by the German Federal Ministry of Transportation and Digital Infrastructure (BMVI) aims at understanding underlying risk-driving factors, their indicators and resulting decision criteria. Using the example of the federal waterways in Germany illustrates the innovative approach.

1 BAW: TECHNICAL EXPERTISE REGARDING WATERWAYS IN GERMANY

With over 100 years of scientific tradition in the field of waterways engineering, the German Federal Waterways Engineering and Research Institute (“Bundesanstalt für Wasserbau”, BAW) deals with a multitude of challenging tasks. The predecessor institution of the BAW was the Royal Research Institute for Hydraulic Engineering and Shipbuilding ("Königliche Versuchsanstalt für Wasserbau und Schiffbau"), which was founded in Berlin in 1903.

The BAW was assigned a technical and scientific mission, which covers all areas of waterways engineering relating to Germany's federal waterways. The BAW was also assigned responsibility for the building of special purpose ships for the Waterways and Shipping Administration (WSV). In addition, the BAW manages the construction planning of special purpose ships for other non-military federal authorities. Today the BAW operates from its headquarters in Karlsruhe and offices in Hamburg.

2 THE BMVI NETWORK OF EXPERTS: AN INTERDISCIPLINARY APPROACH

2.1 Background

In Germany, the infrastructure assets have a capital value of around 430 billion Euros. The consideration of the transport performance makes the added value impressively clear. In addition to passenger services, goods traffic with its approximately 655 billion tonne-kilometres plays a key role. In order to secure the transport performance, investments are urgently necessary. In view of the need to design and built a resilient and environmental-friendly transport system in Germany, the Federal Ministry of Transport and Digital Infrastructure (BMVI) is taking an innovative course of action. It pools the expertise and skills of its departmental research facilities and executive agencies in the BMVI Network of Experts (NoE) under the guiding principles “Knowledge – Ability – Action”. The network, founded January 2016, is a new format of departmental research, which is formed by seven departmental research facilities and executive agencies of the BMVI (c.f. Federal Ministry of Transport and Digital Infrastructure 2017).

[1] Department B Structural Engineering, Federal Waterways Engineering and Research Institute (BAW), Germany, andreas.panenka@baw.de
[2] Department G Geotechnical Engineering, Federal Waterways Engineering and Research Institute (BAW), Germany, julia.sorgatz@baw.de
[3] Department W Hydraulic Engineering in Inland Areas, Federal Waterways Engineering and Research Institute (BAW), Germany, julia.kasper@baw.de

The collaborating institutions are:

- Federal Highway Research Institute (BASt)
- Federal Institute of Hydrology (BfG)
- Federal Waterways Engineering and Research Institute (BAW)
- Deutscher Wetterdienst (German Meteorological Service, DWD)
- Federal Office for Goods Transport (BAG)
- Federal Maritime and Hydrographic Agency (BSH)
- Federal Railway Authority (EBA)

2.2 Organisation of the NoE

The NoE covers five distinctive research topics (see Figure 1). Each of these areas is subdivided into several key topics (KT) dedicated to specific fields of interest. At the administrative level, the steering committee establishes the direct link to high-level governmental and departmental authorities and administrations. Assisted by the scientific task force, the coordination board ensures a smooth cooperation between the involved parties by managing the administrative and organisation work.

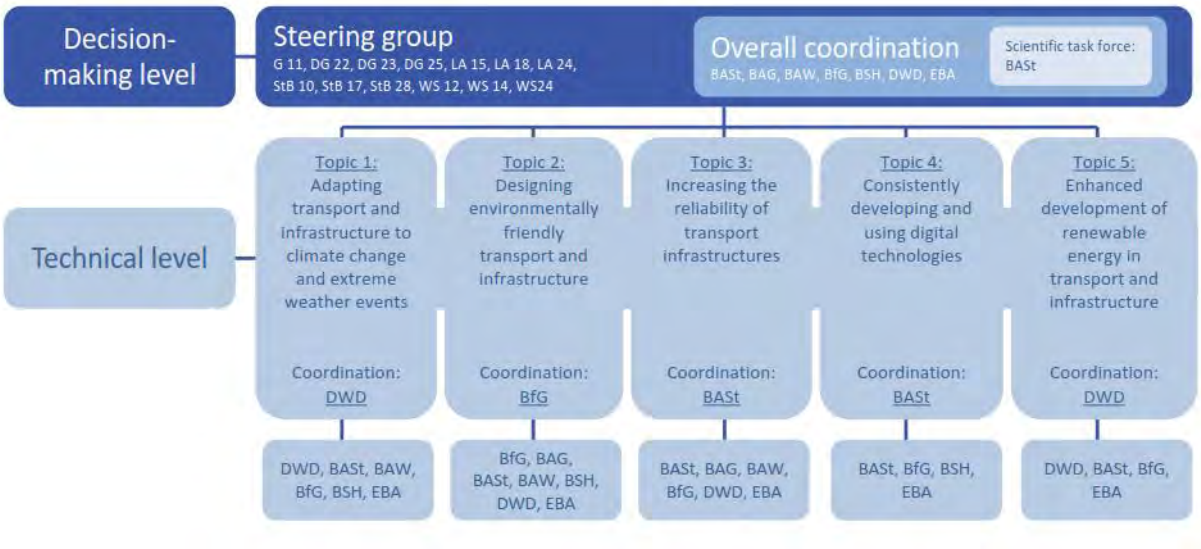

Figure 1: The BMVI Network of Experts Knowledge–Ability–Action

2.3 The BAW as part of the interdisciplinary approach

As technical advisor to the BMVI, the BAW is part of the NoE. The research activities of BAW consider the particular requirements of the waterway infrastructure. The NoE currently funds 10 R&D projects and 12 R&D positions of the BAW. Each of the projects is associated to one specific research area, which covers certain aspects regarding the understanding of risk-driving factors, their indicators and resulting decision criteria in context with civil engineering structures.

Topic 1: Adapting transport and infrastructure to climate change and extreme weather events

Topic 1 identifies the vulnerabilities to traffic and infrastructure caused by climate change and extreme weather events, and then develops appropriate adaptation options. Here, the resilience to extreme weather events and the consequences of climate change as well as the sustainable usability of the transport infrastructure are of particular importance. By linking the expertise of DWD, BSH, BfG, BAW, EBA and BASt, the respective specific knowledge on climate development will be combined with practical knowledge on the three modes of transport: road, rail and waterway.

Topic 1 is divided into nine key topics, which deal with the provision of data as well as concrete hazard scenarios. These include floods, storms, landslides and waterway-specific hazards. The results are included in a risk management system, which will be further developed in this topic. With regard to the projected impacts of climate change, adaptation options are being developed and tested, both for individual modes of transport and across modes of transport. Simulation

models and analysis methods are applied and validated using two focal regions, coast and inland.

The BAW is represented in all key topics and contributes its experience as well as the knowledge gained in the context of the projects, in particular from analyses of numerical model examinations

Topic 2: Designing environmental friendly transport and infrastructure

Topic 2 has the goal to find solutions for a design of transport and infrastructure, which is environmental-friendly and sustainable. This objective is pursued in five key topics, dedicated to

- ∂ biodiversity and structural diversity of transport routes,
- ∂ invasive species (neobiota) being introduced and spread by the transport mode,
- ∂ transport-related material loads,
- ∂ building and construction-related emissions and
- ∂ reducing noise and noise emissions.

The BAW is involved in a project, which works on operational and technical improvements of inland navigation regarding the reduction of emissions. For this purpose, a dynamic vehicle model (FaRAO) is used to simulate inland waterway vessels. This model is extended by a special engine model, which also simulates the emissions of an inland vessel at different operating points of the engine. To calibrate and validate the engine model, vessel and engine data are surveyed under real operating conditions. The first test will be conducted in the area of the port of Duisburg. Eventually, the spread of emissions of all modes of transport using an air pollutant transport model with chemical reaction equations.

Topic 3: Increasing Reliability of Transport Infrastructure

The reliability of the infrastructures is regarded as essential aspect of a resilient transportation system. The bulk of the German transportation network lies on infrastructures that were constructed several decades ago and which actually require continuous maintenance and modernisation. Thus, combined effects of aging infrastructure, altered and generally higher traffic impacts over their lifetime as well as environmental stressors increase risks in terms of the reliability associated with these transportation infrastructures. In this regard, the past efforts in maintaining the infrastructures have been nowhere near sufficient, and have resulted in a considerable investment backlog.

In this context, Topic 3 investigates methods and concepts, which could help in increasing the reliability of the transportation infrastructure again. Reliability is defined as “ability of a structure or a structural member to fulfil the specified requirements, including the design working life, for which it has been designed.” (DIN EN 1990:2010) This definition implies that functional requirements (i.e. limit states), structural behaviour, actual and future live load scenarios, as well as possible deterioration processes are generally known, measureable, and continuously evaluated over the whole operational lifetime of the structure. In a consequence, an effective maintenance management system must also consider inevitable uncertainties associated with these aspects.

Topic 3 consists of four key topics:

- ∂ state-of-the-art field tests methods to assess the condition of the infrastructure
- ∂ modern reliability evaluation tools, both qualitative and quantitative
- ∂ availability and vulnerability of infrastructure under extreme weather events
- ∂ rehabilitation measures under operation

Altogether, these key topics aim at developing a proactive and future-oriented maintenance management system which helps to increase the reliability of the transportation infrastructure in Germany (see PANENKA et. al 2018).

Topic 4: Consistently developing and using digital technologies

The aim of Topic 4 is to positively influence digital technologies through networking of departmental research and BMVI technical authorities. The thematic focus is thus on the consistent use of the possibilities of information and communication technologies with a focus on inter-

agency cooperation in the area of information provision and IT-use. The topic is currently in a conception phase. The BAW observes the development of this topic.

Topic 5: Enhanced development of renewable energy in transport and infrastructure

Topic 5 works on the various application and extraction potentials of renewable energies in an intermodal approach to transport and infrastructure. A cross-cutting pilot project on this topic will initially show the benefits of joint research in this area with the participation of different departmental institutions. The involved higher authorities work together to develop concepts for a significantly increased use of renewable energies in the transport infrastructure. This also includes the operation of maintenance and repair vehicles. Options and recommendations are being developed so that the modes of transport waterway, rail and road can increasingly make their contribution to climate protection in the future. Topic 5 is currently in a conception phase. The BAW observes the development of this topic.

3 INCREASING THE RELIABILITY OF THE WATERWAY INFRASTRUCTURES

The waterway infrastructure features a large number of structures with a high diversity. Thus, the determination of risks emerging from these structures requires profound technical knowledge and adequate evaluation tools. In this regards meaningful structural indicators in combination with additional data sources like geographic information systems (GIS) or advanced metrological weather models are essential for an efficient risk assessment. The combination of all information allows an understanding of risk-driving factors, which helps to define the essential decision criteria. This knowledge evokes an increasing demand for new technologies and methodologies helping to reduce both the actual impact of disruptive metrological events on the infrastructure and the potential risks of possible failure scenarios.

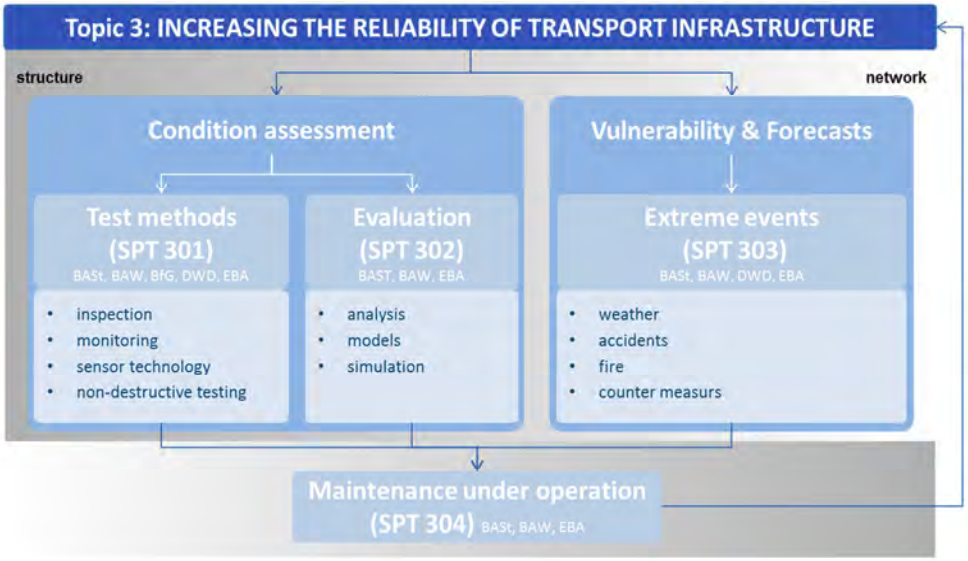

Figure 2: The organisation chart of Topic 3

In this context, the interdisciplinary research activities of Topic 3 in the NoE show first results, which especially support the need for an improvement of the reliability of waterway infrastructures.

3.1 Reducing the impact of disruptive events with smart water level control

The water level of the German waterways is usually subject to a strict water level control. Disruptive events for the automated water level control of impounded waterways are often caused by unknown lateral inflows, such as storm water overflow from urban areas after heavy rainfall events. In order to avoid violations of the water level tolerance and reduce discharge fluctuations, the BAW is developing a new control strategy. A smart water level control should be based on a model of the impounded river section, high-resolution precipitation forecasts for urban catchment areas and communication between neighbouring impoundments (KASPER, J. et al. 2017). The development process of a smart water

level control shows the benefits of a close cooperation between institutions providing competences in meteorology, hydraulic engineering and control technology.

Essential risk factors are the prediction accuracy of extreme rainfall events and, subsequently, the precise control of the resulting discharge. The higher the difference between the summer base discharge and lateral inflow due to extreme weather events, the higher the requirements for the water level control system. The main indicator for the effectiveness of the water level control system is the extent of water level fluctuations in the waterways, which shall be minimized.

Figure 3 shows a schematic representation of smart water level control. A rainfall-runoff model estimates future lateral inflow using probabilistic weather forecast by the DWD. Based on these predictions and on information from upstream impoundments, the model predictive control system, developed by AMANN et al. (2000), calculates ideal water level and discharge trajectories using optimization procedures. In this way discharge fluctuations are homogenized, which increases the reliability of the affected transport infrastructure and thus the safety of shipping. A pilot project is being carried out for the Hofen impoundment at the river Neckar. This area was chosen because the lateral inflow due to extreme rainfall events during summer season may be considerably greater than the summer base discharge of the waterway.

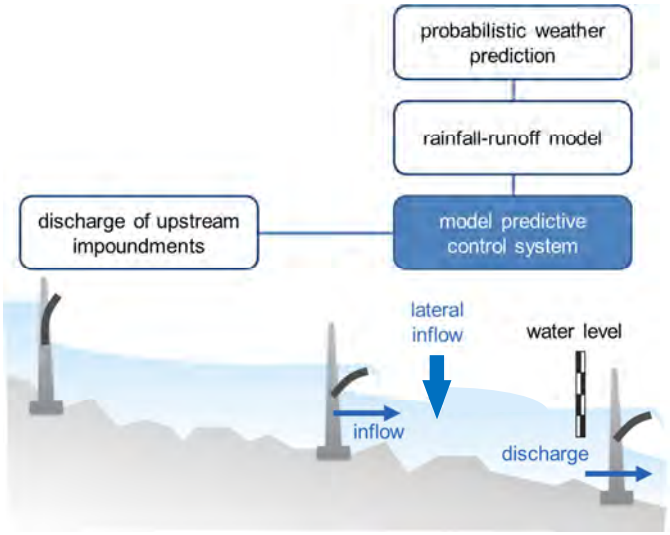

Figure 3: Schematic representation of smart water level control at navigable waterways

3.2 Eliciting expert knowledge about structural deterioration processes and damage scenarios

Assessing deterioration processes and damage development are crucial parts of a reliability analysis. Both they depend on strongly varying initial and boundary conditions. In this regard, the elicitation and usage of available expert knowledge is indispensable. So-called guided expert interviews (e.g. BOGNER, A. et al. 2009; MILES, M. B. et al. 2014) were used during the design process for a full-scale embankment model test. The interviews were conducted to analyse the long-term damage development of loose riprap embankments (SORGATZ, J. 2018). Based on results of the expert interviews, the model test was designed (see Figure 4). The model was finally erected in the wave basin of the BAW, which allows observing degradation caused by hydraulic loads after initial damage. The work is complemented by calculations using state-of-the-art reliability methods in analytical and numerical models (e.g. BAECHER, G.B. & CHRISTIAN, J.T. 2003) as well as a long-term field monitoring campaign. In order to monitor armour stone displacements laser scanner and the structure-from-motion technique are utilised (SORGATZ, J. & LEISMANN, K. 2018).

The project uses state-of-the-art engineering solutions as well as established methods known from social sciences. The interdisciplinary approach of the project attracted great interest within the NoE. Furthermore, it is an excellent example of how different data sources and expert knowledge may be combined to acquire profound technical knowledge, which eventually leads to a well-founded engineering solution.

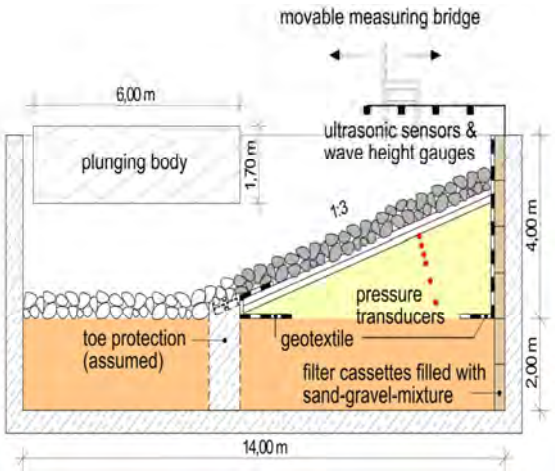

Figure 4: Model test design in the BAW wave basin

3.3 Risk assessment based on the structural condition of civil engineering structures

The detailed, i.e. quantitative, assessment of the structural reliability is a complex task and considered unfeasible when dealing with a large number of structures. In the field of mechanical engineering, qualitative methods are often used to assess the reliability of processes and products on a more general level. These methods are fairly unknown to civil engineers but prove beneficial in analysing inspection data and expert knowledge. The widely used Failure Mode and Effect Analysis (FMEA) was adapted to make use of data already available in the maintenance management system of the BAW (see Figure 5). The FMEA is a systematic and inductive method. Its fundamental idea is the assessment of every possible failure modes within any system, system member or product component. Likewise, possible failure consequences and failure causes are identified. Finally, the procedure leads to a risk assessment and the determination of optimization measures. The method aims at identifying risks and weak spots as early as possible in order to implement improvements early enough (BERTSCHE, B. & LECHNER, G. 2004). Furthermore, the method allows the consideration of both qualitative and quantitative data. The risk assessment results in a ranking of the identified failure modes supporting the prioritization of optimization measures for the most effective improvement in comparison to the actual situation.

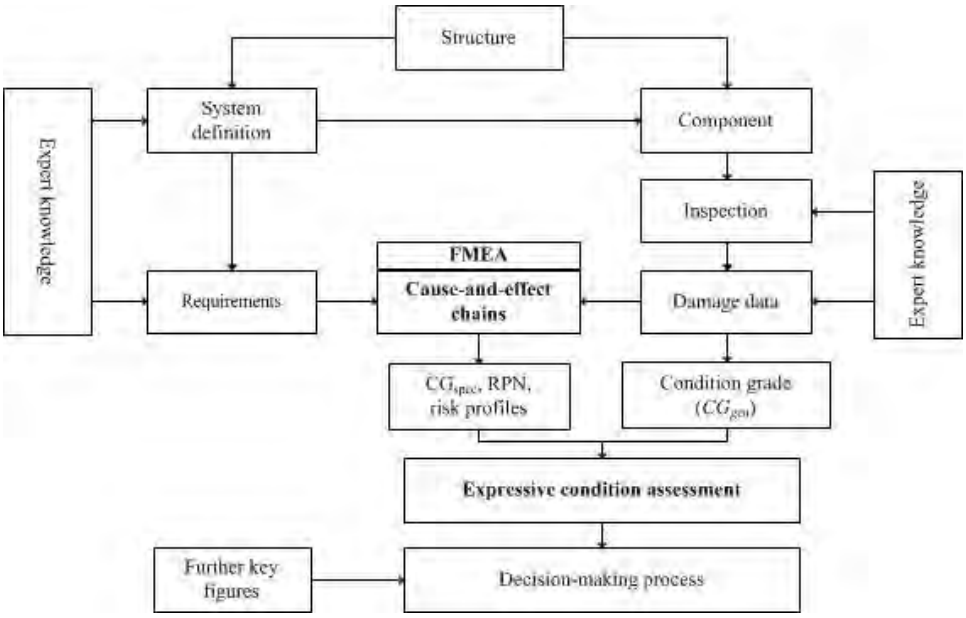

Figure 5: Implementation of FMEA in the condition assessment of civil engineering structures

The FMEA was enhanced with fuzzy logic-based evaluation methods providing comprehensive key figures for a comparative risk assessment on a large number of structures (PANENKA, A. & NYOBEU F., 2018a). In a second step, different structures may be compared based on the results of the first step (PANENKA, A. & NYOBEU F., 2018b). To do so, the results of the first step are summarized in a so-called risk profile of the structure (see Figure 6). The higher the risk profile the more risky is the condition of the structure. Such qualitative risk assessment then helps in the decision process about further actions such as intensifying rehabilitation measures or installing a smart water level control in order to reduce the water load variation on river weirs.

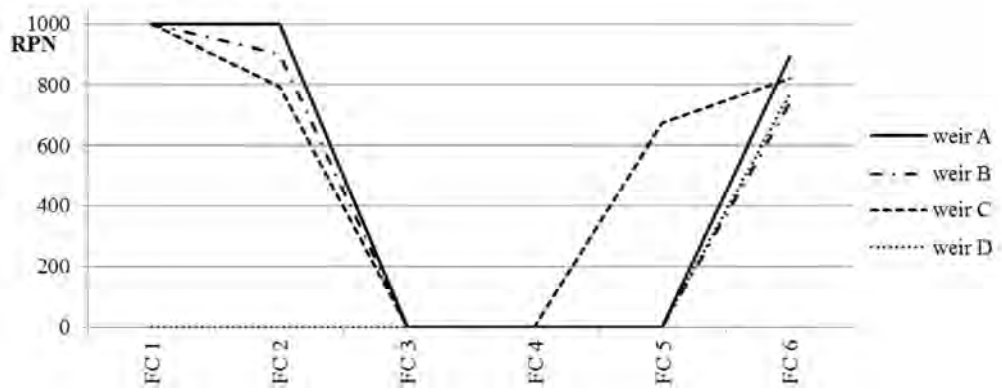

Figure 6: Risk profiles of four different weir structures based on failure causes 1 to 6

4 CONCLUSION

The presented projects demonstrate the benefits of interdisciplinary research approaches with regard to the understanding of risk-driving factors, their indicators and resulting decision criteria. The results achieved so far add profound and comprehensive information to the ongoing discussions about efficient investment strategies in order to reduce the risks emerging from an aging infrastructure. In this way, the research activities of the BAW contributes to the urgently required reduction of the maintenance backlog and, eventually, to a reliable, highly available infrastructure.

The NoE is a future-oriented approach to bundling the strengths of research facilities and authorities. It is accompanied by visionary roadmaps for the individual topics and a comprehensive strategic plan. At the technical level, contacts are established and a common methodological and technological knowledge base is built up. At the decision-making level, the necessary organizational structures and processes are developed and adapted to the needs of the experts involved in the projects. Already in this early phase of the NoE, several obstacles have been overcome in interagency cooperation. First publications at national and international level are in preparation or will be published soon. In 2018 and 2019, scientific and political events will be held more frequently in order to communicate the benefits of the BMVI Network of Experts to transport infrastructure operators and to decision makers in politics.

The projects are continuously presented on www.bmvi-expertennetzwerk.de/EN.

Acknowledgment

The BMVI Network of Experts, a multidisciplinary research program initiated by the German Federal Ministry of Transport and Digital Infrastructure (BMVI), financed and supported the research work outlined in this article.

References

Amann, K.-U., Arnold, E. & Sawodny, O. (2016): Online real-time scheduled model predictive feedforward control for impounded river reaches applied to the Moselle river. In: 2016 IEEE International Conference on Automation Science and Engineering (CASE): 1276–1281. IEEE, Fort Worth, Texas, USA, 21 – 24 August 2016.

Baecher, G. B. & Christian, J. T. (2003). Reliability and statistics in geotechnical engineering. Wiley, Chichester

Bertsche, B. & Lechner, G. (2004). Zuverlässigkeit im Fahrzeug- und Maschinenbau. Ermittlung von Bauteil- und System-Zuverlässigkeiten. Berlin, Springer Verlag, Heidelberg

Bogner, A. et al (Eds.) (2009). Interviewing Experts. Palgrave Macmillan, Basingstoke

DIN EN 1990:2010. Eurocode - Basis of structural design. Beuth, Berlin

Federal Ministry of Transport and Digital Infrastructure (2017). BMVI Network of Experts: Knowledge – Ability - Action. Berlin: printed in-house; available online: http://www.bmvi-expertennetzwerk.de/DE/Publikationen/Medien/Brochure-Expertennetzwerk.pdf

Kasper, J., Simons, F., Belzner, F. & Schmitt-Heiderich, P. (2017): Einfluss von Starkregenereignissen auf die Abfluss- und Stauregelung am Beispiel der Neckarstauhaltung Hofen. In: Modellierung aktueller Fragestellungen zur Wassermengenbewirtschaftung an Bundeswasserstraßen. Bundesanstalt für Gewässerkunde, Veranstaltungen 5/2017, Koblenz, Germany, 13 – 14 September 2016

Miles, M. B. et al. (2014): Qualitative data analysis. A methods sourcebook (3. ed.), Sage Publ, Los Angeles, Calif.

Panenka, A. et al. (2018). Reliability assessment of infrastructure in Germany: Approaching a holistic concept. In Caspeele, R. et al. (ed.): 6th International Symposium on Life-Cycle Civil Engineering (IALCCE 2018). Proc. intern. symp, Ghent, 28 – 31 October 2018; not yet published.

Panenka, A. & Nyobeu, F. (2018a). Maintaining an aging infrastructure based on a fuzzy risk assessment methodology. In Qian, X. D. et al. (ed.): 6th International Symposium on Reliability Engineering and Risk Management. Proc. intern. symp, Singapore, 31 may – 1 June 2018; not yet published

Panenka, A. & Nyobeu, F. (2018b). Condition assessment based on results of qualitative risk analyses. In Caspeele, R. et al. (ed.): 6th International Symposium on Life-Cycle Civil Engineering (IALCCE 2018). Proc. intern. symp, Ghent, 28 – 31 October 2018; not yet published

Schmidt-Bäumler, H. (2017). Risk-based maintenance management system for waterway infrastructures in Germany. In Bakker, J. et al. (ed.) Life-Cycle of Engineering Systems: Emphasis on Sustainable Civil Infrastructure: 559-566. London: Taylor & Francis Group

Sorgatz, J. & Kayser, J. & Schüttrumpf, H. (2018): Expert interviews in long-term damage analysis. In Caspeele, R. et al. (ed.): 6th International Symposium on Life-Cycle Civil Engineering, Ghent, 28 – 31 October 2018; not yet published

Sorgatz, J. & Leismann, K. (2018): Damage assessment of bank revetments using SfM and 3D laser scanning. In Qian, X. D. et al. (ed.): 6th International Symposium on Reliability Engineering and Risk Management. Proc. Intern. Symp, Singapore, 31 May – 1 June 2018; not yet published

Stamatis, D.H. (2003). Failure Mode and Effect Analysis: FMEA from Theory to Execution. ASQ Press, Milwaukee

Westoby, M. J. et al. (2012). 'Structure-from-Motion' photogrammetry. A low-cost, effective tool for geoscience applications. In: Geomorphology 179: 300–314

RIVER INFORMATION SERVICES (RIS) IN GERMANY

by

Nils Braunroth[1], Wieland Haupt[2]

ABSTRACT

Since the first initiatives of the European Commission on River Information Services, this framework on information exchange to support traffic and transport management in inland navigation, has found its way throughout the world.

The PIANC RIS Guidelines are the basis for the RIS Guidelines as formally accepted by the Central Commission for the Navigation of the Rhine (CCNR) and the European Commission. The CCNR has been supporting the development of the technical standards to this day. Since 2005 the development of the technical aspects of River Information Services has been regulated by the European Commission.

River information Services were formally recognized as a concept for harmonized information services to support traffic and transport management in inland navigation, including interfaces to other transport modes.

The added value of River Information Services has found recognition throughout the world.

The standards of Inland ECDIS, Electronical Ship Reporting, Vessel Tracking and Tracing and Notices to skippers were published and the expert groups have been working on them to improve them and to develop new aspects for next versions.

Traffic and transport management in a transport corridor requires an integrated network-approach where the information services to the users are an interactive part of voyage and traffic planning processes. RIS enabled corridor management as support to transport management is becoming more and more an essential and explicit part of RIS.

The last years were very busy. So it is interesting to give a report of the status of RIS in Germany, about what happened in the last years, what is on-going, and which strategy is followed concerning RIS in the future.

---

[1] Federal Ministry of Transport and Digital Infrastructure Bonn, Germany, Deputy Head of Division "Waterway Infrastructure Engineering, RIS", nils.braunroth@bmvi.bund.de
[2] German Federal Waterways and Shipping Administration, Germany, Head of Geographic Information Center South (FGS), wieland.haupt@wsv.bund.de

1. INTRODUCTION

River information services (RIS) is a collective term for a bundle of services: fairway information services, traffic information and traffic management information, informations support of accident management, transport-related services as well as services for waterway and port charges. Different RIS functions and sometimes also RIS sub-functions are available for the individual services. RIS can be implemented according to needs and resources. It is equally possible to realize only single RIS functions or sub-functions available as well as entire services.

Different RIS can be implemented on the basis of a number of existing RIS systems. Such systems are visual or radar reflecting navigation signals, light signals, mobile radio (voice and data), GNSS for ship positioning, VHF radio, internet, ship- or shore-based radar installations, shore-based CCTV cameras, electronic navigational charts (IENC), ship reporting systems or inland waterways tracking and tracing systems (Inland AIS).

Our presentation will give an overview of the actual RIS projects and our future strategy:

- Implementation of AIS at the main waterways of the German inland waterway network and examples of the use of Inland AIS on board at vessels as well as off shore applications
- Pilot lock management and implementation at the main waterways
- ELWIS (Electronic Waterway Information Service), the internet-based fairway information portal of the German Waterways and Shipping Administration
- Safety of Navigation, improved by Inland AIS AtoN
- Prospects for the near future

2. ACTUAL RIS PROJECTS

2.1 Implementation of AIS infrastructure

Following the developments in maritime navigation Europe developed the so called Inland AIS which serves the specific needs for inland navigation while preserving interoperability with maritime AIS. European waterway and shipping authorities in close cooperation with the river commissions are now preparing the mandatory carriage requirement for Inland AIS on European inland waterways or have already introduced the appropriate regulations in their waterways.

Since December 2016 the use of Inland AIS and Inland ECDIS is mandatory for all waterways of class IV and above as well as for selected waterways of class III in Germany. This onboard equipment enables the mutual recognition, identification and display of nearby vessels and their course on an electronic navigational chart. The use of these systems supports onboard navigation and diminishes the risk of accidents; thus, it enhances safety and ease the navigation and contributes to the efficiency and attractiveness of inland navigation.

In recent years, the Federal Waterways and Shipping Administration has set up additional shore-based AIS infrastructure along selected waterways. Today, a total of 3600 km of federal inland waterways are covered by shore-based AIS infrastructure.

In parallel with physically setting up infrastructure, the legislation procedure to adopt the legal basis for processing AIS data entered into force with the adoption of the 3rd amendment to the Inland Shipping (Federal Competences) Act on 5th May 2017.

2.2 Pilot lock management and implementation on the main waterways

To ensure a speedy lock operation, the locking operations should be optimized by minimizing the waiting time for vessels. Therefore it is a necessity to have e.g. an overview about the position of vessels and their sailing directions. Starting from the question of an optimal sequence for a special lock on e.g. the Danube, this question should be expanded to a chain of locks on the Danube. An existing electronic transport diary is intended to be further developed. The aim of this project is to develop a new concept for lock management with an electronic traffic diary using the inland AIS equipment and perform the testing and implementation of the Danube by the middle of 2018. Main task in the development was the usage of AIS data, such as position reports, vessel details. As a consequence the documentation gets more reliable and uninfected. Statistic output is simplified and standardized. The traffic diary is an official document and must be treated accordingly. This pilot should be applied to all other locks on federal inland waterways after its validation.

2.3 ELWIS (Electronic Waterway Information System)

ELWIS (Electronic Waterway Information System) has been the internet-based fairway information portal of the German Waterways and Shipping Administration since 1999. Back then, the service was designed to provide traffic-related information to skippers sailing on inland waterways in order to enhance safety, to ease of inland navigation, and to support voyage planning.

ELWIS is accepted and widely used in the shipping sector **(**see **Figure 1)**.

In 2017, 38 million pages were opened in ELWIS.

ELWIS-ABO is a special additional service that provides subscription-based information. Subscribers must register for this service and specify which kind of information they want to receive (such as water levels at certain gauges, high water/low water forecasts, notices to skippers, or ice reports) and choose a delivery method (email or text message). Information can be received automatically or

based on incidents. In 2017, more than 4.4 million emails were sent via ELWIS subscriptions. The availability of the system in 2017 was 99.96 %.

Since 2011, several improvements have been implemented. At the moment, a route- and chart-based search function is under way.

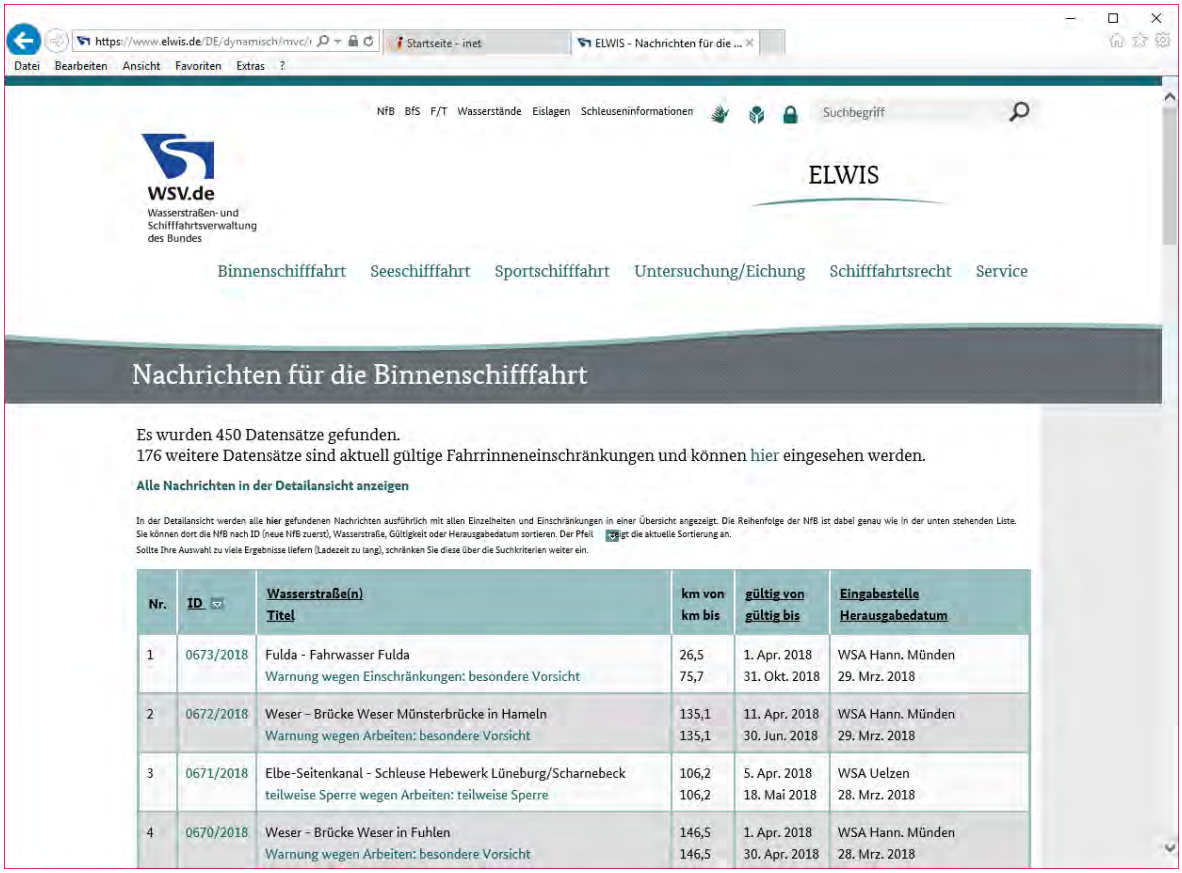

Nr.	ID	Wasserstraße(n) Titel	km von km bis	gültig von gültig bis	Eingabestelle Herausgabedatum
1	0673/2018	Fulda - Fahrwasser Fulda Warnung wegen Einschränkungen: besondere Vorsicht	26,5 75,7	1. Apr. 2018 31. Okt. 2018	WSA Hann. Münden 29. Mrz. 2018
2	0672/2018	Weser - Brücke Weser Münsterbrücke in Hameln Warnung wegen Arbeiten: besondere Vorsicht	135,1 135,1	11. Apr. 2018 30. Jun. 2018	WSA Hann. Münden 29. Mrz. 2018
3	0671/2018	Elbe-Seitenkanal - Schleuse Hebewerk Lüneburg/Scharnebeck teilweise Sperre wegen Arbeiten: teilweise Sperre	106,2 106,2	5. Apr. 2018 18. Mai 2018	WSA Uelzen 28. Mrz. 2018
4	0670/2018	Weser - Brücke Weser in Fuhlen Warnung wegen Arbeiten: besondere Vorsicht	146,5 146,5	1. Apr. 2018 30. Apr. 2018	WSA Hann. Münden 28. Mrz. 2018

Figure 1: **ELWIS – Example of a message overview list for inland navigation**

2.4 Safety of Navigation, improved by Inland AIS AtoN messages

AIS AtoN and Inland ECDIS are suitable technical standards to improve safety of navigation. All the more when these standards are used in combined applications.

Several concrete reference applications on the “Elbe-Weser” corridor, started within the frame of the RIS COMEX project. They will be installed and field tested. Both types of AIS AtoN, the “Real AIS AtoN” and “Virtual AIS AtoN” will be used for specific AIS AtoN messages.

The aim is to inform about the current situations and to visualize it in the Inland ECDIS chart on board of the vessels.

An indicated dangerous situation or a specific recommendation can support safety of navigation. In the “Elbe-Weser” corridor we plan to realize:

- Recommended tracks in specific shallow sections with frequent changes of the river bed, provided by virtual Inland AIS AtoN line messages (see **Figure 2**)

- Indication of a virtual caution area while a ferry (especially a cable ferry) is crossing (shown in **Figure 3**)
- Indication of currently limited vertical clearance under bridges (depending on water level) (see **Figure 4**)
- Indication of the current switching status of signals by the use of application specific messages (**Figure 5** shows an example)

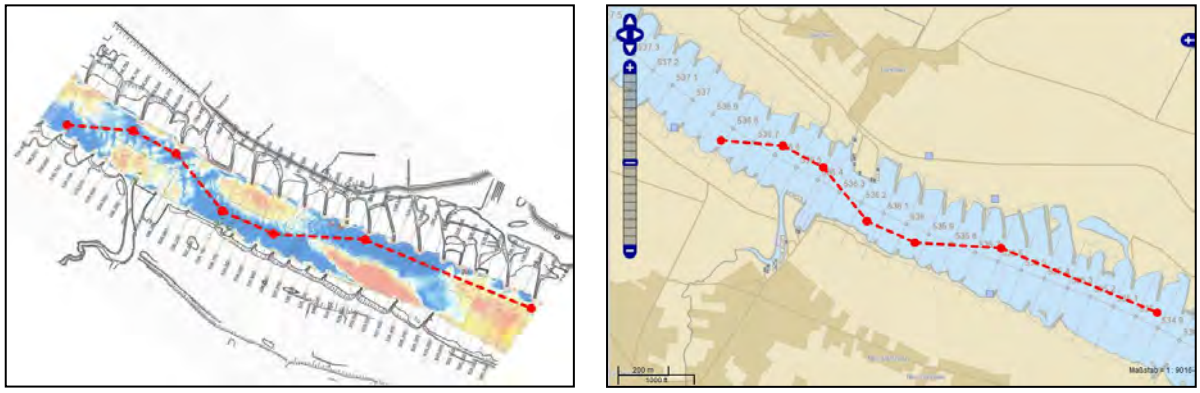

Figure 2: ***Construction of a recommended track, visualized in Inland ECDIS***

Figure 3: ***Cable ferry at the river Elbe, virtual caution area while the ferry is crossing***

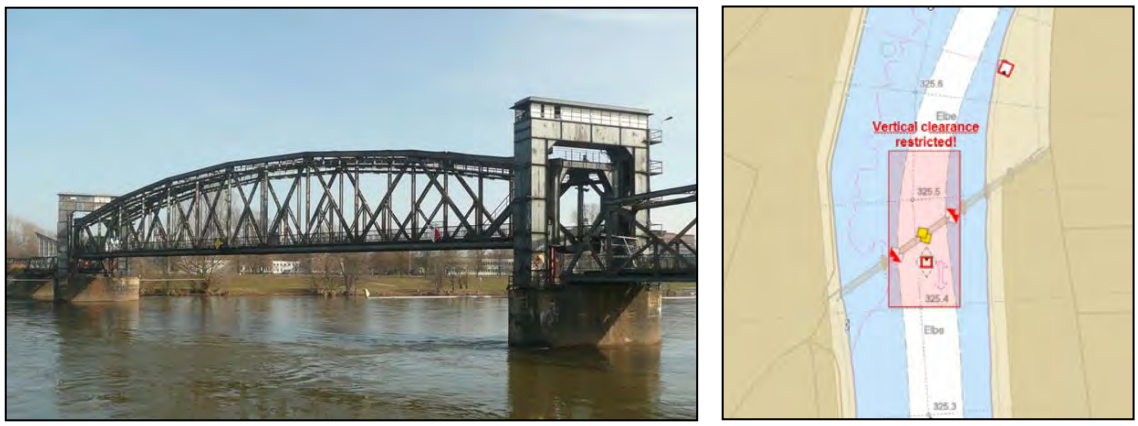

Figure 4: ***Bridge at the river Elbe, virtual caution area is indicating low vertical clearance***

Figure 5: ***Current switching status of signals, visualized in Inland ECDIS***

We invest about 900.000 euro for:

- Extending the existing AIS land infrastructure and realizing the specific AIS AtoN messages for broadcasting (Overview map in **Figure 6**)
- Amending the already existing working environment for managing, providing and monitoring AIS AtoNs in the corridor (System components of the technical infrastructure in **Figure 7**)
- Amending the Inland ECDIS systems in cooperation with the Inland ECDIS manufacturers to receive AIS AtoN messages and visualize them in the system on board
- To test efficiency and effectivity of providing information via incremental IENC updates to the users
- To provide additional the AIS AtoN information via a Web Map Service to reach pleasure craft users who are not legally obligated to use Inland ECDIS on board.

The project is co-financed by the European Union.

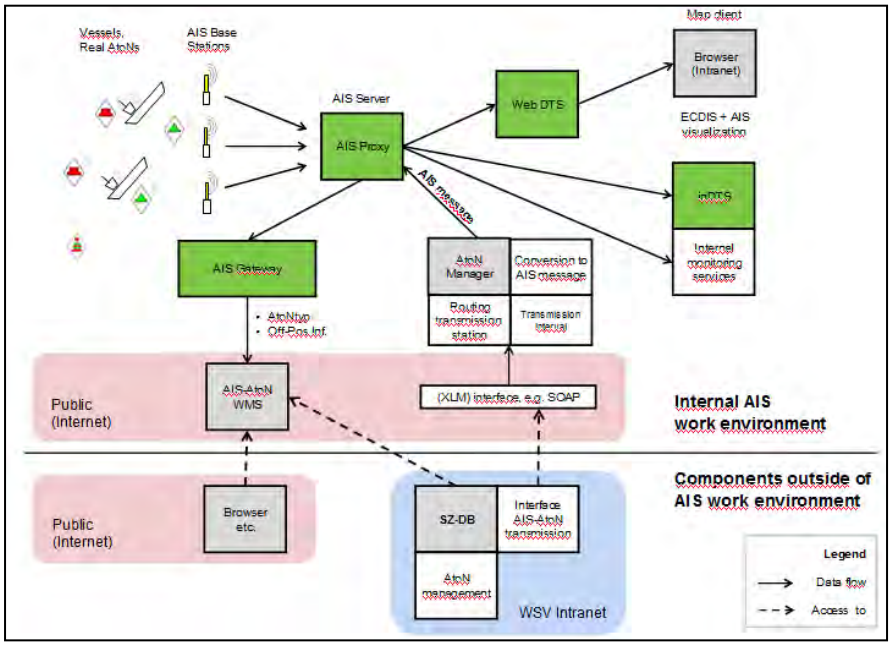

Figure 7: ***AIS data management and AIS services***

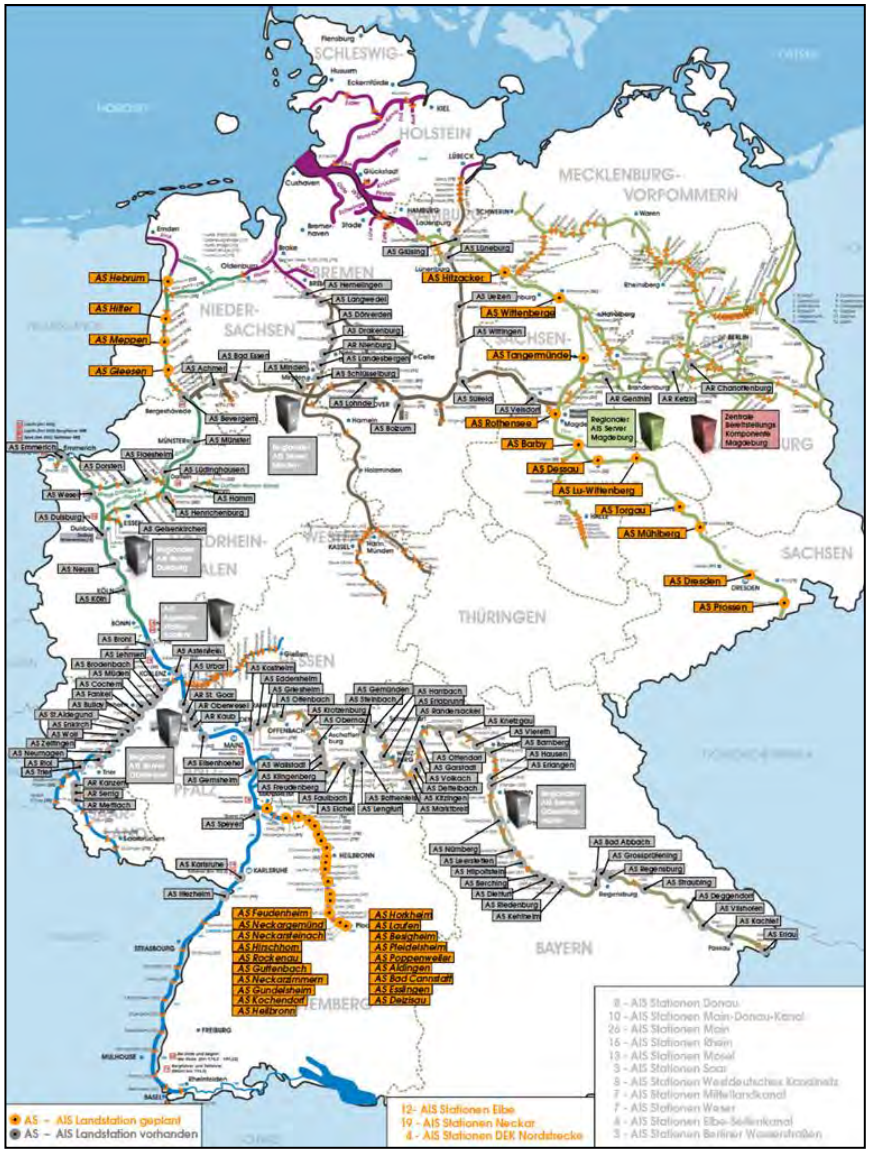

Figure 6: ***AIS land infrastructure in Germany***

3. Prospects for the near future and our strategy

Currently, project work is ongoing to develop a successor to today's reporting and information system, known as MIB and MIB II+.

Particular attention will have to be paid to the efficient use of data. A European RIS concept and a RIS Masterplan will be designed and implemented within the RIS COMEX project in accordance with the specific needs of waterway corridor sections.

New important challenges are automated navigation and digital test fields.

Nowadays, automated navigation covers a very wide range of technical solutions and use cases - ranging from simple navigation assistance to fully automated navigation.

As with maritime or road transport, technological developments aim at automated navigation in inland navigation. Inland navigation international projects, such as LAESSI (Control and Assistance Systems to Enhance the Safety of Navigation in Inland Waterways) is to support the skipper in his tasks of guiding the vessel and thus make inland shipping safer and also more efficient. Beyond evaluating the technical capabilities and associated advantages / disadvantages, implementing demonstrators should enable to gain experience.

Hence the Federal Ministry of Transport and Digital Infrastructure and the City of Hamburg are heading for jointly implementing a digital test field in the port of Hamburg.

Objectives are:

- improvement of infrastructure of the port of Hamburg
- optimal use of transport carriers
- increased digital connection of intermodal supply chains

The existing smart PORT system will offer an appropriate basis for the pilot implementation.

Further initiatives are foreseen on inland waterways.

Unlike other modes of transport, no international definition of automation levels in inland navigation is currently available. First proposals have been presented by the CCNR.

References

CCNR: Automated navigation. Proposed definition of levels of automation in inland navigation, 23.01.2018

CCNR: Electronic Chart Display and Information System for Inland Navigation, Edition 1.02, 16.10.2003, Section 4

CCNR: Vessel Tracking and Tracing Standard for Inland Navigation, Edition 1.0, 31.5.2006

Burchfield, R.W.(2004). Fowler´s Modern English Usage (Revised 3rd ed.). Oxford University Press. ISBN 978-0-19-861021-2.

Recent large dimensions flap gate on Seine River

by

Nathalie Macé[1], Fabrice Daly[2], Xavier Bancal[3], Laurent Vidal [4]

ABSTRACT

Recently, 3 weirs with very large flap gates have been re-built on the Seine River near Paris for VNF-DTBS (*Voies Navigables de France*- Seine Basin): Chatou, downstream of and Le Coudray and Vives-Eaux upstream of Paris. The previous weirs had been built about 80 years ago to increase navigation depth on Seine river. They had lift gates (Chatou) or wicket « Aubert » gates.
The flap gates operated each by 2 hydraulic cylinders are remarkable because they are out of or just at the limit of the proven optimal scope of flap gates compared to other types, according to 2006 PIANC report (design of movables weirs and storm barriers), because of the torsional rigidity limit, or out of the range indicated by standard design guide for flap gates made by VNF-Cerema in 2009. There is no example of both larger and higher flap gate. Their main dimensions are spans around 30 m and a water height from 4.8 to 7.8 m.
However, the reasons why this kind of gates has been chosen are mainly aesthetic, liability, precise regulation and price.
The main design, construction or operating constraints have been the structure, the energy dissipation basin, the cofferdam, the maintenance bulkhead, and fish passes.
The flap gate design will be compared: use of torsion tube or traditional fish belly shape, design and installation of hinges and cardan joint. The large gates have been installed in several parts assembled on place with bolts. The hydraulic cylinders' rods have unusual long strokes, 9.25 m for Chatou weir.
For Le Coudray Weir, a laboratory physical model (scale 1/12) has been made and improved the calculations and design, for discharge, hydrodynamic forces, energy dissipation basin, hydraulic jump and downstream protection, aeration and vibrations prevention.
The hydraulic winter conditions imposed to be able to remove the cofferdam every winter. In addition the soil conditions were difficult: hard limestone or chalk. So, innovative sheet-piles cofferdams have been made: cofferdam without concrete plug in Chatou, sheet-piles set on riverbed with bored piles and injections in rock in Le Coudray to insure stability and watertighting.
For the 3 weirs, the maintenance upstream bulkhead will be floating ones which led to some difficulties in design and operations, because of the large dimensions.

[1] Voies Navigables de France, France
[2] Cerema, France
[3] Tractebel, France
[4] Artelia, France

1. INTRODUCTION

Three weirs with very large flap gates have been built on the Seine River near Paris for VNF-DTBS (*Voies Navigables de France*- Seine Basin): Chatou, 2nd weir downstream of Paris finished in 2013, Le Coudray finished in 2012, and Vives-Eaux finished in 2017, 4th and 5th weirs upstream of Paris. They are remarkable because they are out of or just at the limit of the proven optimal range of flap gates compared to other types like radial gates or lift gates.

The article will focus on specific points of these three works:

- cofferdam and foundations on rock soil
- design of the flap gate and actuators
- hydraulic design of structure
- floating maintenance bulkheads

The 3 old weirs had been built about 80 years ago to increase navigation depth on Seine river. They had lift gates (Chatou) or wicket « Aubert » gates and had been made to replace XIXth century needles gates. « Aubert » gates called after the inventor, have metallic wickets maneuvered by mechanical arm on a carriage moving on a passway several meters above the weir. They have been used in France in the thirties for 6 or 7 weirs including Suresnes weir holding Paris reach. New weirs have been constructed downstream of the former (Chatou and Vives Eaux) or upstream for Le Coudray.

figure 1 - Chatou previous weir - lift gates

figure 2 - Le Coudray Aubert gate

Flap gates have been chosen for several mains reasons:

- feedback on a lot of smaller flap gates on Seine basin, last 20 years
- probably less expensive
- aesthetic: the superstructures are less visible; this point has been very important for Chatou gate because the old lift gate had an industrial aspect no longer desired for the new one
- liability and precise water level regulation

Nevertheless, especially for Chatou, the dimensions were until now considered as just at the limit or out of the range of flap gates. The span are indeed significant as they exceed 30 m with head from 5 to almost 8 m. Until now, it seems that there are no flap gates both larger and higher than the Chatou one: see Erbisti (design of hydraulic gates 2004).

Several types of gates are classically adapted to these dimensions, as radial gates and lifting gates, or even more recently inflatable gates). For the Chatou dimensions, other types of gates were previously regarded as preferable. However, there is no really prohibitive criterion in spite of smaller flap gates resistance to torsional effort.

2006 PIANC report (design of movables weirs and storm barriers), indicated a preferable span range from 1 to 35 m with 2 hydraulic cylinders and a water height from 2 to 5 m with a limit of 7 m because of the torsional rigidity limit. Similarly, the standard design guide for flap gates made by VNF-Cerema in 2009 gave a upper limit of 4 m for the optimal range. Moreover it recommended a fish belly structure for high flap gate.

New weirs project figures

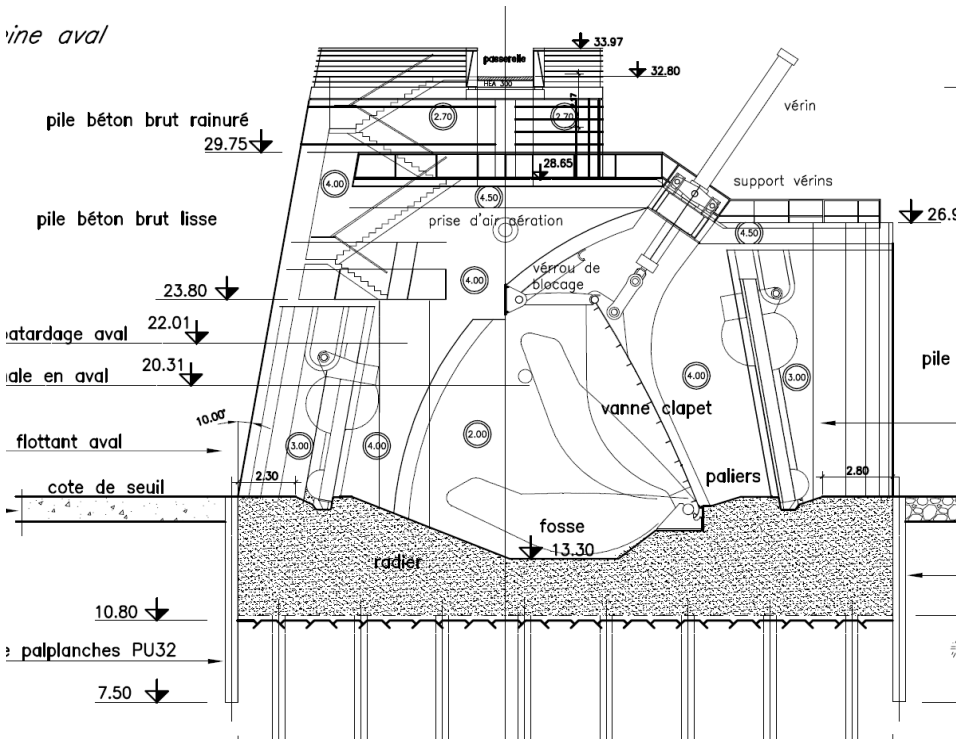

figure 3 - Chatou weir

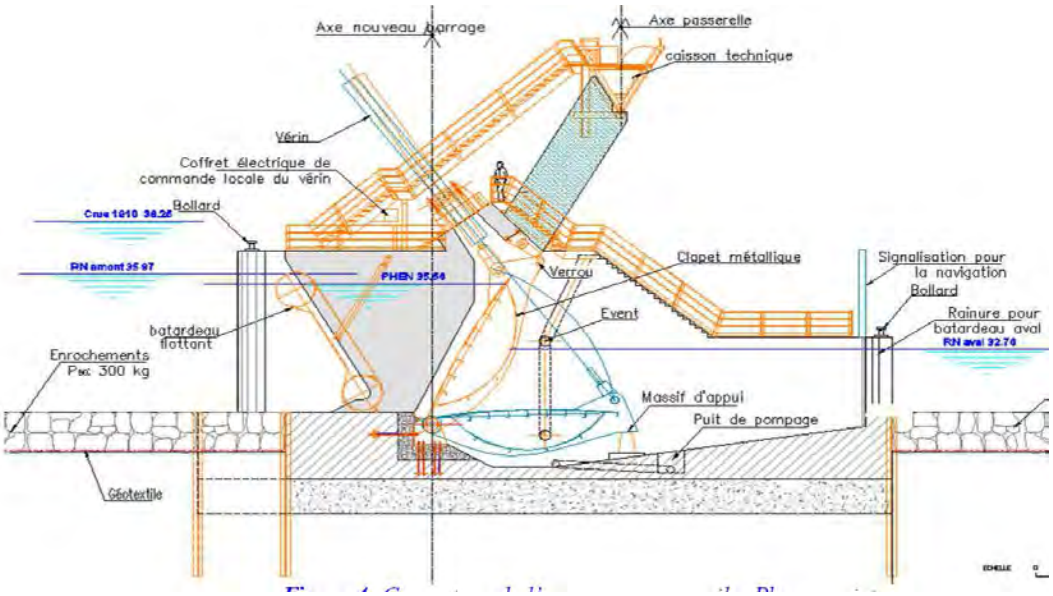

figure 4 - Le Coudray

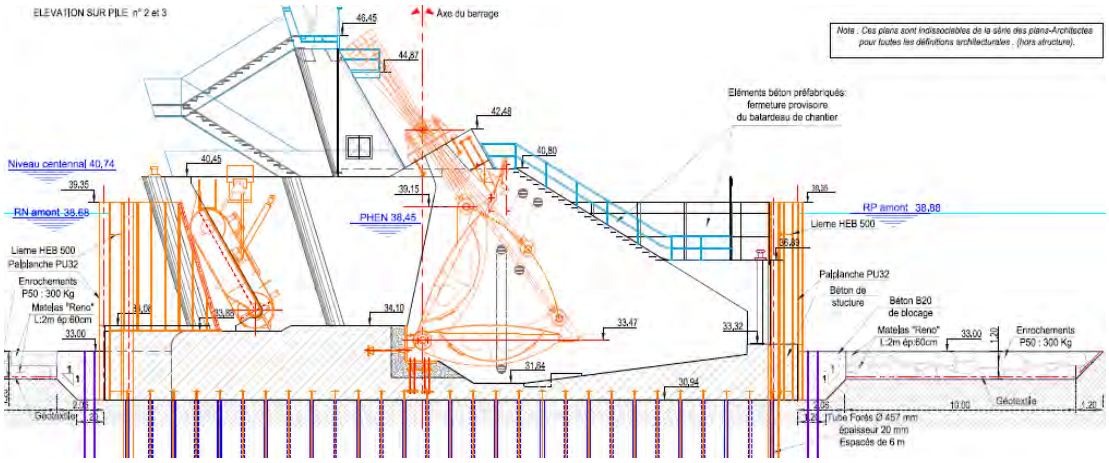

figure 5 - Vives Eaux

2. COFFERDAM AND FOUNDATIONS

2.1 General

The 3 works have been made in complex situations:

- Need to obstruct only 1/3 of the river width to allow flow, and thus to build in 3 years out of the high waters period.
- Need to remove the cofferdam quickly if the discharge is beyond a given limit (for example 10y discharge for Chatou)
- Cracked bedrock close to surface, difficult to watertight .

The bedrock near surface prevented from using the more classical technique for weirs: sheetpiles cofferdam with a underwater concrete plug, to allow the cofferdam stability and watertightness.

The techniques had to be adapted during the final studies or during the work itself, which demonstrate the importance to have, as soon as possible, dense enough geotechnical data on nature of soil and crack density, permeability and capacity to drive sheetpiles.

2.2 Chatou cofferdam

The chalk is covered with a sediment layer from 50 cm to 6m, with a cracked and pervious chalk layer, 1 to 2 m thick. As it was possible to drive sheetpiles on this site, the cofferdam was made up of high inertia PU32 sheetpiles, anchored 7 m in the good chalk, reinforced by a brace systems made of walers and struts. 700 tons of sheetpiles GP PU32 and 400 tons of braces has been implemented to realize retaining structures. The cofferdam excavation bottom was 13 m under the Seine river water level, and the earth volume reached 3700 m3 not including polluted sediments dredging.

In the geotechnical conditions ot Chatou weir, it was audaciously considered, since the design stage, that the cofferdam dimensioning could mainly rely on the intrinsic characteristics of good chalk reached at the excavation bottom. In order to accommodate hydraulic constraints imposing unleash clogging between December 1st to March 31th, Tractebel, the project manager, proposed a cofferdam without prior submerged concrete plug, to guarantee a short execution time with respect to the working volume to realize in 8 months.

This proposal has been maintained during working stage, based on the results of geotechnical investigations showing good and homogeneous characteristics. The stability of cofferdam structure is brought by the bracing system completing the bottom support point, only given by foundation soil, as indicated in the following picture.

Excavation bottom earthworking

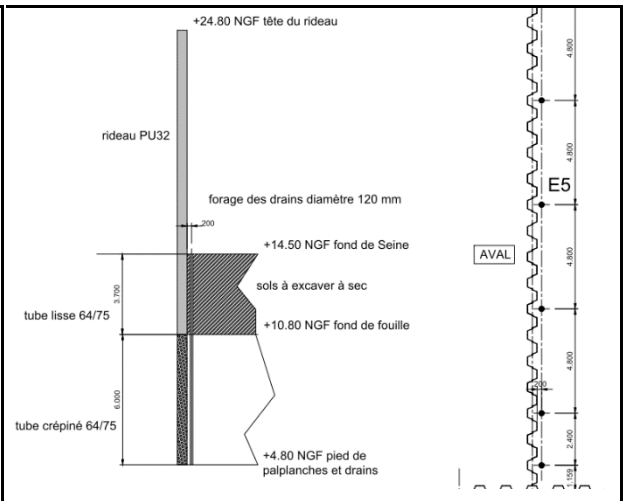

: Piezometer in the periphery of enclosure E5

figure 6 - Vives Eaux excavation bottom Figure: piezometer I the periphery of cofferdam

In order to manage geotechnical and hydraulic remaining risks, piezometers have been implemented around the cofferdam in the recess of sheetpiles wall as indicated in the figure above. These technical arrangements aimed to detect possible lateral leaks in the chalk bedrock potentially created by sheetpiles driving. These leaks can be caused by the sheetpiles detachment and, in the same

time, a separation of the sheetpiles interlocks. This defect can't be detected solely by the interpretation of driving curves, which are not sufficient to assess residual risks.

The cofferdam has been realized in the following order: left bank span (including an abutment and a pier), central span (including one pier), right bank span (including the other abutment). Water pressure on the wall implemented in the flow direction was transmitted to the ground for the left and right banks. For the central span these efforts were transmitted to the pier, already made during the first year, which created difficulties for the support point of the upper waler as it was impossible to install anchoring devices for architecture reasons.

At each work stage, the piezometer measures have been compared to the theoretical profiles in order to detect, as far as possible, increases of water pressure or leaks which could threaten the local stability of an area of the excavation bottom and then the sill integrity. Such phenomenon happened three times during earthwork at the excavation bottom at the contact of banks (and earth retaining elements) which can have local earth peculiarities that are unpredictable before and during works. As soon as a breach happened at an interlock, the required repair consisted in restoring the water level and in setting, with the help of divers, a submerged concrete reinforcement confined behind a steel plate fixed to sheetpiles. If appropriate, this action had to be completed by injections out of the cofferdam enclosure.

On a part of the fish pass cofferdam, indurated chalk was encountered. As it was impossible to drive sheetpiles, an excavation was made under water and submerged concrete was set which slowed the work in progress.

2.3 Le Coudray Cofferdam

The tests carried out during the works showed the great difficulty to drive sheetpiles even with pre-drilling. That's why, after a proposal of the contractor, the cofferdam was made as follows:

- First temporary cofferdam set on the riverbed with head and bottom braces
- Tubular piles bored in the rock and connected to the sheetpiles to insure stability
- Watertighted concrete cordon
- First attempt to dewater the cofferdam.
  It wasn't possible to watertight because dewatering made water come under sheetpiles, and also soil come out of vents, with some risks of piping. A new cofferdam concept was studied and consisted of a cut-off wall with cement injections instead of sheetpiles impossible to drive.
- Injections in the fractured rock in order to watertight it.
  Every 1.2 m on 2 staggered lines, at 50 cm and 1 m around the cofferdam. The depth was 3 m, excepted for 1/6 for which it was 6 m. The goals of these injections were to improve concrete rock contact and to fill and clog cracks.
- First cofferdam cut 1,5 m above ground before floods (tubular tubes let in place)
- 2nd cofferdam made of sheetpiles connected to previous ones

The injected volume has been 122 m^3. 20 m^3 has been injected under the concrete sill to fill the holes created at the first pumping attempt. The injections limited the water inflow at an acceptable value of approximately 550 m3/h.

This new and innovative technique studied and decided during work, led to a 2 years delay and an 40 % additional cost. That's why it was considered at the design studies stage for the Vives Eaux weir located in a similar geotechnical situation.

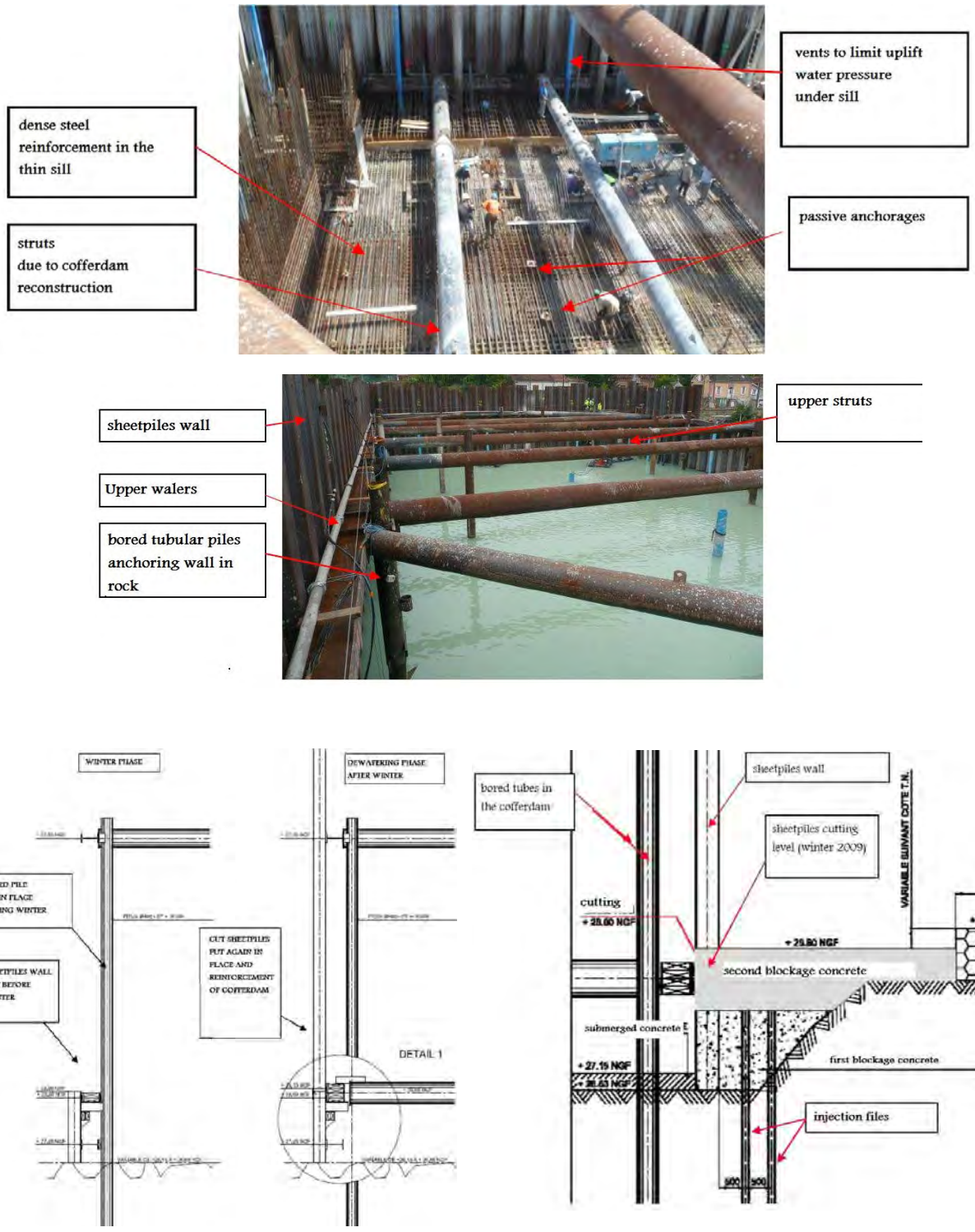

Figure 7 Le Coudray Cofferdam

2.4 Vives Eaux Cofferdam

As it wasn’t possible to drive sheetpiles, the previous and difficult experience of Le Coudray has been used. The cofferdam is made of sheetpiles only set on the riverbed, and held by two lines of walers fixed to bored piles every 6 m. Strut at the upper level reinforced the sheetpiles wall. There was no submerged concrete plug.

Technical characteristics of various cofferdam elements can be described as follows:

- piles: diameter 457 mm, thickness 20 mm, spacing: 6 m
- 2 lines of walers HEB 500
- struts; diameter 610 mm, thickness 16 mm, spacing: 7 m et the level of the upper walers line.

Cofferdam has been realized as follows:

- earthwork, realization of sheetpiles set place
- implementation of a gabion cordon around the excavations
- implementation of bored piles
- implementation of walers lines
- setting of sheetpiles
- casting of concrete at the sheetpiles foundation (using gabions as a formwork)
- injections to form a peripheral wall
- realisation of anchorages
- implementation of struts
- dewatering of the cofferdam

The injections ensure the watertightness and limit the internal erosion and undermining risk. They were made through the concrete foundation at approximately 60 cm from sheetpiles wall, in 3 phases with a 3.6 m spacing (phase 1), then 1.2 m spacing (phase2), and finally in staggered row with phases 1 and 2.

During the work a flood happened and the contractor wasn't able to remove the cofferdam in time. So there was an over water height upstream but without significant consequences.

2.5 Sill design

Concerning the Chatou weir, the sill thickness varies from 2.1 to 4.8 m. It has been anchored in chalk by micropiles 10.3 m deep with spacing of 3.25 x 3.25 m in order to resist to hydrostatic uplift pressure. In 2009 the Eurocode became mandatory. It led to increase significantly the steel reinforcement of concrete sill, to avoid concrete cracking due to tensile stresses

For the Weir of Le Coudray, It wasn’t the best solution to make a thick submerged concrete plug replacing rock which is very difficult to remove. That’s why the concrete plug has been rather thin and strongly anchored by 82 passive micropiles (HA50), 10 m deep, with a grid spacing from 2.5 x 2.5 to 4x4 depending on the location.

3. DESIGN OF FLAP GATES AND OPERATORS

3.1 General

For the 3 weirs, each gate has 2 hydraulic cylinders. However, each cylinder is capable to support alone the whole effort in case of failure of the other one, which is the higher load case. The gates are made of steel S355.

General characteristics

	Chatou	Le Coudray	Vives Eaux
Span width (L)	32.5 m	34.2 m	30.2 m
Water height on sill (H)	7.76 m	6 m	4.8 m
Water fall	3.25 m	3.21 m	2.71 m
Flap gate type	torque tube	fish belly	fish belly
Gate weight : P → P/ L.H → P/ L.H² →	167 tons 662 kg/m² 85 kg/m³	117 tons 570 kg/m² 95 kg/m³	63 tons 435 kg/m² 90 kg/m³
Gate thickness	2.75 m	2 m	1.62 m
Number of hinges	12	12	10
Max deflection	77 mm	34 mm	22 mm
Number of bolts	570 class 10.9	900 class 8.8	534 class 10.9
Max effort on a actuator - normal service - with only 1 operating	 380 tons 700 tons	 230 tons 400 tons	 tons 300 tons
Oil pressure	218 bars	250 bars	250 bars
cylinder rod stroke	9.25 m	7.3 m	6.2 m
Diameter of hydraulic cylinder	670 mm tige:220 mm	480 mm	480 mm

The weight per square meter of closure (considered vertically – P/LH), logically increases with water height. However, P/LH² (linear weight divided by H²) seems to be more stable around 90 kg/m³, which can indicate that the optimisation levels are similar but not equal, especially in the comparison between fish belly and torque tube.

For 3 weirs, the gates have been fabricated in several parts, lifted inside the cofferdam by a crane, precisely implemented and then assembled by bolts.

The procedure described below for Le Coudray is representative of the 2 others.

3.2 Chatou Weir

The gates have been fabricated in 6 identical sections which were 5.5 m wide. They are bound only by the torque tube, but the 6 flap parts of the gate are independent structures only linked by a joint. The 6 torque tubes sections are connected by circular flanges welded on the tubes and assembled together by pre tensioned bolts. Unlike studies, the torque tube gate has been proposed by contractor, who considered that it was too complex to realize 9 m long joint surfaces, with the high precision necessary to a correct transmission of efforts. This tube was watertight reducing the weight and the effort on the hydraulic cylinder. Theoretically, the shortcoming could be a slightly heavier and thicker flap gate (2.75 m instead of 2.5 expected by first studies for fish belly gate). The potential consequence should be a higher recess in the stilling basin, which could lead to lower the whole concrete structure by 25 cm with an effect on cost. In this case, it wasn't a significant design criterion and the concrete structure wasn't modified.

The hydraulic cylinders are mounted on cardan joint supports turning on self-lubricating bronze rings, and allowing rotations in 2 directions to compensate the deformations due to gate bending. In normal service, the gate inclination varies between 3 and 66° with respect to horizontal. During maintenance stops they are supported by special locks, relieving the cylinders.

Figure 8 - Chatou gate sector lifted - Cardan joint

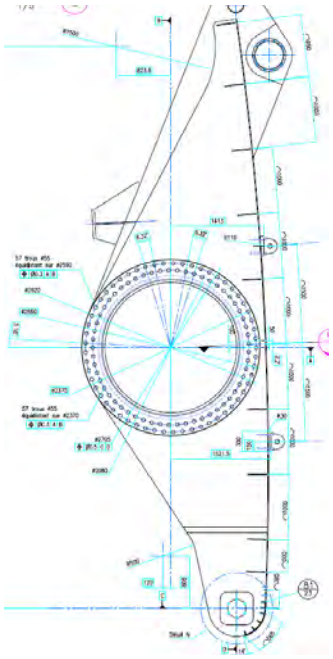

Chatou gate plan

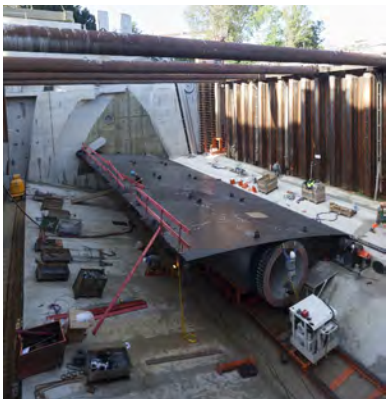

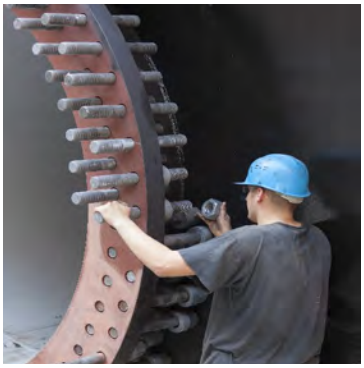

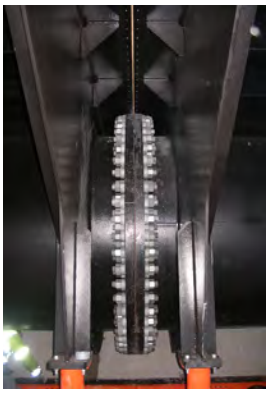

Figure 9 - Chatou gate : gate in the cofferdam - bolting - bound tubes

figure 10 - General view (fish eye)

3.3 Le Coudray weir

It has an optimized fish belly shape. To handle it more easily, the flap gate has been transported in 4 sections. They had approximately the same weights and dimensions, but are not symmetrical. As a matter of fact, it's better to avoid locating the joint surface in the middle of flap gate, on the higher stress plane.

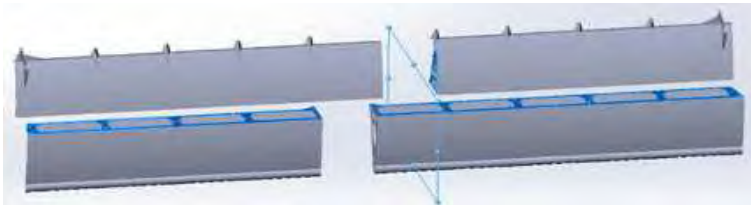

Figure 11 - Le Coudray weir: 4 gate sections

The mounting has been made with following steps:

- Adjustment and sealing of hinges.
  The tolerance was only 1 mm. The hinges had pre-stressed anchorage rods intended to be sealed in concrete with great precision. A perfect alignment was necessary for hinge axes: use of topographic control and piano strings.

- Transport and set up the first section.
  The gates are lifted by the crane on a system of rails in the cofferdam that allows to move them to their final position.
- Coupling: the axes of rotation are put in place
- Set up other sections and bolting.
  The parts are bound by HR bolts (high strength) with controlled tightening using a hydraulic wrench, completed by a sealing bead on each laying plane.
- Tightening
- Dry tests then tests in water

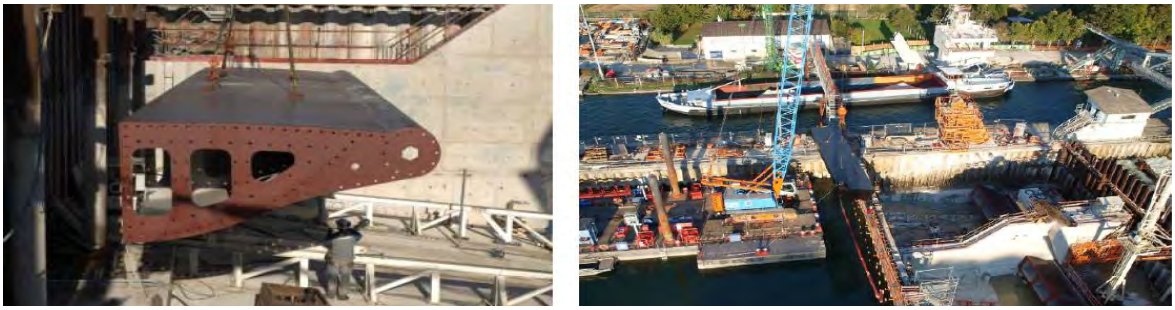

Figure 12 Le Coudray Weir: gate lifted to the cofferdam

Figure 13 Hydraulic cylinders - vents downstrean of the gate - cardans joints

3.4 Vives Eaux Weir

The principle is the same but in the meantime, regulations have evolved, due to the inclusion of Eurocodes. In addition, the weight per m² was reduced by 1/4 between the two weirs thanks to the optimization of the design. However, if we consider that the efforts are generally rather proportional to the square of the height, we find comparable ratios because the height is lower by 20%. The optimization concerns the manufacturing time by reducing the thickness of weld seams and the simplification of parts, as well as on the lightening of certain parts.

Figure 14 : Vives Eaux - gate lifted

4. HYDRAULIC DESIGN OF THE SILL AND STILLING BASIN

4.1 Le Coudray weir

The sill is designed to accommodate the horizontally lowered flap gate. It must also allow the location of the hydraulic jump on the concrete, as long as it is not drowned by downstream level, in order to limit downstream erosion. In order to optimize this design, a 1/12 scale model has been developed for Le Coudray weir. It represents the gate, the energy dissipation basin and the rip-rap protection downstream. The dimensions are 8 m in length and 1.4 m in width, and represent 96 m on 16.8 m in reality, ie. half a gate, which is sufficient because the phenomena are bi-dimensional. The measurements made by sensors are: the flowrate introduced into the model, the water levels upstream and downstream, the pressures under the gate (frequency of 100 Hz), and the forces on the gate.

The model thus made it possible to determine:

- the flowrate according to the position of the gate (relation head-discharge)
- the hydrodynamic efforts.
- the length of the dissipation basin and the length and characteristics of the rip-rap protection.
- the location of hydraulic phenomena: jet plunge and hydraulic jump
- The aeration of the nappe and nappe dividers on the gate (anti-vibration).

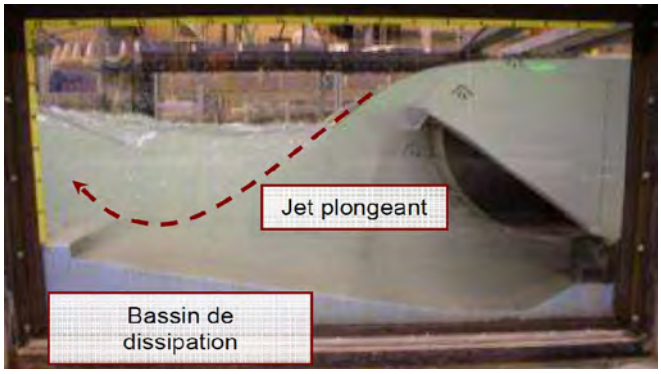

Figure 15 : plunging jet

figure 16 - rip rap

The tests were carried out for 5 possible gate positions (8, 35, 43, 54, 69 °) and 6 possible discharges (representing from 60 to 570 m3 / s on the entire weir). The model has made it possible to visualize the plunging jet, and to check the position of the hydraulic jump, generally in the basin, and sometimes, at the limit of the rip-rap, as well as the stability of the armour stones. Therefore the initial design calculated by classical formulas has not been modified. The maximum hydrodynamic forces on the gate have been evaluated at 200 tons per cylinder by integrating the rapid fluctuations.

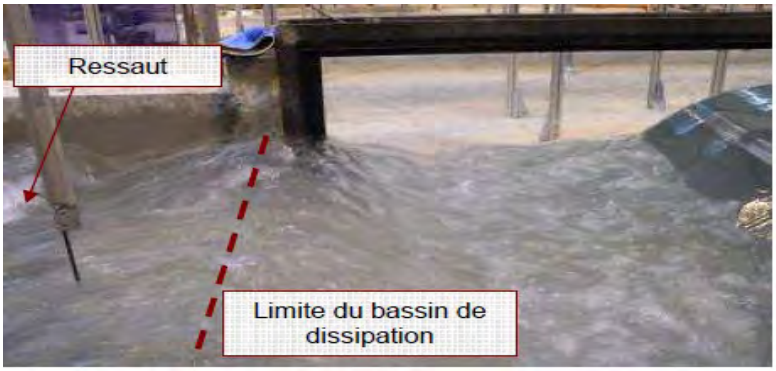

Figure 17 Hydraulic jump after the limit of basin

For an inclination of the gate greater than 35 ° the current dividers installed on the top of the gate are no longer effective. There is then a downstream depression, which causes a vibration of the order of 1.35 Hz. The aeration makes it possible to suppress the vibrations of the gate by resonance. It is made by pipes installed in the wall structure, an connecting the downstream side of the gate to the atmospheric pressure. Three vents have been positioned to provide this function for a maximum of positions. The geometric constraint on these vents is that the exit point is above the downstream level and below the gate.

Dividers have also been optimized by varying their position, shape and number.

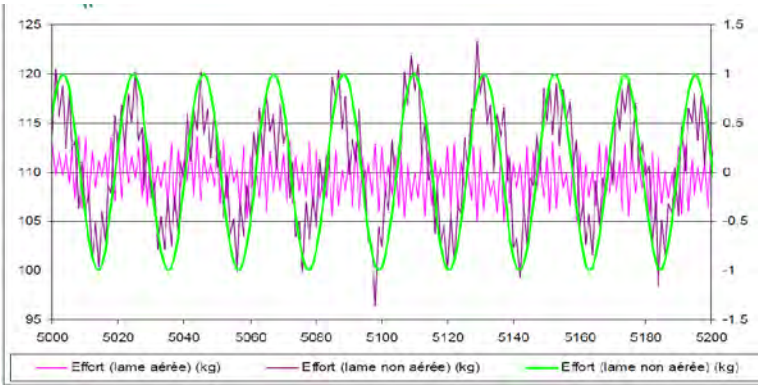

Figure 18 Results: vibration without aeration (green line) and with aeration (red line)

figure 19 View of depression location and position of vents

4.2 Chatou weir

For Chatou, the energy dissipation basin is short, barely longer than necessary to house the lowered valve, which does not allow the top spill to always be well located in the basin. However, the downstream height is important, which favours the dissipation of energy and the ground resistance to scour (chalk).

5. UPSTREAM MAINTENANCE BULKHEAD

The maintenance bulkheads are floating stoplogs, which makes it possible to avoid heavy handling equipment. They are put in final vertical position by filling of the ballasts

Chatou weir Bulkhead

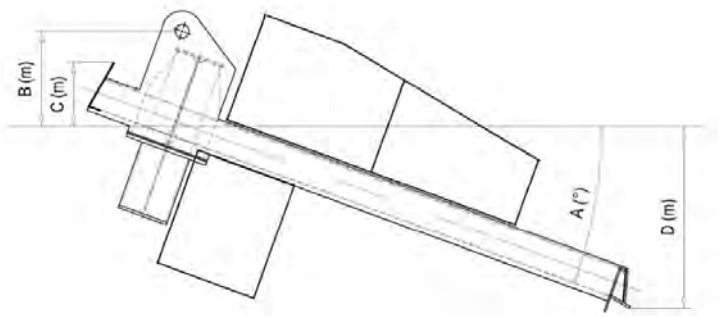

figure 20 - Chatou bulkhead plan with ballasts

figure 21 - Chatou Bulkhead arriving by buoyancy and in final position (first use)

Le Coudray weir

The Le-Coudray bulkhead consists of a stiffened metal decking which is supported on two cylindrical and compartmental longitudinal caissons 1.5 m in diameter. The compartments are equipped with valves and piping for filling / emptying.

For its installation, the bulkhead will be brought by buoyancy. When the roller located on the bulkhead come in contact with the pier equipped with rail guide, the cylinder rods come out so as to allow their attachment to the piers clamps.

In 2018 it is fabricated but not yet in operation. The downstream maintenance bulkhead is simply made up of aluminium beams stacked between vertical H shaped profiles.

For Vives Eaux, old equipment which is also used on 4 other works of the Seine upstream has to be refurbished. For the other 2 the equipment is new.

Figure 23 -Le Coudray bulkhead moored

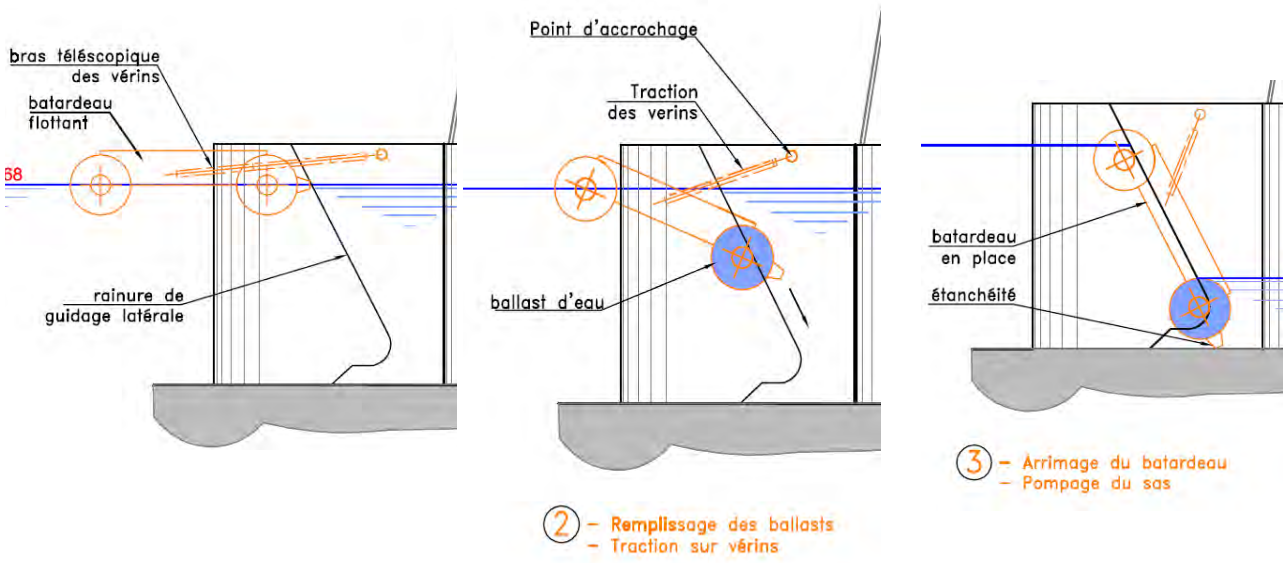

figure 24 - Le Coudray : 3 phases to put the bulkhead in final place

References

[1] Reconstruction du barrage de Chatou : retour d'expériences sur les travaux de génie civil (Reconstruction of the Chatou gated weir: Returns experiences of civil works)
Eric Boidy Colloque CFBR: "Modernisation des barrages" décembre 2013

[2] Duramé N., Debaene C., Un nouveau barrage remplace l'ancien à Chatou, revue Travaux n°887, pp.58-69, mars-avril 2012.

[3] Legras, M (2013) Retour d'expérience sur la reconstruction du barrage de Coudray-Montceaux sur la seine(Feedback from the dam reconstruction of Coudray-Montceaux on the Seine)
Colloque CFBR: "Modernisation des barrages" décembre 2013

[4] Laurent VIDAL - Reconstruction des barrages de Coudray et de Vives Eaux – Vantellerie et contrôle commande (Reconstruction of Coudray and Vives Eaux dams, Gates and control system)
Colloque CFBR: "Vantellerie" décembre 2015

SHIP AND BARGE COLLISIONS WITH BRIDGES OVER NAVIGABLE WATERWAYS

by

Michael Knott[1], P.E. and Mikele Winters[2] P.E.

ABSTRACT

Highway and rail bridges that cross busy navigation channels near coastal ports and inland waterways pose unique risks to a nation's critical transportation infrastructure, and potential bridge collapse due to vessel collision often leads to loss of life and significant economic and political consequences. Recent decades have demonstrated the potential vulnerability of major bridge crossings over navigable waterways to catastrophic collapse due to extreme event loads. This paper will discuss ship and barge collision with bridges over waterways using lessons learned from historical accidents worldwide and analysis procedures for vessel collision assessments for new and existing bridges in the United States (AASHTO 2009 and AASHTO 2014). This paper also discusses the application of ship and barge collision risk analysis procedures to model complex navigation channel geometries near bridges and modern electronic navigation systems and port control procedures that potentially reduce the risk of collision.

1. INTRODUCTION

Vulnerability of critical infrastructures to extreme events have made headlines worldwide in the past decades due to structural failures, loss of life and financial damages associated with earthquakes, hurricanes, storm surge and waves, tsunamis, flooding and scour, vessel collisions, and terrorist attacks. For critical bridges, the risk and magnitude of such extreme events is often the controlling load case for the structure design. It was only after a marked increase in the frequency and severity of vessel collisions with bridges crossing navigable waterways that studies of the collision problem were initiated in the 1980s. Pivotal events spurring the change were collapses in 1980 of both the Sunshine Skyway Bridge (Figure 1) and the Tjörn Bridge (Figure 2).

In the period from 1960 to 2015, there have been 35 major bridge collapses worldwide due to ship or barge collision with a total loss of life of 342 people. The greatest loss of life occurred in 1983 when a passenger ship collided with a railroad bridge on the Volga River in Russia. One hundred and seventy six (176) people were killed when an aberrant vessel attempted to transit through a side span of the massive bridge. Most of the deaths occurred when a filled movie theater on the top deck of the passenger ship was sheared off by the low vertical clearance of the bridge superstructure's side span.

Figure 1: Sunshine Skyway Bridge Collapse, Tampa Bay, Florida, U.S. (1980)

Figure 2: Tjörn Bridge Collapse, Almo Sound, Sweden (1980)

[1] Moffatt & Nichol, Richmond, Virginia, U.S.A., mknott@moffattnichol.com

[2] Moffatt & Nichol, Raleigh, North Carolina, U.S.A., mwinters@moffattnichol.com

Relatively recent ship collision events have included the collapse of the Jiujiang Bridge in 2007 with 9 fatalities (Figure 3) and the Eggner's Ferry Bridge in 2012 (Figure 4). Eighteen (18) of the bridge catastrophes mentioned above occurred in the United States (U.S.), including the collapse of the Sunshine Skyway Bridge in which 396m of the main span collapsed and 35 lives were lost as a result of the collision by an empty 35,000 DWT (deadweight tonnage) bulk carrier (Figure 1). Recent collapse of U.S. bridges due to barge collision on the inland waterway system include the Queen Isabella Causeway Bridge in Texas (2001) which resulted in 8 fatalities, the I-40 Bridge in Oklahoma (2002) which resulted in 13 fatalities (Figure 5), and the Popps Ferry Bridge in Mississippi in 2009 (Figure 6).

Figure 3: Jiujiang Bridge Collapse, Xijiang River, Foshan, China (2007)

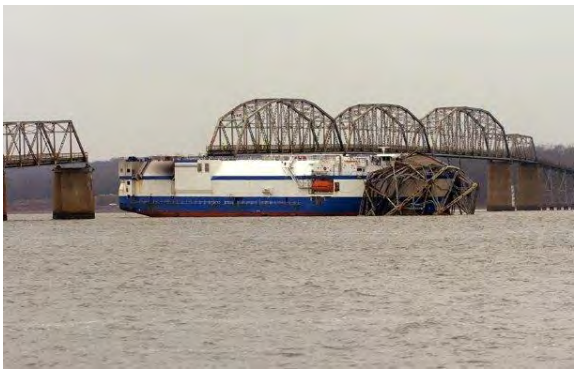

Figure 4: Eggner's Ferry Bridge Collapse, Kentucky, U.S. (2012)

Figure 5: I-40 Bridge Collapse, Oklahoma, U.S. (2002)

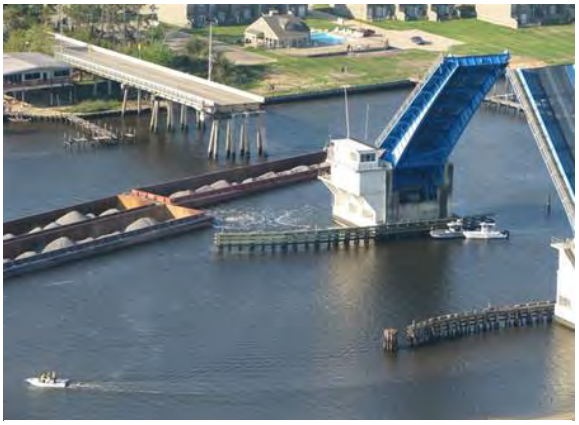

Figure 6: Popps Ferry Bridge Collapse, Mississippi, U.S. (2009)

One of the more publicized tragedies in the United States (U.S.) involved the 1993 collapse of a CSX Railroad Bridge across Bayou Canot near Mobile, Alabama. During dense fog, a barge tow became lost and entered a side channel of the Mobile River, where it struck a low-level railroad bridge causing a large displacement of the superstructure. The bridge collapsed a few minutes later when a fully loaded Amtrak passenger train attempted to cross the damaged structure. Forty-seven (47) fatalities occurred as a result of the collapse and train derailment.

It should be noted that there are numerous vessel collision accidents with bridges which cause damage that varies from minor to significant but does not necessarily result in collapse of the structure or loss of life. During a 2-week period in January 2016, there were 6 separate barge collisions with highway and rail bridges crossing the Mississippi River due to floodwater conditions. None of the collisions were catastrophic, but the bridges had to be closed temporarily for structural inspections and repairs. A United States Coast Guard (USCG) study of towing vessels and barge collisions with bridges located on the U.S. inland waterway system during the 10-year period from 1992 to 2001 revealed that there

were 2,692 accidents with bridges (USCG 2003). Only 61 of these caused bridge damage in excess of US$500,000 (1,702 caused very minor damage with no repair costs to the bridge), and none resulted in fatalities. The study concluded that 90% of the barge tow accidents were related to human performance (78% to pilot error and 12% to other operational factors). Only 5% were related to mechanical problems, and for the remaining 5% there was insufficient information to assign a cause.

In addition to motorist and train disruption, structural damage and potential loss of life, significant environmental damage can also occur in a waterway due to oil and chemical spills as a result of vessel collision. An example includes the spillage of 644,000 liters of fuel oil in the Fore River, Maine in 1996 when a collision occurred with a bascule bridge pier of the Million Dollar Bridge that ripped a 9m hole in a loaded tanker ship (caused by an underwater protrusion of the concrete support pier footing). A large portion of the guide pile fender system was destroyed and the flare of the ship's bow imparted significant damage to the movable bascule leaves, causing closure of the bridge until repairs were made. Although the main cause of the accident was attributed to pilot error, a contributing factor was the limited horizontal clearance of the navigation opening through the bridge (only 29m). Another example includes the spillage of 203,000 liters of fuel oil into San Francisco Bay in 2007 when a container ship hit one of the main pier fender systems of the San Francisco-Oakland Bay Bridge during dense fog.

The 1980 collapse of the Sunshine Skyway Bridge was a major turning point in awareness and increased concern for the safety of bridges crossing navigable waterways in the United States. Investigations and research subsequent to the Sunshine Skyway and other major bridge accidents worldwide ultimately led to the development of the American Association of State Highway and Transportation Officials (AASHTO) *Guide Specification and Commentary for Vessel Collision Design of Highway Bridges* in 1991. For the first time, this landmark publication provided the bridge design community the procedures to evaluate the risk of vessel collision and estimate the magnitude of impact forces associated with ship and barge collisions. A second edition of the Guide Specification was developed (AASHTO 2009) to update and integrate lessons learned from the use of the original 1991 Guide Specification, incorporate Load and Resistance Factor Design (LRFD) bridge design methodologies, and include results from ship and barge collision research conducted since the original vessel collision publication. The Guide Specification provisions were subsequently adopted as a mandatory requirement of the primary U.S. bridge design code (AASHTO 2014). Unless otherwise noted, references to AASHTO vessel collision requirements in the remainder of this paper denote the AASHTO 2009 Guide Specification (AASHTO 2009).

It should be recognized that the USCG refers to ship and barge accidents as "allisions", which is technically correct as it involves an accident between a single moving object (ship/barge) and a stationary object (bridge). Whereas a "collision" is technically an accident between two moving objects. While respecting the technicality of the terms, the use of "collision" for ship/barge accidents with bridges is the publicly accepted usage for transportation-related accidents and is the term adopted by AASHTO in the bridge design specifications.

The AASHTO provisions and requirements represent a simplification of a very complex problem. Many of the requirements are based on lessons learned from historical accidents in which: 1) vessels impact bridges as they are transiting the waterway in the vicinity of the bridge during normal merchant marine operations, and 2) vessels impact bridges as a result of breaking loose from their moorings during a severe storm event and drift in the waterway due to winds and currents. These are two different design scenarios (load cases) in AASHTO and require two separate analyses for evaluating vessel collision impacts on different portions of the bridge.

After a summary of the basic AASHTO risk analysis equation, this paper will discuss: application of the AASHTO vessel collision principles for curved navigation channels near bridges, selection of the appropriate water depth and scour for use in the risk analysis for the evaluation of both tidal and non-tidal waterways, development of protection factors (PF) for use in the risk analysis, and the importance of considering vessel bow crushing when evaluating the consequences of potential local contact between an aberrant ship/barge bow with a bridge pier.

2. VESSEL COLLISION RISK ANALYSIS

2.1 Methodology

AASHTO provides three (3) alternative design methodologies (Methods I, II, and III) in order to furnish the bridge designer flexibility in establishing criteria for ship/barge collisions. Method II is the preferred

design standard for critical structures and the method discussed in detail in this paper. However, there are situations where Methods I and III are appropriately employed.

Method I is a relatively simple, semi-deterministic procedure for selecting a design vessel and subsequently computing collision impact loads. It is particularly useful in shallow draft river waterways transited by barges and barge tows of approximately the same size. The procedure is less accurate (and usually more conservative) than the Method II analysis and is, therefore, not recommended for final design of critical bridges. However, Method I procedures are useful in defining boundaries of the navigation zone used in the Method II risk analysis. Method I procedures are also useful in providing an initial assessment of the magnitudes of impact forces while input data for the significantly more complicated Method II risk analysis procedures are collected and analyzed.

Method III is a cost-effectiveness procedure where benefit/cost analysis is combined with the risk of a potential bridge collapse to determine the applicable design vessel. This procedure is typically used in cases where it is not feasible (economically or technically) to either design a new bridge or retrofit an existing bridge to comply with the Method II risk acceptance criteria.

Method II is a probability based risk analysis procedure that can be used both for directly assessing the risk of collapse from vessel impact and developing vessel impact criteria for design. Using Method II procedures, a mathematical model is developed to estimate the annual frequency of bridge collapse based on the bridge pier/span geometry, ultimate pier strength, waterway characteristics, and the characteristics of the vessel fleet transiting the channel. The estimated risk of collapse can then be compared to predetermined acceptance criteria. Unless otherwise approved by the Owner for special situations, Method II should be used for all new bridge design.

AASHTO provisions specify an annual frequency of collapse of 0.0001 for critical bridges and an annual frequency of collapse of 0.001 for regular bridges based on risk comparisons with natural extreme events and engineering. These annual frequencies correspond to return periods of bridge collapse equal to 1/10,000 years, and 1/1,000 years, respectively. Critical bridges are defined as those bridges that are expected to continue to function after a major impact due to social/survival or security/defense requirements (typically these are iconic long span bridges). This does not imply that the structure is expected to last 10,000 or 1,000 years but that during the normal design life of the bridge (say 100 years) the risk of collapse due to collision by a vessel in the design fleet will be very small. It should be noted that the risk criteria for critical bridges is significantly greater than those for regular bridges and usually results in design impact loads associated with larger vessels transiting the waterway.

Various collision risk models have been developed to achieve design acceptance criteria. In general, the occurrence of a collision is separated into 4 events: 1) a vessel approaching the bridge becomes aberrant, 2) the aberrant vessel impacts a bridge element, 3) the bridge element that is hit fails, and 4) a protection factor based on bridge location and nearby waterway features. The AASHTO risk equation is shown below:

$$AF = (N)\,(PA)\,(PG)\,(PC)\,(PF)\,(GF) \qquad (1)$$

where

AF = Annual frequency of bridge element collapse due to vessel collision;

N = Annual number of vessel trips classified by type, size, and loading condition, that use the channel and can strike the bridge element,

PA = Probability of aberrancy (a measure of how often a vessel might go off-course),

PG = Geometric probability (if it goes off-course, will it hit part of the bridge?),

PC = Probability of collapse (if a bridge component is hit, will the bridge collapse?),

PF = Protection factor (are there land masses or nearby structures to protect the bridge?), and

GF = Growth factor to account for future increase (or decrease) in annual number of vessel trips (projection of vessel traffic to the mid-point of the bridge design life).

Once the input information for the analysis has been collected and developed (usually the most time consuming part of the process) the risk evaluation can be made relatively straightforward by using programs such as Microsoft Excel and Mathcad to automate the repetitive/iterative analysis process. As illustrated in Figure 7, the analysis is typically conducted in a matrix or table. In the first column, various types and sizes of ships/barges are arranged in rows in order of decreasing size. Values for the various risk components are then computed for each specific vessel type and an AF calculated for

each row. This analysis is performed for each bridge pier and/or superstructure span as appropriate for the project as well as for vessels transiting both upbound and downbound (which can have differing speeds and water current conditions depending on transit direction). Once AF for each bridge pier or span component has been computed, the annual frequency of collapse of the total bridge can then be obtained by summing the AF's of each bridge component, vessel, and transit path in the analysis. The inverse of the annual frequency of collapse (1/AF) represents the return period (in years) of the failure event.

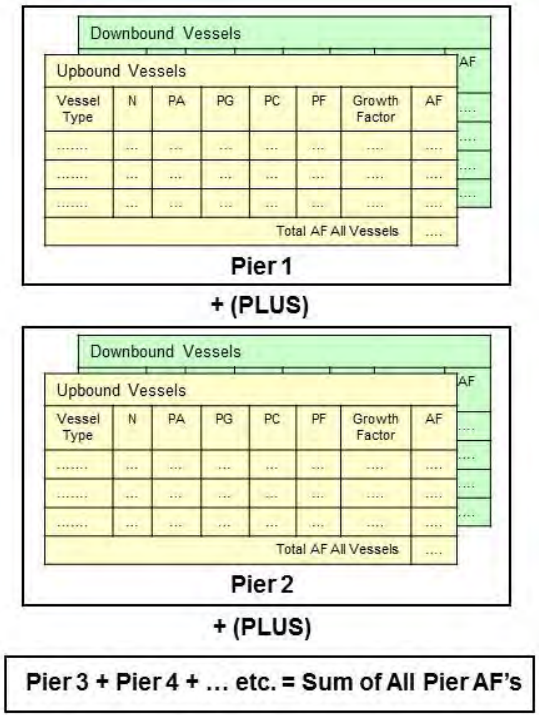

Figure 7: Computation of the Annual Frequency of Collapse (AF)

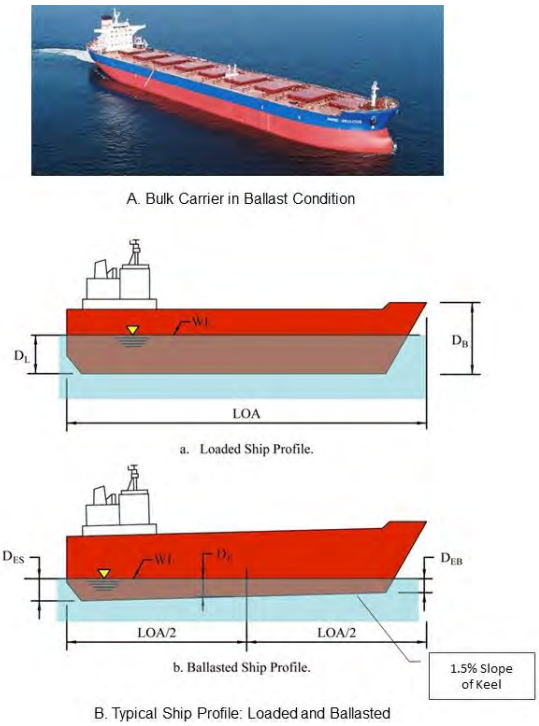

Figure 8: Ballasted Vessels

2.2 Vessel Fleet and Annual Frequency (N)

The number of vessels (N) that could potentially strike a bridge element is based on the available water depth and the actual draft of the aberrant vessel. Vessels transiting with drafts deeper than the available water depth will run aground before contacting the bridge, while those with drafts less than the available water depth have the ability to strike the bridge. The risk assessment must also include the effect of ballasted vessels transiting the waterway, since the draft at the bow is much smaller than the draft at the stern of the ship (Figure 8). The smaller draft at the bow can often reach bridge piers in shallow water at large distances (vessel length overall (LOA)) from where the stern starts to run aground. In general, tanker and bulk carrier vessels transit one-way loaded and one-way ballasted (or empty), whereas container ships, general cargo, and cruise ships are generally transiting loaded (or partly loaded) both upbound and downbound in a harbor or port.

With regards to water depth, the physical ability of a vessel to strike a bridge pier is based on the available water depth at the location of the pier and the draft of the vessel. For example, a loaded ship with a 10m draft would run aground before it could strike a pier in 6m of water, although the same ship transiting ballasted with a 5m draft at the stern and a 2.5m draft at the bow could potentially strike the pier. The ability of a vessel to "plow" through underlying soft soils without a significant decrease in speed must also be considered when establishing available water depths at bridge piers. In the absence of a more detailed vessel grounding analysis, a rule-of-thumb utilized by the authors is to assume an additional 1m of water depth to account for very soft surface material that may exist on the bottom of the waterway.

After waterway data is collected, the vessel fleet (ships and barges) transiting the navigation channel at the bridge location is subdivided into categories (usually 5,000 DWT increments) for the risk analysis. Vessel characteristics are developed for each category including; length overall (LOA), beam (width),

drafts at the bow and stern (loaded and ballasted); displacement tonnage; heights above water level (bow, deckhouse and mast); and transit speeds (upbound and downtbound). Characteristics should also include the layout of ship bow overhangs, particularly for cruise and container ships, which often have large flares of the main deck extending over the bulbous bow at the waterline. Automatic Identification System (AIS) information for vessels transiting a waterway is an important source of data used to estimate the frequency of vessels, vessel tracks in the waterway, and operating speeds as they pass under the bridges. An example of plotted AIS vessel tracks is shown in Figure 9.

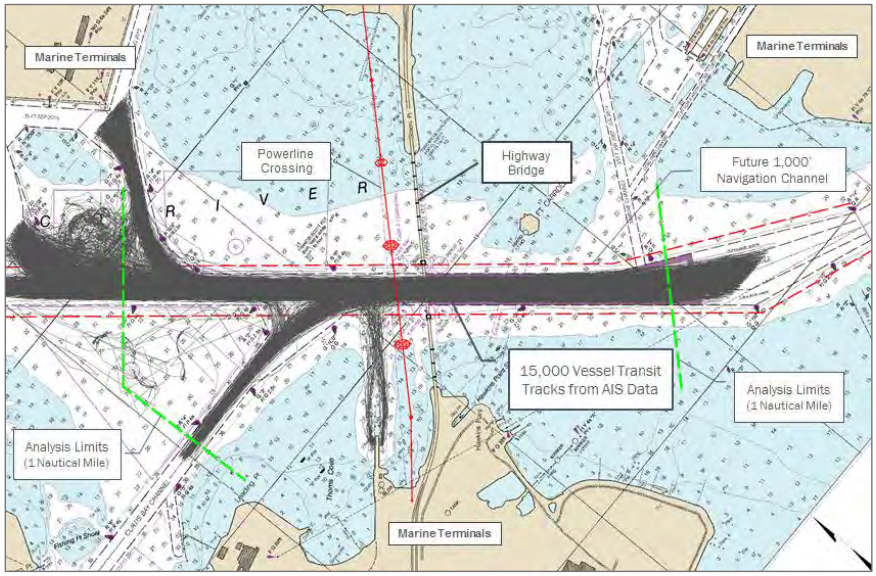

Figure 9: AIS Vessel Tracks at Bridge Location

2.3 Probability of Aberrancy (PA)

The probability of aberrancy (PA) is a measure of risk that a vessel is in trouble and may stray off-course as a result of pilot error, adverse environmental circumstances, or mechanical failure. The most accurate procedure for determining PA is to compute it using long-term vessel accident data (groundings, collisions, and rammings) in the waterway and statistics on the frequency of vessel traffic during the same period of time. An alternate procedure for calculating PA can be performed by using the following AASHTO equation:

$$PA = (BR)\ (R_B)\ (R_C)\ (R_{XC})\ (R_D) \qquad (2)$$

where

BR = Aberrancy base rate developed from historical accident data on waterways worldwide (assumed 0.6×10^{-4} for ships and 1.2×10^{-4} for barges),

R_B = Correction factor for bridge location,

R_C = Correction factor for currents acting parallel to vessel transit path,

R_{XC} = Correction factor for cross current acting perpendicular to vessel transit path, and

R_D = Correction factor for vessel traffic density.

The correction factor for bridge location ($R_{B)}$ is computed based on the relative location of the bridge to one of three waterway regions (straight, transition, and turn/bend).

Correction factors for currents acting parallel (R_C) and perpendicular (R_{XC}) to the vessel transit path are based on equations provided in AASHTO. The parallel current component (V_C) and perpendicular current component (V_{XC}) are computed from the geometric relationship between the orientation of each vessel transit path or independent channel leg (see following discussion related to complex channel geometries) and the direction of the current.

The correction factor for vessel traffic density (R_D) in the immediate vicinity of the bridge is determined by whether the structure is located in a low, medium, or high density area.

Modern Navigation Practices: The AASHTO vessel aberrancy base rate (BR) assumes a single local pilot onboard ships transiting bridges in coastal locations and no tug assistance. The existing AASHTO provisions do not include consideration of new safety measures based on modern navigation systems, vessel design, and regulatory requirements (crew training and certifications, vessel safety inspections, maneuvering restrictions, etc.) that have occurred since the original adoption of AASHTO's vessel collision design provisions published in 1991. The Code also does not provide guidelines for modelling additional navigation restrictions that are sometimes imposed by Government Agencies such as requirements for certain vessels to have multiple pilots, tethered tugs, daylight transits only, speed limits, and visibility restrictions.

For the risk assessment of major bridges, it is important to include the effects of the above factors in potentially reducing the risk of collision. The aberrancy base rates in the risk assessment should be adjusted to reflect site-specific vessel operating practices and regulatory requirements in the navigable waterway. Adjustments to the aberrancy base rate may depend on the size, type and loading condition of the transiting vessels; the number of pilots; vessel operations; tethered tug escort; water currents; traffic density; transit speed and current restrictions; daylight and visibility restrictions; Vessel Traffic Service (VTS); electronic navigation tools (EDIS and other navigation aids and devices); and Port State Control (PSC). The magnitude of each adjustment can be established based on Code recommendations, published research, and previous risk studies that have been accepted by federal agencies as appropriate for similar marine risk analyses. Table 1 shows the site-specific recommended adjustments to BR for vessel collision risk assessments conducted for two highway bridges in Vancouver, Canada (Homes & Knott 2018).

Item/Description	Adjustment Factor	Discussion
Vessel Traffic Service (VTS)	0.80	20% reduction in risk attributed to VTS and mandatory vessel participation (Trans Mountain 2013)
Electronic Chart Display and Information System (ECDIS)	0.81	Compliance with international ECDIS requirements are mandatory for all ships by July 2018. The adjustment is based on 1/2 of the 38% reduction attributed to ECDIS because of the overlap with the reduction due to pilots onboard the vessel (Trans Mountain 2013).
Other Navigation Aids	1.00	Additional potential risk reductions include (Trans Mountain 2013): AIS (2-5%); ENC (0-13%); Conventional ATNs (0-13%); DGPS (0-8%); and PPU (0-10%). For purposes of vessel collision risk analysis, these potential reduction factors are sometimes not included to be conservative.
Port State Control (PSC)	0.94	PSC includes the inspection of foreign ships to verify compliance with international regulations on the condition of the ship, equipment, crew manning and operations (including rest periods). Studies have demonstrated that PSC activities reduce the rate of vessel accidents in waterways. The adjustment is based on 1/2 of the 12% reduction attributed to PSC because of the overlap with the reduction due to pilots onboard the vessel (Trans Mountain 2013).
Pilotage - 1 Pilot	1.00	The code base rate assumes a single pilot; therefore, a further reduction is not applicable.
Pilotage - 2 Pilots	0.54	46% reduction in risk attributed whenever a second pilot is required onboard a vessel (Trans Mountain 2013).
Daytime Only Transit Restriction	0.50	Value based on Larsen 1993 which states that the rate of collision/grounding accidents at night are 4 times the probability of such accidents in daytime (which implies a 75% reduction in risk or a reduction factor of 0.25). For purposes of the vessel collision risk assessment, a conservative value of 0.5 was used.
Visibility Restrictions	0.50	Value based on Larsen 1993 which states that the rate of collision/grounding accidents in fog when the visual range is less than 200m has been found to be 100 times the risk in clear weather. Visibility studies in Dover Strait, United Kingdom by Wheatley (Larsen 1993) found that reduced visibility increased the accident rate by 4.4 times as compared to clear visibility conditions (which implies a 77% reduction in risk or a reduction factor of 0.23). For purposes of the vessel collision risk analysis, a conservative value of 0.5 was used.
Passenger / Cruise Ships	0.17	Value based on Larsen 1993 which states that vessel accident studies in Japanese waters indicate that passenger vessels are 6 times safer than cargo ships and tankers (which implies an 83% reduction in risk or a reduction factor of 0.17).

Table 1: Example of BR Adjustments for Modern Navigation Practices

2.4 Geometric Probability (PG)

The geometric probability (PG) is the conditional probability that a vessel will hit a pier given that it has lost control (is aberrant) in the vicinity of the bridge. The method of computing PG is based on a normal distribution curve, with the mean located at the centerline of assumed vessel transit path and a standard deviation equal to the length overall (LOA) of the design vessel under consideration. Note that bridge elements located beyond 3 standard deviations from the centerline of vessel transit path do not influence the geometric probability of collision. The area under the normal distribution curve bounded by the limits of the centerline of vessel contacting either side of the pier is equal to the geometric probability of collision (Figure 10). As can be interpreted from this figure, increasing the distance between piers can significantly reduce the value of PG since the collision zone would be contained within the tail area of the normal distribution curve.

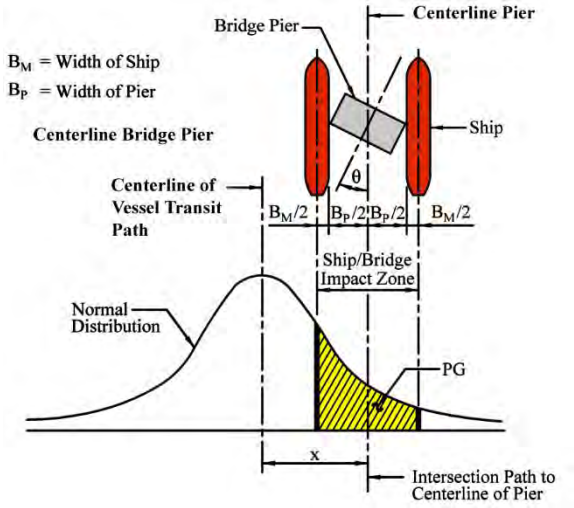

Figure 10: Geometric Probability of Pier Collision

PG Adjustment for Tethered Tugs: In some waterways, tug assistance for ships is required for transiting portions of the navigation channel. Where required during vessel transits, tethered tugs provide an extra measure of security related to potential vessel collision with bridges as tugs assist in keeping an aberrant ship in the navigation channel. For bridges located in areas where mandatory tug assistance is required for ships the AASHTO Method II risk analysis procedures for PG should be adjusted. For purposes of a risk assessment study only tugs tethered to the ship are considered. Because of potential time delays in hooking up with a ship near the bridge location, escort tugs and tugs of opportunity should be excluded from the risk assessment.

Within the context of the AASHTO procedures for estimating the risk of vessel collision, the use of tugs may have a slight benefit in reducing the PA base rate (minor because the major cause of aberrancy is human error onboard the ship). However, the primary benefit will be to the PG factor in reducing the ability of an aberrant vessel to leave the navigation channel as the tugs can push the vessel back into the channel and keep it away from the bridge. The following equation was developed by Moffatt & Nichol based on navigation simulations to model the effect of tethered tugs on PG by introducing an adjustment factor (r_{tug}) to reduce the standard deviation (σ) based on a tug safety factor (f_{tug}), width of the channel (w), vessel LOA, and properties of a standard normal distribution (ϕ).

$$r_{tug} = \frac{0.5w}{loa\Phi^{-1}\left(1 - \frac{1 - \Phi\left(\frac{0.5w}{loa}\right)}{f_{tug}}\right)} \quad (3)$$

A tug safety factor (f_{tug}) of 2.0 has been used in previous vessel collision studies based on Trans Mountain 2013 and other ship navigation studies. It could be argued that the tug safety factor might be much higher (exceeding 3 or 4) for ships with tethered tugs that are moving relatively slowly in the

waterway. Although the tug adjustment factor (r_{tug}) varies based on vessel size, the typical reduction factor for ships in the vessel fleet is a modified standard deviation of approximately 1/3 of LOA (0.33). The effect of the adjustment to PG is shown in Figure 11. The use of a reduced standard deviation causes the spread of the normal distribution to "peak" closer to the mean (channel centerline). This reduces the PG associated with bridge piers and spans when compared to PG estimates without the adjustment. It should be noted that adjustment in the standard deviation used to estimate PG for ships with tethered tugs are also made to the standard deviation used in the vessel speed distribution in AASHTO 2009.

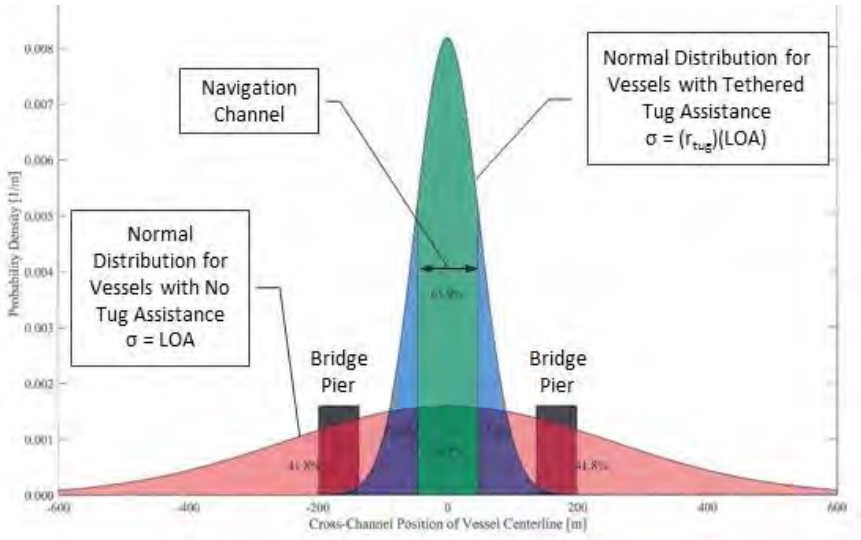

Figure 11: Tethered Tug Adjustment Factor

2.5 Probability of Collapse (PC)

The probability of bridge collapse (PC) once an aberrant vessel has struck a pier is a function of many variables including vessel size, type, bow shape, speed, direction of impact, and mass. It is also dependent upon the ability of the pier to resist collision impact loads. Based on historical accident data, the probability of collapse is computed according to the ratio of bridge element ultimate strength/capacity (H) to the vessel impact force/demand (P) in accordance with equations provided in AASHTO 2009. Note that the ultimate strength/capacity (H) is typically related to the overall "global" resistance of the bridge element being investigated. Therefore, under this criteria, localized damage would be deemed acceptable so long as it does not compromise the structural integrity of the system. From the equations provided in AASHTO, the following observations can be made:

- In cases where the pier capacity exceeds the design vessel impact force (> 100%), the probability of bridge collapse becomes 0.0
- In cases where the pier capacity is in the range of 100% to 10% of the design vessel impact force, the probability of bridge collapse varies linearly from 0.0 to 0.10
- In cases where the pier capacity is in the range of 10% to less than 0.1% of the design vessel impact force, the probability of bridge collapse varies linearly from 0.10 to 1.0

2.6 Protection Factor (PF)

The protection factor (PF) is used in the risk analysis to adjust AF for full or partial protection of individual bridge piers or span components (regardless of the actual water depth) from vessel collision due to protection measures or shielding associated with existing or new site conditions. Examples of protection measures include: an existing upstream or downstream bridge providing protection from impacts in one direction; a feature in the waterway, such as a shoreline or peninsula extending out on one side of the bridge that might block vessels from impacting a pier; a wharf or other structure near the bridge that might protect some of the piers; or protection measures installed at the bridge, such as dolphins or islands placed around piers to reduce the AF to acceptable levels. Values for PF may differ from pier to pier and may also vary depending on the direction of vessel traffic. The use of PF provides

an important tool in evaluating the risk of ship/barge collision with bridges and in the development of effective and cost-effective protection measures if required by the risk analysis.

Similar to geometric probability (PG), the method for computing PF is based on a normal distribution curve, with the mean located at the centerline of assumed vessel transit path and a standard deviation equal to 30 degrees of rotation from the transit path. Therefore, at 3 standard deviations from the centerline of transit path, the vessel would effectively be traveling perpendicular to the bridge element and would no longer influence the protection factor. The area under the normal distribution curve is bounded by the protection angle (Θ) provided on either side.

AASHTO provides an example of how PF is estimated for a large diameter dolphin structure placed in front of a bridge pier. The same protection principle is illustrated in Figure 12 for a bridge located on a narrow inland waterway, where a pier is situated in the water but close to the shoreline. The landside of the bridge provides protection for the pier from collisions in that particular direction, since aberrant barge tows outside of the channel would run aground. The level of protection provided by the landside can be calculated as shown in Figure 12, where vessel collision trajectories are estimated using a normal distribution based on a standard deviation (σ) equal to 30 degrees (0 degrees represents a head-on collision and 90 degrees a complete sideways collision).

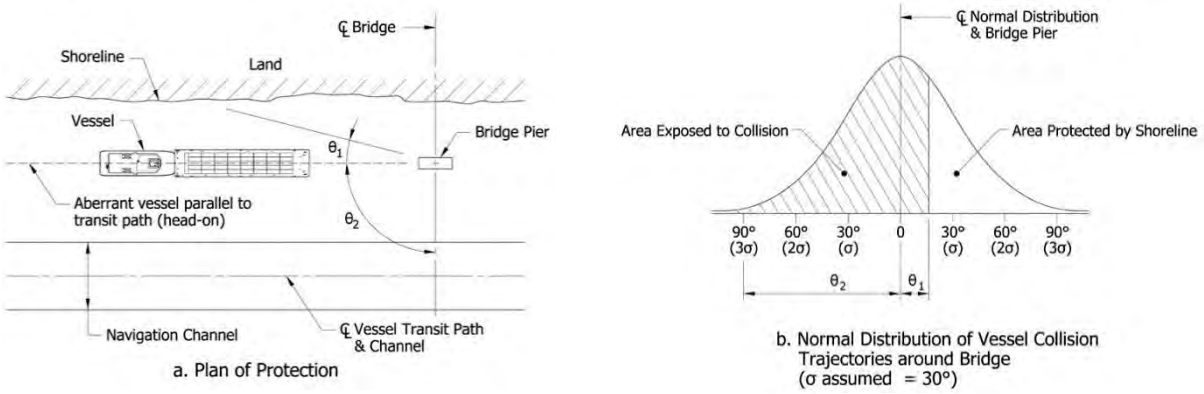

Figure 12: Protection Factor Illustration

In accordance with normal distribution properties, approximately 86% of all events occur within +/- 1σ, 95% within +/- 2σ, and 99% within +/- 3σ. Potential collision exposure angles can be developed based on the waterway/bridge geometry and vessel size. These angles can then be used in the normal distribution curve to estimate the probability of exposure to collision and the area protected by the feature under consideration. The protection provided is utilized to determine a PF value for use in the risk analysis. PF would be developed for each pier or span included in the risk analysis for both the upbound and downbound vessel directions, as applicable.

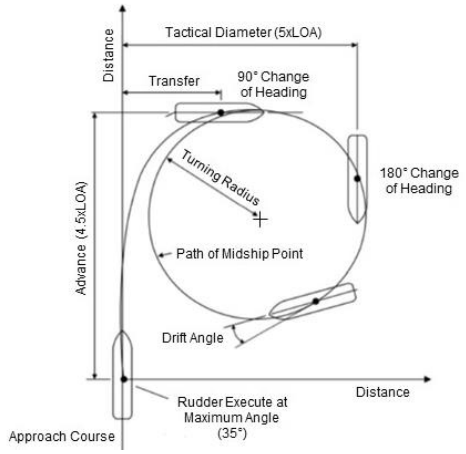

Figure 13: Aberrant Ship Turning Circles

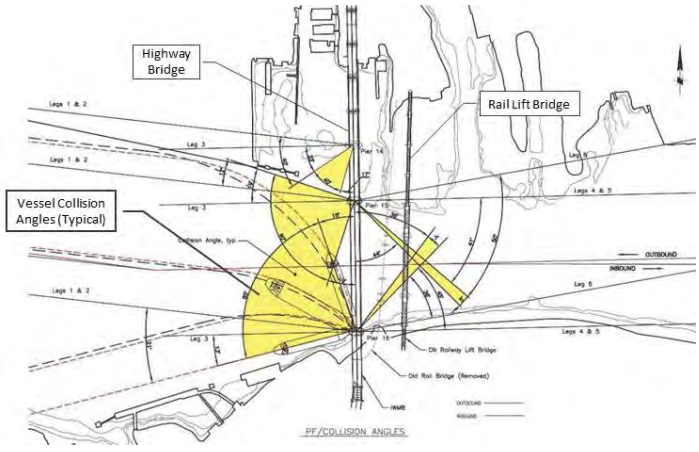

Figure 14: Illustration of Collision Angles for Bridge Protection Factors (PF)

Physical protection features in the waterway near a bridge can be combined with the estimated movements of an aberrant vessel (Figure 13) to develop vessel collision angles used to estimate PF as illustrated in Figure 14. In Figure 14, vessels are transiting a narrow waterway and pass under both a highway bridge and an adjacent rail lift bridge.

2.7 Superstructure (Span) Collision

Vessel collision assessments are usually based on an evaluation of bridge piers in the waterway being hit by an aberrant vessel, however, for arch-shaped bridges an evaluation of potential superstructure collision must also be considered. For arch-shaped bridges the vertical clearance above water is reduced significantly between the edge of the channel and the piers supporting the arching superstructure. As shown in Figure 15, potential superstructure collision could occur between the mast of the vessel hitting the lower chord of the steel truss, the deckhouse of the vessel hitting the truss, or the top of the bow of the ship hitting the truss above water. Figure 15 also illustrates the potential pier collision scenario where the bulbous bow of an aberrant vessel hits the concrete pier supporting the bridge structure.

The location of the point of contact of an aberrant vessel mast, deckhouse or bow with the steel truss varies depending on the vessel size and draft (loaded or ballasted), geometry of the steel truss members, and the water elevation. Multiple water levels significantly complicates the superstructure risk analysis but should be considered in locations where tidal ranges are large. The vessel impact force also varies depending upon which part of the ship contacts the bridge component. Mast impact forces are smaller than deckhouse impacts, which are smaller than flared bow impacts, which are less than the full bow impact force on the pier (the largest impact force). In general the mast of an aberrant ship would contact the bottom chord of the truss before potential contact was made with the ship deckhouse (Figure 15).

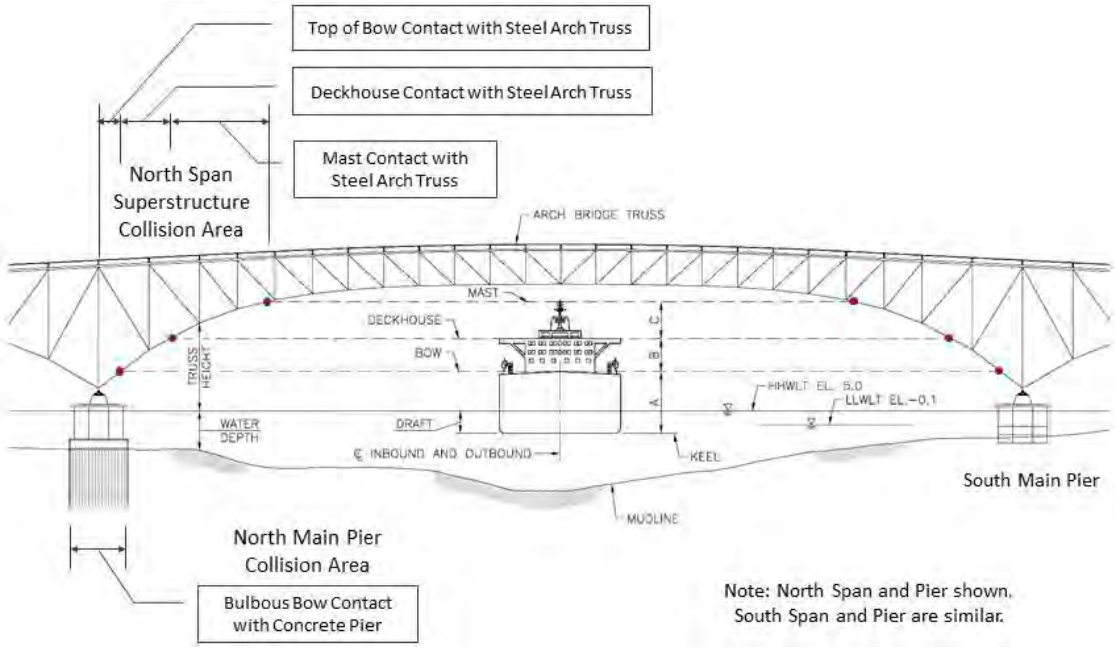

Figure 15: Superstructure (Span) Collision Geometry

3. ANALYSIS OF COMPLEX CHANNEL GEOMETRIES

As indicated throughout AASHTO 2009, the provisions represent an analysis simplification of a very complex problem. Procedures on how to evaluate typical ship/barge impacts are provided and illustrated and general principles are discussed, but it does not explicitly cover every conceivable situation that may be encountered. Therefore, it is left to bridge designers to use engineering judgment to apply the general analysis principles to model site-specific and sometimes complex bridge and navigation channel geometries.

An example of using AASHTO risk analysis principles to model a curved channel alignment near a bridge is shown in Figure 16. In this figure, the downbound vessel transit path is straight as ships/barges

approach the main span of the bridge, but the upbound vessel transit path is highly curved due to existing waterway and navigational constraints. In order to model the curved vessel transit path, the upbound curve is broken into a series of six (6) 305m tangent sections ("legs") measured outward from the centerline of the bridge. The 1830m (6,000 feet) distance on each side of the bridge crossing represents approximately 1-nautical mile and was selected by AASHTO based on historical accident data (the Canadian Bridge Code 2014 uses 2,000m for the analysis limit). The selection of six (6) 305m legs was based on judgment and experience from similar risk analysis models. Another bridge designer might elect to use sixty (60) 30.5m legs to further refine the "mesh" used for analysis (all that would be required is additional computation and model development effort).

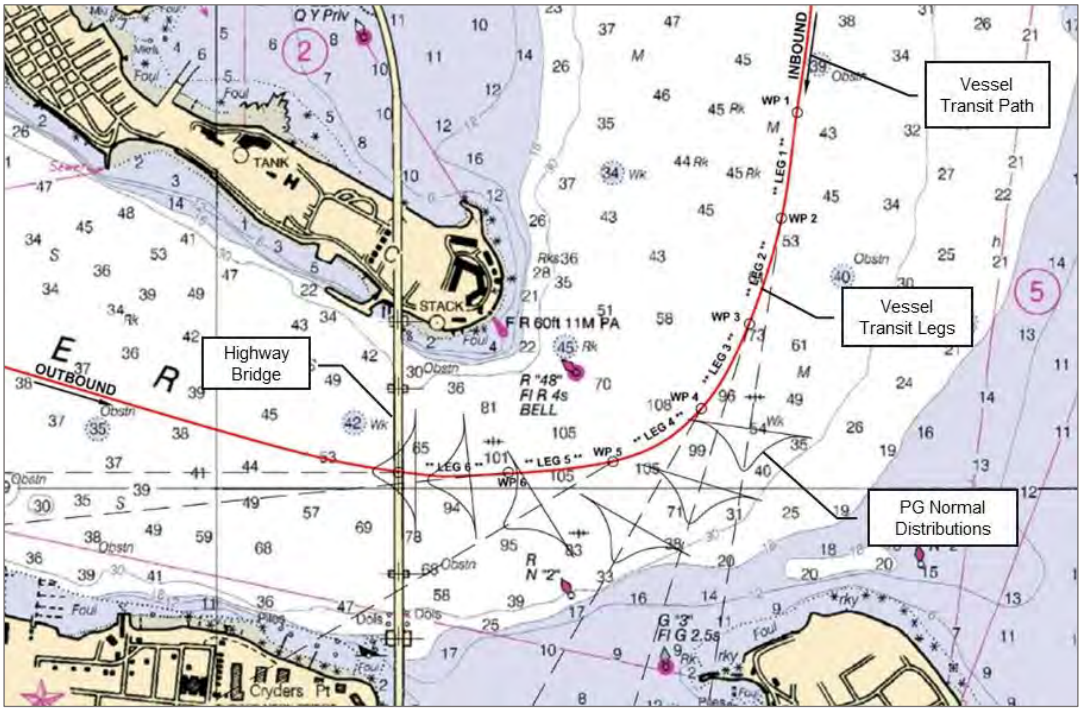

Figure 16: Illustration of Curved Channel Approach to Bridge

To conduct the risk analysis on the curved portion of the inbound transit path, each tangent section is computed as a "straight" section in the risk analysis and the 6 legs are added together to estimate the total inbound transit path AF. As shown in Figure 16, each leg has its own geometric probability (PG) distribution based on AASHTO's normal distribution centered on the tangent direction. The estimate of PG for each specific bridge pier or span component affected by an aberrant vessel is computed based on the bridge and waterway geometry associated with each leg and each vessel type. The legs are combined to estimate the risks due to inbound and outbound vessels, which are in turn combined to estimate the total bridge risk.

A probability of aberrancy (PA) must also be computed for each individual leg when conducting the risk analysis for the curved section. For the curved inbound transit path, the aberrancy base rate (BR) should be equally divided among the number of legs (so for the provided example, each inbound leg would have a base rate of BR/6). The base rates, which represent the minimum rates of accident frequency, are multiplied by correction factors for bridge location relative to bends in the waterway, currents acting parallel to vessel transit path, cross-currents acting perpendicular to vessel transit path, and the traffic density of vessels using the waterway. For each leg and its associated tangent geometry in the waterway, PA correction factors need to be determined, since the effect of currents and cross-currents can vary significantly.

It should be noted that the same aberrancy BR is used for both the inbound and outbound transit paths in the overall risk analysis. It is not divided by two (for each side) and then further divided by six for each tangent leg – that would be an incorrect application of the AASHTO requirements.

As seen in the example bridge in Figure 16, the PG associated with ships/barges that would become aberrant on Legs 1, 2 and 3 of the inbound transit path would not be headed in a direction that would

potentially impact the bridge. They would instead run aground in the southern shallow waters of the river away from the bridge alignment. Inbound vessels becoming aberrant in Leg 4 would be on a principal path headed toward the bridge south main tower and anchor pier locations but away from the piers on the north side. Aberrant vessels in Legs 5 and 6 would be in a principal direction through the main navigation span of the bridge. As seen in the provided example, the AASHTO vessel collision provisions and principles can be adapted to model complex bridge and curved channel geometries.

4. WATER ELEVATIONS AND SCOUR

Available water depths are a key factor in determining which vessel could potentially strike bridge piers in a waterway. AASHTO 2009 states:

> "… As a minimum, the design water depth shall be computed from the bottom of the waterway to the annual mean high water level … In waterways where seasonal flooding represents a significant portion of the high-water activity, judgment must be used to establish the design water level."

The water level shown in AASHTO 2009 for ship and barge impact loads is noted as Mean High Water (MHW). It is certainly true that the terminology used in the current AASHTO requirements are based primarily on tidal waterways, with statements that "judgment" should be used where "seasonal flooding represents a significant portion of the high-water activity." This is an indirect Code reference to non-tidal waterways and represents a potential source of confusion or ambiguity on specifically how to apply the AASHTO collision requirements in a consistent and reasonable manner to non-tidal locations.

4.1 Maximum Impact Loads (Typical Vessel Transits)

Maximum impact loads due to aberrant vessels transiting the waterway at normal speeds should be developed differently between tidal and non-tidal waterways as discussed below.

Tidal Waterways: The water elevation used in determining the design depth for a vessel collision risk analysis is very important. AASHTO recommends using MHW for tidal areas and engineering judgment in non-tidal areas, such as inland rivers. In areas with tidal influence, there are typically 2 high tides per day. As a general simplified explanation, the average elevation of each high tide (each day) over the course of a year provides the MHW elevation. However, typically one of the daily high tides is higher than the other. Therefore, the average elevation of the highest daily tide (each day) over the course of a year provides the Mean Higher High Water (MHHW) elevation. Tides vary in elevation daily, weekly, monthly and seasonally due to the phases of the moon – usually so-called "spring tides" yield the highest tide elevations of the year.

Commercial merchant vessels transit a waterway throughout the year, so the selection of MHW as a design datum by AASHTO was based on a reasonably conservative water elevation that vessels would regularly experience while navigating under "normal" conditions. In general, vessels do not navigate through a waterway during severe storms and flood events but instead are tied-up at a dock or anchored until the high water and associated high current passes and "normal" conditions return. In fact, many inland navigable waterways have a flood level or "stage" established by the USCG and/or the U.S. Army Corps of Engineers (USACOE) that prohibits commercial navigation during an extreme high water event due to safety reasons.

Although the risk analysis is usually conducted using MHW, it is considered over-conservative in waterways with significant tidal fluctuations, such as the coastal areas of Canada where the tide variations exceed 5m on a daily basis. For locations where large tide variations exist, the tidal range is usually divided into 4 equal increments between MHW and Mean Low Water (MLW) levels and the risk analysis is conducted for each water level. This requires that the number of vessel transits (N) for each vessel category be allocated as appropriate to each water level. Although more accurate, there is a significant increase in the computational effort required when using multiple water elevations.

Non-Tidal Waterways: For non-tidal inland waterways, the use of MHW does not apply, but a similar thought process would be recommended in selecting a water elevation for the vessel collision risk analysis. A high water level that covers almost all "normal" conditions in which a commercial vessel may be navigating the waterway should be selected. Some U.S. state Departments of Transportation (DOTs) have adopted the "2% flowline" as the water datum for vessel collision analysis (this would effectively cover 98% of all water levels in the waterway). Flowlines are typically established for a specific waterway location using historical water-gage measurements obtained by federal and state agencies such as the USACOE, DOT, and National Oceanic and Atmospheric Administration (NOAA).

For the “normal” navigation scenario, the authors contend that use of a 2% flowline may be overly conservative when compared to the tidal waterways MHW limit. An exceedance curve developed for a typical tidal location shows that MHW is only surpassed approximately 10% of the time. Therefore, for a non-tidal location, a 10% flowline might be considered similar to the MHW level and more appropriate for use in the vessel collision risk analysis.

In summary, the primary goal for the “Maximum Impact” design scenario is to determine a reasonably conservative “typical/normal/average high water condition” under which vessels are routinely transiting the waterway, excluding water stages where navigation is shut down on the waterway. Water levels associated with extreme storm events should be excluded.

4.2 Minimum Impact Loads (Drifting Barge in a Storm Event)

Minimum Impact Loads due to a drifting barge in a storm event should be developed differently between tidal and non-tidal waterways as discussed below.

Tidal Waterways: Bridges and inland lock structures are routinely hit by vessels after they break loose from moorings during a severe storm event and are carried by winds and currents in the waterway. The vessels are usually empty barges that have broken loose and are drifting in the waterway. As a result, AASHTO has a minimum impact design requirement associated with an empty barge impacting any bridge pier located in water depths greater than 0.6m during a storm event. The barge is usually an empty 10.7m wide by 59.5m long hopper barge that is commonplace on the U.S. inland waterway system (but could be a different barge size depending on the specific waterway barge fleet).

The water level and water current for this situation should be based on the selected extreme storm event. AASHTO requires that all piers located in 0.6m of water (corresponds to the empty hopper barge draft) under the extreme storm event should be designed for the minimum vessel impact force.

For a new bridge, the 100-year design storm is typically selected for evaluation of the drifting barge scenario. On the U.S. East Coast, the 100-year storm is often related to an extreme hurricane event and hydrologic and hydraulic (H&H) models are used to determine both the water elevation and currents for bridge piers in the waterway. Depending on the depth and overall width of the waterway, different current speeds may exist over its width and should be considered for the various pier designs based on their locations.

Non-Tidal Waterways: For non-tidal inland waterways, a similar rationale and design process should be used to determine the extreme storm event and its associated water level and current for the drifting barge collision scenario. Historic records and H&H analysis can be used to establish a 100-year design event (or other alternative design year event as might be required).

5. COMBINATION OF VESSEL IMPACT LOADS AND SCOUR

Discussions concerning vessel collision extreme events also raise critical issues related to scour. The combination of vessel impact loads and scour are discussed in AASHTO 2009 for two design cases: 1) drifting barge during a storm event, and 2) aberrant vessels impacting bridge piers during normal operations while transiting the navigation channel. The following paragraphs are excerpts from AASHTO 2009:

> “Minimum impact loads associated with a drifting empty barge breaking loose from its moorings and hitting a bridge (potentially during storm and high water conditions). The drifting barge impact loads should be combined with one-half of the predicted long-term plus one-half of the predicted short-term scour. For this load case, long-term scour should be taken as the sum of the contraction scour portion of live bed scour and scour due to long-term channel degradation. Short-term scour should be taken as the short-term portion of the live bed scour associated with the 100-year storm/flood event.”
>
> “Maximum impact loads associated with a ship or barge tow striking the bridge while transiting the navigation channel under typical waterway conditions (i.e., not during extreme storm events and high water conditions). The vessel impact loads should be combined with one-half of the predicted long-term scour.”
>
> “Short-term scour includes contraction, local and live bed scour in which river or bay bottom material (sand, clay, gravel, etc.) is removed as a result of increased water velocities caused by flooding conditions in conjunction with the overall bridge geometry and substructure shape on the hydraulic conductivity of the site.”

"In the U.S., historical data indicates that merchant ships and barge tows will not transit river and harbor areas during periods of high water and flood events which cause abnormal and dangerous water currents in the navigation channel. During such flood events, vessels will normally leave the harbor, tie-up at docks, or anchor in designated areas of the waterway. Following the passage of the flood stages of the waterway, and once currents return to normal levels, merchant shipping will recommence in the waterway. By that time it is anticipated that the short-term (live bed) scour areas near the bridge piers will have been significantly refilled by sediment transport mechanisms in the waterway. It is of interest to note that no records of any scour concerns are reported on any of the 31 major bridge collapses mentioned at the beginning of this report."

"At limited locations in the U.S., live bed scour conditions do not exist and instead, clearwater scour conditions may exist. In clearwater scour situations, up-river site conditions are such that there is virtually no particulate matter (soil, gravel, etc.) to transport; therefore, river bed material removed by local contraction scour is not replaced after flood level water velocities subside. Under this special condition, the full depth of scour should be used in the vessel collision analysis."

"Long-term scour includes aggradation and degradation scour and refers to scour across the entire waterway width. This is a permanent site condition with a magnitude (depth) that increases with time and is independent of the presence of a bridge or the structures geometry – this scour will occur regardless of the bridge. Long-term scour (if it is present at all) is usually a gradual deterioration of base support across the waterway."

In a typical bridge crossing, the long-term scour is usually a small value and is often not significant when evaluating the maximum impact load scenario. Of course each site has to be evaluated on its own merits before a specific design decision can be made.

6. VESSEL BOW CRUSHING AND BRIDGE PROTECTION

Based on the risk analysis results, a design vessel or a series of design vessels can be determined for each specific bridge pier location and/or superstructure element. Associated with each design vessel is an impact force and subsequent collision energy, as well as a general determination of the vessel bow geometry. An estimate of bow geometry is critical in determining if any portion of the ship/barge bow overhang can contact and cause damage to the bridge pier foundation or superstructure.

It is important for bridge designers to account for potential crushing of the vessel bow when determining bridge pier foundations (piles), footings, and general pier geometry. Consideration must also be given to not only the bow overhang above water, but also protrusions associated with a vessel bulbous bow below water. As shown in Figure 17 and Figure 18, after initial impact the vessel bow can be crushed a considerable distance and could possibly make contact with a vulnerable portion of the bridge pier, such as the tower (above water) or foundation piles (below water), causing catastrophic damage if not considered in the evaluation of protection measures.

Figure 17: Ship Bow Crushing

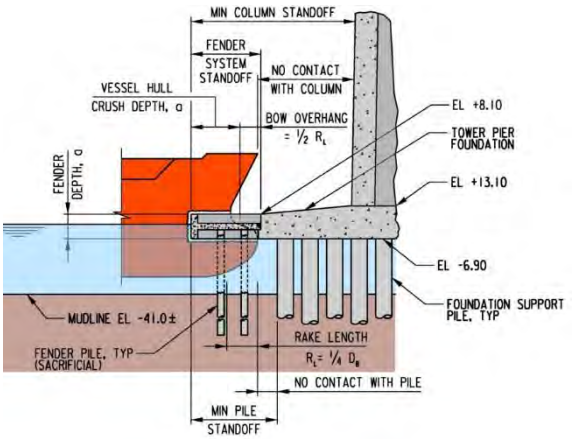

Figure 18: Ship Bow Crushing and Bridge Pier Geometry

In Figure 17, a ship crashed into a container terminal wharf, which effectively sliced through the bow of the ship for a relatively significant distance (until the collision energy was absorbed). The underwater bulbous bow portion of the ship also destroyed numerous piling that supported the wharf structure. The wharf structure and piling where the ship made contact had to be repaired/replaced.

As shown in Figure 18, bridge pier design should consider crushing of the vessel bow under impact conditions to determine the appropriate stand-off distance required for both underwater (piling) and above water contact with bridge pier elements. The amount of bow crushing can be calculated using AASHTO procedures based on the vessel impact force and energy and the geometry and strength of the bridge pier structure. In general, the vessel bow will crush until the impact energy is absorbed, assuming that the pier structure is sufficiently strong to withstand the impact forces both locally and globally. For major bridge projects sophisticated explicit solver finite element models (FEM) of both the design vessel and the bridge piers are usually developed for dynamic impact analysis as part of the design process.

7. CONCLUSIONS

Vulnerability of highway and railroad bridges to potential catastrophic collapse due to ship and barge collisions can be evaluated using AASHTO provisions for both relatively simple and complex bridge and navigable waterway geometries.

This paper illustrated application of the AASHTO vessel collision principles for curved navigation channels near bridges; selection of the appropriate water depth and scour for use in the risk analysis for the evaluation of both tidal and non-tidal waterways; development of protection factors (PF) for use in the risk analysis; adjustments to probability of aberrancy (PA) for modern navigation practices; modifications to the geometric probability (PG) for tethered tug assistance; and highlighted the importance of considering vessel bow crushing when evaluating the consequences of potential local contact between an aberrant ship/barge bow with a bridge pier.

It should be noted that the discussion and recommendations on the application of the AASHTO procedures in this paper represent the personal opinions of the authors only and should not in any way be considered an official position of AASHTO or any other organization or company.

REFERENCES

AASHTO (2009). Guide Specifications and Commentary for Vessel Collision Design of Highway Bridges, 2nd Edition with 2010 Interim Specifications, American Association of State Highway and Transportation Officials (AASHTO), Washington D.C., United States.

AASHTO (2014). LRFD Bridge Design Specifications, 7th Edition, American Association of State Highway and Transportation Officials (AASHTO), Washington D.C., United States.

Canadian Highway Bridge Design Code (CHBDC) (2014), CAN/CSA-S6-14, Canada Standards Association, Toronto.

Homes, K., Knott, M., et al. (2018), Vessel Collision Assessment/Mitigation for Two Vancouver Bridges, CSCE/SCGC/IABSE 10th International Conference on Short and Medium Span Bridges, Quebec City, Canada, July 31 - August 3, 2018.

Larsen, O. (Editor) (1993). Ship Collision with Bridges: The interaction between Vessel Traffic and Bridge Structures. Structural Engineering Document 4, International Association for Bridge and Structural Engineering (IABSE).

Trans Mountain (2013). Termpol Review Process Documents, 15 Volumes (Termpol 3.1 thru 3.19) plus Supporting Documents and Reference Materials, Trans Mountain Expansion Project, Canada.

USCG (2003). American Waterways Operators Bridge Allison Work Group. Report of the U.S. Coast Guard - American Waterways Operators, Inc. Safety Partnership, Washington, D.C.

GENERAL CONSIDERATIONS ON THE USE OF INFLATABLE GATES ON WATERWAYS. A REVIEW OF PIANC WG166.

by

Michael Gebhardt[1], Julien Aubonnet[2], Jean-Luc Berterottière[3], Bart De Heyder[4], Peter Jansen[5], Jan-Willem Lechtenberg[6], Ichiro Maruyama[7], Don Mason[8], Timothy Paulus[9], Philippe Rigo[10] and Thilo Wachholz[11]

1. INTRODUCTION

Inflatable gates are relatively new gate types, and are considered to be innovative hydraulic structures. A rubber gate consists of a multi-ply rubber membrane, which is fixed to the weir sill using clamp plates and anchor bolts. The rubber gate is inflated by pumping air or water inside the rubber body until the design height or pressure is reached. It is deflated by allowing the air or water inside the rubber body to escape. A steel-rubber gate is a row of steel gate panels supported on their downstream side by inflatable air bladders. By controlling the pressure in the bladders, angle and height of the steel gate panel can be controlled, and the upstream water level be kept within a required tolerance. Rubber gates have a number of advantages but the main reasons are the capital and maintenance costs which are supposed to be lower than steel gates. The aim of this contribution is to give a summary at the end of the Working Group lifecycle.

The report of PIANC InCom Working Group (WG) 166 “Inflatable Structures in Hydraulic Engineering” (PIANC 2018) is for owners and operators and focusing on the design, fabrication, construction, operation and maintenance of inflatable gates. A previous report of InCom WG26 focused on the “Design of Movable Weirs and Storm Surge Barriers” (PIANC 2006) which briefly introduces rubber gates (also known as rubber dams, rubber weirs or inflatable dams) and steel-rubber gates (also known as pneumatically actuated gates or Obermeyer gates). It is also referred to the report of WG138 “Mechanical and Electrical Engineering – Lessons Learnt from Navigation Structures” (PIANC 2014), where drive systems are described which are utilized in navigation structures and storm surge barriers.

2. WORKING GROUP

InCom WG166 consisted of 13 members from seven countries (Fig. 1). On September 23rd, 2013 WG166 held its kick-off meeting in Maastricht during the PIANC-SMART Rivers Conference. Since the kick-off seven meetings took place in Hanover (March 2014), in Tokyo and Osaka (May 2014), in Paris and Dijon (October 2014), in Gent and Aachen (March 2015), in Albany and Burlington (July 2015), in Nimes (January 2016) and finally in Utrecht (June 2016).

[1] Federal Waterways Engineering and Research Institute, Germany, michael.gebhardt@baw.de
[2] BRL Ingénierie, France, Julien.Aubonnet@brl.fr
[3] VINCI Construction, France, jean-luc.berterottiere@vinci-construction.fr
[4] De Vlaamse Waterweg nv, Belgium, bart.deheyder@wenz.be
[5] Rijkswaterstaat, The Netherlands. michael.gebhardt@baw.de
[6] Floecksmühle Energietechnik GmbH, Germany, Willi.Lechtenberg@floecksmuehle.com
[7] former employee of Sumitomo Electric Industries, Ltd., Japan, ichiroikomabiz@gmail.com
[8] Dyrhoff Ltd., UK, donmason@dyrhoff.co.uk
[9] U.S. Army Corps of Engineers, USA, Timothy.M.Paulus@usace.army.mil
[10] University of Liège, Belgium, ph.rigo@ulg.ac.be
[11] Generaldirektion Wasserstraßen und Schifffahrt, Germany, thilo.wachholz@wsd-m.wsv.de

The work was influenced by ongoing projects in Belgium, France and Germany where inflatable gates will be applied on water-ways. Guest experts were regularly invited and contributed indirectly to that report. On-site visits to existing weirs, meetings with operators and administrations and technical excursions to manufacturers were arranged. In the end, many more experts contributed in some way to the report.

Figure 1: Members of Working Group 166 at Curtis Dam, USA (from left to right): Philippe Rigo, Julien Aubonnet, Peter Jansen, Michael Gebhardt, Thilo Wachholz, Jan-Willem Lechtenberg, Steve Denton (Atlantic Power Corporation), Ichiro Maruyama, Timothy Paulus, Don Mason, Jean-Luc Berterottière and Bart De Heyder (top right)

3. RELEVANCE OF INFLATABLE STRUCTURES FOR WATERWAYS

Rubber gates have a number of advantages when compared with standard steel gates:

- The simplicity and flexibility of the structure is a key consideration in its wide scope of applications. Generally, capital and maintenance costs are considered to be lower than steel gates.
- Moving parts are eliminated (hinges, bearings); no problems due to corrosion or sealing and no lubricants used, which may be harmful to the environment.
- Inflatable gates have a high reliability and availability, they can always be deflated to prevent blocking and they are far less affected by settlements or earthquakes.
- Drive mechanisms, such as hydraulic cylinders, electrical actuators or chains (which generally require a great amount of maintenance) are not needed. Inflatable gates are controlled by inflating or deflating leading to a significantly lower level of energy demand.
- The effort for recesses and concrete reinforcement (sill, pier) is lower and the transfer of forces into the weir sill is evenly distributed. Many applications show that rubber gates can be an interesting alternative to steel gates, in particular on sites where they are adapted to existing weir structures.
- The rubber membrane can be installed or replaced within a few weeks so that the construction time is considerably reduced and availability of the movable weir is increased.

The majority of these advantages apply also to steel-rubber gates, but compared to rubber gates they require some extra maintenance due to the steel gate panels. The capital and maintenance costs are higher. Generally, steel-rubber gates are also simple structures and slightly advantageous regarding the control of flow and water level.

In spite of the advantages, it must also be stated that there are a small number of experienced suppliers and a limited number of manufacturers. Rubber is a complex product requiring special attention for the jointing process or the rubber formula. The report shows the different manufacturing processes in order to inform the reader of possibly weak points of the membrane structure.

Inflatable gates have been used as water control structures for more than sixty years. The world's first rubber gate was installed in Los Angeles County in the USA in the mid-1950s. The first steel-rubber gate was installed at the end of the 1980s. For navigation purposes, the first rubber gate in the German waterway and shipping administration was installed in 2006. Today, five rubber gates are in operation at German waterways (Fig. 2a & d). In the French administration three steel-rubber gates were installed in 2011 (Fig. 2c), and 29 other rubber gates will be installed until 2020 in Northern France. Currently, steel-rubber gates for navigational purposes are also under construction at two sites in Belgium. The Storm Surge Barrier Ramspol (Fig. 2b) is also a waterway application, but a barrier and thus deflated for most of the year. One of the weir spans is navigable for ships. It is still the largest rubber gate ever made since commissioning in 2001.

Figure 2: Applications of inflatable gates at waterways

Despite the increasing interest in inflatable gates at inland waterways, the vast majority of inflatable gates were installed for other purposes, mainly irrigation, hydropower, or recreational purposes. The longest list of applications can be found in Japan with almost 4,000 installations. Today, an increasing interest can be found in Asia (China in particular). It is obvious that the number of waterway applications is comparatively small. It is being attempted to provide a comprehensive summary of best practices and to discuss knowledge and experience within the constraints of waterways.

4. CURRENT INSTALLATIONS, TYPICAL DIMENSIONS AND LIFETIME

The report provides an overview of current installations based mainly on reference lists of suppliers and manufacturers. It is not intended to be a complete list, because there is lack of information for instance from China and Eastern Europe. But, it can be assumed that about 5,000 inflatable gates are currently installed worldwide. Today, the largest rubber gate for water level control has a height of 6.0 m and the largest steel-rubber gate has a height of 8.5 m. Regarding the total width the largest weir equipped with rubber gates has a total width of about 640 m, the largest width of one span is about 110 m. Apart from the maximum values the analysis of from about 1,000 inflatable gates installed worldwide shows, that for 88% of the installations the height is less than 3.0 m, for 70% the span width is less than 30.0 m. These average values can generally be considered as typical dimensions of inflatable gates, while the maximum values indicate what is feasible at the moment. In general, inflatable gates are most appropriate for wide spans with a small number of piers, which makes them relatively unobtrusive in the landscape. Compared to rubber gates the number of steel-rubber gates is considerably smaller. Less than 10% of the installations are known to be steel-rubber gates.

With regard to the number of applications it can be concluded that inflatable gates are a proven technology up to a certain limit. It is easy to imagine that setting a limit value for the height of inflatable gates even with proven technology is difficult. In general, the inflatable gate technology is proven up to 3.0 m by a very large number of installations. Up to 5.0 m there are still quite a number of gates with good experiences. For comparison, the application range of the Japanese standard for rubber gates (JICE, 2000) is limited by a height of 6.0 m. Since 1978 this standard gives a solid base for the design and material requirements. Although the Japanese standard doesn´t correspond to other standards worldwide it was the basis for a large number of installations even outside Japan.

Inflatable gates can be used for water level control which is generally the case for hydropower and navigation, although the majority is installed for irrigation purposes, where overflow depth is limited and the rubber gate will be fully deflated above that limit. There exist also a large number of hydropower applications, where the constraints with regard to the upstream water level tolerances are comparable but slightly less restrictive. In order to control the upstream water level for a large discharge range, countermeasures against vibrations, such as deflectors or breakers, have to be adapted.

A property of air-filled types is the so-called V-notch phenomena. A V-notch occurs due to the density differences of air and water. The system becomes unstable and the membrane will be folded or dented. The resulting V-shaped "dent" makes flow rate adjustment difficult and results in a large flow rate per unit width. This is the reason why water-filled types were recommended for the French and German waterway applications. Experiences show, that water-filled rubber gates equipped with a row of breakers allow a regulation of the upstream water level within the required tolerances. For these features, steel-rubber gates have a slight advantage because the gate panels behave like a flap gate and provide a stable nappe separation.

Today, rubber membranes are designed to be UV stable, weather, ozone and heat resistant. According to the Japan Institute of Country-ology and Engineering (JICE) the lifetime of a rubber membrane was originally supposed to be about 30 years for moderate environmental conditions. In fact, about 14% of almost 4,000 installations in Japan are operating more than 35 years with the same rubber membrane. In ten years the proportion will reach 42%. Based on these recent experiences it can be stated that aging didn´t affect the durability of the rubber membrane and the lifetime can be even longer (JICE, 2000).

5. CONCLUSIONS

In recent years, the technology of inflatable gates has been improved and standards have been adjusted as soon as a failure has been detected. Therefore, inflatable gates are an interesting alternative to standard steel gates, enabling savings to be made on the capital spending and maintenance costs, in particular on sites where these gate types are adapted to existing weir structures. An increasing benefit of this technology can be observed, however, failures (although small in number) pushed some to return to the “standard steel technology”. Considering this, it is the right time to publish this report and to provide a comprehensive summary of best practices that can be incorporated into the future design of inflatable gates and to aid designers and operators in their preliminary tasks.

WG166 completed about nearly 30 project reviews of inflatable gates which are provided on the PIANC Database (http://www.infrastructure.pianc.directory/index.jsp). Here, projects of inflatable gates are made available next to Navigation Locks and Major Infrastructures.

References

JICE (2000). Technical Standard for Rubber Gates. Japan Institute of Country-ology and Engineering, Tokyo.

PIANC (2006). Report of Working Group 26: Design of Movable Weirs and Storm Surge Barriers. PIANC, Brussels.

PIANC (2014). Report of Working Group 138: Mechanical and Electrical Engineering Lessons Learnt from Navigation. PIANC, Brussels.

PIANC (2018). Report of Working Group 166: Inflatable Structures in Hydraulic Engineering. PIANC, Brussels.

A new in-chamber double longitudinal culverts filling and emptying system for high head and large navigation lock

by

LI Jun[1], LIU Ben-qin[2], ZHAO Gen-sheng[3] and XUAN Guo-xiang[4]

ABSTRACT

Xijin hydro-junction is a key project of the Xijiang Golden Waterway in China, a two-step single-lane lock has already been constructed. The proposed 2nd lane lock is designed for the maximum vessel with the tonnage of 3000t. The new lock is located at the right bank of the river and also the 1st lane lock, and it is designed as a single step lock. The effective dimension of the lock chamber is 280.0m×34.0m×5.6m (length × width × water depth over the sill), and its maximum lift height is 20.3m, the designed filling time is 12min. Due to its large dimension and high lift, the comprehensive hydraulic characteristics of the new lock is close to the Three Gorges Locks and the Gezhouba Locks on Yangtze River, so it is quite necessary to determine and improve the layout of the filling and emptying system both by hydraulic analysis and model test study.

The lock chamber is quite wide, so the transverse flow distribution in the chamber during the filling run is the main influencing factor of the ship berthing safety due to the previous experiences. At the beginning, the In-chamber longitudinal culvert system (ILCS) invented by the U.S. Army Corps of Engineers is been adopted for the new lock. A physical model with the scale 1:30 was built for the hydraulic study. The test results of the initial layout indicate that: under the ILCS layout, the transverse flow distribution in the chamber during the filling run especially with single valve opened is quite uneven, there is obvious water surface slope and the transverse hawser forces of the vessel far exceeded the allowable valve.

Based on the test results, we changed the energy dissipating type from flow jet collision to open ditch, which means a “T” type baffle was set between the two bottom culverts, and the height of the holes in the “T” type baffle was adjusted to improve the transverse flow distribution. At the same time, considering the uneven flow distribution problem under single valve opened or asynchronous double valves opening, the layout of the two separate culverts in the ILCS was adjusted that two converged sections were set for the two culverts near the lock heads. The test results under the new layout indicate that the optimizations greatly improved the flow conditions in lock chamber, the transverse hawser forces of the designed vessel reduces nearly by 50%, and the hydraulic characteristics under different conditions all satisfied the requirements of design and standards.

The new in-chamber double longitudinal culverts filling and emptying system has many advantages, such as obvious energy dissipation efficiency, high hydraulic efficiency, simple structure, economic construction and maintenance, and it is a safe and efficient filling and emptying system for high head large navigation lock. Compared to the ILCS, the new system adapts to more lift height, which is recommended under 12m by the U.S. Army Corps of Engineers, and also has more efficiency and safety.

Key words：navigation lock, filling and emptying system, in-chamber culvert, energy dissipation, hydraulics;

1. INTRODUCTION

Xijiang River is one of the high level waterways which are being constructed in recent years, and it is as important as Yangtze River in Chinese inland water transportation. The Chinese government has planned to make Xijiang River become a golden waterway with the annual traffic capacity over 100 million tonnage. A lot of large navigation locks have been or being constructed to achieve the above goal. Among these

[1] Nanjing Hydraulic Research Institute, Key Laboratory of Navigation Structure Construction Technology, Ministry of Transport, lijun@nhri.cn, China
[2] Nanjing Hydraulic Research Institute, bqliu@nhri.cn, China
[3] Nanjing Hydraulic Research Institute, gszhao@nhri.cn, China
[4] Nanjing Hydraulic Research Institute, xuan@nhri.cn, China

locks, the Xijin 2nd lane lock has the second highest hydraulic characteristics, ranked only behind the Datengxia lock (LI Jun et al, 2016) [1].

The designed vessel for Xijing 2nd lane lock is 3000t single vessel and 2×2000t push train. The effective dimension of the lock chamber is 280.0m×34.0m×5.6m (length × width × water depth over the sill), the lock's maximum lift height is 20.3m, the designed filling time is 12min. Due to its large dimension and high lift, the comprehensive hydraulic characteristics of the new lock is close to the Three Gorges Locks and the Gezhouba Locks on Yangtze River, so it is quite necessary to determine and improve the layout of the filling and emptying system both by hydraulic analysis and model test study.

2. SELECTION OF THE FILLING AND EMPTYING SYSTEM

2.1 Selection criteria

According to the Chinese Industry Standard "Design code for filling and emptying system of shiplocks (JTJ306-2001)" [2], the selection coefficient for lock filling and emptying system is as follows:

$$m = \frac{T}{\sqrt{H}} \tag{1}$$

in which, m is the selection coefficient, T(min) is the designed lock filling time, and H(m) is the lock lift height. For Xijin 2nd lane lock, H is 20.3m, T is 10~12min, so its selection coefficient m is 2.22~2.66. According to the design code, when m is between 1.8 and 2.5, the lock filling and emptying system can be simple through culverts system including side-port system, in-chamber longitudinal culvert system and in-chamber laterals system; when m is between 2.5 and 3.5, the lock filling and emptying system can be through heads system or above through culverts systems.

2.2 System selection and layout

Because the important role and high hydraulic characteristics of Xijin 2nd lane lock, and considering its large chamber dimension, great geological condition, safety, economy and maintenance, the in-chamber longitudinal culvert system becomes an appropriate selection.

Stockstill (1998) first invented a new In-chamber Longitudinal Culvert System (ILCS) for the McAlpine project and carried out a 1:25 model test, numerous culvert designs with various port arrangements were evaluated, some design criteria for this system were given according to the investigation [3]. Hite (1999,2000) carried out the second ILCS model investigation for the Marmet Navigation Project and the second ILCS model study, and also gave some design suggestions and valve operation suggestions [4,5]. Based on the above studies, John E. Hite (2003) carried out further and detailed studies of ILCS, and gave the detailed design guidance for this new system [6], this guidance was written in the U.S. Army Corps of Engineers Engineer Manual "Hydraulic Design of Navigation Locks(EM 1110-2-1604)" (2006) [7]. The investigation of the ICLS showed that this type of filling and emptying system was feasible from a hydraulic performance point of view, and can reduce construction costs associated with large concrete gravity walls, but this system is suggested to be used only in low to medium lift height (3m~12m) large locks.

For studying the applicability of ILCS in high lift large lock, according to the design guidance by U.S. manual and our design experiences of similar system, we designed the ICLS for Xijin 2nd lock, the layout of the system is shown in Figure 1 and Figure.2, and the key characteristics of the system are shown in Table.1.

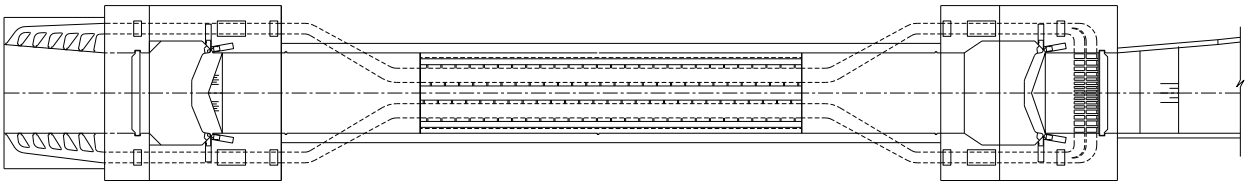

Figure 1: Initial layout of In-chamber Longitudinal Culvert System for Xijin 2nd lane lock

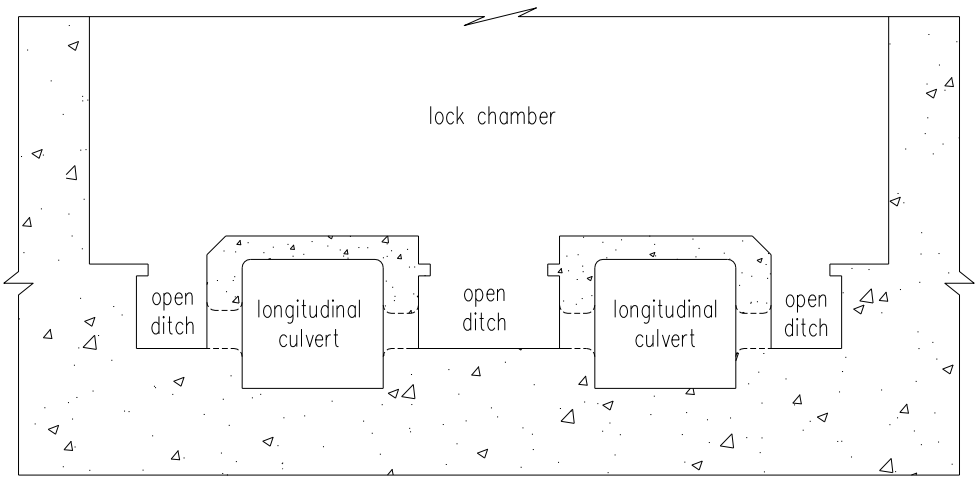

Figure 2: Cross section of lock chamber for Xijin 2nd lane lock

No.	Position	Description	Area (m^2)	Area ratio to valve section
1	Valve section culvert	submerged depth under maximum lift height condition: 7.82m.	2-4.5×6.0=54.0	1.00
2	Intake	6 vertical side ports on guide wall, throat section height of each port is same, throat section width of each port reduces along the flow direction.	2～6×4.5×7.2=388.8	7.20
3	In-chamber longitudial culvert	2 longitudinal culverts, side ports on each side of the culvert. Length of the side port section is 162.0m which is 57.9% of the chamber usable length.	2～6.0×5.5=66.0	1.22
4	Side ports	There are 27 side ports on each side of the bottom culvert. Dimension of the port from upstream to downstream are: 0.50m×1.50m (9 ports, width × height), 0.46m×1.50m m(9 ports), 0.42m×1.50m m(9 ports), port spacing is 6.0m, length of the port is 1.5m, inlet and outlet of the port should be round out, the trimming circle radius is 0.3m.	2～2×9×1.50×（0.5+0.46+0.42）=74.52	1.38
6	Open ditches in lock chamber	Width of open ditches at lock wall sides is 3.0m and open ditche in the center of lock chamber is 6.0m, the depth of the open ditch is 3.6m.	/	/
7	Outlet	Double of the culvert area, inside guide walls should be set up.	2～2×4.5× 7.2=129.6	2.40
8	Energy dissipation chamber	Manifolds in lower sill with 32 top ports and 16 side ports.	Top:4×（2+2+1.5+1.5+1+1+0.8+0.8）×4.5=190.8 Side:2×（2+2+1.5+1.5+1+1+0.8+0.8）×6=127.2	3.53 2.36

Table 1: key characteristics of In-chamber Longitudinal Culvert System for Xijin 2nd lane lock

3. MOEDL TEST INVESTIGATION OF THE INITIAL ILCS

3.1 Model design

A 1:30 scale model is established for studying the hydraulic characteristics of the filling and emptying system. The accepted equations of hydraulic similitude, based on the Froudian relations, were used to express mathematical relations between the dimensions and hydraulic quantities of the model and prototype. General relations for the transference of the model data to prototype equivalents, or vice versa, are presented in Table 2.

Parameter	Ratio	Scale relations
Length	$L_r = L$	1:30
Area	$A_r = L_r^2$	1:900
Velocity	$V_r = L_r^{1/2}$	1:5.48
Discharge	$Q_r = L_r^{5/2}$	1:4929.5
Time	$T_r = L_r^{1/2}$	1:5.48
Force	$F_r = L_r^3$	1:27000

Table 2: Model test similitude

The model reproduced part of the upstream approach channel, the entire filling and emptying system including intakes, valves, culverts, outlet, lock chamber, and part of the downstream approach channel.

The lock chamber was constructed of steel sheet, the culverts were constructed of polyethylene(PE) plastic, the valve section culvert and one side of the lock wall were constructed of methyl methacrylate(PMMA) for the convenience of observing hydraulic phenomenon, the upstream and downstream approach channels were constructed of concrete precast slab with cement sand plaster. The model vessels were constructed of glass fiber reinforced plastics. The real model is shown in Figure.3 and Figure.4.

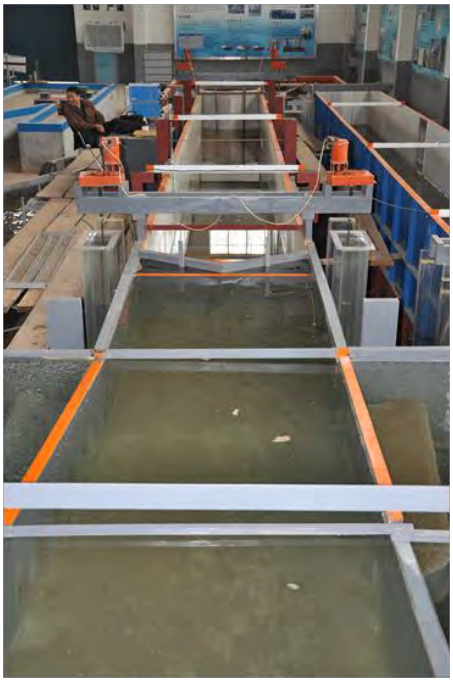

Figure 3: Overall model

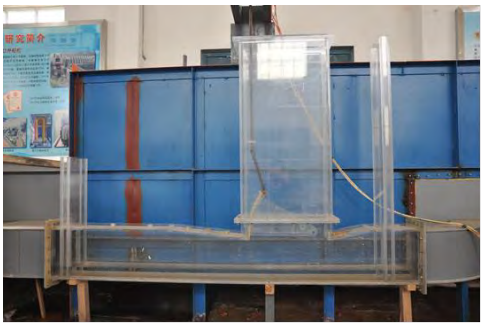

Figure 4: Model of valve section

3.2 Instruments and equipment

The upstream and downstream water level are controlled by overflow tank, the valve are driven by stepper motor which can achieve stepless speed regulation. The water level in lock chamber and the local transient or fluctuating pressures in culvert are measured by resistance-type pressure sensor, the local average piezometric pressures are measured by piezometric tubes. The vessel's hawser forces are measured by full-circular resistance-type dynamometer invented by Nanjing Hydraulic Research Institute. The discharge is measured by rectangle measuring weir. All the data are collected by WaveBook 516E high-speed data acquisition system.

3.3 Test results and analysis

The vessel berthing condition test was firstly carried out. The hawser forces of 2×2000t push train were measured during the filling run, and the results are shown in Figure 5.

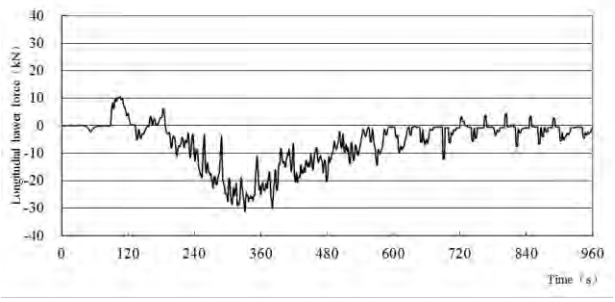

a longitudinal hawser force

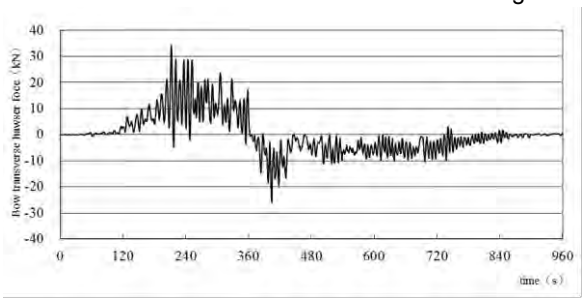

b bow transverse hawser force

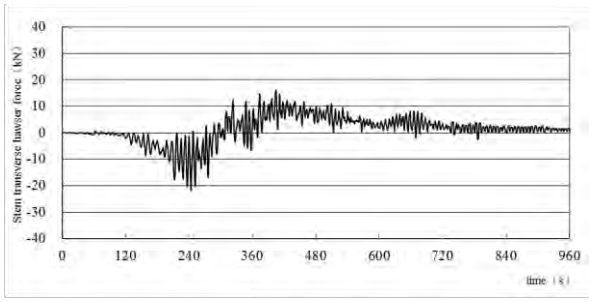

c stem transverse hawser force

Figure 5: Hawser forces of 2×2000t push train under initial layout (double valves operation)

The test results indicate that under the initial ILCS layout, when double filling valves opening in 6min continuously and synchronously, the maximum longitudinal hawser force of the designed 2×2000t push train is 30.9kN, the maximum transverse hawser force is 34.3kN. According to the design code [2], the longitudinal hawser force satisfied the safety need (no more than 40kN), but the transverse hawser force far exceeded the controlling value (no more than 20kN).

Due to the outflow adjustment and energy dissipation by grouped side ports layout and longitudinal open ditches, the longitudinal flow distribution in lock chamber is relatively even, there is no obvious longitudinal water slope, so the maximum longitudinal hawser force of the push train is only 75% of the allowable value. However, because the middle open ditch is wider than side ones, even though the side ports are staggered in the middle open ditch, the outflow in middle open ditch is more than side ones, so there is obvious transverse water slope in lock chamber which induced the large transverse hawser force. Besides, the transverse flow distribution in the chamber during the filling run with single valve opening will be more uneven than double valves opening. Therefore, the initial ILCS must be improved.

4. IMPROVED ILCS AND ITS TEST RESULT

4.1 Improvement of the initial ILCS

Based on the test results of the initial layout, the energy dissipation efficiency was not enough in the middle open ditch which induced more outflow around the center of the lock chamber, so we set a “T” type baffle in the middle open ditch to divide the large open ditch into two smaller ones, which will increase the energy dissipation strength, besides, we set several holes in the baffle to let the flow in the two small open ditches can exchange and mixing, which will further strengthen the energy dissipation efficiency and also can readjust the flow distribution in the two open ditches. The height of the holes in the baffle is the key parameter to improve the transverse flow distribution, and after several tests, we gave the recommended layout of the baffle which is shown in Figure 6.

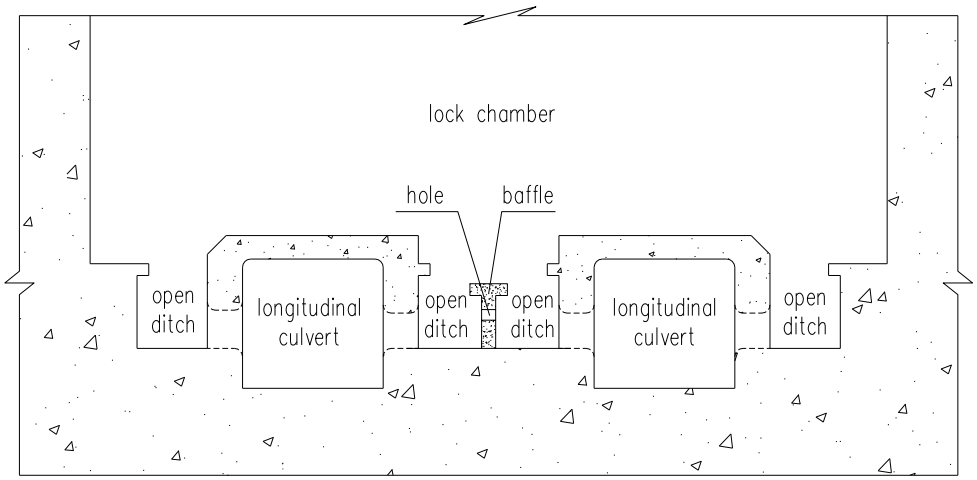

Figure 6: Cross section of lock chamber after improvement

At the same time, considering the uneven flow distribution problem under single valve opened or asynchronous double valves opening, the layout of the two separate culverts in the ILCS was adjusted that two converged sections were set for the two culverts near the lock heads. The recommended layout of the improved ILCS is shown in Figure 7.

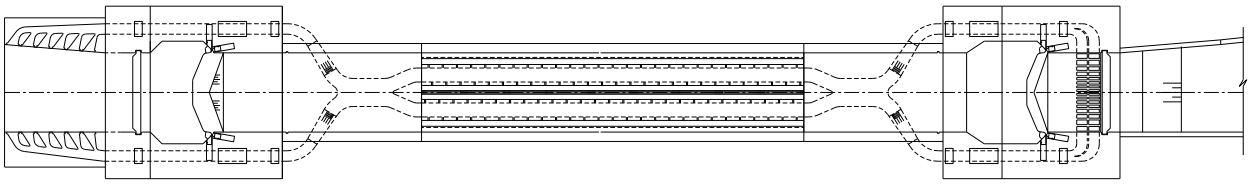

Figure 7: Layout of improved In-chamber Longitudinal Culvert System for Xijin 2nd lane lock

4.2 Test results and analysis

4.2.1 Vessel’s berthing condition

The test results of vessel’s hawser forces under the new layout are shown in Table 3. It indicates that the optimizations greatly improved the flow conditions in lock chamber, the flow distribution in lock chamber became more even, the transverse hawser forces of the designed push train reduces nearly by 50%, the maximum longitudinal hawser forces of push train and barge have further reduced and are only 64% and 67% of allowable value respectively, all of the forces satisfied the code. The improvements of the system have obvious effects.

Vessel type	Valve operation pattern	Vavle opening time (min)	Berthing position	Longitudinal hawser force (kN)	Bow transverse hawser force (kN)	Stem transverse hawser force (kN)
2×2000t push train	Double valve continuous opening	5	Upper chamber	23.0	16.8	17.7
			Middle chamber	25.5	18.6	18.6
			Lower chamber	23.9	13.0	11.8
	Single valve continuous opening	5	Upper chamber	17.7	16.0	17.8
			Middle chamber	15.7	18.0	14.4
			Lower chamber	16.5	14.1	9.5
3000t barge	Double valve continuous opening	5	Upper chamber	24.7	14.5	21.7
			Middle chamber	31.0	11.3	16.6
			Lower chamber	9.6	14.9	17.7
	Single valve continuous opening	5	Upper chamber	13.2	11.2	17.7
			Middle chamber	31.0	14.2	19.3
			Lower chamber	14.3	16.7	14.3

Note: According to the Chinese Standard, the allowable longitudinal hawser force for 2000t and 3000t vessel are 40kN and 46kN respectively, the allowable transverse hawser force for 2000t and 3000t vessel are 20kN and 23kN respectively.

Table 3: Hawser forces of designed vessels under improved layout

4.2.2 Hydraulic characteristics of filling and emptying runs

The main hydraulic characteristics under maximum lift condition (lift height: 20.3m) are shown in Table 4 and Fig8.

Operation pattern		t_v (min)	H (m)	T (min)	Q_{max} (m^3/s)	U_{max} (m/min)	U_a (m/min)	d (m)
Filling	Double valves Continuous opening	5	20.3	11.92	653	3.33	1.70	+0.62
		6	20.3	12.63	625	3.18	1.61	+0.62
		7	20.3	13.20	592	3.02	1.54	+0.62
	Single valve Continuous opening	5	20.3	16.75	479	2.44	1.21	+0.46
		6	20.3	17.47	460	2.34	1.16	+0.46
		7	20.3	18.00	441	2.25	1.13	+0.46
Emptying	Double valves Continuous opening	5	20.3	12.96	601	3.06	1.57	-0.43
		6	20.3	13.50	566	2.88	1.50	-0.43
		7	20.3	14.04	530	2.70	1.45	-0.43
	Single valve Continuous opening	5	20.3	18.21	437	2.23	1.11	-0.38
		6	20.3	18.80	426	2.17	1.08	-0.38
		7	20.3	19.39	418	2.13	1.05	-0.38

Note : t_v is the valve opening time, H is the lock lift height, T is the filling or emptying time, Q_{max} is the maximum filling or emptying discharge, U_{max} is the maximum rate-of-rise or rate-of-fall of the water level in lock chamber, U_a is the average rate-of-rise or rate-of-fall of the water level in lock chamber, d is the overfill or overempty.

Table 4: Hydraulic characteristics of filling and emptying runs under improved layout

The test results indicate that:

1) If the filling and emptying valves both open in 5min continuously and synchronously, the average operation time is 12.44min, considering the scale effect of lock hydraulic model test, the prototype discharge coefficient will increase compared with model, the prototype operation time will decrease, so the prototype operation time will less than 12min.
2) When double filling and emptying valves all open in 5min continuously and synchronously, the maximum filling discharge are 653m^3/s and 601m^3/s respectively. The velocities in different sections of the improved system all can satisfy the code (flow velocity in culvert should not exceed 15m/s, average velocity of intake should not exceed 2.5m/s) and operation safety.
3) The overfill and overempty under different conditions are both over 0.30m which are higher than the allowable value (0.25m) according to the code. In prototype, we can use the countermeasure to reduce the overfill and overempty that opening the miter gate when the water levels become equal on both sides of the gate, and this countermeasure has been successfully used in the Three Gorges Locks.

4.2.3 Resistance coefficient and discharge coefficient

According to the steady flow test results we can calculate the resistance coefficients and discharge coefficients under different conditions. The filling and emptying discharge coefficients under double valves open are 0.841 and 0.729 respectively, and the filling and emptying discharge coefficients under single valve open are 1.027 and 0.979 respectively.

5. Conclusion

The new in-chamber double longitudinal culverts filling and emptying system has many advantages, such as obvious energy dissipation efficiency t, high hydraulic efficiency, simple structure, economic construction and maintenance. Compared to the ILCS, the new system adapts to more lift height, which is recommended under 12m by the U.S. Army Corps of Engineers. So it is a safe, efficient and economic filling and emptying system for high head large navigation lock.

6. REFERENCES

[1] LI Jun, XUAN Guo-xiang, et al. (2016). Application of two-section four-manifold total-balanced filling and emptying system in 40m-grade single-step giant ship lock. Port & Waterway Engineering. 2016(12). (in Chinese)

[2] Chinese Industry Standard, Design code for filling and emptying system of shiplocks (JTJ306), 2001. (in Chinese)

[3] Stockstill, R. L. (1998). “Innovative lock design; Report 1, Case study, New McAlpine Lock filling and emptying system, Ohio River, Kentucky,” Technical Report INP-CHL-1, U.S. Army Engineer Waterways Experiment Station, Vicksburg, MS.

[4] Hite, J. E., Jr. (1999). “Model study of Marmet Lock filling and emptying system, Kanawha River, West Virginia,” Technical Report CHL-99-8, U.S. Army Engineer Waterways Engineer Station, Vicksburg, MS.

[5] Hite, J. E., Jr. (2000). “New McAlpine Lock filling and emptying system, Ohio River, Kentucky,” Technical Report ERDC/CHL TR-00-24, U.S. Army Engineer Research and Development Center, Vicksburg, MS.

[6] John E. Hite, Jr. (2003). “In-Chamber Longitudinal Culvert Design for Lock Filling and Emptying System”, Technical Report ERDC/CHL TR-03-8, Coastal and Hydraulics Laboratory, U.S. Army Engineer Research and Development Center, Vicksburg, MS.

[7] Hydraulic Design of Navigation Locks (EM 1110-2-1604), US Army Corps of Engineers,2006.

A new in-chamber double longitudinal culverts filling and emptying system for high head and large navigation lock

by

LI Jun[1], LIU Ben-qin[2], ZHAO Gen-sheng[3] and XUAN Guo-xiang[4]

ABSTRACT

Xijin hydro-junction is a key project of the Xijiang Golden Waterway in China, a two-step single-lane lock has already been constructed. The proposed 2nd lane lock is designed for the maximum vessel with the tonnage of 3000t. The new lock is located at the right bank of the river and also the 1st lane lock, and it is designed as a single step lock. The effective dimension of the lock chamber is 280.0m×34.0m×5.6m (length × width × water depth over the sill), and its maximum lift height is 20.3m, the designed filling time is 12min. Due to its large dimension and high lift, the comprehensive hydraulic characteristics of the new lock is close to the Three Gorges Locks and the Gezhouba Locks on Yangtze River, so it is quite necessary to determine and improve the layout of the filling and emptying system both by hydraulic analysis and model test study.

The lock chamber is quite wide, so the transverse flow distribution in the chamber during the filling run is the main influencing factor of the ship berthing safety due to the previous experiences. At the beginning, the In-chamber longitudinal culvert system (ILCS) invented by the U.S. Army Corps of Engineers is been adopted for the new lock. A physical model with the scale 1:30 was built for the hydraulic study. The test results of the initial layout indicate that: under the ILCS layout, the transverse flow distribution in the chamber during the filling run especially with single valve opened is quite uneven, there is obvious water surface slope and the transverse hawser forces of the vessel far exceeded the allowable valve.

Based on the test results, we changed the energy dissipating type from flow jet collision to open ditch, which means a “T” type baffle was set between the two bottom culverts, and the height of the holes in the “T” type baffle was adjusted to improve the transverse flow distribution. At the same time, considering the uneven flow distribution problem under single valve opened or asynchronous double valves opening, the layout of the two separate culverts in the ILCS was adjusted that two converged sections were set for the two culverts near the lock heads. The test results under the new layout indicate that the optimizations greatly improved the flow conditions in lock chamber, the transverse hawser forces of the designed vessel reduces nearly by 50%, and the hydraulic characteristics under different conditions all satisfied the requirements of design and standards.

The new in-chamber double longitudinal culverts filling and emptying system has many advantages, such as obvious energy dissipation efficiency, high hydraulic efficiency, simple structure, economic construction and maintenance, and it is a safe and efficient filling and emptying system for high head large navigation lock. Compared to the ILCS, the new system adapts to more lift height, which is recommended under 12m by the U.S. Army Corps of Engineers, and also has more efficiency and safety.

Key words：navigation lock, filling and emptying system, in-chamber culvert, energy dissipation, hydraulics;

1. INTRODUCTION

Xijiang River is one of the high level waterways which are being constructed in recent years, and it is as important as Yangtze River in Chinese inland water transportation. The Chinese government has planned to make Xijiang River become a golden waterway with the annual traffic capacity over 100 million tonnage. A lot of large navigation locks have been or being constructed to achieve the above goal. Among these

[1] Nanjing Hydraulic Research Institute, Key Laboratory of Navigation Structure Construction Technology, Ministry of Transport, lijun@nhri.cn, China
[2] Nanjing Hydraulic Research Institute, bqliu@nhri.cn, China
[3] Nanjing Hydraulic Research Institute, gszhao@nhri.cn, China
[4] Nanjing Hydraulic Research Institute, xuan@nhri.cn, China

locks, the Xijin 2nd lane lock has the second highest hydraulic characteristics, ranked only behind the Datengxia lock (LI Jun et al, 2016) [1].

The designed vessel for Xijing 2nd lane lock is 3000t single vessel and 2×2000t push train. The effective dimension of the lock chamber is 280.0m×34.0m×5.6m (length × width × water depth over the sill), the lock's maximum lift height is 20.3m, the designed filling time is 12min. Due to its large dimension and high lift, the comprehensive hydraulic characteristics of the new lock is close to the Three Gorges Locks and the Gezhouba Locks on Yangtze River, so it is quite necessary to determine and improve the layout of the filling and emptying system both by hydraulic analysis and model test study.

2. SELECTION OF THE FILLING AND EMPTYING SYSTEM

2.1 Selection criteria

According to the Chinese Industry Standard "Design code for filling and emptying system of shiplocks (JTJ306-2001)" [2], the selection coefficient for lock filling and emptying system is as follows:

$$m = \frac{T}{\sqrt{H}} \tag{1}$$

in which, m is the selection coefficient, T(min) is the designed lock filling time, and H(m) is the lock lift height. For Xijin 2nd lane lock, H is 20.3m, T is 10~12min, so its selection coefficient m is 2.22~2.66. According to the design code, when m is between 1.8 and 2.5, the lock filling and emptying system can be simple through culverts system including side-port system, in-chamber longitudinal culvert system and in-chamber laterals system; when m is between 2.5 and 3.5, the lock filling and emptying system can be through heads system or above through culverts systems.

2.2 System selection and layout

Because the important role and high hydraulic characteristics of Xijin 2nd lane lock, and considering its large chamber dimension, great geological condition, safety, economy and maintenance, the in-chamber longitudinal culvert system becomes an appropriate selection.

Stockstill (1998) first invented a new In-chamber Longitudinal Culvert System (ILCS) for the McAlpine project and carried out a 1:25 model test, numerous culvert designs with various port arrangements were evaluated, some design criteria for this system were given according to the investigation [3]. Hite (1999,2000) carried out the second ILCS model investigation for the Marmet Navigation Project and the second ILCS model study, and also gave some design suggestions and valve operation suggestions [4,5]. Based on the above studies, John E. Hite (2003) carried out further and detailed studies of ILCS, and gave the detailed design guidance for this new system [6], this guidance was written in the U.S. Army Corps of Engineers Engineer Manual "Hydraulic Design of Navigation Locks(EM 1110-2-1604)" (2006) [7]. The investigation of the ICLS showed that this type of filling and emptying system was feasible from a hydraulic performance point of view, and can reduce construction costs associated with large concrete gravity walls, but this system is suggested to be used only in low to medium lift height (3m~12m) large locks.

For studying the applicability of ILCS in high lift large lock, according to the design guidance by U.S. manual and our design experiences of similar system, we designed the ICLS for Xijin 2nd lock, the layout of the system is shown in Figure 1 and Figure.2, and the key characteristics of the system are shown in Table.1.

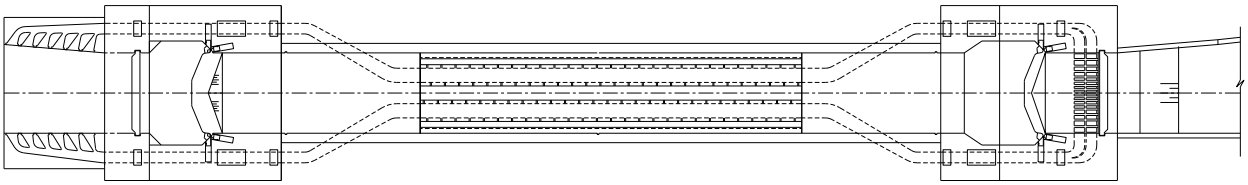

Figure 1: Initial layout of In-chamber Longitudinal Culvert System for Xijin 2nd lane lock

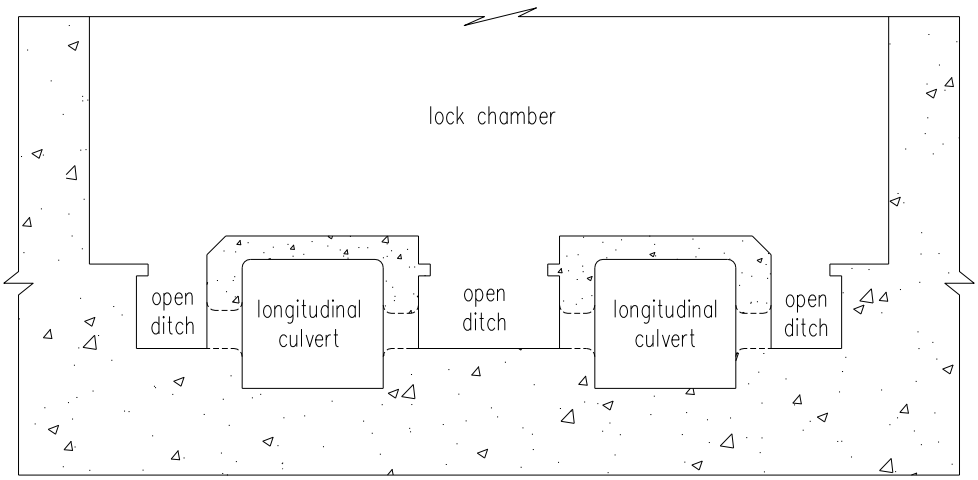

Figure 2: Cross section of lock chamber for Xijin 2nd lane lock

No.	Position	Description	Area (m^2)	Area ratio to valve section
1	Valve section culvert	submerged depth under maximum lift height condition: 7.82m.	2-4.5×6.0=54.0	1.00
2	Intake	6 vertical side ports on guide wall, throat section height of each port is same, throat section width of each port reduces along the flow direction.	2～6×4.5×7.2=388.8	7.20
3	In-chamber longitudial culvert	2 longitudinal culverts, side ports on each side of the culvert. Length of the side port section is 162.0m which is 57.9% of the chamber usable length.	2～6.0×5.5=66.0	1.22
4	Side ports	There are 27 side ports on each side of the bottom culvert. Dimension of the port from upstream to downstream are: 0.50m×1.50m (9 ports, width × height), 0.46m×1.50m m(9 ports), 0.42m×1.50m m(9 ports), port spacing is 6.0m, length of the port is 1.5m, inlet and outlet of the port should be round out, the trimming circle radius is 0.3m.	2～2×9×1.50×（0.5+0.46+0.42）=74.52	1.38
6	Open ditches in lock chamber	Width of open ditches at lock wall sides is 3.0m and open ditche in the center of lock chamber is 6.0m, the depth of the open ditch is 3.6m.	/	/
7	Outlet	Double of the culvert area, inside guide walls should be set up.	2～2×4.5× 7.2=129.6	2.40
8	Energy dissipation chamber	Manifolds in lower sill with 32 top ports and 16 side ports.	Top:4×（2+2+1.5+1.5+1+1+0.8+0.8）×4.5=190.8 Side:2×（2+2+1.5+1.5+1+1+0.8+0.8）×6=127.2	3.53 2.36

Table 1: key characteristics of In-chamber Longitudinal Culvert System for Xijin 2nd lane lock

3. MOEDL TEST INVESTIGATION OF THE INITIAL ILCS

3.1 Model design

A 1:30 scale model is established for studying the hydraulic characteristics of the filling and emptying system. The accepted equations of hydraulic similitude, based on the Froudian relations, were used to express mathematical relations between the dimensions and hydraulic quantities of the model and prototype. General relations for the transference of the model data to prototype equivalents, or vice versa, are presented in Table 2.

Parameter	Ratio	Scale relations
Length	$L_r = L$	1:30
Area	$A_r = L_r^2$	1:900
Velocity	$V_r = L_r^{1/2}$	1:5.48
Discharge	$Q_r = L_r^{5/2}$	1:4929.5
Time	$T_r = L_r^{1/2}$	1:5.48
Force	$F_r = L_r^3$	1:27000

Table 2: Model test similitude

The model reproduced part of the upstream approach channel, the entire filling and emptying system including intakes, valves, culverts, outlet, lock chamber, and part of the downstream approach channel.

The lock chamber was constructed of steel sheet, the culverts were constructed of polyethylene(PE) plastic, the valve section culvert and one side of the lock wall were constructed of methyl methacrylate(PMMA) for the convenience of observing hydraulic phenomenon, the upstream and downstream approach channels were constructed of concrete precast slab with cement sand plaster. The model vessels were constructed of glass fiber reinforced plastics. The real model is shown in Figure.3 and Figure.4.

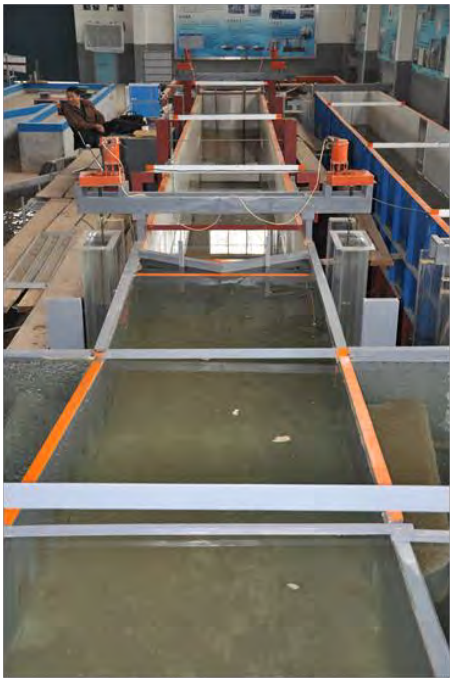

Figure 3: Overall model

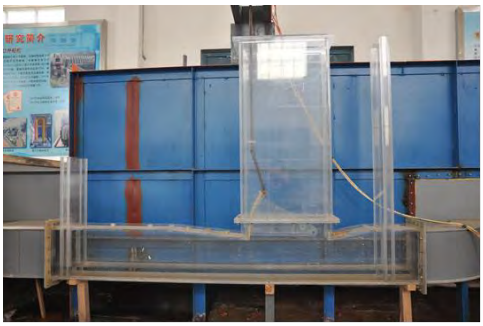

Figure 4: Model of valve section

3.2 Instruments and equipment

The upstream and downstream water level are controlled by overflow tank, the valve are driven by stepper motor which can achieve stepless speed regulation. The water level in lock chamber and the local transient or fluctuating pressures in culvert are measured by resistance-type pressure sensor, the local average piezometric pressures are measured by piezometric tubes. The vessel's hawser forces are measured by full-circular resistance-type dynamometer invented by Nanjing Hydraulic Research Institute. The discharge is measured by rectangle measuring weir. All the data are collected by WaveBook 516E high-speed data acquisition system.

3.3 Test results and analysis

The vessel berthing condition test was firstly carried out. The hawser forces of 2×2000t push train were measured during the filling run, and the results are shown in Figure 5.

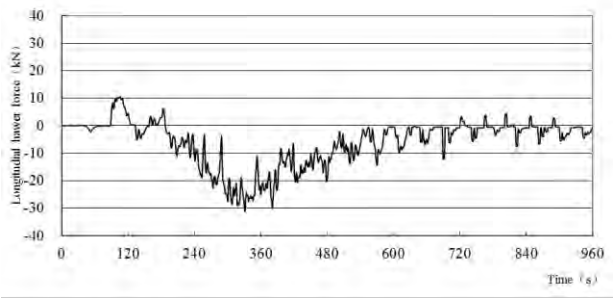

a longitudinal hawser force

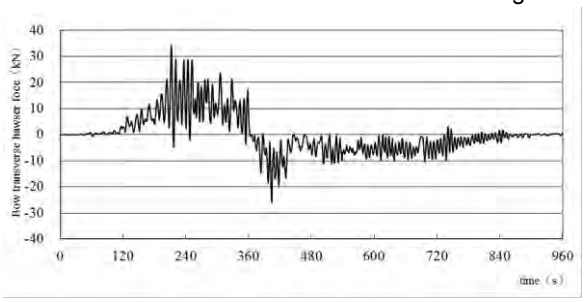

b bow transverse hawser force

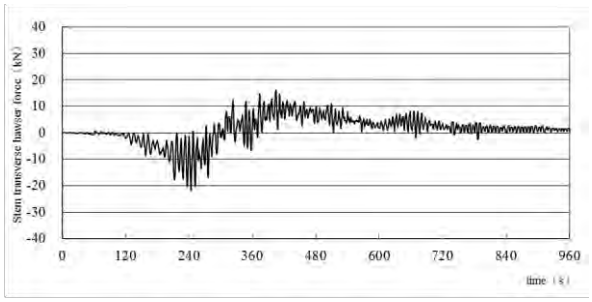

c stem transverse hawser force

Figure 5: Hawser forces of 2×2000t push train under initial layout (double valves operation)

The test results indicate that under the initial ILCS layout, when double filling valves opening in 6min continuously and synchronously, the maximum longitudinal hawser force of the designed 2×2000t push train is 30.9kN, the maximum transverse hawser force is 34.3kN. According to the design code [2], the longitudinal hawser force satisfied the safety need (no more than 40kN), but the transverse hawser force far exceeded the controlling value (no more than 20kN).

Due to the outflow adjustment and energy dissipation by grouped side ports layout and longitudinal open ditches, the longitudinal flow distribution in lock chamber is relatively even, there is no obvious longitudinal water slope, so the maximum longitudinal hawser force of the push train is only 75% of the allowable value. However, because the middle open ditch is wider than side ones, even though the side ports are staggered in the middle open ditch, the outflow in middle open ditch is more than side ones, so there is obvious transverse water slope in lock chamber which induced the large transverse hawser force. Besides, the transverse flow distribution in the chamber during the filling run with single valve opening will be more uneven than double valves opening. Therefore, the initial ILCS must be improved.

4. IMPROVED ILCS AND ITS TEST RESULT

4.1 Improvement of the initial ILCS

Based on the test results of the initial layout, the energy dissipation efficiency was not enough in the middle open ditch which induced more outflow around the center of the lock chamber, so we set a “T” type baffle in the middle open ditch to divide the large open ditch into two smaller ones, which will increase the energy dissipation strength, besides, we set several holes in the baffle to let the flow in the two small open ditches can exchange and mixing, which will further strengthen the energy dissipation efficiency and also can readjust the flow distribution in the two open ditches. The height of the holes in the baffle is the key parameter to improve the transverse flow distribution, and after several tests, we gave the recommended layout of the baffle which is shown in Figure 6.

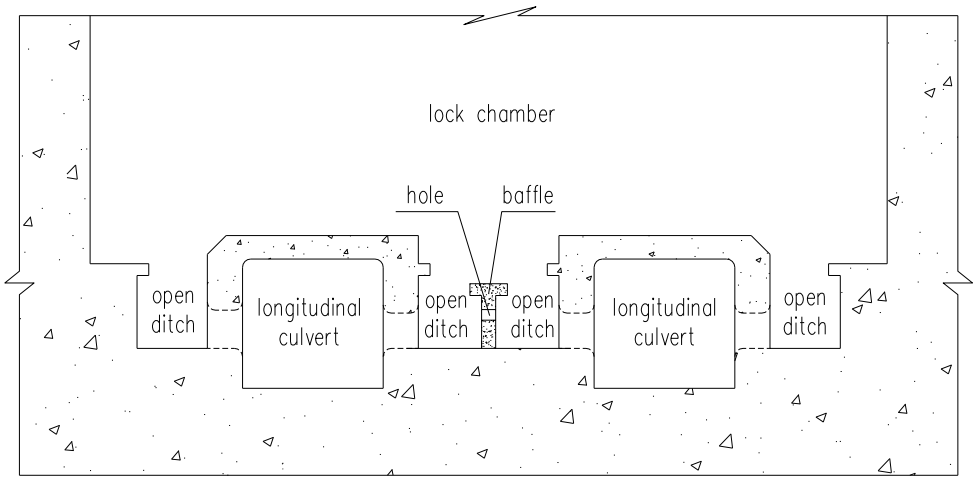

Figure 6: Cross section of lock chamber after improvement

At the same time, considering the uneven flow distribution problem under single valve opened or asynchronous double valves opening, the layout of the two separate culverts in the ILCS was adjusted that two converged sections were set for the two culverts near the lock heads. The recommended layout of the improved ILCS is shown in Figure 7.

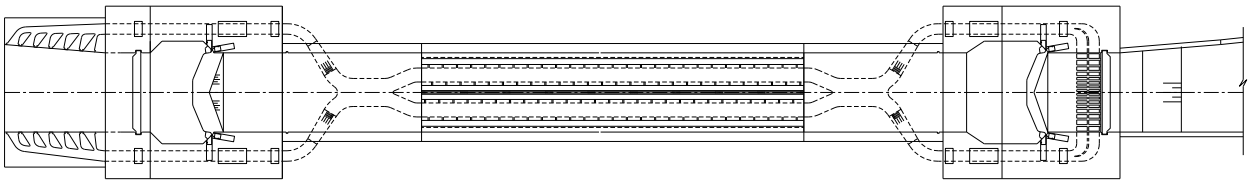

Figure 7: Layout of improved In-chamber Longitudinal Culvert System for Xijin 2nd lane lock

4.2 Test results and analysis

4.2.1 Vessel’s berthing condition

The test results of vessel’s hawser forces under the new layout are shown in Table 3. It indicates that the optimizations greatly improved the flow conditions in lock chamber, the flow distribution in lock chamber became more even, the transverse hawser forces of the designed push train reduces nearly by 50%, the maximum longitudinal hawser forces of push train and barge have further reduced and are only 64% and 67% of allowable value respectively, all of the forces satisfied the code. The improvements of the system have obvious effects.

Vessel type	Valve operation pattern	Vavle opening time (min)	Berthing position	Longitudinal hawser force (kN)	Bow transverse hawser force (kN)	Stem transverse hawser force (kN)
2×2000t push train	Double valve continuous opening	5	Upper chamber	23.0	16.8	17.7
			Middle chamber	25.5	18.6	18.6
			Lower chamber	23.9	13.0	11.8
	Single valve continuous opening	5	Upper chamber	17.7	16.0	17.8
			Middle chamber	15.7	18.0	14.4
			Lower chamber	16.5	14.1	9.5
3000t barge	Double valve continuous opening	5	Upper chamber	24.7	14.5	21.7
			Middle chamber	31.0	11.3	16.6
			Lower chamber	9.6	14.9	17.7
	Single valve continuous opening	5	Upper chamber	13.2	11.2	17.7
			Middle chamber	31.0	14.2	19.3
			Lower chamber	14.3	16.7	14.3

Note: According to the Chinese Standard, the allowable longitudinal hawser force for 2000t and 3000t vessel are 40kN and 46kN respectively, the allowable transverse hawser force for 2000t and 3000t vessel are 20kN and 23kN respectively.

Table 3: Hawser forces of designed vessels under improved layout

4.2.2 Hydraulic characteristics of filling and emptying runs

The main hydraulic characteristics under maximum lift condition (lift height: 20.3m) are shown in Table 4 and Fig8.

Operation pattern		t_v (min)	H (m)	T (min)	Q_{max} (m^3/s)	U_{max} (m/min)	U_a (m/min)	d (m)
Filling	Double valves Continuous opening	5	20.3	11.92	653	3.33	1.70	+0.62
		6	20.3	12.63	625	3.18	1.61	+0.62
		7	20.3	13.20	592	3.02	1.54	+0.62
	Single valve Continuous opening	5	20.3	16.75	479	2.44	1.21	+0.46
		6	20.3	17.47	460	2.34	1.16	+0.46
		7	20.3	18.00	441	2.25	1.13	+0.46
Emptying	Double valves Continuous opening	5	20.3	12.96	601	3.06	1.57	-0.43
		6	20.3	13.50	566	2.88	1.50	-0.43
		7	20.3	14.04	530	2.70	1.45	-0.43
	Single valve Continuous opening	5	20.3	18.21	437	2.23	1.11	-0.38
		6	20.3	18.80	426	2.17	1.08	-0.38
		7	20.3	19.39	418	2.13	1.05	-0.38

Note : t_v is the valve opening time, H is the lock lift height, T is the filling or emptying time, Q_{max} is the maximum filling or emptying discharge, U_{max} is the maximum rate-of-rise or rate-of-fall of the water level in lock chamber, U_a is the average rate-of-rise or rate-of-fall of the water level in lock chamber, d is the overfill or overempty.

Table 4: Hydraulic characteristics of filling and emptying runs under improved layout

The test results indicate that:

1) If the filling and emptying valves both open in 5min continuously and synchronously, the average operation time is 12.44min, considering the scale effect of lock hydraulic model test, the prototype discharge coefficient will increase compared with model, the prototype operation time will decrease, so the prototype operation time will less than 12min.
2) When double filling and emptying valves all open in 5min continuously and synchronously, the maximum filling discharge are 653m^3/s and 601m^3/s respectively. The velocities in different sections of the improved system all can satisfy the code (flow velocity in culvert should not exceed 15m/s, average velocity of intake should not exceed 2.5m/s) and operation safety.
3) The overfill and overempty under different conditions are both over 0.30m which are higher than the allowable value (0.25m) according to the code. In prototype, we can use the countermeasure to reduce the overfill and overempty that opening the miter gate when the water levels become equal on both sides of the gate, and this countermeasure has been successfully used in the Three Gorges Locks.

4.2.3 Resistance coefficient and discharge coefficient

According to the steady flow test results we can calculate the resistance coefficients and discharge coefficients under different conditions. The filling and emptying discharge coefficients under double valves open are 0.841 and 0.729 respectively, and the filling and emptying discharge coefficients under single valve open are 1.027 and 0.979 respectively.

5. Conclusion

The new in-chamber double longitudinal culverts filling and emptying system has many advantages, such as obvious energy dissipation efficiency t, high hydraulic efficiency, simple structure, economic construction and maintenance. Compared to the ILCS, the new system adapts to more lift height, which is recommended under 12m by the U.S. Army Corps of Engineers. So it is a safe, efficient and economic filling and emptying system for high head large navigation lock.

6. REFERENCES

[1] LI Jun, XUAN Guo-xiang, et al. (2016). Application of two-section four-manifold total-balanced filling and emptying system in 40m-grade single-step giant ship lock. Port & Waterway Engineering. 2016(12). (in Chinese)

[2] Chinese Industry Standard, Design code for filling and emptying system of shiplocks (JTJ306), 2001. (in Chinese)

[3] Stockstill, R. L. (1998). “Innovative lock design; Report 1, Case study, New McAlpine Lock filling and emptying system, Ohio River, Kentucky,” Technical Report INP-CHL-1, U.S. Army Engineer Waterways Experiment Station, Vicksburg, MS.

[4] Hite, J. E., Jr. (1999). “Model study of Marmet Lock filling and emptying system, Kanawha River, West Virginia,” Technical Report CHL-99-8, U.S. Army Engineer Waterways Engineer Station, Vicksburg, MS.

[5] Hite, J. E., Jr. (2000). “New McAlpine Lock filling and emptying system, Ohio River, Kentucky,” Technical Report ERDC/CHL TR-00-24, U.S. Army Engineer Research and Development Center, Vicksburg, MS.

[6] John E. Hite, Jr. (2003). “In-Chamber Longitudinal Culvert Design for Lock Filling and Emptying System”, Technical Report ERDC/CHL TR-03-8, Coastal and Hydraulics Laboratory, U.S. Army Engineer Research and Development Center, Vicksburg, MS.

[7] Hydraulic Design of Navigation Locks (EM 1110-2-1604), US Army Corps of Engineers,2006.

HOW TO POWER NAVIGATION LOCKS WITH ELECTRICITY

by

***George Berman Alemán*[1]**

1. WHY WE NEED AN "AIR LIFT LOCK" DEVICE?

The need to power navigation locks with electricity is simply being able to operate the locks when hydropower is not available. This technology is developed considering Panama's need for more revenues from the Canal and population's need for more potable water. Panama's water resources, primarily from Lake Gatun, are abundant but several droughts made the population aware of its limits. The record for most annual transits was set in 1971, 14,500 transits or nearly 40 transits per day. This number of transits is essentially the limit to Canal operations set by the availability of hydropower. The Panama Canal Authority has increased its revenues by increasing the size, not the number, of ships that transit the Canal daily. The Neo Panamax Locks increased the average ship size and revenues but has not increase the total number of transits. In 2017, the total transits were 13,549 or 37 transits per day.

The technology to power navigation locks with electricity will allow Panama to exploit its principal resource, it's geographic location, to its full potential without the limit imposed by the availability of water. It will eliminate draft restrictions on shipping through the Canal during droughts, and it will guarantee the population potable water without compromising canal operations. This technology is developed in Panama because water conservation has become one of our country's greater needs.

2. DESCRIPTION OF DEVICE

The device that powers navigation locks with electricity is described first, for the clarity of further explanations. The intent is to incorporate this technology first as a retrofit to the Panamax Locks. Therefore, the device presented here as the "Lock Air Lift" is designed specifically for this purpose. Figure 1 is a photograph of a physical model, scale 1/60, of the device. The device is shown, both in its closed and open positions. The device consists of two shells that slide in a telescoping manner to form a parallelepiped. The parallelepiped has a square top and bottom, 3.50 m wide, top and bottom surface and rectangular sides 11.00 meters high. The device is made of steel, and is powered by a hydraulic piston, 60 cm in diameter located along the centerline. The top of the device is flush with the lock floor, it expands vertically 8.6 meters met in a telescoping manner. The vertical expansion of the device corresponds to the level the water needs to rise in the lock chamber.

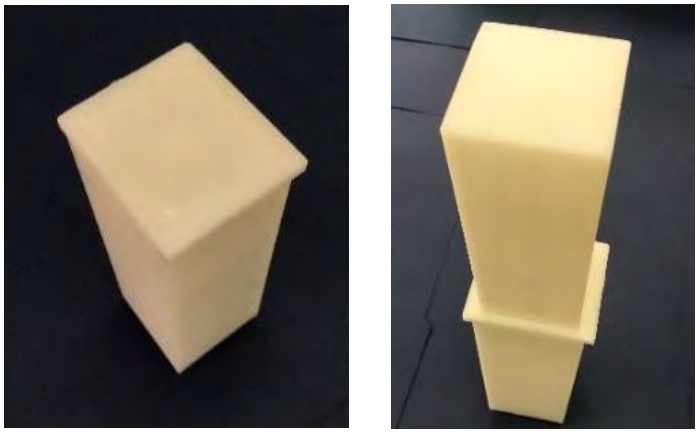

a) closed **b) opened**

Figure 1: Physical Model of Lock Air Lift Device, Scale 1/60. a) closed, b opened

[1] Geotechnical Engineering Consultant, Ingenieros Geotécnicos, S.A., gberman@ingeotec.net

The Panamax locks present suitable conditions for the introduction of this technology:

- The Panamax Locks have two lanes, so one lane can be shut down for the installation of the device while the other lane allows the locks to operate at a reduced capacity.
- These locks are not currently used to their maximum capacity of 45 ships per day. Their current use, 30 ships per day, is set by the availability of hydropower for canal operations.
- The device can be installed without compromising the lock's hydraulic culverts providing the locks a dual energy system.
- The author's experience as construction supervisor on "Overhauls" of the Panamax Locks provides a reference to the design proposals herein presented.

3. A THERMODYNAMIC SYSTEM FOR THE PANAMA CANAL

The Canal will be considered as a Thermodynamic system to envision the addition of another source of energy to power the operation of the Panamax Locks. The amount of energy required to lift one ship through one step of a Panamax Lock is shown in equation 1.

$$E=m*\left(H+\frac{\Delta H}{2}\right) \quad (1)$$

Where:

E: energy, kg-m (kWh)

m: mass, kg

H: height of water, m

ΔH: increase in height, m

$$E=33.54*304.88*15.24*1000*\left(15.24+\frac{\Delta 8.61}{2}\right)=5{,}420{,}869\ kg\text{-}m\ (14.77\ \ kWh)$$

For reference, the cost of this energy would be $1500, if this energy were electricity. The expenses of using electricity are calculated at the rate of $0.10-kilowatt hour. However, this modest energy requirement is coupled to a huge power requirement. The time stipulated to raise the water level in the lock chamber is 15 minutes. The power is calculated by equation 2. This huge power requirement precludes the use of water pumps to recirculate the water in the locks. The device that powers the locks with electricity must meet this power requirement.

$$P=\frac{E}{t} \quad (2)$$

Where:

P: power, kW

t: time, h

$$P=\frac{14.77\ kWh}{0.25h}=59\ kW$$

Figure 2 depicts the Canal as a Thermodynamic System. The total amount of energy available per year to the Canal and how it is expended is shown. The energy, hydropower, can be described in terms of the volume of water, at the elevation of Gatun Lake, as Mm3. The energy calculated for one lock step is multiplied by three, corresponding to the three steps from ocean to lake of the Panama Canal locks, to obtain the energy of one transit. The Neo Panamax Locks consume 7% less than the Panamax Locks because of the water savings basins.

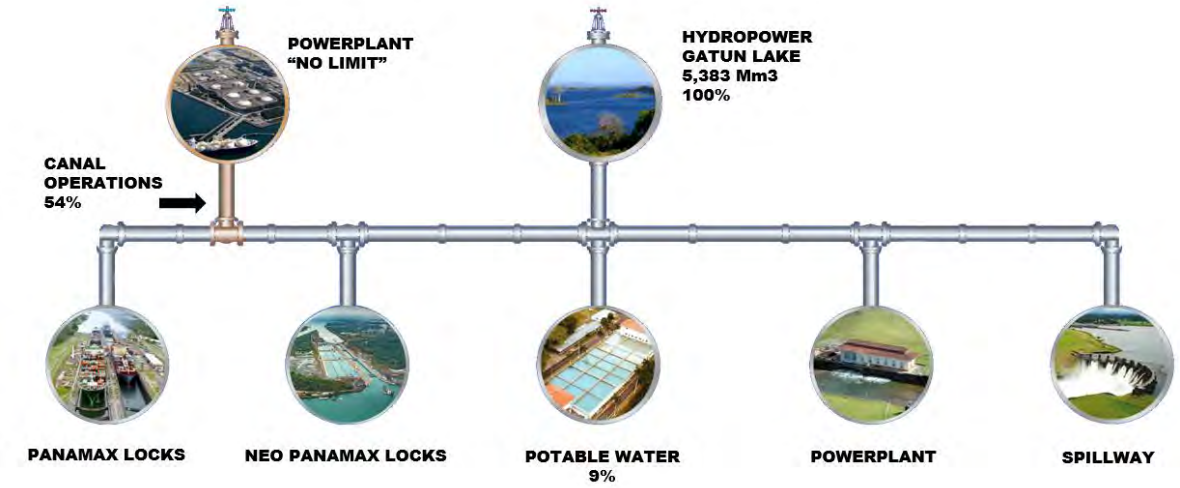

Figure 2: The Panama Canal as a Thermodynamic System

The total available hydropower in Gatun Lake, is 5,383 Mm3. The principal use of the hydropower of Gatun Lake is to power the canal's operations, 2,897 Mm3 (54%). Gatun Lake is also the population's principal source of potable water, it consumes 485 Mm3 (9%). A large part of the total energy cannot be used, 1,991 Mm3 (37%), this water is used to generate electricity at the Gatun Power Plant or is spilled at Gatun Spillway, because of the limited storage capacity of Gatun Lake and the limited spilling capacity of Gatun Dam.

The energy is sold by the Panama Canal Authority at vastly different prices. For comparison, the unit price of the energy at each distribution point follows - at the Neo Panamax Locks, up to $1,200,000 per transit ($447,000 average), at the Panamax Locks up to $400,000 per transit ($121,000 average), for municipal consumption, $40,000 per transit and at the Gatun Power Plant $1,500 per transit. One transit consumes 196,841 m3 of water. Note that the value of water for electrical generation is the theoretical value of the energy needed to lift the ships, as corresponds when the energy loss is minor. The revenues at each distribution point cannot respond to market demand because of the limit imposed by the availability of water.

The opportunity to increase the fresh water resource to the Canal is limited. The current proposal for a new dam and reservoir at Rio Indio would only increase the available energy a fractional increment where the introduction of a new energy source could increase the available energy without any limits. Although providing water for the population's consumption is not profitable when compared to the Panama Canal's operations, this activity is of great priority. The population's growth rate has required the construction of additional potable water plants on Gatun Lake. This increasing demand for water compromises the efficiency of the Panama Canal's operations. It also puts in jeopardy the revenues to the government that it must increase.

4. THEORETICAL BASIS FOR OPERATION

The operation of the device is based on three fundamental principles: the first law of thermodynamics, Archimedes' principle and Pascal's principle. These principles are well known.

The idea that electricity can power navigation locks is validated conceptually by the first law of thermodynamics - energy cannot be created or destroyed, it can only be transformed. The purpose of this device is to transform electricity into hydropower. The energy of hydropower is simply the water's potential energy as defined by its elevation. Devices that transform one form of energy to another have changed history, most notable is the steam engine which started the industrial revolution.

Archimedes' principal validates that the water level in the open vessel of the lock chamber can be raised by placing a solid at the bottom of the vessel. The placement of the solid at the floor of the locks is the function of the device. The solid emerges from the floor of the lock chamber as the result of the expansion of the device. The solid displaces the water and the water level rises within the enclosed vessel of chamber. The flotation line on the ship remains constant, so the ship rises as the water level

rises. The rate of emergence of the solid is less than the rate at which the flotation level rises such that the device never encounters the ship bottom. For the level of water in the chamber to rise the amount needed to transit the ship without adding any water would require full coverage of the floor with these devices. Think of these devices as tiles on a floor, the more of the floor that is covered with tiles the less water needs to be added to operate the locks. Figure 3 depicts an idealized cross section of a navigation lock chamber where the water level is raised with this device.

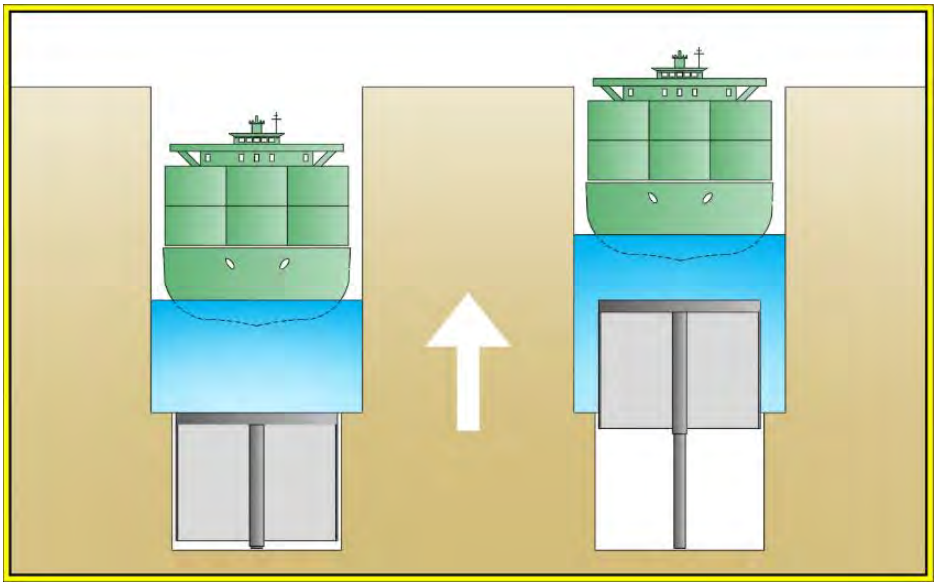

Figure 3: Operation of Device

As stated earlier, although the energy requirement to lift the ship in the lock chamber is moderate, the power requirement is huge. The expansion of the device is achieved with hydraulic power. The center of the device is a hydraulic cylinder / piston. The hydraulic fluid within the cylinder is at high pressure to achieve high forces. Pascal's principle is the basis for hydraulic power technology. Hydraulic power systems are also powered by electrical pumps. The volume of hydraulic fluid required to operate the device, compared to the volume of water needed to fill the lock is reduced proportionally, up to100 times, by the ratio of the hydraulic pressure to the ambient pressure. The reduced volume transfer requirement of the hydraulic power system compared to recycling the water with pumps, makes them practical.

5. DESIGN OF THE DEVICE

The device and its operation has been described. The design of the device has been advanced so that the components can be sized and their cost estimated. The device has two main components, the steel shells with the telescoping mechanism, and the hydraulic power circuit.

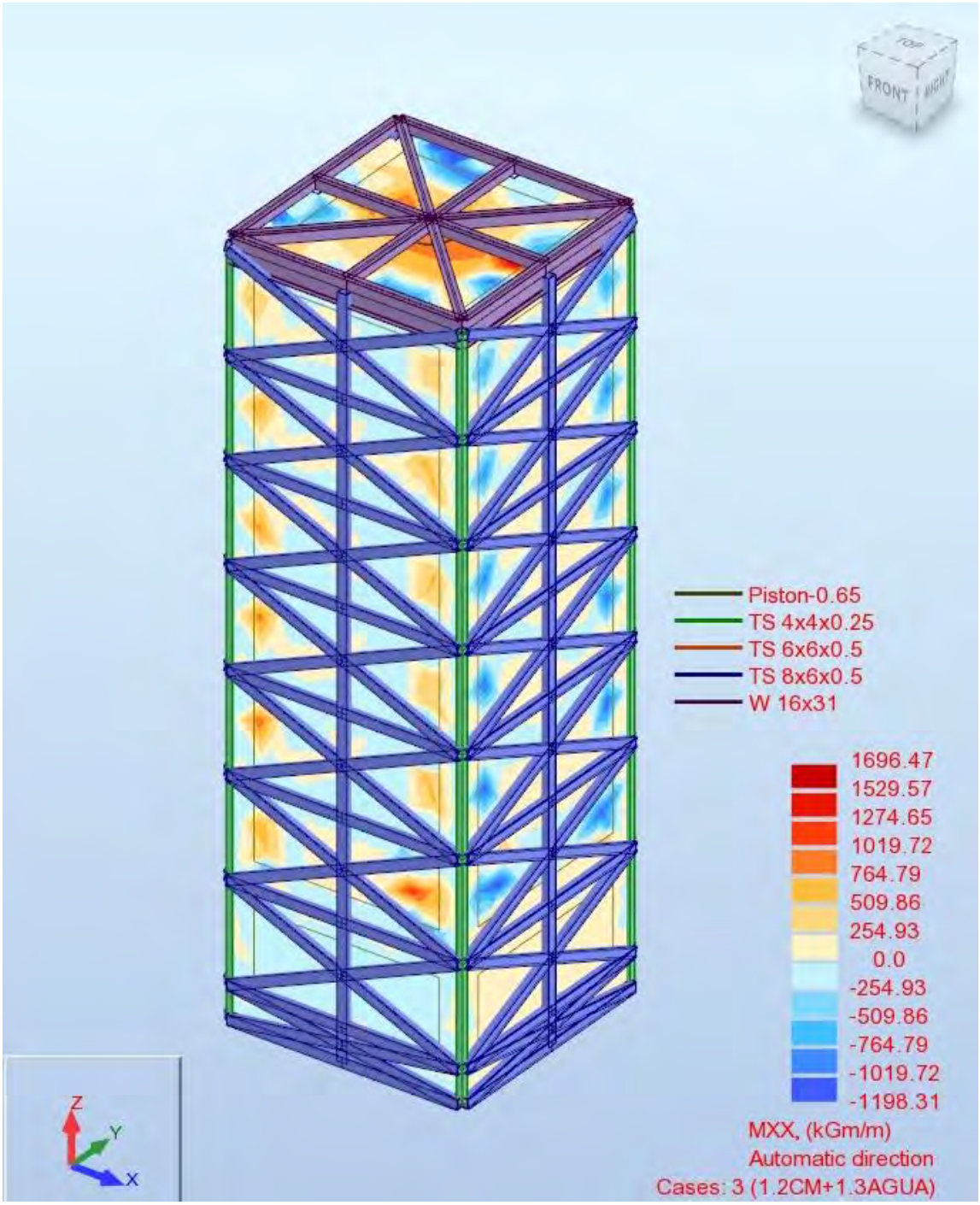

Figure 4: Stresses on Surface of Expanded Device

The square piston's shell is subjected to hydrostatic pressures corresponding to a depth of up to 24.00 meters. Figure 4 depicts the stresses on the square pistons shell. The design was accomplished with the structural design software ROBOT. The stresses are quite high on this shell because air at ambient air pressure fills the inside of the shell through an open standpipe. Figure 5 presents the structural details for the telescoping mechanism, the total amount of steel needed to make this device is 55 tons for the square piston and 40 tons for the square sleeve.

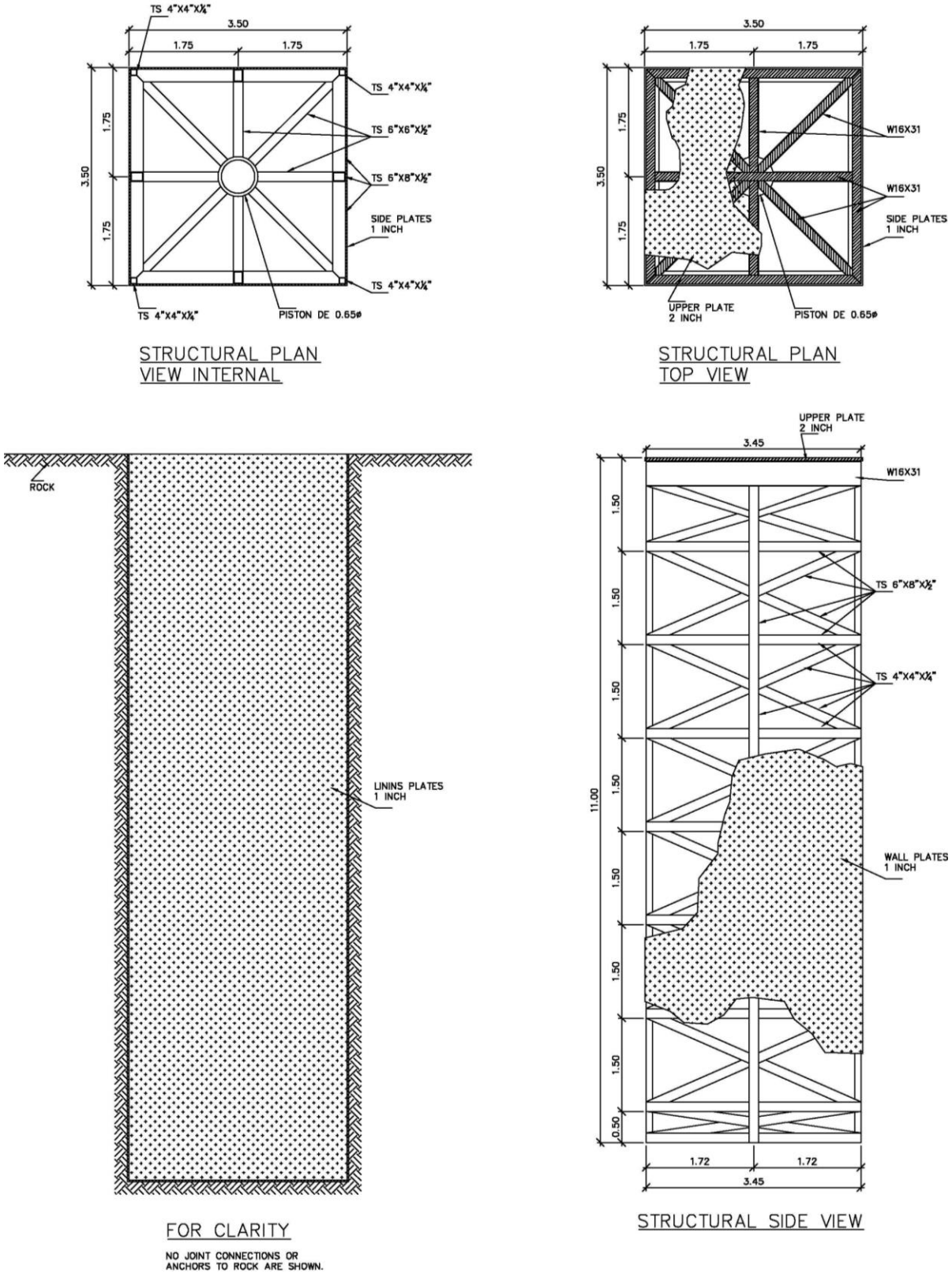

Figure 5: Structural Plans of Device

The hydraulic power circuit includes a pump, a storage cylinder, and an energy accumulator. The hydraulic piston is 60 cm in diameter and has a travel of 8.6 meters, the piston has a capacity of 250 tons. The energy accumulator allows the pumps to run continuously further reducing the power requirement.

The device interior is at ambient pressure. There is a stand pipe open to the atmosphere to the device. The square piston must slide in an out without leaking water from the locks. A sump pump is added to address minor leaks.

6. INSTALLATION OF THE DEVICE

Figure 6 are the installation plans of the device at the Panamax Locks, both the plan view and the cross section are shown. The plans depict the installation scheme to achieve maximum floor coverage without disrupting the locks hydraulic filling system of culverts. The number of units per lock chamber is 384. The floor coverage is 40%. The portion of the floor, where the units are installed, corresponds directly to the water savings achieved through the use of the units. Saving all of the water added to raise the ships in the lock chamber requires the complete coverage of the floor. The water savings can be expressed as water saved without increasing the number of transits or as additional transits if the same amount of water is consumed. The construction time is mostly devoted to the excavation.

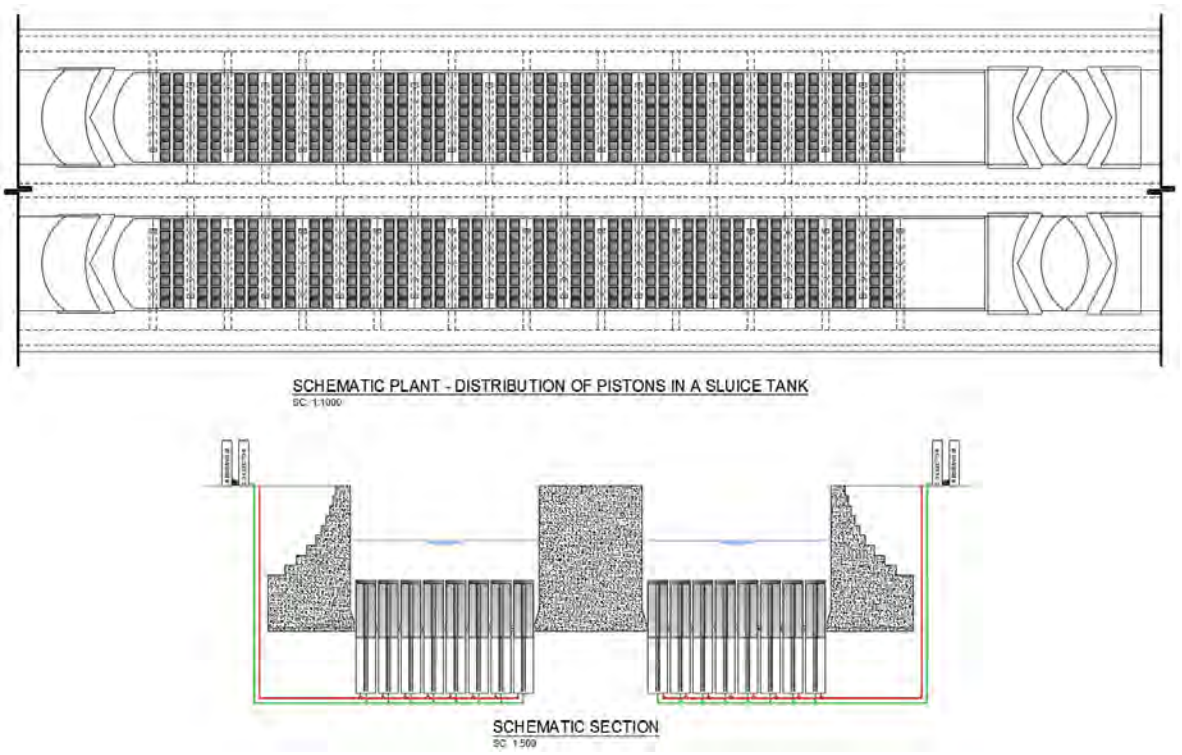

Figure 6: Plan View of Complete Installation at Panamax Locks (40% of floor area results in 40% water savings)

The installation of the device has important considerations. The unit is prefabricated before installation. The lock lane is taken out of operation for the excavation of the hole in which to place the device, the construction of the piping network and the installation of the prefabricated device. The lane outages, for installation, should be limited to less than 15 days.

The foundation material is agglomerate rock for the Pacific Panamax Locks and Gatun rock at the Atlantic Panamax Locks. The excavation starts with the construction of a slurry wall along the perimeter of the excavation. The slurry wall is anchored, where necessary, such that the excavation will not harm the existing lock structure. Figure 8 depicts stresses on the anchored slurry wall and the existing lock structure. The excavation will encompass the installation of one or more units. The calculations of stresses on the slurry wall were calculated with finite element geotechnical software PLAXIS.

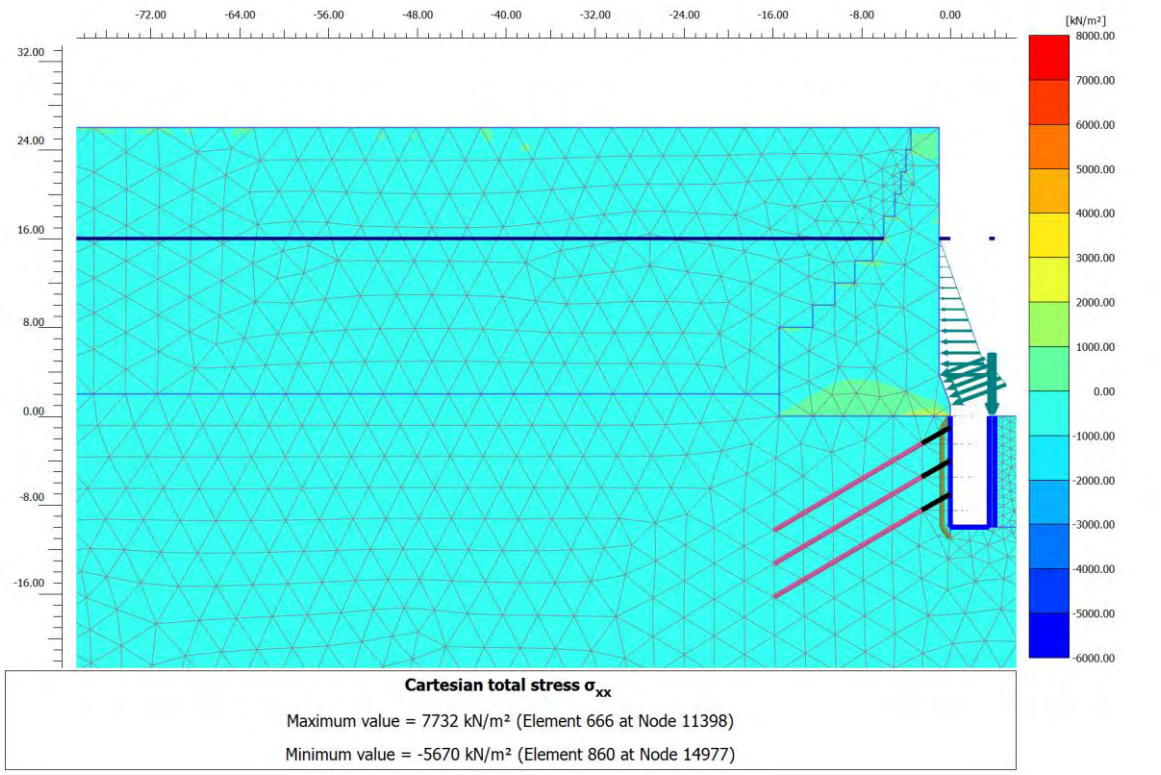

Figure 8: Stresses on Lock Wall and Slurry Wall during Construction

A key issue is system reliability. A malfunctioned unit can simply be taken out of operation in the closed position without any meaningful effects on lock operations. The units can be repaired simply by replacing the piston with a prefabricated unit. However, workers can also enter the device through a hatch to fix effectively minor repairs without removing the unit.

7. BENEFITS AND COST CONSIDERATIONS

The volume of water saved by one-unit is 103 m3. The benefit from the device is cumulative, the benefit is directly proportional to the number of units installed. Full coverage of the chamber floor with these units would allow raising the water level in the chamber without adding water. However, only one unit needs to be installed at each of the six Panamax Locks to achieve savings in water usage.

Table 1 presents the construction costs estimated for the fabrication and installation of the device. The cost of each unit is estimated at $2,000,000. The operating costs are not estimated but they are considered to be lower. The cost of electricity is a small fraction of the sales price. The main component of the operating costs will be equipment maintenance.

	Quantity	Unit Cost	Cost
Fabricated Steel Device	95 Ton	10,000 $/Ton	950,000 $
Hydraulic Power System	1 Unit	500,000 $/unit	500,000 $
Excavation	200 m3	2,000 $/m3	400,000 $
Installation	1 unit	150,000 $/unit	150,000 $
Total Cost			2,000,000 $

Table 1: Installed Cost for a Single Unit

The benefits obtained from this device have already been described in a general way. However, in order to evaluate the viability of installing the device, the economic benefit is estimated. For this simple analysis, the only economic benefit considered is obtained from using the now idle capacity of the Panamax Locks, 15 transits per day. The installation considers the maximum coverage of 40% of the chamber floor, which provides the water savings for these 15 additional transits.

Two investment schemes are considered. The first scenario aims for the minimal investment, namely, the installation of only one unit per lock, 6 total. The second scenario aims for maximum water savings, without compromising the locks existing hydraulic system. This scenario requires the installation of 384 units per lock, 2304 total. The total costs are obtained multiplying the number of units by the unit cost of the installed unit. The benefit is obtained by multiplying the price of an average transit by the number of additional transits possible with the device, or only a fraction (1/384) of a transit possible with the minimal investment strategy. The cost of an average transit for this analysis is considered $300,000 which is less than the maximum toll possible. Table 2 presents the cost and benefits of the two investment schemes. The scope of the investment, between these two extremes would depend on traffic projections.

	Units ()	Cost ($)	Additional (transits/day)	($/transit)	Annual Revenue ($)
Minimum Investment	6	12,000,000	0.04	121,000	1,725,195
Maximum Benefit	2,304	4,608,000,000	15	121,000	662,475,000

Table 2: Revenues and Construction Costs for Two Scenarios

8. CONCLUSIONS

- The ratio of initial costs to annual benefits appears to show that investment in this technology promises favorable returns, regardless of the scope of the investment.
- The installation of this device will make the operation of the Panama Canal more reliable by eliminating the interruptions due to droughts.
- The installation of this device will also increase the reliability of the potable water supply.
- The device can be installed without any delay because there will not be an adverse environmental impact.
- This device can be adapted to the Neo Panamax Locks, where the value of water is greater.
- The device could be incorporated in the construction of smaller locks to incorporate regional commerce.
- The device can be adapted to navigation locks elsewhere, where hydropower is limited, if only seasonably.

The author has patented the device “Air Lift Lock” at the Ministry of Commerce of the Republic of Panama. Also, the process to obtain international patents is currently underway. The intellectual property rights for the device belong to the author.

REFERENCES

Panama Canal Authority (Through FY 2009). Canal Transits / Capacity. Chart published by Panama Canal Authority.

Panama Canal (FY 2017). Panama Canal Annual Report. Reference for Data on Panama Canal.

PARANA- PARAGUAY RIVERS INLAND WATERWAY
by

Sebastian García[1], *Raul Escalante*[2]

ABSTRACT

The Paraguay – Paraná Rivers Inland Waterway (from now on HPP, by its acronym in Spanish) is located in South America and flows through five countries: Brazil, Bolivia, Paraguay, Argentina and Uruguay. The HPP is an inland waterway 3.442 km long counted from Caceres Port in Brazil to Nueva Palmira in Uruguay where it has its nominal end. The Paraná River section of HPP is in one of the more populated and industrialized area of South America so it is a strategic link to facilitate trade between the southern Brazil, Bolivia and Paraguay and Rosario (Argentina) from where it can connect with deep draught ships with the Atlantic Ocean.

In the stretch Sanfa Fe- Corrientes the project required a final navigable channel of 12 feet draught (including 2 feet of under keel clearance) that was achieved in 2012 and since then has been maintained that way.

Capital dredging required the mobilization of approximately 1.5 M cubic meters of sediment. It was installed a modern aids to navigation (AtoN) system integrated by 330 lighted buoys and beacons, all of them designed according to IALA guidelines.

The intervention included the realization of frequent bathymetric surveys, the installation and maintenance of a 12 automatic water level measuring stations network and the installation of antennae for the reception of AIS signals (Automatic Identification System).

The paper will focus on the description of this important South American Waterway, the improvements in transportation infrastructure already achieved, the works to be done to transform the whole waterway in a modern navigation system that can produce an important effect on navigation costs and safety.

1. INTRODUCTION

The Paraguay – Paraná Rivers Inland Waterway (from now on HPP, by its acronym in Spanish) is located in South America and flows through five countries: Brazil, Bolivia, Paraguay, Argentina and Uruguay. Its catchment area is about 2.605.000 km2 (950.000 km2 from Parana River (Corrientes) + 1.095.000 km2 from Paraguay River +560,000 km2 (from Middle Paraná River south of Corrientes) but without considering the part corresponding to Uruguay River) which integrates a bigger one or about 3.100.000 km2 well known as Plata Basin, as it's finally discharge in Río de la Plata and the Atlantic Ocean.

The HPP is an inland waterway 3.442 km long counted from Caceres Port in Brazil to Nueva Palmira in Uruguay where it has its nominal end. In this length the 700 Km pertaining to the Upper Paraná from Corrientes to Iguazu (Figure 1) are not included. In spite of this end of HPP project in Nueva Palmira, the connection between this inland waterway and open deep waters at the Atlantic Ocean is done by sailing from ports of Rosario area through Parana de las Palmas and Río de la Plata (red line in Figure 1) with deep draught ships for a channel 600 km long. This connection is not included in this description.

---

[1] Aids to Navigation Deputy General Manager, Hidrovia S.A., Agentina. sgarcia@gba-hidrovia.com.ar
[2] Aids to Navigation General Manager, Hidrovia S.A., Agentina. rescalante@gba-hidrovia.com.ar

Figure 1- Navigable waterway in Paraguay – Paraná – Plata river system

The Paraná River section of HPP is in one of the more populated and industrialized area of South America so it is an strategic link to facilitate trade between the southern Brazil, Bolivia and Paraguay and Rosario (Argentina) from where it can connect with deep draught ships with the Atlantic Ocean. It is considered the most important integration way of MERCOSUR since it is one of the most important way of transport needed to facilitate physical integration of the five countries mentioned. Its commercial area of direct influence (hinterland) is estimated at about 720.000 km2 and about 3.500.000 km2 of indirect influence with a population of more than 40 million inhabitants.

From north to south, the HPP passes through important local ports as Caceres, Corumbá and Puerto Murtinho in Brazil; Puerto Suarez (Bolivia); Concepción, San Pedro, Asunción (Capital City) and Villeta in Paraguay; Puerto Pilcomayo, Formosa, Corrientes, Barranqueras, Paraná, Santa Fe, San Martín – San Lorenzo and Rosario in Argentina and finally Nueva Palmira in Uruguay.

We are dealing with a waterway that crosses five countries, as can be seen in Figure 1.

2. PHYSICAL CHARACTERISTICS

Physical characteristics and depths along Paraguay and Paraná rivers determine what kind of vessels can navigate on them and accordingly is determined the allowed draught.

As can be observed in Figure 2, from Caceres to Santa Fe Port navigation is allowed with barges loaded up to 10 feet; from Santa Fe Port to Rosario Port the allowed draught is 25 feet and from Rosario to Atlantic Ocean, including Buenos Aires Port, is 34 feet. Nowadays the biggest ship that has been arriving at Buenos Aires is a containership of 10.200 TEUs of capacity and 330 m Loa.

Figure 2- Allowed draft along Paraná - Paraguay Rivers Inland Waterway

3. CARGO TRANSPORTATION

Main cargoes for this route are iron ore and grains with some participation of containers and fuel. It is important to notice that two countries, both Paraguay and Bolivia, have this waterway as their main and more convenient international trade connection due to their condition of land locked countries.

The hinterland of the waterway has a very big agriculture potential as well as reserves of iron ore and manganese that are of worldwide importance.

Soybean, byproducts and recently also vegetable oil, iron ore and fuels gather at least 87 % of total freight.

In Table 1 it is shown tonnage passed through the waterway from 2010 to 2016 and a forecast for year 2021 of around 25 M tons.

Products	Total Cargos [tons]							
	2010	2011	2012	2013	2014	2015	2016	2021
Soybeans (& derivates)	6.517.544	6.966.184	4.225.150	7.978.427	7.757.154	7.721.289	8.322.094	10.715.904
Other Grains	1.462.169	1.449.211	2.230.112	2.327.078	2.756.674	4.214.646	633.464	3.360.156
Iron ore	3.850.348	5.269.551	4.273.014	5.313.151	6.625.000	4.126.000	3.564.751	3.500.000
Liquid Cargo	2.940.419	2.833.960	2.314.998	3.047.732	3.456.864	4.064.111	3.679.247	4.314.390
General Cargo	608.384	1.052.533	777.521	1.423.752	1.306.260	1.460.559	1.075.810	1.504.545
Container [tons]	1.040.000	1.120.000	792.000	1.104.000	1.360.000	1.400.000	1.440.000	1.664.000
[TEUs]	130.000	140.000	99.000	138.000	170.000	175.000	180.000	208.000
Total **	**16.418.864**	**18.691.439**	**14.612.795**	**21.194.140**	**23.261.952**	**22.986.605**	**18.715.366**	**25.058.995**

*** Total does not include figures in TEUs.*

Table 1: Cargoes tonnage passed through the waterway. Years 2010 – 2015 and forecast for 2021

The increasing tonnage of cargo transported through the waterway in following years will put a strong demand of additional barges and pushers.

For a long time aged Mississippi barges had been imported from EEUU for being used in HPP but later this practice was forbidden in some countries by new legislation. Therefore several local shipyards are supplying these barges and also recently a couple of new shipyards have been installed in Paraguay.

4. NAVIGATION THROUGH THE WATERWAY

The Santa Fe–Confluence waterway handles both domestic and international commercial river traffic to and from Argentina, Uruguay, Paraguay, Bolivia and southern Brazil.

The transport of cargo is done by a fleet composed by barges and pushers. These barges are formed in convoys of different sizes pushed by tugs (pushers) of adequate power.

Most bulk barges are “Mississippi” type, so their dimensions are: Loa = 60 m; B = 11 m; D = 10 feet and DWT = 1,500 ton. Since several years ago, a new type has been developed and is called “Jumbo” barge. These ones have Loa = 66 m; B = 15 m; D = 10 feet and DWT = 2,500 ton. In Figure 3 both types of barges are shown.

A majority of the fleet is under Paraguayan flag. This is a problem arising from having the countries different policies on fundamental aspects such as labor regulations, taxes and others.

Cargo is transported in convoys of barges with different configurations for each stretch of the river as can be seen in Figure 4.

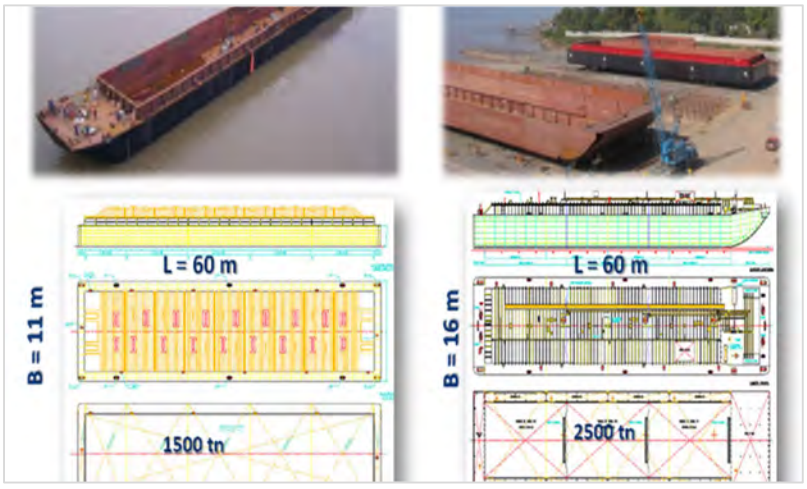

Figure 3 – Dimensions of “Mississippi” and “Jumbo” barges

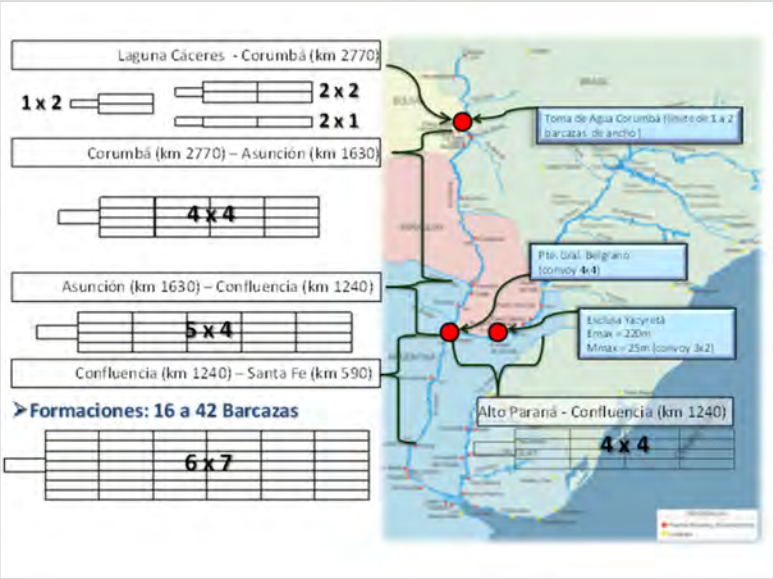

Figure 4- Configuration of convoy

Maximum convoy size is a 6 x 7 barges with a pusher of more than 7,000 HP with a total length of approximately 410 m. A barge convoy of such characteristics is shown in Figure 4 and a photo of one of them in Figure 5.

Figure 5: Example of a 6 x 7 barges convoy

The number of barges and tugs present in the waterway, period 2010 – 2016, are shown in Figures 6, 7 and 8. It can be observed that there are an important number of barges that goes out of service and that are replaced by new units every year. This happens due to the high average age of the fleet. This fact also explains the recently installation of new shipyards in Paraguay to satisfy this market.

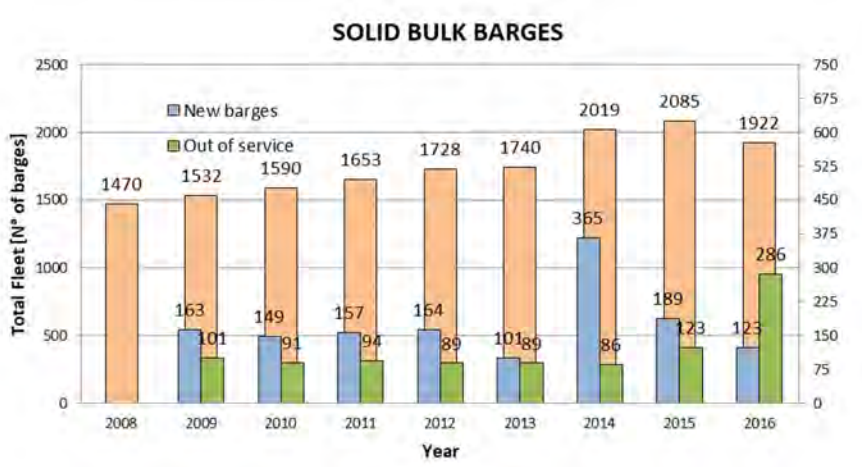

Figure 6: Solid Bulk barges fleet. Period 2010-2016

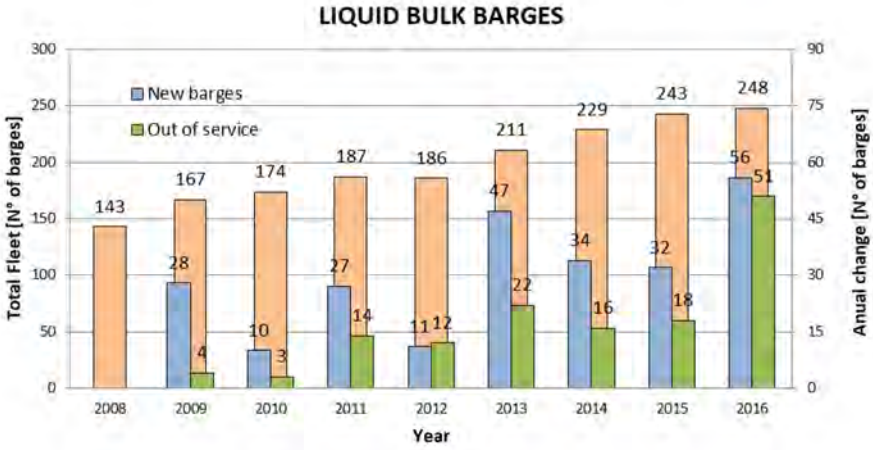

Figure 7: Liquid Bulk barges fleet. Period 2010-2016

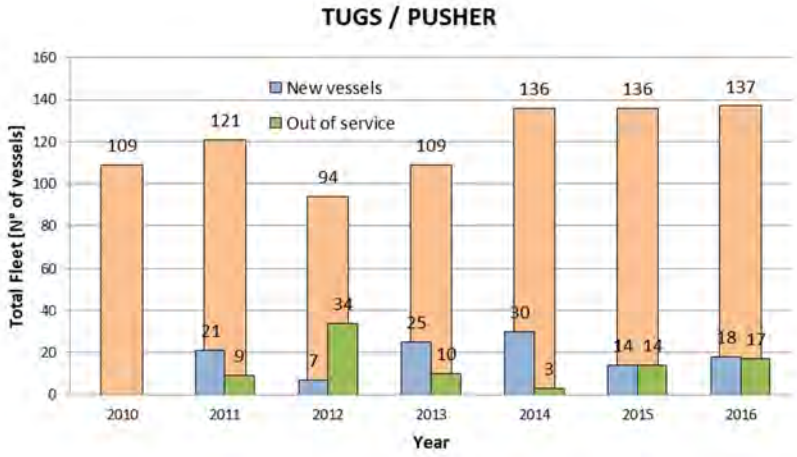

Figure 8: Tug fleet. Period 2010-2016

5. INFRASTRUCTURE INVESTMENTS ALREADY DONE

Between 2010 and 2012, investments were realized in Argentinian Paraná river section from Santa Fe port up to the confluence of Parana and Paraguay rivers. This project section, 640 km long connects Santa Fe port with Barranqueras and Corrientes ports at the North and is known as “Santa Fe – Confluencia” section of the HPP waterway.

The project here requires a final navigable channel of 12 feet draught (including 2 feet of under keel clearance) that was achieved in 2012 and since then has been maintained that way.

Capital dredging required the mobilization of approximately 1.5 M cubic meters of sediment. It was installed a modern aids to navigation (AtoN) system integrated by 330 lighted buoys and beacons, all of them designed according to IALA guidelines.

The intervention includes the realization of broad and frequent bathymetric surveys, the installation and maintenance of a 12 automatic water level measuring stations network and the installation of antennae for the reception of AIS signals (Automatic Identification System).

In Figure 9 it is shown the stretch from Santa Fe to Confluencia (Corrientes), with the position of water level measuring stations, AIS receiving stations, and places of main shallow waters.

Figure 9 – Stretch from Santa Fe to Corrientes

A longitudinal profile of the river measured on the dredged axis of the Santa Fe- Confluencia waterway can be seen in Figure 10 where a stretch of 100 km has been represented as an example. Areas with depths up to 80 feet are present along most of the route but there are also stretches with depths lower than 12 feet. The last ones account for about 60 km of the 640 km of the total length of the waterway. These shallow areas are denominated “fords” (or “*pasos*” in Spanish). Number of shallow areas is

around 37 in the 640 length of the waterway. In these shallow areas is where dredging works have to be performed in order to allow safe navigation of convoys. Minimum design depths are to be guaranteed 92.5 % of the time

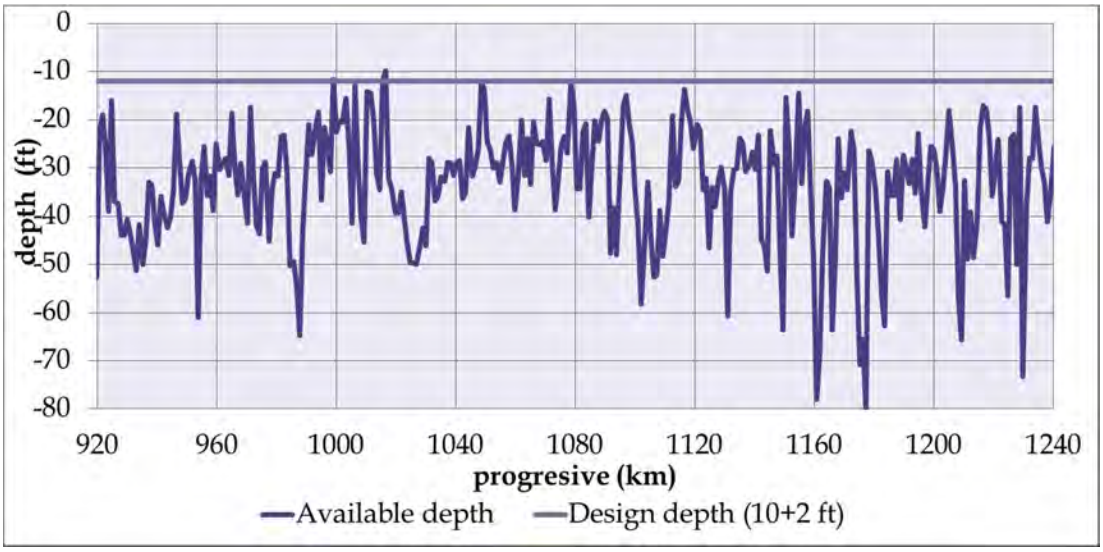

Figure 10 - Longitudinal profile of the river

Due to the intense sedimentological activity, in addition to the dredging works needed, one very important task that has been realized is the continuous adjustment of waterway axis following the river thalweg that allowed to reduce significantly the amount of dredging carried out. Detailed bathymetric surveys and continuous buoytenders assistance to adjust the aids to navigation position that marked the route have been done. In table 2 is possible to appreciate the importance of the job that has been done.

	Waterway axis							
	2011	2012	2013	2014	2015	2016	2017	
Fords	25	28	26	43	40	38	57	257
In between fords	13	15	15	20	22	19	15	119
TOTAL	38	43	41	63	62	57	72	376

Table 2: Waterway route axis adjustments

Accordingly to actual legal requirements an important and conscious Environmental Impact Assessment (EIA) process took place before beginning the intervention in this stretch. In that process, the Environmental Impact Study (EsIA) considered the fluvial ecosystems in river flow and its floodplain, aquatic and riparian biota, nature conservation, water and sediment quality as well as social aspects like other uses of the system. That EsIA took in consideration that the waterway is close to 14 natural protected areas, 2 wetlands RAMSAR Sites, 2 bird conservation areas and fish aquatic reserves. This EsIA was carried out in order to identify, predict and evaluate the environmental impacts of doing the projected dredging works and installment of aids to navigation (AtoN) along the waterway. Based on the results of this EsIA management actions and mitigation measures were proposed.

6. ACHIEVEMENTS & LESSONS LEARNED

As conclusion of the work done it can be said that there were several navigation restrictions that existed previous to the systematization of the stretch that were solved with the improvements done. For example:

- In some places (due to several problems as water depths) big barge convoys had to be disassembled and moved from one point to another in repeated movements. This practice required additional times and efforts. Nowadays convoys are not disassembled any more.
- Convoys had no possibilities of doing night navigation due to the lack of lighted AtoN. This shortcut has been removed.
- In times of low water barges had to be loaded several feet less than the design draught due to lack of enough depth in critical zones. Actually the design depth is guaranteed for the 92,5 % of time along a year.
- All aspects mentioned previously have an important economic effect.

Continuous adjustment of waterway axis following the river thalweg, allowed to reduce significantly the amount of dredging carried out.

Once the improvements in the waterway were done, several difficulties caused by local traditions were evidenced:

- Many of the pushers do not have satellite navigators installed.
- Captains do not have experience in the use of electronics charts.
- At the time of the project, there were no electronic charts available for the area. Today some barges companies have their own digital charts (not S 57 format)
- Most of the navigation is done loaded downstream and on ballast upstream. In the second case there is a tendency of using shortcuts in curves as navigating upstream.
- Previous to the works on the area no bathymetric surveys were available. Therefore convoys used small boats navigating in front of them to determine depths. Nowadays as updated charts are available, there are almost no convoys still using the old procedure in Santa Fe-Confluencia stretch. This aspect denotes more trust in the information provided.

7. FINAL REMARKS

Although this stretch of the river is 640 km long, it is only a minor part of the whole Parana - Paraguay River waterway and others waterways of the region.

Very important is to take notice that despite the work is completed, time is needed for the captains to fully use it. Special training programs are needed.

Local traditions need time for education and training the community so as to pass from a semi artisanal way of navigation to a technical supported way of doing so.

All aspects of the project conforms a virtuous circle. Now we have a waterway with dredged depths and modern AtoN. The investment in infrastructure works is the first step. For doing that, water level measuring stations have being installed and regular bathymetric surveys are being done. With this information it is possible to draw navigation charts and to make it electronic. AIS receiving antennae permit the following of convoys movements that allows both to control the navigation and to improve the design of the waterway.

From this intervention it can be seen that the improvement of the waterway is possible applying the appropriate working methodologies and the results are worth the money required to do the job because there are ways of solving the difficulties to make inland navigation more effective and efficient.

If this effort is spread upstream, a time will come when the whole waterway will be upgraded to a modern system of navigation and therefore having an important effect on navigation costs and safety.

As PIANC WG 201 is developing a classification system for Latin American waterways, and one point of discussion is the main parameter to take into consideration as basis for the classification, from the description presented in this paper for the HPP waterway can be concluded that the main parameter used is clearly the natural and dredged depth.

DEVELOPMENT OF ROMANIAN INLAND WATERWAYS AND HYDRO CONNECTION WITH EUROPE

by

Romeo Ciortan[1], Eugeniu Vasilache[2]

1. INTRODUCTION

Transportation is one of the main components of the social and economic life for any human society. It is part of processing products and to take them to their place of consumption.

Favorable conditions were created to promote the extension of European and intercontinental exchanges, as well as to integrate the regional transport network into the continental network.

These charts will put a strong logistic pr[3]essure on transports and on their infrastructure. The coherence of the regional systems could also be facilitated by stimulating intermodal transport.

Given its geographic location Romania is bordered by the Danube River to south and by the Black Sea to the south-east Fig.1.

This geographical position enabled over time the construction of sea and river ports which currently ensure the performance of a major traffic of import and export goods.

The total capacities of these ports in million tones/year are 134, respectively 83.1 for maritime ones, 33.5 for river-maritime, 16.1 for the river ones and 1.3 for canal ports.

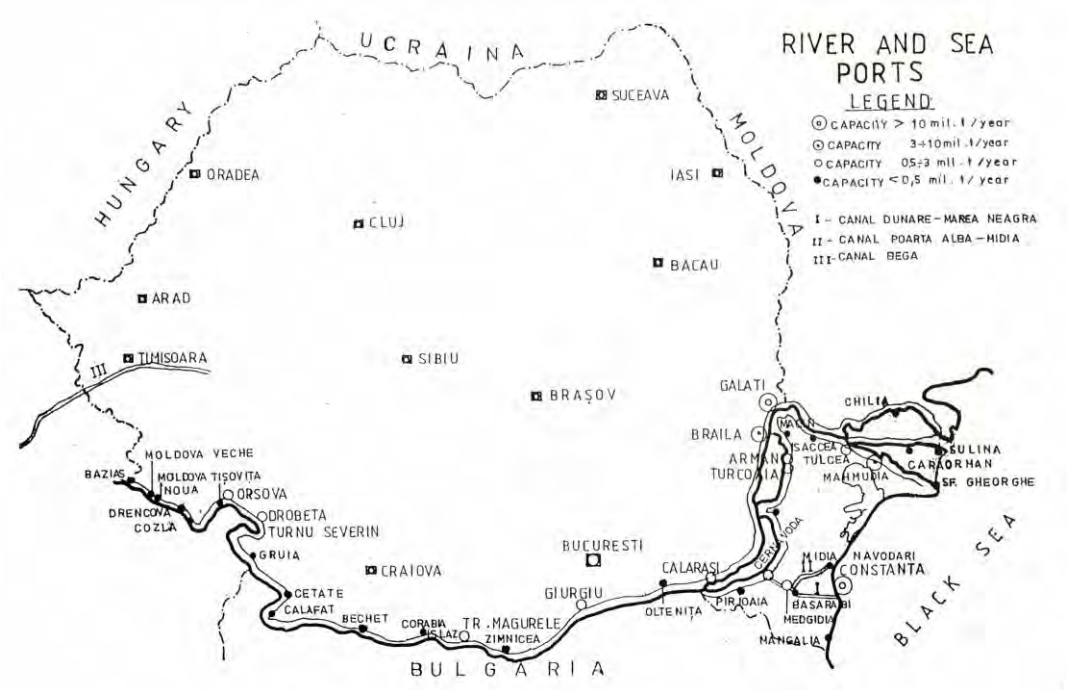

Figure 1: Ports and waterways in Romania

2. THE PORTS

Strategy for the development of the navigation infrastructure includes the foresights for modernization of maritime, river ports and waterways in an integrated concept.

[1] Ph.D, Corresponding Member of the Romanian Academy of Technical Sciences, Professor at Ovidius University, Constanta, Romania: ciortanromeo@yahoo.com
[2] M.Sc., Civ.Eng.; General Manager, Proinginer Construct, Complexului street No.5, Bucharest, Romania; eugeniu.vasilache@yahoo.fr

2.1 Maritime ports

On the Romanian shores of the Black Sea are located three seaports: Constanta, Mangalia, at about 22 miles to the south, and Midia, at about 10 miles to the north.

Constanta Port

The most important of those is Constanta Port, Fig.2, located at about 182 miles to the Bosphorus strait and about 85 miles to the main navigable Danube outlet into the sea, namely the Sulina arm. It spreads out over about 10 km of shoreline and advances about 5.5 km into the sea.

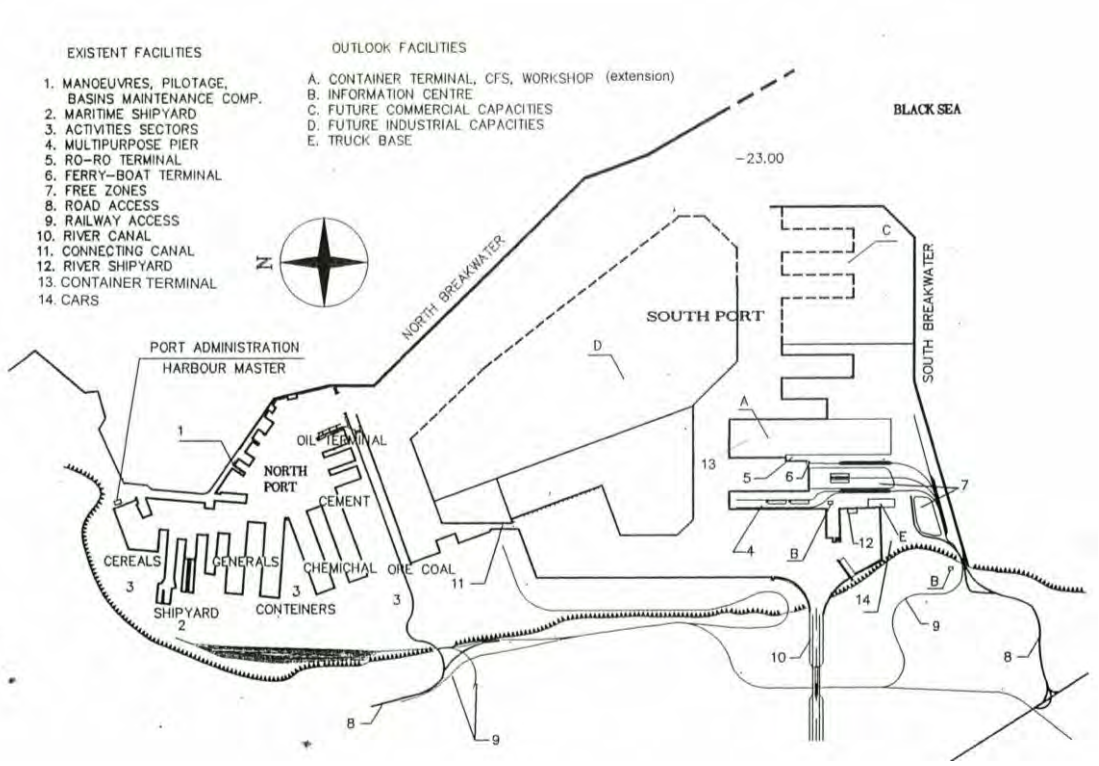

Figure 2: Constanta Port

The development of the Port of Constanta has been carried out in several phases.

The phase derives from the necessity of providing new port capacities to handle the constantly growing cargo traffic carried by high-capacity ships which for the time being have no access to the port. This large-scale development would be capable in the end to allow the berthing of ships up to 250,000 dwt.

The Danube – Black Sea Canal, which is connected to the Danube in Cernavoda, starts in the port area. The ships transporting goods on this channel to and from the Danube ports have also access to Constanta Port.

By its location and size, Constanta Port has real perspective for attracting new volumes of traffic and for developing economic activities, both in domestic trade and in international transit.

Constanta Port, being the largest trade port within the Black Sea area, has very high development capabilities in four possible directions:

- As a main transit port, between the Black Sea area and Western Europe.
- As a hub for traffic of goods to Europe.
- As an important terminal for navigation services to the countries of the Black Sea basin.
- As a loading and unloading center for large ships in relation to the goods trade among the surrounding markets.

Port of Midia

It has been developed in front of Lake Tasaul to receive vessels up to 10,000 dwt capacity. Infrastructures include berths for traffic of livestock, general cargo, liquid oil products, liquefied gases, ocean fishing activities and a shipyard.

The connection of the port with the Poarta Alba-Midia Navodari Canal ensures economic shipment of some goods, to the countries of Central Europe.

2.2 Inland Ports

Inland ports are located on the Danube River and on its inland waterways Fig.1.

Four river-maritime ports are situated on the Danube lower course also known as Maritime Danube, that allow access of ships with a capacity of about 7,500 dwt (the draught allowed on the Sulina branch of the Danube River).

River ports are developed along the entire Danube watercourse and on the navigable canal. Given the volumes of raw materials to be transported each port serves an area of the country and some industrial plants developed near the waterways.

3. DEVELOPMENT OF ROMANIAN TRANSPORTATION SYSTEMS AND THEIR CONNECTION WITH EUROPE

Due to its good access to major communication routes and strategic position Romania may become the easterly focus point for East-West trading.

The Romanian transportation system is connected to the transfer subsystems of transportation types, having basic monitoring position involving the development of transports and in particular of the intermodal ones.

3.1 Rail Transportation

An important percentage of cargo transportation through Romania is by rail. Romania also has widely dispersed of 40 inland terminals for the handling of containers.

The railway transportation subsystem is appointed with the enhancement of the main national railways in order to increase the travel speed up to 150-200 km/hour and even up to 250 km/hour with an improvement of the related equipment. The Romanian railway network will then integrate with the European one to ensure the conditions for the increase in exchange of goods.

3.2 Road Transportation

The road transport subsystem to which is appointed the enhancement of the whole national roads and an extra program to highways and express routes. All the previous enumerated works are mixing with the European transport system with its western capitals and major cities connections.

3.3 Inland Water Transport

Inland waterways in Romania are well developed. Constanta Port is linked by the Danube Canal and the Danube to an international hinterland including Ucraine, Moldova, Bulgaria, Serbia, Hungary, the Czech Republic, Slovakia, Germany and Austria.

Danube Fig.3 is navigable from Ulm to the Black Sea, measuring 2,588 km, out of which 1,075 km are in Romania. Along its course the Danube crosses the territory of 9 countries and 4 capitals and it represents an important historical waterway.

The Danube flows into the Black Sea, trough 3 main branches. The main way of access is Sulina Chanel, 63 km long, which ensures, the navigation of 7.0 m draught maritime vessels up to Braila. Except the navigable sector of the Danube between Braila and Sulina, the minimum navigable depth kept by maintenance dredging is between 2.0 – 2.5 m.

With the opening of the Rhin – Main – Danube Canal in September 1992, there is a physical connection with the Rhine and the hinterland is potentially extended to Germany and to the Netherlands.

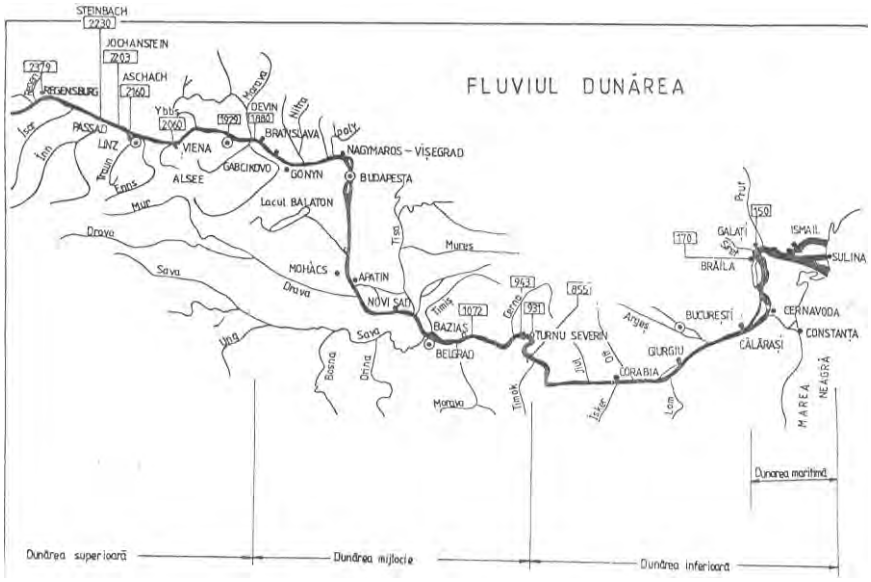

Figure 3: Danube River

The peripheral location of Danube induces a limited influence of its ports, restricted to the southern part of the country. Considering this, the strategy for the Territorial Arrangements Plan stipulates the turning into navigable waters of some Danube tributaries.

The same purpose has been considered in accomplishing navigable canals, such as:

- The Danube – Black Sea Canal, connecting Danube to Constanta port.
- The Poarta Alba – Midia, Navodari Canal, connecting the port Midia to Danube.
- The Bega Canal assisting the western part of the country.

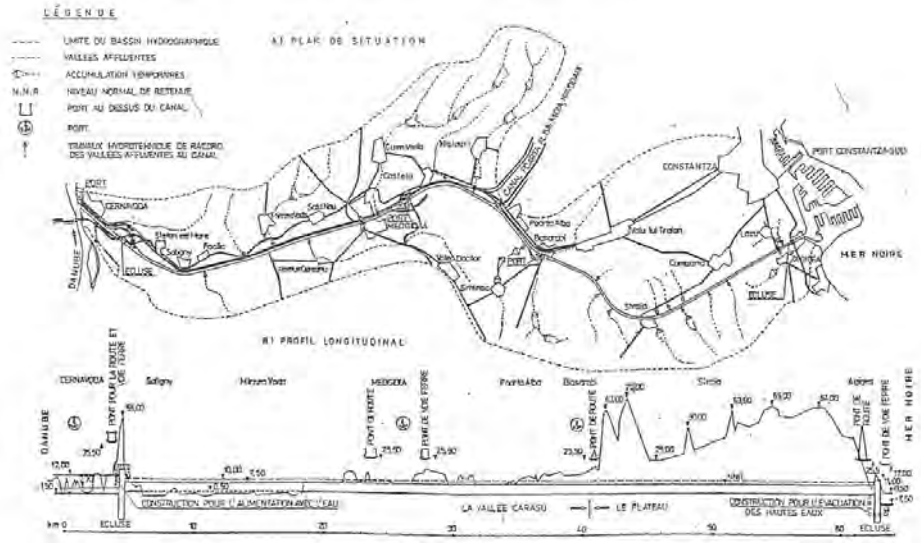

Figure 4: Danube – Black Sea Canal

The Danube – Black Sea Canal Fig.4: Its capacity is 75 million tones/year. The Danube – Black Sea Canal has complex functions, such as: navigation and water administration, irrigations, electric energy supply, drinking and industrial water supply, drainage of the adjacent lands, regularization of the water flow and their transit towards the sea. The navigable canal is 64.4 km long and 7.0 m water depth. The longitudinal profile, the hydro technical scheme of the canal, respectively, comprises a unique water race between the two hydro-technical systems of Cernavoda and Agigea Fig.5

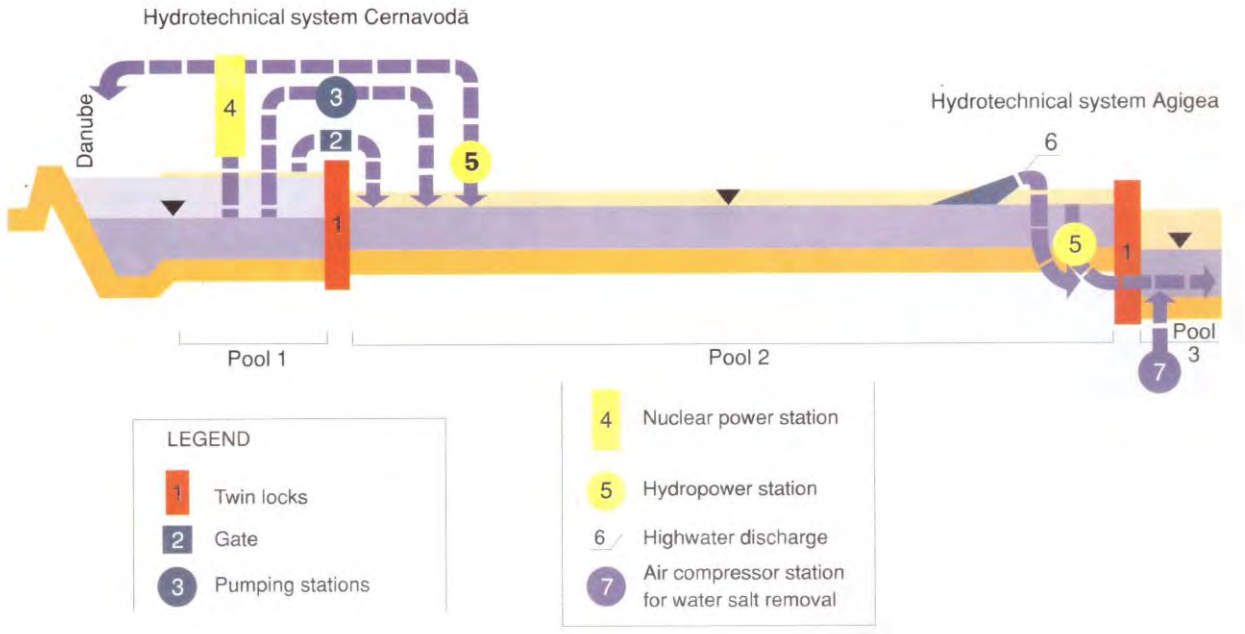

Figure 5: Danube Black Sea Canal. Hydrotechnical diagram.

The calculation convoy is made up of 6 barges and a pusher of 2,400 – 3,200 HP. The access of river – maritime vessels of 5,000 – 6,000 dwt of this waterway is also possible.

The twin locks have chambers of 310 m length, 25 m wide and a minimum depth of 7.5 m Fig.6.

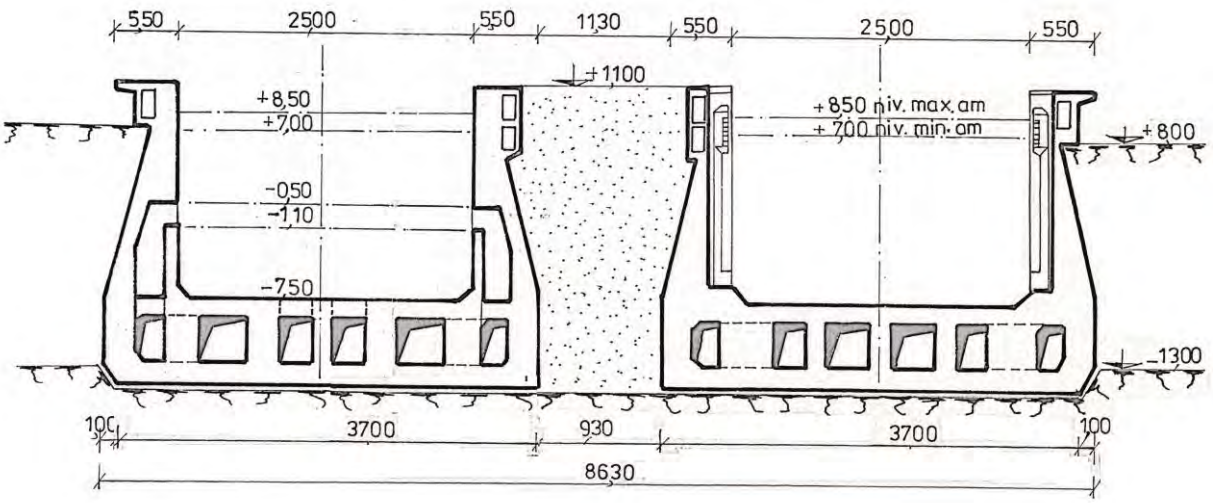

Figure 6:Twin locks

To prevent penetration salted water in the lock have been provided two solutions:

1. Fill the lock above the salty water level only from the freshwater canal through a drain located above the port basin (salted water).
2. at the downstream end of the lock is provided a compressed air curtain which prevents entering water from the port basin. This curtain is created before barge entrance and stops after the lock has been partially included.

Poarta Alba – Midia, Navodari Canal: This is the northern embracement of the navigation system in Dobrogea, the navigable waterway detaches itself from the main Danube – Black Sea Canal on km 36 and flows into Midia maritime port and Tasaul Lake

The technical characteristics adopted for this navigable waterway allow the usage of 3,000 tones type barges, used on the Danube – Black Sea Canal, the convoy consisting of only one barge and a pusher, based on the reduced traffic.

The twin lock chambers has a useful length of 145 m, 12.5 m width and minimum water level at the apron 6.0 m.

4. METHODS FOR DEVELOPING PORT ACTIVITIES

Currently the exploited port capacity is 60% and the revenues from cargo handling have decreased. Therefore as described below a number of actions are to be taken that will lead to an increased efficiency of the facilities and aim to increase volume of handled goods. Some of these measures have been applied but necessary adjustments have to be constantly undertaken.

4.1 Extension of the hinterland of a port

In order to achieve this, easy connections to distant areas must be created. Therefore European transport corridors are considered Fig.7.

Figure 7: European transport corridors

A series of aspects concerning the need of a new infrastructure in Eastern Europe, the Black Sea Region and the Balkans included alongside with the possibilities or realizing the transport corridors for road and rail corridors, which are to meet the transport and multi-modal transport needs on local, regional or national level, as well as on pan-European level.

Most of the European rivers are improved for navigation. In addition, a network of artificial navigable canals linking the major rivers and the rivers in the area has been developed for covering as much territory as possible.

As far as the waterborne transport is concerned, development of inland waterway networks efficient form the energy consumption point of view, having a less impact on the environment. The inland waterway network must be integrated into the intermodal traffic systems. The actions for the further development of the waterborne transport on short sea shipping must be also put into force.

These new routes enlarge, considerably, the Danube hinterland. Also, all the corridors have a port as extreme point, such as Constanta in Romania, Varna and Burgas in Bulgaria, Istanbul in Turkey and Odessa in Ukraine.

The maritime Port of Constanta is linked by the Black Sea – Danube Canal and the Danube itself to an international hinterland including 10 European countries Fig.8.

Figure 8: Constanta – Rotterdam corridor

4.2 Promoting small distances navigation in the Black Sea

The Black Sea has an area of 411,540km^2 and together with the Azov Sea, the area amounts to 461,540km^2. The maximum distance between coasts is 1,125km on the East-West direction and 600km on the North-South direction.

Navigation is possible all the year round, except the Northern part of the Azov Sea, where, during some winters, icebreakers are needed for about two months. Three important navigable rivers flow into the Black Sea, Danube, Niper, Don Thus extending considerably, the hinterland of the sea Fig.9.

Figure 9: Black Sea hinterland

There are more than 35 ports on The Black Sea and Azov Sea coast. The Volga – Don Canal allows the navigation of ships up to the Caspian Sea and then, on the inland waterways in Russia, up to the White Sea, passing by the Moscow area and St. Petersburg, the latter being one of the biggest ports on Baltic Sea.

By creating the logistic zone of the Black Sea, the efficient connection of the European flows with the Asian flows can be realized. International companies consider the Black Sea region a significant business area. The new political, economic and commercial conditions have generated an attractive and favorable context for business.

The Black Sea is connected to the Mediterranean Sea through the Bosphorusand Dardanelles and then, to the Atlantic basin through Gibraltar, while the navigation to the Asia – Pacific region is realized Suez Canal.

5. INTERNATIONAL COLLABORATION REGARDING THE DANUBE RIVER

5.1 European Community Collaboration

Extension of the hinterland of a port requires connection to distant areas and European Transport Corridors are considered. The Corridor VII represents, in fact, a waterway of the Danube. Nevertheless, it is mentioned that other corridors cross the Danube: Corridor V, Corridor IX.

These routes enlarge considerably the Danube hinterland. In addition, all the corridors end to a port, such as Constanta Port in Romania.

5.2 The International Convention (I.C.) regarding the protection of the Danube

This convention was adopted in 1994 in Sofia. Its purpose is to increase the collaboration regarding prevention and control of transboundary pollution, sustainable management of the Danube and the rivers along its hydrographic basin, as well as, rational exploitation and conservation of water resources. This will contribute to the protection of the Black Sea and assist the efforts of the United Nations Economic Commission for Europe (UNECE) and European Community.

5.3 The Danube Commission (D.C.)

The Danube attracted the attention of many economic, political and military authorities of different countries. Following a series of discussions, the “Convention regarding the rules governing the navigation on the Danube” was signed in Belgrade in 1954 by the countries having direct access to the Danube.

Danube Commission’s (D.C.) purpose is to standardize the regulation for navigation; for example, establishing the manner for performing the maintenance works, signalling, and so on.

D.C. cooperates with CEE, with the International Committee regarding the protection of the Danube convention and Rhine Commission in order to be in line with the regulations, due to the fact that the navigation takes place both on the Danube and Rhine Fig.10.

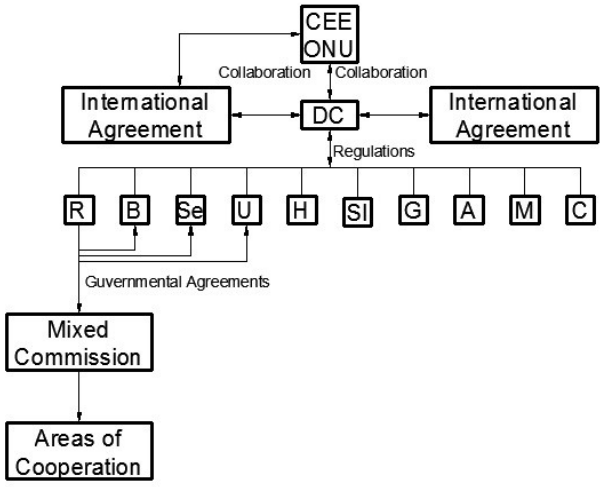

Figure 10: International collaboration regarding Danube River exploitation

5.5 Cooperation between countries

Government agreements that took into consideration the D.C. regulations enacted between Romania and its neighbours Conventions. As a result, Mixed Committees were found Fig.11.

The members of these committees meet periodically to discuss all issues at stake along the common sections of the Danube.

In order to address any navigation issues all Danube riparian countries adopt the C.D. regulations, which issues fundamental Provisions. Some aspects are developed by the governmental Mixed Commissions.

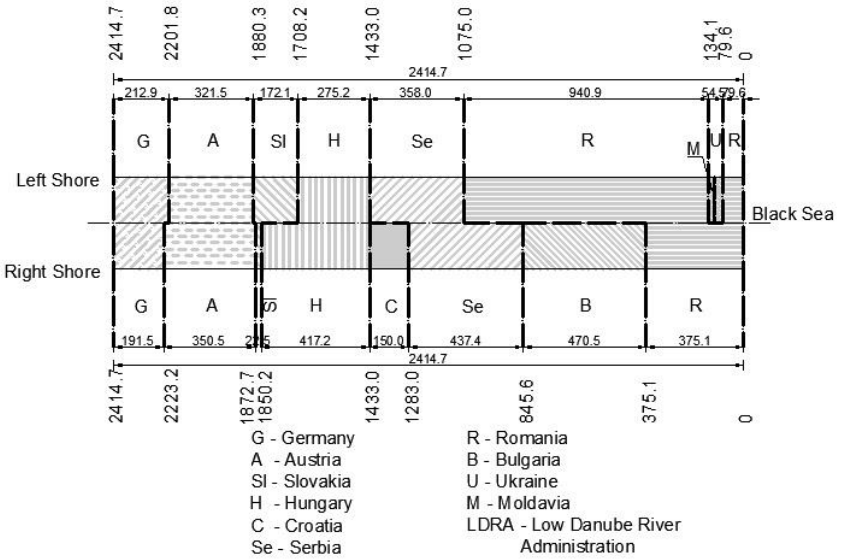

Figure 11: Sections of the Danube

5.6. Studies on the Danube Waterway

A number of studies have been conducted to improve the navigation conditions along the Danube River.

Consequently, Danube as a traditional European waterway corridor for passengers and cargo alike, has a major impact on the development of its adjacent countries. However, the transport patterns in the River are in decline compared to other modes of transport such as road, rail, and air.

Increased Danube Transportation will support further European Integration, social stability and economic growth by means of reduced costs and reduced environmental damage at an attractive investment cost.

6. CONCLUSIONS

In order to improve the performance of a port should be considered the development of its activities in three directions: cargo manipulation, industrial activities and services.

Is required an integrated transportation system for an area as big as possible in order to have reduced shipping costs. The transportation networks must lead to the port hinterland expansion.

To increase efficiency, the watercourse infrastructure must fulfill several functions: flow regularization, irrigations, water supply, drainage, power generation, etc.

Implementation of the zone of logistic activity concept (ZLA) will develop and will increase the efficiency of the port activities.

References

Alderton, P.M. (1999). Port management and operation, London.

Ciortan R., Romanian navigation infrastructure as part of an integrated transportation system, PIANC World Congress San Francisco, USA 2014

Ciortan R., International collaboration concerning the use of Danube River in Romania, SMART RIVERS Conference Buenos Aires, Argentina 2015

DESIGN OF A LOCK TO REDUCE SALT INTRUSION IN THE VILAINE ESTUARY

by

Olivier Bertrand [1], Olivier Cazaillet [2]

ABSTRACT

The Vilaine estuary is located in South Brittany, along the French West coast. Arzal dam is located eight kilometers upstream from the mouth of the Vilaine in the Atlantic Ocean. It is primarily intended to regulate the flow of the Vilaine and provide drinking water during the tourist season.

In order to reduce the salt intrusion upstream of the Arzal dam, the solution proposed by Artelia and its partners consists essentially in reducing very considerably the quantities of sea salt that enter the reservoir at each lock operation. The tests on the 3D physical model showed that this abatement can be obtained operating the substitution of the brackish waters contained in the lock by fresh water taken from the reservoir before the opening of the upstream doors. The effectiveness of this substitution was confirmed by the physical model of the new lock, which allows to refine the design and operating rules of the lock. A 3D numerical model has also ensured that the residual salinity of the lock operation could not cause any problem in the future in the reservoir.

The substitution of brackish water by fresh water in the lock is fundamental for the proper functioning of the new lock. A withdrawal of the brackish waters near the bottom of the lock chamber combined with a soft introduction of fresh water in the upper part makes it possible, by minimizing the mixing between the two flows thanks to the difference of density. The physical model at scale 1/12 allowed assessing the lock water supply system, the duration of the lock chamber emptying, the crest level setting of the outlet ports, the curves of decay of the salinity in the lock as a function of time. The model also assessed the impact of door opening on freshwater and brackish water trapped below the upstream lock's threshold.

The numerical model of the whole reservoir upstream of the dam allowed evaluating the impact of the new lock on the saline intrusion. The 3D model in place allows to analyse all the processes and to test different configurations of operation of the structures.

1. INTRODUCTION

The Vilaine estuary (Figure 1) is located in South Brittany, along the French West coast. The Vilaine River has a flow discharge ranging between 2 and 1500 m3/s. Arzal dam is located eight kilometers upstream from the mouth of the Vilaine in the Atlantic Ocean. It is primarily intended to regulate the flow of the Vilaine and provide drinking water during the tourist season. This is one of the rare estuarine dams in the world.

[1] ARTELIA Eau & Environnement, France, olivier.bertrand@arteliagroup.com
[2] ARTELIA Eau & Environnement, France

Figure 1: the Vilaine estuary (sea on the left; from the left riverbank to the right: the dam, sluice gates and the lock)

The “Institution d’Aménagement de la Vilaine” (public organization created to carry out the necessary structural adjustments) has initiated design studies for the construction of a second lock at the Arzal dam. This lock must fulfil different and sometimes even contradictory set of functional objectives (protection against floods, drinking water reservoir, river navigation, road crossing, fish crossing, flushing ...). Among these, maintaining and preserving a water resource for the production of drinking water is the major objective of the project. Currently, desalination is carried out by a siphon system which pumps the brackish water in a pit located upstream the dam and evacuates water further downstream. This system is highly water consuming and poses problems especially during the summer.

In order to study the feasibility of the project, two complementary models were used:

- A physical model of the lock to evaluate its efficiency and to optimize some components,
- A numerical model to analyse the saline intrusion in the Vilaine.

2. THE PHYSICAL MODEL OF THE LOCK

2.1 Objectives

The principle of the substitution was developed on the basis of a preliminary 3D numerical model of the lock chamber, which allowed to show that an extraction of brackish water associated with an introduction of fresh water in the upper part would enable to rapidly lower the salinity present in the lock.

However, the complexity of the process requires that a physical scale model be built in order to:

- validate the operating principle and its effectiveness,
- set up the inlet ports crests,
- confirm dimensioning of the inlet and outlet aqueducts,
- define the pumping times according to the desired abatement,
- if necessary, define any rules for valve opening,
- assess any risk to the boats moored in the lock chamber caused by the fresh water filling.

This modelling should also allow a better understanding and visualization of the velocity field within the fresh water flow introduced into the lock chamber, above and after the lateral water gate.

2.2 Conception of the model

Flow dynamics at the scale of the physical model should follow the Froude similitude. This similitude ensures the conservation of the main forces involved in the flow (gravity, inertia, turbulent friction). The densimetric Froude number is also conserved because salt water on the sea side is represented with salt concentrations equal to those of nature. Thus the dynamic effects related to the freshwater/saline water density gradient, whatever the value of this gradient, are also well reproduced in the model.

It is also important that the friction forces in aqueducts and lateral water gate are correctly reproduced, which assumes that the Reynolds number is high enough and that the universal coefficient of friction is conserved. This imposes a fairly large scale.

The geometric similitude and the Froude similitude lead to the following scales:

- Scale of lengths, heights and pressures: 1/12
- Volume scale: $1/12^3$, or 1/1728
- Time and speed scale: $1/12^{1/2}$, or 1/3.46
- The salt concentration scale is 1.

2.3 Model construction

The model represents all the hydraulic components of the lock:

- The lock chamber
- The upstream radial gate of the lock chamber
- The upper and lower aqueducts on each side of the lock chamber: lower aqueduct for salt water intake by gravity or for pumping of brackish water from the lock chamber, upper aqueduct for fresh water supply from the reservoir
- The bottom outlet ports between the lock chamber and the lower aqueducts (9 on each side)
- The upper inlet ports between the upper aqueduct and the lock chamber (10 on each side with adjustable crest)
- The intake radial gates of the upper aqueducts
- Pumps of the lower aqueducts

2.4 Lock operation

The model works like the prototype (the real size lock). During lock operation, salt water is pumped by adjustable pumps at the downstream end of the lower aqueducts to a storage basin (representing the maritime estuary). At the same time, the fresh water is brought into the lock chamber by gravity by opening the gates of the upper aqueducts.

The initial salinity in the lock is adjusted according to the characteristics of the test (3 salinities tested): the salinity is prepared in the storage basin and introduced into the lock chamber by the aqueducts and bottom gates. The salt water is firstly mixed to obtain a good homogenisation.

Each test is initialized in terms of initial water level and salinity in the lock chamber before the gate operation (Figure 2).

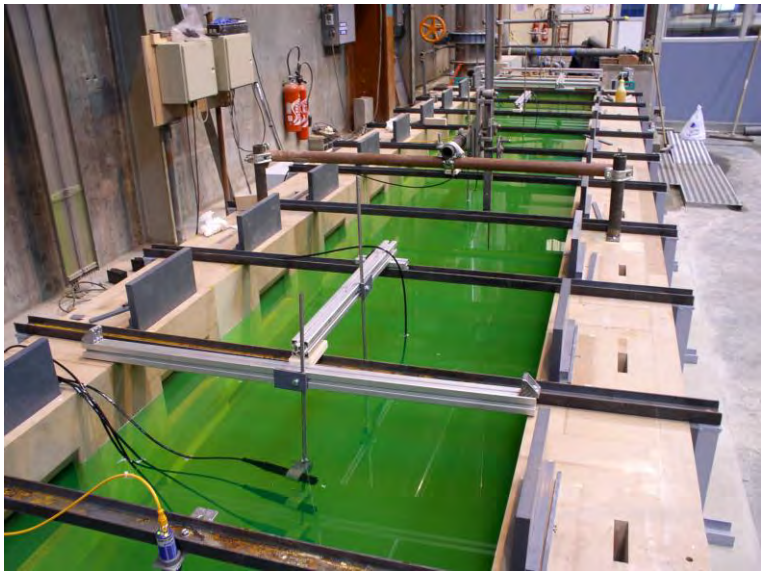

Figure 2: impoundment of the physical model

The measurements concern:

- the discharge of each lower aqueduct: these variable flows are measured downstream of each pump by means of an electromagnetic flow meter
- Water levels: these water levels are measured at four points by echo-sounding sensors: in the upstream basin representing part of the reservoir upstream of the dam, in the lock chamber (upstream, central, downstream)
- Salinity is measured in twelve points distributed vertically and along the lock chamber

All the measurements are recorded at the required frequency and stored in a computer. The radial gates and pumps are also computer-driven (open and closing time of each device, opening and closing velocity, discharge variation)

2.5 Tests

The variables that it was necessary to test are:

- The upstream level (in the fresh water reservoir) which is a boundary condition of the model.
- The downstream level (tidal range downstream the dam). In practice, it can be seen that these levels have no effect on the substitution mechanisms since they are only engaged after the equilibrium of the levels with the upstream reservoir.
- The salinity of the water introduced into the lock chamber (initial condition). The minimum value is 2.50 PSU and the maximum value is 35 PSU, intermediate values are 15 and 32 PSU.
- The position of the crest of the small vertical gates of the inlet ports which has been pre-dimensioned to satisfy two objectives:
    - Minimize turbulence associated with the introduction of fresh water into the lock chamber so as to reduce the risk of mixing fresh and brackish water. This condition is linked in particular to a minimisation of the fresh water introduction with a most possible laminar flow and with the lowest possible vertical velocity field component.
    - Minimize transverse currents on the hulls of boats in the lock chamber by trying to keep velocities below 30 cm/s.

- The pumping rate. By default Q_{max}=4 m^3/s per aqueduct in the prototype (possible variation +/- 1.6 m^3/s) during around 15 mn with a slow rising from 0 to Q_{max} to prevent the mixing.
- The opening rate and the closing rate of the radial gates at the upper aqueduct intake.

2.6 Results

The results are:

- The head losses in the aqueducts between the reservoir and the inlet ports: around 0.36 m for a supplied discharge of 8 m^3/s
- The opening height of the inlet ports according to the discharge and consequently the crest level setting: 0.7 m up to 0.9 m according to the discharge. An opening of 0.6 m appears to be insufficient
- The minimal substitution time to avoid water mixing according to the discharge of the operation: between 15.1 mn and 16.6 mn
- The value and repartition of the salinity at the end of the test: the final salinity remains always below 2 g/l, and mainly below 1.6 g/l, between the water surface and the crest of the sill of the upstream lock chamber gate, whatever the initial conditions with the defined gate opening und pumping conditions
- The influence of the upstream and downstream water levels, initial salinity, pumping rate on the final salinity: the pumping rate is to be between 8 and 9.6 m^3/s. A discharge less than 8 m^3/s is insufficient to lower the salinity. Initial salinity has almost no influence on the final salinity
- The influence of the upstream lock chamber gate opening after a test on the residual salinity dispersion into the reservoir: the opening of the gate does not increase the salinity upstream of the lock above 2 g/l. However a 9.6 m^3/s discharge gives a better security on this residual salinity as the limit between fresh water and brackish water stabilises at the end of the test 1 m below the gate sill. This limit stabilises only at the sill level with 8 m^3/s substitution rate. For that reason, the impact of the boats propellers (not studied in the model) on a local re-mixing, when the boats sail out of the lock, will be much better controlled by a 9.6 m^3/s rate.

The following Figure 3 presents the salinity sensor records of one of the tests with the following conditions: pumping discharge 8 m^3/s, initial reservoir level equal to the mean reservoir level observed in summer season, initial salinity of the water in the estuary 32 g/l, outlet port opening 0.70 m, appropriate opening and pumping increase velocity at the beginning of the substitution. Sensors Sonde 1, Sonde 8, Sonde 9 are located around 1 m above the bottom of the lock chamber.

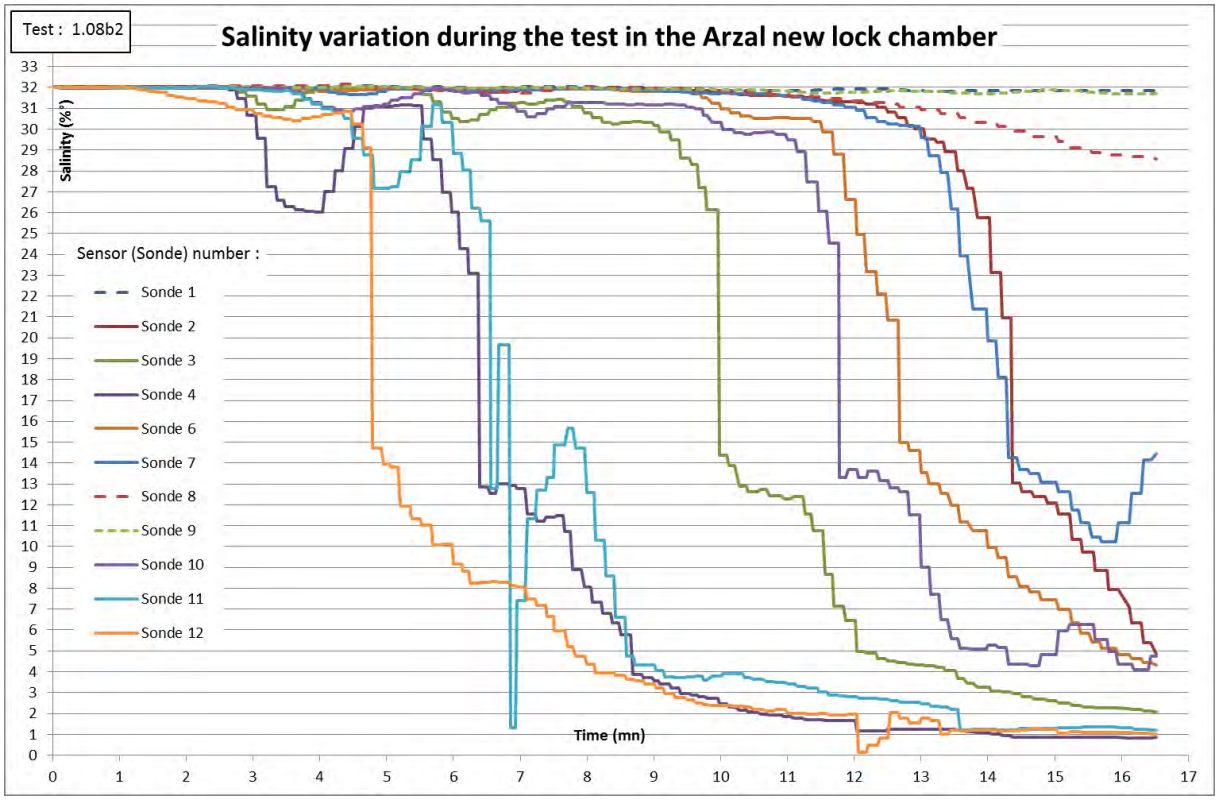

Figure 3: salinity variation during a test – physical scale model

All these variables and the tests carried out allow to specify the characteristics of the lock. The work obtained meets well the requirements of saline water substitution. The impact of the structure on upstream reservoir is then studied by numerical modelling.

3. THE NUMERICAL MODEL OF THE RESERVOIR

The built model allows the calculation, at all points of the reservoir, of the water flow patterns under the influence of upstream water inflows, water outlets at the dam as well as withdrawals and losses (evaporation, water intake from the Férel plant, leaks...), the effects of wind on the surface but also under the influence of the quantity of salt dissolved in the water which is variable.

This variation of dissolved salt causes water density differences and thus internal currents, the saltiest waters, and consequently the densest, tend to flow under fresh water and thus accumulate at the bottom. It is the amount of salt dissolved (its concentration) that is the main concern of the process to answer the questions asked.

For all these reasons, the model is a three-dimensional (3D) one and we have used the TELEMAC-3D software. It covers a territory which, initially limited to a length of about 4 km upstream from the dam, has been extended to the Cran bridge to ensure a more accurate representation of the phenomena and allow a better understanding (Figure 4).

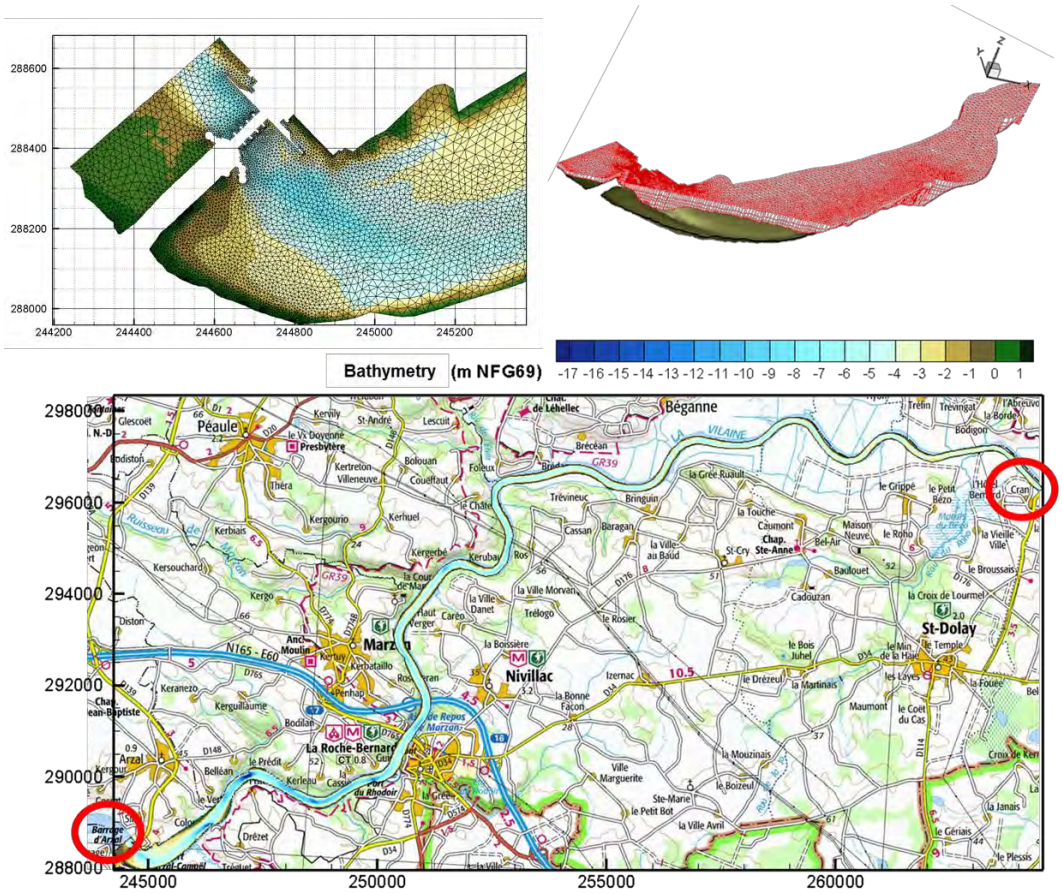

Figure 4: extend and mesh of the numerical model

One of the difficulties of the project is that the precision of certain data is of the same order of magnitude as certain expected results.

2.3 Boundary conditions and calibration

Boundary conditions

Different conditions are imposed at the model boundaries. What goes into the reservoir:

- The natural flow of the Vilaine, upstream from the reservoir and measured at the Pont de Cran, with some secondary inflows. These data are provided by the Pont de Cran station which, since its creation, has contributed to the knowledge of the estuary but which is inaccurate for measuring low flows in summer. Winter floods (slow plains floods due to heavy rains) show flowrates greater than 400 m3/s, whereas in summer low flow is almost null (flowrate less than 2 m3/s).
- Brackish water from the estuary that flows through the dam through the lock at each lock opening (fairly easy to determine) or through leaks at the sluices gates when the sea level is higher than the level in the reservoir. These last are not known and can only be very roughly estimated at a few hundred l/s at most.

What comes out:

- The overflow at the dam. Almost null in summer, these surverses aim to manage water levels in the Arzal reservoir. They are highly variable depending on upstream water contributions. They are not measured but can be approximated based on the recorded levels and the position of the dam gates.
- The locks. These quantities of water leaving the lock can be calculated with correct accuracy. During the year 2005 corresponding to the calibration period, the average flow discharged at the lock is estimated at 9,500 m^3/d (0.11 m^3/s).
- Siphoned waters. The two siphons capture most of the parasite salt water brought by the sluices and redirect it towards the estuary. In low water, a large part of the resource is thus lost by siphons (300,000 to 400,000 m^3/d) at a time when drinking water needs are most high.
- The fish pass. The fresh water flow lost by the fish channel averaged 0.9 m^3/s (over 80 000 m^3/d) in 2005 and 0.3 m^3/s in the summer months alone.
- Evaporation. Over the 2005 calibration period, the volume of water evaporated is greater than the volume of water brought by precipitation. Water loss (obtained by subtracting the volume brought by precipitation from the volume of water evaporated) can reach 42 000 m^3/d (July 11, 2005).
- The Drezet plant has expanded its drinking water production capacity from 30,000 m^3/day in 1972 to 100,000 m^3/day today. This growth is linked to tourist pressure and the development of the industrial basin of the Lower Loire. The plant produces between 15 and 20 million m^3 of drinking water each year. For 2005, the volume of untreated water pumped at Drezet averaged 66,000 m^3/d (0.77 m^3/s) with a peak of over 92,000 m^3/d (July 15) and a minimum of 39,500 m^3/d (January 31). Peak demand is therefore in the middle of the summer period, which obviously corresponds to the low flow period of the Vilaine.

Water levels

Knowledge of the levels in the Vilaine and in the estuary is essential because it makes it possible to establish exchanges through the dam and also to take into account the variability of the quantity of water stored in the upstream reservoir.

The water level in the Arzal reservoir is controlled by opening the gates and dam sluices. It is between +2 and +2.4 m NGF (general levelling of France) during low-water periods (during floods, this level can be much lower). The water level downstream of the dam is influenced by the tide. It varies between -3 and +3.5 m NGF. The data provided by the IAV are measurements taken on both sides of the dam.

Salinity

Salinity varies according to several parameters including:

- the natural flow of the Vilaine (the higher this flow is and the more salinity is pushed towards the sea),
- wind, time and tide level...

This salinity can vary greatly between the surface of the water body and the bottom. Various measurement campaigns have been carried out to better understand these values, one of which was carried out in 2007.

To summarize, we can consider that this salinity varies in very important proportions from 0 to 35 g/l thus passing from a freshwater profile to a seawater profile and that an average value of the order of 13 to 18g/l is representative of the salinity of the waters at the base of the dam without that we can put in evidence a relation with the parameters that influence it.

The "drinking water" requirement involves a normative concentration value for chlorides of less than 200 mg/l (0.2 g/l for approximately 20 g/l for sea water). Local industrial uses may require values below 100 mg/l.

The calibration was carried out by optimizing the setting and the tuning of a set of phenomena such as the refined evaluation of the mass flow of salt rejected by the siphons, a better treatment of the density effects reflecting the mobility of the water masses as a function of their saline concentration, the representation of the volume of salt entering each sluice, the average salinity of the estuary which is representative of the period, the extrapolation of the upstream flowrate for periods without data... By adjusting all these parameters, we obtain, in fine, a simulation of the phenomena rather close to the measurements available at the plant (Figure 5 below).

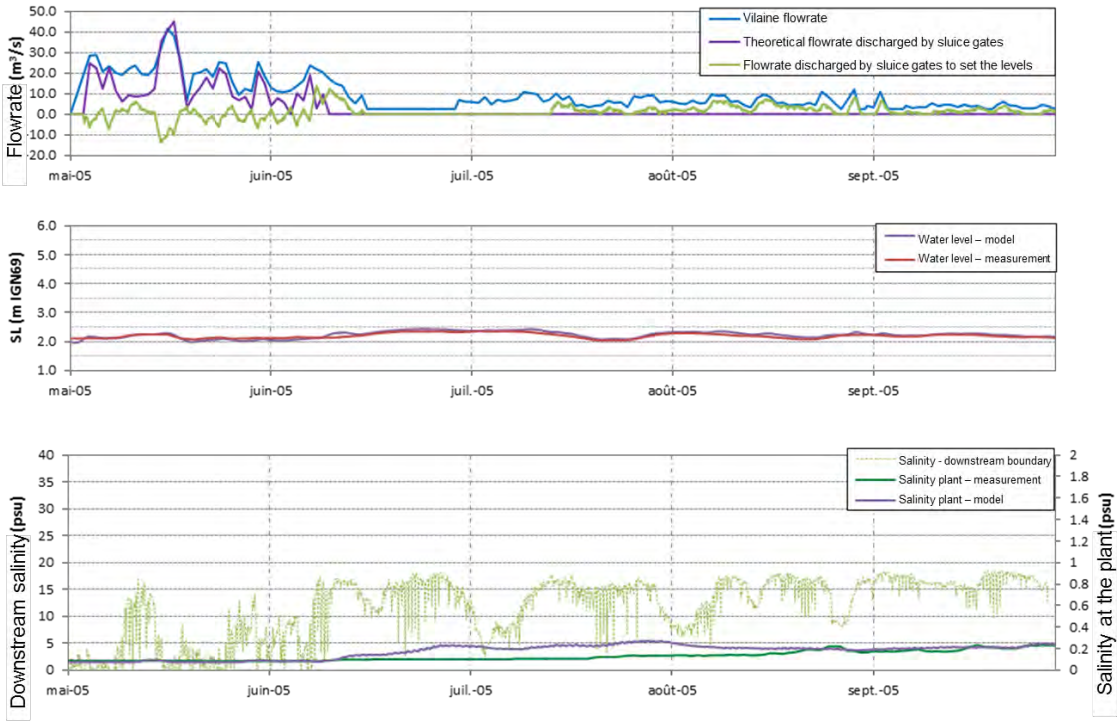

Figure 5: calibration of the numerical model

For the later tests, however, we retained a more unfavourable situation and in particular one where siphons played a more active part. This allowed us to place ourselves in a conservative situation to evaluate the impact of the siphon shutdown.

2.3 Exploitation

The longitudinal profile and the horizontal view of the reservoir, Figure 6 hereafter, show the extent of the salinity front for the configuration selected at the end of the calibration.

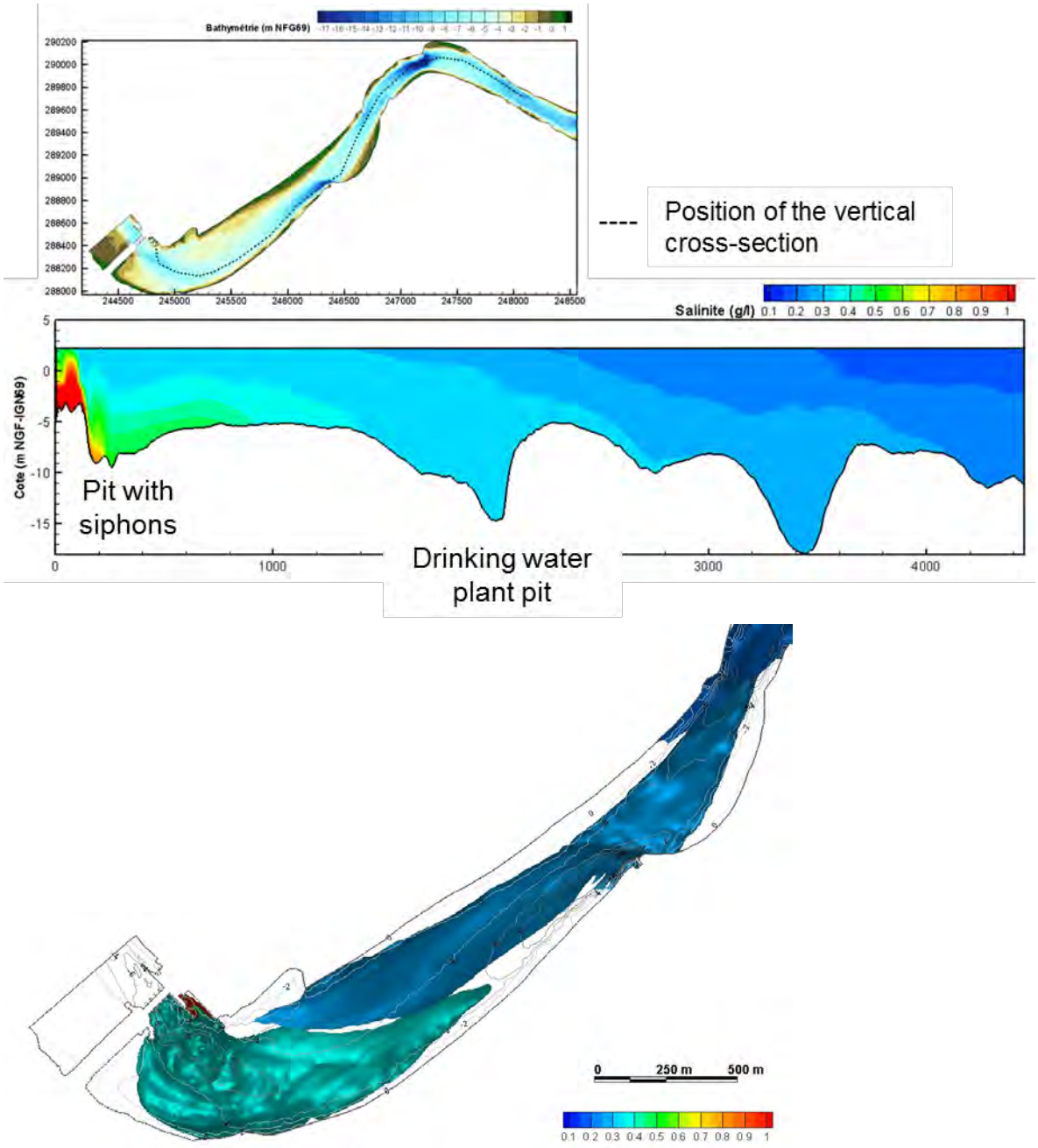

Figure 6: salt intrusion cartography – present state (iso-concentrations fixed at 1 - 0.5 - 0.4 - 0.3 - 0.25 psu)

The figures show that there is a brackish wedge downstream of the reservoir that reaches its maximum concentration near the dam (in red on the longitudinal profile). This high salinity is maintained by saline intrusions linked to the locks opening. Away from the dam, concentrations decrease quite rapidly over the first few hundred meters and then more slowly, even very slowly. Water extends with concentrations above 0.05 g/l upstream from the Roche-Bernard (first town upstream the dam), at least near the bottom, as the salt concentration spreads under the effect of density currents.

The projected lock will significantly reduce the quantities of salt that will enter the upstream reservoir. It remains to determine whether its effectiveness will be sufficient to achieve the fixed objectives.

Tests on the mathematical model of the lock enabled a correlation to be established between the substitution pumping times of the water in the lock and the salinity reduction obtained. To test the effectiveness of the solution, a pumping time of 11 minutes at each ascending lock was assumed. This corresponds to a coherent time with regard to the constraints of passing ships through the structure. The tests were carried out with the siphons maintained (because we know they are effective), then we wanted to know if the new lock would allow us to do without them.

New lock with siphons

The above cross-sections (Figure 7) and graphs (Figure 8) show the efficiency of the new lock with very high salinity reductions in the reservoir.

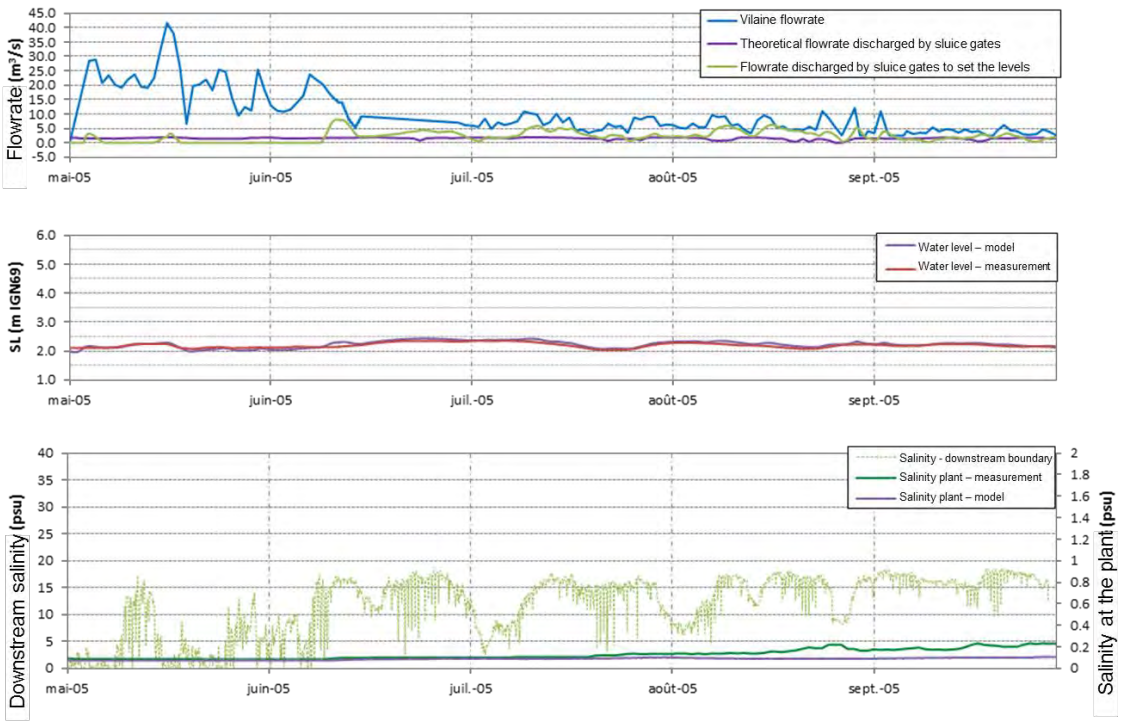

Figure 7: results obtained with the new lock with siphons

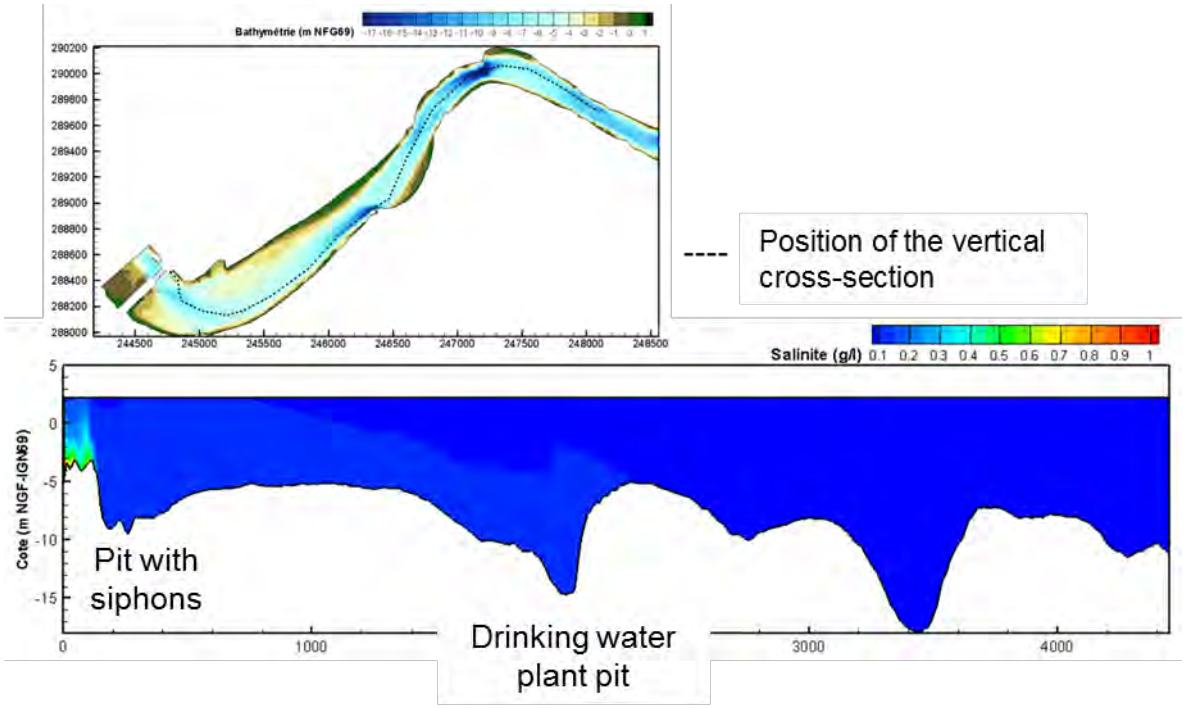

Figure 8: salt intrusion cartography – new lock with siphons

New lock without siphon

Having noted the effectiveness of the system, it is a legitimate question to know whether the new lock can be sufficient to obtain the expected result without having to use siphons that consume water.

The same calculation was done, assuming this time that the siphons are stopped (Figure 9 & Figure 10).

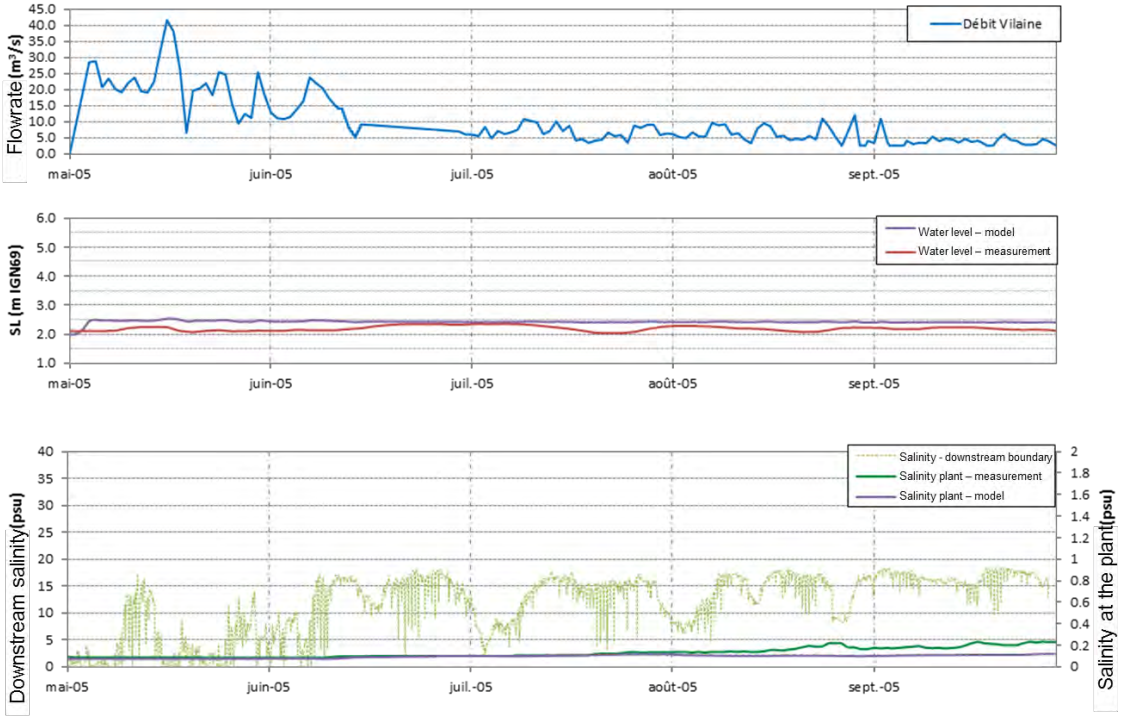

Figure 9: results obtained with the new lock without siphon

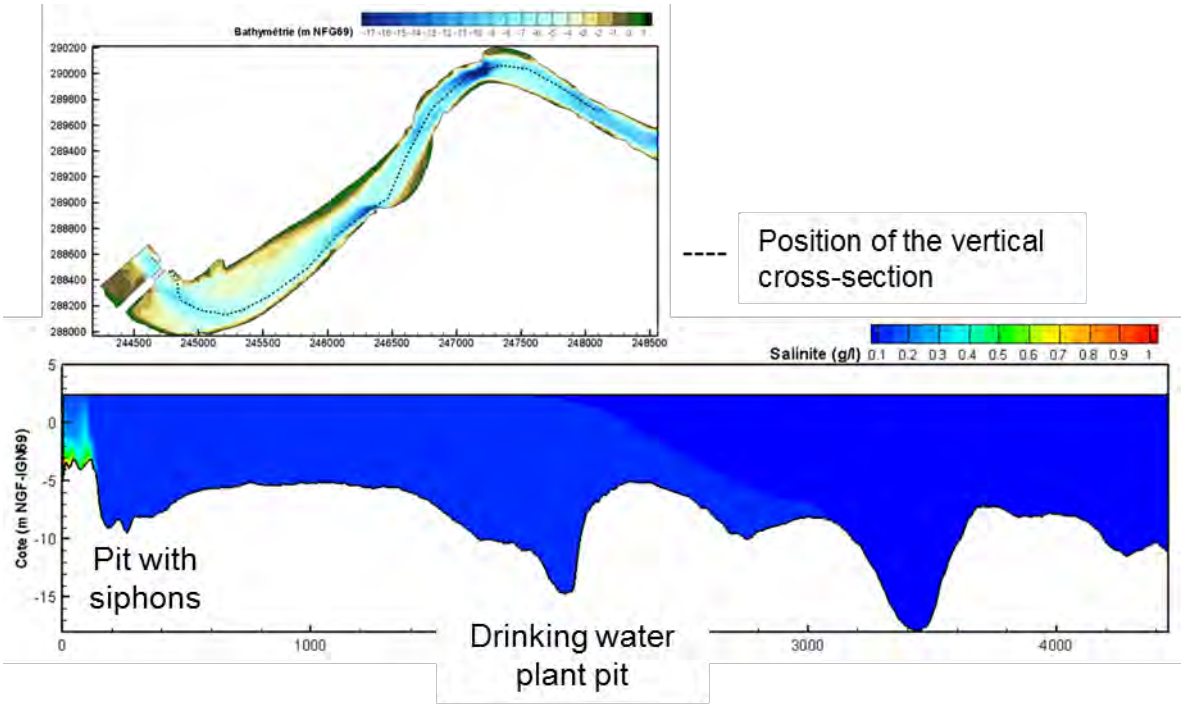

Figure 10: salt intrusion cartography – new lock without siphon

The differences between these two series of graphs do not appear clearly and show that the contribution of siphons remains marginal if the new lock is built.

This clearly indicates that, under conditions similar to those in 2005, the installation of the proposed lock alone would be sufficient to contain the salinity in the reservoir at very low levels without the need to use siphons or move the drinking water intake.

4. CONCLUSION

The Arzal dam is one of the rare estuarine dams in the world. In order to reduce the salt intrusion upstream the dam, two complementary models were used:

- A physical model of the new lock to evaluate its efficiency and to optimize some components,
- A numerical model to analyse the saline intrusion in the Vilaine.

The physical scale model represents all the hydraulic components of the lock and works like the prototype (the real size lock). During lock operation, salt water is pumped by adjustable pumps at the downstream end of the lower aqueducts, at the same time the fresh water is brought into the lock chamber by gravity by opening the gates of the upper aqueducts.

The studies realised shows that the lock meets well the requirements of saline water substitution. The impact of the structure on upstream reservoir is then studied by numerical modelling.

The three-dimensional numerical model covers a large territory upstream from the dam to ensure a more accurate representation of the variation of dissolved salt and the water flow patterns. After a calibration on the current situation, the exploitation of the model for the project state differs by taking into account the new lock which reduces saline intrusions.

The use of the new lock makes it possible to limit saline intrusions very strongly. Two calculations in this project state were performed. These two calculations are distinguished by the use of siphons as is currently the case or the complete stop of siphons during the whole simulated period. It is difficult to differentiate between the two calculations performed, especially given the uncertainty on all input data. This shows that, with the new lock, maintaining the siphons in operation does not bring any significant gain on the salinity reduction.

In conclusion, the proposed solution, i.e. the anti-salt lock, seems relevant and self-sufficient since it addresses the problem of salt intrusion into the reservoir even when the siphons are stopped. However, it seems reasonable to keep and maintain the siphons as they are, which would provide the additional efficiency that may be necessary in the case of a shutdown of the new lock or to compensate for the operation of the existing lock. Indeed, it was recognized that it could be used, on an exceptional basis, on peak summer days.

5. ACKNOWLEDGEMENTS

The authors would like to thank the IAV “Institution d’Aménagement de la Vilaine” for the funding of the studies, the technical exchanges and the sharing of field data.

GUIDELINES FOR RIVER INFORMATION SERVICES (RIS) EDITION 2018 – PIANC WG125

Jürgen Trögl[1], Mario Sattler[2], Cas Willems[3], Jeffrey van Gils[4]

1. Historical Background

PIANC recognized already in 1999, the importance of the development of River Information Services (RIS) and installed a working group on this topic with the task to develop the first edition of the Guidelines for River Information Services. These first RIS Guidelines were published in 2002. The PIANC RIS Guidelines were an important corner stone of the Directive on River Information Services of the European Commission that came into force in 2005. It is applicable to all waterways of class IV or higher with binding rules for authorities on the implementation of RIS within the European Union.

The RIS Guidelines describe the principles and general requirements for planning, implementing and operational use of River Information Services and related systems. They are equally applicable to the traffic of cargo vessels, passenger vessels and pleasure craft. They should be used in conjunction with international regulations, recommendations and guidelines, such as:

- Guidelines and Criteria for Vessel Traffic Services in Inland Waters,
- Technical specifications for Inland ECDIS,
- Technical specifications for vessel tracking and tracing systems, such as Inland AIS,
- Technical specifications for Electronic Ship Reporting in inland navigation,
- Technical specifications for Notices to Skippers in inland navigation

Since the publication of the RIS Guidelines versions 2002 and 2004, further developments on services and standards as well as the technical and practical experience have taken place. PIANC established in 2010 the Permanent Working Group 125 with the task to keep the Guidelines for River Information Services up to date. As a first result of this Permanent Working Group, PIANC published in 2011 an update of the RIS guidelines after having analysed the world-wide status of the implementation of River Information Services.

The PIANC RIS guidelines 2011 were formally accepted by the United Nations Economic Commission for Europe (UNECE) and all European River Commissions.

Since the last technical report of PIANC on RIS the development in the implementation of River Information Services has been considerably. The PIANC working group is preparing the next generation of RIS guidelines that will be published by PIANC in 2018

In the PIANC *"Technical Report on the Implementation Status of River Information Services status 2010"* of Working Group 125, it was stated that the development and use of RIS services in a logistics environment was still in his infancy. Since this report the following developments were recognised as relevant reasons for the update of the RIS guidelines. These developments are:

- RIS enabled corridor management
- The Maritime e-Navigation development
- The need for globalisation of the RIS guidelines

The described RIS services since until 2011 are:

Mainly traffic related

1 Fairway information Services (FIS)

2 Traffic information (TI)

a) Tactical traffic information (TTI)

[1] via donau - Oesterreichische Wasserstrassen-Gesellschaft mbh, Austria, Juergen.Troegl@viadonau.org

[2] via donau - Oesterreichische Wasserstrassen-Gesellschaft mbh, Austria, Mario.Sattler@viadonau.org

[3] Smart Atlantis, The Netherlands, caswillems@me.com

[4] Ministry of Transport and Water management, Rijkswaterstaat, The Netherlands, Jeffrey.van.gils@rws.nl

b) Strategic traffic information (STI)

3 Traffic management information (TM)

a) Local traffic management (vessel traffic services - VTS)

b) Lock and bridge management (LBM)

c) Traffic Planning (TP)

4 Calamity abatement support (CAS)

Mainly transport related

5 Transport logistics Information(ITL)

a) Voyage planning (VP)

b) Transport management (TPM)

c) Port and terminal management (PTM)

d) Cargo and fleet management (CFM)

6 Law enforcement information (ILE)

7 Statistics information (ST)

8 Waterway charges and harbour dues (CHD)

Figure 1: RIS services

2. RIS enabled Corridor Management

Since 2010 studies have been conducted on RIS enabled Corridor Management. The concept of Corridor Management is recognised as the next step in the deployment of RIS services in Europe.

> *"Corridor Management is defined as information services among waterway authorities mutually and with waterway users and related logistic partners with the goal to optimise use of inland navigation corridors within a network of waterways"*

Corridor Management requires sharing of information between authorities and the cooperation of public and private partners is necessary to improve both the performance of inland navigation and the use of the existing infrastructure.

Besides the necessary technical and procedural harmonisation, the basic principle of Corridor Management is the mutual agreement between the fairway authorities in a specific transport corridor on the services and functions they are planning to provide in that corridor.

Three distinctive levels of Corridor Management have been defined:

- Level 1: Corridor Management at this level provides a set of services to enable reliable route planning by supplying – dynamic and static – infrastructural information.
- Level 2: Corridor Management at this level provides a set of services to enable reliable travelling times for voyage planning and for traffic management, by providing traffic information:
    - Level 2a: considering the actual use of the waterway network (e.g. actual waiting times)
    - Level 2b: considering predictions during a voyage (e.g. predicted waiting times on the corridor) where considered reasonable
- Level 3: Corridor Management at this level provides a set of services to support transport management of the logistic partners.

Enhancing inland navigation with the concept of RIS enabled Corridor Management will lead to benefits for inland waterborne transport in the logistic chain e.g.:

- Reliable voyage planning to improve the operation of skippers, terminal and port operators;
- Improved added value of Vessel Traffic Management Services in the logistic chain;
- Simplification of the administration procedures by the usage of an intelligent information management.

The PIANC RIS guidelines are essential for the further development and implementation of RIS enabled Corridor Management being an essential corner stone towards smart multimodal transport management solutions. During the evolution of the PIANC RIS Guidelines and its revision towards a version 2018 a possibility is sought for incorporating the concept of Corridor Management in such a way that it can be applied on a world-wide scale and provides also added value to the regions of the world where national borders don't play such a dominant roles as in Europe.

3. RIS in the intermodal transport domain and Maritime e-Navigation development

The PIANC Working Group 125 on RIS analysed the above-mentioned developments but also took up the lessons that can be learned from information technologies and services in other transport domains, like there are e-Navigation in the maritime world and Intelligent Transport Systems (ITS) in the road sector.

In the RIS Guidelines 2018 special attention is given to the relation between RIS and the maritime concept of e-Navigation and the benefits of these developments for inland navigation.

The PIANC working group 156 on the relation between RIS and e-Navigation published their final report in 2017. As the harmonization between the inland and maritime world is very important, several recommendations of this working group will be of importance for the RIS guidelines 2018.

It is expected that RIS Flagship projects will take into consideration the developments in e-Navigation in order to pave the way for a coordinated implementation of RIS and e-Navigation in Inland Waterways.

These Flagships projects will cope with challenges that need to be solved:

- Standardisation, interoperability, interconnectivity and proprietary solutions
- Improve the quality and reliability of traffic and transport data
- Innovative solutions (IoT, Blockchain)
- Short and medium-term solutions (autonomous sailing)
- Privacy and building confidence, stakeholder acceptance ("legal" issues)
- Cooperation between private & public partners
- Cybersecurity

More than ten years after the adoption and transposition of the RIS Directive in Europe, an important level of experience has been accumulated at EU, Member State and stakeholder's level. At the same time, important IT and technological developments took place. RIS has been recently included in the Digital Inland Waterway Area strategy (DINA), whose aim is to interconnect and unlock the potential of information systems on infrastructure, people, vessels, management and cargo components of inland waterway transport.

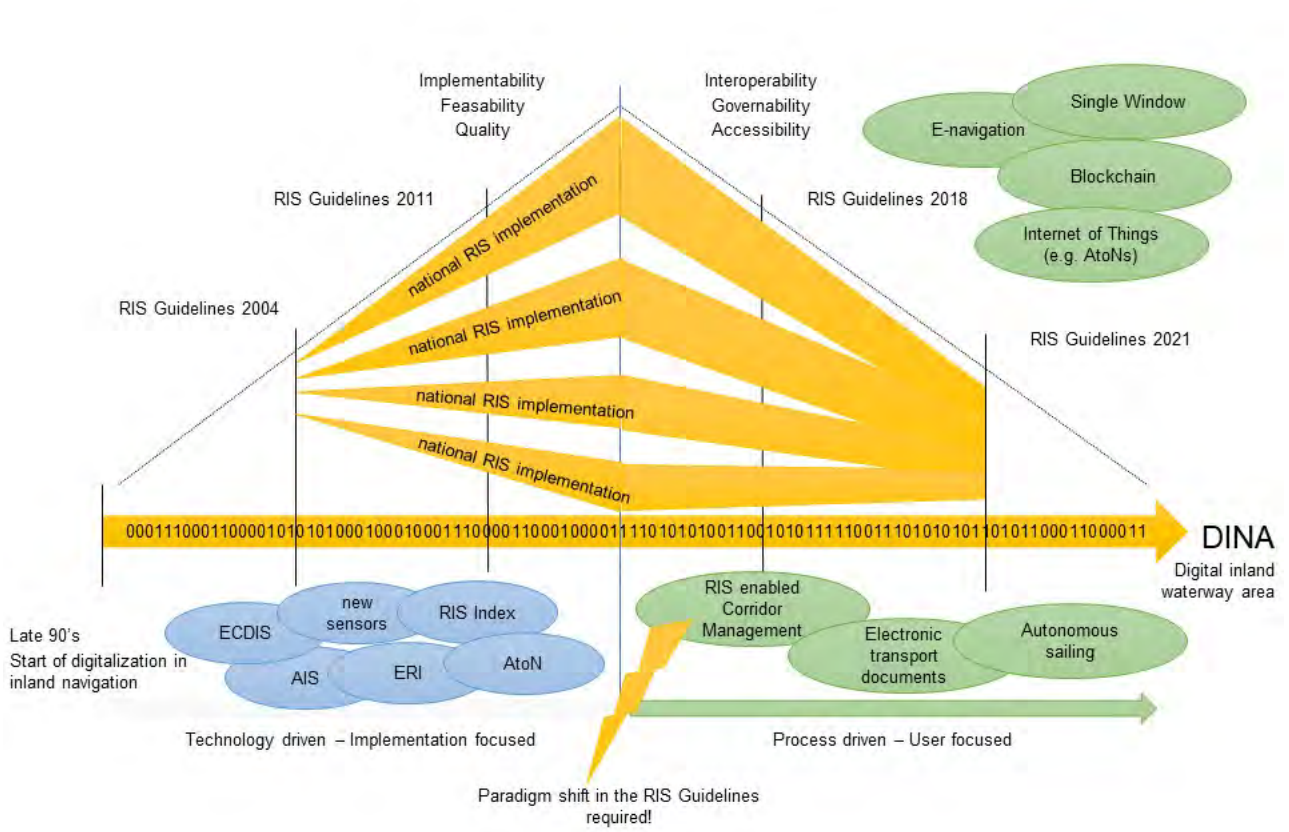

Figure 2: The evolution of the RIS Guidelines towards DINA

4. Globalisation of the RIS guidelines

The concept of River Information Services has originated from Europe, and so does the principle of RIS enabled Corridor Management. It was soon recognized that RIS can also bring benefits to waterway users on other continents, thus waterway authorities around the world started with the implementation of RIS in their domain. In the framework of PIANC there has always been a good cooperation between Europe and the USA on the development of RIS towards a worldwide concept.

It became obvious that the RIS Guidelines need to become a tool suitable for guiding the worldwide implementation of RIS and taking due consideration of developments in other transport domains. For this reason, the new RIS Guidelines 2018 are currently transformed into guidelines for stakeholders in the inland waterborne transport domain all over the world.

In those cases where RIS are deemed to be necessary for the safety of traffic flow, the protection of the environment, the efficiency of transport and to augment the traffic on the waterways while keeping the safety at least on the same level, the competent authority should provide the necessary expertise and arrange funding to provide the desired levels of technology and expertise to meet the objectives.

The RIS services, and their relation with the RIS Key Technologies, can be seen as a layered model presented in Figure 3. The implementation of RIS should contain a least Fairway Information Services and in the next step it can be extended with traffic information, then with traffic management as the primary services. Based on these three primary services the other services can be implemented.

Figure 3: RIS Services implementation sequence

Eventually RIS can be part of a Multi-modal cloud for traffic and transport information services enabling efficient transport throughout the different modalities available at and during the transport of goods. The information needed before, during and after transport will be an open information infrastructure with role based access for registered and controlled information sharing.

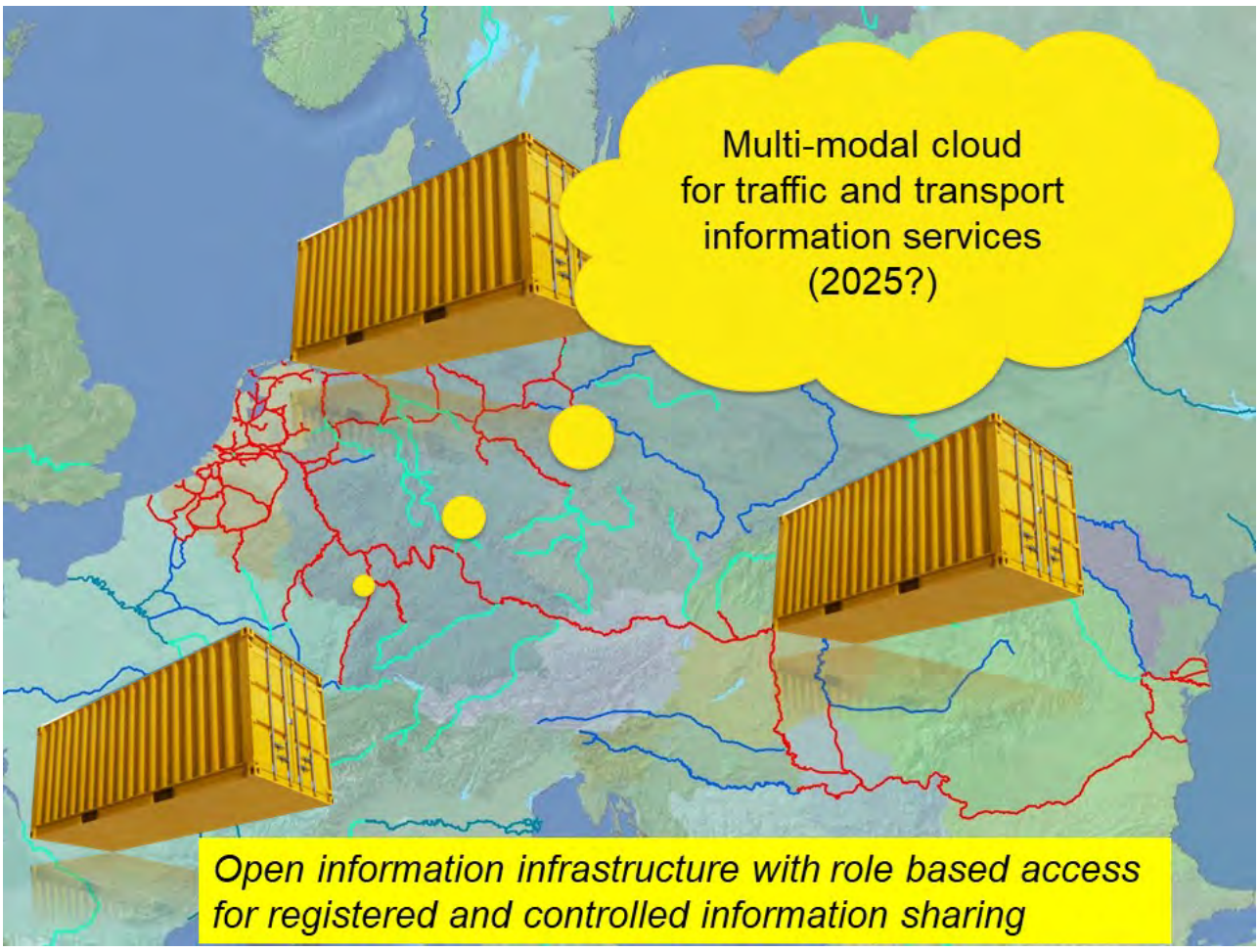

Figure 4: Multi-modal cloud

5. Presentation of the Guidelines edition 2018 in their practical context

The contribution of the PIANC WG125 team to the PIANC World congress provides insights into the recent developments of RIS in Europe and the USA, and the important role of PIANC WG125 in transforming the concept of Corridor Management into a practical guideline for the application of RIS in smart transport management solutions in the inland waterborne transport domain. The presentation will not be restricted to the theory of the Guidelines but will be highlighted with an inside view of practical and operational systems and application.

Presented by: Jürgen Trögl

Topics: 1.7 - River Information Services (RIS, IAS, ...)

LEVELLING THE NEW SEA LOCKS IN THE NETHERLANDS; INCLUDING THE DENSITY DIFFERENCE

#103

Wim Kortlever[1], A.J. van der Hout [2], T. O'Mahoney[3], A. de Loor[4], T. Wijdenes[5]

ABSTRACT

In the Netherlands two deep sea locks are being built, one at IJmuiden and one at Terneuzen. Since these locks maintain the transition between the fresh water in the canal and the salt water in the outer approach, density currents will occur in the lock during levelling. When designing the levelling systems of the new locks the additional forces on the moored vessel caused by these density currents have been taken into account. Extensive scale model studies have shown that for the IJmuiden Lock a system with openings in the lock gates is possible and safe, while for the Terneuzen Lock a more complex system is needed which fills and empties the lock through separate grids in the lock floor.

1 INTRODUCTION

To allow larger sea-going vessels to call in at the main ports of Amsterdam and Ghent, two deep sea locks are being built, the New IJmuiden Lock and the New Terneuzen Lock. The realization of the New IJmuiden Lock started in September 2016. According to the original planning the lock will be opened around the end of 2019. The New Terneuzen Lock will be built in the years 2017 to 2022.

This paper describes the design process which was followed to come to the reference designs of the lock levelling system that is safe for the vessels and at the same time allows for a short levelling time.

The IJmuiden locks are in the northwest of the Netherlands, at the entrance of the North Sea Canal, the canal which connects the Port of Amsterdam with the North Sea. The Terneuzen locks are in the southwest of the Netherlands, at the entrance of the Ghent-Terneuzen Canal, the canal which connects the Port of Ghent with the Western Scheldt Estuary and the North Sea. At both locations the new lock is built next to the existing lock for sea-going vessels. These two locks are the North Lock in IJmuiden and the West Lock in Terneuzen.

Firstly, in the next sections, the design and functioning of the levelling systems of the two existing locks are shortly examined, to find the reasons for choosing the specific type of levelling system. The North Lock uses short culverts in the lock heads, whereas the West Lock uses a bottom filling system. In the following section the design approach for the new locks is drawn up, which includes both numerical and scale modelling. In the last sections the resulting reference designs for both new locks are described following this design approach.

Principally, the choice of a type of levelling system is determined by the maximum head difference, the required levelling time, main vessel dimensions and mooring configurations. Since these locks maintain the transition between fresh (brackish) and salt water, density currents in the lock during levelling lead to additional hydrodynamic forces on the moored vessel. Therefore, this density effect must be included when engineering the levelling system.

---

[1] Hydraulic Engineer, Rijkswaterstaat, Ministry of Infrastructure and Water Works, The Netherlands, wim.kortlever@rws.nl
[2] Researcher/consultant, Deltares, The Netherlands
[3] Researcher/consultant, Deltares, The Netherlands
[4] Researcher/consultant, Deltares, The Netherlands
[5] Hydraulic Engineer, OpenIJ, The Netherlands

2 IJMUIDEN NORTH LOCK

The North Lock was built in the nineteen twenties. The lock chamber is 400 m long and 50 m wide. The sill lies 15 m below mean sea level. At IJmuiden the head difference when levelling varies between about 4 m and -1.5 m. As the maximum head difference during mean springtide varies between only 1.6 m and -0.3 m, differences during normal conditions are relatively small.

The design of the levelling system for this lock was based on the designs of the German sea locks built at that time. A scale model study was carried out in Germany to study the behaviour of several levelling systems considering different culvert lay-outs (Ringers, J.A. and Josephus Jitta, J.P.,1927). In these model tests the density difference was not considered. Based on the test results, a system with short culverts in the lock heads was chosen (Figure 1). Levelling through gate openings was regarded as not feasible, mainly because of the impact on the steel construction of the gate, but also due to the expected flow forces on the moored vessel in the lock.

While the size of the vessels has increased by a factor of two (maximum blockage ≈ 0,8) since it was constructed, the levelling system works satisfactorily.

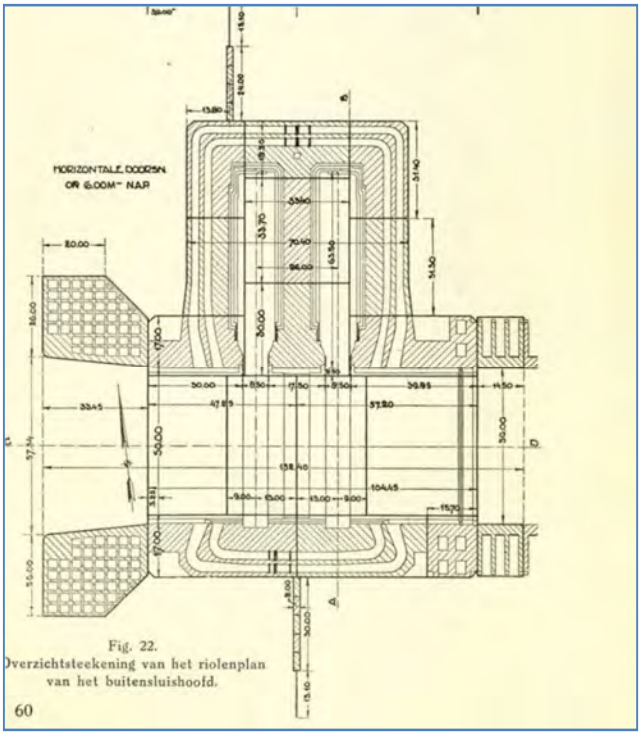

Figure 1: North Lock Outer Head: Horizontal Section of Short Culverts

3 TERNEUZEN WEST LOCK

The outlines of the West Lock, which was built in the nineteen sixties, are shown in Figure 2. The lock chamber is 355 m long and 40 m wide. The sill lies almost 13 m below mean sea level. The water level on the canal is about 2 m above mean sea level. The head difference when levelling varies between 1.5 m and -4.8 m. Compared to IJmuiden the daily maximum absolute value of the head difference is considerably larger, 4 m versus 1.4 m, corresponding to a mean water level on the canal of 2.1 m and mean low tide of -1.9 m outside.

Taking into account these higher head differences, it has been decided to fill and empty the lock through two bottom grids, located at about one quarter and three quarters of the chamber length (Philpott, K.L., 1961). By distributing the discharge over these two grids, the resulting translatory waves are significantly reduced, and the corresponding forces as well. This concept was originally worked out without considering the density effects. However, when this system was tested in a scale model, in a later phase also including a density difference, it showed that the density forces did not lead to extra-long levelling times. Not only the translatory waves are significantly reduced, but also the density currents. In practice, the levelling system at the West Lock has proven to be safe and reliable.

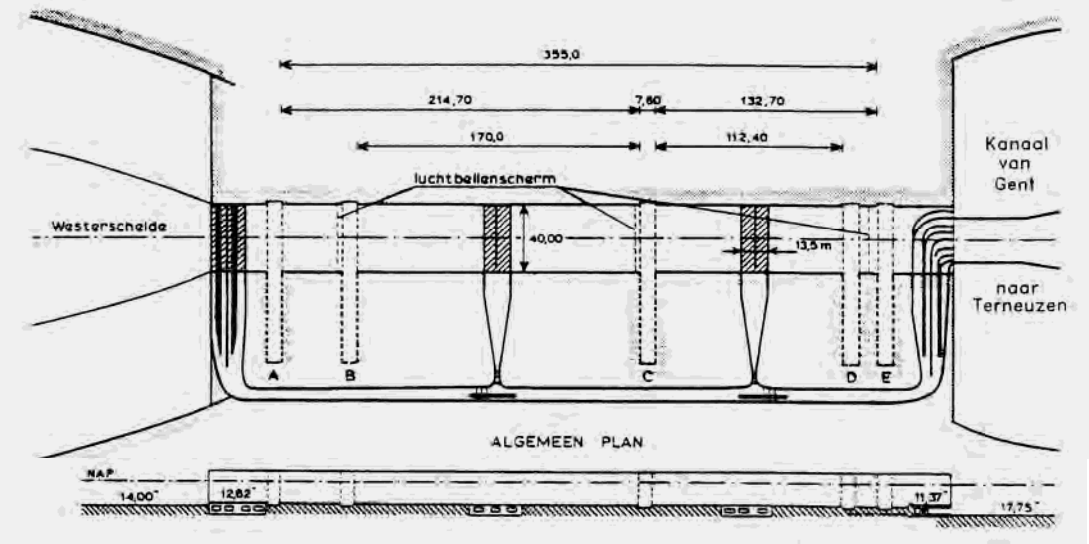

Figure 2: General Plan West Lock: Two Bottom Grids Centered Between Inner Gates

4 GENERAL DESIGN APPROACH

4.1 Choosing the Type of Levelling System

Several large sea locks have a levelling system which consists of short culverts in the lock heads, with culverts built around the gate recesses and culvert in-/outlets in the lock walls, like the IJmuiden North Lock and the Belgian locks with special outlets just above the lock chamber floor (Berendrecht, Kieldrecht). A through-the-gate filling system with openings or ducts in the gate, which is the most common for inland navigation locks, is the most simple system. Because of both the relatively high flow forces on the moored vessel and the impact on the gate structure, this system is less common for large sea locks (Kaiserschleuse, Zeebrugge). A more complex system is the longitudinal system, with culverts along the entire lock chamber and well distributed outlets or ports along the chamber wall or floor. This type of system has been chosen for the old and new locks at the Panama Canal. The levelling system of the Terneuzen West Lock is also a longitudinal system, but the outlets in the lock chamber are concentrated at the two bottom grids.

It is a well-known fact that for relatively low head differences and long levelling times a through-the-gate system may be sufficient. Although the lock is filled or emptied from one side the hydraulic forces on the vessel stay within acceptable limits. Compared to this gate system, a system with short culverts may be hydraulically advantageous when the jets from the outlets in the wall collide and lose their energy. However, using short culverts still means that the lock is filled or emptied from one lock head, leading to fluctuating water slopes along the chamber. Thus, short culverts are also only applicable for limited head differences. An important difference between a through-the-gate system and short culverts is the combination of functions when using the gate system, which may have consequences for the availability and maintenance of the gates. In the case of high head differences and/or short levelling times, a longitudinal system may be considered.

As the daily maximum head difference for IJmuiden and Terneuzen is 1.4 m and 4 m respectively, and the acceptable levelling time is about 15 to 20 min, the starting point for the design of the new locks was a through-the-gate system or short culverts.

4.2 Dimensions and Vertical Position of the System

If the lock chamber is filled or emptied at the lock head, through ducts in the gate or short culverts, the total cross-sectional area of these ducts or culverts can be determined by using the one-dimensional flow-force model LOCKFILL (Deltares, 2015), which includes the translatory waves, the effect of the jets and the force component due to the density currents (stratified flow). It has been assumed that the incoming flow from the ducts or outlets is well distributed over the width of the lock chamber. The chosen dimensions of the system and the valve opening program determine the flow curve and the levelling time. On the basis of this flow curve, LOCKFILL calculates the longitudinal hydrodynamic force on the vessel in the lock. The valve opening program is adjusted, resulting in a different flow curve, until the maximum hydrodynamic force meets the force criterion. The additional result is the attainable levelling time. As long as the force curve stays below the criterion, the levelling time may be shortened further by increasing the dimensions of the system.

A similar approach can be followed when choosing a longitudinal culvert system. First, after the dimensions and culvert losses (inlet, valves, bends, junctions, friction, outlet) have been estimated, the nonstationary flow through the culverts is calculated by using a one-dimensional flow model for nonstationary flow and pressures in closed conduits, e.g. WANDA (Deltares). The inflow in the lock will not only depend on the total resistance of the system but also on the inertia of the water in the system. Second, WANDA may be combined with a one-dimensional model for the flow in the lock chamber. With this combination, accounting for the blockage of the vessel in the lock chamber, a first estimate can be given of the water slopes in the chamber and the resulting horizontal forces on the vessel. As for filling, the effect of the density difference is not included.

Mostly, at the end of levelling, the gate is opened when the flow through the levelling system has decreased and the water level difference or the residual forces on the gate are below a certain threshold. However, when there is a density difference between the outer and the inner lock approach, the water level difference at the end of levelling will be determined by this density difference and the level of the openings of the levelling system. Naturally, the levelling stops when the pressure difference at the level of the gate openings or between the culvert inlets and the outlets is close to zero. Figure 3 shows the equilibrium state, with no flow.

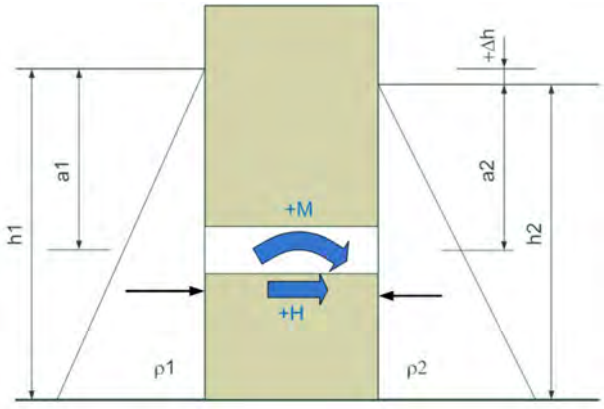

Figure 3: Water Level Difference at Equilibrium State; No Flow Through Openings

The water level difference is determining for the residual moment and horizontal force on the gate at the moment that the gate opening starts, and thus has an impact on the gate stability, the capacity of the gate opening system and the friction on the gate supports. Also, when opening the gate, the level difference can cause a translatory wave propagating into the lock chamber which exerts a short-lasting force on the vessel in the chamber.

It can be shown that both the residual horizontal force on the gate and the incoming translatory wave will be minimal if the level of the openings or the culvert in-/outlets is located at half the water depth at the end of levelling. It also follows that for a longitudinal levelling system with ports or outlets just above or in the chamber floor, one should take into account a larger level difference and higher residual forces on the gate. The drawback of a higher level of the openings or outlets in the chamber, when the vessel is moored close to the active gate, is the relatively high level of the incoming jets and the subsequent higher flow forces on the vessel. Balancing the forces on the gate, the incoming translatory wave and the flow forces on the vessel may lead to the choice of an intermediate location of the levelling openings, between half the water depth and the lock floor.

4.3 Hydraulic Design

When the layout and main dimensions of the levelling system are known, the next step is the hydraulic design, i.e. the streamlining and shaping of the system, especially the culvert systems. This is done on the basis of two-dimensional and three-dimensional flow models in CFD (Computational Fluid Dynamics), including turbulence, e.g. STAR-CCM+, Fluent, OpenFOAM. For a culvert system, it is possible to study a number of different culvert shapes by assuming stationary flow conditions, and neglecting any free water surface ('rigid lid') and the density difference. In the larger models the levelling system is combined with a part of the lock approach and the chamber. A vessel is not included. Attention has to be paid to the flow conditions in the culverts or ducts, the detachment points of the flow and the distribution of the incoming flow over the cross-section and length of the chamber. In this way, the loss coefficients of all specific parts of the system can be determined.

Using the more accurate loss coefficients resulting from the CFD, the LOCKFILL or WANDA one-dimensional calculations of the levelling process, which is nonstationary, can be repeated for a better prediction of the flow curve and the levelling times.

The hydraulic design is not always fully optimized, because of the interface between the hydraulic design and the steel or concrete structure of the gate or lock. Especially in the Netherlands where the lock is often not built in a dry building pit and lock walls are constructed with combi-walls or diaphragm walls there is usually a trade-off between the hydraulic design and the structural design.

4.4 Density Currents

It is emphasized that, when there is a density difference, density currents will develop in the chamber during levelling, and the entire flow pattern in the lock may be different. Because of the additional forces due to the density currents the maximum hydrodynamic force on the vessel will be larger than without the density difference. Additional longitudinal and transverse forces on the vessel will develop due to differences in stratification between fore and aft, and between port and starboard. It is advisable to carry out a CFD simulation of the density currents in the chamber for a first indication of the flow pattern. An example of the calculated flow through a gate with a density difference is shown in Figure 4 (De Loor, A., and O'Mahoney, T., 2014).

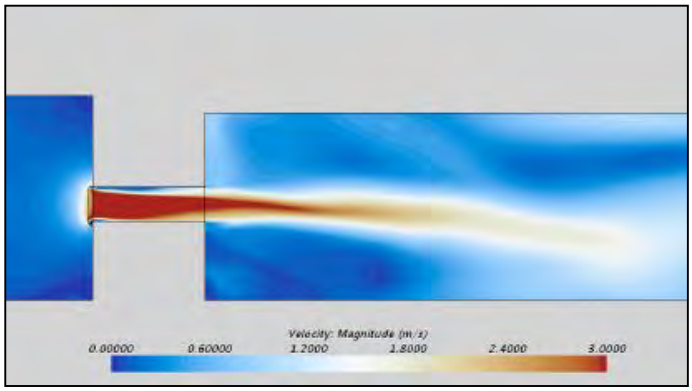

Figure 4: CFD Simulation, Flow Through Gate Ducts, Valve Fully Open, $\Delta\rho$ = 20 kg/m^3

Apart from levelling, when the density difference is large and the lock gate is opened to either of the sides, the water in the chamber starts to exchange with the water in the approach. These density or exchange currents are characterized by a fresh (brackish) water flow at the surface and a salt water flow below (stratified flow). Fresh water in the chamber will be exchanged for salt water from the outer approach, or salt water in the chamber will be exchanged for fresh water from the inner approach. The time needed for a full exchange is determined by the density difference and the length and the depth of the chamber. For the IJmuiden North Lock (Figure 5) the time needed for a full exchange is about 20 minutes. The exchange current will be delayed when a vessel with a large blockage is in the lock. When the gate has opened at the sea side, the outflow of fresh water from the stern is obstructed by the vessel. Thus, for a long time salt water is at the bow and fresh water at the stern (or vice versa). This condition creates a longitudinal force on the vessel, directed towards the sea side, and a transverse force, directed to the central axis of the lock, for a certain time (10-30 min for long locks).These forces will probably be higher than the forces due to the filling and emptying process.

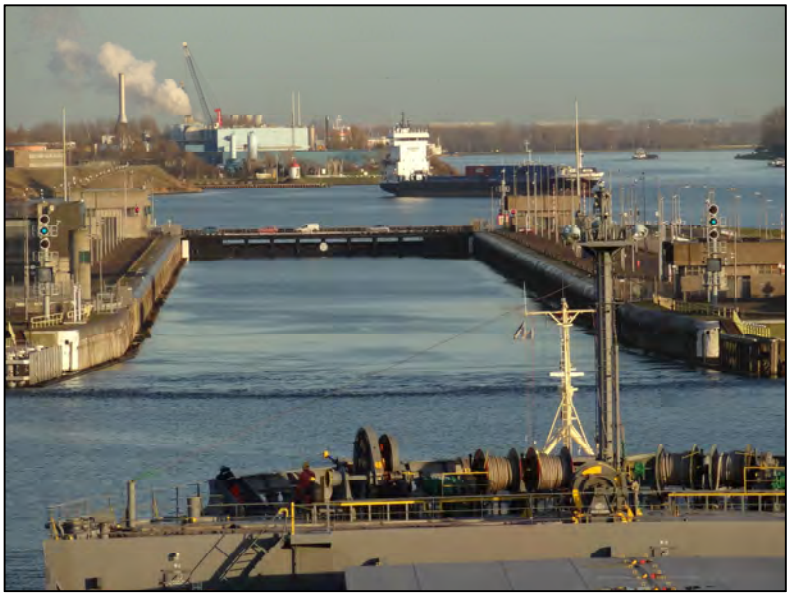

Figure 5: Lock Exchange at the North Lock; Fresh Water Flowing out of the Lock

4.5 Scale Model

The layout, the dimensions and the shapes of the levelling system can be determined based on the results of the numerical models. However, it is recommended that for nonstandard locks the design of the levelling system is validated in a scale model of the lock, because in such a physical model all hydraulic phenomena may be included. In a numerical simulation it is practically not yet feasible to combine the nonstationary flow in the lock chamber, possible density currents, the rising or falling water level and the vessel present in the lock.

The locks and the levelling system for the Panama Third Set Locks had been built on a scale of 30 to 1. The effects of the density difference and density currents were not included. More recently, the new sea locks of IJmuiden and Terneuzen have been built on scales between 40 to 1 and 30 to 1. In these models the density effects are included. Given these scales, scale effects, which are related to the larger influence of the viscosity, are expected to be limited, when compared to the prototype.

The scale model that is used for the new locks of IJmuiden and Terneuzen is shown in Figure 6 (Nogueira, H.I.S., et al., 2018, Van der Hout, A. et al., 2018).

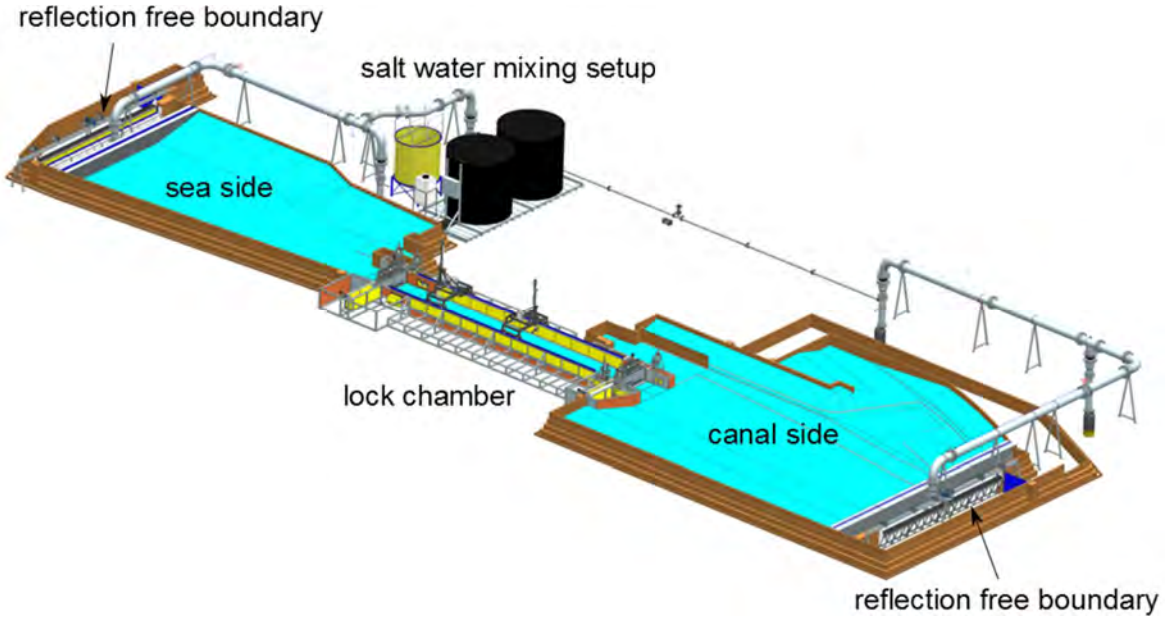

Figure 6: Scale Model Design IJmuiden Lock and Terneuzen Lock

The zigzag weirs at the model ends are used to adjust the water levels in the lock approaches. To avoid reflections of the translatory waves a constant flow is maintained over the weirs by using an adapted pipe system. The approaches in the model have been made approximately 600 m long (40 to 1), to avoid the disturbance of the measurements by the reflected density waves. To establish a density difference over the lock, the density of the water in the outer approach can be increased by mixing fresh water with brine.

Main parameters which are measured during the model tests: (1) water level; during levelling the water slopes in the chamber are a measure for the forces on the vessel, (2) water density; the density forces on the vessel are primarily determined by the differences in stratification between the sides of the vessel, between bow and stern, and between port and starboard, (3) force; the longitudinal force and the transverse forces on the bow and the stern of the vessel are measured, and the yawing moment can be derived from the transverse forces. The vessel is held still in the lock such that displacements in the horizontal plane are prevented.

In the scale model both the nonstationary levelling process and the lock exchange following after the opening of the gate can be simulated.

4.6 Hydrodynamic Force Criterion

In reality, the mooring lines have to withstand the hydrodynamic force on the vessel. When the forces in the lines become to high, the displacements of the vessel will be too large and the lines may break. In order to avoid this situation, the hydrodynamic force during levelling has to be lower than a certain force criterion. This force criterion is used to evaluate the results of the scale model tests.

Moreover, the mooring lines have to be handled to account for the vertical displacement of the vessel during levelling. If the lines are not slacked, then the forces in the lines due to the vertical displacement alone may already be higher than the maximum allowable force in the line. To evaluate the effect of different line handling scenario's and the changing water level on the line forces and the vessel displacements, numerical simulations have been carried out with a dynamic model, using the measured hydrodynamic force from the scale model as input (Rietveld, M.W.J., et al., 2016).

This dynamic model, called SCHAT, simulates the vessel movement and the forces in the mooring lines for a given input hydrodynamic force. For different head differences these line forces and the displacements of the vessel have been compared with the threshold values that were determined in advance. Thereby, not only different handling scenario's which were based on information received from the pilots, but also different mooring line configurations, line types and winch capacities have been considered.

5 NEW LOCK IJMUIDEN

5.1 Introduction

The reference layout of the new lock is shown in Figure 7. The entrance from the sea is on the west side, and the North Sea Canal to Amsterdam is on the east side. In this layout, the lock head at the sea side has two rolling gates, and the lock head at the canal side has one. The gate recess of the eastern gate in the western lock head is used as a maintenance dock. In the final design made by the contractor this maintenance dock has been removed to the canal side of the lock chamber.

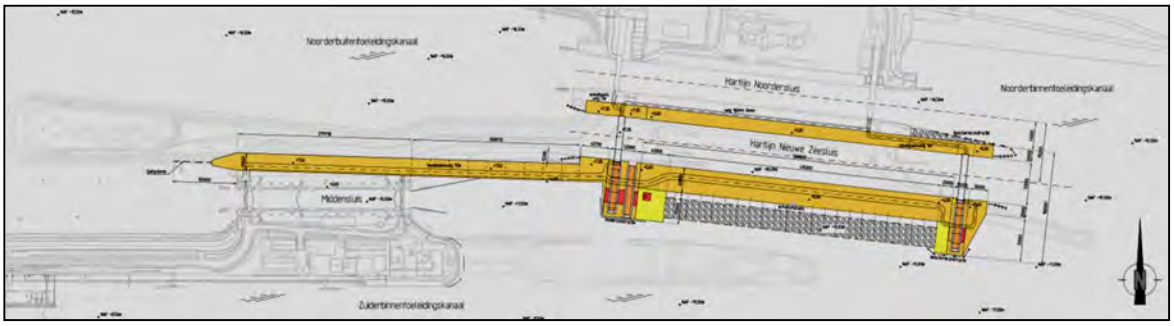

Figure 7: Reference Layout

The new lock chamber which is now under construction will have the following dimensions:

- Chamber length between outer gates: 545 m.
- Overall chamber width: 70 m.
- Sill level: NAP – 17.25 m (NAP: Amsterdam Ordnance Datum).
- Chamber floor level: NAP – 17.75 m.
- Design vessels: bulk carrier: Loa x B x T = 330 x 52 x 19 m, container vessel: Loa x B x T = 366 x 52 x 14.5 m.

The maximum allowable vessel draft in salt water is 13.75 m, due to canal restrictions.

Characteristic water levels:

- Mean high tide: NAP + 1.01 m (mean spring: NAP + 1.16 m).
- Mean low tide: NAP – 0.68 m (mean spring: NAP – 0.72 m).
- Lock closed when sea side above: NAP + 3.90 m.
- Lock closed when sea side below: NAP – 1.65 m.
- Target water level North Sea Canal: NAP – 0.40 m.

The maximum head during levelling, with the sea at high water and the canal at low water, is 4.95 m and the minimum head, with the canal at high water and the sea at low water, is -1.75 m.

The maximum water density difference between the approach harbours is about 20 kg/m^3. The average density difference may be estimated at 14 kg/m^3.

5.2 Type of Levelling System

While creating the reference design of the new lock, two types of levelling system were considered: a system with ducts and valves in the rolling gates and a system with short culverts in the lock heads. At the time of the construction of the North Lock it was not considered feasible to level with openings in the gates, because these openings would weaken the gate structure too much. Also, it was expected that during levelling the flow forces on the vessel in the lock might be too high. Now, based on the current state of knowledge in gate construction and lock hydraulics, and considering the daily maximum head difference of about 1.4 m, both options seem possible.

As mentioned before, hydraulically, the system with ducts in the gate and the system with short culverts are comparable, because the lock is filled or emptied from one side, leading to fluctuating water slopes along the chamber. The short culverts may be advantageous when the jets from the outlets in the wall collide and lose their energy. Being comparable, it was assumed that the development of the density currents during the levelling would not lead to a different behaviour between the two types of system. Therefore, it was likely that the levelling times of the gate system would only be longer to some degree than if short culverts were applied.

5.3 Dimensions and Vertical Position

For both types of system, ducts in the gate and short culverts, the initial one-dimensional LOCKFILL-calculations have resulted in a total cross-sectional area of 80 m^2: twelve gate ducts of b x h = 2.2 m x 3 m or four culverts (two on the south side, two on the north side) of b x h = 4 m x 5 m (Jongeling, T.H.G., 2014). To limit the residual horizontal force on the gate and the translatory wave, when opening the gate, it has been decided to put the ducts and in-/outlets near NAP – 8.5 m, halfway the mean water column of 17 m.

5.4 Hydraulic Design

Based on these dimensions of the levelling systems, a number of alternatives for the layout of the culvert system have been considered. At the sea side head, it is impossible to build the south side culverts around the gate recesses, due to a lack of space. It is regarded as not feasible to pass below these gate recesses, because of the soft soil conditions. As a consequence, all four culverts pass the gate on the north side of the gate (Figure 8). Two culverts come out into the chamber through the north wall, and two culverts cross below the chamber floor and come out into the chamber through the south wall. At the canal side head, two culverts pass the gate on the north side of the gate, and two culverts pass through the gate recess (Figure 8), comparable to the inner head of the existing North Lock.

The shaping and streamlining of especially the culvert system has been done on the basis of flow models in CFD, with STAR-CCM+ (De Loor, A. and O'Mahoney, T., 2014). The design of the north side culverts was adapted to decrease the difference in loss coefficients between the short north side culverts and the longer south side culverts. The culvert inlets in the lock chamber were enlarged to reduce the flow velocities and improve the flow distribution at the foremost position of the bow of the vessel. The openings between the beams and columns in the chamber inlets on the sea side have a cross-sectional area of about 80 m^2 (north) or 103 m^2 (south), and on the canal side a cross-sectional area of about 56 m^2 on both sides.

With respect to the gate ducts, 'breaking' bars have been placed at the end of all openings in the sea side gate, to improve the distribution of the inflow into the chamber when the valves are not fully open. In addition, the number of gate openings has been increased from 12 to 14.

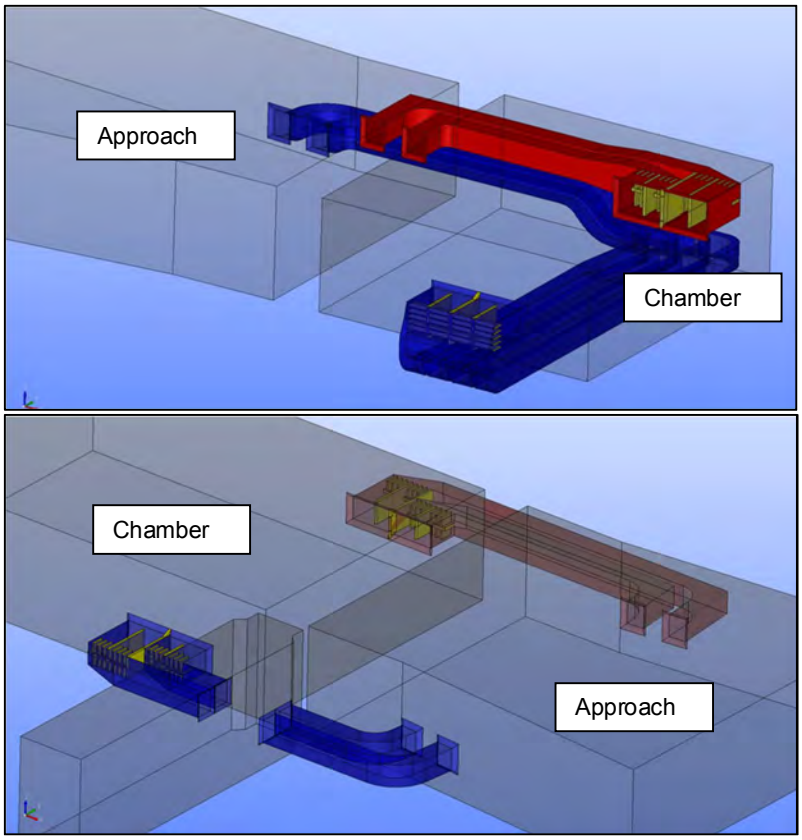

Figure 8: Reference Design of Short Culverts
Upper: sea side, lock lead, two short culverts (red), two long culverts (blue)
Lower: canal side, lock head, south culverts connected to gate recess

5.5 Scale Model

Based on the dimensions and the layout of the levelling systems resulting from the numerical models, a scale model of the lock has been built, on a scale of 40 to 1, including both systems (Figure 6). An extensive scale model study has been carried out (Nogueira, H.I.S., et al., 2018, Van der Hout, A. et al., 2018).

First, tests were carried out with a stationary flow to determine the loss coefficients of both levelling systems. Then, levelling tests were performed, in fresh water only and at a maximum density difference of 20 kg/m^3, with and without the main bulk carrier. In the levelling tests, both the levelling times and the hydrodynamic forces were measured. In a number of density tests, at the end of the levelling, the lock gate was opened to simulate the lock exchange.

It proved that the one-dimensional flow-force model LOCKFILL had to be adjusted to fit with the measurements of the forces on the vessel. The maximum force in the longitudinal direction at the moment of high flow rate was higher in the scale model. Also, it showed that the damping of the translatory waves in the chamber is less in the case of levelling through ducts in the gate than levelling through the culvert system. The influence of the density differences on the forces on the vessel is considerable. In the density tests, both the longitudinal and the transverse forces on the vessel in some cases exceeded the criterion as a result of this extra density component.

After levelling, when the gate is opened, the lock exchange flow, given the high density difference, brings about very high forces on the vessel, directed towards the side with the higher density. Then, both longitudinal and transverse forces are much higher than the criteria. These forces are independent of the type of levelling system.

5.6 Reference Design: Conclusion

After the model in LOCKFILL had been calibrated, this numerical model has been used to determine the maximum levelling times, allowing for the inaccuracy of the model (De Loor et al., 2015). It proved that these required levelling times are longer in case of levelling through the gate, when compared with levelling through the culverts. In consequence of the density difference the transverse forces during levelling may be higher than the criterion. The transverse forces prove to be higher for the gate system than the short culvert system.

The phase in which the vessel is leaving the lock, when the gate has been opened and the lock exchange results in very high forces on the vessel, is regarded as a special operational phase during which additional tug assistance should be available to assist the vessel (Van der Hout, et al., 2018).

5.7 Final Design by Contractor

On the basis of the results of the reference design the building consortium (OpenIJ) has chosen for the same gate system, though with 16 instead of 14 ducts, each with a net opening width of 2.2 m and a net opening height of 3.0 m (Van Lierop, 2018). These ducts are well distributed over the length of the gate, in order that the levelling discharge is evenly spread over the width of the lock chamber. The centerline of the gate openings is at NAP – 10.25 m, more or less at half of the water depth. This means that the residual horizontal force on the gate and the translatory wave, both related to the moment that the gate is opened, are limited.

The lifting valves, which are driven by hydraulic cylinders, are located at the center of the gate. To improve the distribution of the inflow into the chamber, breaking bars have been placed at the end of all ducts. Although these bars are more effective at the chamber side of the gate, the bars are installed on both ends of the ducts, so that the two operational gates are directly interchangeable with the only spare gate. Due to the symmetrical shape with respect to the center of the gate, the discharge coefficients for filling and emptying are equal. Figure 9 shows a cross-section of the gate.

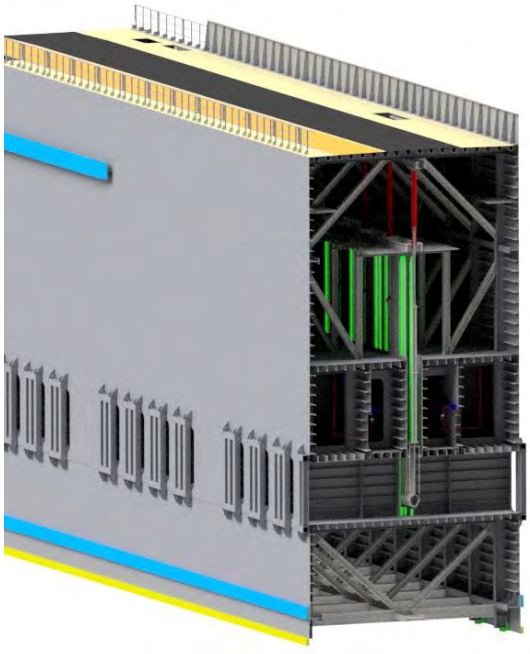

Figure 9: Cross-section Rolling Gate

To determine the discharge coefficient of the ducts, and to find the best shape and location of the breaking bars, OpenIJ carried out flow simulations with CFD, with package Flow3D (Figure 10, Van Goolen et al., 2017).

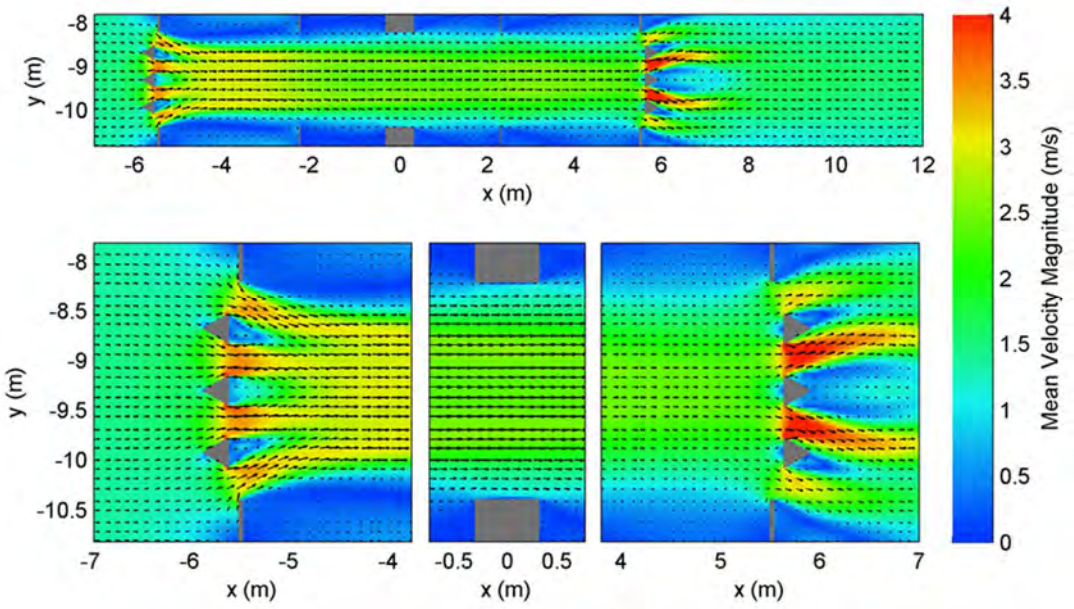

Figure 10: Horizontal Cross-section of Duct; Flow Pattern: Water Flows to the Right

It proved that the pattern of the inflow in the chamber improves when the breaking bars are placed just outside the gate and are given a triangular cross-section. The flow resistance in the ducts is mainly determined by the breaking bars at the entrance and the exit of the duct, the valve in the middle, the stiffeners at the valves, and the stiffeners in between the valves and the entrance or exit. Using the results of the numerical simulations the discharge coefficients have been calculated for different valve positions.

The final design has been assessed in the scale model which is shown in Figure 6. Again, the discharge coefficients have been determined accurately. It showed that the values resulting from the measurements correspond to the ones from the numerical simulations. With the valves lifted above the duct, the net discharge capacity (μA) is 44.4 m^2 (0.42 x 16 x 2.2 x 3 m^2). Subsequently, the valve lifting programs for the different head differences were determined based on the required levelling times and the maximum permitted hydrodynamic forces on the vessel. The tests showed that with the more extreme head differences the density currents during levelling produce the highest forces on the vessel.

The 1D flow-force model LOCKFILL was further calibrated with the scale model tests. Since it was not possible to carry out the scale tests over the entire range of head differences, the calibrated LOCKFILL was used to establish the intermediary valve programs. When emptying, the 16 valves will be operated simultaneously with a constant lifting speed or the valve speed will be varied in time. When filling, it will often be necessary to operate only 8 valves at a time, evenly distributed over the gate, except for the smallest head differences. Additionally, in the case of filling at more extreme head differences, the valves will be lifted in stages, which means that all valves will be stopped and remain standing for a specified period. This is due to the relatively high density forces in those circumstances.

When the gates are delivered, the final valve programs will be adjusted in accordance with a number of site tests of the levelling process. By means of measuring the levelling discharges against time the discharge coefficients will be validated and the levelling times will be verified.

6 NEW LOCK TERNEUZEN

6.1 Introduction

The building contract for the new lock has been awarded in the summer of 2017. The reference layout of the new lock is shown in Figure 11. The entrance from the sea and the Western Scheldt Estuary is on the north side (left), and the Ghent-Terneuzen Canal to Ghent is on the south side. The contract requires that each lock head will include two rolling gates. It has to be possible to carry out the maintenance to each gate in the own gate recess.

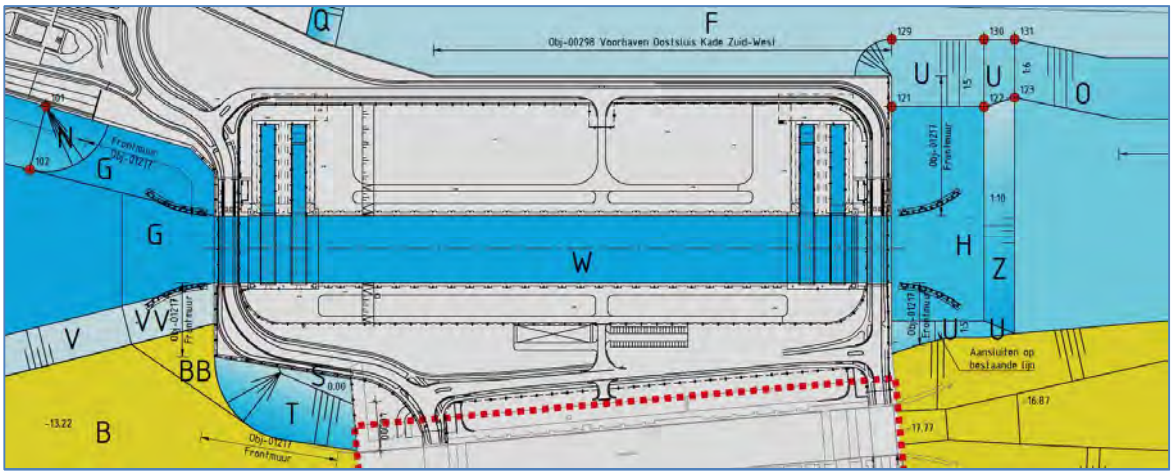

Figure 11: Reference Layout

The dimensions of the New Terneuzen Lock are:

- Overall lock length: 550.60 m.
- Chamber length between outer/inner and outer/inner gates: 452/427/402 m.
- Overall chamber width: 55 m.
- Sill level at outer head: NAP – 16.44 m, sill level at inner head: NAP – 14.12 m.
- Chamber floor level: NAP – 16.80 m.
- Design vessels with respect to levelling system design: bulk carrier: Loa x B x T = 257 x 40 x 16.3 m, container vessel: Loa x B x T = 366 x 49 x 14.5 m.

Given the sill level at the outer head and a minimum water level for locking of NAP – 2.69 m, a vessel can pass the lock irrespective of the tide level, when the draft of the vessel in fresh water is 12.50 m or less. A vessel with a draft of 14.5 m can pass the lock when the water level is NAP – 0.44 m or higher.

Characteristic water levels:

- Mean high tide: NAP + 2.29 m (mean spring: NAP + 2.67 m).
- Mean low tide: NAP – 1.89 m (mean spring: NAP – 2.13 m).
- Lock closed when sea side above: NAP + 4.60 m.
- Lock closed when sea side below: NAP – 2.69 m (LAT).
- Target water level Ghent-Terneuzen Canal: NAP + 2.13 m.

The maximum head during levelling, with the sea at high water and the canal at low water, is 2.72 m and the minimum head, with the canal at high water and the sea at low water, is -5.07 m.

The maximum water density difference between the approach harbours is about 20 kg/m^3. The average density difference may be estimated at 14 kg/m^3.

6.2 Type of Levelling System

Since it had been decided that the final design of the levelling system for the New IJmuiden Lock will be a through-the-gate system, this type of system has also been chosen as a starting point for the reference design of the New Terneuzen Lock. First, a comprehensive study has been carried out to assess the feasibility of a through-the-gate-system with 12 circular ducts, considering an absolute value of the daily maximum head difference of 4 m and an acceptable levelling time of about 15 to 20 min.

An important distinction has to be made between IJmuiden and Terneuzen, because the prevailing condition at IJmuiden is the filling of the lock with salt water from the outer harbour, and the prevailing condition at Terneuzen is the filling of the lock with fresh (brackish) water from the canal (Figure 12). Initially, it was assumed, also based on preliminary flow-force calculations with a 1D-model in LOCKFILL, that the different development of the density currents would not lead to significantly higher forces or longer levelling times for Terneuzen. An exploratory scale model study has been carried out to determine the shortest levelling times which could be attained, and to solve the uncertainty regarding the density currents. These model tests indisputably showed that the density forces when filling during low tide, i.e. filling with fresh water, could only be reduced by prolonging the levelling times outside the acceptable range.

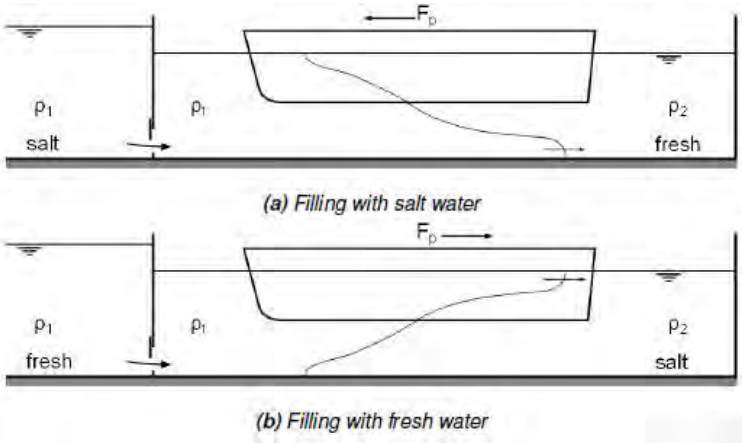

Figure 12: Force Due to Density Currents; Filling with Salt or Fresh Water

As a system with short culverts could be slightly advantageous, because of the colliding jets, additional tests were carried out with this type of system. It proved that even with shorts culverts it is not possible to meet, at the same time, the force criterion and the required levelling time.

Therefore, it has been decided to specify in the requirements for the tender a levelling system which is more comparable with the system of the existing West Lock. In the requirements two alternatives were specified: the West Lock System with two bottom grids, located at about one quarter and three quarters of the chamber length, and the Baalhoek System with four wall grids, two per lock head located in the walls, opposite each other. The Baalhoek System was subject of a scale model study, but has never been built. In both longitudinal systems the levelling discharge is distributed over two parts of the lock, thus reducing the hydrodynamic forces due to both the density currents and the translatory waves.

6.3 Dimensions and Vertical Position

In the preliminary case of the through-the-gate system consisting of 12 circular ducts the μA-value, i.e. the net discharge capacity, is about 28 m^2 for filling, which has been determined in the scale model. As a starting-point, the required dimensions of the reference system with bottom grids have been based on the capacity of the existing West Lock, adjusted for the width of the New Lock: $\mu A \approx 35\ m^2$.

The longitudinal culvert consists of two parallel culverts of 8 m x 4 m, which come together in one connecting culvert in between the bottom grids (Figure 13). In both lock heads, at the position of the gates, there is a valve house between the culverts and the outlet or inlet, having four valves, two valves per culvert. The maximum opening at each valve is b x h = 5 x 3 m^2, so that the total available area at the valves is 60 m^2. It has been decided to place the culverts within 25 m from the lock chamber wall to make it possible to combine the culverts and the chamber wall into one structure. As at the West Lock, the culverts connect to bottom grids, which are spaces under the lock floor with a perforated ceiling. The diameter of the holes is 0.3 m. Due to the relatively low position of the bottom grids, the residual horizontal force on the gate and the translatory wave, when opening the gate, have to be considered.

The second option, the Baalhoek system, with four wall grids is not considered in this paper, because the winning bid in the tender was based on the West Lock system.

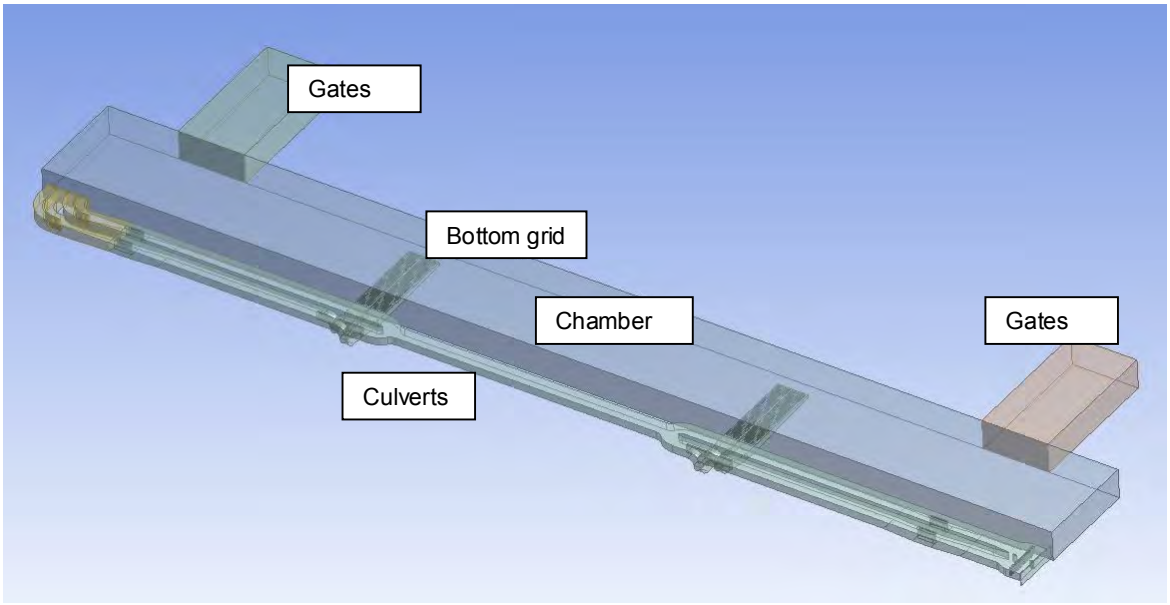

Figure 13: 3D CAD Rendering of Culvert System

6.4 Hydraulic Design

Given the dimensions, the next step focused on the hydraulic design of the bottom grids, the connection between the horizontal culverts and the bottom grids, and the in-/outlets. Again, the shaping and streamlining of the culvert system has been done on the basis of flow models in CFD, with STAR-CCM+ (O'Mahoney, T. et al., 2018).

The layout and the connection to the lock head of the in-/outlets have been varied to improve the distribution of the outflow when emptying and to direct the flow away from the approaches of the neighbouring West Lock, to limit the hindrance for vessels approaching this Lock. The emptying discharges will be higher at the outer lock head than at the inner lock head, because of the larger head differences at low tide. Furthermore, the lock may be used to discharge water from the canal. The fresh water flowing out of the lock to the outer harbour takes the form of a density current concentrated near the surface. Because of these conditions, the in-/outlet at the outer head has been given a 90°-bend towards the lock entrance.

Figure 14 shows the culvert connection to the bottom grid that has been chosen, based on the feasibility from both a hydraulic and a structural perspective. The CFD-simulations proved that a uniform flow distribution at the grid can be reached with a total area of the perforations of 60 m^2 per bottom grid, including a sloping bottom and a dividing wall in the longitudinal direction of the space under the grid.

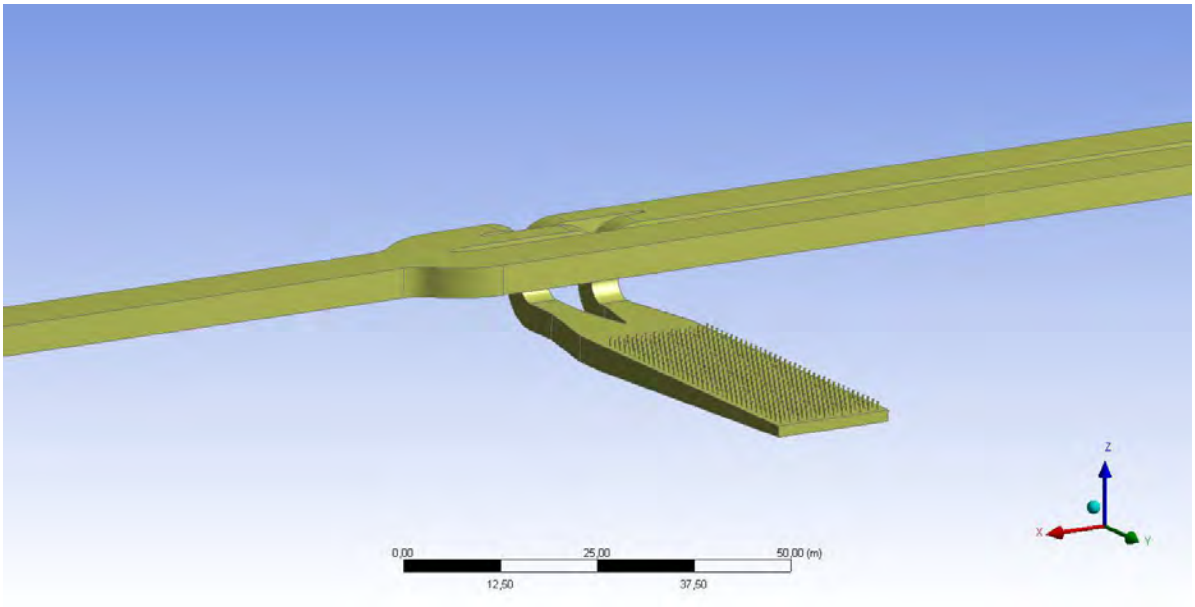

Figure 14: Culvert Connection to Bottom Grid

Based on the loss coefficients of all system components, the discharge coefficient of the total system was estimated. Next, simulations have been carried out with the one-dimensional flow model WANDA, intended for nonstationary flow and pressures in closed conduits, to provide an indication of the attainable levelling times and the evenness of the discharge distribution between the two bottom grids.

6.5 Scale model

The through-the-gate system was tested in a scale model, and subsequently rejected. Since there was insufficient time to test the longitudinal culvert system with bottom grids before the tendering process, it has been decided to prescribe the minimum net discharge capacities (μA), which had been determined in the CFD-study. The minimum μA-values for filling and emptying are 34.5 m^2 and 33 m^2 respectively. In addition, when filling the lock, during the 25% time interval around the maximum flow rate the ratio between the flow discharge through the nearby bottom grid and the far bottom grid has to be between 45/55 and 55/45. For emptying, the same ratio has to be applied, but then during the 15% time interval around the maximum flow rate. The skewness during emptying is less critical due to the absence of the density currents and the related force component.

Eventually, the final design by the contractor has to be verified in a scale model, which means that the net discharge capacity and the evenness of the levelling through the grids has to be proven. Then, given these required capacity and evenness of the levelling, the attainable levelling times while meeting the force criteria will be determined by Rijkswaterstaat, using the same scale model.

6.6 Reference Design: Conclusion

Since the daily head differences can amount to 4 m and the maximum levelling time should be approximately 20 min, a through-the-gate system is not feasible. Therefore, a longitudinal system has been considered, with two filling grids in the floor of the lock chamber or four filling grids, two per lock head located in the walls, opposite each other.

For the tendering-process, it has been decided to prescribe the minimum net discharge capacities (μA), which had been determined in the CFD-study. The minimum μA-values for filling and emptying are 34.5 m^2 and 33 m^2 respectively. Additional requirements apply to the skewness of the inflow along the lock chamber and the maximum overtravel at the end of levelling.

6.7 Final Design by Contractor

The contractor of the new lock has chosen for the West Lock System. As the layout of the in-/outlets and the bottom grids had been largely prescribed, except for the total area of the perforations in the grids, the main degrees of freedom in the design of the contractor were the dimensions and layout of the culverts, and the connections to the bottom grids and the valve houses. Now, the hydraulic design based on the numerical simulations is completed. In July 2018, the net discharge capacities and flow distributions will be verified in a scale model of this design. When the hydraulic design meets the requirements, the final scale model tests will be carried out, under the responsibility of Rijkswaterstaat, to determine the valve lifting programs and achievable levelling times, meeting the force criteria related to the vessel in the lock.

In essence, in the final design chosen by the contractor, the culverts are replaced by one large culvert, which is connected to both bottom grids. The flow into the lock can only be balanced as long as the flow losses are dominated by the losses at the perforations in the bottom grids and not by the losses in the in-/outlets, culverts and connections.

7 CONCLUSIONS

- Density currents in the lock during levelling lead to additional hydrodynamic forces on the moored vessel. Therefore, this density effect must be included when engineering the levelling system.
- The levelling systems of the existing large sea locks at IJmuiden and Terneuzen are a system of short culverts and a longitudinal culvert system with bottom grids respectively. At first, these systems were designed without considering the density currents during levelling. Practice has shown that for the occurring head differences these systems are adequate for these locks.
- When there is a density difference between the outer and the inner lock approach, the water level difference at the end of levelling will be determined by this density difference and the level of the openings of the levelling system. It can be shown that both the residual horizontal force on the gate and the incoming translatory wave will be minimal if the level of the openings or the culvert in-/outlets is at half the water depth at the end of levelling.
- Apart from levelling, when the density difference is large and the lock gate is opened to either of the sides, the water in the chamber starts to exchange with the water in the approach. This exchange flow creates density forces on the vessel, directed towards the salty side, which are most probably higher than the forces due to the filling and emptying process.
- It is recommended that for the nonstandard locks the design of the levelling system is validated in a scale model of the lock, because in such a physical model all hydraulic phenomena may be included.
- The scale model of the reference design of the New IJmuiden Lock proved that both a system of short culverts and a system of gate ducts are feasible, owing to the limited head differences, provided that the levelling times for the gate system may be longer to some degree.
- The final design of the gate system of the New IJmuiden Lock consists of 16 ducts (16 x 2,2 x 3 m^2), with breaking bars at both ends. When filling, it will often be necessary to operate only 8 valves at a time, evenly distributed over the gate. Additionally, in the case of filling at more extreme head differences, the valves have to be lifted in stages. This is due to the relatively high density forces in those circumstances.
- An important distinction has to be made; the prevailing condition at IJmuiden is the filling of the lock with salt water from the outer harbour, and the prevailing condition at Terneuzen is the filling of the lock with fresh (brackish) water from the canal. This fact, in combination with a daily maximum head difference of 4 m and an acceptable levelling time of about 15 to 20 min, meant that for Terneuzen a longitudinal levelling system is required, comparable to the system of the West Lock.
- The final design of the levelling system of the New Terneuzen Lock shows one large culvert along the lock chamber which is connected to two bottom grids. On the one hand the losses at the perforations in the bottom grids have to be dominant to balance the flow into the lock. On the other the total head loss has to be limited to meet the required flow capacity.

8 REFERENCES

De Loor, A., O'Mahoney, T., and Weiler, O., (2015). Nieuwe Zeesluis van IJmuiden, Maatgevende nivelleertijden. Deltares. By order of Rijkswaterstaat. In Dutch.

De Loor, A., and O'Mahoney, T. (2014). Hydraulische vormgeving nivelleersysteem zeesluis IJmuiden. Deltares. By order of Rijkswaterstaat. In Dutch.

Deltares (2015), LOCKFILL User and Technical Manual. Deltares, the Netherlands.

Deltares. WANDA: one-dimensional flow model for nonstationary flow and pressures in closed conduits. Deltares, the Netherlands

Jongeling, T.H.G. (2014). Zeetoegang IJmond Nieuwe Zeesluis, Analyse van het nivelleringssysteem met behulp van rekenprogramma LOCKFILL. Rijkswaterstaat, the Netherlands. In Dutch.

Nogueira, H.I.S., Van der Ven, P., O'Mahoney, T., De Loor, A., Van der Hout, A., and Kortlever, W.C.D. (2018). Effect of Density Differences on the Forces Acting on a Moored Vessel While Operating Navigation Locks, Journal of Hydraulic Engineering. ASCE, 144(6): 04018021.

O'Mahoney, T., Heinsbroek A., De Loor, A., Kortlever, W.C.D. and Verelst, K. (2018). Numerical Simulations of a Longitudinal Filling System for the New Lock at Terneuzen. PIANC World Congress 2018, Panama City, Panama.

Philpott, K.L. (1961). Progress Report on the Terneuzen Lock Investigation, Waterloopkundig Laboratorium Delft, the Netherlands, M667.

Rietveld, M.W.J., De Loor, A., Van der Hout, A. and Kortlever, W.C.D. (2016). A dynamic approach to the determination of force criteria for lock operations in large sea locks; using scale model test results and the dynamic mooring analysis tool SCHAT. Submitted to PIANC to compete for the Paepe-Willems Award 2016.

Ringers, J.A., and Josephus Jitta, J.P. (1927). Proeven en beschouwingen, welke geleid hebben tot het vaststellen van het systeem van vulling en lediging van de kolk der nieuwe schutsluis te IJmuiden, Rapporten en mededelingen van den Rijkswaterstaat, No. 23, Algemeene Landsdrukkerij, 's Gravenhage, the Netherlands. In Dutch.

Van Goolen, D., Wijdenes, T., Adema, J., Voortman, H., and Richardson, J. (2017). DO Ontwerpnota Nivelleerstudie. OpenIJ. By order of Rijkswaterstaat. In Dutch.

Van der Hout, A.J., Nogueira, H.I.S., Kortlever, W.C.D., and Schotman, A.D. (2018). Scale model research and field measurements for two new large sea locks in the Netherlands, PIANC World Congress 2018, Panama City, Panama.

Van Lierop, P. (2018). No Standard Lock Gates for the New Sea Lock in IJmuiden, the Largest Lock in the World. PIANC World Congress 2018, Panama City, Panama.

34th PIANC World Congress

Panama 2018

May 7- 12 2018

Connecting Maritime Hubs Globally

Theme: Inland navigation, waterways, ports and terminals

Authors:

Javier D. Ho Panama Canal Authority Balboa, Panama 272-1669
jho@pancanal.com

Paul Bernal Panama Canal Authority Balboa, Panama 272-1824
PaulBernal@pancanal.com

Presenter: Javier D. Ho

The Importance of the U.S. Inland Transportation and Navigation System for the Panama Canal Grain Trade

I. Introduction- the U.S. Grain Trade and the Panama Canal

Traditionally for the Panama Canal Authority, grain flows fight for the number one position in terms of commodities transiting the waterway, ranging between 33.4 and 53.2 million metric tons in the last five fiscal years and representing a significant 20% of total cargo tonnage on average (Figure 1)[1]. Fiscal year 2015 was a record setting for grains thanks to the record flows of soybeans and sorghum, along with the good flows of corn. At the same time, about 81% of the total grain trade through the Panama Canal originates in ports located along the U.S. Gulf, including export terminals in Corpus Christi, Houston, Galveston and several terminals along the Mississippi River, perhaps the most important export outlet for crops shipped out of the U.S. Midwest. As a matter of fact, only the U.S. Gulf to Asia route represents 60% of total grain cargo flows through the waterway (Figure 2).

[1] Based upon Panama Canal Authority Datawarehouse, comparing with USDA data.

Main Commodities through the Panama Canal (metric tons)

Commodity	FY 2013	FY 2014	FY 2015	FY 2016	FY 2017
Petroleum and Products	41.6	41.3	47.3	41.7	59.9
Container Cargo	51.2	47.6	40.7	41.4	55.6
Grains	33.4	49.4	53.2	41.5	36.8
Coal and Coke	16.5	14.5	10.3	8.3	17.6
Chemicals and Petroleum Chemicals	12.9	12.7	13.9	16.7	15.1
Ores and Metals	14.5	15.3	14.6	11.2	11.9
Nitrates, Phosphates and Potash	7.2	7.8	7.8	7.4	8.3
Manufactures of Iron and Steel	6.8	6.8	7.1	5.3	6.8
Others	31.4	35.8	37.9	34.5	32.9
Total	**215.5**	**231.2**	**232.8**	**208.0**	**244.9**

Figure 1. Source: Panama Canal Authority. Fiscal years goes from October to September.

Main Routes for Grains through the Panama Canal (metric tons)

Route	FY 2013	FY 2014	FY 2015	FY 2016	FY 2017
Gulf USA- Asia	22.7	34.3	35.1	21.3	17.5
Gulf USA- West Coast South America	2.2	4.7	6.1	7.1	7.0
Gulf USA- West Coast Central America	2.1	3.1	3.8	4.5	4.5
South Atlantic USA- Asia	0.7	0.8	0.7	0.9	0.9
Mexico (Pacific)- East Coast South America	0.4	0.4	0.5	0.7	0.8
Others	5.3	6.1	7.0	7.0	6.1
Total	**33.4**	**49.4**	**53.2**	**41.5**	**36.8**

Figure 2. Source: Panama Canal Authority. Fiscal years goes from October to September.

In 2016, about 31% of total U.S. grains exports, that is, 44.1 million metric tons out of a total of 141.4 million metric tons, transited through the Panama Canal[2]. The main destination region for the U.S. Gulf grain trade is East Asia, mainly China, Japan, South Korea and Taiwan, although there are significant flows to ports located at both the West Coast of Central and South America. The U.S. Gulf trade, however, competes with grains originating in the U.S. Pacific Northwest

[2] Here year 2016 is from September to August.

(PNW) and with alternative grains sources such as Brazil, Argentina, Eastern Europe, Russia and Australia. In 2012, Brazil surpassed the United States as the main exporter to China (Figure 3).

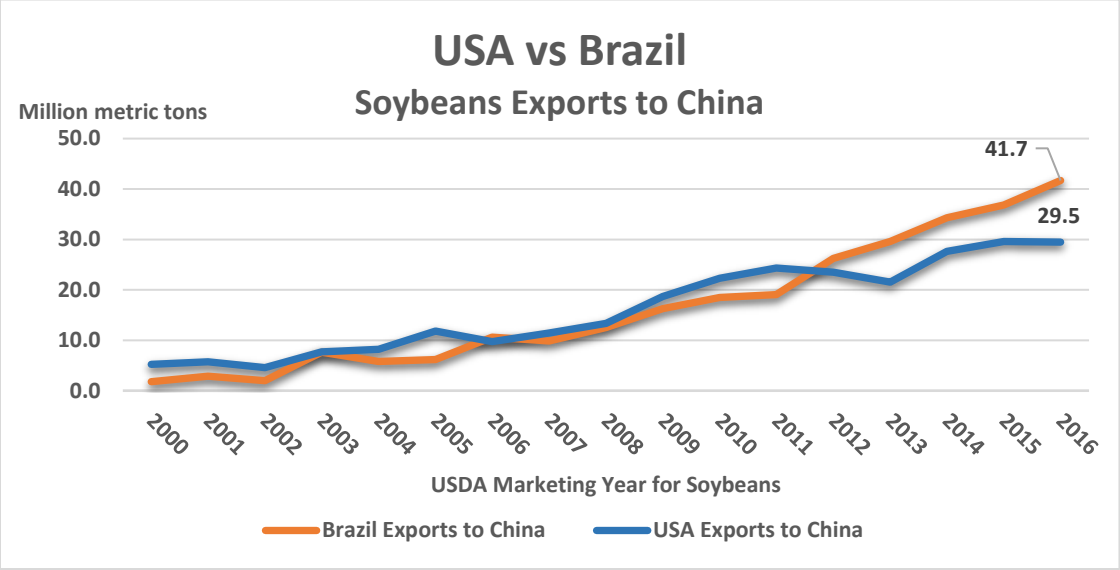

Figure 3. USA vs Brazil Soybeans Exports to China. Source: USDA and Secex Brazil data converted to U.S. marketing years.

In order for grains originating in the U.S. Midwest and transiting through the Panama Canal to remain competitive against the PNW and alternative sources in other countries, it is very important that the grain trade from this region have a reliable and economical means of transportation. This fact highlights the importance of a safe and reliable transportation system, including inland navigation waterways, railroads and port terminals.

Given the significant participation of grains in the total Panama Canal cargo tons and the importance of the U.S. Gulf as the main origin for this commodity, this paper will first explain the main transportation modes U.S. grains utilized, from the hinterland to the main grain export regions, where the choice of transportation mode depends mainly on the geographical location of crops such as wheat, corn, sorghum and soybeans. Next, the dynamic interaction truck-barge-train for grain deliveries, both domestically and for exports, will be discussed, a relationship that results in a contested area for grains, especially for exports. Once the importance and participation of the transportation modes for grains are understood, the report will highlight the importance of the Mississippi River System to the Panama Canal grain trade and the need for maintenance, investment and steady funding for the Inland Waterway System. Finally, a list of top priorities of infrastructure work by advocacy groups will be included in this paper.

II. Transportation Modes of Grains in the United States and Geography of Crops

Regarding the main transportation modes for U.S. grain exports, about 48% is transported on barges, 36% through rail and 16% is mobilized through trucks[3]. Soybeans and corn cargo movements are dominated by barges, followed by rail. Wheat is highly dominated by rail, then

[3] Based upon *Transportation of U.S. Grains : A Modal Share Analysis* (Oct 2017 update)- USDA- AMS

followed by barges. In terms of sorghum, this grain is mostly transported by rail and trucks[4]. Any transportation mode needs to be competitive and is highly depended on crop location. For example, corn and soybeans are highly concentrated in the Midwest region, including Iowa, Minnesota, Illinois, Wisconsin, Missouri, Nebraska and North and South Dakota and wheat is mostly concentrated in areas closer to the Pacific Northwest and center USA (Figure 4). In other words, the geographical location of crops often determines the mode of transportation and the port outlets for U.S. grain exports.

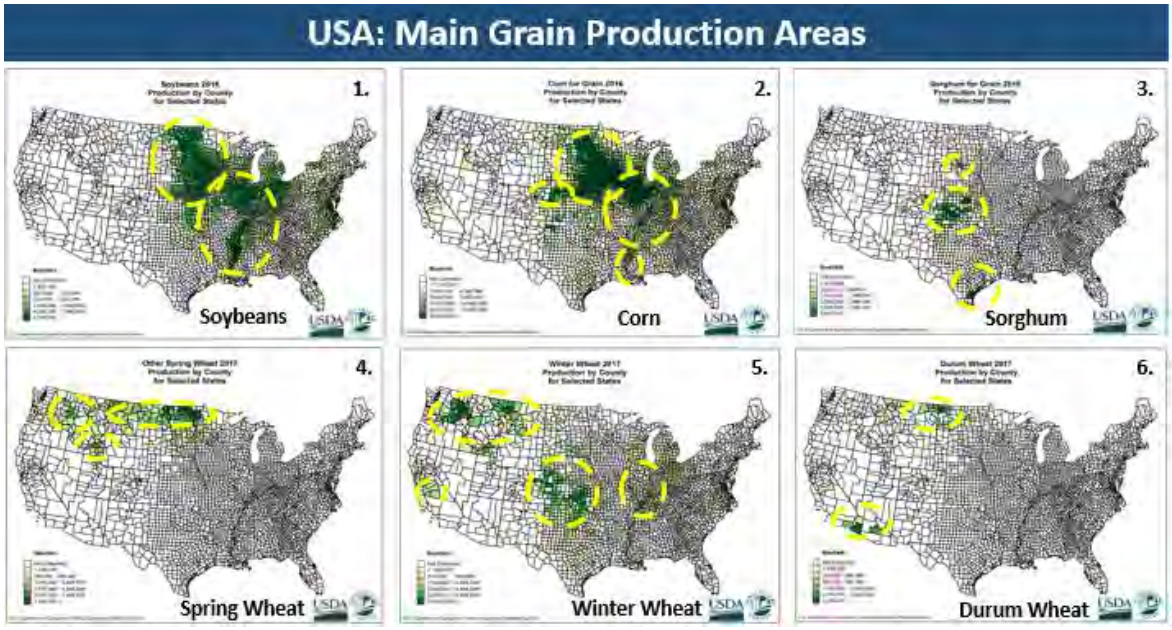

Figure 4. Source: www.nass.usda.gov.

From the same source and in terms of train carloads participation by main port region, the Pacific ports receive the majority of the grain shipments for exports, followed distantly by Texas and the Mississippi River port regions. In other words, some grain flows on trains move to export terminals along the Mississippi River. On the other hand, corn and soybeans represent the majority of grain movements through the Mississippi River System. These movements include grains through Mississippi Lock 27 (Granite City, IL), Ohio River Lock 52 and Arkansas River Lock 1[5]. Soybeans and corn are mostly exported through the Mississippi Gulf port region. Likewise, wheat is mostly exported through the Pacific and Texas (Figure 5). Because of the growing investment in export elevators in the PNW, shuttle trains and biotechnology, a growing number of corn and soybeans are also exported through this port region.

[4] Ibid.

[5] USDA- GTR Dataset (Table 10: Barge Grain Movements). Weekly data from USDA- GTR was converted to calendar years.

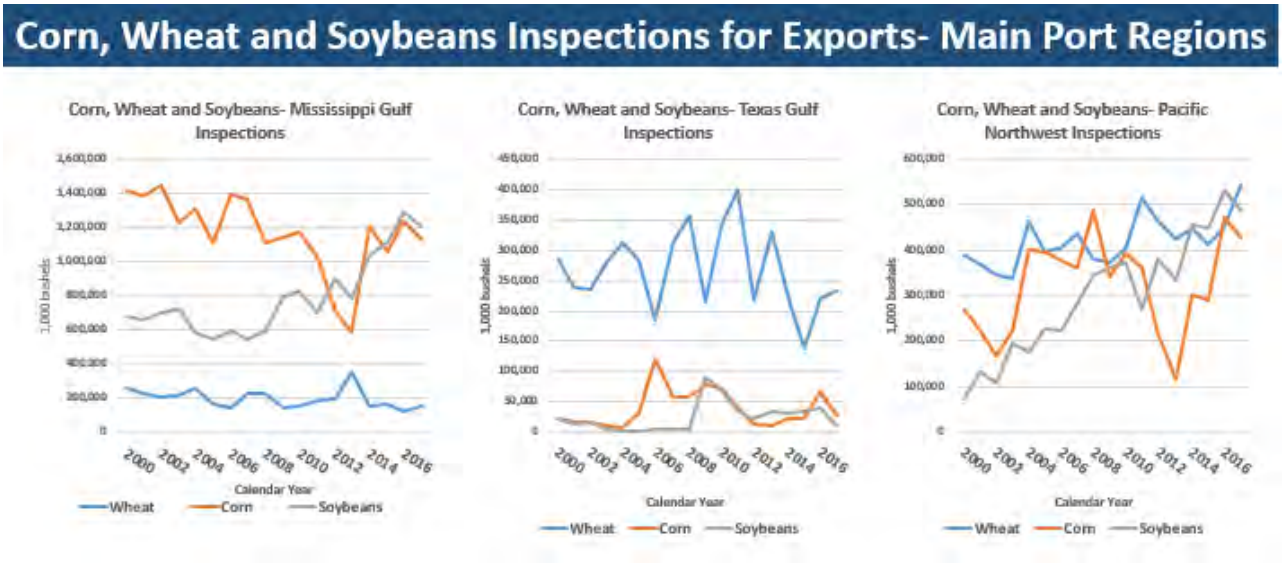

Figure 5. Source: USDA- GTR Dataset (Table 16: Grain Inspections for Exports by Port Region).

In simple words, corn and soybeans are mostly transported through barges and exported through the Mississippi River port system while wheat is mostly transported by trains to PNW and Texas Gulf export terminals. Sorghum is transported by rail, - and to a lesser extend trucks- to export terminals in Texas. Nonetheless, it is very important to keep in mind the growing amount of corn and soybeans transported by rail, especially to the PNW, and some deliveries destined to the U.S. Gulf. At the same time, the availability of weekly data from the U.S. Department of Agriculture regarding rail deliveries to ports, grains inspections, grain barges unloaded in the New Orleans region and vessel loading activity in port provides an opportunity to attempt a forecast of weekly grain transits through the Panama Canal. In our case we attempted to forecast weekly grain transits through the Panama Canal using a TBATS model (TBATS (0.375, {0, 0}, 0.919, {<52, 6>}), employing as exogenous variables barge movements with corn and wheat, which proved to be statistically significant. It is worth mentioning that this parameters are preliminary estimates, and in the future parameters are prone to change. Furthermore, since this is an on-going project, other forecasting and time series models may be used instead, such as VARMAX, NNET AR, and others.

III. Trucks, Barges and Train Services for Grains and the Geographical Approximation- Gulf versus Pacific Northwest

Most of the grains exported through the PNW from the U.S. hinterland involve railroads while grains exported through the U.S. Gulf from the hinterland involve barges or railroads in some areas. Depending on the location of an American farmer, he may decide to sell his grain to a local elevator, delivering it by trucks. Otherwise, if the basis and grain prices are advantageous, the same farmer may sell his grain directly or indirectly to an grain elevator with access to a railroad yard that can reach either or both the U.S. Gulf ports or the Pacific Northwest[6], or may sell his grain to an elevator that reach barge terminals connecting to export elevators located on

[6] Examples of such locations are Minneapolis, MN and Council Bluff, Iowa. Source: USDA-GTR, Table 7: Tariff Rail Rates for Unit and Shuttle Trains.

the Mississippi River (See Diagram 1). To keep it simple, this interaction is dictated by the relative prices that a grain producer may receive for his product and by the cost of transportation from origin to destination.

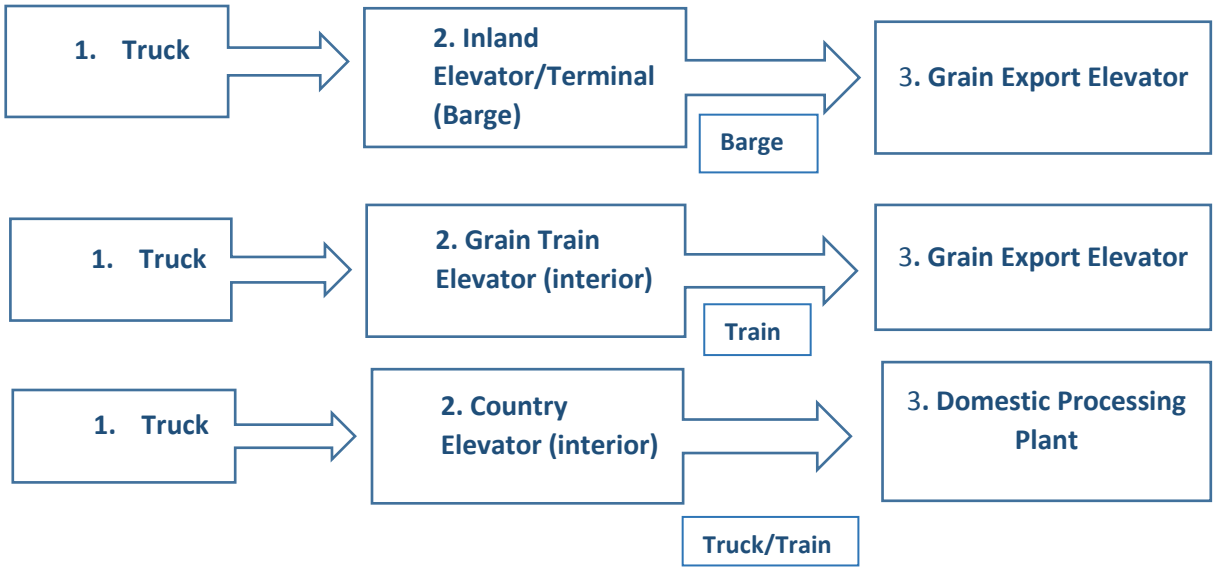

Diagram 1.[7]

Grains can be delivered to inland barge terminals located in regions such as Twin Cities, Mid-Mississippi, Lower Illinois River, Saint Louis, Cincinnati, Lower Ohio and the Cairo- Memphis area (Table 1)[8]. Depending on supply and demand conditions during the marketing year, barge rates may fluctuate during a time span. For example, the following table presents weekly barge rates for November 14, 2017, in the middle of the 2017/18 harvest season, and for January 9, 2018 in the lower part of the same harvest season:

Table 1. Weekly Barge Rates: Southbound Only

	Twin Cities*	Mid-Mississippi*	Lower Illinois River	St. Louis	Cincinnati	Lower Ohio	Cairo-Memphis
Nov. 14, 2017	$25.26	$19.58	$17.63	$10.17	$22.04	$18.99	$7.38
Jan. 9, 2018	-	-	$18.19	$10.97	$13.46	$11.59	$5.90

*Source: USDA-GTR Table 9: Weekly Barge Freight Rates: Southbound Only. In $/short tons. * Locks closed for winter.*

Barge rates may fluctuate depending on the month of the year, supply and demand for barges in particular locations, and issues related to the navigability of barges through the system. Those barge rates represent price approximations for grains that are to be delivered into the Mississippi port region between Baton Rouge and New Orleans. Many of these inland barge

[7] Diagram 1 is a simplification of the transportation choices for grain deliveries.
[8] USDA-GTR, Table 9: Weekly Barge Freight Rates: Southbound Only.

terminals may receive grains, either through trucks or short haul railroads. Depending on the basis point, that is, the difference between the price of grains in the local market and price in the next future market, this is an indicator to either buyers or sellers as to the best time to engage in a grain delivery transaction[9].

In terms of trucks, and also taking into consideration the basis point of a particular delivery location, they are mostly the initial transportation mode for grain exports. For instance, grains delivered to elevators with shuttle trains services to export terminals begin with a truck haul. Also, trucks may be the primary delivery mode for inland barge terminals along the Mississippi River (See Diagram 1). Then those barge terminals along the Mississippi River may deliver grains to export terminals located in the New Orleans region. According to Mike Steenhoek, executive director of the Soy Transportation Coalition[10], "The average rail haul for soybeans and grain is 900 miles. Also, emphasizing the importance of trucking we have the following: "Trucking is mostly utilized to feed into the long-haul modes — like rail and barge — vs. competing with them"[11]. According to the same source, this is a consequence of the business model adopted by railroads in which long haul transportation of commodities is a priority.

There are information tables that compare short and long haul rates for truck deliveries, based on vehicles with 80,000 lbs. gross vehicle weight limit and assuming a truck carrying 55,000 lbs or 25 metric tons of grain (Table 2 and 3)[12]. The same source explains that rates per metric ton per mile can be calculated from rates per truckload. This same information is used by the U.S. Department of Agriculture as part of the calculation of landed costs to export destinations.

Table 2. U.S. Grain Truck Market, 4th Quarter 2017

	25 Miles	100 Miles	200 Miles
North Central Region	$4.90	$3.59	$3.29
Rocky Mountain	NA	NA	NA
South Central	$4.50	$3.21	$3.10
West	NA	NA	NA
National Average	$4.64	$3.49	$3.15

[9] Based upon *Understanding Basis. Chicago Board of Trade*. https://www.gofutures.com/pdfs/Understanding-Basis.pdf

[10] The Soybean Transportation Coalition (STC) is an organization consisting of representatives from the United Soybean Board (USB), the American Soybean Association and 12 state soybean boards, striving to make U.S. transportation more effective, reliable and competitive as it is essential to the success of U.S. soybean farmers.
[11] The Trucker.Com.
https://www.thetrucker.com/News/Story/Soycoalitionwantsheaviertrucksallowedoninterstates

[12] Grain Truck and Ocean Rate Advisory: Quarterly Updates. USDA-AMS.

Table 3. U.S. Grain Truck Market, 1st Quarter 2017

	25 Miles	100 Miles	200 Miles
North Central Region	$3.98	$2.78	$2.54
Rocky Mountain	NA	NA	NA
South Central	$4.18	$3.04	$2.71
West	NA	NA	NA
National Average	$4.12	$2.95	$2.61

Note: Rate per mile, per truckload.

Truck rates for grain deliveries are a function of the delivery distance, fuel price (diesel), truck availability and utilization as well as expectation on future truck usage[13]. The distances afforded by trucks are an important component of the inland transportation system. For example, inland barge terminals and grains elevators with shuttle trains services may be fed by trucks as far as 200 miles away. This is an important component in the eventual competition among export terminals along the U.S. Gulf and Pacific Northwest regions. It also gives an idea of the range within the U.S. grain hinterland in the competition between elevators with shuttle trains services and inland barge terminals. Nonetheless, trucks needs adequate roads and bridges to fulfill their roles in the transportation system.

What could be the *contested area* for grains moving from the U.S. hinterland to either U.S. Gulf or Pacific Northwest grain export elevators? To answer that question, it is important to understand the truck range for delivery into the Mississippi River system. From the truck tables we can infer that inland barge terminals along the Mississippi River can be fed by trucks in a 200 miles radius east and west of the Mississippi River. This explain the possibilities of inland barge terminals along the Mississippi River obtaining grains from most part of the state of Iowa, Minnesota and Missouri, states that are located west of this river system. Inland barge terminals can also obtain grains 200 miles east of the Mississippi River from the states of Illinois, Wisconsin, Kentucky, Tennessee and parts of Indiana. Those states east and west of the river rank among the main producers of corn and soybeans in the United States.

In the case of regions more than 200 miles away west of the Mississippi River, railroad services become a part of the delivery equation. The following table from the U.S. Department of Agriculture published in the Grain Transportation Report provides monthly train rates from particular routes, many origins beyond the reach of the inland barge system on the Mississippi River (Table 4)[14]. We are only including some in order to have an idea of the possible *contested area* between U.S. Gulf versus Pacific Northwest. The table includes the train service, rail rates (in $ per metric tons) and the grain type transported.

[13] Ibid.

[14] Based on Table 7: Tariff Rail Rates for Unit and Shuttle Train Shipments, USDA-GTR. The information is voluntarily provided by Class I railroads.

Table 4. Tariff Rail Rates for Unit and Shuttle Train Shipments

Origin	Destination	Train Service	Grain Type	Nov. 2017 Rate ($/mt)	Jan. 2018 Rate ($/mt)
Minneapolis, MN	New Orleans, LA	Unit Train	Soybeans	$37.32	$37.61
Council Bluff, IA	New Orleans, LA	Shuttle Train	Soybeans	$49.03	$49.38
Lincoln, NE	Galveston/Houston, TX	Shuttle Train	Corn	$36.74	$36.74
Wichita, KS	Galveston/Houston, TX	Shuttle Train	Wheat	$41.42	$41.42
Amarillo, TX	Los Angeles, CA	Unit Train	Wheat	$51.75	$52.15
Grand Island, NE	Portland, OR	Shuttle Train	Soybeans	$58.98	$59.47
Sioux Falls, SD	Tacoma, WA	Shuttle Train	Corn	$49.26	$49.26
Fargo, ND	Tacoma, WA	Shuttle Train	Soybeans	$54.62	$54.62
Grand Forks, ND	Portland, OR	Shuttle Train	Wheat	$55.72	$55.72

Although not perfect in terms of including all trains services from the U.S. hinterland to export elevators, the tariff rail rates table for unit and shuttle train shipments provides a good approximation of the *contested area* for grains in the interior of the United States. Thanks to this table, we are able to draw a map with the approximated area in which U.S. Gulf *fights* for grain shipments against the Pacific Northwest (Figure 6). The *contested area* is about the size of Ecuador, that is, 295,605 km2. Railroads also adjust rates according to supply and demand for services, and take into consideration U.S. Gulf- Pacific Northwest freight rate differential to Asia and barge rates[15]. The same source also mentions studies related to barge and rail competition, stating that without competition between barge and railroads, grain exporters may pay higher railroad rates, especially the farther exporters are from the inland waterway system.

[15] *A Reliable Waterway System is Important to Agriculture*. USDA-AMS. February 2017.

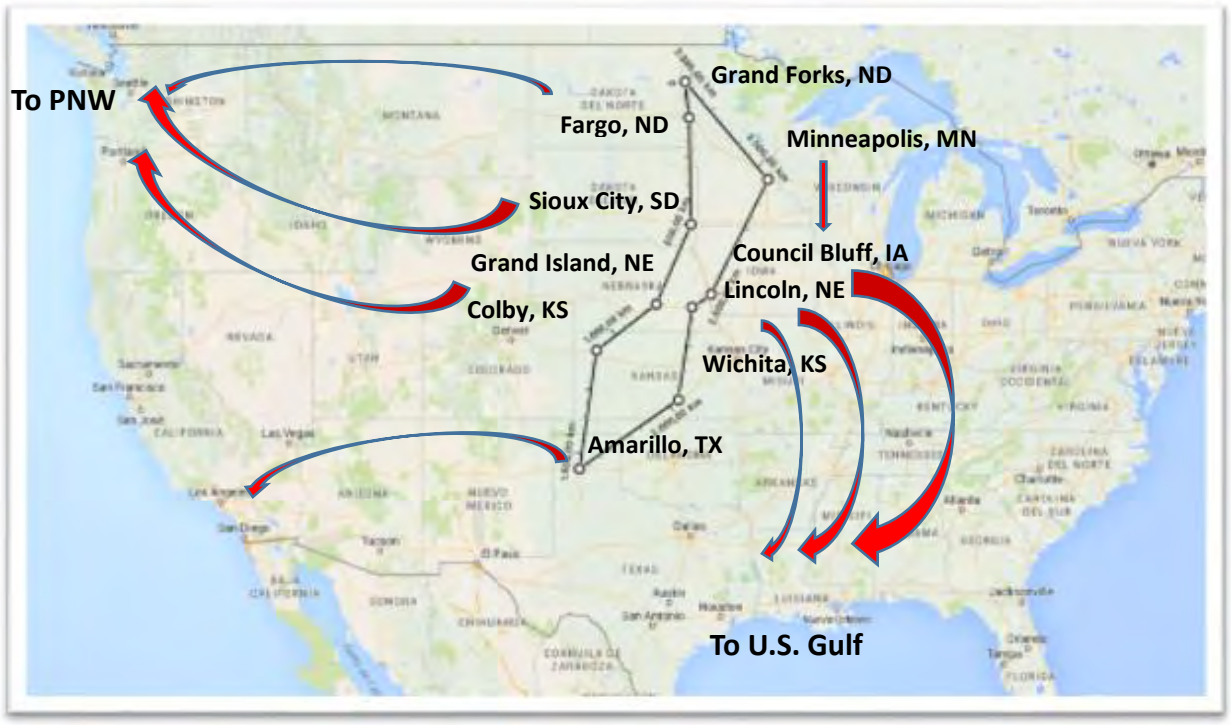

Figure 6. Map showing the approximate contested area between U.S. Gulf vs PNW in the U.S. hinterland. Drawing and calculations from Google Maps, derived from data used from Table 4. Developed by J Ho[16].

IV. The importance of the Mississippi River System to the Panama Canal Grain Trade- Maintenance and Funding for the Inland Waterway System

According to *A Reliable Waterway System Is Important to Agriculture* developed by the U.S. Department of Agriculture, "Agriculture will provide a $21.5 billion trade surplus to the American economy" and "Exports are responsible for 20 percent of U.S. farm income, also driving rural economic activity and supporting more than one million American jobs on and off the farm".[17] In other words, world trade is key to the agricultural sector of the United States, representing one of the economic activities in which the United States has a competitive advantage compared to other countries. In terms of reducing the U.S. trade deficit with China, U.S. grains and energy, including oil, LNG and LPG products, could be goods that may be purchased more by China in order to reduce this deficit[18].

Given the importance of the U.S. Gulf as the main origin of grains to the Panama Canal, -the U.S. Gulf to Asia is the main grain route-, it is very important to discuss the importance of the Mississippi River Inland System to the Panama Canal Grain Trade. The main export elevators along the Mississippi system include terminals between Baton Rouge and the Delta of the Mississippi River such as Belle Chase, Convent, Darrow, Ama, Paulina, Destrehan, Reserve,

[16] Figure 6 is only an approximation based upon the availability of unit and shuttle trains to the U.S. Gulf and PNW.
[17] Ibid. USDA, February 17, 2017.
[18] *U.S. commodity exports to China to raise amid trade talks, but volumes are capped*. Reuters, May 22, 2018.

Port Allen and Westwego. They are controlled by large trading firms such as Cargill, Archer Daniels Midland (ADM), Bunge, Louis Dreyfus, CHS and Zen-Noh.

Previously, we mentioned that corn, soybeans and sorghum are the main grain flows through the waterway and that the majority of the corn and soybean exports through the Mississippi River port system are transported through barges. However, it is important to recognize that the Mississippi River system, -the older operating locks in the United States belong to the Kentucky River locks 1 and 2 and were built in 1839[19]- , is in dire need of repairs. There are 29 locks on the Upper Mississippi River and maintenance is performed by the U.S. Army Corps of Engineers. Most of the locks were built in the 1920´s and 1930´s, thus exceeding their lifespan. According to Walter Kemmsies of Moffatt and Nichol, there have been an increase in the number of unscheduled lock outages and unscheduled breakdowns in the system[20].

One example of unscheduled incidents occurred on October 11, 2011, when a 280-foot section of the Lockport Wall in Illinois collapsed into the river[21]. Scheduled and unscheduled closures for repairs are costly both in terms of money spent and reliability of the system[22]. Furthermore, some studies estimate that disruptions at Mississippi River Lock 25 and Illinois River LaGrange Lock could result in 7,000 jobs loss and a negative impact of $2.4 billion in economic activity[23]. Given the importance of the Mississippi River System to the U.S. grain trade and other commodities, several trade associations advocate upgrading the overall inland system, including the Columbia River system in the Pacific Northwest.

Advocacy groups such as the Soy Transportation Coalition and Waterways Council, Inc. have written about the impact of unscheduled lock outages and have released a list of top ten priorities of infrastructure work. This list includes improvements in bridges, roads, rail tracks and waterway systems and the recommendations are the following[24]:

- Maintenance and rehabilitation of locks and dams to significantly reduce the potential for unexpected, widespread, and prolonged failure. Priority should be devoted to ensuring the reliability of locks and dams along the nation's inland waterways. Available funding for new construction of locks and dams should be directed first to locks and dams 20-25 on the Mississippi River.

---

[19] United States Army Corps of Engineers: *The U.S. Waterway System- Transportation Facts,* page 4. December 2005.
https://web.archive.org/web/20070703141148/http://www.iwr.usace.army.mil/ndc/factcard/fc05/factcard.pdf

[20] Presentation in the *Ag Transportation Summit 2015*, Rosemont, Illinois, August 4-5 2015.

[21] Waterways Council Inc. http://waterwayscouncil.org/key-issues/improve-system-reliability-through-infrastructure-maintenance/.

[22] Presentation in the Ag Transportation Summit 2015, Ibid. Also, *The Impacts of Unscheduled Locks Outages* prepared for the National Waterway Foundation and U.S. Maritime Administration is a good reference study for the impact of unscheduled outages. October 2017.

[23] The Agricultural Transportation Working Group, May 2017. http://www.nopa.org/wp-content/uploads/2017/05/5.1.17-ATWG-Inland-Waterways-and-Port-Priorities-.pdf

[24] American Soybean Association. https://soygrowers.com/soy-transportation-coalition-releases-top-10-wanted-list-infrastructure-priorities/

- Dredging the lower Mississippi River between Baton Rouge, Louisiana, to the Gulf of Mexico to 50 ft.
- Ensuring the Columbia River shipping channel from Portland, Oregon, to the Pacific Ocean is maintained at no less than 43 ft.
- Permit six axle, 91,000 lbs. semis to operate on the interstate highway system.
- Increase the federal tax on gasoline and diesel fuel by ten cents a gallon and index the tax to inflation. Ensure rural areas receive proportionate, sufficient funding from the fuel tax increase.
- Provide greater predictability and reliability of funding for the locks and dams along the inland waterway system.
- Provide block grants to states to replace the top twenty most critical rural bridges.
- Provide grants to states to implement rural bridge load testing projects to more accurately diagnose which bridges are sufficient and which bridges are deficient.
- Ensure full utilization of the Harbor Maintenance Trust Fund for port improvement initiatives.
- Permanent (or at least multi-year) extension of the short line railroad tax credit.

According to the Soybean Transportation Coalition, the appropriate maintenance and overhaul of locks and dams will greatly reduce the potential for unexpected and prolonged breakdowns of the system. The coalition notes that "Priority should be devoted to ensuring the reliability of locks and dams along the nation's inland waterways"[25]. They also point out that funding priority for new construction of locks and dams shall prioritize Locks 20-25 on the Mississippi River. According to the coalition, "These lock and dam sites are among the most widely utilized by the soybean and grain industries"; consequently, any failure or entanglement in these locks during harvest could severely impact the competitiveness and reliability of the U.S. grain industry. Any event that may risk the movement of grains, -including other commodities through the Mississippi River Locks System-, will have an effect on the grain flows through the Panama Canal, impacting grains destined to Asia and the West Coast of Central and South America. Failure in the Mississippi River System may favor alternative sources of grains such as the U.S. Pacific Northwest, Brazil, Argentina and others. Therefore, a reliable and competitive grain transportation system is beneficial for both American farmers and for Panama Canal grain trade.

The Soybean Transportation Coalition also release a press note and a full study about the need to provide funding for locks and dams in a more reliable manner, a study that explains "the cost escalations and project delays resulting from the current unpredictable and piecemeal funding approach", currently applied on the inland waterway system[26]. The report also identifies "potential best practices that if implemented, will enhance the likelihood of lock and dam construction and rehabilitation efforts being completed on time and within budget"[27]. In the report, researchers compared a hypothetical lock and dam project built with the current piecemeal and unpredictable funding approach compared with another project constructed with

[25] Soy Transportation Coalition. http://www.soytransportation.org/newsroom/Top10MostWantedListSummary(1-29-18).pdf

[26] Soy Transportation Coalition News Release, April 16, 2018, originating from *Predictable Funding for Locks and Dams*, *Final Report*. April 2018. Prepared by the Texas A&M Transportation Institute, for the Soy Transportation Coalition.

[27] Ibid.

a more predictable and reliable funding. According to the same source, projects could be completed on time with no cost overruns if funding from Congress is constant and reliable. On the other hand, significant cost overruns may occur if funding is unpredictable and comes bit by bit.

In terms of current funding for the inland infrastructure, the Inland Waterway Trust Fund provides around $110- $120 million per year of matching fund with revenues from the U.S. Treasury, totaling up to $220- $240 million between the two sources. The Inland Waterway Trust Fund comes from a $0.29 per gallon charge on diesel fuel used on 27 stretches of the Inland Waterway System. The inland system is 12,000 miles including the Mississippi, Ohio, Illinois, the lower Missouri rivers and the Gulf and Atlantic Intercostal waterways.

V. Conclusion- The Inland Waterway System is Important but Needs Investment

Historically speaking and into the future, cargo to and from the U.S. Gulf are very important to the Panama Canal. Grains, mostly originating from the U.S. Gulf region, will remain as one of the most important commodities for the waterway, fighting for the number one spot with petroleum products and containerized cargo. However, in order for the Panama Canal to remain relevant to the U.S. grain trade, it is important that the United States authorities provide the necessary and reliable funding for the improvements of the U.S. inland waterway system, mainly the Mississippi River locks system. This system of locks and dams, which govern traffic on the Ohio River and the Mississippi north of St. Louis, is aging. Lock failures could cripple river traffic and drag down the U.S. economy with it.

Without competitive and reliable grain flows from the U.S. hinterland to export terminals located on the U.S. Gulf to final destination in Asia, the grains flows through the Panama Canal will be severely impacted. Therefore, further investment in transportation infrastructure is necessary and will be positive to the Panama Canal. The Mississippi waterway system is an important artery for grains coming from the U.S heartland to the world market. If the United States wants to remain the supermarket to the world, this country needs to take action before it is too late. In other words, the Mississippi River and Inland System is key to the Panama Canal, not only in terms of the grain trade but also in terms of other commodities that are transported up and downriver.

Advocacy groups such as the Soy Transportation Coalition and the Waterways Council have put forward a list of top infrastructure priorities and studies related to the reliability of funding for the inland waterway in order for the U.S. to remain a viable competitor in the world market. They are keeping an eye on competition, especially Brazil, a country that, although still behind the United States in terms of infrastructure, has made progress in terms of infrastructure investment and managed to displace the former as the number one soybean supplier to the Chinese market.

Greater investment in the U.S inland waterway system will not only provide benefits to grains but will also be positive for other commodities such as coal, iron and steel, chemicals, petroleum products, project cargo and containers. Likewise, further dredging on the lower Mississippi River between Baton Rouge, Louisiana, to the Gulf of Mexico is an extra benefit for the competitiveness of U.S. exporters. Definitely, America’s economy benefits from the cost efficiencies barge transportation provides compared to transportation by truck or rail.

Finally, it is important to remember the amount of jobs dependent on the inland waterways, which, according to Tim Parker, CEO and President of Parker Towing Company and Chairman of the Waterways Council is around 541,000 jobs[28] . In terms of reducing the U.S. trade deficit with China, any possibility of increasing U.S. export commodities to China will need greater improvement in the current infrastructure. Finally, it is worth mentioning the benefits to the U.S. construction industry in terms of a regular maintenance program, and the positive impact on the U.S. energy renaissance as a result of the fracking revolution.

[28] Waterways Council Inc. Ibid.

Preferred Bibliography

- Ag Transportation Summit 2015, Rosemont, Illinois, August 4-5 2015. Presentation by Walter Kemmsies of Moffatt and Nichol.
- American Soybean Association. https://soygrowers.com/soy-transportation-coalition-releases-top-10-wanted-list-infrastructure-priorities/
- A Reliable Waterway System is Important to Agriculture. USDA-AMS. February 2017.
- Grain Truck and Ocean Rate Advisory: Quarterly Updates. USDA-AMS.
- The Agricultural Transportation Working Group, May 2017. http://www.nopa.org/wp-content/uploads/2017/05/5.1.17-ATWG-Inland-Waterways-and-Port-Priorities-.pdf
- Predictable Funding for Locks and Dams, Final Report. Prepared by Texas A&M Transportation Institute for the Soy Transportation Coalition. April 2018.
- Reuters. *U.S. commodity exports to China to raise amid trade talks, but volumes are capped*. May 22, 2018.
- Soy Transportation Coalition. http://www.soytransportation.org/newsroom/Top10MostWantedListSummary(1-29-18).pdf
- Soy Transportation Coalition News Release. April 16 2018.
- The Trucker.Com. https://www.thetrucker.com/News/Story/Soycoalitionwantsheaviertrucksallowedoninterstates
- *The Impacts of Unscheduled Lock Outages*, Center for Transportation Research, University of Tennessee and Vanderbilt Engineering Center and Operational Resiliency, Vanderbilt University. Prepared for the National Waterways Foundation and the U.S. Maritime Administration. October 2017.
- Transportation of U.S. Grains: A Modal Share Analysis (Oct 2017 update)- USDA- AMS
- Understanding Basis. Chicago Board of Trade. https://www.gofutures.com/pdfs/Understanding-Basis.pdf
- United States Army Corps of Engineers: The U.S. Waterway System- Transportation Facts, page 4. December 2005. https://web.archive.org/web/20070703141148/http://www.iwr.usace.army.mil/ndc/factcard/fc05/factcard.pdf
- USDA-GTR Dataset Table 7: Tariff Rail Rates for Unit and Shuttle Trains.
- USDA-GTR, Table 9: Weekly Barge Freight Rates: Southbound Only.
- USDA- GTR Dataset (Table 10: Barge Grain Movements).
- Waterways Council Inc. http://waterwayscouncil.org/key-issues/improve-system-reliability-through-infrastructure-maintenance/

REENGINEERING VALVE OPENING LAW TO OPTIMISE LOCK LEVELLING: SOME CASE STUDIES

by

D. Bousmar[1]

ABSTRACT

When designing a new lock, detailed hydraulic studies are usually executed to fix the layout of the filling and emptying system in order to achieve safe and efficient levelling conditions. During the lifetime of the lock, the concrete works and the culvert layout remain usually stable. On the other hand, it is often observed that the valve opening schedule evolves, as a consequence of successive maintenance or replacement. This results in a lock working in non-optimal conditions. This paper presents case studies illustrating how an abnormal working process can become standard operation, and how reengineering can restore lock performances. It highlights the benefits of a reengineering of the valve schedule, with the input of field measurements.

1. INTRODUCTION

The hydraulic design of a lock levelling has to fulfil several criteria like: (1) short levelling duration; (2) acceptable mooring forces; (3) limited levelling wave amplitude. Usually, reducing the levelling time increases the forces acting on the vessels. In some cases, modifying the design of the levelling culverts enables shorter levelling time, through e.g. longitudinally distributed or even through equal distribution filling systems. This increased culvert complexity may nevertheless impact the building cost of the lock (PIANC, 2015).

The hydraulic design usually results in an optimised design of the levelling culverts and a proposed schedule for opening the valves. During lock commissioning, the valve opening laws are implemented, tested and validated. Then, during the lifetime of the lock, it is often observed that the valve opening schedule evolves. During maintenance or replacement of electro-mechanical parts, performances and settings are not always perfectly replicated. Some technicians may adapt or tune the schedule, without refereeing to the hydraulic design team. In some cases, the reports from the original design are forgotten or even lost. As a result, the lock does not work anymore optimally.

In the last years, the Hydraulic Research Laboratory of the Service Public de Wallonie has been involved in some reengineering studies for such locks on the Walloon waterways network, Belgium. The report from these case studies illustrates how an abnormal working process can become standard operation, and how reengineering can restore lock performances. Field measurement can also provide relevant information in the absence of extensive documentation.

This paper will first present the methodology behind the case studies: flow modelling for valve schedule efficiency assessment; field measurement for data collection; and design criteria. Then, several case studies will be developed, highlighting methodological aspects and results: Lock of Havré on the Canal du Centre; Locks of Pommeroeul and Hensies on the Canal Pommeroeul-Condé (Bousmar & Libert, 2016); and three old locks (Leers-Nord, Estaimpuis, Warcoing) on the Canal de l'Espierres (Bousmar & Libert, 2017). Table 1 summarizes the main characteristics of these locks.

Lock	Dimensions	Drop	Levelling system
Havré	124 m x 12.5 m	10 m	Trough the floor
Pommeroeul	151.7 m x 12.5 m	13.5 m	Trough the floor
Hensies	149 m x 12.5 m	4.6 m	Filling: short culverts with dissipation chamber / Emptying: sluice valves in gates
Leers-Nord, Estaimpuis, Warcoing	38.5 m x 5.15 m	1.8, 2.7, 2.5 m	Sluice / grid valves in gates

Table 1: Lock dimensions and levelling systems

[1] Hydraulic Research Lab., Service Public de Wallonie, Châtelet, Belgium, didier.bousmar@spw.wallonie.be

2. METHODOLOGY

2.1 Modelling of the levelling process

For the sake of simplicity, the levelling process has been modelled in a non-coupled way. Discharge and head losses are first estimated in the culvert system, using a one-dimensional pipe model and assuming a horizontal water level in the lock chamber. The water surface evolution in the lock chamber is then estimated from a one-dimensional or a two-dimensional free surface model, using the discharge hydrogramme as an inlet condition.

The flow in each levelling culvert section *i* can be modelled using an unsteady pipe flow equation:

$$\frac{L_i}{gA_i}\frac{\partial Q_i}{\partial t} + H_{i,downstr.} - H_{i,upstr.} + \frac{\zeta_i Q_i^2}{2gA_i^2} = 0 \quad (1)$$

where Q_i is the discharge in the culvert section; L_i and A_i are the length and wetted area or the culvert; $H_{i,upstr.}$ and $H_{i,downstr.}$ are the head values at both ends of the section; and ζ_i is the head loss coefficient for the section. At each junction between culvert sections, the discharges have to comply with the continuity equation:

$$\sum Q_i = 0 \quad (2).$$

A pipe equation (1) and a discharge value Q_i are set for each culvert section; and a continuity equation (2) and a head value $H_{i,upstr./downstr.}$ are set for each junction. The number of equations equals thus the number of unknown.

This non-linear equation system is solved in an implicit way, using the following discretization with time and linearization (UCL, 2013):

$$\frac{L_i}{gA_i}\frac{Q_i^{t+\Delta t} - Q_i^t}{\Delta t} + H_{i,downstr.}^{t+\Delta t} - H_{i,upstr.}^{t+\Delta t} + \frac{\zeta_i Q_i^{t+\Delta t}\left|Q_i^t\right|}{2gA_i^2} = 0 \quad (3),$$

$$\sum Q_i^{t+\Delta t} = 0 \quad (4).$$

For symmetrical parts of the levelling system, only one side is modelled and the discharges are counted twice.

At the beginning of the simulation, all discharges Q_i are set equal to zero. For a filling simulation, the initial head values at junctions are set equal to either the head in the upstream reach $H_{upstr.}$ or in the lock chamber H_{lock}, depending on the location of the junction with regard to the closed valve. For emptying simulation, the initial head values are similarly set equal to the head in the lock chamber H_{lock} or in the downstream reach $H_{downstr.}$.

During the simulation, the head in the upstream, resp. downstream, reach are kept constant. In the lock chamber, the water level is adapted after each time step, as a function of the total incoming (positive) or exiting (negative) discharge Q_{tot}:

$$H_{lock}^{t+\Delta t} = H_{lock}^t + \frac{Q_{tot}^t \times \Delta t}{S} \quad (5)$$

where S is the lock chamber horizontal surface.

The head loss coefficients ζ_i were estimated a priori from tables (Idel'cik 1969) for friction and for singularities like contractions, expansions, bifurcations, confluences, trash racks, outlets, etc. These coefficients were kept constant during all the simulations, assuming a large Reynolds number.

Variable head loss coefficients were used only for the valves. The head loss coefficient values were dependent on the actual valve position at the given time, according to the valve opening schedule:

- Havré and Pommeroeul locks are equipped with butterfly valves Pratt-Hanrez 1B, for which a original head loss diagram from the manufacturer could be recovered;
- Hensies lock is filled through vertical lift cylinder valves. Data could be recovered from an old scale modelling study on a similar valve (LRH, 1954). Emptying is operated through flat sluice valves. The head loss coefficient for the latter was estimated as for an orifice flow;

- The 3 locks on the Canal de l'Espierres are equipped with flat sluice valves and grid valves. The head loss coefficients were estimated a priori for an orifice flow; and then fitted on field measurements (see paragraph 6).

2.2 Field measurements

As only limited data could be recovered from original design studies, field measurements were planned on each lock, excepted Hensies which is currently out of service. Measurement objectives were twofold: (1) confirming the existing valve opening schedule; and (2) recording the current filling and emptying hydrogrammes, for numerical model calibration and validation purpose.

The valve opening schedules were recorded using either a cable-actuated distance sensor fixed temporarily on the valve hydraulic jack; either a stopwatch and a measuring tape. On the Canal de l'Espierres, video recording was used to support stopwatch measurements. Water levels in the lock chamber were recorded with a temporary pressure sensor "Diver" with integrated data logger. The sensor was fixed either on a lock ladder, either on a concrete block immerged in the water. Details on such measurement methods can be found in Bousmar et al. (2017).

2.3 Design criteria

As quoted above, a proper hydraulic design of a lock filling/emptying has to fulfil several criteria (PIANC 2015): levelling duration; maximum discharge; forces exerted on vessels; cavitation risk. The levelling duration has to be limited. In the present case studies, it is wanted that the levelling duration remains identical or decreases after reengineering. Target values are listed in Table 2. The maximum discharge should also be limited, to reduce levelling wave amplitude in the adjacent reach. Target values were set according to field measurements of wave propagation (Swartenbroekx et al., 2014); or to estimations of waves amplitude, based on actual discharge values and consideration on reach lengths. The lower maximum filling discharge at Havré lock is due to the presence of Strépy ship lift at the other end of the upstream reach. The water level in the mobile chambers of the ship lift has to be kept in a limited range, to keep the balance with the counter weight. Accordingly, it is necessary to reduce levelling waves amplitude in this reach.

Forces acting on vessels during the levelling process can be estimated by different approaches: actual forces in mooring lines; total hydrodynamic forces; total hydrostatic forces; or estimation based on water surface slope (PIANC 2015). In the present case studies, the forces were estimated from the water surface slope, computed without vessel in the lock chamber. For Havré, Pommeroeul and Hensies locks, the target vessel is a CEMT Class Va vessel. Recommended maximal forces are fixed to 0.85 to 1.15 ‰ of the weight of the water displacement of the vessel, depending of the presence of floating or fixed bollards (PIANC 2015). To account for the modelling simplification, the criteria was fixed to a maximum water slope S_w = 0.50 ‰ (see Table 2). For the Canal de l'Espierres locks, the recommended maximal forces for a CEMT Class I vessel would be in the range 1.50 .. 2.00 ‰. Accordingly, a criteria was fixed for the global water slope $S_{w,glo}$ computed on the whole lock length (end to end). However, these locks are mainly used by smaller recreational boats. For these, the admissible force can raise up to 3 ‰ (PIANC 2015). This criteria is applied to a local water slope $S_{w,loc}$ computed on a length of 10 m, considering the maximum local value along the lock length.

Lock	Duration		Max. discharge		Max. water slope
	Filling	Emptying	Filling	Emptying	
Havré	10 min	9 min	40 m³/s	60 m³/s	0.5 ‰
Pommeroeul	9 min	9 min	75 m³/s	75 m³/s	0.5 ‰
Hensies	9 min	9 min	30 m³/s	30 m³/s	0.5 ‰
Leers-Nord, Estaimpuis, Warcoing	8 min (6 min)	8 min (6 min)	4.5 m³/s (3.0 m³/s)	4.5 m³/s (3.0 m³/s)	Glob.: 1.5 ‰ (1.0 ‰) Loc.: 3.0 ‰ (2.0 ‰)

Table 2: Design criteria. Optimal target values in parenthesis.

Cavitation risk is only to be considered at the valves of Havré and Pommeroeul locks, who present the largest total head. Cavitation risk is estimated through a cavitation number C (Savary & Libert, 2013):

$$C = \frac{H_2 - H_{vap}}{\Delta H_{1-2} + v_2^2/2g} \tag{6}$$

where H_2 and v_2 are the head and the mean velocity in the section downstream the valve; $H_{vap} \approx 0.30$ m is the vapour tension of water; and ΔH_{1-2} is the head loss at the valve. $C < 2.5$ means cavitation inception; and $C < 1$ means developed cavitation with damage inception.

A last design constraint is the compatibility of the recommended valve schedule with the electromechanical equipment characteristics. For Havré, Pommeroeul and Hensies locks, the electromechanical parts will be replaced. Valve schedules can therefore be fixed more easily. Valves are operated by hydraulic jacks. Constant opening rates will be preferred. Different successive opening rates can also be considered if required. At the locks on the Canal de l'Espierres, no replacement of the electromechanical equipment is foreseen. As the hydraulic jacks have a very short stroke and operate too fast, the valve schedule will be discontinuous with stepwise openings. Such an opening schedule is however known to generate significant waves in the lock chamber and is not to be preferred when possible (PIANC 2015).

3. LOCK OF HAVRÉ

3.1 Available data

Figure 1 shows the lock of Havré. The chamber is 124 m long and 12.5 m wide. An intermediate gate enables locking in a half chamber, to save water. The levelling is operated through a distribution system located in the lock floor. Figure 2 shows the central culvert and a floor diffuser. This system is supplied through longitudinal culverts in the lock walls. Due to the intermediate gate, the distribution system is actually split in an upstream and in a downstream part. Discharge is controlled through 6 butterfly valves of diameter 3 m, symmetrically located in the upstream, intermediate and downstream heads.

Although this lock dates from the early 1970ies, no original design report could be recovered. Only the original valve opening schedule was recovered in the as-built files. This schedule is plotted in red on Figure 3. It is a complex multispeed schedule. It starts with a fast opening till 45°, followed by two lower speed phases. The last 10° are eventually operated at the fast initial speed.

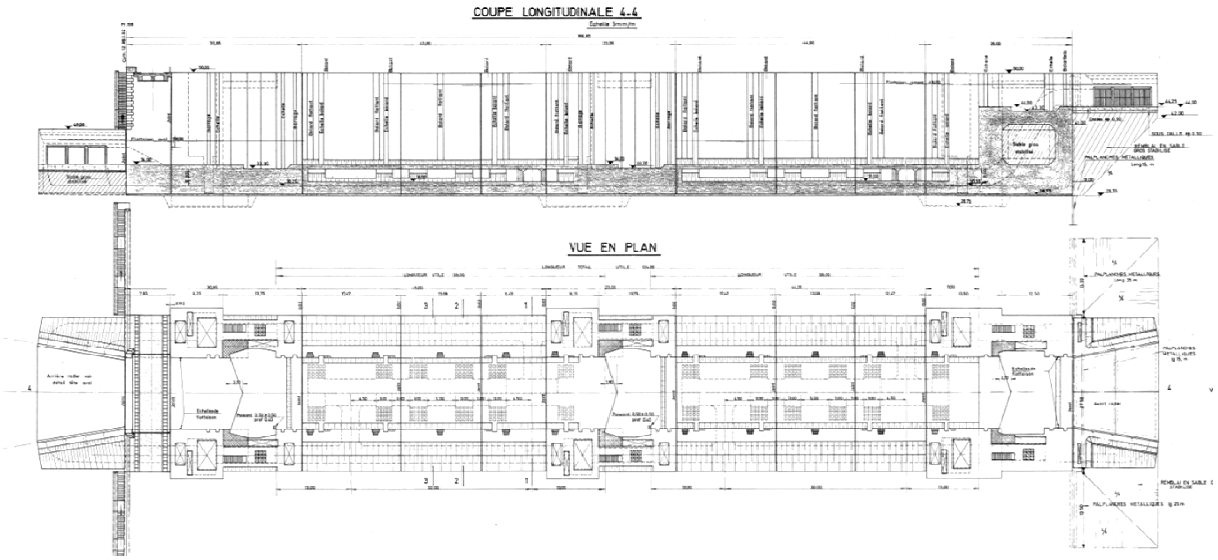

Figure 1: Lock of Havré. Elevation and plan.

Figure 2: Lock of Havré. Views from inside the central diffusion culvert.

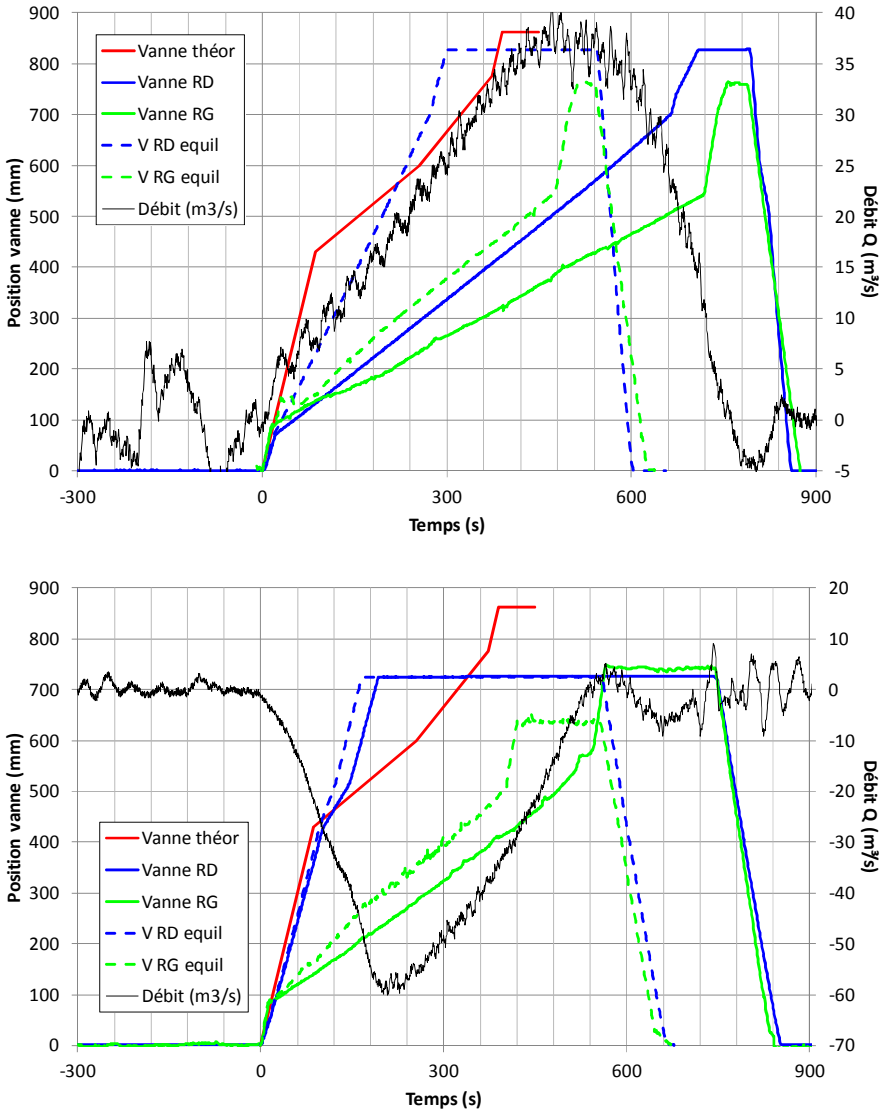

Figure 3: Lock of Havré. (a) Filling; and (b) emptying. Measured hydrogramme in black. Valve opening schedule (given as hydraulic jack position): theoretical curve (red), measured for right (RD-blue) and left (RG-green) valves. Plain curve is during levelling, while dashed curve is measured at equilibrium with no head on the valve.

Field measurements were organised to collect the actual valve opening schedule and the levelling hydrogrammes for both filling and emptying. Those data are also plotted on Figure 3. It clearly appears that the actual valve schedule differs significantly from the original one found in as-built files. Significant discrepancies even appear between left and right side valves. The only similarities between the actual and the theoretical schedules are their multispeed aspect and, up to a certain extent, the fast and low speeds of the different phases. Surprisingly, it was also observed that the valves operated faster when the lock chamber was at equilibrium (thus with no head and discharge) than during actual levelling. As the hydraulic jacks are operated at a constant speed, fixed by a constant oil discharge, no explanation was found for this last observation.

3.2 Modelling of the lock levelling

In a first stage, the culverts of the levelling system were schematized as a succession of prismatic culverts and singularities. Head loss coefficients were estimated for each part, as depicted in § 2.1. Before going through the actual culvert flow modelling by solving the pipe equations system, a simplified analysis of the lock filling was done. This analysis was done for an estimated maximum discharge of 60 m³/s with the valve fully opened and assuming a uniform distribution of the flow through the 24 floor diffusers. Figure 4 shows the head loss estimated in each culvert part for these idealised discharge values.

The culvert system looks like a longitudinally distributed filling system similar to the ones depicted in the literature (PIANC, 1986; 2009). From this simplified analysis, it appears that the system is not equilibrated: (1) the head loss in the longitudinal culvert from inlet to junction with the central culvert is lower for the first half chamber than for the second half chamber; (2) the head loss from the inlet to this junction is lower in the right side culvert; and (3) the head loss in the floor diffusers is much lower than in the longitudinal culverts. As a result, the discharge will be unevenly distributed between the central culverts; and, as the head loss is not large enough in the diffusers, no discharge control can be anticipated at this level.

A last observation from this simplified analysis is that the total head loss at peak discharge with the valves fully opened is lower than 2 m; whereas the total drop of the lock is 10 m. If the valves are opened too fast, the actual discharge resulting from this high drop will be much higher than 60 m³/s. In other words, the valves seem oversized.

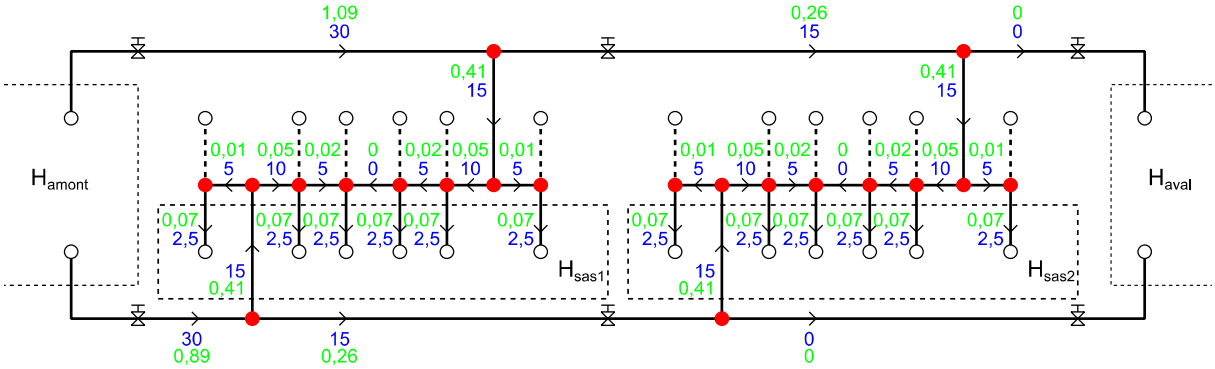

Figure 4: Lock of Havré. Simplified estimation of head losses (in green) and discharges (in blue). Dashed lines in the culvert system are symmetrical parts. White nodes are connected with boundary levels; red nodes are internal junctions.

A detailed numerical modelling was accordingly necessary for a deeper analysis. Figure 5 shows the hydrogramme obtained with the actual valve schedule (“Q insituV”). This hydrogramme is very close to the measured one. This validates the modelling done and the setting of the head loss coefficients. Figure 6 shows the actual discharges from each floor diffuser, also computed for the actual valve schedule. As anticipated from the simplified analysis, the distribution is uneven, with more discharge in the first half chamber, and also with different discharges between diffusers in the same half chamber. This uneven discharge distribution generates waves in the lock chamber. The water surface slope, computed on the total lock length is shown on Figure 7. The maximum values are in the range 0.15 ‰. Such values are acceptable with regard to the design criteria.

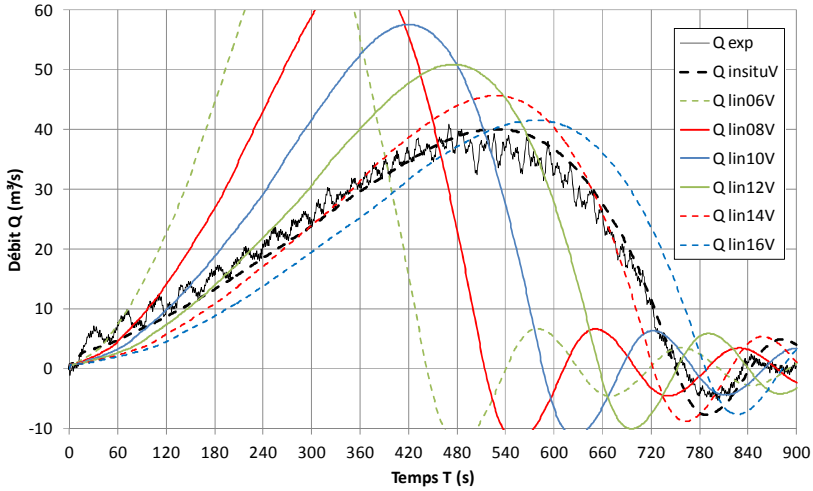

Figure 5: Lock of Havré. Filling hydrogramme, computed for the actual valve opening schedule ("Q insituV") and for linear valve openings ("Q linXXV") in XX minutes.

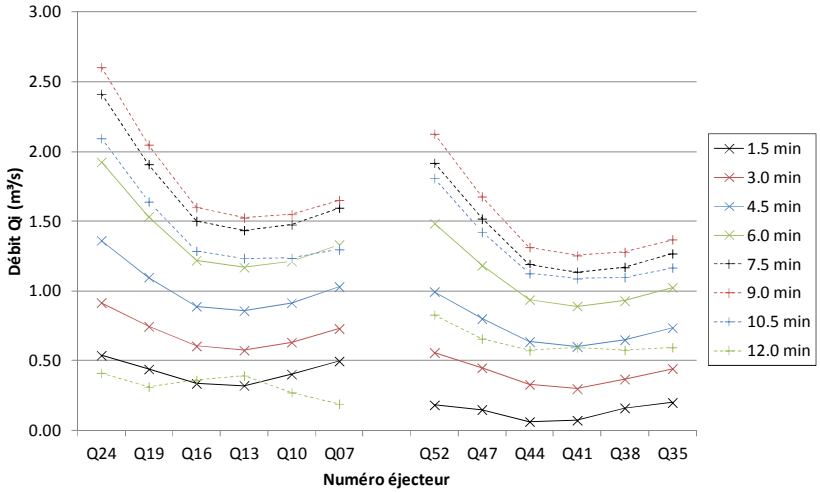

Figure 6: Lock of Havré. Discharge distribution between floor diffusers. Filling computed with the actual valve opening schedule.

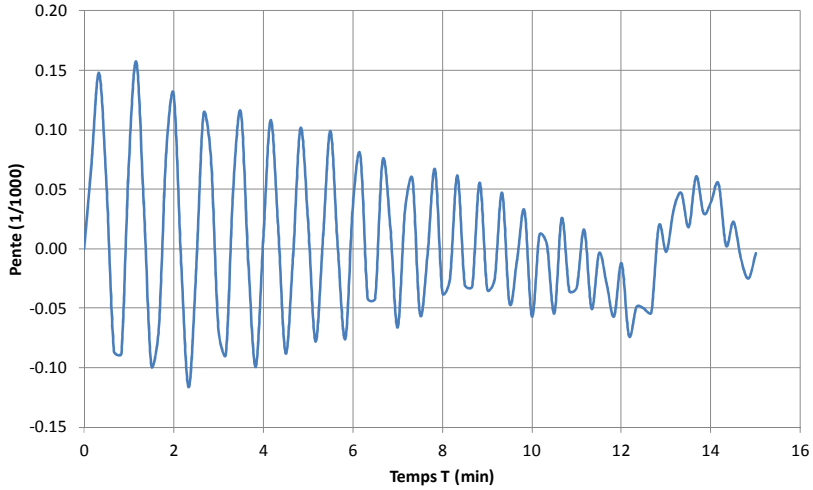

Figure 7: Lock of Havré. Water surface slope in the lock chamber. Filling computed with the actual valve opening schedule.

Using this validated numerical model, different valve opening schedules were then tested for the lock filling. At first, for the sake of simplicity, linear openings were tested, operated at a constant speed. Figure 5 shows the results obtained with a total opening duration varying from 6 to 16 minutes. For the fastest valve opening (6 minutes), the maximum discharge is significantly larger than the admissible discharge as listed in Table 2. This confirms that the total head losses in the filling system are too low and that the valve is probably oversized. The maximum discharge remains too high up to a linear valve opening in 14 minutes. A linear opening is 16 minutes results in an acceptable maximum discharge. But, with such a valve schedule, the levelling duration equals 13 minutes, which is too long. Additionally, the valve movement continues for 3 minutes after the levelling is completed. This again confirms that the valve is oversized. From a technical point of view, such a schedule is also not acceptable, as the hydraulic group that operates the jacks of the valves has to be available as soon as the levelling is finished, to operate the lock gate jacks.

As no optimal solution could be found with a unique valve opening speed, further tests were performed with a bilinear valve schedule, starting with an opening at high speed, followed by a second step at lower speed. With such schedules, no filling time is lost during the first opening step, as the valve is operated fast at the angles were the opening is too low to be efficient. The opening rate is then reduced to avoid too large discharge at a more efficient opening angle. Figure 8 shows the optimized hydrogramme ("Q opti4") compared to the existing one. The filling duration is reduced by more than 2 minutes. The corresponding valve schedule is shown on Figure 9: the valve is opened at 0.30°/s till an angle of 36°. The opening rate is then divided by 5 to 0.06°/s. As the valve opening duration is again longer than the filling time, a third opening step at high velocity is introduced to open the last 30° at the high speed (0.30°/s, "Q opti4f").

With this optimized valve schedule, the computed water surface slope remains below S_w = 0.17 ‰. The minimum value of the cavitation number computed with (6) is C = 1.63. C remains below 2.5 during 204 s indicating possible cavitation, but with limited risk of damage.

A similar optimized valve schedule could be found for lock emptying, with a longer first opening step till an angle of 54°, as the maximum allowed discharge is larger than for filling.

The analysis of the levelling process for the lock of Havré resulted in complex valve opening schedules presenting three speed steps. These schedules present a shape similar to the schedule found in the as-built files but they were re-optimized for the actual design criteria. Notably, the lower maximum discharge during filling imposes a shorter first opening step compared to emptying. The analysis also highlighted that these complex schedules probably result from oversized levelling valves.

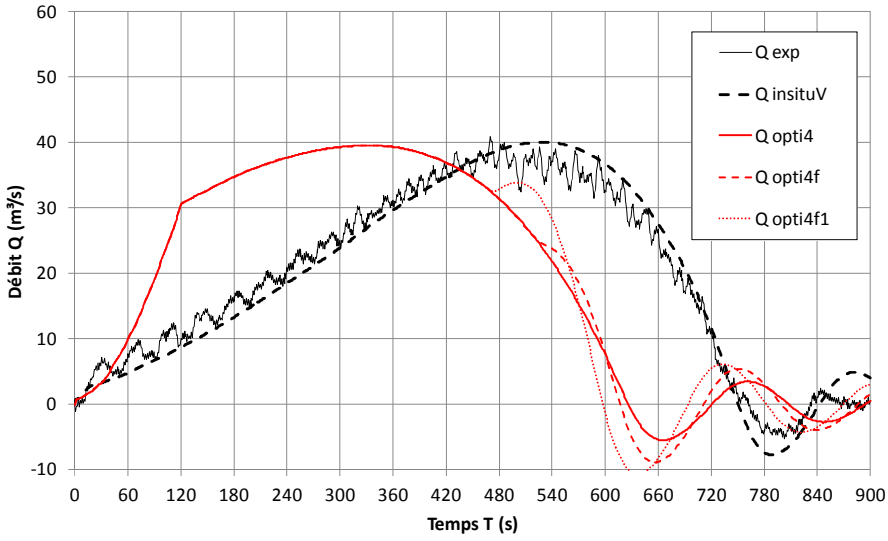

Figure 8: Lock of Havré. Filling hydrogramme, computed with the optimized valve opening schedule ("Q opti4").

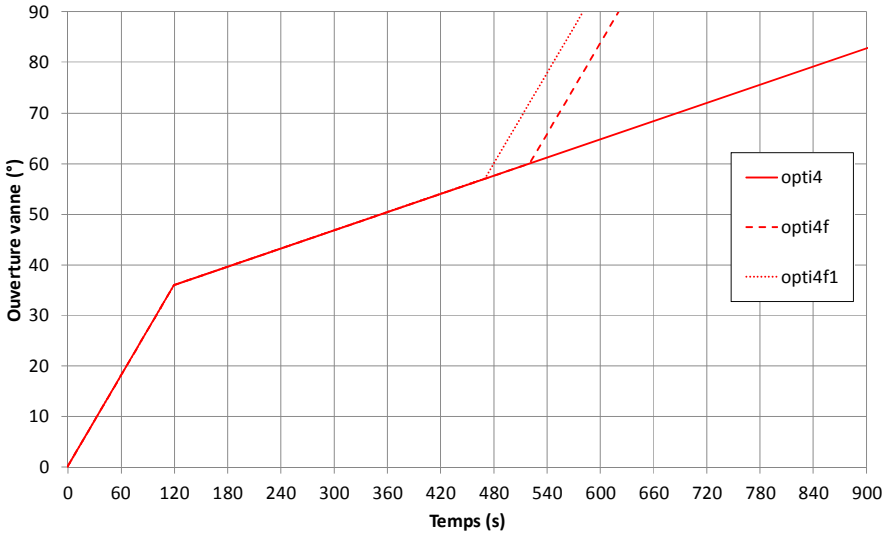

Figure 9: Lock of Havré. Optimized valve opening schedule for filling hydrogramme.

3.3 Robustness of the valve schedule

Field measurement of the current valve opening schedule showed that this schedule had been significantly altered since the lock commissioning. Specific control procedures will have to be implemented in the planning of the maintenance operations to ensure that the proposed schedule won't be affected similarly. Additionally, a sensitivity analysis was performed to check whether small tuning errors could affect the levelling hydrogramme. Two parameters were tested for the first opening step: (1) the duration was increased or decreased by 10 s, resulting in a 3° angle error; and (2) the opening speed was increased or decreased by 10 %. The error on the opening step duration was the most significant, with an impact of up to 5 m³/s on the maximum discharge; and of 30 s on the levelling duration. These results should provide guidance on the acceptable tolerances of the electro-mechanical system tuning.

The hydrogramme was also computed for several special levelling cases, to further check its robustness: (1) operation with one valve out of order; (2) operation on a half-chamber, using the intermediate gate and valves; and (3) emergency stop. When levelling with only one valve, the levelling duration is logically found longer, but the maximum discharge and water slope remain compliant with the acceptance criteria. When operating a half chamber, it was found that the intermediate gates should be operated with the same schedule than the upstream valves. Using the schedule of the downstream valves results in a too large maximum discharge.

An emergency stop may be requested if for example one vessel line is blocked on a fixed bollard. The valves should then be closed at their maximum speed (here 1.5°/s) to minimize the residual water level rise in the lock chamber. The resulting discharge gradient will cause large wave and water surface slope in the chamber. Two cases were tested for an emergency stop during lock filling: at the end of the first opening step (36°), to maximum the discharge gradient, and at the peak discharge, to maximise the residual level rise. Both cases were investigated at maximum closing speed (1.5°/s), and at half closing speed (0.75°/s).

The largest residual level rises were observed when stopping at the peak discharge: 0.28 m at the maximum closing speed, and 0.54 m at half speed. Figure 10 shows the resulting water surface slope. The sudden discharge gradient causes significant waves, notably for a closing at maximum speed starting at 36° ("opti4Ur"). The maximum slope S_w = 1.5 ‰ is 3 times larger than the acceptance criteria. Closing at half speed reduces this maximum slope to S_w = 0.9 ‰. However, regarding the residual level rise, such a slope was found acceptable for an exceptional situation like an emergency stop.

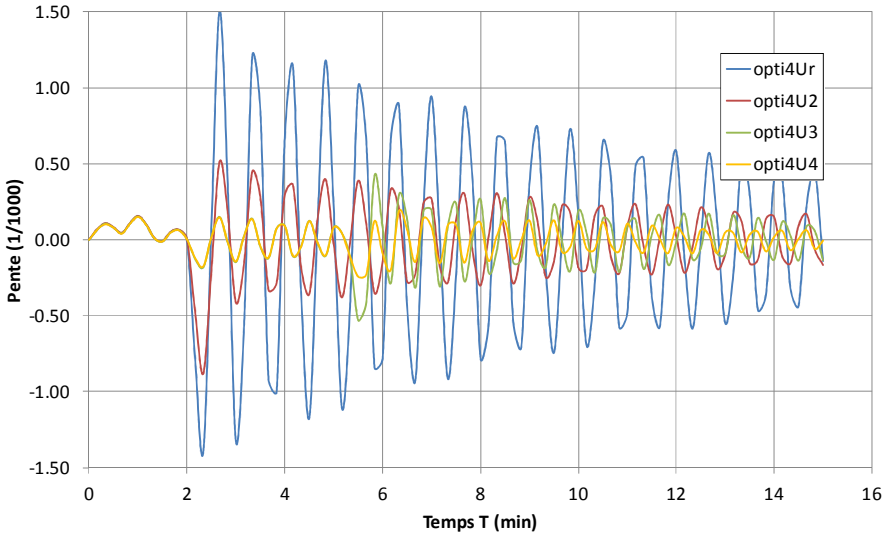

Figure 10: Lock of Havré. Water surface slope in the lock chamber. Emergency stop during filling (Ur, U2: at 36°; U3, U4: at 48°; closing speed: Ur, U3: 1.5°/s, U2, U4: 0.75°/s).

4. LOCK OF POMMEROEUL

The lock of Pommeroeul is 151.75 m long and 12.5 m wide (Figure 11). An intermediate gate enables locking in two half chamber, of non-equal length. As in Havré, the levelling is operated through a distribution system located in the lock floor. Discharge is controlled through 4 butterfly valves of diameter 3 m. The central culvert is separated in two parts. It is connected to the right side longitudinal culvert in the upstream half lock; and to the left side longitudinal culvert in the downstream half lock. Accordingly, the levelling in a half chamber is obtained by operating only one valve, and no intermediate valve is needed.

As for Havré, only the valve opening schedule could be recovered from the original studies. It is a 4 steps multispeed schedule. Field measurements highlighted that this schedule has also been significantly altered with time.

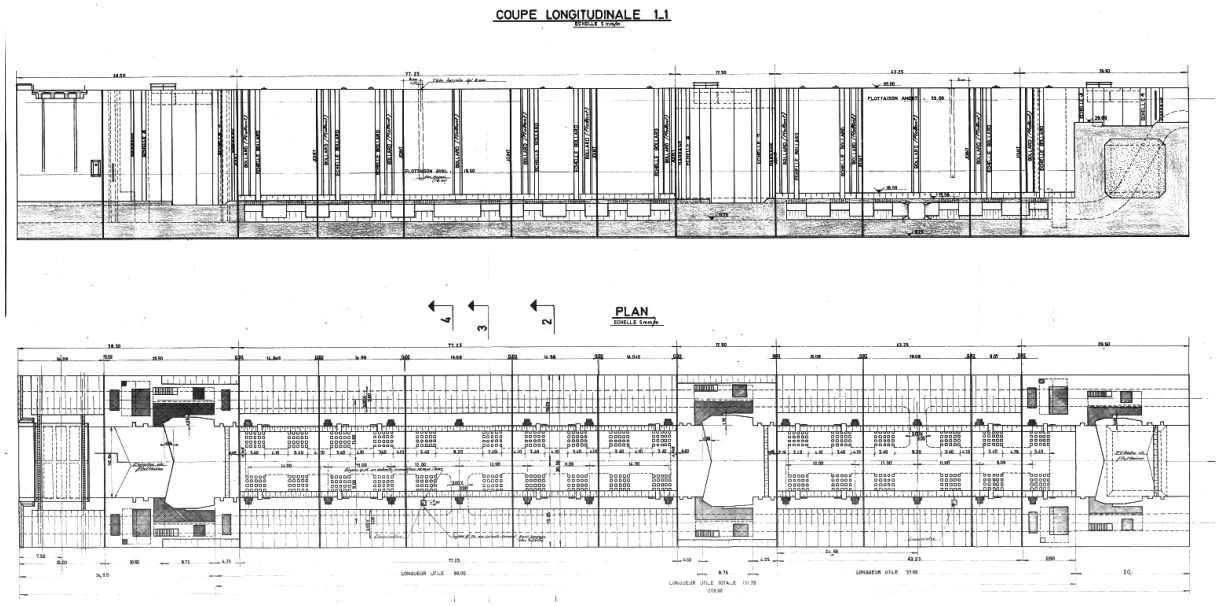

Figure 11: Lock of Pommeroeul. Elevation and plan.

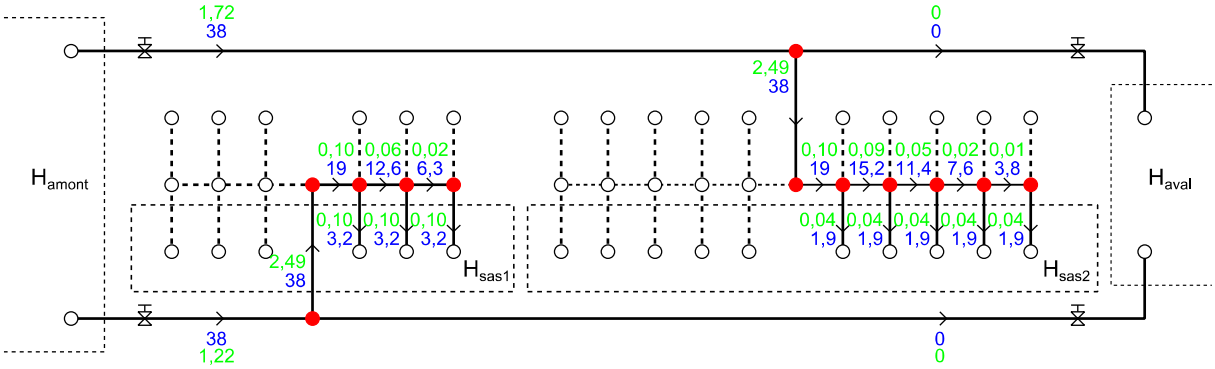

Figure 12: Lock of Pommeroeul. Simplified estimation of head losses (in green) and discharges (in blue). Dashed lines in the culvert system are symmetrical parts. White nodes are connected with boundary levels; red nodes are internal junctions.

Figure 12 shows the results of the preliminary estimation of head losses in the levelling system. In this simplified modelling of the lock filling, a peak discharge Q = 76 m³/s is equally distributed between both longitudinal culverts and the upstream valves are fully open. As for Havré lock, it appears that the system is not equilibrated: (1) due to the different lengths of both half-chambers, the discharge distribution between different number of diffusers won't be equilibrated; (2) the head loss from the inlet to the junction with the central culvert is lower in the right side culvert; and (3) the head loss in the floor diffusers is much lower than in the longitudinal culverts. No uniform discharge distribution can be expected from such a layout. Additionally, the total head loss at peak discharge with the valves fully opened is lower than 4.5 m, for a total drop of the lock equal to 13.5 m. Again, the valves seem oversized.

As for Havré lock, a more comprehensive analysis was performed through numerical modelling. First simulations were run for the existing valve opening schedule. Some limited tuning of a head loss coefficient was necessary to optimise the quality of the results compared to field measurements: on the transverse culvert that links the longitudinal and central culverts, the local head loss coefficient was reduced from ζ = 2.55 to ζ = 1.55 for both filling and emptying.

Figure 13 shows the distribution of discharge between the floor diffusers during a filling simulation. Obviously, the upstream diffusers contribution is larger than the contribution from downstream diffusers in the beginning of the filling; while the trends invert during the filling. As a result, significant waves are observed in the lock chamber.

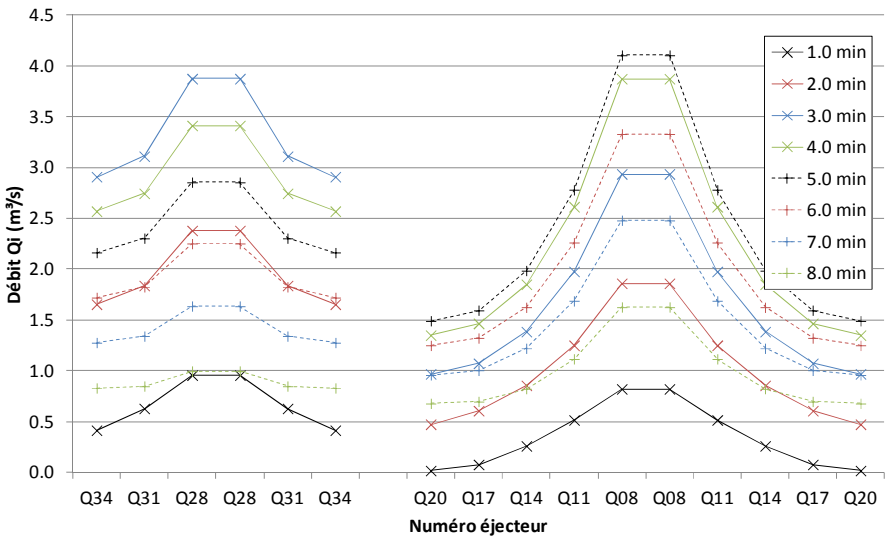

Figure 13: Lock of Pommeroeul. Discharge distribution between floor diffusers. Filling computed with the actual valve opening schedule.

The calibrated and validated numerical model was then used to define an optimized valve opening schedule. Due to the valve oversizing, linear opening turned out to be inefficient, resulting either in a too large discharge, either in a too long levelling duration. A complex schedule with 3 steps similar to Havré was eventually adopted: high opening speed in the beginning (180 s at 0.30°/s, till 54°); lower speed to control the peak discharge (280 s at 0.075°/s, till 75°); high speed to conclude the valve opening within the levelling duration (50 s at 0.30°/s). Compared to Havré, the transition between high and low speed occurs later: the total head loss is indeed higher; and the admissible peak discharge is also higher. The valve opening schedule for emptying is similar to the one for filling, as the admissible peak discharges are equal.

The robustness of the valve opening schedule was also tested. Sensibility analysis leads to results quite similar to Havré. As could be expected from the levelling system layout, asymmetric filling with only one valve leads to non-uniform discharge distribution. Thanks to the reduced total discharge, resulting water slopes remain below S_w = 0.30 ‰. Good results are also obtained when levelling on a half-chamber. Due to its shorter size, the upstream half-chamber is filled faster than the downstream half-chamber.

In case of emergency stop, the residual level rise is 0.49 m at maximum valve closing speed, and 0.93 m at half closing speed. These values are higher than at Havré, due to the larger peak discharge. On the other hand, maximum water slope at maximum speed is S_w = 0.67 ‰. This value remains admissible in such an exceptional case.

5. LOCK OF HENSIES

The lock of Hensies differs from Havré and Pommeroeul by its lower drop of 4.6 m and by the simpler layout of its through-the-head levelling system (Figure 14). The filling is operated through short culverts and a dissipation chamber located under the head floor. The filling discharge is controlled by a lifting cylindrical valve. The intermediate and downstream mitre gates are fitted with sluice valves. This lock is out of service since the mid 1990ies. It was therefore not possible to measure in-situ the valve opening schedule. Only the theoretical schedule for downstream sluice valve could be recovered in the as-built files. This schedule includes 3 phases operated at 3 different opening speeds.

An accurate modelling of the levelling requires a good knowledge of the head loss at the cylindrical valve and in the dissipation chamber. The variation of the head loss coefficient of the valve with its opening was estimated from scale model measurements done on a similar valve for Marchienne lock as depicted on Figure 15 (LRH, 1954). The loss coefficient for the dissipation chamber was set to ζ = 10, according to scale model measurements done on a similar geometry (UCL, 2013).

Linear valve opening at constant speed are tested in a first stage. Figure 16 shows the filling curves and hydrogrammes for openings in 120, 180, 240, 300 and 360 s. The “theor” curve corresponds roughly to the opening schedule of the downstream sluice valve found in the records. Increasing the duration of the valve opening has an impact on the peak discharge. When the opening duration is longer or equal to 180 s, the peak discharge is below the maximum admissible discharge. On the other hand the opening duration has only a limited impact on the filling duration: +95 s, when opening in 360 s instead of 120 s. This shows that the head losses are mainly controlled by the culverts and not by the valve.

As Hensies lock is filled through the head, longitudinal waves will be more important and the water slope criteria will be more significant. Discharge gradients should be avoided to reduce wave amplitude (PIANC, 2015). Figure 17 clearly shows that the speed step at 75 s in the “theor” opening schedule generate large waves in the lock chamber. With the linear opening schedule, the larger waves are observed at the beginning of the filling process. For a valve opening in 120 s, the peak water slope S_w = 0.64 ‰ is larger than the admissible criteria. When the valve is opened in 180 s, the peak water slope reduces to S_w = 0.42 ‰. Accordingly, a linear valve opening in 180 s is an optimal solution.

A similar analysis showed that an optimal emptying can be obtained with a linear opening of the sluice valves in 360 s.

The robustness of these two valve schedules was also tested. As the opening is operated at a constant speed, and as the culvert head losses control the filling process, the sensitivity to the schedule setting is very low. Asymmetrical filling was also less sensitive as the levelling is operated through the head. For an emergency stop, the residual rise is 0.40 m, with a maximal slope S_w = 1.32 ‰.

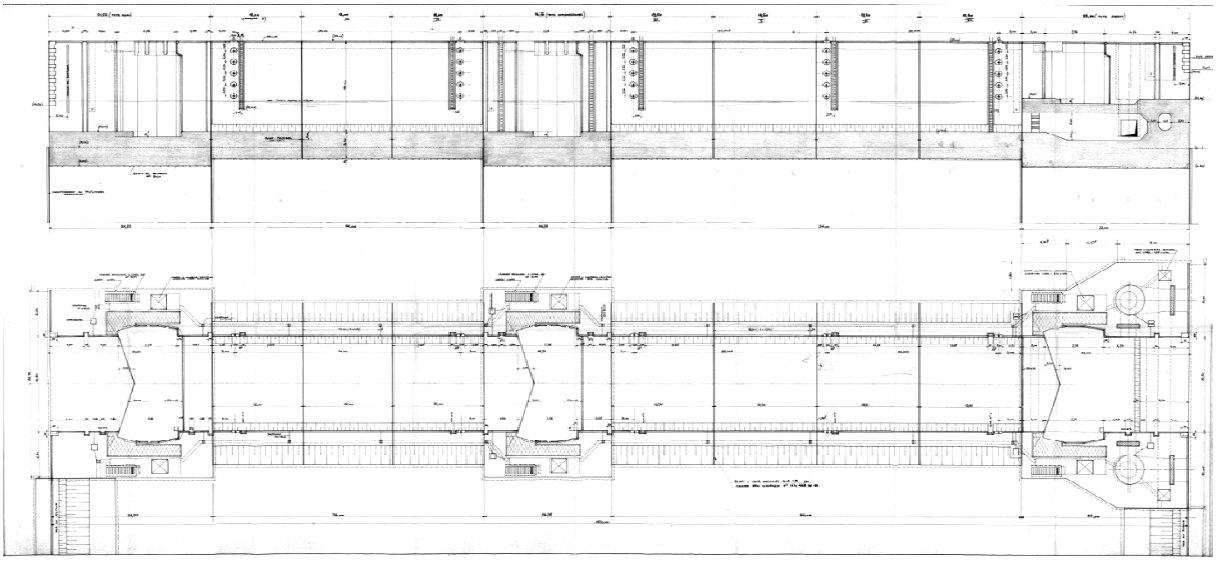

Figure 14: Lock of Hensies. Elevation and plan.

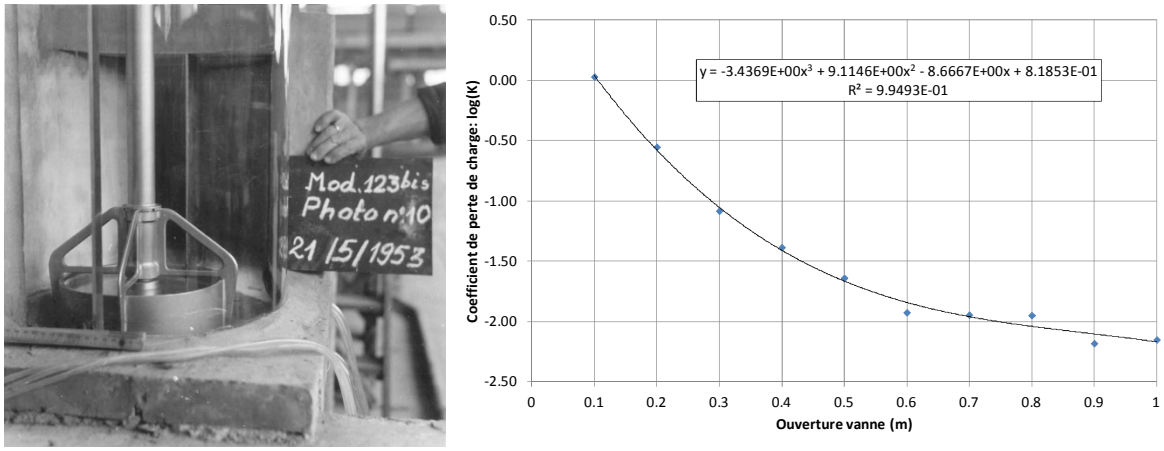

Figure 15: Scale modelling of Marchienne lock cylindrical valve. (a) Model (LRH, 1954); and (b) measured head loss parameter $K = \zeta/2gA$.

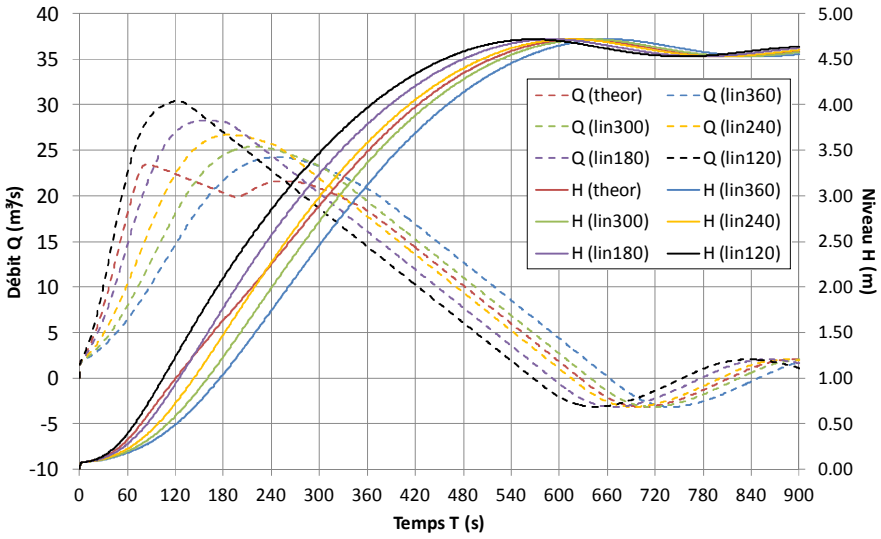

Figure 16: Lock of Hensies. Filling curves and hydrogrammes, computed for linear valve openings ("Q linXXX") in XXX seconds.

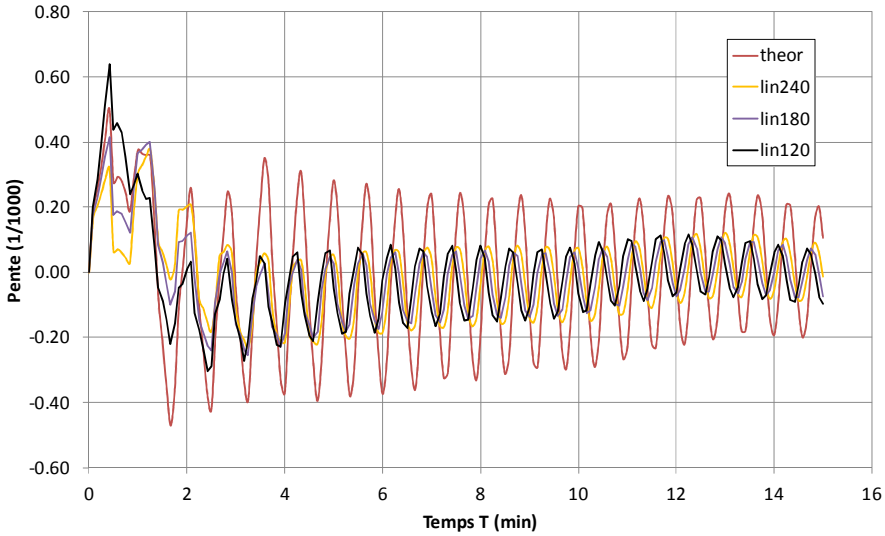

Figure 17: Lock of Hensies. Water surface slope in the lock chamber, computed for linear valve openings.

6. LOCKS ON THE CANAL DE L'ESPIERRE

The last case study covers three old locks (38.5m x 5.15m x H 1.8 .. 2.7m) on the Canal de l'Espierres (Figure 18a). These lock dates from the 19th century. They are equipped with either grid valves with a very short stroke of 150mm (Figure 18b), either with sluice valve with a stroke of 450mm, both located in mitre gates. Twelve years ago, the manual gears system actuating the valves was replaced by hydraulic jacks. According to as-built files, the opening speed of these jacks is 25 mm/s. Position is controlled by automate. The jack is operated in successive steps, with opening phases duration fixed in seconds, and stand-by phases duration fixed in minutes.

Local staff complained about poor levelling conditions: too long valve opening schedule during filling, and too large water movement in the lock chamber during emptying. These complaints were quite inaccurate and possibly subjective. This justified field measurements to obtain a reliable diagnosis before further analysis and reengineering.

Figure 18: Lock of Leers-Nord: (a) General view; and (b) grid valve in the upstream gate

Figure 19 shows the recording of a filling and an emptying sequence at Warcoing lock, operated in automatic mode (450 mm high sluice valves in the upstream gate, and 3 x 150 mm high grid valves in the downstream gate). The upstream valves open in 4 steps. It is nevertheless observed that the 2 last steps occur after the filling is completed. The filling lasts 8'18''; while the valve opening sequence lasts 14'15". The emptying lasts only 3'21". Significant waves were visually observed in the lock chamber. Due to technical problems (end of travel sensor not closed, valve blocked in partially opened position),

it was not possible to record fully automated sequences at Leers-Nord and Estaimpuis. Similar observations could nevertheless be collected on valve schedules and filling curves.

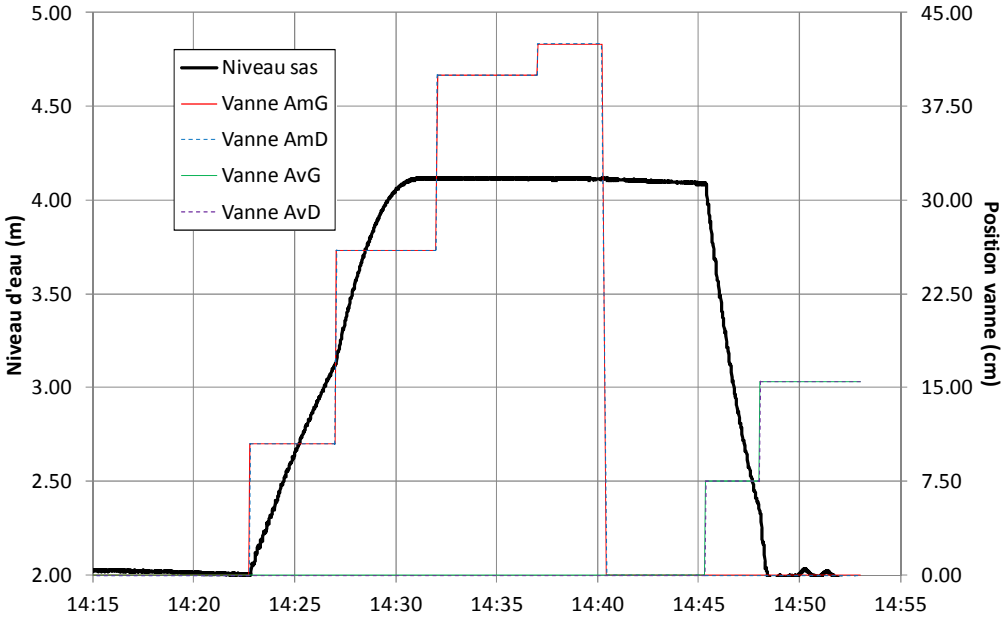

Figure 19: Lock of Warcoing: filling and emptying curve, and valves position.

For the modelling of the lock levelling, the flow equation (1) reduces to a single equation and the inertia term is almost negligible. All the head losses are concentrated at the valves modelled as orifices. According to Idel'cik (1969), the head loss coefficient for an orifice similar to the sluice valve could be in the range $\zeta = 2.7 .. 2.9$. The grid valve in fully opened position could be assimilated to a rack with cylindrical bars and $\zeta = 1$.

From the levelling measurements, it was possible to identify the values of the head loss coefficients that give the best fit between recorded and modelled levelling curves. Figure 20 shows an example of such a fitting for the downstream grid valves at Estaimpuis. The best fit is obtained with a value of $\zeta = 4.17$ at an opening of 90 mm, and $\zeta = 1.31$ at full opening. Similar fitting were obtained for all measurements, leading to a range of ζ values. Additionally, uncertainties up to 20 mm have to be considered on the initial valve position, and accordingly on all valve positions. This results in uncertainty on the ζ value. Figure 21 summarizes the observed values of the head loss parameter $K = \zeta/2gA$, as a function of the valve position, compared to values computed with different values of the head loss coefficient ζ. Eventually, it has been assumed that ζ varies linearly with the valve position, from $\zeta = 4$ for a closed valve to $\zeta = 1$ for a fully opened valve. Similar fittings were obtained for the sluice valves, with a head loss coefficient varying linearly in the range $\zeta = 2.85 .. 4.00$.

With the so-computed levelling hydrogrammes, it was possible to compute water movements in the lock chamber. Figure 22 shows the global and local maximum water slopes recorded during Warcoing lock emptying. These results confirm the visual observation of large waves occurring in the lock chamber. Local slopes up to $S_{w,loc} = 8$ ‰ are observed. A first peak corresponds to the first valve opening step that generates a first discharge burst. A second peak is observed at the second opening step.

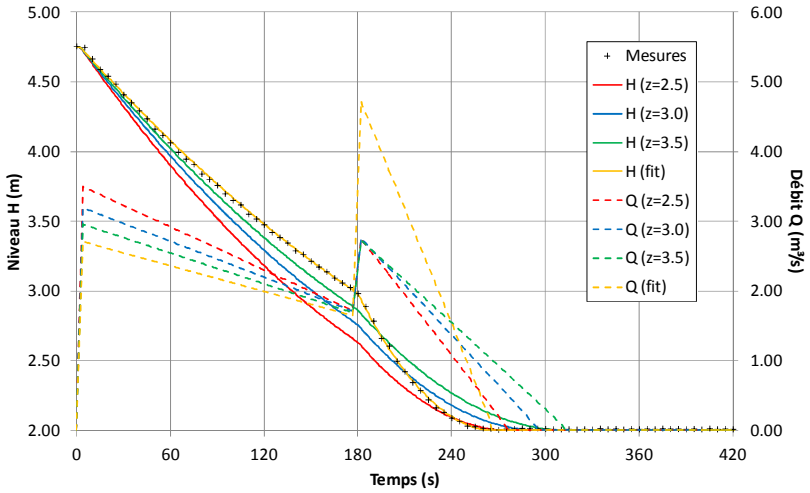

Figure 20: Lock of Estaimpuis: emptying curve, measured and computed for different values of ζ (noted z on the graph legend).

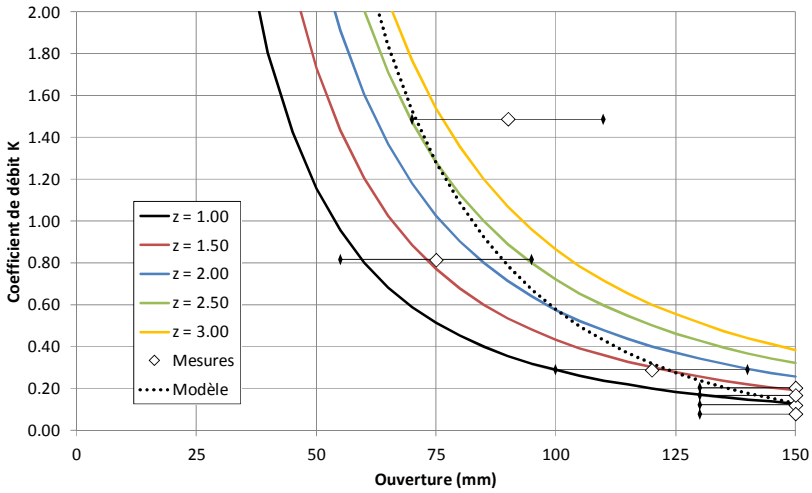

Figure 21: Grid valves on Canal de l'Espierre locks. Best fit head loss parameter $K = \zeta/2gA$, and associated values of ζ (noted z on the graph legend).

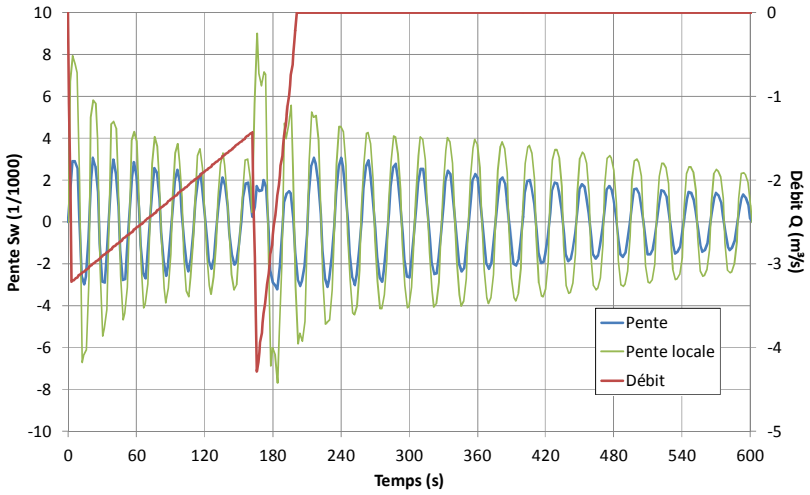

Figure 22: Lock of Warcoing. Global and local water surface slope in the lock chamber during emptying, computed for current valve schedule.

The measurements also roughly confirmed that the hydraulic jacks operate at a speed of 25 mm/s. Due to this high speed, an accurate setting of valve position is difficult, mainly for the grid valves: the full stroke is covered in only 6 s. An inaccuracy of 1 s on the step control results in a 15% error on the valve position. The number of possible step sequences is also limited accordingly: one step of 6 s; two of 3 s; three of 2 s or six of 1 s (see Figure 23). Only a few more schedules are possible for the sluice valves with a total travel time of 18 s.

Figures 24 and 25 show typical results obtained for the filling of Estaimpuis lock, through 450 mm sluice valves. Modelling were done for different steps opening schedules, and for an idealized linear opening, taken as reference. The levelling duration slightly varies with the total duration of the opening sequence. Large local and global water slopes are observed in all cases, except the linear opening. The largest slopes are logically observed for the longer opening steps (9 s) that generate the higher discharge bursts. For longer opening steps, the ratio between local and global slopes decrease, as the wave length is longer compared to the lock length. In any case, the less bad results were obtained for the shortest opening steps: with six steps of 3 s, separated by a 1 min stand-by, the filling duration is 6'02", the maximum global slope equals $S_{w,glo}$ = 1.4 ‰, and the maximum local slope $S_{w,loc}$ = 3.8 ‰.

The only way to improve results and to reduce local slope is to decrease the valve opening speed. Figure 26 shows that dividing the jack speed by two reduces the maximum local slope to $S_{w,loc}$ = 2.3 ‰, while the maximum global slope and levelling duration remain almost unchanged. With a speed divided by 4, the maximum local slope is almost equal to the maximum global slope.

Quite similar results were obtained with the grid valves, with a preferred schedule in six steps of 1 s. These results are not detailed here for conciseness. From this analysis, it was concluded that the existing situation could be improved by reducing the valve travel at each step and by multiplying the steps. This improvement can be obtained by a simple change in the control automated parameters. Further improvement could be obtained by reducing the valve opening speed, but this will imply a mechanical intervention on the hydraulic system.

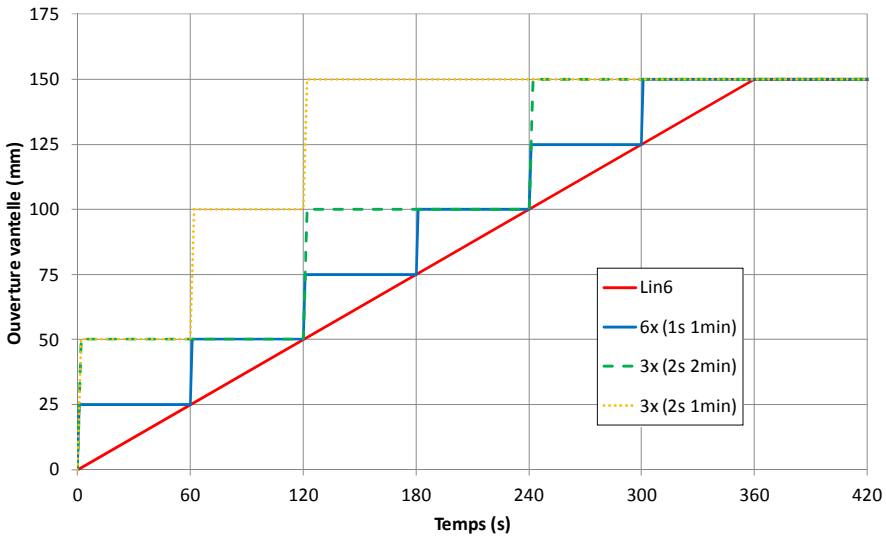

Figure 23: Grid valve on Canal de l'Espierre locks. Technically admissible opening schedules.

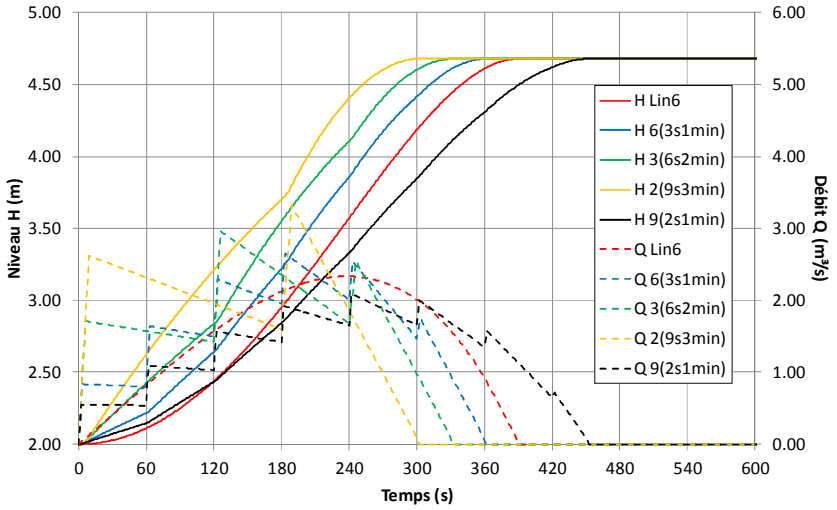

Figure 24: Estaimpuis lock: filling curve and hydrogramme, for different valve opening schedules.

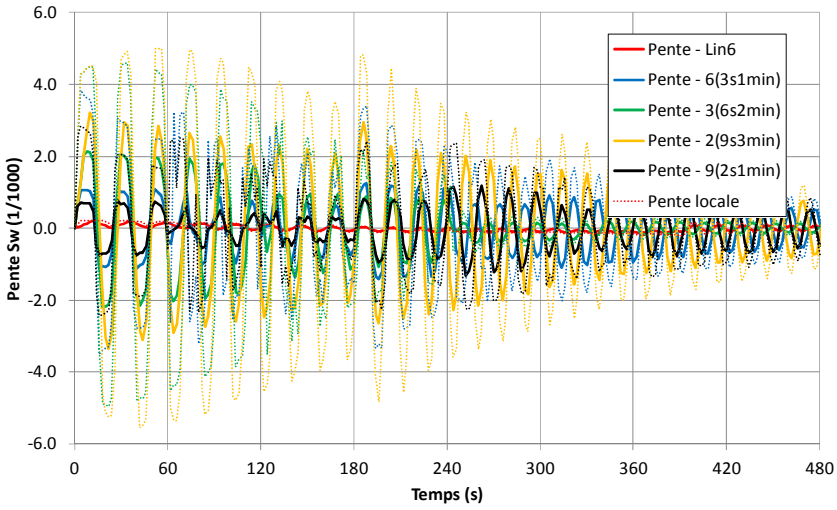

Figure 25: Estaimpuis lock: water surface slope, for different valve opening schedules.

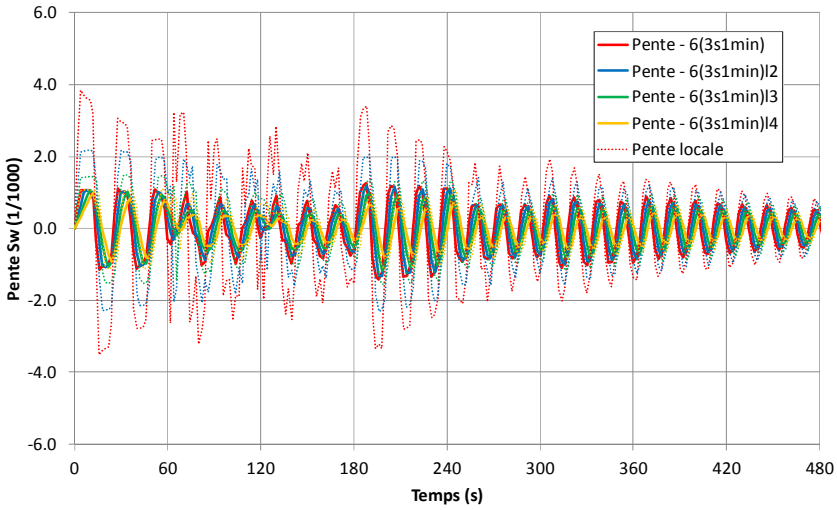

Figure 26: Estaimpuis lock: water surface slope, influence of the valve opening speed.

7. CONCLUSIONS: LESSONS LEARNT

Four case studies of lock levelling systems reengineering were presented, focusing on the adaptation of the valve opening schedule. In three cases, the electro-mechanical equipment is to be fully replaced. This let some freedom for the levelling design. In the last case, the electro-mechanical equipment is on site and severely constrains the possible valve schedules.

For all cases, only limited documentation was available. No hydraulic studies for the levelling could be recovered. The objectives and design criteria of the engineers who designed those locks levelling are therefore unknown. With a new regard and with new modelling tools, some of their choices seem questionable now:

- At Havré and Pommeroeul, a very complex system of levelling culverts was developed. This system looks like a fully equilibrated levelling system, but is not. Also, the butterfly valves seem definitively oversized.
- At the Canal de l'Espierres, the electro-mechanical system has been designed to open the valve, apparently as fast as possible, without consideration for the wave generation in the lock chamber.

These observations confirm the need to consider all flow processes and to perform a careful hydraulic design of any lock. As highlighted by PIANC (2015), all stakeholders should be aware of the possible consequences of their interventions on the vessel safety during levelling.

PIANC (2015) also highlighted the risk of an uncontrolled long term evolution of the valve opening schedules. Field measurements at Havré and Pommeroeul confirmed this risk. Hopefully, on the Canal de l'Espierres, electro-mechanical engineers in charge of the project requested a hydraulic study prior to any modification of the valve schedules. Again, one should conclude by highlighting the need for contacts between people in charge of the design and of the maintenance; and for appropriate maintenance and control procedures, in order to ensure the lasting quality of an optimal lock operation.

8. REFERENCES

Bousmar, D. & Libert, Y. (2016). "Liaison Seine Escaut-Est. Ecluses d'Havré, Pommeroeul et Hensies. Détermination des lois de sassement". Mod. 058/10, Final report, SPW-DO.222, Châtelet, Belgium.

Bousmar, D. & Libert, Y. (2017). "Canal de l'Espierres. Diagnostic du sassement des écluses de Leers-Nord, Estaimpuis et Warcoing. Mesures in-situ de janvier et février 2017, modélisation du sassement". Avis 2016/08, Final report, SPW-DO.222, Châtelet, Belgium.

Bousmar, D., Savary, C., Swartenbroekx, C. & Zorzan, G. (2017). "Field measurement on navigation locks for hydraulic diagnosis". HydroSenSoft, International Symposium and Exhibition on Hydro-Environment Sensors and Software, IAHR, Madrid, Spain.

Idel'cik, I.E. (1969). "Mémento des pertes de charge". Eyrolles, Paris.

LRH (1954). "Canal de Charleroi à Bruxelles. Vannes de la tête amont de l'écluse 1F". Mod. 123bis, Final report, Min. Travaux Publics, Borgerhout-Anvers, Belgium.

PIANC (1986). Final report of the International Commission for the study of locks. PIANC, Brussels.

PIANC (2009). Innovations in navigation lock design. Report 106. PIANC, Brussels.

PIANC (2015). "Ship behaviour in locks and lock approaches". Report 155. PIANC, Brussels.

UCL (2013). "Ecluse 225 m x 25 m d'Ampsin-Neuville. Assistance à l'étude par modélisation physique et numérique du système d'alimentation en eau du sas". MS 222/11/01, Final report, Pôle Génie Civil et Environnemental, Louvain-la-Neuve, Belgium.

Savary, C. & Libert, Y. (2013). "Quatrième écluse de Lanaye. Evaluation du risque de cavitation au droit des vannes de sassement". Mod. 019/5, Final report, SPW-DO.222, Châtelet, Belgium.

Swartenbroex, C., Bousmar, D. & Savary, C. (2014). "Superposition of lock generated waves in the Seine Sheldt East network in Belgium". PIANC World Congress, San Francisco, USA.

DESIGN AND CONSTRUCTION OF A CELLULAR COFFERDAM FOR THE PACIFIC ACCESS CHANNEL

by

Antonio A. Abrego Maloff[1], Gonzalo De León[2], Maximiliano De Puy[3]

ABSTRACT

As part of the Panama Canal Long Range Master Plan, the Panama Canal Authority (ACP) initiated in 1997 the expansion of the capacity of the waterway. The Expansion Project included the construction of additional locks and navigation channels to allow the transit of Post-Panamax vessels. This project required a new navigation channel to connect the Gaillard Cut with the new Pacific Locks. This channel was designated as the Pacific Access Channel (PAC). The channel is approximately 7.8 km long and 218 m wide, with a water elevation at 26.82 m PLD (Precise Level Datum for the Panama Canal) and is separated from the Miraflores Lake (elevation 16.45 m PLD) by a new dam. ACP divided the Pacific Access Channel works into four separate construction packages.

One of those packages, named PAC-4 included the construction of one of the two embankment dams required to separate the new access channel from the Miraflores Lake, that have a difference elevation of almost ten meters. These dams were designated as Borinquen 1E and 2E; the last one was included in the Locks Contract while the Borinquen 1E dam was built during the PAC-4 contract. The design of the PAC-4 required that the contractor excavate to ground elevations below the Miraflores Lake level. Therefore, it was required the construction of a cellular cofferdam and an embankment cofferdam in order to provide the adequate conditions for the required excavation works. This cofferdam was designed by the ACP design team and the review process was performed by URS Corp., who was the consultant in charge of the design of the embankment 1E. The paper describes the design criteria assumed; the possible additional uses of this structures; and the construction process itself.

1. INTRODUCTION

In 1997, the Panama Canal Authority (ACP) initiated the expansion project of the waterway in order to increase its capacity. The Expansion Project included the construction of additional locks and navigation channels to allow the transit of Post-Panamax vessels. This project required a new navigation channel to connect the Gaillard Cut with the new Pacific Locks. This channel was designated as the Pacific Access Channel (PAC). The new channel is approximately 7.8 km long and 218 m wide, with a water elevation at 26.82 m PLD (Precise Level Datum for the Panama Canal) and is separated from the Miraflores Lake (elevation 16.45 m PLD) by a new dam.

ACP divided the Pacific Access Channel works into four separate construction packages. The first three contracts, denominated PAC-1, PAC-2 and PAC-3, were executed from 2007 until 2009, and the design contemplated to excavate from the natural ground elevation down to elevation 30.00 PLD. The last excavation contract, named PAC-4, was designed to remove all the remaining material down to elevation 9.14m PLD (bottom of navigation channel); this contract also included the construction of one of the two embankment dams required to separate the new access channel from the Miraflores Lake, that have a difference elevation of almost ten meters. These dams were designated as Borinquen 1E and 2E; the last one was included in the Locks Contract while the Borinquen 1E dam was built during the PAC-4 contract. The design of the PAC-4 required that the contractor excavate to ground elevations below the Miraflores Lake level; therefore, it was required the construction of a cellular cofferdam and an embankment cofferdam in order to provide the adequate conditions for the required excavation works. This cofferdam was designed by the ACP design team and the review process was performed by URS Corp., who was the consultant in charge of the design of the embankment 1E.

[1] Panama Canal Authority, Panama, AAbrego@pancanal.com
[2] Panama Canal Authority, Panama, GDeLeon@pancanal.com
[3] Geotechnical Consultant, Panama, Maxdepuy@gmail.com

Most cofferdams can be built either on rock or on sand and gravel; and the design varies depending on the soil condition. For the structure required in this project, given the geology of the area, the cofferdam was designed for the case where is resting on rock. It is important to note that the cofferdam was built as a separate structure from dam 1E, which will not depend on the cofferdam for its own stability.

The paper describes the design criteria assumed for the cofferdam, including its alignment, geological conditions under the structure and a summary of the design procedure used. In addition, the paper will address the construction process from the owner's point of view, including some changes proposed by the design team and also by the contractor due to problems at foundation levels.

2. PROJECT DESCRIPTION

The new Borinquen Dam 1E was part of the works for the Pacific Access Channel (phase 4), and begins at the Pedro Miguel Locks in the north and extends south across Miraflores Lake to Fabiana Hill, a rocky hill outcropping north of the Miraflores Locks (see Figure 1). This dam and the other three included in the Locks Contract, separates the Miraflores Lake (at elevation 16.75m PLD approximately) from the new navigation channel (at elevation 25.90m PLD approximately). Since the construction of this dam involved excavation of the foundation down to elevation 0.00m PLD, it was necessary that the contractor built a cofferdam in order to allow excavation in the dry.

The cofferdam was required where Dam 1E construction would extend into or near Miraflores Lake, between approximately Stations 1+000 and 2+700 (see Figure 1). The north end of the cofferdam was tied into the west approach wall of the Pedro Miguel locks. The south end of the cofferdam was tied into existing ground. The 1.8 km long cofferdam has a maximum height of about 17.00m.

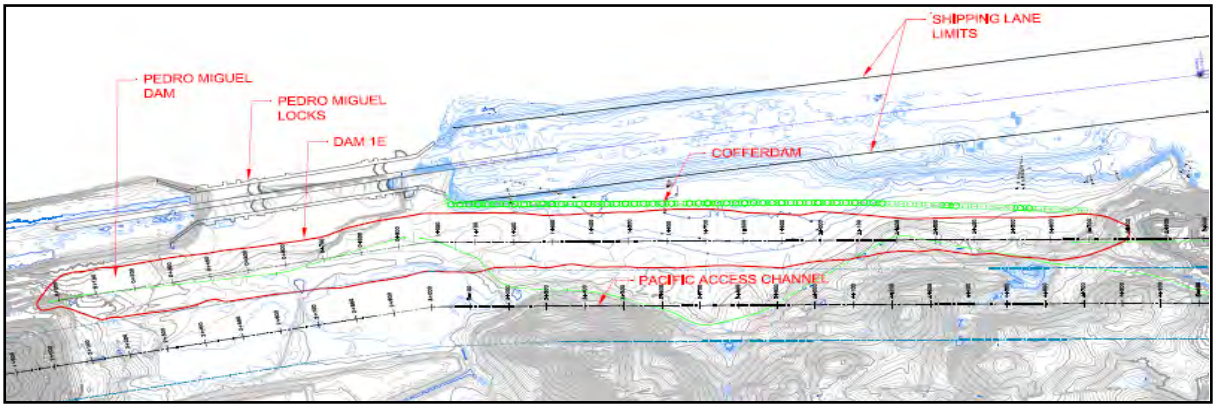

Figure 1: Dam 1E and cofferdam location

3. DESIGN CRITERIA

Most cofferdams can be built either on rock, where little or no overburden exists, or on sand and gravel; and the design varies depending on the soil condition. For the structure required in this project, given the geology of the site, the cofferdam was designed for the case where is resting on rock. It is important to note that the cofferdam was built as a separate structure from Dam 1E, which does not depend on the cofferdam for its own stability.

In general, the design of a cofferdam must satisfy the following criteria:

a. The structure must be able to withstand all the various loads applied to it;
b. The quantity of water entering the cofferdam must be controllable by pumping;
c. At every stage of construction the formation level must be stable and not subject to uncontrolled heave, boiling or piping;
d. Deflection of the cofferdam walls and bracing must not affect the permanent structure or any existing structure adjacent to the cofferdam;
e. Overall stability must be shown to exist against out of balance earth pressures due to sloping ground or potential slip failure planes;

3.1 Alignment

In order to accomplish the performance described above, the design of the cofferdam needs to consider several design criteria. One of them is the final alignment. This alignment was first outlined based on the design of Dam 1E (URS, 2008) and the final surface of the outcropping rock (weathered and sound).

The cofferdam was originally located approximately 30.00 m east of the outboard toe of Dam 1E and west of the shipping channel. The cofferdam was located in such a way not to interfere with the construction of Dam 1E and the shipping channel in Miraflores Lake. Due to the preliminary design of Dam 1E, the original cofferdam alignment required a PI between stations 3P+494.08 and 3P+778.71. This was done in order to maintain the cofferdam structure close to the toe of the dam and to reduce construction costs.

The final alignment of the cofferdam was defined based on various aspects as describe below:

a. The cofferdam must be located to avoid interference with construction of Dam 1E and the shipping channel in Miraflores Lake;
b. Minimum clearance between the cofferdam and the outboard toe of Dam 1E shall be 10 m;
c. The cofferdam must satisfy the operation requirements. In the middle section of the cofferdam, the structure will be used as a tie-up station (see fig. 2). The Cofferdam shall be straight in the area of the tie-up station. (approx. 500 m);
d. The northern closure will be the south end of Pedro Miguel Locks;
e. In the southern closure the cofferdam will extend until top of weathered rock reach elevation 18.00m PLD.

The final alignment in figure 2 shows the north and south ends and also where the structure changes it size and type. It changes size because the structure may be used as a tie-up station only in its middle portion. The rest of the structure will not be treated as such and therefore a more economical design has been implemented. On the other hand, as shown in Figure 2, the cellular cofferdam extends from the north end up to a point south of station 4P+249 where the geology allows a change in the type of cofferdam to be used. At this point, the rock is above elevation 18.00m PLD (see Section 4) and therefore a cellular cofferdam in uneconomical and an embankment cofferdam with sheet piles cutoff may be used as describe in Section 3.2.

In addition, since the cofferdam structure is required to keep the excavation area for the dam foundation completely dry, it was decide that in the north (Pedro Miguel Locks) the cofferdam would be extended and tied into an existing slope to reduce the risk of flooding. In order to ensure the water-tightness of the system, it was also decided to design a grout curtain or a similar structure extending from the cofferdam to the locks wall as shown in Figure 3. In the south end, the cofferdam will tie into the existing ground at Point #5 (see Figure 2).

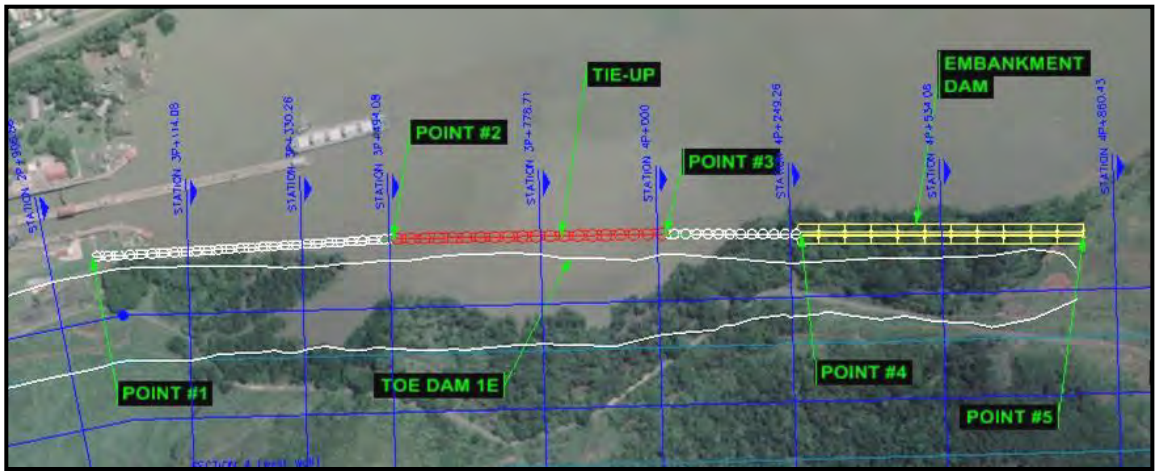

Figure 2: Cofferdam final alignment

Figure 3: North tie-in of cofferdam (at Pedro Miguel Locks)

3.2 Cofferdam Alternatives

The original cofferdam concept required for the construction of Dam 1E consisted of a single-diameter cellular cofferdam to be built throughout the entire 1.8 km long alignment. However, analysis of the possible future uses of the structure and the geology of the area, lead the Design Team to consider two different alternatives along the alignment in order to allow tying up operations and also to reduce the cost of the structure:

a. Embankment cofferdam with sheet pile cutoff

This first alternative was considered for those areas where the rock elevation was above 18.00m PLD and the driving of the flat sheet piles (required for cellular cofferdams) was determined to be unnecessary (as well as impractical). Evaluation of the geology of the area (see Section 4) suggested that south of Station 4P+429 the rock elevation was above the required 18.00m PLD; therefore, and to avoid any seepage through the rock, it was decided that an embankment cofferdam with a sheet pile cutoff (see Figure 4) was enough to guarantee impervious condition during the excavation works required.

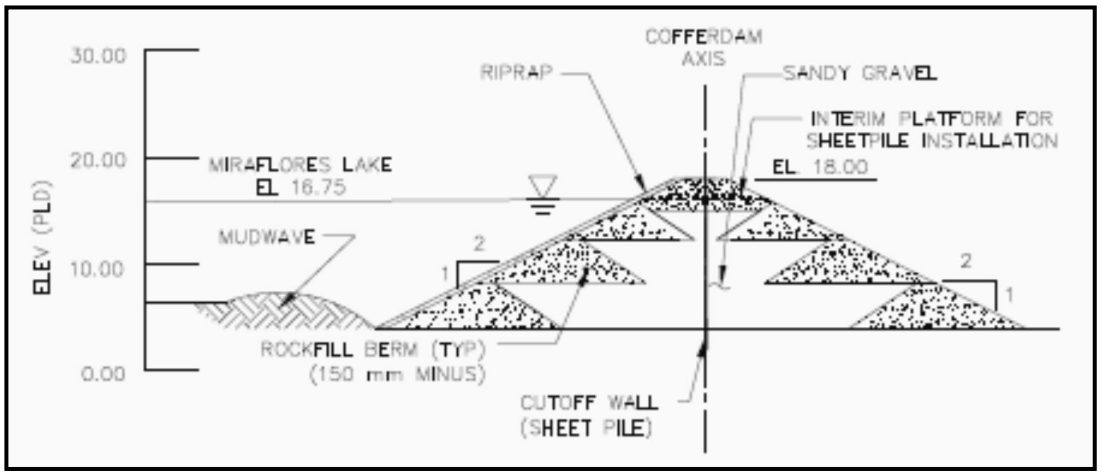

Figure 4: Typical Section of the Embankment cofferdam with sheet pile cutoff

This type of cofferdam was constructed in the south part of the cofferdam alignment, specifically from Station 4P+429 up to the south end where the structure must tie into the existing ground at Fabiana Hill.

b. Cellular sheet pile cofferdam

Those areas where the weathered rock elevation is below 18.00m PLD, the cellular sheet pile cofferdam alternative was used. This alternative was chosen over the Float-in-place concrete caisson cofferdam because is more economical and also because ACP has already design this type of structures in the past.

The Panama Canal operates another tie-up station in the Gaillard Cut which was design under the same concept. Having ACP the experience of designing a similar structure and considering that this existing cofferdam is presently being used as a tie-up station, the Design Team proposed that the remaining cofferdam was design as a cellular cofferdam instead of float-in-place concrete caisson. In addition the Team proposed that a portion of such a cofferdam might be used as a tie-up station.

The new cofferdam structure is located in the Miraflores Lake, a few hundred meters west of the existing navigation channel and north of the existing Miraflores Tie-up station. The existing tie-up station is composed of several buoys anchored to the lake floor and therefore there is no land access to this facility. The idea of having this structure design as a future tie-up station was extensively accepted because it would provide land facilities to the actual operation crew and an additional anchoring capacity at Miraflores, which may increase the vessel transit through these locks.

Therefore, it was decided that the middle portion of the structure, between station 3P+494 and 4P+000 (approximately 500m), were designed for the appropriate tie-up station loads and additional earth fill to be placed on top of the cells to reach the required freeboard.

3.3 General Design Criteria

In addition to the alignment the cellular sheet pile cofferdam design needed to consider several other general design criteria as shown in Table 1.

Feature/Issue	Criteria	Remarks
1. Cofferdam Crest Elevation	18.00 m.	The area between Dam 1E and the cofferdam will be backfilled to the cofferdam crest level.
2. Miraflores Lake Operating Levels	• Maximum: elevation 16.75 m • Minimum: elevation 16.45 m	
3. Operations	• For tie-up station, foundation level must allow for Panamax vessel draft. o Dredge line on Miraflores Lake side of cofferdam will be elevation 2.90 m. • Construction of the cofferdam shall minimize impact on shipping operation	A deck will be constructed on top of the cofferdam to allow for ship tie-up station.
4. Foundation	• Residual soils or rock: o Sheet pile refusal on weathered rock, or o At least 2 m below SPT N-value of 50. • Seepage cutoff must be adequate to prevent piping o Foundation to be non-erodible, or hydraulic gradient to be less than 0.3 in erodible materials.	• Materials must have sufficient strength for static and seismic stability, eliminate liquefaction potential, and minimize settlement. • All fill, alluvium, Pacific Muck and unsuitable soils will be removed from the cofferdam foundation in place under wet conditions.
5. Backfill	• Between Dam 1E and Cofferdam: Zone 3 rockfill.	Sheet pile cell fill is ACP specification.

Feature/Issue	Criteria	Remarks
	• Within sheet pile cells: Free-draining rockfill (minus 150 mm)	
6. Stability	• Must have adequate static and seismic stability. • Check overall cofferdam stability at tie-up station (draft to allow for Panamax vessel)	Ref: *Design of Sheet Pile Cellular Structures, EM 1110-2-2503*. U.S. Army Corps of Engineers, September 1989.
7. Dead Loads (Static)	• Loads from rockfill on west side of cofferdam. • Hydrostatic loads.	
8. Live Loads	• Ship berthing forces from a Panamax ship. • Operational deck loads. • Construction loads.	Loads to be determined during preliminary design of the cofferdam.
9. Seismic Loads	• Backfill loading. • Inertial loads of the cofferdam itself. • Hydrodynamic loads from Miraflores Lake.	
10. Drainage of Seepage	Provide for drainage of seepage from Dam 1E through cofferdam to Miraflores Lake.	Consider Miraflores Lake operating levels to set drainage invert elevation through cofferdam.
11. Corrosion Resistance	Must resist corrosion in brackish water conditions.	Consider wave splash and fluctuating Miraflores Lake levels.

TABLE 1: Design criteria for the cofferdam

4. FOUNDATION CONDITIONS

The proposed cofferdam footprint is underlain by varying depths of fill. Beneath the fill, the cofferdam is primarily underlain by the La Boca formation, and Pedro Miguel agglomerate. The designers of the Dam 1E concluded that the fill and residual soil materials are not suitable for dam foundation, so they will be stripped before construction of the embankment. However, for the case of the cofferdam this material is soft enough so the sheet piles will be driven through them until reaching hard rock (top of weathered rock), or the predefined elevation.

Once the cells are constructed and ready to be backfilled, this material will be removed. Only in the portion where the Tie-Up station will be constructed, this soft material will be dredged prior to the construction to avoid future interference of the dredge operations with the final structure.

4.1 Geological cross sections

Along the alignment of the cofferdam ACP drilled several boreholes to better characterize the geology right underneath the cofferdam structure. These new boreholes complemented many others already drilled in the area. As a result, ACP geologist developed a longitudinal cross section showing the location of the fill, overburden, top of weathered rock and top of sound rock. In addition, several cross sections were developed along the cofferdam alignment in order to provide the designer with more precise details on how the cofferdam would be founded on the soil. In this paper only two cross section are shown.

Using this longitudinal cross section, the Design Team was able to determine the location where the cofferdam would be switched from a cellular structure into an embankment cofferdam. It was decided that from station 4P+249.26 extending south across low lands to Fabiana Hill the rock elevation was

high enough so a cellular cofferdam is no longer required. Therefore, in this section an embankment cofferdam would be used instead.

All the cross section developed by ACP were evaluated and analyzed by the Design Team. It was concluded that section 3P+330.26 (figure 5) was the most critical one within the non tie-up portion of the cofferdam, while section 3P+778.71 (figure 6) was the most critical within the portion assigned to the tie-up station.

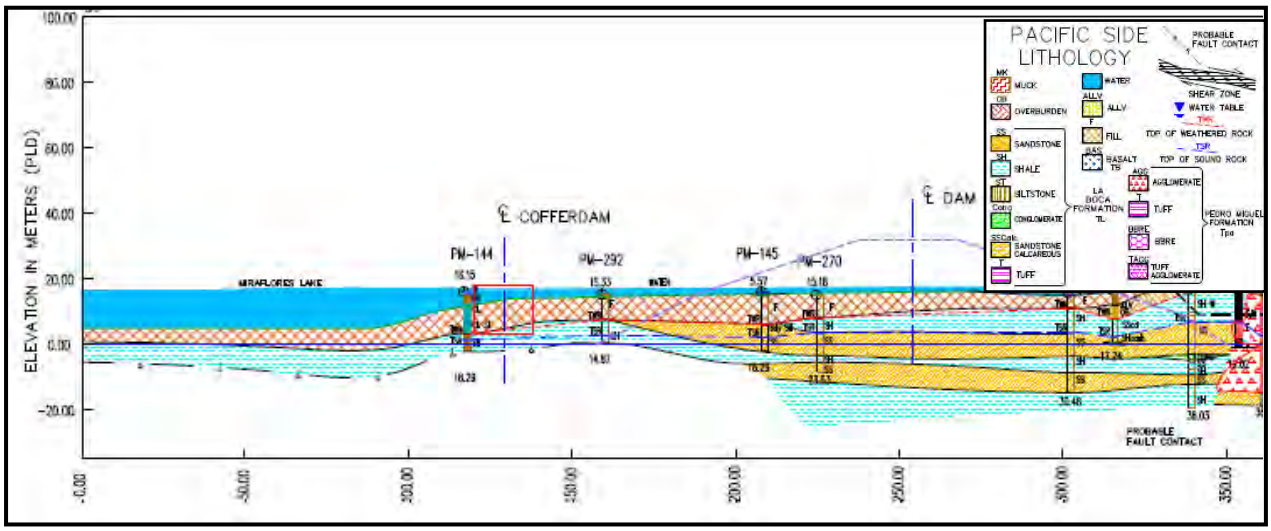

Figure 5: Cross section at station 3P+330.26 (non tie-up station)

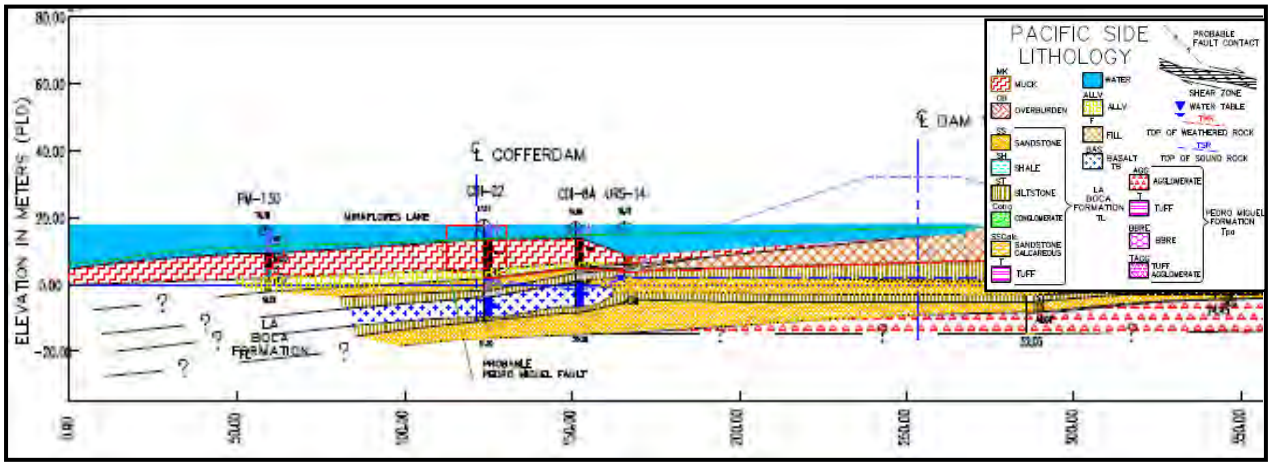

Figure 6: Cross section at station 3P+778.71 (tie-up station)

5. COFFERDAM DESIGN

The design of the cofferdam was done following the standard procedure developed by the Tennessee Valley Authority (TVA), also known as the Terzaghi's Method. Although there are other methods available, the TVA procedure is simple and one of the most commonly used around the world.

Basically, a cellular cofferdam is a gravity retaining structure formed from the series of interconnected straight web steel sheet pile cells filled with soil, usually sand, or sand and gravel. The interconnection provides water-tightness and self-stability against the lateral pressures of water and earth. The circular one (as the one being design), consists of individual large diameter circles connected together by arcs of smaller diameter. These arcs generally intercept the circles at a point making an angle of 30, 45 or even 90 degrees with the longitudinal axis of the cofferdam. The prime feature of the circular type cofferdam is that each cell is self-supporting and independent of the next.

The design of a cellular cofferdam proceeds much the same as that of an anchored wall. Before the design can be initiated, the necessary controlling dimensions must be set. In this case, the height of the structure is a known value so the next step was to choose an approximate diameter, D, and the equivalent width, B.

One additional parameter that needed to be defined was the location of the water table inside the cell, or the so called saturation line. This basically refers to the degree of saturation within the cell fill and its location is influenced by a number of factors including the condition of the pile interlocks, the permeability of the cell fill, whether a berm is used, and the number and position of weep holes on the inside row of piling. In the present design, a horizontal line, at an elevation so chosen as to represent the average expected condition of saturation, was assumed in order to simplify computations.

Once all these parameters were defined, the next step was to verify the stability of the cells. Since the cells will be founded on rock, several types of failures were needed to be checked: a) Sliding on the base; b) Overturning; c) Shear failure on centerline of cell; d) Horizontal shear; e) Excessive interlock tension; and f) Loss of internal stability

5.1 Design of the non Tie-Up and tie-up sections

The non tie-up section of the cofferdam applies to those areas that will not be used for berthing vessels. These areas have been identified as those close to the Pedro Miguel Locks (between point 1 and 2 in figure 2), and to the southern portion of the alignment inside the Miraflores Lake (between point 3 and 4 in figure 2). A review of the geological cross-section in these areas revealed that the most critical is the one identified as 3P+114.08; therefore, this section has been adopted as typical and the design will be performed based on its features.

On the other hand, the tie-up section of the cofferdam applies to that area that will be used for berthing vessels. This area has been identified in the middle section of the cofferdam alignment, between point 2 and 3 in figure 2. A review of the geological cross-section in this area revealed that the most critical is the one identified as 3P+778.71; therefore, this section has been adopted as typical and the design will be performed based on its features.

The design of the cofferdam has considered two different loading conditions that control the cell geometry and stability of the structure:

a. *Construction condition*: Condition that applies during the time the cofferdam is being constructed;
b. *Long term condition*: Condition that applies once the construction of the cofferdam has finished and all the permanent loads are applied.

For the evaluation in either condition, the material properties were maintained exactly the same. Table 2 shows a summary of these properties, while Table 3 summarizes all the assumptions made for the cofferdam design.

Material	Condition	Friction Angle (ϕ)	Cohesion (kN/m^2)	K_a	K_o	γ_{sat} (kN/m^3)	γ' (kN/m^3)
Fill/Muck	All	17°	0.00	0.548	-----	16.60	6.79
Cell fill	All	34°	0.00	0.254	-----	20.60	10.80
Backfill	All	42°	0.00	0.183	0.331	22.00	12.19
La Boca Found. (seismic)	All	32°	0.00	-----	-----	-----	-----
La Boca Found. (static)	Non Tie-up constr.	27°	0.00	-----	-----	-----	-----
La Boca Found. (static)	Non Tie-up long term	29°	0.00	-----	-----	-----	-----
La Boca Found. (static)	Tie-up constr.	26°	0.00	-----	-----	-----	-----
La Boca Found. (static)	Tie-up long term	27°	0.00	-----	-----	-----	-----

TABLE 2: Material properties

Parameter	Section Analyzed			
	Non Tie-Up		Tie-Up	
	Construction	Long Term	Construction	Long Term
Berm outboard	Not included	Not included	Not included	Not included
Passive resistance included	Not included	Not included	Not included	Not included
Pulling force from vessel	---	---	---	563.8kN
Loading from compaction surcharge	---	Not included	---	Not included
Aditional Surcharge	---	Not included	---	Not included
Height of cell	14.70m	14.70m	16.70m	16.70m
Additional height (for loading evaluation)	---	---	---	3.65m
Miraflores Lake Level (outboard side)	16.75m PLD	16.45m PLD	16.75m PLD	16.45m PLD
Saturarion level (inside cell - midpoint)	10.05m PLD	16.45m PLD	9.05m PLD	16.45m PLD
Unit Weight γ_{wet} assumed	γ_{sat}	γ_{sat}	γ_{sat}	γ_{sat}
Friction coefficient δ (outboard side)	0^o	---	0^o	---
Friction coefficient δ (inside cell)	22^o	22^o	22^o	22^o
Backfill condition	---	At Rest	---	At Rest
Water inside fill/muck (seismic design)	Restrained	---	Restrained	---
Water inside backfill (seismic design)	---	Free	---	Free

TABLE 3: Assumptions made for the design of the cofferdam

5.1.1 Construction stage condition

During this stage the cofferdam is analyzed assuming that the inboard side of the cofferdam has been fully excavated and the water on the Miraflores Lake exerts the maximum pressure on the structure. In addition, the overburden or fill material in the lake contributes to increase the active pressure. Figure 9 shows the typical cross-section assumed for this portion of the structure.

It is important to note from Table 3, that there is a difference in the height of the cell between the non tie-up and tie-up section. This difference results from the geological exploration, which indicated that at station 3P+778.71 (tie-up section), the top of the weathered rock was located at elevation 1.30m PLD and not at elevation 3.30m PLD.

As for the saturation line inside cell, it was assumed with a slope 1:1 from lake level to TWR; therefore the water elevation at the mid-point inside the cell are different for both cases. This slope is based on the filling material as shown in the USACE EM-1110-2-2503 manual (USACE, 1989);

In figure 7 it is shown the typical cross section used for design. Since the structure is located in a seismically active area, the stability of the cofferdam was verified for the static condition and also the seismic condition. Figures 8 and 9 show the load distribution on the cell for both conditions.

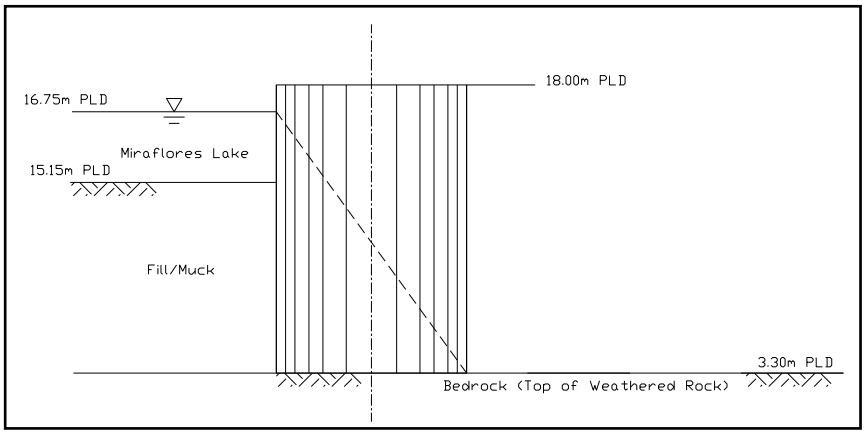

Figure 7: Typical cross-section for the non Tie-Up section during the construction stage

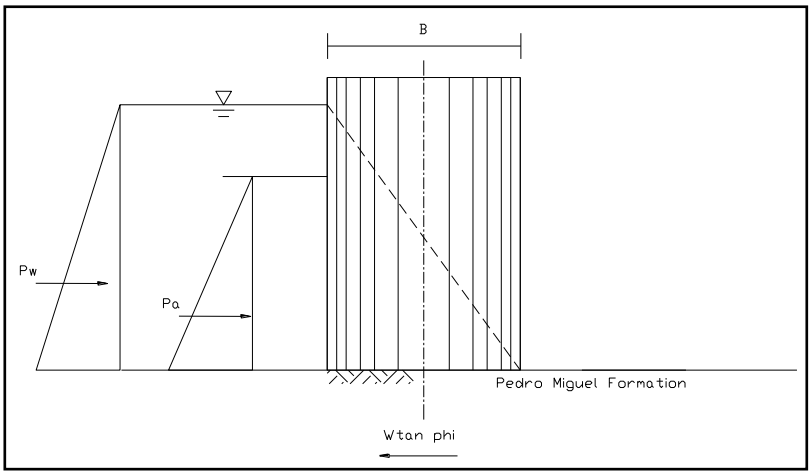

Figure 8: Horizontal pressure components acting on the cofferdam during the construction stage (static loading)

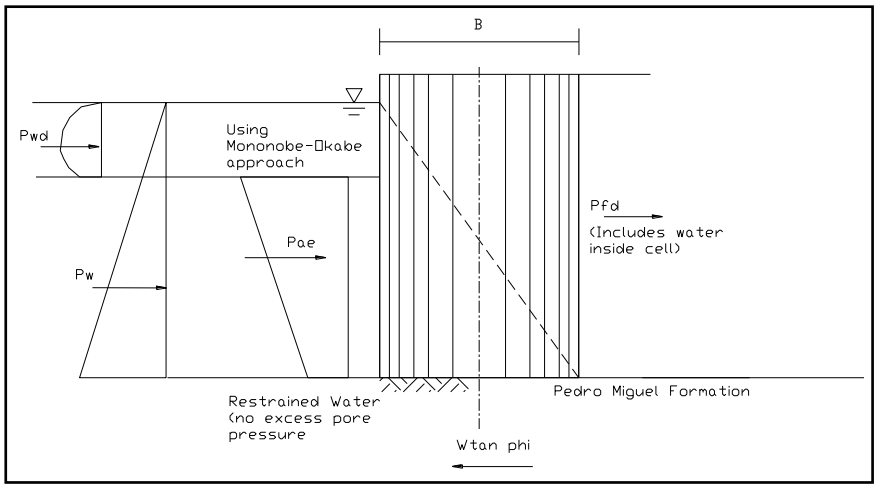

Figure 9: Horizontal pressure components acting on the cofferdam during the construction stage (seismic loading)

5.1.2. Long term condition

During this stage the cofferdam is analyzed with all permanent loads applied to the structure. The area between Dam 1E and the cofferdam has been backfilled to the cofferdam crest level. It is also assumed that on the inboard side of the cofferdam all the material (fill/muck) has been removed. This is assumed since this condition might happen in the future as part of normal operating procedures Figure 10 shows the typical cross-section assumed for this portion of the structure.

One significant difference at this stage between the non tie-up section and the tie-up section is the pulling force from vessels. For the non tie-up section, no pulling forces exerted from vessels is considered. For the tie-up section, the pulling force exerted on the future dock has been calculated assuming a Panamax ship with a DWT = 100,000 tons. The formulation of the load components has been derived from the literature (Tsinker, 1997). The resulting value is 563.8 kN (total load normal to the dock), which has been estimated assuming an horizontal angle (α) = 30^o, a vertical angle (β) = 20^o, a pulling force (QB) = 1,000 kN and a 20% increase due to non-uniformities.

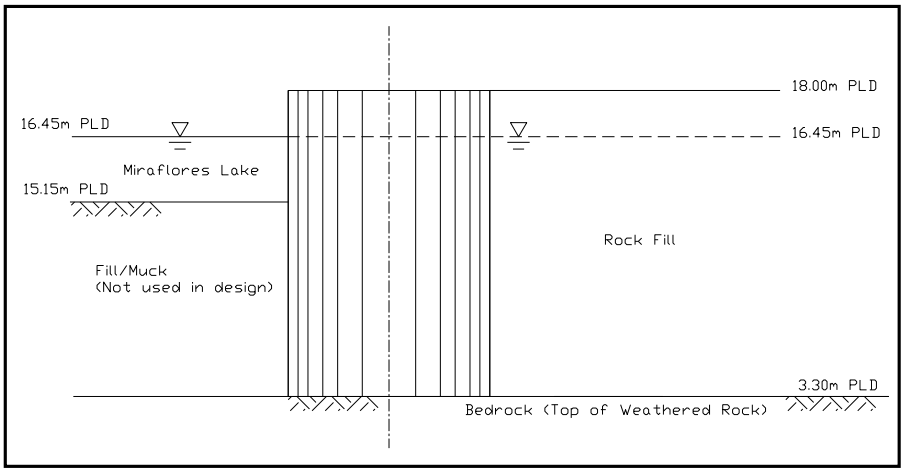

Figure 10: Typical cross-section for the non Tie-Up section for the long term condition

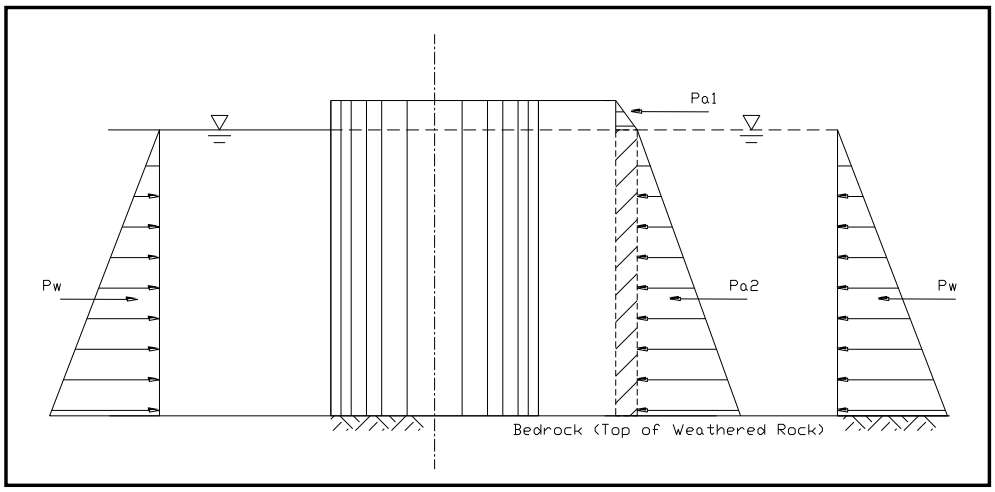

Figure 11: Horizontal pressure components acting on the cofferdam for the long term condition (static loading)

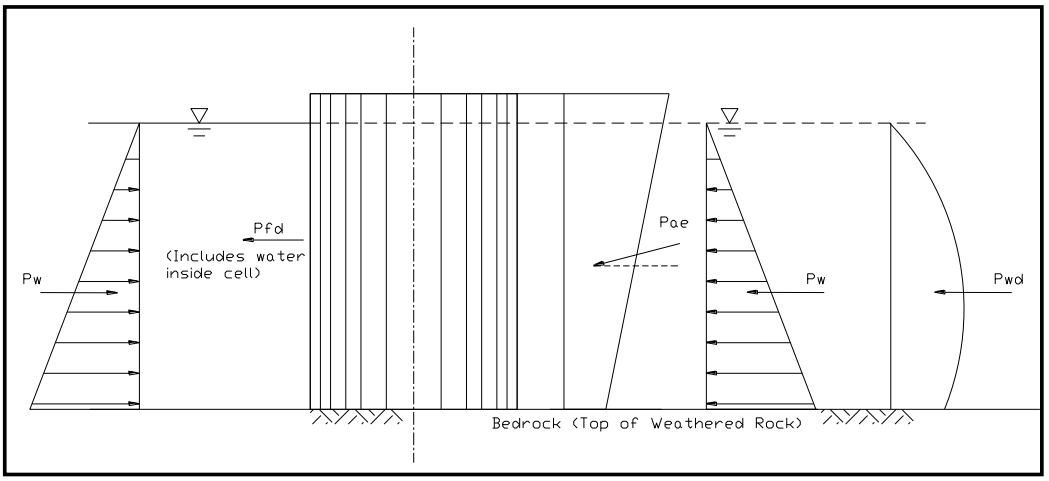

Figure 12: Horizontal pressure components acting on the cofferdam for the long term condition (seismic loading)

5.3 Results

Once the loading conditions have been established and the material properties chosen, the Design Team proceeded to evaluate and design the structure according to the criteria and procedures given above. It should be noted that following recommendations of USACE (1989), the stability of the structure has been evaluated for three different factors of safety, depending on the loading condition:

a) F.S. = 1.50 for the long term stage (permanent condition)
b) F.S. = 1.25 for construction stage (temporary condition)
c) F.S. = 1.10 @ 1.30 for seismic evaluation (see Tables 4 and 5)

All the stability analysis performed to the different cross-section and loading conditions were implemented in an Excel worksheet. In order to verify the accuracy of such worksheets, the stability analyses were also performed by hand and the results cross-checked with the computer results. It is important to note that such calculations were performed assuming an equivalent B=0.875D, where D=1.25H. The only fixed dimension was the height of the cell, which was a known value before the analysis was performed.

A summary table with all the final stability analysis results is shown in Tables 4 and 5. In addition to the resulting factor of safety, it is also presented the minimum strength required by the sheet piles and junction elements to comply with stresses imposed on the structure.

Failure Mode	Min. F.S. Required (1)	Construction Stage	Min. F.S. Required [1]	Long Term
Sliding Stability	*1.25*	1.72	*1.50*	1.77
Overturning	*Middle 1/3*	Middle 1/3	*Middle 1/3*	Middle 1/3
Vertical Shear	*1.25*	2.17	*1.50*	3.61
Horizontal Shear	*1.25*	1.83	*1.50*	2.41
Bursting (piles of cell)	*< tu/r*	Req. Min. 3000 kN/m	*< tu/r*	Req. Min. 3000 kN/m
Bursting (Tees of cell)	*< tu/r*	Req. Min. 3000 kN/m	*< tu/r*	Req. Min. 5000 kN/m
Seismic Sliding Stability	*1.30*	1.42	*1.30*	1.09 (3)
Seismic Overturning Stability	*Middle 1/2*	Middle 1/2	*Middle 1/2*	Middle 1/2
Seismic Vertical Shear	*1.10*	1.20	*1.10*	0.77 (3)
Seismic Horizontal Shear	*1.10*	1.01 (2)	*1.10*	1.25

Notes:
[1] According to TVA, USS Steel Sheetpiling Design Manual & others
[2] Analysis does not include effect of berm located in the inboard face, which will increase the FS above 1.1
[3] Values below the minimum required factor of safety

TABLE 4: Summary of results for the non tie-up section

Failure Mode	Min. F.S. Required (1)	Construction Stage	Min. F.S. Required [1]	Long Term
Static Sliding Stability	*1.25*	1.82	*1.50*	1.77
Overturning	*Middle 1/3*	Middle 1/3	*Middle 1/3*	Middle 1/3
Vertical Shear	*1.25*	2.37	*1.50*	2.89
Slipping between piling & fill	*1.25*	1.62	*1.50*	1.77
Horizontal Shear	*1.25*	2.07	*1.50*	2.16
Bursting (piles of cell)	*< tu/r*	Req. Min. 3000 kN/m	*< tu/r*	Req. Min. 3500 kN/m
Bursting (Tees of cell)	*< tu/r*	Req. Min. 3000 kN/m	*< tu/r*	Req. Min. 5500 kN/m
Seismic Sliding Stability	*1.30*	1.52	*1.30*	0.98 (2)
Seismic Overturning Stability	*Middle 1/2*	Middle 1/2	*Within Base*	Within Base
Seismic Vertical Shear	*1.10*	1.28	*1.10*	0.63 (2)
Seismic Horizontal Shear	*1.10*	1.12	*1.10*	0.85 (2)

Notes:
[1] According to TVA, USS Steel Sheetpiling Design Manual & others
[2] Values below the minimum required factor of safety

TABLE 5: Summary of results for the tie-up section

It is important to note that in Table 4 and 5 the footnotes 2 and 3 indicates that these values are below the minimum factor of safety required. This is due that the seismic analysis was done assuming that the response of the cell fill is governed by its drained strength. However, during an earthquake, its short-term strength is greater than the drained strength, suggesting that the real dynamic factor of safety is likely to be greater than the static one.

Once the equivalent width (B or w_e) was determined, the geometry of the cells was then defined. This was done with the help of tables or with computer programs. Several solutions are possible for the circular cells with a given equivalent width. In order to determine the final layout of the cells, the Design Team based the actual geometry of the cell on the ARCELOR's geometrical parameter tables found in the literature (Arcelor, 2005). The final equivalent width was chosen to be the closest to the one determined by empirical relationships; therefore, assuming a fixed B matching the ones presented in the table, the rest of the parameters were easily defined. The final values can be found in Table 6 and 7, and the corresponding definition in Figure 13.

Parameter	Value
Height (H)	14.70 m
Diameter (D)	17.93 (≈ 1.22H)
Equivalent Width (B)	16.34 (≈ 0.911D)
Radius of main cell (r_m)	8.97 m
Radius of connecting arcs (r_a)	5.98 m
System Length (x)	20.86 m
Junction Tipe	90°
Angle α	48.21°
N° of sheetpiles in cell (include 4 junction piles)	112 pcs
N° of sheetpiles in arc	19 pcs
Min. Interlock strenght requirement cell piles	3,000 kN/m
Min. Interlock strenght requirement T piles	5,000 kN/m

TABLE 6: Final layout for the non tie-up section

Parameter	Value
Height (H)	16.70 m
Diameter (D)	21.77 (≈ 1.30H)
Equivalent Width (B)	19.84 (≈ 0.911D)
Radius of main cell (r_m)	10.89 m
Radius of connecting arcs (r_a)	7.86 m
System Length (x)	26.29 m
Junction Tipe	90°
Angle α	47.65°
N° of sheetpiles in cell (include 4 junction piles)	136 pcs
N° of sheetpiles in arc	25 pcs
Min. Interlock strenght requirement cell piles	3,500 kN/m
Min. Interlock strenght requirement T piles	5,500 kN/m

TABLE 7: Final layout for the tie-up section

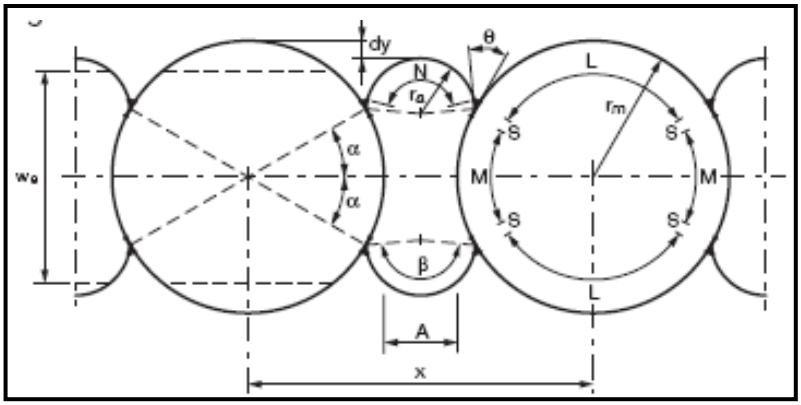

Figure 13: Geometrical values for circular cells

6. CONSTRUCTION OF THE COFFERDAM

The final layout of the cofferdam resulted in a structure consisting of 58 cells, 57 pairs of connecting arcs and 462 linear meters of cutoff wall (figure 14 and 15). The cellular cofferdam was designed for two different uses, therefore, the size of the cells varies according to the use. In the portion to be used as a tie-up station (Section “C” in figure 14) the final cell diameter is 21.64 m and the length is 499.51 m, which result in 20 cells. On the other hand, in the portion of the cofferdam not used as a tie-up station (Section “B” and “D”), the final cell diameter is 17.83 m and the total length is 667.52 m, which results in 33 cells. The remaining 4 cells, are located in the north end of the cofferdam, specifically built in an existing slope to reduce the risk of flooding (Section “A”). This 4 cells were also constructed with a cell diameter of 21.64 m.

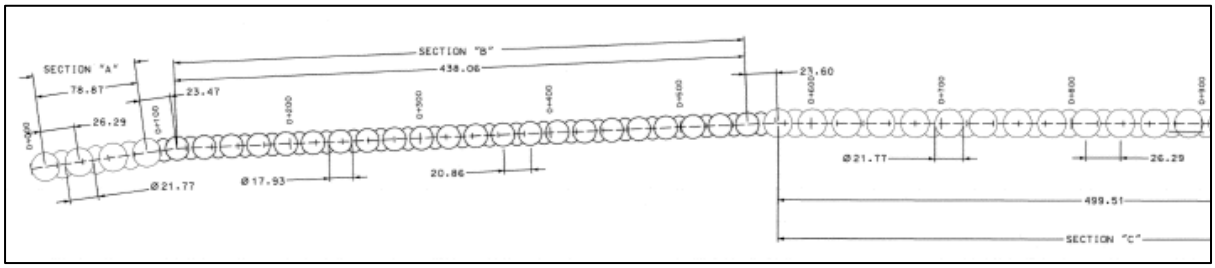

Figure 14: Final layout of the cofferdam (north end)

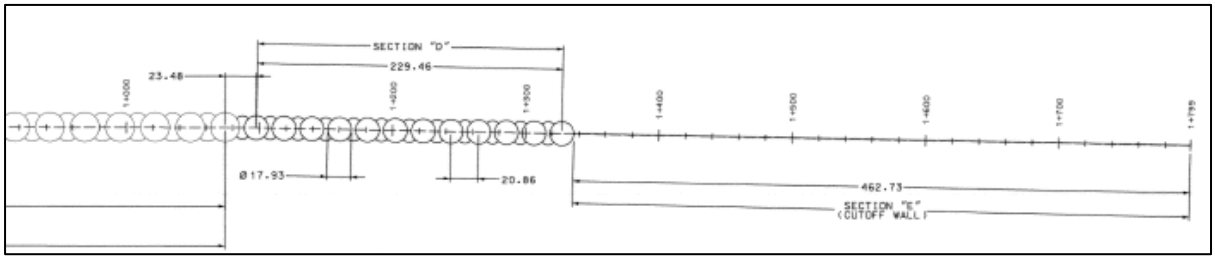

Figure 15: Final layout of the cofferdam (south end)

The south end of the cofferdam, was built using an embankment cofferdam with Z piles driven to refusal through the middle portion of the embankment (Section “E”). This portion of the structure has a length of 462.73 m and the average length of the piles is approximately 15.00 m.

6.1 Construction Methodology

The PAC-4 contract was awarded to the consortium ICA-FCC-MECO, and they subcontracted the consortium GOETTLE – ICONSA for the construction of the cellular cofferdam and the embankment cofferdam. Before this contract was awarded to the fore mentioned contractor, ACP had already purchased all the sheet piles required for the project, including the straight web piles for the cellular cofferdam and the Z piles for the embankment cutoff wall.

Works began in 2010 and the construction methodology proposed by the consortium was in accordance with international practice. First, all unsuitable material within the cell footprint was removed by the dredging work. Then, a bathymetric in-survey of the cofferdam installation area was perform to compare to the post-dredge bathymetric survey of the dredging subcontractor. This work was performed to anticipate the expected volume of cell fill.

6.1.1 Templates

In order to construct the cofferdam cell, it was necessary first to design and fabricate the templates which are used to drive the piles around. The templates consisted of two steel rings spaced vertically 3.0 m, which can be anchored into the correct position by means of ten spuds (tubular piles).

For this project, four different type of templates were required: a) for the 21.77 m cells, b) for the 17.93 m cells, c) for the connecting arcs between the same size cells, and d) for a special condition connecting arcs between two cells of different diameters. The templates were fabricated in New Orleans, USA, and then transported on barges to the project site in Panama; in figure 16 it is shown the templates.

Figure 16: Templates being transported

6.1.2 Marine cellular cofferdam

There were four cofferdam construction fronts: three fronts working from barges for cells in the dredged area, and one front working on land for cells outside the dredged area (cells 1-4 and 54-58). Each of the three marine teams were equipped with two floating templates. These templates were designed in such a way that the top ring of the template floated some 0.46 m above the water surface. The use by each marine crew of two templates with associated spud piles enabled the crews to work on a new cell while the previous cell were backfilled.

Once the template was floated to the cell footprint the spud piles were installed through spud wells to fix template on location; then, four sheet key (H-piles welded to a sheet pile) were driven into weathered rock to completely fix the template (see figure 17).

For the installation of the sheets between key sheets, the contractor first attached some of them to the template using spot welding directly to the template, then, in a sequential order, the sheet piles were vibrated into top of weathered rock ("near" refusal or to design tip elevation, whichever occurred first). This procedure was done in multiple passes, each pass was approximately 1.50 m in vertical length, and in a circular pattern. At the end, to reach the refusal criteria or to reach the design tip elevation, an impact hammer was used, centering the hammer over the sheet interlocks at the hammer's high impact energy and in conformance with the approved pile refusal criteria (see figure 18).

After reaching the refusal criteria or design tip elevation, the sheet piles were cut as required to install the cell fill using a conveyor. Initially, the cut off sheet were handled by the piling crane and later, after some cells were completely filled, a track excavator or other suitable equipment handled the cut off sheets.

Figure 17: Template in position

Figure 18: Driving piles in a cell by vibration

For the placement of the backfill, three temporary earthen access ramps were constructed prior to start of the works: one at cell 5, one at cell 14, and one at cell 46. At the end of each ramp there was a temporary access trestle that served as bridge between the fill and the cofferdam. These trestles were designed such that trucks and equipment could access the cell without damaging the sheet piles at that juncture.

The filling procedure of a given cell was only possible when such cell was closed and driven to refusal. Only the first cell of each working front was filled directly from the trestle using a 30.00 m long conveyor. The rest of the cells were filled using the same conveyor placed on top of the adjacent finished cells, with the discharge end over the center of the cell. The conveyor was fed by either a front-end loader or an excavator. Figure 19 shows this operation. Important to note that material from the conveyor was deposited in the cell at the center at all times, so the backfill was distributed evenly to avoid differential stresses or excessive development of interlock tensions.

Figure 19: Filling operation of the cells

At each cell, a drainage system was install according to the drawing plans and specifications. The drainage system consists of two 0.30 m diameter PVC pipes with filter fabric wrap placed in the inboard and outboard face of the cofferdam with the pipe discharge invert located at 17.00 m, PLD.

6.1.3 Connecting arcs

These structures are required to tie in independent cells all together, and are joined to the main cells by special T-piles. The placement of sheet piles in these arcs required the use of special templates also fabricated in New Orleans and transported in barges to the project site.

Prior to beginning the fill of the main cell, it is required to install two starter sheets at each of four SWC Weldon locations. The SWC is the point at which the arcs connect to the circular cell. The template was not used to set these starter sheets, which are not driven to refusal prior to initiating adjacent cell fill placement. The connecting arc template was only placed after completion of cell fill placement for both adjacent cells and was used to set the remaining sheets within the connecting arcs.

Only after the two adjacent cells were completely backfilled and the connecting arcs were driven to refusal, the connecting arcs were backfilled either directly from a front-end loader or excavator, or using chute, in both cases discharging at the center of the segment, so that the material was distribute evenly within the segment.

6.1.4 Landside cofferdams

For the construction of the landside cofferdam, the land crew utilized the same template as the marine crews. They began the construction in the north side of the alignment, in other words, the 4 land side 21.64 m diameter cells and then the same land crew built the remaining five 17.83 meter diameter land-side cofferdams located in the south end.

First, a trench was excavated the approximate width of the cofferdams to a depth sufficient to verify that no unsuitable material was encountered within the cells. This depth was approximately 4 m. The cofferdam template was then built in place, as shown in figure 20.

Figure 20: Landside cofferdam in the south end

Figure 21: Landside cofferdam in the north end after cutting off sheet piles

Unlike the cell built in water, no backfill was required for these cells and only driving the sheet piles to the refusal criteria or the design tip elevation was required. Once the crew finished using the template, it was removed in pieces and then re-used on the next and adjacent land-side cell, and so on (see figure 21).

6.1.5 Embankment cutoff wall

The work consisted in the construction of 464.45 meters (6.975 m2) of a sheet pile “Z-wall” using 15.00m long PZC-26 sheets, and the construction of embankment along sheet pile Z-wall.

The sheet piling was installed in a sequential manner from north (junction with the southernmost cellular cofferdam cell) to south. A template was installed at the starting location, and the surveyors were given the correct alignment and centerline of the wall.

The template consisted of a 24” steel I-beam whaler that lied down on the ground along the alignment of the face of the wall. This whaler was supported off the ground by 14” beams, 1.80m long, which lay on the ground, perpendicular to the whaler and all welded together as a unit. This frame, in turn, was fixed to the ground by driving steel H-piles, approximately 6.00 m long, vibrated into the ground adjacent to intersections of the whaler and support beams.

Figure 22: Driving sheet piles for the embankment cutoff wall

The sheets piles were driven in pairs. After 10 pairs are set on the template, the crane and hammer vibrated the sheets in a staggered pattern, so that the tip of every sheet was not more than 1.20 to 1.50m below that of any adjacent pile. After all the piles were driven to near refusal with the vibratory hammer, they were later impacted with the impact hammer to the required design elevation or to refusal, whichever occurred first.

6.1.6 Berm

After the construction of the cofferdam was finalized during the first quarter of 2011, the contractor was instructed to build a berm in the inboard side of the cofferdam before dewatering. This berm was originally included in the drawings and specifications of the contract, but not was a requirement for the design of the structure. In figure 23 it can be seen the structure finalized and the excavation works as they progressed later that same year. Note the berm already in place in the inboard side of the cofferdam. This is condition known as “construction stage”, where all the loads are acting from the Miraflores lake side.

Figure 24 shows the same cofferdam but working in the so called “long term” condition, where all the load is acting from the Borinquen dam side. The Panama Canal Authority has been monitoring the behavior of the cofferdam since it was built. For this, several prism are located in both sides of the cells and they are being monitored monthly using robotic instruments that read the real position of the prisms, triggering an alert if a displacement threshold previously set, is exceeded.

Figure 23: View of cofferdam from the south side (construction stage)

Figure 24: View of cofferdam from the south side (long term condition)

References

Arcelor (2205) “Piling Handbook,” Eight Edition

Tsinker, G. (1997) “Handbook of port and harbor engineering: geotechnical and structural aspects,” Published by Chapman & Hall.

URS (2008) Task Order No. 4, Borinquen Dam Design, Task B.1.8: Preliminary Design, Dam 1E, Draft Report, September 2008.

USACE (1989) “Design of Sheet Pile Cellular Structures Cofferdams and Retaining Structures,” EM1110-2-2503, September 1989.

Technical management of the cyber-physical waterway: it's all about managing complexity.

by

MSc. Eng. Michiel Coopman[1],

ABSTRACT

Organizations that manage inland waterway infrastructure (IWI), are rapidly introducing cyber-physical technologies or will do so in the next decade. They are evolving towards the cyber-physical waterway (CPW).

There is not one perfect way to manage the CPW but not all ways are equally effective. Managing a CPW, means managing complexity. Evolving to the CPW increases the overall system complexity rapidly. If not well managed, complex systems are vulnerable systems that are hard to maintain and expensive to modify.

Cyber-physical technology allows for remote-control of locks and bridges, predictive maintenance, optimal and automated adjustments of weirs, optimized traffic control etc.

These technologies are fundamentally different from classic waterway technology. We analyze these differences between classic waterway technology and cyber-physical technology on both a component and a system level.

We provide insight in the relation between technology characteristics and technical management. Understanding this relation is crucial to successfully implement cyber-physical technologies on the waterway. Based on this relation we explore the technical management and procurement strategy for the CPW.

We argue that technical management of the cyber-physical waterway reduces and manages complexity by aligning itself on system-boundaries and system-life-cycles.

We recommend organizing your technical management the way you want your overall CPW-technical system design to be.

1. Background

De Vlaamse Waterweg (Flemish Waterway) is a newly formed government agency in Belgium. It was formed at the beginning of 2018 out of merger of 2 existing agencies with different territories; *Waterwegen en Zeekanaal* in the West and centre of Flanders and *De Scheepvaart* in the East of Flanders.

De Vlaamse Waterweg NV now manages almost all inland waterways and infrastructure in Flanders, Belgium.

Over the last 2 to 3 decades, both Flemish agencies have invested heavily in cyber-physical technology for remote control and monitoring of Inland Waterway Infrastructure. In the time leading up to the merger, the different existing technical infrastructure was mapped, as well as the organizational structures and technical management, with the aim of integration.

The ambition of the newly formed De Vlaamse Waterweg, is to invest and utilize cyber-physical technologies on a large and organization-wide scale. A central question during the merger was, on how to do this in the most effective and efficient way. This paper builds on this analysis.

[1] De Vlaamse Waterweg NV (Hasselt, Belgium), coopmanmichiel@gmail.com

Although at first, technical analysis and organizational mapping were separate paths, it was soon found that both were in fact leading up to almost identical schematics. Borderlines between technical infrastructure and differences in implementations where near to identical to borders between organizational entities. The technical infrastructure had copied the shape of the organizational borders.

One might think this insight is trivial, little surprising and of little use. However, we will show that although this may be true for classic waterway infrastructure, it is of utmost importance to keep this in might when implementing cyber-physical technologies and re-designing your organisation. It can be used to your advantage.

We first describe the cyber-physical waterway. Next, we analyze the differences between classic waterway technology and the technology applied in the CPW on two levels: the component level and the system level. Based on this, we provide some guidelines on how to effectively and efficiently organize the technical management of the CPW.

2. The Cyber-Physical Waterway

2.1 General

In cyber-physical systems, physical and software components are deeply intertwined, each operating on different spatial and temporal scales, exhibiting multiple and distinct behavioral modalities, and interacting with each other in a myriad of ways that change with context. (US National Science Foundation,2009).

Some interrelated and overlapping terms that are used around the world for cyber-physical technologies are smart-technologies or Industry 4.0 technology. It is the combination of IT-related and networked components into physical infrastructures such as locks, weirs, movable bridges and waterway-infrastructure in general.

2.2 Applications of the Cyber-Physical Waterway

The cyber-physical waterway (CPW) is a waterway where for example:

- ➔ Infrastructure is connected with different communication networks such as fiber-networks and wireless networks (GPRS, VHF, RF, …)
- ➔ level sensor data is combined with weather forecasts to predict water levels and to automatically adjust weirs in the whole area in the most optimized mode
- ➔ bridge, locks and weirs are remotely operated from one or more central control rooms
- ➔ traffic flows are optimized based on tracking and tracing of vessels and all other relevant information, estimated times of arrival are calculated and used for lock-management
- ➔ infrastructure is continually monitored to allow for predictive maintenance, such as, bridge-openings, brake-pad wear, vibrations, engine-temperatures
- ➔ safety is guaranteed by smart safety devices, such as ship-bridge collision detection systems and vehicle detection

3. Characteristics of the CPW on a component level

3.1 CPW components

Traditionally, IWI comprises of steel or concrete structures and electrical and electromechanical components. The components used to implement a CPW are IT-related such as embedded computers, software and network components. As such, they inherently have IT-related characteristics. As such, there is a difference in complexity.

3.2 Complexity of CPW components

One way of quantifying complexity is based on information theory. Based on Zander and Kogut (1995); with increasing complexity of knowledge, the speed at which this knowledge can be spread within the organisation diminishes. This speed relates with the speed at which the technology can be implemented. They distinguish several properties that determine this speed.

Based on these properties, we list the differences between traditional IWI-components and CPW-components.

Traditional IWI components	Cyber-Physical Waterway components
Slow technological development	Fast technological development
Long product life cycles (>10 years)	Short product life cycles (<10 years)
Compatibility forms not a big issue	Compatibility issues supplier depended
Knowledge largely supplier independent	Knowledge largely supplier depended
Knowledge relatively easily codifiable	Knowledge difficult to codify
Wide variety of possible contractors	Specialized contractors

Complexity is built in, in the use of CPW components. First because dynamics increases. Secondly because without proper standardisation, variety becomes very high aswell, even for components with almost identical function and purpose.

With cyber-physical components, component-life-cycles are much shorter. Time from design, to implementation, maintenance, modification and finally disposal can range between 2 to 20 years.

For example, a new concrete structure now and 10 years ago, will be more or less built and calculated in the same manner. It won't need much maintenance in the first 10 years and will last for 50 to 100 years. If you want to change it, you can use the expertise from a number of contractors which can provide the same composition of concrete. The technical drawings can be read and modified to the new situation by any qualified engineer.

When you install a Supervisory Control And Data Acquisition-software (SCADA), you'll need to choose from a large number of suppliers which each offer almost identical functions and feautures but require completely different knowledge and training to implement.

You will need the latest operating system and computer-hardware not older than 3 years. Immediately after installation, you'll need to install patches and updates and repeat this half-yearly.

You won't be able to connect to random brands of PLC, especially not when they are older than 10 to 15 years. During the product life-cycle of the SCADA system, hardware and operating system may change 3 times.

You may have the best documented project, if you want some extra functionalities, chances are you'll find nobody except the original programmer to help you.

Characteristics of the CPW on a system level

4.1 Component breakdown structure vs system-engineering

Traditionally, IWI is analyzed by decomposing the infrastructure in a physical bounded component-breakdown-structure; the waterway is composed of several locks and bridges, which in their turn are composed of several structural elements and a drive system, with an engine and brakes, with brake-pads which are mounted by nuts and bolts and so on.

In a CPW, several components are networked with components that are located outside the physical boundary of the object. Therefore, to analyze the CPW, a purely geograpical and physically bounded breakdown is impossible and a system perspective is more suited. This is the aproach found in the field of system-engineering. Each sub-system has a role to play and provides a service to the other sub-systems and combined they achieve a higher goal then just the services added.

You can distinguish functional systems such as a CCTV-system, an access-control-system, a dynamic traffic sign-system, an IP-based radio communication-system etc. but also underlaying and supporting systems such as the IP-network-infrastructure and components, operating systems, virtual servers, storage-facilities etc.

4.2 Complex (infra)systems

Another broadly accepted meausure of complexity, is the degree of interconnectivity. What is the effect of a change in one part of the overall system on other parts?

Traditional IWI isn't much interconnected and the behavior on a system level is straightforward. Only a few important minimal specifications are needed to describe the waterway and its structures: maximum width and length of the vessels, underpass height and depth of the waterway. The design of the lock or bridge itself may vary almost freely. A failure of one component, usually has only a local effect.

The subsystems of the CPW have multiple interactions, they continuously exchange information and are interdepend. Give the fast technological evolutions and short life cycles, the sub-systems vary over time, as do the interactions. The effect of a change in one area often has an unpredicted effect on other systems.

To fulfil its purpose, for example remote control, the CPW needs to fulfil multiple functions (radio-communication, control, vision, etc.) with a diversity of systems that are not usually designed to be combined and interoperable.

These are the characteristics of a high complexity (Jacobs, M. A.,2013). The CPW is a complex infrasystem.

4. Technical Management of the CPW

A complex system that isn't well designed and managed, becomes very vulnerable. A single failure or well-intended change can result in failure of the whole system.

The preferred way to manage complexity, is to reduce it. Reducing complexity can be done on a technical level and on an organizational level.

5.1 Managing complexity on a technical level

Reducing complexity on a technical level can be done by:

- Modular design
- Clearly identifying and defining interfaces between (sub)systems
- Using minimal specifications for the services and interfaces between (sub)systems
- Creating multipurpose, open in between-layers
- Utilizing open widely used technical standards
- Separating functions/services
- If unavoidable, proprietary brand-based standardization

To summarize, we need to design the system to allow for continuous, fast and easy updates, upgrades, adaptions, modifications, … in contrast with building something that will last unaltered for 100 years.

5.2 Managing complexity on an organizational level

Willem and Buelens (2009) argue that technical dependency runs parallel with knowledge dependency. The need to share knowledge between organizational entities is a function of the interdependency of these entities.

Otherwise stated: (Conway, 1968): "Any organization that designs a system will inevitably produce a design whose structure is a copy of the organization's communication structure."

A frequent form of technical management of IWI uses an organizational structure roughly based on two dimensions: by geographical location and by technological life-cycle phase, usually study, construction and maintenance.

This is rational for classic IWI. Coordination between geograpical location is easy, because of the very limited minimal waterway specifications. Coordination between life-cycle phases is relatively easy aswell, because of supplier independency, ease of codification, long life cycles etc.

Given the characteristics of the CPW-system and its components, this strategy becomes problematic.

To reduce and manage complexity for cyber-physical systems on an organizational level, organizational structure should be at least partially aligned with a divison into (technical) subsystems. This reduces the need to transfer knowledge and reduces variety. At the same time, this will automatically result in more transparant system borders, clearer system-interfaces and modularity.

To further reduce the need to transfer knowledge and to cope with the high dynamics it is favorable to manage the different life-cycle phases of the components of the same system from the same organizational entity.

These implications hold true, wether the organisation uses in-house staff or outsources most tasks. When using outsourcing, procurements for a subsystem should comprise and integrate the different life-cycle phases such as implementation, maintenance and renewal.

5. Conclusion

Technical management of waterway infrastructure used to be little dynamic and coördination was relatively easily done by dividing technical management into geographical bounded areas and using minimal technical specifications inbetween.

Inland waterways are now rapidly evolving towards complex systems. If not well managed, complex systems are vulnerable systems that are hard to maintain and expensive to modify.

Successful technical management of the CPW is done by reducing complexity and aligning technology and organizational strategy by adapting for specific technological and system characteristics. Use organizational entities that manage the whole life cycle of a subsystem accros a the geograpical borders.

In conclusion; design your technical management the way you want your overall CPW-system design to be.

References

1. Conway E. Melvin (1968) How Do Committees Invent, Datamation magazine, April 1968
2. Jacobs, M. A. (2013). Complexity: Toward an empirical measure. Technovation, 33(4-5)
3. US National Science Foundation (2009) Cyber-Physical Systems (CPS) nsf08611
4. Hermann, M., Pentek, T. & Otto, B. (2015). Design Principles for Industrie 4.0 Scenarios - A literature Review (Working paper). (01), 13.
5. Willem, A. & Buelens, M. (2009). Knowledge sharing in inter-unit cooperative episodes: The impact of organizational structure dimensions. International Journal of Information Management, 29(2), 151–160.
6. Zander, U. & Kogut, B. (1995). Knowledge and the Speed of the Transfer and Imitation of Organizational Capabilities - an Empirical-Test. Organization Science, 6(1), 76–92.

Paper 124 – St-Lawrence Seaway Modernization

NOLET B.; P. Eng.
St-Lawrence Seaway Management Corporation (SLSMC), Canada

Email (1st author): bnolet@seaway.ca

ABSTRACT: The SLSMC is modernizing its current mode of operation through the use of various key technologies: (1) Hands-Free Mooring ("HFM"); (2) Vessel Self-Spotting ("VSS"); (3) Remote Operation and (4) Leveraging AIS. HFM employs vacuum technology to secure a vessel to the lock wall at the touch of a button, instead of the traditional manual tie-up process. The project complements existing technology and enables the SLSMC to continue providing safe and reliable transits while improving its financial position through reduced costs and increased revenues.

1 INTRODUCTION

In its effort to tighten its operating costs, the St-Lawrence Seaway Management Corporation (SLSMC) had to look at technology in order to leverage its productivity and efficiency, and ensure its sustainability for the long term. In researching different technologies to achieve this, the SLSMC had to align with the interests of its stakeholders who use the system, to ensure that gains are also realized on their side.

As a result of stakeholder consultations, it was deemed essential that the "modernized" Seaway had to be:

- as safe or safer to transit through,
- as fast or faster to transit through,
- able to reduce the need for manual labor during lockages and improve staff efficiency, and
- able to alleviate some of the requirements for specific seaway fittings in order to potentially allow more vessels access into the Seaway.

2 MODERNIZATION

2.1 Hands Free Mooring (HFM)

2.1.1 Holding Capacity

The process of going through the St-Lawrence Seaway locks can be demanding. The need to deploy mooring wires (28mm diam.) to stabilize vessels during turbulent lockages not only puts a strain on vessel components, equipment and personnel, but can also place both lock and ship personnel in harm's way. Vessels are traditionally subjected to intense hydraulic forces within a very confined lock, and all involved personnel must apply a high level of awareness to ensure a smooth and safe transit.

There have been cases of mooring wires breaking, which can endanger the safety of all personnel in the vicinity. Mooring wires typically break when attempting to stop vessels, or during an upbound lockage, when the turbulence is at its highest.

One of the main goals of HFM was to reduce or eliminate the need for handling mooring wires, in order to eliminate some of the biggest hazards of vessels transiting the seaway system. As well, the elimination of handling mooring wires would not only eliminate time consuming tasks, but would also translate into personnel no longer having to execute heavy labor, and instead, being available to execute other tasks. The challenge resided in the deployment of a mooring system which would surpass the holding capacity of four mooring wires and hold all vessels almost completely in place throughout all the lockages.

For the large commercial vessels (up to 225.5m in Length) four mooring wires are required to secure the vessel inside the locks during the lockages, two at the bow, and two at the stern.

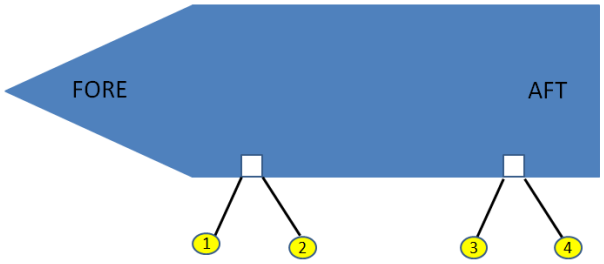

Figure 1: Four Mooring Wires are required for lockages

Mooring wires and associated winches may have a pull capacity of up to 10 Tons each, providing, at best, 20 Tons of holding force in either of the fore-aft direction (assuming wires are parallel to the vessel). Still, it was common to see vessels drifting forward and aft a few meters during a lockage, allowing possible impacts with neighboring structures, causing damage. A typical deep lock in the Seaway has 14metres difference between upper pool and lower pool, and the fill times vary between 8 to 10 minutes. This creates high turbulence around vessels in low pool, with beams sometimes only 600mm less than the width of the lock. The highest forces were measured either at the start of a fill for an upbound vessel, or when the lower mitre gates open prior to releasing a lowered vessel (the lower end mitre gates open swinging towards the vessels).

Any new mooring system not only had to be able to raise and lower with the moored transiting vessels, but also had to be recessed into the existing lock walls when not used. Vessels with beams of 23.77m are common in a lock 24.38m wide leaving no room to accommodate for the equipment, This substantially restricted the allowable fore-aft movement of the new mooring system once moored to the vessels, since vertical slots had to be cut in the existing lock walls to install the new mooring equipment. The need for the HFM equipment to be able to move vertically was emphasized by the high number of vessels who have thick steel rub bars, usually positioned near the waterline. The mooring system had to have the ability to position the different units at a variety of desired heights in order to avoid any rub bars, even if the vessel is in ballast, with a deep draft at the stern and a shallow draft at the bow.

As prototypes were developed and installed, equipped with load cells and strain gauges, along with new water level sensors in strategic locations, data started to be collected for upbound lockages and downbound lockages. Different fill profiles and different locks presented different force patterns over time, which required some HFM equipment adaptation. It was not financially viable to implement a system with sufficient capacity to hold all vessels with zero fore-aft movement allowed. It became evident that a balance between holding capacity and allowable vessel movement had to be achieved. Allowing some vessel movement during lockages drastically reduced the forces on the HFM equipment. Different concepts of energy absorption were explored, ending on the selection of hydraulic cylinders anchored horizontally behind the vacuum pads,

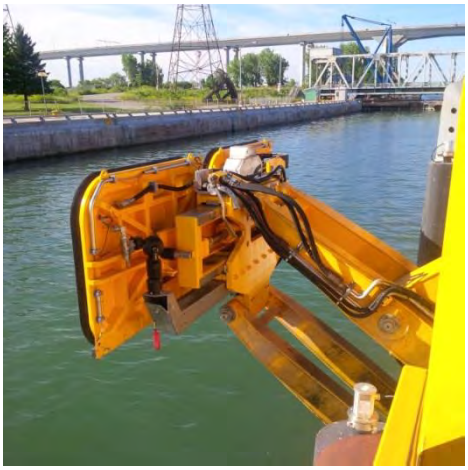

Figure 2: Double Unit extended in to the lock

A standard vacuum pad draws a vacuum of up to -95 KPA, which translates into a coupling force of 20 tons per pad in the pull away direction. The main part of the pad which makes contact with the vessel hull is the neoprene seal on the perimeter of each vacuum pad. The coefficient of friction between the neoprene seal of the vacuum pad and the steel hull is such that the holding force in the vessel's fore-aft direction is approximately 10 Tons per vacuum pad. Any forces in different directions are to be added when considering the overall holding capacity

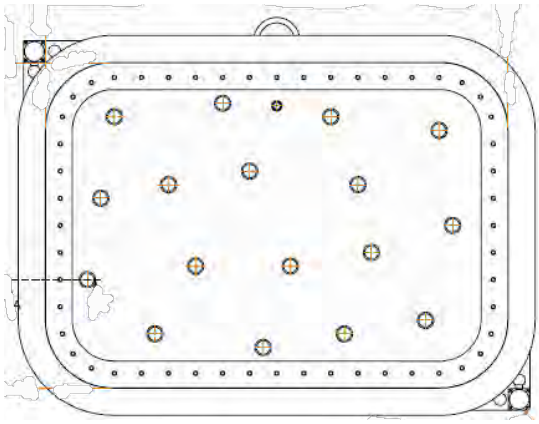

Figure 3: Typical Cavotec MoorMaster [tm] vacuum pad

The final mooring system being deployed at all deep locks of the St-Lawrence Seaway system is made up of a total of six (6) vacuum pads, providing an overall holding capacity of 120 Tons, or 60 Tons in the fore-aft direction. The layout chosen comprises of three (3) double units, each unit is recessed inside a slot in the lock wall, to minimize civil installation costs. Each pad can move up to 300mm in either direction (downstream or upstream, moored or unmoored).

Allowing a maximum fore-aft movement of 300mm in either direction while moored has been deemed appropriate, keeping the forces within the system capacity for the majority of the vessels. It has also been deemed sufficient to withstand the forces in the reverse direction immediately after mooring upbound vessels in low pool, as a result of the piston effect experienced by large upbound vessels entering the locks with speed.

In some cases, the timing of opening of the intake valves to fill the locks has been adapted to ensure that the main forces on the mooring equipment are vessels pushing into the vacuum pads as opposed to pulling on them, and balancing the fore-aft forces. As well, as a new standard, vessels are now held 300mm away from the lock walls, to preserve the vessel hulls and the lock walls. This change has had an impact of water movements during lock filling, which required some customization of the valve timing opening sequences.

Figure 4: Three double units recessed in a lock wall

2.1.2 Layout of the Mooring system

When establishing the layout of the equipment, a balance had to be reached between spacing the double units as far as possible to provide them with the best leverage while holding the vessel, and the need to be able to attach to as many vessels as possible using the Seaway system. Commercial vessels as short as 100m in length and as long as 225.5m use the system, and the 6 pads need parallel body to secure the vessels. Based on the profile of the fleet using the Seaway system, it was decided that the optimal layout was to place all three units 25m apart from each other, for an overall footprint of 50m, and centered along the lock wall. Any vessel with approximately 60m of parallel body will be secured with three double units. Shorter vessels may be processed with only two units (4 pads) since the forces on the vessels during the lockages are much less, with the water having more room to move around the vessel.

Figure 5: Mooring units centered in the lock wall, 25 m apart from each other

2.1.3 Warping and positioning vessels

As prototypes were being refined, it also became evident that, for the narrower vessels using the Seaway, the use of wires for positioning close to the lock wall was going to require the provision of an equivalent method, if wires were no longer going to be used. The latest mooring units were designed with the ability to extend close to 2m into the lock, capture the vessel, bring it close to the lock wall and hold it off the concrete face. This added feature has been very well received by the Seaway stakeholders, with the added benefits of safety and time savings.

With the tight tolerances between vessel length and lock dimensions, there was sometimes the need to have vessels move forward 4-5 metres after being stopped, in order to properly fit within the confines of the locks. With the removal of mooring wires, which was the preferred method of finalizing the positioning of vessels, the mooring system had to gain the ability to move vessels a set distance in a set direction (fore or aft). A "Warping" sequence, a Cavotec patented active control technology developed for other installations was modified for this application. It is made up of a series of "attach /

move sideways / detach /re-position /re-attach / etc". The Warping function makes it possible for the Hands Free Mooring system to not only capture the vessels, but also place them in their final position longitudinally in order to proceed with the lockage.

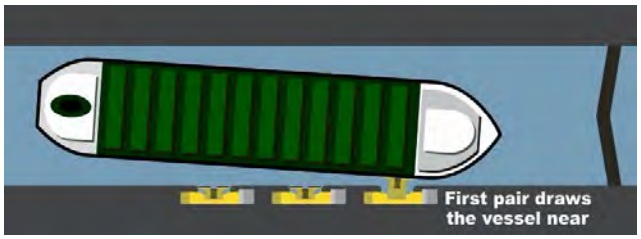

Figure 6: Hands Free Mooring units bring vessels close to the lock wall, and hold them off the concrete wall during the lockage

2.2 Vessel Self-Spotting (VSS)

Vessel clearances at either the stern or the bow can be as short at 3-4 metres. This forces the need for accurate positioning inside the lock before the lockage can proceed.

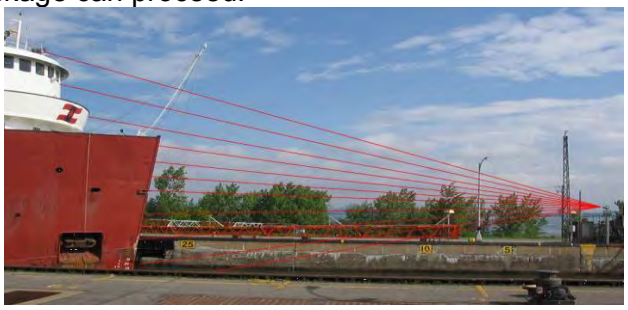

Figure 7: Laser Scanner to spot vessel into lock

VSS uses innovative three-dimensional Class 1, eye-safe laser scanning and image recognition techniques to detect and track the position of the most forward portion of the vessel. It indicates to the vessel the distance it has to go to reach its final mooring position in the lock. The vessel's position is updated dynamically and displayed to the vessel on LED panels, as it progresses to its final mooring position.

Figure 8: Laser Scanner and Display Panel

VSS is currently implemented and proven operational at all the SLSMC deep locks.

2.3 Remote Operation

With the implementation of Hands Free Mooring, the presence of personnel at the lock is no longer required. The operation of the lock can now be done from any site, and are being centralized into the Seaway's traffic control centres. This allows lock operators to be in charge of different locks at different times, depending on traffic patterns.

The Modernization Project also consists of implementing remote operations for all locks and bridges of the St-Lawrence Seaway Management Corporation. More specifically, the lock operation and associated tasks are being transferred to central control points where operations can be executed and monitored remotely. The ability to touch, hear and see is being replaced by modern cameras, microphones and sensors; in order to ensure smooth transition. The functions being transferred to remote operation will include the following lock equipment:

- VSS;
- gates that allow vessels entry and exit from a lock;
- valves filling and emptying locks;
- ship arrestors, which are used for protection of gates in case vessels do not stop at the appropriate position; and
- the HFM equipment

Remote operation has already been implemented for all movable bridges and has been working successfully for several years.

Figure 9: Remote Operations of Locks and Bridges

2.4 AIS Leveraging

In a remote operation environment, ensuring a high level of situational awareness becomes more challenging, as the operator no longer has all the clues he/she is familiar with, from being on site. Therefore better failsafes need to be developed to better safeguard against operational errors.

It is a Seaway requirement that every commercial vessel entering the Seaway must have a fully functional Automated Identification System (AIS). This allows vessels to broadcast their position and see other vessels' positions. Geofencing is being created around the vicinity of seaway structures. When vessels approach structures such as bridges or locks, the AIS position is tracked. When the vessel enters the pre-determined geofenced perimeter of the structure, the operator will be prevented from lowering a bridge or closing lock gates just ahead of an oncoming vessel.

Figure 10: Leveraging AIS to protect Lock Gates

3 BENEFITS DELIVERED

3.1 Safety

As more and more compatible vessels are using the HFM system, the use of mooring wires is also disappearing (one of the major injury factors on board a ship). This translates not only into a reduction of frequency of wire breaks and associated hazards, but also a reduction of manual labor which translates in an improvement in the working conditions of all personnel involved.

The process of transiting through the Seaway locks has gone from being very labor intensive to being automated with machinery executing the hard work.

Additional benefits in safety cost savings related to the avoidance of lost time injury are also anticipated over time.

With the addition of AIS failsafes, transiting through the Seaway will remain the safest mode of transportation of goods.

3.2 Staff efficiency

With the HFM equipment securing the vessel safely in position, the tasks of tending to the winches and mooring wires are no longer required, freeing up personnel to execute other tasks.

With increased regulations around work hours and mandatory rest periods, the automation of the mooring has provided some flexibility for vessel crews to facilitate compliance to regulation, by being available during the lock transits, either for other tasks or for resting

.

3.3 Time savings

With the requirement of four mooring wires for each commercial vessel, the tasks of deploying handlines, tying up mooring wires, hoisting up the mooring wires with car haulers and placing them on bollards was time consuming. The mooring and releasing of vessels with the HFM system only takes a few seconds.

3.4 Other benefits

With the requirement to use four (4) mooring wires at each lock, the wear and tear on vessel-mounted equipment such as winches and wires, and its related maintenance and replacement costs, can be substantial. The implementation of HFM at every deep lock completely eliminates that portion, lengthening the equipment life, and spreading the related maintenance.

A review of the current mandatory requirement for vessels to be equipped with mooring wires and roller fairleads will be done, once the system is fully converted. Alleviating this requirement may facilitate Seaway access to some vessels not currently equipped with wires and roller fairleads.

In addition, in the Great Lakes environment, the absence of salt water means that vessels may expect to have a longer service life than salt water vessels. It is common to see vessels with considerable age transit through the Seaway. Sliding on approach walls and lock walls has

translated into hulls with poor surface quality on older vessels. With vessels no longer required to tighten their mooring wires to ensure contact with the lock wall during the lockage, the hulls no longer rub the concrete walls with extensive pressure. Not only does this extend the condition and life of both the vessel hulls and the lock walls, but it becomes an important factor, as fleet renewal is currently taking place in the Great Lakes area.

4 CONCLUSION

A 2011 study called "The Economic Impacts of the Great Lakes – St-Lawrence Seaway System" revealed the following global contributions of the Seaway system:

- 227,000 jobs
- $34.6Billion (CAD) Economic Contribution
- $14.5Billion (CAD) Personal Income
- $4.7Billion (CAD) in taxes paid to Federal, State,Provincial Governments

These findings emphasized the importance of keeping the vital St-Lawrence Seaway system healthy, competitive and efficient for years to come.

A total of $7.1 Billion (CAD) is currently being invested globally (between 2009 and 2018) in different parts of the Seaway system, of which $1.2Billion (CAD) has been targeted for ships, as part of a global fleet renewal program.

The leveraging of technology to control operating costs allows the St-Lawrence Seaway Management Corporation to remain an efficient and competitive transportation choice.

The recent deployment of technologies such as Hands Free Mooring and Vessel Self Spotting has been very well received by Seaway stakeholders. The improvements in transit times, in safety, the reduction of potential hull damages, the avoidance of extensive maintenance of ship-based equipment, and the flexibility provided in resource allocation has translated into our stakeholders now asking for a faster implementation throughout the Seaway system.

REFERENCES

"*The Economic Impacts of the Great Lakes – St-Lawrence Seaway System*", Martin Associates, Lancaster, PA, October 18, 2011

A PLANNING FRAMEWORK FOR IMPROVING RELIABILITY OF INLAND NAVIGATION ON THE MADEIRA RIVER IN BRAZIL

by

Calvin T. Creech[1], R.S. Amorim[2], A.N.A.O. Castañon[2], S.A. Gibson[3], W.C. Veatch[4], T.J. Lauth[5]

ABSTRACT

The Madeira River Waterway is an important transportation link between the agricultural production areas of western Brazil and the deep draft ports on the Amazon River, where commodities are transferred for domestic consumption or international export. However, navigation reliability is limited, especially during low-flows. In addition, current economic studies predict that the demand for the waterway is expected to increase, especially for agricultural commodities. A primary impedance to navigation on the Madeira River is sand shoals in thalweg crossings, especially near split flows at islands. These bottlenecks in the system require navigators to light-load their barge convoys to tonnages less than 25% of loads transported during high water levels. A secondary impedance is associated with rock outcrops near the navigation channel, which combined with a lack of aids to navigation, increase risks of accidents for the convoys.

To address navigation reliability and safety, a planning study framework has been developed on the Madeira River. This framework aims to design alternatives that will provide economically justifiable engineering solutions for improved waterway reliability and reduced navigation risk (safety) during low-flow conditions. The planning study implements the USACE 6-step planning process, which includes identifying navigation opportunities; forecasting future navigation conditions; and formulating, evaluating, comparing, and ultimately selecting a recommended plan. The planning study evaluates alternatives consisting of maintenance dredging, rock excavation, river training structures, and bank stabilization using engineering tools that were developed to assess design effectiveness. Alternatives were analyzed by combining five primary studies; namely, a statistical analysis of navigation reliability; a fluvial geomorphology study, a hydraulic model to determine low water datum conditions; development of a design barge configuration and associated channel dimensions; and a sediment transport model to evaluate channel response due to the proposed measures and alternatives.

The statistical analysis developed a framework for the determination of the navigational low water reference level. This information was used to calculate the low water reference plane in a hydraulic model between observed gage locations. The model was calibrated to known sand shoal depths under low-flow conditions as well as moderate and flood flows. The design barge configuration task was combined with a fluvial geomorphology study to demonstrate the navigability of a 3x3 barge convoy (60m long x 11m wide per barge) configurations during low-flows and a maximum of 5x4 barges during high flows. The channel alignment associated with these design barge configurations was determined to fit within the current sinuosity of the Madeira River, which does not require channel straightening in the system. Finally, the sediment transport model was developed and applied to predict the future conditions associated with the proposed alternatives and to evaluate the effectiveness of dredging, river training structures, and other measures for improved navigation. The planning study analyzes alternatives that will provide the maximum cost-benefit ratio over the 50-year economic life-cycle of the Madeira River Waterway Project.

Keywords: Inland Navigation, South America, Planning, Reliability

---

[1] U.S. Army Corps of Engineers, Mobile District, Calvin.T.Creech@usace.army.mil
[2] Brazilian National Department of Transportation Infrastructure, Brazil
[3] U.S. Army Corps of Engineers, Hydrologic Engineering Center, USA
[4] U.S. Army Corps of Engineers, New Orleans District, USA
[5] U.S. Army Corps of Engineers, St. Louis District, USA

1.0 INTRODUCTION

The Madeira River is an important navigation thoroughfare in western Brazil. Barges transport about 8 million tonnes annually of agricultural and other commodities, primarily downbound, along the Madeira River. Madeira navigation is limited by the geomorphology and sediment processes in the river, which include localized shoaling, shallow channels, and rock outcrops, which force barges to light load during the dry season.

In 2016, the Brazilian National Department of Transportation Infrastructure (DNIT – Departamento Natcional de Infraestructura de Transportes) and the US Army Corps of Engineers (USACE) began an intergovernmental agreement which includes joint contributions to the Madeira Waterway Planning Study and Executive Design (MWPSED). The MWPSED study is a multi-stage planning investigation of navigational alternatives on the Madeira River.

1.1 Site Conditions

The Madeira River is the largest tributary on the Amazon, with its 1,400,000 km^2 drainage area constituting 19% of the total Amazon basin (see Figure 1). The Madeira's navigable reach is approximately 1,080 km, from its junction with the Amazon approximately 150 km downstream of Manaus, to the Santo Antônio dam, just upstream of Porto Velho.

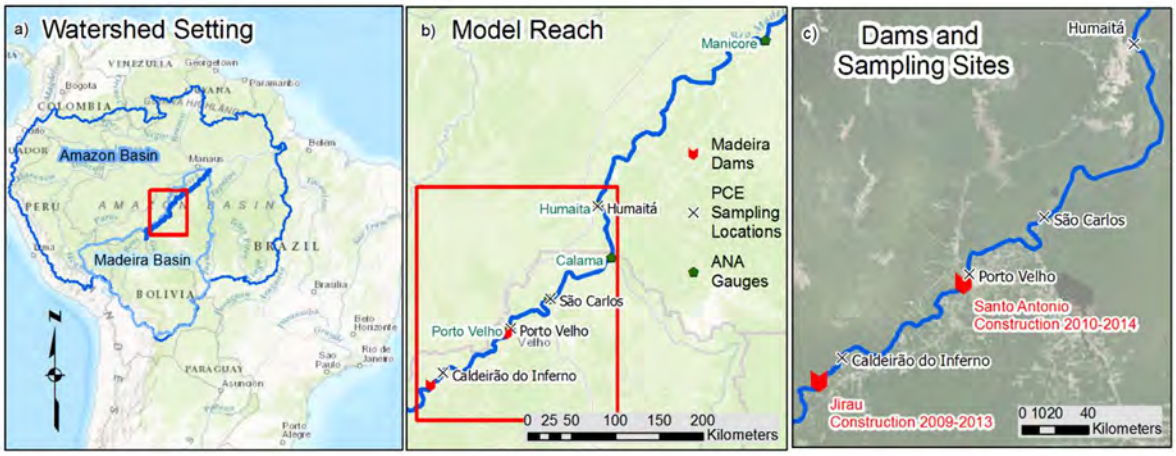

Figure 1: Project site map, including two dams built between 2012 and 2014, ANA gages, and PCE (2015a and 2015b) sampling sites.

The navigational reach of the Madeira can be divided into two, morphologically distinct sub-reaches, of approximately equal length, upstream and downstream of Manicoré, Amazonas (Teixeira and Maia, 2009). The "Lower Madeira Waterway" (Segment I) is straight and more confined, with a narrower floodplain contained by Pleistocene terraces (DNIT/USACE, 2017). The "Upper Madeira Waterway" (Figure 1b) about 600 km from Manicoré to Porto Velho (Segment II), which is much more sinuous, and winding across a much wider floodplain.

Two dams upstream of the Porto Velho were constructed between 2008 and 2014 (Figure 1c). Construction on the Jirau dam began in 2008. The Jirau dam was mostly completed in 2013, when it began generating electricity, though construction continued until 2015. Santo Antônio dam construction lagged the Jirau by about a year. Construction began in 2009 and finished in 2014, just before the flood of record. Both dams are "run-of-river" with little water storage. Neither dam currently has a lock, which prevents any commercial navigation upstream of Porto Velho, Rondônia.

1.2 Current Navigation Conditions

The Madeira Waterway is primarily used for the transport of agricultural commodities (soy and corn) that originate from the central-west region of Brazil (Mato Grosso and Rondônia). The current transportation fluxes throughout any reach of the Madeira from the years 2010 to 2012 are shown in Table 1 (LEME/PETCON, 2014). Approximately 73% of the goods shipped on the Madeira River consist of soy (56.6%) or corn (16.2%) although the Madeira waterway is used for numerous other commodities.

Commodity	Tonnes/year	Percentage
Soy	4,720,902	56.6%
Corn	1,353,436	16.2%
Roll-on / Roll-off, Miscellaneous, and Containers	953,163	11.4%
Fuels, Mineral Oils and Products	557,879	6.7%
Fertilizers	307,875	3.7%
Cement	250,846	3.0%
Machinery	103,628	1.2%
Sugar	32,149	0.4%
Other	53,848	0.6%
Total	8,333,727	100.0%

Table 1: Annual Tonnage of Commodities Shipped on the Madeira River from 2012-2014

Due to the low water levels during the dry season, navigation drafts are significantly impacted in critical reaches of the navigation channel. As a result, navigation companies adjust both the barge configuration and the per barge tonnage in order to achieve safe navigation during the dry period. According to a recent navigation feasibility study (LEME/PETCON, 2014), during the months of August through October the barge companies typically use 9 barges (3x3), whereas during the rest of the year the companies typically transport with either 16 barges (4x4) or 20 barges (5x4) as shown in Figure 2.

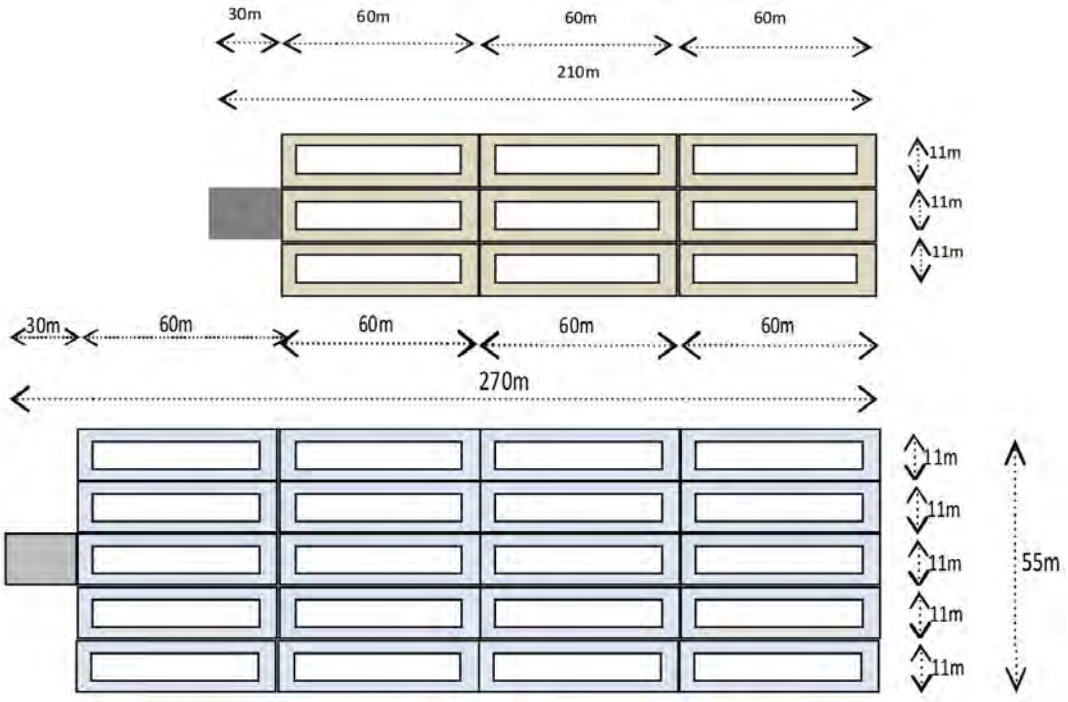

Figure 2: Tow Configuration during Low Flows (above) and High Flows (below)

Light-loading of the individual barges is currently necessary during the low water season to reduce navigation drafts. A fully loaded 60m x 11m barge can carry approximately 2,000 tonnes, which corresponds to a navigation draft of approximately 3.5 meters (although some companies load the barges up to 2,500 tonnes per barge or more during the wet season). However, during the dry season many companies light-load individual barges to 1,000 tonnes or less. During the dry season, drafts can be as low as 1.8 to 2.0 meters in the most critical reaches of the navigation channel. Finally, the travel times are also increased in the low water months. During high flows, the downbound travel time from Porto Velho, Rondônia to the deep draft port at Itacoatiara, Amazonas is approximately 60 hours, whereas during the low flows, downbound travel time is approximately 92 hours (see Table 2). During extreme lows, the downbound travel time can be even longer due night travel restrictions and additional delays associated with breaking up the tow in dangerous rocky sections of the river.

Period	Convoy	Loading per barge	Total Convoy Load	Depth	Itinerary	Travel Time
Wet	20 barges full	2,000 tonnes	40,000 tonnes	3.5 meters	Porto Velho – Itacoatiara	60 hours
	20 barges empty				Itacoatiara – Porto Velho	130 hours
Dry	9 barges full	950 tonnes	8,550 tonnes	1.8 to 2.0 meters	Porto Velho – Itacoatiara	92 hours
	9 barges empty				Itacoatiara – Porto Velho	100 hours

Table 2: Typical Travel Times During the Wet and Dry Seasons on the Madeira River

2.0 METHODS

The objective of this study is to develop a planning framework, which will be implemented to improve navigation reliability on the Madeira River. In this approach, alternatives are developed to economically address navigation inefficiencies due to the rock outcrops and alluvial shoals in the navigation channel. The technical approaches used to evaluate the effectiveness of the alternatives are based on five primary studies, which include a statistical hydrologic analysis, a fluvial geomorphology study, a hydraulic study of the low water conditions, a navigation channel study, and a long-term sediment transport model. In future phases of the planning study, an economic analysis will evaluate the feasibility of the proposed alternatives. This paper presents the technical (engineering) methods used to develop and evaluate proposed alternatives for improved navigation reliability.

2.1 Hydrology

Flow on the Madeira is very consistent from year to year. The average hydrograph is smooth and symmetrical (Figure 3). The wet season runs from February to May, with peak flows generally in March or April. Flows drop from May to September, with the lowest flows (and the critical navigational condition) in September and October.

Stage and discharge data were downloaded from the ANA (Agência Nacional de Águas, National Water Agency) HidroWeb website (ANA, 2017), which is a sub-system within the SNIRH Sistema Nacional de Informações sobre Recursos Hídricos, National System of Water Resources Information, http://www.snirh.gov.br/). Both observed and computed discharge data were downloaded. Data were imported in HEC-DSS software and visually checked for obvious errors (e.g. extreme outliers, zeroes in place of missing data, etc.), with such points removed rather than interpolated.

The Porto Velho gage has a nearly complete record from April 1967 to present, with two data gaps in 2010 and 2011. These gaps correspond to periods of gradual change, on the falling limb of the hydrograph. Therefore, interpolating these flows with HEC-DSS does not introduce much uncertainty

into the low flow hydrology model. These daily flows (with the two interpolated patches) became the upstream model boundary condition in the Hydraulic and Sediment Transport Models.

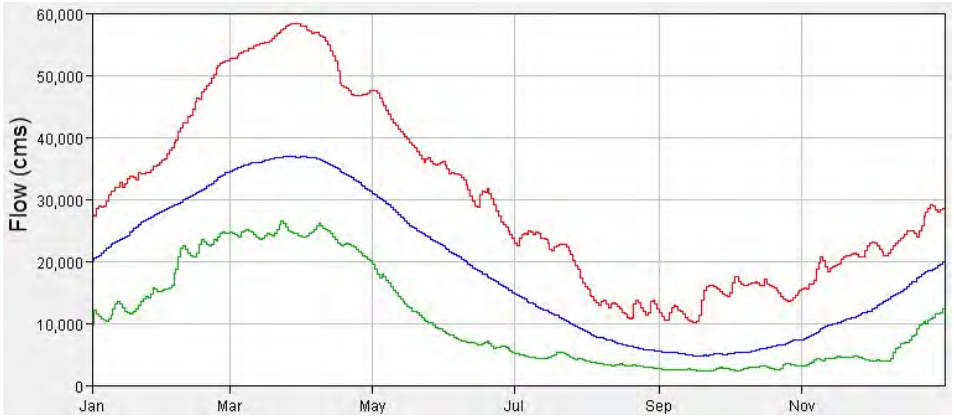

Figure 3: Average Flow at Porto Velho (blue) with Daily Maximum (red) and minimum (green) Flow for each Calendar Day

The majority of the navigation shoals and rock outcrops exist on the upper 600 km of the Madeira River between Manicoré, Amazonas and Porto Velho, Rondônia. The Brazilian Navy uses three gages (Porto Velho, Humaitá, and Manicoré) to established a 90% exceedance stage, and these gages (as well as other ANA gages within the focus area of the study) are shown in Figure 4.

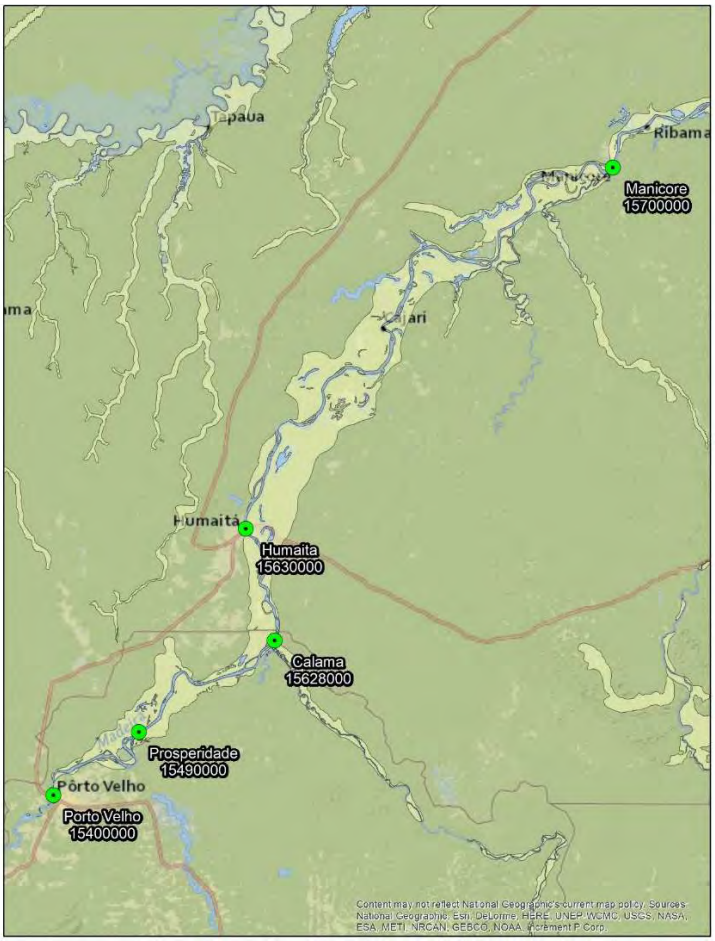

Figure 4: ANA Gages Located within the HEC-RAS Model Domain

2.2 Fluvial Geomorphology and Hydraulics

An analysis of the general quaternary geology was conducted in order to determine overall geologic conditions influencing the fluvial geomorphology and navigability of the Madeira River. Representative maps of the surficial geology for both Segment I (downstream waterway) and Segment II (upstream waterway) are shown in Figure 5 (from Quadros et al., 2007). In Segment I, the Madeira River is generally straighter than Segment II (sinuosity in Segment I is approximately 1.18 compared to approximately 1.4 in Segment II). The Holocene alluvial deposits and floodplains are generally narrower in Segment I than in Segment II. In Segment I, the Madeira River is often adjacent to older Pleistocene era terraces (N3i in Figure 5). The geology map shows that the river oscillates between being adjacent to an older more competent surficial geology on either bank (especially between Borba and Manicoré, Amazonas). This was confirmed in the field where a high, cemented (competent) terrace was often observed on one of the two banks along this reach. Figure 5 demonstrates a relatively narrow Holocene era alluvial deposits in Segment I. This condition results in relatively low rates of erosion of either bank between the mouth of the Madeira River and Manicoré due to the relative stability of the older, semi-cemented Pleistocene valley. Segment II (upstream of Manicoré) generally has wider areas of alluvial deposits than Segment I and is associated with more navigation shoals. The Madeira River does not encroach upon older, more stable terraces in Segment II as often as it does in Segment I. The Holocene alluvium has been deposited more recently than the Pleistocene terraces and this alluvium is more easily eroded, leading to more active morphological features such as avulsions (one has occurred upstream o Manicoré), higher rates of bank erosion, and the migration of meanders moving downstream in the upstream segment II.

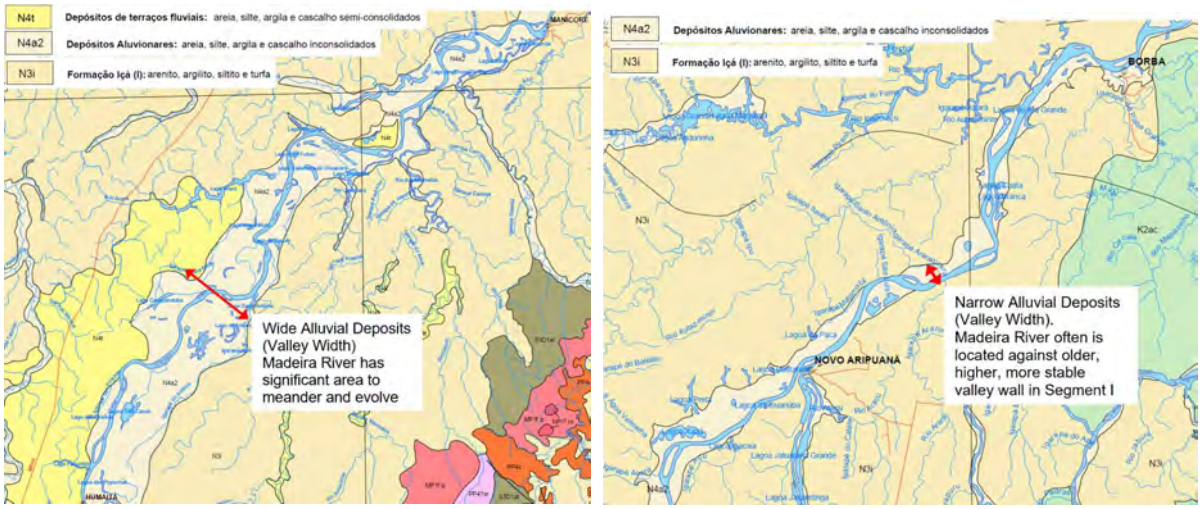

Figure 5: Typical Fluvial Geomorphology Conditions of Segment II between Porto Velho and Manicoré (left) and in Segment I between Manicoré and the Amazon River (right)

Most of the navigation impedances are located in Segment II. Therefore, this reach was the focus of the modeling efforts performed for the study. The Madeira River was first modeled in HEC-RAS to analyze the low-flow steady state hydraulic conditions between the cities of Porto Velho, Rondônia and Manicoré, Amazonas. The main purpose of the numerical modeling completed on the Madeira River is to define a low water condition surface profile for the evaluation of channel reliability.

Hydraulic calculations were performed using the Hydraulic Engineering Center's River Analysis System (HEC-RAS) version 5.0.4. HEC-RAS is an integrated system of software, comprised of a graphical user interface (GUI), separate hydraulic analysis components, data storage and management capabilities, graphics and reporting facilities. The open channel steady-state hydraulic functionality of HEC-RAS was used to model the Madeira River between Porto Velho and Manicoré. Water surface profiles are calculated using a standard-step backwater calculation utilizing the energy equation, momentum equation, conservation of mass, Manning's equation, and other hydraulic equations.

River depths (reducted to a low water datum) were collected by the Brazilian Navy in February and March of 2016. These depths was reduced by using three long-term stage gages along the Madeira River within the model boundary (Porto Velho, Humaitá and Manicoré). At each gage a 90% exceedance stage has been calculated (the values of the Navy recognized 90% stage at each of the three gages are shown in Table 3).

Station	ANA Station Code	Navy Published Level [cm]
Porto Velho, Rodônia	15400000	327.6
Humaitá, Amazonas	15630000	1018
Manicoré, Amazona	15700000	1059.1

Table 3: Brazilian Navy Reduction Level Stages

2.3 Sediment Transport Modeling

A sediment transport model was used to assess the existing conditions of the sediment dynamics, and was used as a primary tool to address long-term impacts to the navigation channel depths based on the proposed alternatives. This model was built using data primarily from the hydraulic model as well as recent studies on sediment conditions (sediment gradations, sediment load estimates, boundary conditions, etc) collected by the Santo Antônio Energy Company (PCE, 2015a and PCE, 2015b). Figure 6 shows typical gradations of the bed collected by these studies, and demonstrates that bed gradations along the navigation channel are generally uniform fine to medium sands with a d_{50} between 0.2mm and 0.4mm. Figure 6 also shows that gradations do not significantly change in either the distribution or size in the downstream direction. The flow-sand concentration data for Porto Velho (upstream boundary of the sediment transport model) are plotted in Figure 7 with temporal traces associated with the 2010 (left) and 2014 (right) events. The 2014 event was the flood of record on the system and was approximately a 300-year event.

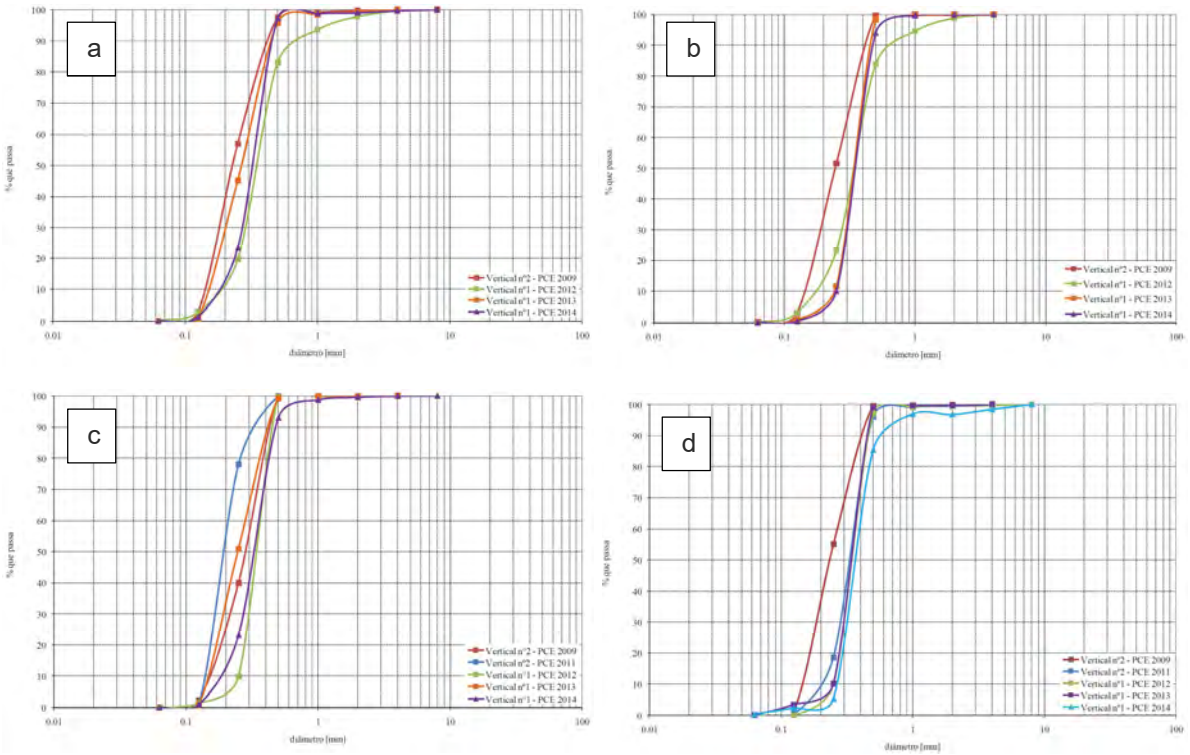

Figure 6: Bed Gradations between 2009 and 2014 of the Madeira River at Distances downstream from Porto Velho. a) 252 km; b) 202 km; c) 152 km; and d) 22 km

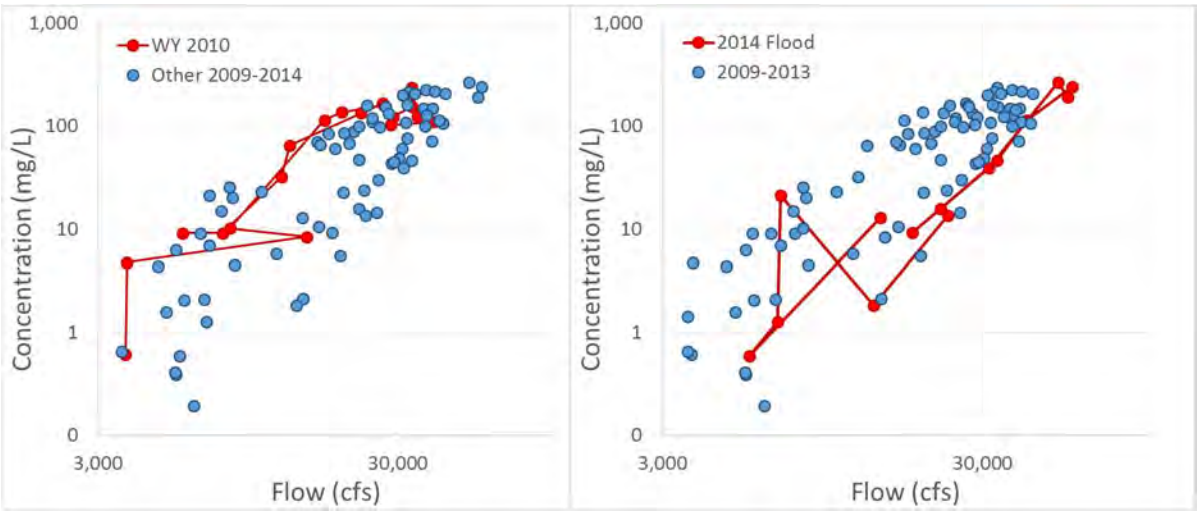

Figure 7: Temporal Trace of the Sand Rating Curve for the 2010 Water Year (WY) and 2014 Flood

2.4 Navigation Channel Planning and Design

The evaluation of current navigation maneuverability and reliability are important to understand the magnitude of interventions (dredging, river training structures, canalization, etc.) necessary to meet the desired level of service. The navigation channel dimensions have been classified for the Madeira River, which consist of a design tow convoy of 210m x 33 m and a navigation channel depth of 3.5 meters (DNIT, 2016). The reliability associated with this waterway design is not specifically identified in Brazilian policy; however, a common level of reliability associated with Brazilian waterways is 90% (or 36.5 days below the defined hydrologic conditions).

Both the Brazilian and USACE systems for defining navigation channel dimensions put restrictions on what is a navigable bend, with the Brazilian system being more conservative for tight bends. For the Brazilian system, a meander or curve in the river is defined as having a radius of less than or equal to 10 times the design tow length. In addition, if the radius is less than 4 times the design tow length, the channel is not considered navigable. Since the design tow length for the Madeira is 210 m then the smallest allowable radius in the Brazilian system is 810 m.

In the Brazilian system, the width of the waterway (for straight reaches) is based on the following:

- One-way traffic the Waterway Width (W) = 2.2 x Maximum Vessel Width (B)
- Two-way traffic the Waterway Width (W) = 4.4 x Maximum Vessel Width (B)

Additional waterway widths for curve sections are not codified in the Brazilian policy, but in practice, the following formula (Equation 1) is generally used for additional widths in curves:

$$B_m = B + \frac{L^2}{2R} \qquad \text{Equation 1}$$

Where, B_m = Channel Width in a meander or curve

B = Channel Width in a straight reach

L = Length of the design vessel or convoy

Additional design elements of the Brazilian system include:

- Distances between curves must be a minimum of 5 x the tow length
- Dredging sites require minimum side slopes of 1:8 for alluvial channels
- Rock excavation sites require minimum side slopes of 1:1

3.0 RESULTS

3.1 Hydrology

The current Nível de Referência (literally “reference level,” meaning benchmark) along the Madeira River, is computed by the Brazilian Navy from stage data at several gages along the river. According to Navy publications, the reference level is the stage that is exceeded by 90% of the observed stages over the specified period of analysis. These levels were recomputed in this study, and as shown in Table 4, the recomputed values did not match the published values, which were all more conservative (lower stages) than the recomputed values.

For the development of the hydraulic model, it was necessary to use the Brazilian Navy published level in order to calculate the low-water datum depths associated with the survey; however, calculated reliability of various flow and stage conditions use the revised calculations in this study. A flowrate associated with the navy reduced stage was applied in order to calculate the recognized low water datum. These flows were calculated by investigating the rating curves at each of the gages (an example is shown in Figure 8 – the Porto Velho gage rating curve). The resulting flows used to develop the calibrated hydraulic model are shown in Table 5. In addition to the flows at each of the gages along the Madeira River, tributary inflows were added to the model at their respective locations. The three main tributaries are the Rio Jamari, Rio Ji-Paraná, and Rio Marmelos. The Rio Jamari is a regulated river with a hydroelectric dam approximately 90 river kilometers upstream of the confluence with the Madeira River. Comparisons of the flowrates between the Rio Jamari and Ji-Paraná show that the distribution of flows is approximately evenly split with the Rio Jamari contributing approximately 47.5% of the increase in flow and the Ji-Paraná contributing approximately 52.5%. This corresponds to a flow increase of 292 cms at the Rio Jamari tributary and an increase of 323 cms at the Rio Ji-Paraná tributary. The 90% exceedance flow for the remaining major tributary (the Rio Marmelos) was calculated as 145 cms. A summary of the flows at all stations used in the reduced depth model are shown in Table 5.

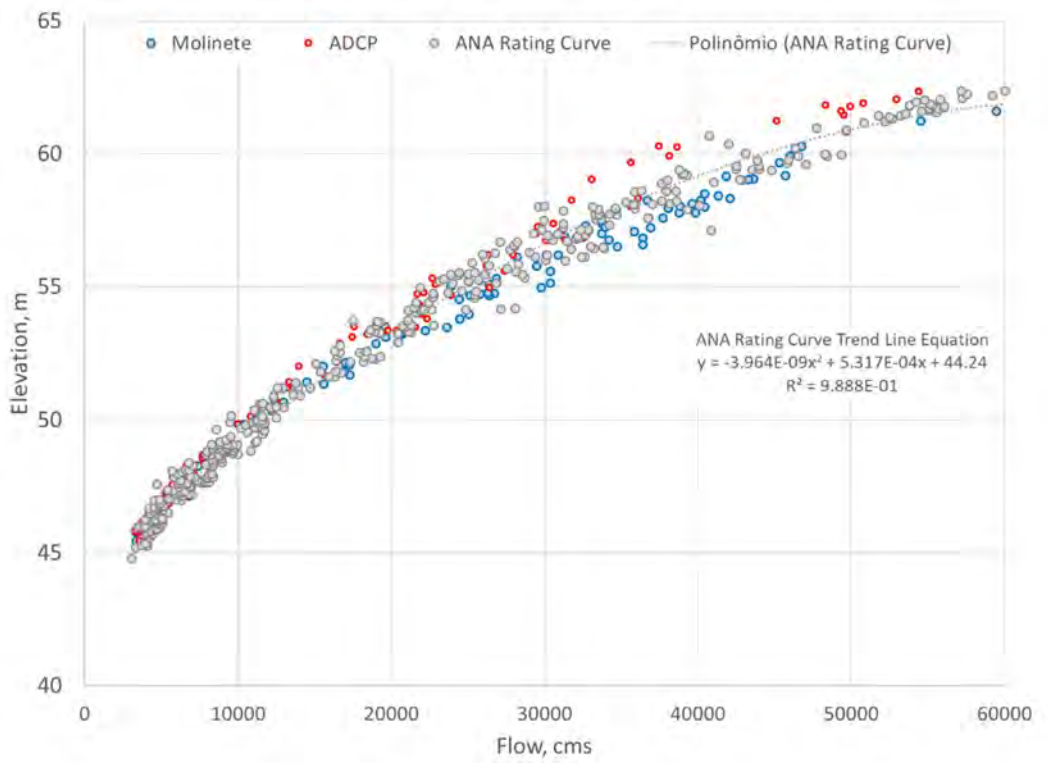

Figure 8: Elevation-Flow Rating Curve at Porto Velho (ANA Gage 15400000)

Station	Navy Published Level [cm]	90% Re-Computed Level [cm]	Actual Duration of Navy Level
Porto Velho	327.6	398	95.8%
Humaitá	1018	1071	94.7%
Manicoré	1059.1	1157	94.0%
Fazenda Vista Alegre	1010	1090	94.3%
Novo Aripuana	905	962	94.7%
F.V. Alegre	1010	1090	94.3%
Borba	1030	1121	94.1%
Nova Olinda D.N.	920	1015	94.3%

Table 4: Comparison of Navy Published Reference Levels to Computed Stages

HEC-RAS Station	Description	90% Exceedance Flow, cms	Estimated Tributary Flow Increase, cms
613.98	Porto Velho Gage	4308	
524.80	Jamari Tributary	4600	292
427.76	Ji-Paraná Tributary	4923	323
360.76	Humaitá Gage	4923	-
92.59	Marmelos Tributary	5068	145
0.00	Manicoré Gage	5068	-

Table 5: Flowrates Supplied to the Low-Flow HEC-RAS Model Representing the Brazilian Navy Reduction Level Condition

3.2 Hydraulic Modeling

The hydraulic model was calibrated by confirming stage elevations observed at the intermediate gage at Humaitá (252 km downstream of Porto Velho) and at the upstream Porto Velho gage. These values are shown in Table 6 and the differences have a maximum of 0.54 m between computed and observed. It is important to note that the original rating curves for Humaitá and Porto Velho have approximately +/- 0.6 m of spread in the observed stage values at a given flowrate. The output of the low water reference plane is shown in Figure 9.

Name	Station, km (upstream of Manicoré)	Observed Low Water Surface Elevation Gage, m	Calculated Water Surface Elevation, m	Difference, m
Porto Velho	609.18	45.95	45.41	-0.54
Humaitá	360.76	34.47	34.67	+0.20

Table 6: Low Water Calibration of the Madeira River HEC-RAS Model

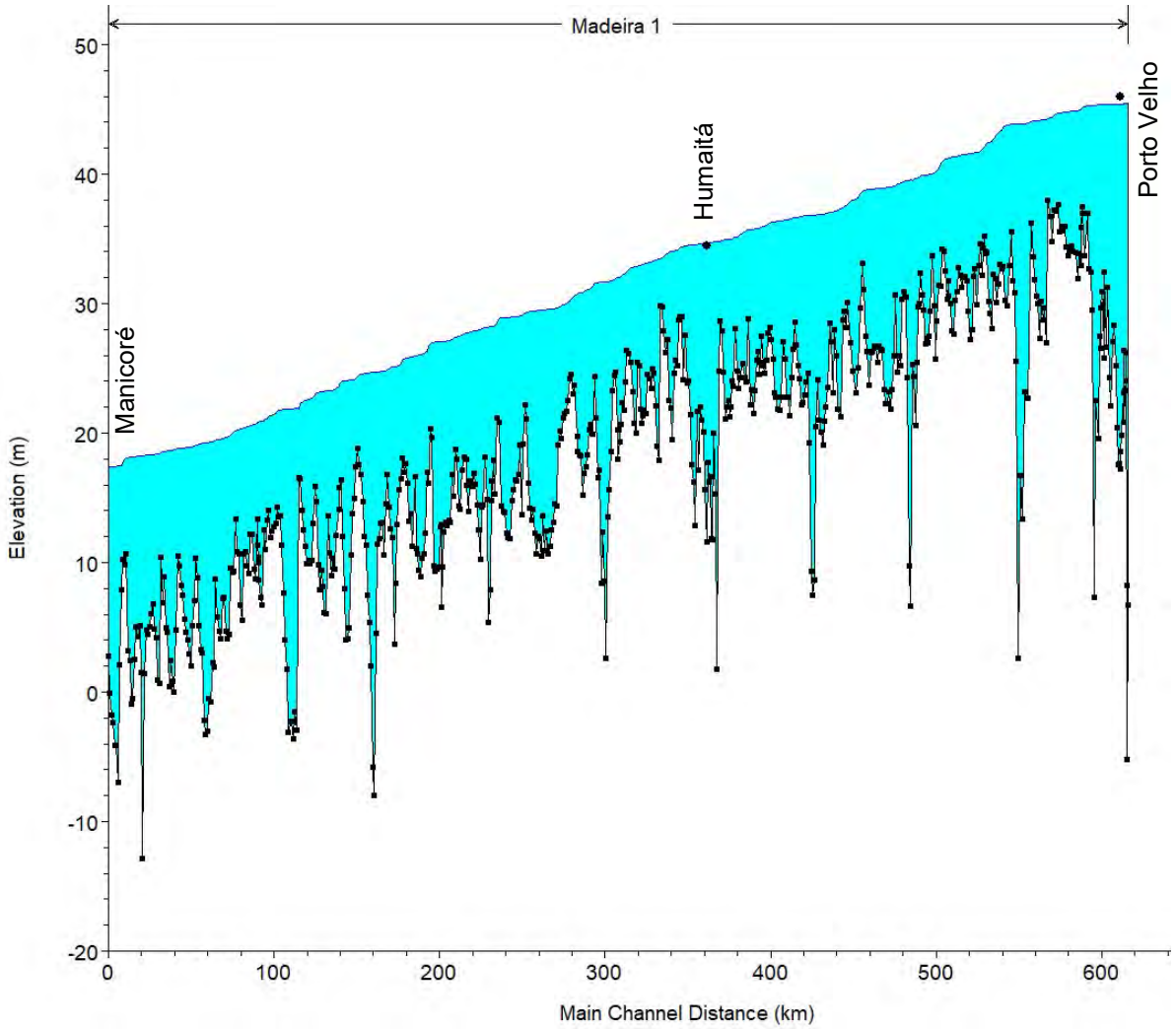

Figure 9: HEC-RAS Low Water Condition Calculated Reference Level

The hydraulic model was then used to calculate dredging removal volumes as a function of navigation channel depth and reliability. The current navigation channel is classified as having a 3.5 meter deep channel. Combining the statistical hydrology data with the hydraulic model an evaluation of the current reliability was made. Simulating the associated steady flow conditions from each flow-stage rating curve within the model boundary, it was found that a 3.5 meter deep channel is available 75% of the time (representing current reliability of 75%). In critical shoal locations, dredging a one-way channel has been proposed by DNIT and would require approximately 250,000 m^3 to achieve 90% reliability and approximately 550,000 m^3 to achieve a 95% level of reliability (95% corresponds to the approximate actual navy reduction level based on the recalculation in the hydrologic analysis). Additional dredging volumes can be found in Figure 10 for various percent exceedance values and design channel depths.

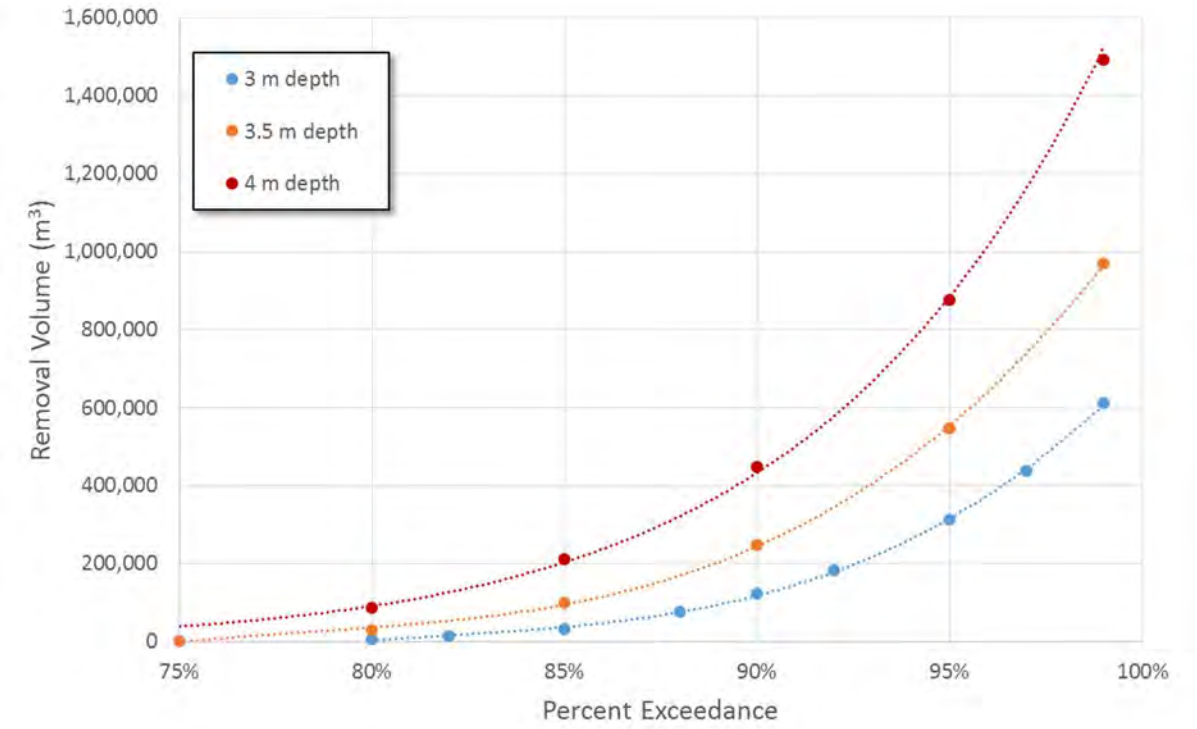

Figure 10: Current Dredging Volumes for One-Way Traffic Through Critical Shoals for Various Levels of Reliability and Navigation Channel Depths

3.3 Sediment Transport Model

For the Madeira River, watershed delivery processes and bed scour introduce sediment as the hydrograph rises. This sediment is the source of many of the navigation impedances on the Madeira Waterway. The watershed sources tend to be finer than bed sources. But regardless of the sediment source, hysteresis occurs in most rivers when these sources are exhausted over the course of a flood, shifting to a supply limited regime, often before the hydrograph peaks. The Madeira River follows this model, transporting very large concentrations at moderate flows early in the wet season, but exhausting the fine sediment sources before the flow peak. However, this supply limitation applies mainly to wash load (silt and clay). As the river exhausts fine sediment sources the sand fraction of the suspended sediment increases, since more of the transported sediment is entrained locally from the bed.

A sediment budget schematic was developed showing the relative inputs of the tributaries to the Madeira River reach downstream of the Santo Antônio dam (Figure 11). Sediment yield from the Santo Antonio dam (and sources upstream) are more than two orders of magnitude greater than the estimated inputs from tributaries between Porto Velho and the confluence of the Madeira River with the Amazon River.

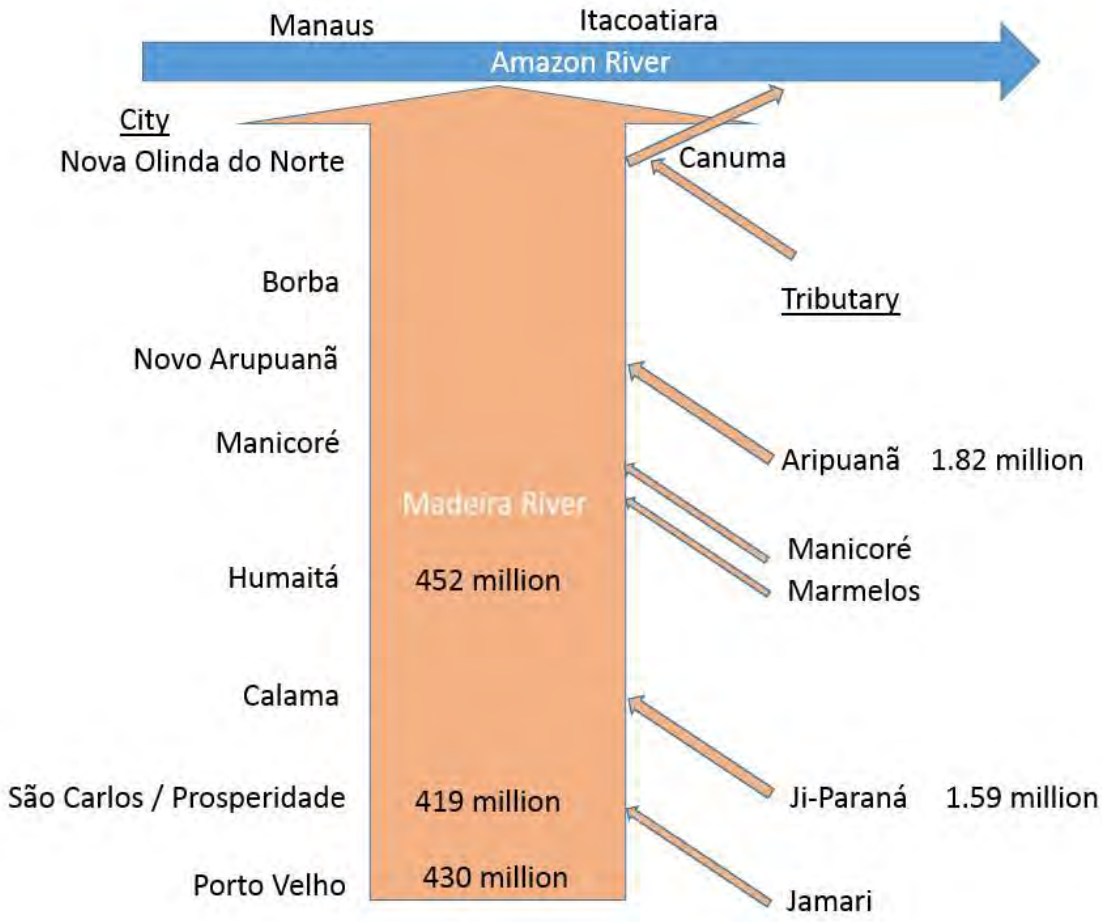

Figure 11: Average Annual Suspended Sediment Budget of the Madeira River (in tonnes)

Collected sediment data was analyzed to determine annual patterns associated with sediment loads versus river flow. Almost all of the PCE (2015b) suspended sediment measurements include a sand-silt split, reporting the percentage of the sample larger than 63 microns. The sand percentage measurements (at Porto Velho) are also plotted against flow and concentration in Figure 12. The suspended sediment concentration and sand content time series are plotted with the Porto Velho hydrographs in Figure 12. The concentration peak leads the flow peak (Figure 12 – top) and the sand content peak tends to lag the flow peak (Figure 12 – middle). Combining the concentration and sand fraction data into a time series of sand load (Figure 12 – bottom) reveals that the sand sedigraph neither leads nor lags the flow hydrograph. Sand transport tends to track flow, peaking at approximately the same time as the hydrograph.

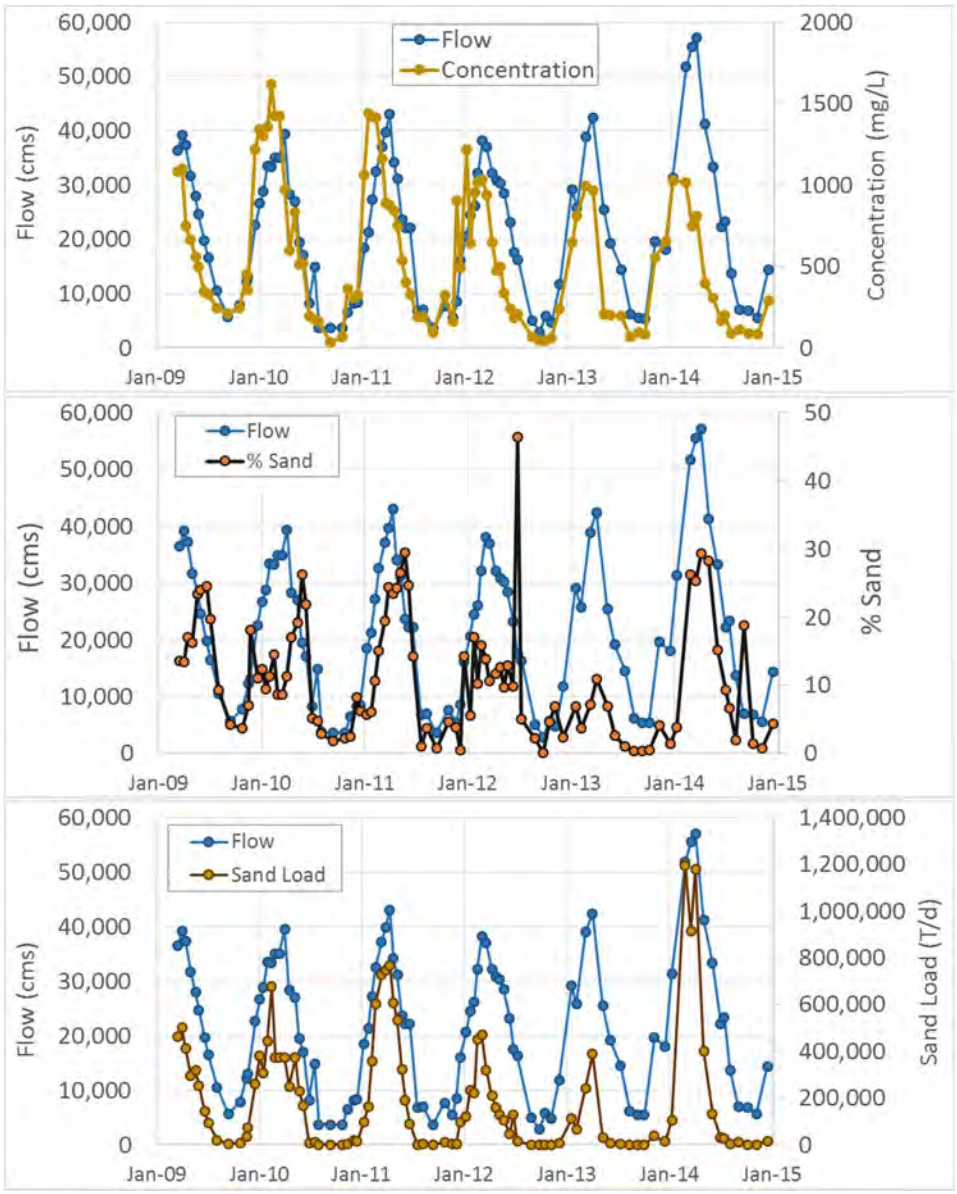

Figure 12: Sediment Concentration (top), Sand Fraction (middle), and sand load (bottom) Time Series at Porto Velho plotted with Hydrograph

The sediment model leveraged these boundary conditions and the model performed well during the quasi-equilibrium credibility test. The model ran the 1967-2014 flow time series with the best estimate algorithms and historic sediment boundary conditions. To test model credibility, the study team evaluated the period of record mass change along the reach against the assumption that the Madeira was in a long-term, decadal scale, equilibrium before the dams. This assumption was tested with the Longitudinal Cumulative Mass Curve (LCMC) which sums the mass change from upstream to downstream. The LCMC for the period of record, mobile bed, sediment transport analysis on the Madeira is included in Figure 13.

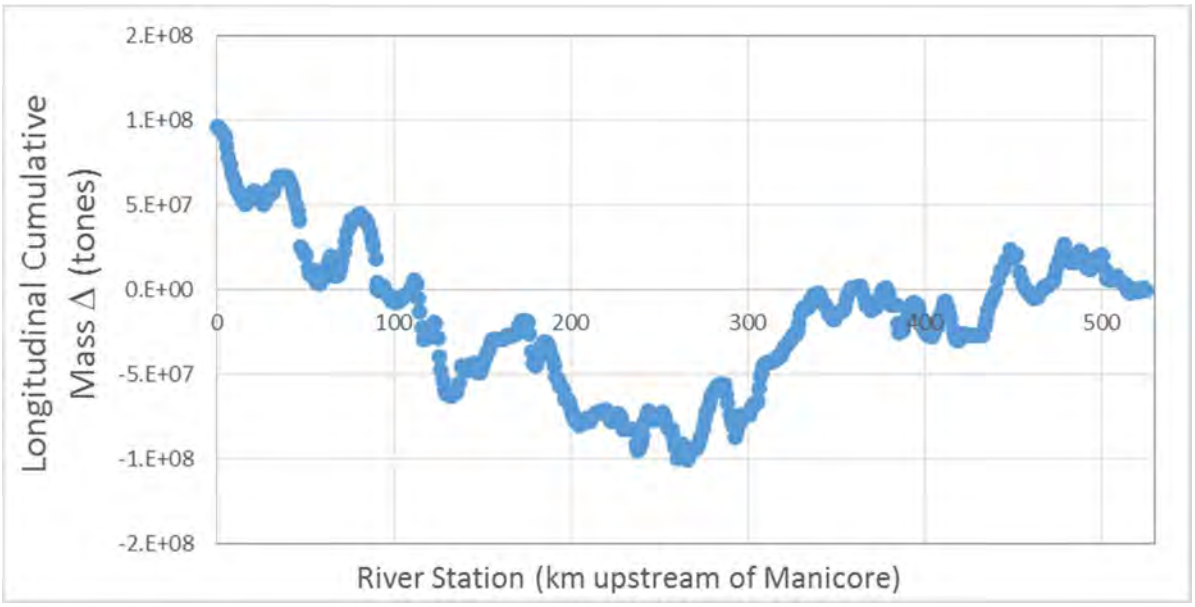

Figure 13: Longitudinal Cumulative Mass Curve (LCMC) for the Madeira River Upstream of Manicoré

The LCMC in Figure 13 shows the modeled reach is roughly in equilibrium on the reach scale. The model scours and deposits around Humaitá and deposits at the downstream model boundary (Manicoré). It is important to note that Manicoré is the only location in the model boundary where aggradation (deposition) was noted in the rating curve.

The model sand flux at Humaitá was slightly higher than observed data (particularly for low flows) but the observed data was within the variability of the computed results. The monthly sand flux that HEC-RAS computed over the 47 year historic period of record (in tonnes per day) is plotted against flow in Figure 14. The measured sand flux is also plotted against flow in this figure for comparison. The observed flux falls mostly within the simulated values and performs particularly well over the moderate flow range (10,000-30,000 cms). However, the model concentrations are high for flows less than 10,000 cms and greater than 30,000 cms. On the whole; however, the best estimate model assumptions performed very well, reproducing a roughly equilibrium condition during a 47 year simulation, increasing confidence in the model's potential for relative alternative analysis.

3.4 Navigation Channel Planning and Design

To have navigation reliability on the Madeira River waterway, the planform geometry must exist that allows for navigation, e.g. sufficient depth, navigable bends, etc. The geologic and fluvial geomorphologic analyses has provided guidance for the proposed plan-form of the navigation channel. From the analyses, it was determined that the Madeira is a dynamic system, with banklines actively aggrading and degrading. There is not significant geologic control to prevent localized planform change, though control does exist in limited locations. Due to terraces, the general planform has some level of constraint. The system is roughly in equilibrium, so that while the system may be active, it can be anticipated that the changes will reflect current standards of geometry in the system. From this, it can be assumed that a) while the same shoaling locations may not always exist, the number and type of shoaling locations are representative, and b) while the radius of the bends may change, the existing radii are reflective of the bends that would develop in the future.

When designing river training structures, the goal is often to approximate the natural width of a self-maintaining (or limited-dredging) channel. This width is referred to as the channel stabilization width. By matching the channel stabilization width for a reach, practice has shown that the newly altered section will likely also self-maintain. The width is matched by constructing structures such that the width

of maintaining sections of the river is roughly matched by the width between the riverward end of structures on one bank and the bankline or riverward end of structures on the opposite bank.

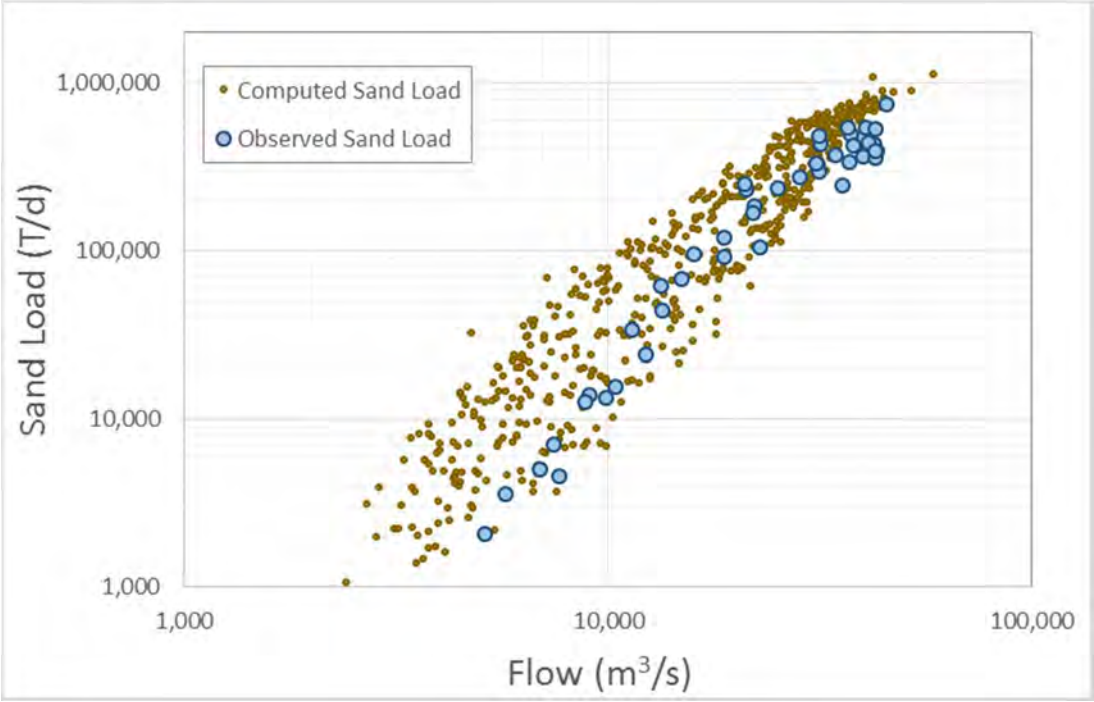

Figure 14: Computed and Measured Sediment Loads at Humaitá, Amazonas

An estimate for the channel stabilization width was developed for the Madeira River between Porto Velho, Rondônia and Manicoré, Amazonas. The reach was treated as a single reach and not sub-divided because the Madeira dwarfs its joining tributaries, showing no sign of increasing channel stabilization width as tributaries join. The width of contiguous sufficient depth was measured every 10 kilometers, measured perpendicular to the draft channel alignment centerline. Measurements were not taken in areas where split flows existed in the channel, or where shoaling prevented contiguous sufficient depth. In total, 39 width measurements were taken. The median width was approximately 630 m; the maximum and minimum were approximately 1070 m and 450 m, respectively. The 75th and 25th percentiles were approximately 810 meters and 570 meters. The measured channel widths are plotted below in Figure 15.

The Madeira River does not naturally maintain sufficient navigation depth for a width much wider than 1,000 meters. This would serve as an upper bounds of what could be considered a channel stabilization width. In practice, choosing a width closer to 800 m, would increase the likelihood of the channel being self-maintaining after the construction of river training structures. It is worth noting that, in practice, it is better to over-estimate the channel constriction width than under-estimate it; while both cases may force undesirable secondary construction, the placement of additional material is easier than recycling existing material. Over-constriction is also more expensive and can also lead to downstream deposition, as the bed over-scours and deposits in the next, less efficient reach.

Approximately 12 historical navigation critical sites have been identified by the engineers and stakeholders navigating the Madeira River. A classification system of prioritization was developed based on magnitude of navigation difficulty and channel stability (see Figure 16). Locations that have a high level of priority and are relatively stable are the primary candidates for implementing river training structures to maintain a self-scouring channel.

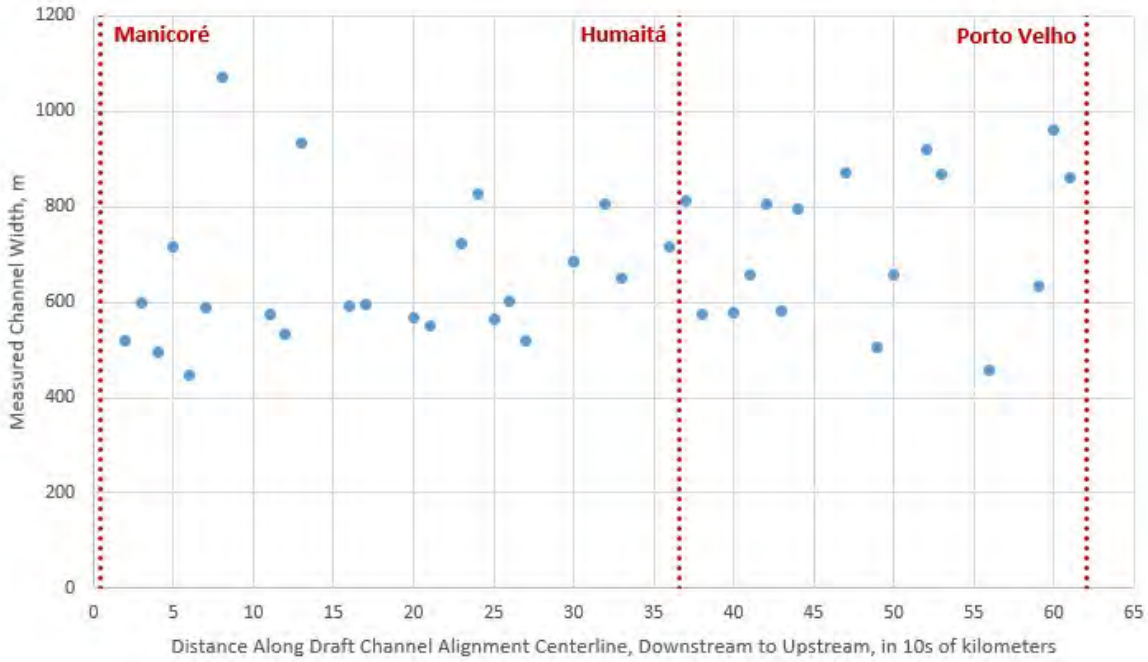

Figure 15: Measured Navigation Width from Porto Velho to Manicoré

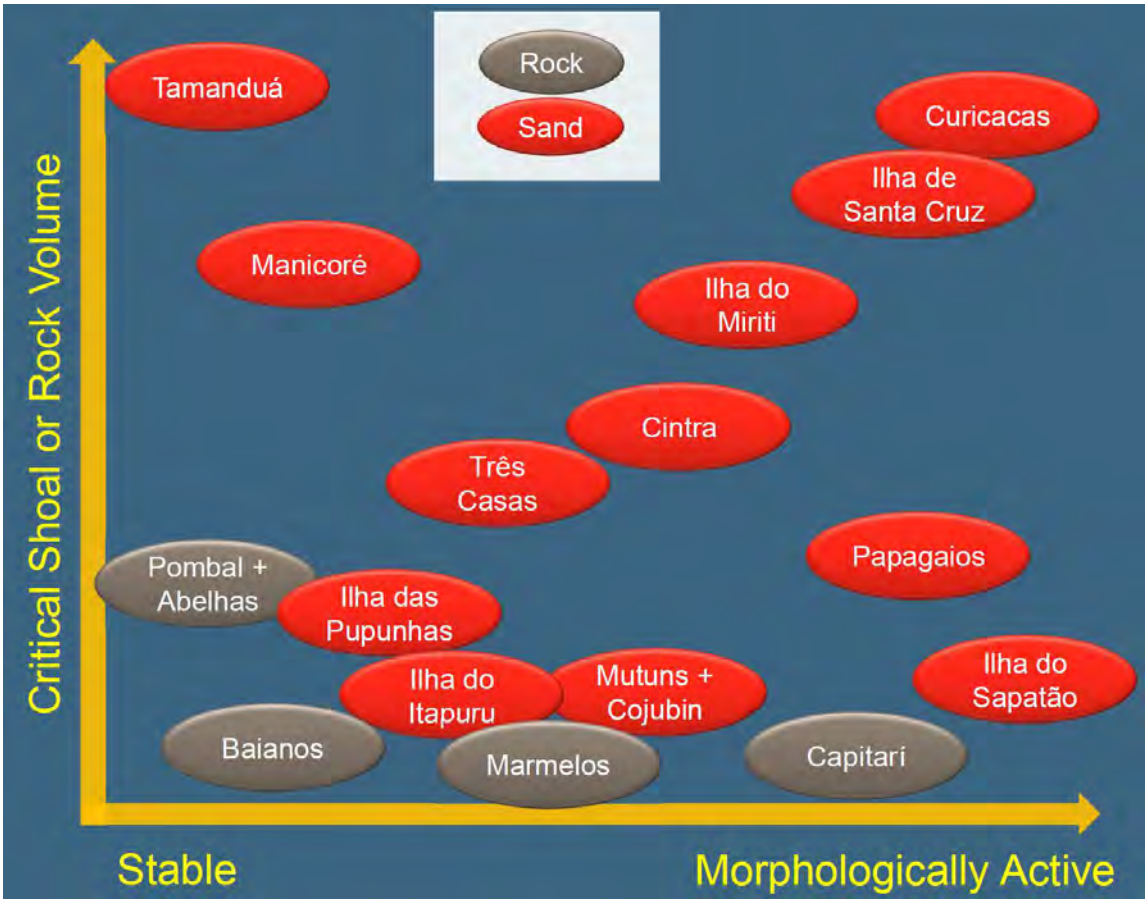

Figure 16: Classification of Navigation Impedances based on Scale of Volume and Stability

In March 2018 DNIT, USACE, and the navigation sector stakehlders held a planning charette to aid in the design of alternatives at each of the sites. Based on this planning charette, several (nine) alternatives were developed to improve navigation reliability on the Madeira River. Measures that were considered for improved navigation included aids to navigation, rock removal, river training structures, dredging, log booms for wood management, among others. Many of the alternatives included river training structures as primary measures for some of the priority sites, especially where the sites are geomorphically stable. The primary sites that were considered to design river training structures include Tamanduá, Mutuns, Curicacas, and Pupunhas. The remaining sites considered rock removal or maitenence dredging as primary measures for improved navigation reliability. Example designs of some of the river training structure solutions are shown in Figure 17.

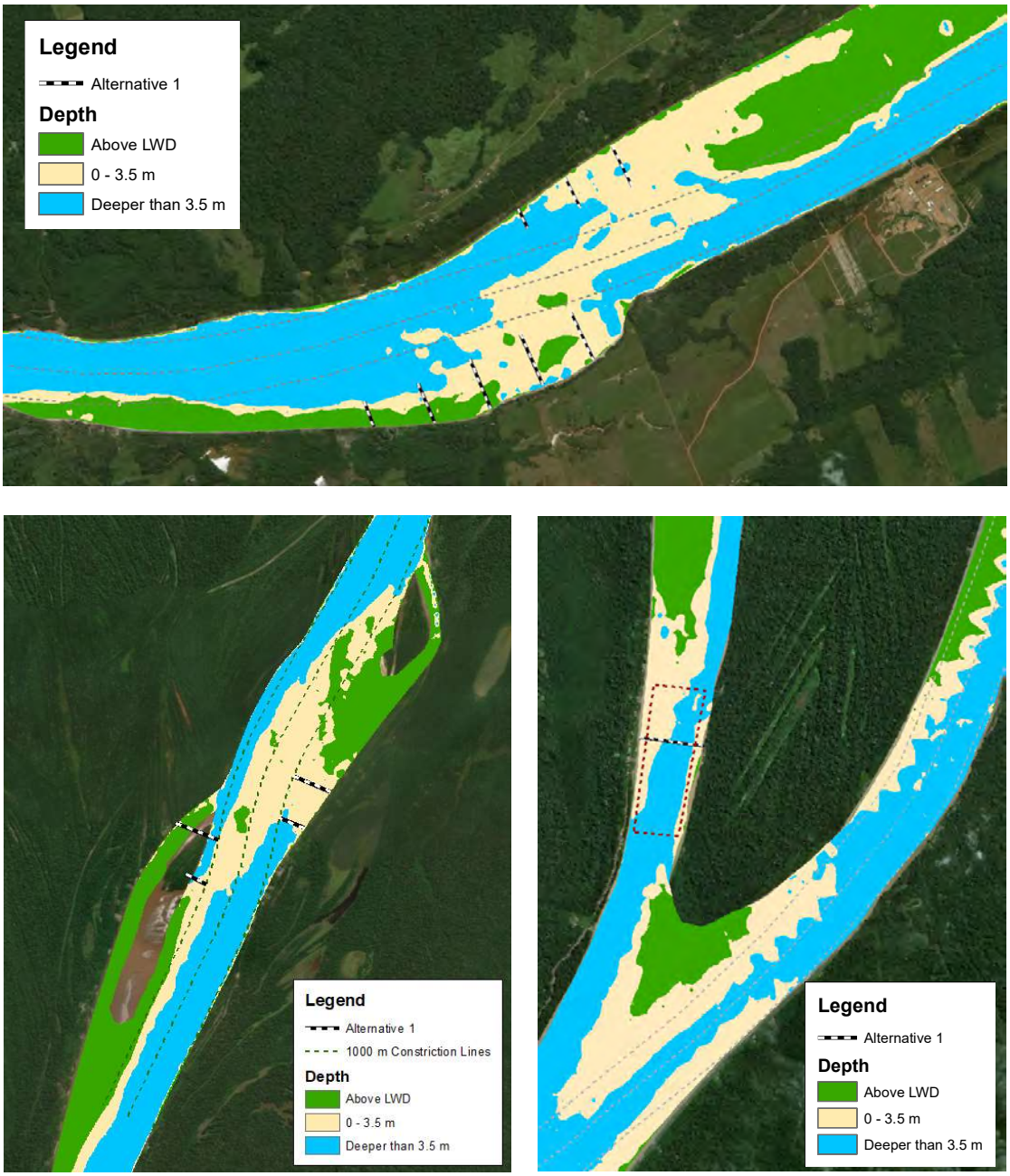

Figure 17: Example River Training and Dredging Alternative Designs at Tamanduá (upper), Curricacas (left), and Pupunhas (right)

4.0 CONCLUSIONS

The Madeira River Waterway is currently used for commercial navigation and is particularly important for transporting agricultural commodities. Despite the lack of waterway improvements, year-round navigation occurs on the Madeira River. However, navigation is significantly less efficient during the low water conditions (when compared to the high water season) due to sand shoals and rock outcrops. These navigation impedances require commercial navigators to travel with less barges, light load each barge, break up convoys in dangerous reaches, and travel only during the day, which increases travel time. As a result of demand, the Brazilian government has initiated studies to identify solutions for improved navigation reliability on the Madeira Waterway.

The planning framework developed for the Madeira River Waterway improvement combines several engineering and technical studies into a decision framework for evaluating economic feasibility of implementing alternatives. These alternatives consist of several measures that include river training structures, aids to navigation, dredging, rock removal, among other measures. The studies that were designed for evaluating the success of the designs include a statistical hydrology study, which is used to define the statistical reliability of the channel conditions. This information was combined with a hydraulic model, which was used to calculate dredging volumes under a range of design channel depths and channel reliabilities. The navigation channel alignment was combined with a fluvial geomorphology study to determine navigation maneuverability for various hydrologic conditions and barge configurations. These studies were also combined in order to define a stabilization width, which aided the design of river training structures. A sediment transport model was then applied to demonstrate the effectiveness of the river training structure design and to calculate long term maintenance dredging.

Several sites were identified as candidate locations for river training structures due to the high volumes of shoals and the persistence (stability) of the shoals. The Madeira River currently exhibits natural morphological evolution (bank erosion and bar development) and is not fixed in place due to its geology or anthropogenic modifications to the channel. Therefore, many navigation impedances (due to sand shoals) are temporary on the engineering scale and may not be ideal candidates for river training structures. However, other sites are stable and exhibit persistent problems with large volumes of dredging necessary to meet current reliability goals. These stable sites were analyzes for the feasibility of using river training structures. The proposed designs are currently preliminary and the next phases will include analysis of environmental feasibility. These designs will significantly limit dredging needs over the life-cycle of the project, and will likely provide significant economic benefit to the navigation sector, which will be evaluated in future phases of this project.

5.0 REFERENCES

ANA, 2017. Hidroweb Gage Data, http://www.snirh.gov.br/hidroweb/publico/apresentacao.jsf. Accessed January 2018.

DNIT, 2016. Administrative Bulletin Nº 172, Portaria Nº 1.635

DNIT/USACE, 2017. Fluvial Geomorphology Study of the Madeira River. FMS Case S6-B-HAO.

LEME/PETCON, 2014a. *Serviços de Consultoria Técnica para a Elaboração de Estudos de Viabilidade Técnico-Econômica e Ambiental – EVTEA e Projeto Básico e Executivo para Melhoramentos na Hidrovia do Rio Madeira, Mamoré e Guaporé*. Volume 1, Resumo Executivo.

PCE, 2015a. *Levantamento Topobatimétrico do Rio Madeira para Acompanhamento da Evolução do Leitoa Jusante da UHE Santo Antônio* (Topo-Bathymetric Survey of the Rio Madeira to Evaluate the Evolution of the Bed Downstream of the Santo Antônio Hydroelectric Power Facility). PJ0955-X-H41-GR-RL-0002-0A.

PCE, 2015b. *Consolidação e Análise dos Dados Hidrossedimentológicos do Rio Madeira – Janeiro de 2008 a Dezembro de 2014* (Consolidation and Analysis of the Hydrologic and Sediment Data of the Madeira River – January 2008 through December 2014). PJ0955-X-H41-GR-RL-0004-0A.

Quadros, M.L. do E.S.; Rizzotto, G.J. (Orgs.). 2007. Mapa Geológico e de Recursos Minerais do Estado de Rondônia,escala 1:1.000.000. Programa Geologia do Brasil (PGB), Integração, Atualização e Difusão de Dados da Geologiado Brasil, Subprograma Mapas Geológicos Estaduais. CPRM-Serviço Geológico do Brasil, Residência de Porto Velho.

Teixeira, S.G., and Maia, M.A.M. 2009. Análise da Dinâmica das Marges do Rio Madeira (AM) no Período de 1987 à 2007, A Partir de Imagens de Sensores Remotos Òpticos. XIV Simpósio Brasileiro de Sensoriamento Remoto, Natal, Brasil, 25-30 abril 2009, INPE, p. 1559-1566.

RECOMMANDATIONS DU WG141 SUR LA CONCEPTION DES VOIES NAVIGABLES - LE CAS DE BRAY-NOGENT

par

Jean-Marc Deplaix[1]

Le groupe de travail 141 de l'AIPCN a remis son rapport fin 2017. Il sera publié au début du 2ème trimestre 2018.

Un des résultats importants de WG141 est un tableau montrant les dimensions recommandées des voies navigables en fonction de la largeur du bateau (voir ***Tableau 10,*** et Söhngen, 2015).

Pour le décideur désireux de comprendre ce qu'il signe, pour un ingénieur confronté pour la première fois à une conception de voie navigable, ou pour les béotiens, ce tableau est d'un grand intérêt, mais ils manquent de compréhension sur la façon de choisir une valeur plutôt que l'autre, et comment on en était arrivé à ces chiffres.

Éléments-clé d'analyse

Il y a quatre éléments essentiels auxquels il faut répondre avant de commencer un projet.

Tout d'abord, quel est le bateau de projet, sa largeur, son tirant d'eau, sa longueur et son "tirant d'air". Presque tous les calculs dépendent de ce bateau de projet. (Mais pour choisir la taille du bateau de projet, vous devrez peut-être étudier le cours d'eau, d'abord, voir ci-dessous).

Deuxièmement, s'agit-il d'une rivière à courant libre, d'une rivière canalisée ou d'un canal? Le tableau à utiliser est différent dans chaque cas, bien que la référence habituelle soit le tableau pour les canaux.

Troisièmement, quel est le trafic de projet, calculé en bateau/année. En effet, alors que les marges de sécurité ne sont pas les mêmes pour un trafic léger ou très élevé, ces tableaux sont souvent utilisées comme si le trafic était de 200Mt/an (qualité A), alors qu'il peut être inférieur à un million (qualité C).

Quatrièmement, en supposant que la voie navigable soit un canal, quelle est sa forme? Trapézoïdal, rectangulaire, RT[2]? Pour chacun, la vitesse obtenue par le bateau de projet pour une même consommation sera différente.

Parfois, nous connaissons la taille de la voie navigable plutôt que la taille du bateau, et nous essayons d'évaluer quel sera le plus grand bateau de conception qui puisse y être logé. Les mêmes tableaux s'appliquent, utilisés en sens inverse.

Il peut arriver que ce soit seulement un goulot d'étranglement qui limitera ou dimensionnera le bateau de projet, un pont ou une écluse; encore une fois, nous pouvons utiliser les mêmes références, lues de manière spécifique, pondérant l'impact du goulot d'étranglement dans le voyage global.

Application au projet Bray-Nogent

Pour bien expliquer cela, on va appliquer la méthodologie à un exemple précis, le projet de mise à grand gabarit de la liaison fluviale Bray/Seine-Nogent/Seine. Ainsi, il sera facile pour les nouveaux venus d'utiliser pleinement le rapport WG141, où ils trouveront tous les détails des calculs, des formules, du processus de modélisation, etc. La méthodologie appliquée pour déterminer le niveau de qualité et de sécurité nécessaire pour toute voie navigable est assez simple, et peut être appliquée à cette voie d'eau entre Bray et Nogent (Projet Bray-Nogent).

[1] Consultant, Paris, jm.deplaix@free.fr. Membre de la Commission CoCom de l'AIPCN

[2] Profils proposés par les recommandations allemandes, vertical d'un côté et trapézoïdal de l'autre.

Il convient d'abord de distinguer les partie du trajet en canal et celles en rivière, et ensuite de déterminer le niveau actuel de qualité et de sécurité. En deuxième lieu, on détermine le niveau nécessaire pour atteindre les objectifs visés sur le plan du gabarit. Enfin, on applique ce niveau dans le tableau synthétique qui permet d'en déduire les dimensions du chenal à respecter sur l'itinéraire, selon que l'on recherche une voie unique ou à double sens.

Il est nécessaire par ailleurs de situer le projet au sein d'un itinéraire, afin d'éviter de se fixer des normes trop élevées par rapport au reste de l'itinéraire, tout en respectant les possibilités d'évolution futures.

Le projet Bray-Nogent comporte 2 trajets en canal, le Canal de Beaulieu et le canal à l'aval de l'écluse de Jaulnes, et 3 trajets en rivière. On se contentera de deux analyses, une en canal, l'autre en rivière.

Itinéraire Haute Seine

Par contre, il s'intègre dans un itinéraire, la Seine dans Paris, la Haute Seine et la Petite Seine, de Paris Bir-Hakeim à l'écluse de la Grande Bosse, entièrement en rivière, qu'il convient d'analyser en premier, car il conditionne les caractéristiques d'accès au projet.

Dans la méthodologie AIPCN, il y a 3 groupes de critères d'analyse, liés aux conditions nautiques, à la vitesse et au trafic. Leur analyse détaillée est faite dans le powerpoint présenté au Congrès.

Le Tableau 1 synthétise l'analyse.

Suite à des réflexions faites lors de l'application de la méthodologie au réseau de canaux Freycinet, en France, on y a modifié l'un des critères concernant la vitesse, en utilisant la distance parcourue en 6 heures plutôt qu'un critère très technique sur la gamme de vitesse, mais sans modifier dans un premier temps les pondérations du WG141.

		HAUTE SEINE & PETITE SEINE / Critères	La facilité de navigation est élevée si les arguments suivants sont vérifiés		Dans les cas suivants, la facilité de navigation est mauvaise		Note	Poids	Poids global	Commentaire
1er groupe de notes: Critères liés à la voie navigable		Règles de notation pour les critères liés à la voie navigable: La note est +1, si l'affirmation dans la colonne de gauche, verte, est vraie, -1 si c'est celle de la colonne de droite, rouge. Si aucun des deux n'est vrai, ou si les 2 sont vrais, la note est 0.							7/20 = 35%	**1,5**
	1	Profondeur, type de marchandises et de mode d'exploitation	Bateaux vides ou ballastés, pas de marchandises dangereuses, profondeur d'eau suffisante		Bateaux chargés, en particulier de marchandises dangereuses, dans des voies d'eau peu profondes		-0,5	1/7	-0,5	Pied de pilote faible (0,4m), peu de march. dangereuses
	2	Niveau d'entraînement, habileté et experience des pilotes	Pilotes hautement qualifiés et expérimentés		Pilotes peu entraînés, mauvaise connaissance des particularités de la voie et de l'infrastructure		1	1/7	1	Peu d'accidents, bons pilotes
	3	Niveaux d'attention, distraction et stress des pilotes	Faible nombre de manoeuvres, peu de croisements ou de ponts		Longs biefs, navigation lénifiante ou au contraire fréquentes manoeuvres		0	1/7	0	Navigation moyennement difficile
	4	Largeur, situation, niveaux de danger, dommages possibles	Chenal confortable, berges en pente, murs guides, digues et petits épis		Chenal étroit, immeubles à proximité, berges verticals, bateaux amarrés, danger élevé en cas d'accident		-0,5	1/7	-0,5	Chenal plutôt étroit, berges rocheuses par endroits
	5	Stabilité et qualité des conditions de navigation	Berges régulières, faites de sable ou de gravier, avec des vents faibles ou abrité		Turbulences, courants traversiers, berges irrégulières, longs épis, lit rocheux, vent et brouillard fréquents		0	1/7	0	Chenal régulier mais rocheux
	6	Type de traffic, croisements, proximité de la berge	2 ou plus de lignes de navigation, interactions avec la berge acceptées		Voies à sens unique, ou au contraire beaucoup de manoeuvres et de dépassements		1	1/7	1	Chenal à 2 lignes de navigation
	7	Equipements et instruments de navigation du bateau	Forts bouteurs actifs ou passifs, forte puissance, 2 lignes d'arbre, systèmes d'information optimaux		Gouvernail arrière seul, ou trop petit bouteur, bateaux de mer, faibles moteurs, pas de systèmes d'information		+0,5	1/7	+0,5	Matériel adéquat mais ancien
2ème groupe de notes: critères liés à la vitesse du bateau		Règles de notation pour les critères liés à la vitesse, selon la vitesse d'objectif (1ère ligne ci-dessous) ou la gamme de vitesse nécessaire (2ème ligne ci-dessous), appliquez la note qui figure entre parenthèses, ou interpolez si besoin							4/20 =20%	**3**
	8	Vitesse d'objectif par rapport à la berge	≥ 13 km/h (1)	10 – 12 km/h (0.5)	5 – 9 km/h (0)	< 4 km/h (-1)	1	2/4	2	Aucune limitation de vitesse
	9	Distance parcourue en 6h, avalant	≥ 75 km (+1 ; +0,7)	≥ 40 km (+0.69 ; 0)	≥ 25 km (-0,01 ; -0.74)	< 25 km (-0,75 ; -1)	+0,3	2/4	0,6	Présence d'écluses, qui diminuent la distance parcourue en 6h (54km)
3ème groupe de notes: facteurs liés à la densité du trafic		Règles de notation selon la densité de traffic : appliquez la note figurant entre parenthèses ci-dessous							9/20 =45%	**2,5**
	10	Gêne due aux bateaux de plaisance, en particulier ceux à rames	Pas d'influence sur la vitesse (+1)	Gêne de faible importance à la navigation commerciale (0)		Fort effet négatif sur la vitesse moyenne (-1)	0	4/9	0	Peu de trafic de plaisance
	11	Limitation de la vitesse en cas de forte densité du traffic commercial	< 5,000 bateaux par an (+1)	5,000 – 15,000 bateaux par an (+0.5)	15,000 – 30,000 bateaux par an (-0.5)	> 30,000 bateaux par an (-1)	+0,5	5/9	+2,5	10.000 bateaux/an
Score total: somme des notes individuelles multiplies par le poids, à reporter dans la dernière colonne = 7/20 = **+0,35**										

Tableau 1 : Analyse de l'état actuel du trajet Paris-La Grande Bosse

Dans la méthodologie AIPCN (Tableau 2 ci-dessous), une telle notation correspond à une voie d'eau de qualité A, mais juste à la limite du B, ce qui dénote une voie à grand gabarit de caractéristiques réduites. Ceci correspond assez bien au ressenti des bateliers. On a légèrement modifié les limites des notes, 0,33 au lieu de 0,40 dans le rapport du WG141, afin que chaque qualité couvre une gamme de notes égale à 0,66.

	restrictions:	
presqu'aucune	légères à notables	fortes
A	**B**	**C**
	facilité de navigation	
navigation facile	pas vraiment facile	secteur piégeux
	Note	
.+1,0 +0,8 +0,6	+0,34 +0,2 0,0 -0,2	-0,33 -0,6 -0,8 -1

Tableau 2 : Classes de facilité de navigation

Les critères de notation qui ont été suivis pour les interpolations sont les suivants :

Pour le trajet parcouru en 6 heures :

Km/6h	1	90	80	75	70	65	60	55	50	45	40	35	30	25	20
note	1	0,9	0,8	0,7	0,6	0,5	0,4	0,3	0,2	0,1	0	-0,25	-0,50	-0,75	-1
La note est la même pour la situation actuelle ou future															

Tableau 3 : Notation détaillée pour le trajet parcouru en 6 heures

: Pour le niveau de trafic :

Trafic en milliers de bateaux/an	30	25	20	15	14	13	12	11	10	9	8	7	6	5
Note pour situation actuelle	-1	-0,66	-0,33	0	0,1	0,2	0,3	0,4	0,5	0,6	0,7	0,8	0,9	1
Note pour situation future	1	0,66	0,33	0	-0,1	-0,2	-0,3	-0,4	-0,5	-0,6	-0,7	-0,8	-0,9	-1

Tableau 4 : Notation détaillée pour le niveau de trafic

Comme il n'est pas prévu d'améliorer la Haute Seine ni la partie aval de la Petite Seine, de Montereau à la Grande Bosse, il n'est pas nécessaire d'évaluer le niveau de qualité et de sécurité d'un projet futur pour cette voie d'eau.

On peut donc passer directement à l'évaluation de la partie en canal et de la partie en rivière du projet Bray-Nogent (Petite Seine Amont).

Analyse de l'état actuel de la voie d'eau

Pour se rendre compte des caractéristiques de l'endroit, il est utile de quantifier la qualité de l'infrastructure actuelle. On valide ainsi la pertinence des clés d'analyse. On recherchera ensuite le niveau de qualité et de sécurité nécessaire pour le nouveau projet de voie d'eau Bray-Nogent à grand gabarit. On en déduira ensuite les caractéristiques de dimensionnement à recommander pour respecter ce niveau.

La partie en rivière, lorsqu'elle est évaluée avec les pondérations précédentes, correspond au tableau suivant, qui reviendrait à estimer que la Petite Seine Amont, au milieu de la catégorie A, est infiniment plus facile à naviguer que la Haute Seine, ce qui est assez loin du ressenti des bateliers.

Les notes individuelles des 11 critères ne sont pas en cause :

- La profondeur est très réduite, mais meilleure que celle du réseau Freycinet
- Le niveau d'entraînement des pilotes est le même que celui de la haute Seine

- Le niveau de stress est moyen, car même si la voie est étroite et oblige à une forte attention, le trafic est très faible et ne nécessite que rarement des manœuvres. Il n'y a par ailleurs qu'un seul pont problématique, en virage
- Le chenal est étroit ; par contre il y a peu d'enjeux potentiels et les berges sont sablonneuses
- Les conditions de navigation sont stables, avec brouillard fréquent et forts courants en crue, dans un chenal étroit mais peu dangereux
- Il y a officiellement 2 lignes de navigation, mais avec les grands bateaux qui y passent actuellement seule la faiblesse du trafic permet une navigation aisée, semblable à une navigation unidirectionnelle, car les berges ne sont pas dangereuses et peuvent être touchées sans dommages
- Enfin, les bateaux sont de bonne qualité, bien équipés mais anciens pour la plupart. La note globale de ce groupe de critères est de 0,8 sur 7
- La vitesse autorisée est de 12 km/h
- La distance parcourue en 6 heures est de l'ordre de 40 km. La note globale de ce groupe de critères est ainsi de 1 sur 4
- La gêne due à la plaisance est insignifiante, même s'il existe un stade de vitesse sur l'un des biefs
- Et le trafic inférieur à 5.000 bateaux/an font que ce groupe de critère devient décisif, avec une note de 9 sur 9

PETITE SEINE AMONT - ETAT ACTUEL / Critères			La facilité de navigation est élevée si les arguments suivants sont vérifiés		Dans les cas suivants, la facilité de navigation est mauvaise		Note	Poids	Poids global	Commentaire
1er groupe de notes: Critères liés à la voie navigable	Règles de notation pour les critères liés à la voie navigable: La note est +1, si l'affirmation dans la colonne de gauche, verte, est vraie, -1 si c'est celle de la colonne de droite, rouge. Si aucun des deux n'est vrai, ou si les 2 sont vrais, la note est 0.								7/20 = 35%	**0,8**
	1	Profondeur, type de marchandises et de mode d'exploitation	Bateaux vides ou ballastés, pas de marchandises dangereuses, profondeur d'eau suffisante		Bateaux chargés, en particulier de marchandises dangereuses, dans des voies d'eau peu profondes		-0,9	1/7	-0,9	Chenal étroit et peu profond, peu de march. dangereuses
	2	Niveau d'entraînement, habileté et experience des pilotes	Pilotes hautement qualifiés et expérimentés		Pilotes peu entraînés, mauvaise connaissance des particularités de la voie et de l'infrastructure		0,9	1/7	0,9	Peu d'accidents, voie difficile même pour de bons pilotes
	3	Niveaux d'attention, distraction et stress des pilotes	Faible nombre de manoeuvres, peu de croisements ou de ponts		Longs biefs, navigation lénifiante ou au contraire fréquentes manoeuvres		0	1/7	0	Navigation assez difficile, oblige à une forte attention
	4	Largeur, situation, niveaux de danger, dommages possibles	Chenal confortable, berges en pente, murs guides, digues et petits épis		Chenal étroit, immeubles à proximité, berges verticals, bateaux amarrés, danger élevé en cas d'accident		-0,2	1/7	-0,2	Chenal plutôt étroit, berges sableuses, forts virages, faible dommages potentiels
	5	Stabilité et qualité des conditions de navigation	Berges régulières, faites de sable ou de gravier, avec des vents faibles, ou biefs abrités		Turbulences, courants traversiers, berges irrégulières, longs épis, lit rocheux, vent et brouillard fréquents		0	1/7	0	Chenal régulier, forts courants en crue, vents faibles, brouillard fréquent
	6	Type de traffic, croisements, proximité de la berge	2 ou plus de lignes de navigation, interactions avec la berge acceptées		Voies à sens unique, ou au contraire beaucoup de manoeuvres et de dépassements		0,5	1/7	0,5	Chenal à 2 lignes de navigation, peu de trafic
	7	Equipements et instruments de navigation du bateau	Forts bouteurs actifs ou passifs, forte puissance, 2 lignes d'arbre, systèmes d'information optimaux		Gouvernail arrière seul, ou trop petit bouteur, bateaux de mer, faibles moteurs, pas de systèmes d'information		0,5	1/7	0,5	Matériel adéquat mais ancien
2ème groupe de notes: critères liés à la vitesse du bateau	Règles de notation pour les critères liés à la vitesse, selon la vitesse d'objectif (1ère ligne ci-dessous) ou la distance parcourue (2ème ligne ci-dessous), appliquez la note qui figure entre parenthèses, ou interpolez si besoin								4/20 =20%	**1**
	8	Vitesse d'objectif par rapport à la berge	≥ 13 km/h (1)	10 – 12 km/h (0.5)	5 – 9 km/h (0)	< 4 km/h (-1)	0,5	2/4	1	12 km/h
	9	Distance parcourue en 6h, avalant	≥ 75 km (+1 ; +0,7)	≥ 40 km (+0.69 ; 0)	≥ 25 km (-0,01 ; -0.74)	< 25 km (-0,75 ; -1)	0	2/4	0	Présence d'écluses, qui diminuent la distance parcourue en 6h (40km)
3ème groupe de notes: facteurs liés à la densité du trafic	Règles de notation selon la densité de traffic : appliquez la note figurant entre parenthèses ci-dessous								9/20 =45%	**9**
	10	Gêne due aux bateaux de plaisance, en particulier ceux à rames	Pas d'influence sur la vitesse (+1)	Gêne de faible importance à la navigation commerciale (0)		Fort effet négatif sur la vitesse moyenne (-1)	1	4/9	4	Peu de trafic de plaisance
	11	Limitation de la vitesse en cas de forte densité du trafic commercial	< 5,000 bateaux par an (+1)	5,000 – 15,000 bateaux par an (+0.5)	15,000 – 30,000 bateaux par an (-0.5)	> 30,000 bateaux par an (-1)	1	5/9	5	3.000 bateaux/an
Score total: somme des notes individuelles multiplies par le poids, à reporter dans la dernière colonne = 10,8/20 = **+0,54**										

Tableau 5: Evaluation initiale de l'état actuel du trajet Bray-Nogent

L'application des mêmes coefficients de pondération que ceux retenus par le Groupe d'études de l'AIPCN, notamment celui de densité de trafic, conduit ainsi à des notes de qualité ne correspondant pas au ressenti des navigants. Comme indiqué dans le rapport du Groupe d'études, il convient alors de modifier les pondérations pour pouvoir se rapprocher du ressenti local.

Après plusieurs tests, on en est venu à proposer une pondération inversée entre les critères liés à la vitesse (qui passent de 4 à 9 points) et ceux liés à la densité de trafic (qui

passent de 9 à 4 points). Sans modification des notes individuelles, le tableau (indice « ter ») devient alors (**Tableau 6**) :

PETITE SEINE AMONT - ETAT ACTUEL ter / Critères			La facilité de navigation est élevée si les arguments suivants sont vérifiés		Dans les cas suivants, la facilité de navigation est mauvaise		Note	Poids	Poids global	Commentaire
1er groupe de notes: Critères liés à la voie navigable	Règles de notation pour les critères liés à la voie navigable: La note est +1, si l'affirmation dans la colonne de gauche, verte, est vraie, -1 si c'est celle de la colonne de droite, rouge. Si aucun des deux n'est vrai, ou si les 2 sont vrais, la note est 0.								7/20 = 35%	**0,8**
	1	Profondeur, type de marchandises et de mode d'exploitation	Bateaux vides ou ballastés, pas de marchandises dangereuses, profondeur d'eau suffisante		Bateaux chargés, en particulier de marchandises dangereuses, dans des voies d'eau peu profondes		-0,9	1/7	-0,9	Chenal étroit et peu profond, peu de march. dangereuses
	2	Niveau d'entraînement, habileté et experience des pilotes	Pilotes hautement qualifiés et expérimentés		Pilotes peu entraînés, mauvaise connaissance des particularités de la voie et de l'infrastructure		0,9	1/7	0,9	Peu d'accidents, voie difficile même pour de bons pilotes
	3	Niveaux d'attention, distraction et stress des pilotes	Faible nombre de manoeuvres, peu de croisements ou de ponts		Longs biefs, navigation lénifiante ou au contraire fréquentes manoeuvres		0	1/7	0	Navigation assez difficile, oblige à une forte attention
	4	Largeur, situation, niveaux de danger, dommages possibles	Chenal confortable, berges en pente, murs guides, digues et petits épis		Chenal étroit, immeubles à proximité, berges verticals, bateaux amarrés, danger élevé en cas d'accident		-0,2	1/7	-0,2	Chenal plutôt étroit, berges sableuses, forts virages, faible dommages potentiels
	5	Stabilité et qualité des conditions de navigation	Berges régulières, faites de sable ou de gravier, avec des vents faibles, ou biefs abrités		Turbulences, courants traversiers, berges irrégulières, longs épis, lit rocheux, vent et brouillard fréquents		0	1/7	0	Chenal régulier, forts courants en crue, vents faibles, brouillard fréquent
	6	Type de traffic, croisements, proximité de la berge	2 ou plus de lignes de navigation, interactions avec la berge acceptées		Voies à sens unique, ou au contraire beaucoup de manoeuvres et de dépassements		0,5	1/7	0,5	Chenal à 2 lignes de navigation, peu de trafic
	7	Equipements et instruments de navigation du bateau	Forts bouteurs actifs ou passifs, forte puissance, 2 lignes d'arbre, systèmes d'information optimaux		Gouvernail arrière seul, ou trop petit bouteur, bateaux de mer, faibles moteurs, pas de systèmes d'information		0,5	1/7	0,5	Matériel adéquat mais ancien
2ème groupe de notes: critères liés à la vitesse du bateau	Règles de notation pour les critères liés à la vitesse, selon la vitesse d'objectif (1ère ligne ci-dessous) ou la distance parcourue (2ème ligne ci-dessous), appliquez la note qui figure entre parenthèses, ou interpolez si besoin								9/20 =45%	**2,5**
	8	Vitesse d'objectif par rapport à la berge	≥ 13 km/h (1)	10 – 12 km/h (0.5)	5 – 9 km/h (0)	< 4 km/h (-1)	0,5	5/9	2,5	12 km/h
	9	Distance parcourue en 6h, avalant	≥ 75 km (+1 ; +0,7)	≥ 40 km (+0.69 ; 0)	≥ 25 km (-0,01 ; -0.74)	< 25 km (-0,75 ; -1)	0	4/9	0	Présence d'écluses, qui diminuent la distance parcourue en 6h (40km)
3ème groupe de notes: facteurs liés à la densité du trafic	Règles de notation selon la densité de traffic : appliquez la note figurant entre parenthèses ci-dessous								4/20 =20%	**4**
	10	Gêne due aux bateaux de plaisance, en particulier ceux à rames	Pas d'influence sur la vitesse (+1)	Gêne de faible importance à la navigation commerciale (0)		Fort effet négatif sur la vitesse moyenne (-1)	1	2/4	2	Peu de trafic de plaisance
	11	Limitation de la vitesse en cas de forte densité du trafic commercial	< 5,000 bateaux par an (+1)	5,000 – 15,000 bateaux par an (+0.5)	15,000 – 30,000 bateaux par an (-0.5)	> 30,000 bateaux par an (-1)	1	2/4	2	3.000 bateaux/an
Score total: somme des notes individuelles multipliées par le poids, à reporter dans la dernière colonne = 7,3/20 = +0,365										

Tableau 6 Evaluation finale de l'état actuel du trajet Bray-Nogent en rivière

On obtient ainsi une évaluation plus proche du ressenti des bateliers. Bien que facile à naviguer, sa profondeur insuffisante et beaucoup de virages serrés placent la partie en rivière de l'itinéraire Bray-Nogent dans la catégorie A, mais très proche de la catégorie B, une appréciation cohérente avec la note donnée à la Haute Seine.

Pour la partie en canal, ci-après, la nouvelle pondération permet une adéquation correcte de la notation avec l'opinion des bateliers. L'ancienne notation plaçait ce canal dans le haut de la catégorie B, alors que c'est un goulot d'étranglement sur le plan du gabarit et une voie difficile à négocier. La nouvelle pondération le place juste au milieu de la catégorie B, peut-être même légèrement au-dessus du ressenti des bateliers.

Figure 1 Croisement dans le canal de Beaulieu (Photo Céline Dobbelaere)

Il est clair qu'aujourd'hui ces canaux ne correspondent pas à la taille des bateaux qui les empruntent, rendant les croisements difficiles pour les bateaux de plus de 7,50 m de large (Canal de Beaulieu, voir **Figure 1** avec bateaux de seulement 8 et 9 m de large). Les croisements sont même impossibles dans la coupure de Jaulnes, en courbe.

Avec ces nouvelles pondérations, on aboutit au tableau suivant :

Parties en CANAL entre BRAY et NOGENT Etat actuel ter / Critères			La facilité de navigation est élevée si les arguments suivants sont vérifiés		Dans les cas suivants, la facilité de navigation est mauvaise		Note	Poids	Poids global	Commentaire
1er groupe de notes: Critères liés à la voie navigable		Règles de notation pour les critères liés à la voie navigable: La note est +1, si l'affirmation dans la colonne de gauche, verte, est vraie, -1 si c'est celle de la colonne de droite, rouge. Si aucun des deux n'est vrai, ou si les 2 sont vrais, la note est 0.							7/20 = 35%	1
	1	Profondeur, type de marchandises et de mode d'exploitation	Bateaux vides ou ballastés, pas de marchandises dangereuses, profondeur d'eau suffisante		Bateaux chargés, en particulier de marchandises dangereuses, dans des voies d'eau peu profondes		-1	1/7	-1	Chenal très étroit et peu profond, croisements chargés difficiles
	2	Niveau d'entraînement, habileté et experience des pilotes	Pilotes hautement qualifiés et expérimentés		Pilotes peu entraînés, mauvaise connaissance des particularités de la voie et de l'infrastructure		1	1/7	1	Peu d'accidents, bons pilotes
	3	Niveaux d'attention, distraction et stress des pilotes	Faible nombre de manoeuvres, peu de croisements ou de ponts		Longs biefs, navigation lénifiante ou au contraire fréquentes manoeuvres		0	1/7	0	Navigation peu difficile
	4	Largeur, situation, niveaux de danger, dommages possibles	Chenal confortable, berges en pente, murs guides, digues et petits épis		Chenal étroit, immeubles à proximité, berges verticals, bateaux amarrés, danger élevé en cas d'accident		0	1/7	0	Chenal très étroit, berges sableuses, peu de danger en cas d'accident
	5	Stabilité et qualité des conditions de navigation	Berges régulières, faites de sable ou de gravier, avec des vents faibles, ou biefs abrités		Turbulences, courants traversiers, berges irrégulières, longs épis, lit rocheux, vent et brouillard fréquents		0,3	1/7	0,3	Chenal régulier mais étroit, peu de vent, brouillards fréquents
	6	Type de traffic, croisements, proximité de la berge	2 ou plus de lignes de navigation, interactions avec la berge acceptées		Voies à sens unique, ou au contraire beaucoup de manoeuvres et de dépassements		0,2	1/7	0,2	Chenal peu adéquat pour 2 lignes de navigation
	7	Equipements et instruments de navigation du bateau	Forts bouteurs actifs ou passifs, forte puissance, 2 lignes d'arbre, systèmes d'information optimaux		Gouvernail arrière seul, ou trop petit bouteur, bateaux de mer, faibles moteurs, pas de systèmes d'information		0,5	1/7	0,5	Matériel adéquat mais ancien
2ème groupe de notes: critères liés à la vitesse du bateau		Règles de notation pour les critères liés à la vitesse, selon la vitesse d'objectif (1ère ligne ci-dessous) ou la gamme de vitesse (2ème ligne ci-dessous), appliquez la note qui figure entre parenthèses, ou interpolez si besoin							9/20 =45%	-3
	8	Vitesse d'objectif par rapport à la berge	≥ 13 km/h (1)	10 – 12 km/h (0.5)	5 – 9 km/h (0)	< 4 km/h (-1)	0	5/9	0	6 km/h
	9	Distance parcourue en 6h, avalant	≥ 75 km (+1 ; +0,7)	≥ 40 km (+0.69 ; 0)	≥ 25 km (-0,01 ; -0.74)	< 25 km (-0,75 ; -1)	-0,75	4/9	-3	Présence d'écluses et faible section mouillée, d'où faible distance parcourue (24km)
3ème groupe de notes: facteurs liés à la densité du trafic		Règles de notation selon la densité de traffic : appliquez la note figurant entre parenthèses ci-dessous							4/20 =20%	2
	10	Gêne due aux bateaux de plaisance, en particulier ceux à rames	Pas d'influence sur la vitesse (+1)	Gêne de faible importance à la navigation commerciale (0)		Fort effet négatif sur la vitesse moyenne (-1)	0	2/4	0	Peu de trafic de plaisance
	11	Limitation de la vitesse en cas de forte densité du trafic commercial	< 5,000 bateaux par an (+1)	5,000 – 15,000 bateaux par an (+0.5)	15,000 – 30,000 bateaux par an (-0.5)	> 30,000 bateaux par an (-1)	1	2/4	2	3.000 bateaux/an
Score total: somme des notes individuelles multiplies par le poids, à reporter dans la dernière colonne = 0/20 = +0,0										

Tableau 7 : Evaluation finale de l'état actuel du trajet Bray-Nogent en canal

On peut noter qu'il apparaît presque impossible, avec un tel tableau d'analyse, que la note baisse jusqu'à la qualité C : il y aura toujours l'un des critères suffisamment favorable pour renforcer la note. Le critère de vitesse paraît en particulier trop favorable : à un seul exemple près, et encore sur une faible longueur, il n'existe pas de voie navigable en Europe de l'Ouest dont la vitesse de parcours soit inférieure à 4 km/h. Le contre-exemple en question, le canal du Rhône à Sète, était fréquenté par des bateaux 2 fois plus gros que son bateau de projet initial, ce qui ramenait la vitesse à 3,5 km/h sur une dizaine de kilomètres. Des travaux ont d'ailleurs été réalisés récemment pour élargir le canal et augmenter la vitesse vers 6 km/h, ce qui a permis d'augmenter sensiblement la taille du bateau de projet, pour l'amener à ce qui se pratiquait déjà, mais avec de meilleures vitesses.

Niveau de qualité nécessaire pour le futur projet Bray-Nogent

En réalisant cette analyse de l'existant, on a testé la validité des pondérations de notation, et modifié celles qui ne paraissaient pas adéquates. En se basant sur ces pondérations, on peut maintenant estimer quel niveau de qualité devrait être recherché pour le projet à réaliser.

Tout d'abord, il faut signaler que pour définir le degré de qualité nécessaire à un projet de voie navigable, il faut tenir compte en même temps de la voie d'eau actuelle et en même temps de l'objectif souhaité.

Ainsi, dans le tableau suivant, la plupart des cases du premier groupe de critère seront renseignées en se basant surtout sur l'existant d'où l'on part, que l'on souhaite modifier, tandis que les autres groupes prendront surtout en compte l'état futur souhaité, le gabarit ou la situation à obtenir.

Même dans le premier groupe, on retrouve cette dichotomie : par exemple, la largeur du chenal, la plus ou moins grande facilité de croisement, les conditions locales plus ou moins favorables et le type de trafic sont le point de départ pour les travaux qui permettront d'atteindre le gabarit voulu. Ils obligent à une augmentation de qualité proche de A. Par contre, la qualité des pilotes, le niveau de stress, la stabilité des conditions de navigation et les équipements du bateau sont évalués en fonction de la situation future attendue, et peuvent être cotés C si ces éléments sont déjà suffisamment favorables sans travaux.

On obtient alors le tableau suivant :

PETITE SEINE AMONT - ÉTAT PROJETÉ / Critères			Arguments conduisant à augmenter le niveau de qualité des normes de conception		Cas où des normes moins élevées peuvent être appliquées pour la conception		Note	Poids	Poids global	
1er groupe de notes: Critères liés à la voie navigable	Règles de notation pour les critères liés à la voie navigable: La note est +1 si l'affirmation dans la colonne de gauche, rouge, est vraie, -1 si c'est celle de la colonne de droite, verte. Si aucun n'est vrai, ou si les 2 sont vrais, la note est 0.								7/20= 35%	0
	1	Profondeur, type de marchandises et de mode d'exploitation	Bateaux chargés, en particulier de marchandises dangereuses, dans des voies d'eau peu profondes, même après projet (fleuves à courant libre)		Bateaux vides ou ballastés, pas de marchandises dangereuses, profondeur d'eau suffisante		0,7	1/7	0,7	Bateaux chargés, voies peu profondes, mais peu de marchandises dangereuses
	2	Niveau d'entraînement, habileté et experience des pilotes	Pilotes peu entraînés, mauvaise connaissance des particularités de la voie et de l'infrastructure		Pilotes hautement qualifiés et expérimentés		-1	1/7	-1	Qualité des pilotes conditionnée par la Haute Seine
	3	Niveaux d'attention, de distraction et de stress des pilotes	Longs biefs, navigation lénifiante ou au contraire obligation de manoeuvrer sans cesse		Faible nombre de manoeuvres, peu de croisements ou de ponts		0,7	1/7	0,7	Pas de longs biefs, mais fréquentes manœuvres et 1 pont dangereux
	4	Largeur, situation, niveaux de danger, dommages possibles	Chenal étroit actuel et/ou dans le projet, immeubles à proximité, berges verticales, bateaux amarrés, danger élevé en cas d'accident		Chenal actuel confortable, berges en pente, murs guides, digues et petits épis		0,9	1/7	0,9	Chenal étroit actuel, quelques enjeux en cas d'accident
	5	Stabilité et qualité des conditions de navigation	Turbulences, courants traversiers, berges irrégulières, longs épis, lit rocheux, vent et brouillard fréquents		Berges régulières, faites de sable ou de gravier, avec des vents faibles ou biefs abrités		-0,8	1/7	-0,8	Conditions locales favorables, parfois des courants
	6	Type de traffic, croisements, proximité de la berge	Voies actuellement à sens unique, ou au contraire beaucoup de manoeuvres et de dépassements envisagés		Voies avec actuellement 2 ou plus de lignes de navigation, interactions avec la berge acceptées		0	1/7	0	Croisement et manœuvres possibles
	7	Equipements et instruments de navigation du bateau	Gouvernail arrière seul, ou trop petit bouteur, bateaux de mer, faibles moteurs, pas de systèmes d'information		Forts bouteurs actifs ou passifs, forte puissance, 2 lignes d'arbre, systèmes d'information optimaux		-0,5	1/7	-0,5	Bateaux assez modernes prévus
2ème groupe de notes: critères liés à la vitesse du bateau	Règles de notation pour les critères liés à la vitesse du bateau: Selon la vitesse d'objectif (1ère ligne ci-dessous) ou la distance d'objectif (2ème ligne ci-dessous), appliquez la note qui figure entre parenthèses, ou interpoler si besoin								9/20 =45%	6
	8	Vitesse d'objectif par rapport à la berge	≥ 13 km/h (+1)	10 – 12 km/h (0,5)	5 – 9 km/h (0)	< 4 km/h (-1)	+0,8	5/9	4	Actuellement 12 km/h autorisé l'objectif serait 12 km/h réel
	9	Distance parcourue en 6heures, avalant	≥ 75 km (+1 ; +0,7)	≥ 40 km (+0.69 ; 0)	≥ 25 km (-0,01 ; -0.74)	< 25 km (-0,75 ; -1)	0,5	4/9	2	Amélioration de la distance prévue (40km/6 devient 65km/6h)
3ème groupe de notes: facteurs liés à la densité du trafic	Règles de notation selon la densité de trafic: appliquez la note figurant entre parenthèses ci-dessous								4/20 =20%	-1,8
	10	Gêne due aux bateaux de plaisance, en particulier ceux à rames	Fort effet négatif sur la vitesse moyenne (+1)	Gêne de faible importance à la navigation commerciale (0)		Pas d'influence sur la vitesse des bateaux de commerce (-1)	0	2/4	0	Peu d'influence prévue
	11	Limitation de la vitesse en cas de forte densité du traffic commercial	> 30,000 bateaux par an (+1)	15,000 – 30,000 bateaux par an (+0.5)	5,000 – 15,000 bateaux par an (-0.5)	< 5,000 bateaux par an (-1)	-0.9	2/4	-1,8	6100 en 2025
Note totale: somme des notes individuelles multipliées par le poids, à reporter dans la dernière colonne									4,2/20	= + 0,21

Tableau 8 : Niveau de qualité recherché pour le trajet en rivière du projet Bray-Nogent

Au vu de ce calcul, il ne semble pas nécessaire d'atteindre le niveau de qualité A pour les parties en rivière de l'itinéraire Bray-Nogent : à part plusieurs virages ou passages problématiques, et une profondeur actuelle insuffisante, la navigation sera assez aisée, compte tenu de la faible densité de trafic, et ne nécessite pas des mesures d'amélioration drastiques. C'est d'ailleurs une constatation du même type qui a conduit à écarter, dans le projet, de longues coupures de méandres, qui auraient amené la rivière en catégorie A supérieure, mais qui, par ailleurs, n'étaient pas souhaitables au plan environnemental et hydraulique.

Il est vrai que la largeur de la rivière au miroir n'est pas suffisante pour permettre une circulation dans les deux sens d'après la circulaire. Pourtant, des bateaux de 120 m de

long circulent actuellement sur ce trajet, malgré un chenal très limité, et cela sans incident notable, sans doute du fait du faible trafic, ce qui fait que la section est pratiquement exploitée comme si elle était unidirectionnelle.

Le même type de calcul donne le résultat suivant pour les parties en Canal de l'itinéraire Bray-Nogent :

Parties en CANAL entre BRAY et NOGENT - Etat projeté bis/ Critères			Arguments conduisant à augmenter le niveau de qualité des normes de conception		Cas où des normes moins élevées peuvent être appliquées pour la conception		Note	Poids	Poids global	
1er groupe de notes: Critères liés à la voie navigable	Règles de notation pour les critères liés à la voie navigable: La note est +1 si l'affirmation dans la colonne de gauche, rouge, est vraie, -1 si c'est celle de la colonne de droite, verte. Si aucun n'est vrai, ou si les 2 sont vrais, la note est 0.								7/20= 35%	1
	1	Profondeur, type de marchandises et de mode d'exploitation	Bateaux chargés, en particulier de marchandises dangereuses, dans des voies d'eau peu profondes, même après projet (fleuves à courant libre)		Bateaux vides ou ballastés, pas de marchandises dangereuses, profondeur d'eau suffisante		0,7	1/7	0,7	Bateaux chargés, voie actuelle peu profonde, mais peu de marchandises dangereuses
	2	Niveau d'entrainement, habileté et experience des pilotes	Pilotes peu entraînés, mauvaise connaissance des particularités de la voie et de l'infrastructure		Pilotes hautement qualifiés et expérimentés		-1	1/7	-1	Qualité des pilotes conditionnée par la Haute Seine
	3	Niveaux d'attention, de stress et de distraction des pilotes	Longs biefs, navigation lénifiante ou au contraire obligation de manoeuvrer sans cesse		Faible nombre de manoeuvres, peu de croisements ou de ponts		0,7	1/7	0,7	Pas de longs biefs, mais fréquentes manoeuvres
	4	Largeur, situation, niveaux de danger, dommages possibles	Chenal étroit actuel et/ou dans le projet, immeubles à proximité, berges verticales, bateaux amarrés, danger élevé en cas d'accident		Chenal actuel confortable, berges en pente, murs guides, digues et petits épis		0,8	1/7	0,8	Chenal étroit actuel, mais peu d'enjeux en cas d'accident
	5	Stabilité et qualité des conditions de navigation	Turbulences, courants traversiers, berges irrégulières, longs épis, lit rocheux, vent et brouillard fréquents		Berges régulières, faites de sable ou de gravier, avec des vents faibles ou abrité		-0,7	1/7	-0,7	Conditions locales favorables mais casiers à aménager
	6	Type de traffic, croisements, proximité de la berge	Voies actuellement à sens unique, ou au contraire beaucoup de manoeuvres et de dépassements envisagés		Voies avec actuellement 2 ou plus de lignes de navigation, interactions avec la berge acceptées		+1	1/7	1	Croisement des bateaux de projet impossible actuellement
	7	Equipements et instruments de navigation du bateau	Gouvernail arrière seul, ou trop petit bouteur, bateaux de mer, faibles moteurs, pas de systèmes d'information		Forts bouteurs actifs ou passifs, forte puissance, 2 lignes d'arbre, systèmes d'information optimaux		-0,5	1/7	-0,5	Bateaux assez modernes prévus
2ème groupe de notes: critères liés à la vitesse du bateau	Règles de notation pour les critères liés à la vitesse du bateau.: Selon la vitesse d'objectif (1ère ligne ci-dessous) ou la distance d'objectif (2ème ligne ci-dessous), appliquez la note qui figure entre parenthèses, ou interpoler si besoin								9/20 =45%	2,5
	8	Vitesse d'objectif par rapport à la berge	≥ 13 km/h (+1)	10 – 12 km/h (0,5)	5 – 9 km/h (0)	< 4 km/h (-1)	+0.5	5/9	2,5	Actuellement 6 km/h; l'objectif serait 10 km/h
	9	Distance parcourue en 6heures, avalant	≥ 75 km (+1 ; +0,7)	≥ 40 km (+0.69 ; 0)	≥ 25 km (-0,01 ; -0.74)	< 25 km (-0,75 ; -1)	0	4/9	0	Amélioration de la distance prévue (24km/6h devient 40km/6h)
3ème groupe de notes: facteurs liés à la densité du trafic	Règles de notation selon la densité de trafic: appliquez la note figurant entre parenthèses ci-dessous								4/20 =20%	-1,8
	10	Gêne due aux bateaux de plaisance, en particulier ceux à rames	Fort effet négatif sur la vitesse moyenne (+1)	Gêne de faible importance à la navigation commerciale (0)		Pas d'influence sur la vitesse des bateaux de commerce (-1)	0	2/4	0	Peu d'influence prévue
	11	Limitation de la vitesse en cas de forte densité du traffic commercial	> 30,000 bateaux par an (+1)	15,000 – 30,000 bateaux par an (+0.5)	5,000 – 15,000 bateaux par an (-0.5)	< 5,000 bateaux par an (-1)	-0.9	2/4	-1,8	6100 en 2025
Note totale: somme des notes individuelles multipliées par le poids, à reporter dans la dernière colonne								1,7/20 = 0,085		

Tableau 9 : Niveau de qualité recherché pour le trajet en canal du projet Bray-Nogent

Ici, la pondération ne met pas assez en valeur l'augmentation de largeur du canal, qui permettra un croisement facile en tout point. Il faut se rappeler que, en canal, il est très difficile de dépasser une vitesse de croisière de 8 km/h, le futur projet Seine-Nord y atteint à peine, et que 10 km/h en canal est une valeur qui mériterait d'être classée en catégorie A supérieure. Il faudrait sans doute modifier les valeurs du tableau à l'avenir, en différenciant les vitesses en rivière et celles en canal.

A la lecture de ces 2 tableaux, et compte tenu du faible trafic, il apparaît possible d'atteindre un niveau de sécurité et de facilité de navigation adéquat tout en n'appliquant que des dimensions de voie d'eau relativement restreintes. Ceci est intéressant, car il n'est pas exclu que la mise en alternat ne soit plus nécessaire sur certains tronçons avec ce référentiel.

Dimensions recommandées pour le projet Bray-Nogent

Une fois ces notes obtenues, reste à en déduire les dimensions à réaliser dans le projet en cause.

Dans la méthodologie du WG141, la correspondance entre niveaux de qualité et dimensions se fait par le biais de 2 tableaux, l'un, très complet, pour les canaux, l'autre, plus lacunaire, pour les rivières.

En ce qui concerne les canaux, les recommandations de l'AIPCN sont les suivantes :

Voie d'eau	Largeur du chenal pour voie unique en alternat				Largeur du chenal pour double sens			
	degré de facilité			Remarques	degré de facilité			Remarques
	C	B	A		C	B	A	
Largeur minimale - W_f section droite en canal	2 B[1] *1.9·B 2.1·B*		*2.3·B*	pour raisons de sécurité	3 B[2] *2.8·B*	4 B[3] *3.5·B*	*4.5·B*	2.5 Bpourrait endommager le canal
n minimal	2.5	3.5	4.5	pour améliorer la vitesse	3.5	5	7	pour améliorer la vitesse
profondeur D minimale (sur toute la largeur du fond)	1.3 d			A cause du squat & pour préserver l'efficacité des bouteurs	1.3 d		1.4 d	A cause du squat & pour préserver l'efficacité des bouteurs
rayon R minimal	4 L	7 L	10 L	ΔF si $R \neq \infty$	4 L	7 L	10 L	ΔF si $R \neq \infty$
courant max v_{flow} (longitudinal)	0.5 m/s				0.5 m/s			
courant max v_{cross} (transversal)	0.3 m/s (moyenne sur L)			ΔF requis si $v_{cross} \neq 0$	0.3 m/s (moyenne sur L)			ΔF requis si $v_{cross} \neq 0$
vent de projet v_w dans les terres	5-6 BF *(8.0 – 13.9 m/s; 10.5 m/s normes hollandaises)*			ΔFrequis pour bateau vide ou ballasté ou porte-conteneur si $v_w \neq 0$	5-6 BF *(8.0 – 13.9 m/s; 10.5 m/s normes hollandaises)*			ΔFrequis pour bateau vide ou ballasté ou porte-conteneur si $v_w \neq 0$
vent de projet v_w près des côtes	6-7 BF *(10.8 – 17.2 m/s; 13.5 m/s normes hollandaises)*			ΔFrequis pour bateau vide ou ballasté ou porte-conteneur si $v_w \neq 0$	6-7 BF *(10.8 – 17.2 m/s; 13.5 m/s normes hollandaises)*			ΔFrequis pour bateau vide ou ballasté ou porte-conteneur si $v_w \neq 0$

Tableau 10 : dimensions de base pour les canaux en ligne droite (Source : AIPCN, Groupe d'Etudes 141, traduction de l'auteur)

Les notes sont les suivantes

1) Ces largeurs de base intègrent 3 distances de sécurité (2 fois 0,3 B avec les berges et 0,4 B pour l'instabilité directionnelle)
2) Les largeurs de base intègrent 4 distances de sécurité (2 fois 0,2 B avec les berges, 0,2 B entre bateaux et $\sqrt[2]{0,3B}$ pour l'instabilité directionnelle)
3) Les largeurs de base intègrent 4 distances de sécurité (2 fois 0,5 B avec les berges, 0,3 B entre bateaux et $\sqrt[2]{0,4B}$ pour l'instabilité directionnelle)

A noter que B est la moyenne des largeurs des bateaux en cas de trafic à double sens.

Pour la largeur d'un chenal bidirectionnel, on appliquera l'interpolation :

note	1	0,9	0,8	0,7	0,6	0,5	0,4	0,3	0,2	0,1	0	-0,33	-0,66	-1
Largeur	4,5	4,4	4,3	4,2	4.1	4	3,9	3,8	3,7	3,6	3,5	3,2	3,0	2,8

Tableau 11 : Interpolation des largeurs en chenal bidirectionnel

Pour la largeur d'un chenal unidirectionnel :

note	1	0,9	0,8	0,7	0,6	0,5	0,4	0,3	0,2	0,1	0	-0,33	-0,66	-1
Largeur	2,3	2,27	2,23	2,2	2,18	2,15	2,13	2,1	2,08	2,065	2,05	2	1,95	1,9

Tableau 12 : Interpolation des largeurs en chenal unidirectionnel

Pour le coefficient n bidirectionnel

note	1	0,9	0,8	0,7	0,6	0,5	0,4	0,3	0,2	0,1	0	-0,33	-0,66	-1
Largeur	7	6,8	6,6	6,4	6,2	6	5,8	5,6	5,4	5,2	5	4,5	4,0	3,5

Tableau 13 : Interpolation de n en chenal bidirectionnel

Pour le coefficient n unidirectionnel

note	1	0,9	0,8	0,7	0,6	0,5	0,4	0,3	0,2	0,1	0	-0,33	-0,66	-1
Largeur	4,5	4,4	4,3	4,2	4.1	4	3,9	3,8	3,7	3,6	3,5	3,16	2,83	2,5

Tableau 14 : Interpolation de n en chenal bidirectionnel

Par ailleurs, l'augmentation de largeur dans les courbes suit la formule de Graewe,

$$\Delta Fc = C_C L^2/R \qquad (1)$$

avec les coefficients C_C suivants :

C_C= 0,25 pour bateaux chargés de classe Vb, 0,5 pour bateaux lèges.

C_C= 0,3 pour bateaux chargés de classe Va, 0,6 pour bateaux lèges.

Pour les fleuves, les choses sont plus floues, du fait de l'influence du courant. Le groupe d'étude se limite à ne recommander que 3 grandeurs :

Rivières	Largeur du chenal pour voie unique en alternat				Largeur du chenal pour double sens			
	degré de facilité			Remarques	degré de facilité			Remarques
	C	B	A		C	B	A	
Largeur minimale - W_f en ligne droite [1]	**2.8 B** [3]	**3.2 B** [3]	**3.4 B** [3]	pour raisons de sécurité	**4 B**	**5 B**	**6 B**	3 B pourrait endommager la berge
profondeur D minimale (sur toute la largeur du fond)	**1.2 d**	**1.3 d**	**≥ 1.3 d**	A cause du squat & pour préserver l'efficacité des bouteurs	**1.2 d**	**1.3 d**	**1.4 d**	A cause du squat & pour préserver l'efficacité des bouteurs
rayon R minimal (ΔF si $R \neq \infty$) [2]	**2 L**	**3 L**	**4 L**	Selon les conditions locales	**2 L**	**3 L**	**4 L**	Selon les conditions locales

Tableau 15 : dimensions de base en rivière (Source : WG 141, traduction de l'auteur)

Ces chiffres sont valables pour un bateau de marchandises normalement équipé et disposant des instruments habituels. Le courant ne doit pas dépasser 1,5m/s et le vent ne doit pas dépasser 5 à 6 BF.

Les notes sont les suivantes :

1) Les largeurs de base intègrent 2 ou 3 distances de sécurité (3 fois 0,5 B à vitesse normale pour la catégorie C, 3 fois 0,8 B pour la catégorie B et 3 fois 1,1 B pour les bateaux rapides – catégorie A) : une avec chacune des berges, et une entre bateaux Ces distances incluent les facteurs humains et l'effet du vent. (…) S'y ajoute une instabilité directionnelle de 0,5 à 0,7 B.

2) En ce qui concerne l'augmentation des largeurs de chenal existantes dans les courbes, les largeurs de base devraient être augmentées d'au moins $\Delta F_C = 0{,}5 \cdot L^2/R$ pour une voie et $1{,}0 \cdot L^2/R$ pour un trafic bidirectionnel. Notez que ces largeurs minimales se réfèrent à des bateaux vides, utilisant tous les moyens de navigation disponibles, et que la largeur supplémentaire dans les courbes dépend fortement du style de conduite, des moyens de navigation disponibles et de d/D (ou T/h).

3) B indique la largeur du bateau de projet pour le trafic à une seule voie, ou la moyenne de largeur des deux bateaux en cas de circulation dans les deux sens. Les

multiplicateurs de largeur (2.8, 3.2 et 3.4) ont été obtenus en multipliant les valeurs en canal par un facteur 3/2.

L'augmentation des diverses distances de sécurité entre les canaux et les rivières correspond à un doublement de ces sécurités. Les coefficients qui en résultent aboutissent à des valeurs trop élevées pour le projet actuel, où la vitesse est limitée, ainsi que pour la plupart des rivières canalisées européennes. On rappelle que la Circulaire française ne prévoit qu'un facteur de 1,1 pour la largeur du chenal en rivière par rapport aux valeurs en canal, alors que dans la proposition du WG141 ce facteur est supérieur à 1,5.

On propose donc de créer un autre tableau, spécifique aux rivières canalisées, généralement plus étroites et plus tranquilles que les rivières à courant libre.

Au cas où une telle catégorie ne serait pas acceptée de façon universelle, elle a en tous cas vocation à s'appliquer en France, puisque la circulaire 76-38 prévoit ce facteur de 1,1 entre les dimensions à prévoir en rivière par rapport à celles en canal, et que toutes les rivières naviguées en France sont canalisées[3].

On obtient alors le tableau suivant :

	Largeur du chenal pour voie unique en alternat				Largeur du chenal pour double sens			
	degré de facilité			Remarques	degré de facilité			Remarques
	C	B	A		C	B	A	
Largeur minimale - W_f en ligne droite	2 B [1)]	2,3 B [2)]	2,5 B [3)]	pour raisons de sécurité	3,3 B [1)]	3,9 B [2)]	5 B [4)]	3 B pourrait endommager la berge
profondeur D minimale au plafond	1,15 d	1,2 d	≥ 1.3 d	A cause du squat & pour préserver l'efficacité des bouteurs	1,15 d	1,25 d	1.4 d	A cause du squat & pour préserver l'efficacité des bouteurs
Rectangle de navigation	$W_f \times d$				$W_f \times d$			
rayon R minimal (ΔF si $R \neq \infty$)	2 L	3 L	4 L	Selon les conditions locales	2 L	3 L	4 L	Selon les conditions locales

Tableau 16 : dimensions de base en rivière canalisée (proposition de l'auteur)

Ici, les notes correspondent à :

1 Ces largeurs de base intègrent 3 ou 4 distances de sécurité (2 fois 0,3 B avec les berges, 0,3 B entre bateaux et 0,4 B pour l'instabilité directionnelle)
2 Les largeurs de base intègrent 3 ou 4 distances de sécurité (2 fois 0,4 B avec les berges, 0,6 B entre bateaux et 0,5 B pour l'instabilité directionnelle)
3 La largeur intègre 3 distances de sécurité (2 fois 0,5 B avec les berges, et 0,5 B pour l'instabilité directionnelle)
4 La largeur intègre 4 distances de sécurité (2 fois 0,65 B avec les berges, 0,7B entre bateaux et 1 B pour l'instabilité directionnelle)

A noter que B est la moyenne des largeurs des bateaux en cas de trafic à double sens.

On atteint environ un facteur de 1,1 par rapport aux valeurs en canal, ce qui semble adéquat aux vitesses actuelles et projetées, et correspond à la pratique française actuelle.

Si l'on traduit les notes de qualité calculées pour Bray-Nogent avec les mêmes multiplicateurs, il faudrait les dimensions suivantes (profil trapézoïdal à 3/1), d'après les interpolations des tableaux 11 à 14 :

[3] A l'exception de la Loire, de la Seine Maritime et d'une partie du Rhin, fleuve frontalier

Bateau 110x11,40x2,8m	Note	Largeur W (m)	Mouillage T (m)	Miroir (m)	Plafond (m)	Ac (m²)	n	ΔW (m) R=220
Rivière bidirectionnelle	0,21	47,08	3,2	63,88	33,68	173,7	5,42	49,5
Rivière unidirectionnelle	0,21	26,70	3,635	43,50	21,69	118,5	3,71	33
Canal bidirectionnel	0,085	40,87	3,5	57,67	36,67	165,09	5,17	41,25
Canal unidirectionnel	0,085	23,51	4,075	40,31	15,86	114,46	3,58	27,5

Tableau 17 : Dimensions recommandées pour le Projet Bray-Nogent

La surlargeur à appliquer a été calculée pour le bateau de projet, grand rhénan de 110 m de long et 11,40 m de large, à 2,80 m d'enfoncement, et pour la courbe la plus serrée, de 220 m de rayon, correspondant à deux fois la longueur du bateau de projet. Ces valeurs sont très trompeuses :

Les seules valeurs exactes sont celles des canaux unidirectionnels, mais on ne peut pas y additionner la surlargeur avec la largeur du chenal : en effet, les bateaux qui nécessitent le plus d'espace sont les bateaux lèges, mais ils disposent d'une plus grande largeur disponible, puisque leur enfoncement n'est que de 1,10 à 1,30 m, voire 1,80 m pour les très grands Rhénans ballastés.

En Petite Seine, on retiendra 1,30m d'enfoncement, ce qui permet de disposer de 9 m de chenal unidirectionnel supplémentaire dans la voie d'eau, à déduire donc du miroir nécessaire. Dans le virage le plus limitant, au lieu de 67,80 m, il suffira d'un miroir de 58,80 m dans un canal unidirectionnel, pour un bateau lège ballasté et de 67,50 m au lieu de 76,50 m dans une rivière unidirectionnelle, en franchissement du virage le plus serré de l'itinéraire par un bateau lège ballasté.

Les largeurs nécessaires au miroir pour un bateau chargé sont sensiblement plus faibles, et dans le même virage ne devraient pas dépasser un miroir de 54,06 m en canal unidirectionnel et 60 m en rivière unidirectionnelle.

Cela revient en quelque sorte à diminuer le chenal nécessaire de 9 m.

Pour les chiffres en bidirectionnel, il est également superflu d'additionner, comme traditionnellement, les surlargeurs nécessaires à un bateau chargé dans un sens et un bateau lège dans l'autre. L'expérience montre en fait que les bateaux manoeuvrent instinctivement pour minimiser l'espace nécessaire au moment du croisement. On a observé que, généralement, l'un des bateaux se remet dans l'axe du chenal le temps du croisement, ce qui est équivalent à offrir à l'autre bateau sa propre surlargeur. Une analyse poussée de ce phénomène a été menée (Eloot, 2013), il en résulte une diminution de la piste balayée d'environ un tiers grâce à ces manœuvres, sans qu'une règle précise ait été proposée.

Par contre, en bidirectionnel, on ne peut utiliser que la moitié des 9 m précédents, car le bateau chargé occupe l'autre moitié du chenal.

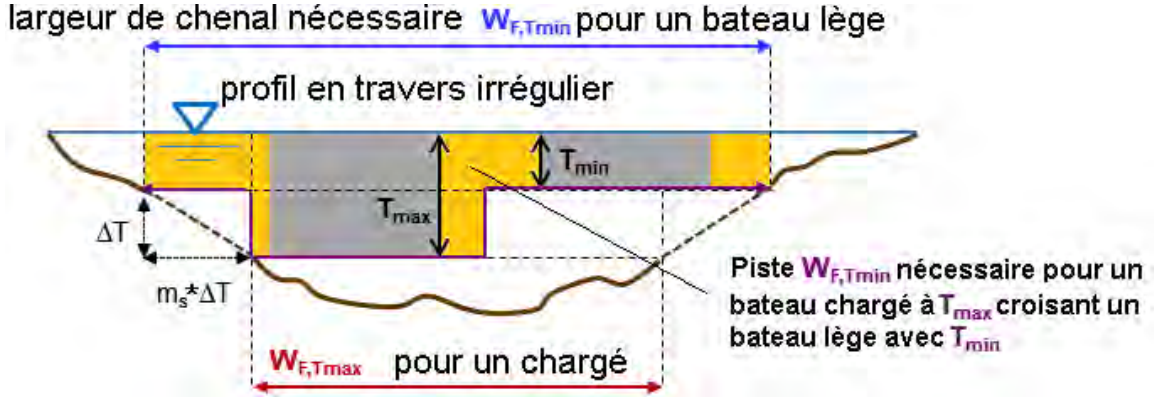

Figure 2 : Coupe d'une voie d'eau lors du croisement d'un bateau chargé et d'un bateau lège (source : WG141, traduction de l'auteur)

Grâce à ces diminutions, et comme la rivière a souvent plus de 60 m au miroir, on propose un calcul approché de la largeur en rivière bidirectionnelle pour vérifier si un alternat pourrait être évité, en supposant une réduction de 30% des valeurs théoriques, et en déduisant la moitié des 9 m signalés plus haut.

Les chiffres sont les suivants en voie d'eau bidirectionnelle :

Type/ dimensions (m)	Courbe de Rayon 220m	Courbe de Rayon 550m	Courbe de Rayon 850m	Courbe de Rayon 1000m	Courbe de Rayon 1500m
ΔW Rivière lège	33	13,2	8,54	7,26	4,84
ΔW Rivière chargé	16,5	6,6	4,27	3,63	2,42
Total ΔW -30%	34,65	13,86	8,96	7,62	5,08
Piste totale	77,23	56,44	51,55	50,20	47,66
ΔW Canal lège	27,5	11	7,12	6,05	4,03
ΔW Canal chargé	13,75	5,5	3,56	3,02	2,02
Total ΔW -30%	28,88	11,55	7,47	6,35	4,24
Piste totale	65,24	47,92	43,84	42,72	40,60

Tableau 18 : Grandeurs caractéristiques d'une voie d'eau bidirectionnelle

On voit que, sauf dans les cas extrêmes, une piste de 60 m est suffisante pour inscrire un croisement de bateaux de 110 m dans tous les virages du trajet Bray-Nogent. La limite se calcule, elle se situe à un rayon de 437 m en rivière et 268 m en canal.

Il se trouve d'ailleurs qu'avec une méthodologie différente, l'application de la circulaire française 76-38 aboutit à des chiffres assez voisins[4].

Par contre, le trajet Ecluse de la Grande Bosse-Bray sur Seine présente aujourd'hui plusieurs courbes d'un rayon inférieur à 220 m. La piste utilisée par les bateaux lèges d'aujourd'hui, ayant jusqu'à 120 m de long dans des courbes très serrées, est cependant plus large que celle qui sera nécessaire aux bateaux lèges du projet, qui auront le même enfoncement lège qu'aujourd'hui, alors même que les courbes seront rectifiées pour respecter 220 m de rayon . Ce seront donc seulement les bateaux chargés à 2,80 m (au lieu de 2 m) qui nécessiteront un recalibrage de cette partie du trajet.

Il est alors particulièrement intéressant de constater que cette succession de courbes serrées est parcourue par les bateaux actuels sans qu'aucun incident n'y soit signalé. Le niveau de trafic actuel, et la présence d'une écluse à l'une des extrémités, rend cela possible. L'écluse agit en effet comme un cadenceur d'alternat, en ne laissant entrer un bateau dans cette section qu'une fois toutes les 30 minutes, au mieux, ce qui correspond exactement à la durée du parcours Bray-La Grande Bosse. Il suffit donc aux bateaux avalants de vérifier l'heure de passage des bateaux montants dans l'écluse pour être sûrs de ne croiser personne. Cette particularité pourra être mise à profit dans le projet en cours de réalisation pour diminuer les dragages sur cette partie du trajet, sans qu'il soit besoin d'instaurer un alternat officiel, toujours pénalisant.

Pour diminuer encore les reprises de berges, il serait possible d'utiliser un profil RT[5], tel que réalisé en Belgique sur la Lys dans le cadre du projet Seine-Escaut (Eloot, 2013). Ce profil, qui présente une berge verticale sur un côté et une pente à 3/1 de l'autre, a l'avantage de permettre une meilleure interaction entre les bateaux lors de leur croisement. Il n'a besoin que d'un miroir égal à la largeur de piste plus 3,90 m.

Conclusions sur l'utilisation des recommandations du WG141

Comme le rapport lui-même le précise, il est nécessaire d'adapter les recommandations mondiales au réseau étudié.

Par rapport aux tableaux proposés dans le rapport du WG141, on a procédé aux ajustements suivants :

[4] Sans doute parce que la surlargeur $L^2/2R$ y est implicitement calculée en voie d'eau unidirectionnelle.
[5] Profil proposé par les recommandations allemandes

- Remplacement du critère « gamme de vitesses praticables » par un critère « distance parcourue en 6 heures »
- Modification du poids des critères, le groupe de critère « trafic » n'ayant plus qu'un poids de 4, et le groupe de critères « vitesse » obtenant un poids de 9
- Utilisation de tableaux d'interpolation, pour faciliter l'estimation des notes (tableaux 3, 4, 11, 12, 13 et 14)

On a présenté également des suggestions d'amélioration des tableaux, en proposant que le critère « vitesse d'objectif par rapport à la berge » soit apprécié différemment en rivière et en canal, une vitesse d'objectif supérieure à 10 km/h n'étant possible en canal qu'au prix d'investissements très élevés.

On pourrait envisager une interpolation comme suit :

note	1	0,9	0,8	0,7	0,6	0,5	0,4	0,3	0,2	0,1	0	-0,33	-0,66	-1
Vitesse (km/h)	>12	11	10	9	8,5	8	7,5	7	6,5	6	5,5	5	4,5	<4

Tableau 19 : Interpolation de vitesse en canal

A comparer avec celle pour la vitesse en rivière

note	1	0,9	0,8	0,7	0,6	0,5	0,4	0,3	0,2	0,1	0	-0,33	-0,66	-1
Vitesse (km/h)	>13	13	12,5	12	11,5	11	10,5	10	9	8	7	6	5	<4

Tableau 20 : Interpolation de vitesse en rivière

Chaque pays, voire chaque voie d'eau, devra procéder ainsi à un réglage fin des pondérations et des critères pour obtenir une bonne adéquation avec les conditions locales.

Grâce à cette souplesse, la méthodologie du Groupe d'Etude 141 peut être d'application mondiale. Cela été l'un des critères qui a guidé ses travaux tout du long, ainsi que l'avait souhaité la Commission CoCom de l'AIPCN.

REFERENCES

Eloot, 2013 : Eloot, K., Verwilligen J., Vantorre M. 2013. Workshop Design Guidelines for Inland Waterways - Detailed Design for Inland Waterways: The Opportunities of Real-Time Simulation, *Smart Rivers Conference 2013, Maastricht*

Söhngen, 2015: Söhngen, B. Workshop Design Guidelines for Inland Waterways, Application of WG 141 approach including elaboration of field data and fast time simulation for Class Va-vessel passing narrow Jagstfeld bridge in the German Neckar River, *Smart Rivers Conference 2015, Buenos Aires*

MOTS CLE

Navigation fluviale
Chenal navigable
Dimensions des voies navigables
WG 141
Classification des voies navigables

Remote-control, set the standard by designing a simulator and professionalize!

by

MSc. Eng. Michiel Coopman[1]

ABSTRACT

This paper considers the goals, challenges, process and results of a reference design for remote operation of locks and bridges. By building a simulator for remote lock- and bridge operation, we set the standard and we can use it as a reference to professionalize the way remote control is designed and implemented.

The goal is to develop technical, functional and operational standards for remote operation of bridges and locks, integrating them into a training simulator and setting up a training course for operators.

We address the critical success factors for remote control; standardization and the combined optimization of human and technological factors.

A virtual world of waterways with different types of locks and bridges is created within the simulator. These virtual locks and bridges can be operated from a reference control room, serving as a realistic representation of a real control room.

The road during development and implementation of this simulator forces both engineers and operators to thoroughly reflect on each small operational and technical aspect of remote control.

Apart from the obvious benefits of standardization, such as increased flexibility in scheduling of workforce, cost-cutting, standardized training, speeding-up implementation of remote control projects and reduced design efforts, we point out some less evident benefits.

We are evolving towards a mesh-like overall control system, dispersed throughout the full territory. We are evolving towards a complete IP-based set-up, where data/server-center and control-room are not necessarily in each other's vicinity. We need the control centers to be interoperable. This allows for back-up and fail-over scenarios as well as shifting between smaller daytime and larger 24/7 control rooms according to demand or weekly and seasonal variations. At the same time, this allows to invest efficiently on redundancy and availability, not on a local level but on a system-wide level.

All this is possible, only when having a clear shared vision on how things should be done. Developing and building a simulator allows to develop and mature this shared vision.

1. Background

Remote operation of inland waterway infrastructure has been around for about 2 to 3 decades. It is now time to evolve towards a reference design so we can professionalize the way remote control is designed and implemented and benefit from the opportunities that lie ahead in the future of remote control.

De Vlaamse Waterweg (Flemish Waterway) is a newly formed government agency in Belgium. It was formed at the beginning of 2018 out of merger of 2 existing agencies with different territories; *Waterwegen en Zeekanaal* in the West and center of Flanders and *De Scheepvaart* in the East of Flanders.

De Vlaamse Waterweg NV now manages almost all inland waterways and infrastructure in Flanders, Belgium.

[1]De Vlaamse Waterweg NV (Hasselt, Belgium), coopmanmichiel@gmail.com

Over the last 2 to 3 decades, both Flemish agencies have invested already heavily in technology for remote operation of Inland Waterway Infrastructure. The ambition of the newly formed De Vlaamse Waterweg, is to invest even more and utilize remote-control on a large and organization-wide scale.

De Vlaamse Waterweg NV has developed and built a simulator for the remote control of locks and bridges. The simulator will be placed in a special designated AWATAR-center.

2. Why do we not yet have a reference design?

2.1 Past

Each bridge or lock is typically designed for its specific boundary conditions and reflects the state of the art of technology at the time of construction. This leads to a wide variety of design and implementations of structures and systems. They were never designed to be connected. This is major technical challenge when implementing remote control.

2.2 Present

Currently, history repeats itself. Several locks and bridges are combined into increasingly larger corridors, operating from a specifically designed control center. When building these centers, several design choices are made based on the involved structures and systems. Often, these projects are the sum and connection of several legacy systems present in the involved area.

Then again, this leads to a wide variety of design and implementations of control centers and Human-Machine-Interfaces (HMI). Therefore, these centers are not designed to be interoperable.

We make design choices based on the task at hand, the technology at our disposal and we search for the best fit. We don't take the bigger picture and the future ahead into account, but we should.

3. Why do we need a reference design?

The introduction of remote operation is historically justified by two main arguments: increasing efficiency by saving manpower and expanding operating hours for waterways with lower volumes of traffic.

However, if we can evolve towards interoperable control centers and interchangeable HMI's, several more advantages can be achieved:

- Increased safety by systematically reviewing and auditing both technical and operational standards
- Speed up implementation of remote control projects by reduced design effort
- Cost-cutting by standardization
- Allow for standardized and professional training of operators instead of on-the-job training
- Allow for back-up and fail-over scenarios for control centers in a mesh-like overall system
- Even more efficiency gains by flexibility in the scheduling of workforce

We need the control centers to be interoperable. This allows for back-up and fail-over scenarios as well as shifting between smaller daytime and larger 24/7 control rooms according to demand or weekly and seasonal variations.

At the same time, this allows to invest efficiently on redundancy and availability, not on a local level but on a system-wide level.

All this is possible, only when having a clear shared vision on how things should be done. Developing and building a simulator allows to develop and mature this shared vision.

4. What are the challenges in establishing a reference design?

Usually, standardization efforts are mainly paper exercises, performed by technical experts. Paper exercises have the risk of not addressing the real-life problems and discussions experienced in the field during construction and operations. They are often open-ended.

Operational personnel often have useful practical knowledge about problems experienced during operations. They need to be involved. However, they sometimes lack skill to interpret technical drawings and documents. Thus, we need more than texts and drawings to communicate and discuss. We need to experience.

In the beginning, trust needs to be built and this is a slow process. This can only be achieved if the intentions are genuine and respectful.

Buy-in of higher management and understanding and support of the goals and intentions is a prerequisite

5. How do we establish a reference design?

De Vlaamse Waterweg NV has set up the AWATAR project. AWATAR stands for Automation of Waterways: Training and Reference.

The 3 main goals of AWATAR are:

- to establish and maintain the technical and operational reference
- to allow for standardized and professional training
- facilitate, professionalize and mature the way remote control is implemented

We made virtual 3D models of several lock and bridges, together with models of ships, cars, pedestrians, … inside a gaming engine. We connected these virtual models with real PLC and SCADA software and simulated different camera-viewpoints, traffic situations and weather conditions.

This allows us to discuss and try very different HMI designs, camera-view points, functional behavior, operational procedures, … all without disturbing any real-life operation and in great detail.

Operators are forming a crucial part in the engineering and construction of the AWATAR-center and simulator. We organized multiple participation sessions, workshops and feedback-loops with both engineers and operators. This process is supported by combining the most modern tools such as 3D modelling and Virtual Reality Glasses to design the operator desk.

6. What is the result?

- A dominant design well documented by technical and operational standards, manuals … supported by both operators and engineers
- A design thoroughly checked on safety issues
- A detailed design and working prototype of the training-simulator
- A camera-simulator, to test camera-viewpoints
- A fully developed training program
- A solid foundation of thrust between engineers and operators

- A modular design, to allow for future changes and technological advancements.

7. What are the lessons learned?

- It takes time and effort to build trust and understanding and to get the right persons involved, but it is worth it;
- Integration of knowledge and experience from operators in an early stage, results in a more useful design;
- The more tangible and life-like the simulator, the more detailed and interesting the discussions get;
- To keep the engineers involved and the results usable in the field, built it with real automation components and software as much as possible;
- Use a contractor with experience in automation of waterway infrastructure;
- The real value of training on a simulator vs on the job training lies in the training of exceptional circumstances or actions that intervene with normal operations, such as emergency situations and technical failures.

8. What is the future?

This simulator will be placed in an operator training center. This center is the meeting point where engineers and operators can thoroughly discuss issues, whereas the conclusions will then form the reference point for the whole organization. It is a physical location but at the same time, it forms a dynamic body of knowledge.

By having a clear and up-to-date reference, we professionalize our technology management. It allows to evolve to an interoperable and thus robust mesh-like setup of control centers. We will build a network of control centers, rather than separate islands.

Driving Assistance Systems for Inland Vessels based on High Precision DGNSS (Research Project LAESSI)

by

Rainer Strenge[1], Michael Hoppe[1], Dr Martin Sandler[2], Dr Anja Hesselbarth[3], Dr Ralf Ziebold[3], Maik Uhlemann[3], Jürgen Alberding[4], Martin Bröschel[1] and Larisa Burmisova[1]

ABSTRACT

Inland shipping is an important key element of the German transport system. The growth in traffic, increasing ship dimensions, reduced maneuver space etc. place high demands on the responsible skippers. It is expected that future driving assistance systems can contribute to safe navigation.

The project LAESSI (Guiding and Assistance Systems to Improve Safety of Navigation on Inland Waterways) aims to develop efficient navigation assistance functions for inland waterway transport. Therefore, nautical information like position, height and heading has to be determined. One main task of the project is the development of a bridge collision warning system, which could provide a timely alert to the skipper, whenever the vessel, particularly the wheelhouse or radar mast, will not safely pass the bridge.

A feasibility study has identified Global Navigation Satellite System (GNSS) technologies as basis for the reliable height determination for such a bridge collision warning system. This approach requires information about the vertical clearance of the bridge superstructure as well as precise height information at least 300 m before the vessel will pass the bridge. The high accuracy level of less than 10 cm in the vertical position requires the use of high precision DGNSS.

The paper will present the derived requirements for inland waterway assistance functions as well as an overview about the overall system architecture. In addition the paper provides information about the high accuracy positioning system, which is based on real-time kinematic (RTK) technology including integrity information. The correction and integrity data in combination with other waterway information will be broadcasted using the new frequency bands offered from VDES (VHF Data Exchange System). Finally the paper will describe first results gained in demonstration areas at the Moselle and Main Rivers.

[1] German Federal Waterways and Shipping Administration, Traffic Technologies Centre, rainer.strenge@wsv.bund.de, Koblenz, Germany
[2] in – innovative navigation GmbH, martin.sandler@innovative-navigation.de, Kornwestheim, Germany
[3] German Aerospace Center, anja.hesselbarth@dlr.de, Neustrelitz, Germany
[4] Alberding GmbH, alberding@alberding.eu, Wildau, Germany

1. INTRODUCTION

Inland navigation plays an important role in transportation of goods in Germany. Although inland navigation is a relatively safe mode of transport, accidents like collisions of wheelhouses with bridge superstructures happen from time to time and can have dramatically consequences. It is expected that this type of accident can be reduced by a system warning that is generated when the ship's height is too large for the bridge passage. In addition, even the daily navigation of a large ship, e.g. a 185 m push tow, in confined waters is a demanding task for a scipper and indicates the need for support.

The aim of the project LAESSI is to support the skipper in his tasks of navigating a vessel and thus make inland shipping safer and also more efficient. To reach this goal, LAESSI makes use of latest GNSS navigation technology and data transmission developments. Within the project LAESSI research was done to add elaborated integrity information to the result of GNSS processing. Providing high precision navigation data with high reliability is a prerequisite to set up advanced driver assistance functions.

The joint research initiative LAESSI was pursued in a unique combination of core competences from in-innovative navigation GmbH, Alberding GmbH, DLR (German Aerospace Center) Institute of Communications and Navigation and Traffic Technologies Centre of German Waterways and Shipping Administration (WSV).

The paper will provide information about the derived requirements for inland waterway assistance functions as well as an overview about the overall system architecture. In addition the paper informs about the high accuracy positioning system, which is based on RTK technology including integrity information. The correction and integrity data in combination with other waterway information will be broadcasted using the new frequency bands offered from VDES (VHF Data Exchange System). Finally the paper will present first results gained in demonstration areas at the Moselle and Main Rivers.

The project was funded by the Federal Ministry for Economic Affairs and Energy (BMWi) under grant number 03SX402.

2. THE CONCEPT OF LAESSI

2.1 Assistance functions

The project focuses on the development of:

- A Bridge Collision Warning System providing a timely alert signal to the skipper, whenever the vessel, particularly the wheelhouse or the radar mast, will not safely pass under a bridge.
- A Berthing Assistant provides an accurate display of the actual situation, in particular highly accurate distances to quay walls and other vessels.
- An Automatic Guidance System reducing stress on the skipper during on route navigation. Highly accurate and integrity tested positioning and heading information are the basis for this functionality, especially on narrow waterways.
- A Conning Display presenting clearly the motion of the ship. For this purpose it is also important to incorporate information from the propulsion systems as well as the influence of wind and water currents.

2.2 System requirements

In the following table accuracy as well as integrity requirements are listed for the different assistance functions. The basic idea of a bridge collision warning is to compare the geodetic height of the vessel with the geodetic height of a bridge. This results in requirements for the height measurement. The algorithm will further be divided into two parts, a long distance part starting about 10 minutes before the bridge passage and a close up part within the last two minutes. The first lines in Table 1 in column bridge collision warning refer to the close up part. A warning in the close up part requires immediate action of the skipper. Therefore, higher integrity requirements have to be taken into account. Also the time to alarm is lower there.

Position and heading are used as a basis for prediction of the ship´s movement in the close up part. High requirements for position and heading accuracy are necessary for the berthing assistant. These are based on the requirement that each point on a 185 m convoy shall be known with 10 cm accuracy. The integrity risk is based on the assumption, that one non detected error within three years of normal operation can be tolerated. The time to alarm requirement takes into account, that on the one hand berthing is a critical operation for the skipper. On the other hand the vessel is moving at low speed in this situation.

	Bridge collision warning	Automatic guidance	Berthing assistant	Conning display
Position accuracy [cm]	20	30	10	20
Height accuracy [cm]	10	not relevant	not relevant	not relevant
Heading accuracy [°]	0,3	0,17	0,07	0,1
Integrity risk	$10*10^{-5}$ / 2 min $30*10^{-5}$ / 8 min	$0,55*10^{-5}$ / 3 h	$18*10^{-5}$ / 10 min	$18*10^{-5}$ / 1 h
Time to alarm [s]	4 6	2	6	6

Table 1: Accuracy and integrity requirements of assistance functions

The integrity requirements for the conning display are quite similar, when the vessel operates in confined waters, but most times not close to walls or other vessels. Thus accuracy requirements are lower. Also the time of using a conning display is longer compare to a typical berthing situation. For automatic guidance of the vessel no especially high accuracy is required. In contrast to the other assistance functions, the skipper is not part of the control and action loop. His functions are monitoring the system as well as tactical trajectory planning. Jumps due to errors in the position measurement might have immediate impact on the rudder commands. Thus the function has to be very reliable. Basis for the proposed integrity risk is the assumption that within one year of 100 vessels operation only one case of not detected integrity problem may occur. Also a very short time to alarm is required.

2.3 Overall system architecture

The required level of accuracy (dm – cm) cannot be achieved by currently used code based positioning techniques. Therefore, phase based GNSS positioning (RTK) needs to be applied. Furthermore exact and valid electronic charts, as well as information regarding the actual situation in the navigational area (e.g. temporary restrictions at construction sites) are required.

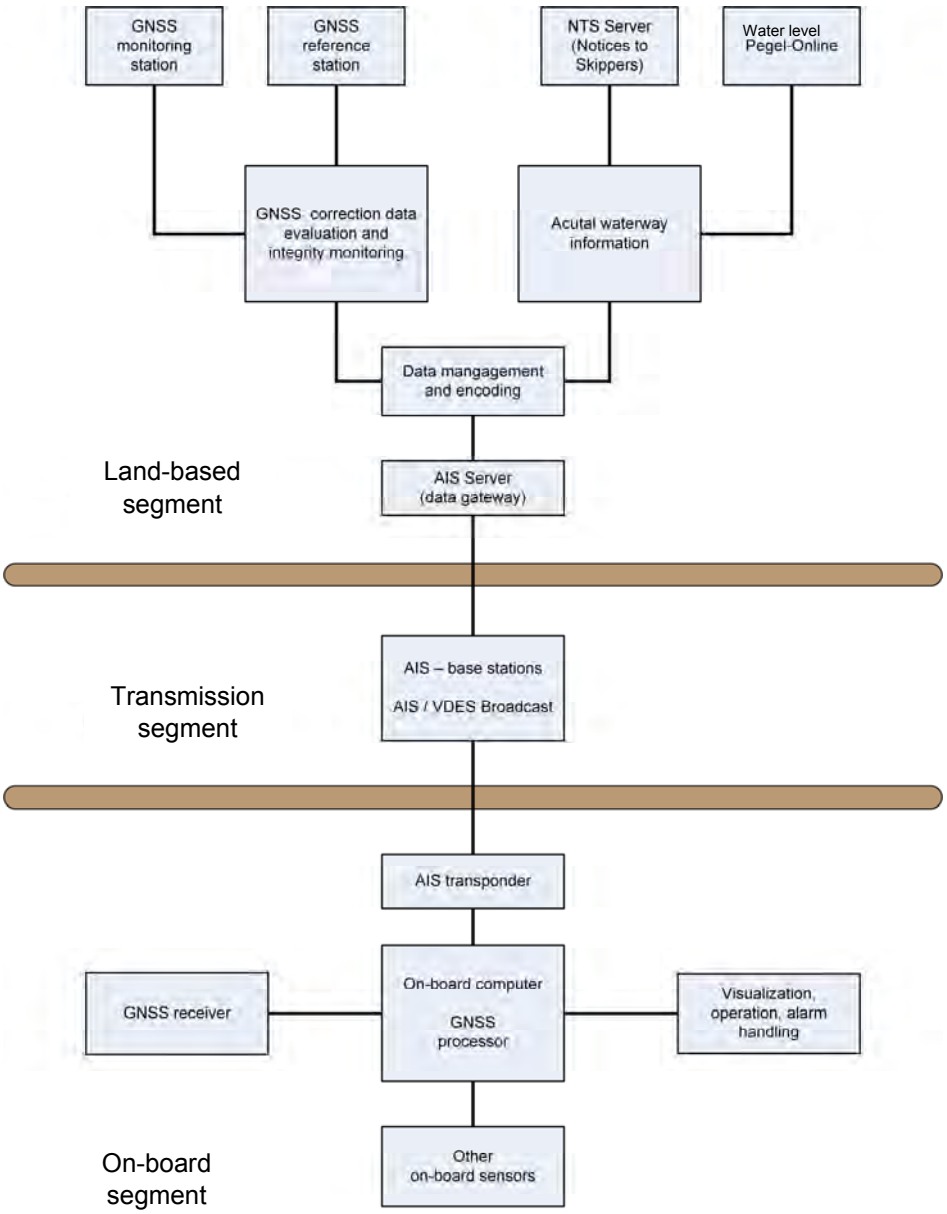

Figure 1: Overall system architecture

Fig. 1 shows a schematic overview of the system architecture of the project LAESSI. The land based segment provides GNSS correction data necessary for the RTK processing on-board the vessel. These correction data are integrity checked before they are transmitted. Any problems are reported to subsequent processing steps and are the first step of the integrity control framework of this project. Also information about actual waterway conditions is prepared.

It is important to provide up-to-date information about waterway restrictions, e.g. construction works at bridges. Such information should be provided timely and to the relevant locations.

Transmission of these data to the vessels shall be done by AIS and its future enhancement VDES. Finally the on-board segment realizes the assistance function. A GNSS receiver, augmented by the correction data generated in the land segment provides high precision GNSS solutions. Processors on the vessel monitor the integrity of the solution and realize the assistance functions. Further on-board sensors are inertial measurement unit (IMU), rate of turn indicator, laser distance scanners etc.

3. DATA PROCESSING AND TRANSMISSION

3.1 Land-based data processing

The on-board assistance functions, which shall support the skipper in a reliable manner, require both precise position information and also actual water way information. This information is generated and collected by the land-based service and broadcast to the vessel. An overview of the design of the service is given in Fig. 2.

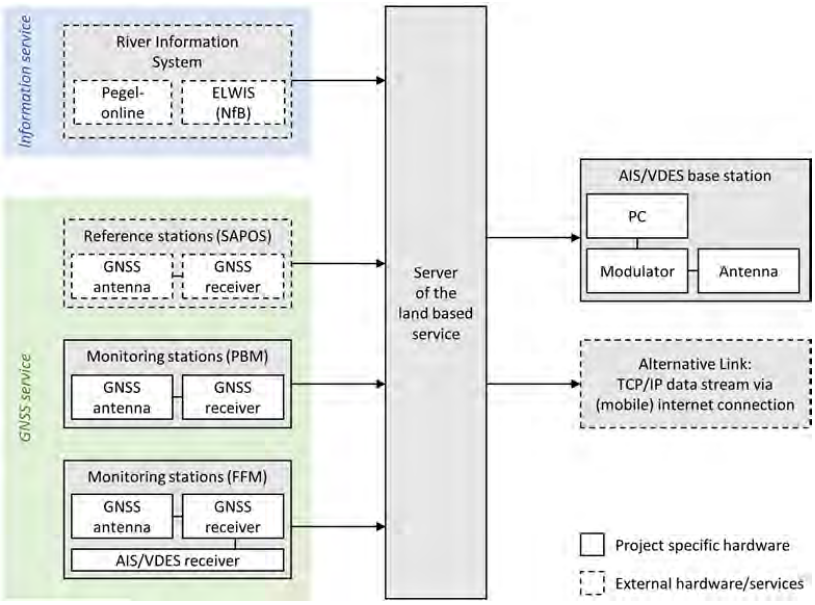

Figure 2: Design of the land-based service

The use of GNSS signals and appropriate measuring techniques for precise positioning are well-established in geodesy. For this purpose the real-time kinematic (RTK) technique will be applied to achieve cm-level position accuracies based on carrier phase GNSS observations and on the corresponding correction data.

Therefore, a network of permanent GNSS reference stations is needed to derive RTK correction data. This network should have an appropriate spatial distribution and the data should be accessible in a standardized way for the central processing server. A state-of-the-art network RTK data processing algorithm will derive the GNSS correction data for the vicinity of the current position of the vessel. As the project aims to support safety critical applications, these GNSS corrections will be checked for their integrity before they will be broadcasted (Pre-Broadcast Monitoring) to the vessel via a standardized communication channel, implemented along the inland waterways. The result of this integrity check will also be transmitted to the user in order to have a full quality assessment of the service and correction data at the vessel.

Additionally a verification of the calculated corrections will be conducted at some Far Field Monitoring stations, which will processed the received corrections. In addition these monitor stations may also provide performance indicators for quality controll of the system perfomance. The requirements of the land-based GNSS service are derived from the needs of the assistance functions:

- The accuracy of the calculated GNSS position on-board shall be below 10 cm for the horizontal and height component.
- The service shall detect erroneous satellite ephemeris/clock or correction data within a certain limit of time and transmit this integrity information to the vessel.
- The availability of the service shall follow the definition of IMO standards (IMO Res. A.953 (23). Furthermore the service has to ensure, that the integrity data transmitted to and via used communication system is error free (checksum).
- The broadcast GNSS correction data shall refer to the latest version of the ETRS89 coordinate reference system, as it is also used in the official German surveying and mapping administrations. Due to this, a homogeneous data basis can be established and the comparison to external surveying data like bridge shapes and harbour maps is ensured.

Besides the precise position the skipper is interested in up-to-date notices about the waterways, like temporarily closed sections, construction work at a bridge or water level information. In Germany this information is provided via web-based portals like ELWIS or PEGELONLINE. From these web services the information needed will be requested, checked for plausibility and broadcasted to the skipper as Application Specific Messages (ASM) via AIS/VDES. This broadcast will be issued in a regional specific manner, so that only relevant notices are transmitted to the on-board device.

3.2 Data transmission

As described above phase based GNSS corrections together with integrity information need to be broadcasted to on-board unit to fulfill the high accuracy requirements of the LAESSI driver assistance applications. Such data are based on carrier phase observations for GPS and GLONASS. The amount of data is expected in a range of about 7 kbit/s using an update rate of 1-2 seconds. In addition to the GNSS corrections waterways information data will be additionally broadcasted for providing up to date information of water levels and relevant notices to skippers (NTS) to the assistance functions.

The NTS data include information of present restrictions of the navigable water as well as information of current bridge clearance. The GNSS corrections as well as the waterway information will be broadcasted to dedicated areas.

To summarize the following requirements for the data transmission can be deviated:

- Data rate: > 9.6 kbit/s enabling an update rate of < 2 sec
- Coverage: complete coverage (partly overlapping) along inland waterways
- Standardization: international standardized communication is required to enable harmonized data transmission

AIS (Automatic Identification System) is already standardized in the maritime and inland waterway domain for the exchange of navigational data between ships, between ship and land and land to ship. For this purpose a number of countries have already installed land-based networks to enable data exchange. The German WSV has installed an AIS network which covers the coast as well as major inland waterways. In connection with a mandatory carriage requirement AIS is a viable candidate for the planned transmission of corrections and waterway information. Nevertheless, the existing AIS is limited within its data capacity. Especially the high demand on the update rate would cause a significant AIS data load. At present an AIS message type #17 is standardized for the transmission of code based GPS corrections. However, this message cannot be used for RTK messages. Within the LAESSI project VDES (VHF data exchange system) is considered for data transmission from land to ship accordingly. VDES provides additional terrestrial frequency channels within the same frequency band and therefore can provide higher data transmission capacity.

As an alternative GSM which is nowadays a standard for mobile data transmission. GSM would be a feasible candidate. However, GSM has not a full coverage along inland waterways and may not be usable under certain circumstances (e.g. when a large number of users is blocking the network). Thus the availability of this service may not fulfill the requirements. However GSM will be used within LAESSI as a backup to AIS (VDES).

The driver assistance applications were tested in selected areas at Moselle and Main Rivers. Inside these areas the existing AIS infrastructure has been modified to enable a simulation of the future VDES. For this purpose future available VDE frequency channels will be used by additional AIS base stations that cover the test bed areas. This system concept enables the use of standard AIS equipment at land and on-board using future frequency channels prevent from any adverse effects with the operational AIS system during the test periods. The use of AIS technique means limiting the data rate to 9600 Bit/s. It is planned that the new developed ASM will be used to support the current development of such messages aligned to the ongoing international standardization process of VDES.

Due to the limited coverage along waterways and the general availability GSM mobile communication was only used as a backup to AIS (VDES) within LAESSI. The concept of VDES comprises the functions of the existing AIS, an additional communication link for the exchange of ASM and an additional communication link enabling higher capacity of VHF digital data exchange (VDE).

4. SHIPBORNE INTEGRITY MONITORING

4.1 Carrier phase processing

Usually code-based techniques (like IALA Beacon DGNSS) are used for inland waterway navigation and achieve accuracies of few meters or less. However, the described assistance functions indicate significantly higher requirements. As a consequence a transition of code observations to the more accurate phase observations (by a factor of 100) is necessary. The challenge by using carrier phase observations is to solve the unknown number of waves phase cycles, the ambiguities. If the ambiguities can be estimated as float values, a dm-accuracy of the position can be achieved. If the carrier phase ambiguities are fixed to integer numbers, cm accuracy is reachable.

Several influences like signal interruptions, multipath, cycle slips and measurement noise affect the ambiguities resolution of the carrier phase and consequently the determination of positioning and velocity information. These special station dependence effects cannot reduce by the land based correction data. Furthermore the atmospheric effects caused by ionosphere and troposphere effects can impact the positioning solution, depending on distance between land based station and the remote station on the vessel. Nevertheless, to provide high accurate (less than 10 cm in horizontal and vertical position) and reliable PNT data a tightly-coupling of the GNSS observations (phase and code) with other sensors like inertial measurement unit (IMU), rate of turn etc. processed by an Extended Kalman Filter (EKF) is required. This combination has the advantage that on the one side short GNSS outages due to obstacles like bridges and buildings near the ship path can be bridged. On the other side more sensor data and the combination of all sensors outputs enable integrity information of higher quality. The described functions are integrated in the on-board PNT unit that was developed by DLR (Fig. 3).

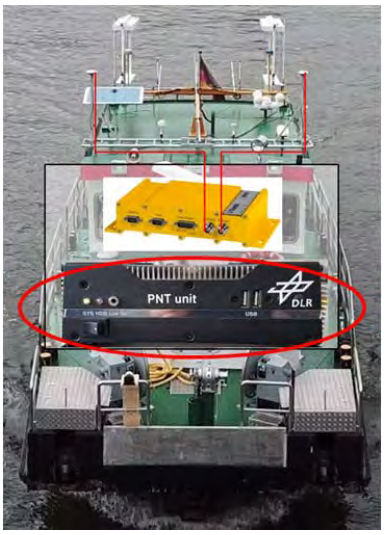

Figure 3: PNT on-board unit developed by DLR

4.2 3-stage integrity concept

Fig. 4 explains the integrity concept on ship-side that consists of three components. At first the parameters from the EKF-based RTK processing were analyzed. This includes a validation of the fixed ambiguities and the variances from the adjustment algorithms. In the next step similar output data like length of the antenna baseline, velocity, heading and height difference from different sensors or procedures will be compared. Furthermore the integrity information from the land based service is used to evaluate the position accuracy on the ship. All individual parameters have specified thresholds based on the assistance function requirements. If all parameters are below their thresholds, the integrity for this event will be assessed positively and the PNT data can be considered as reliable.

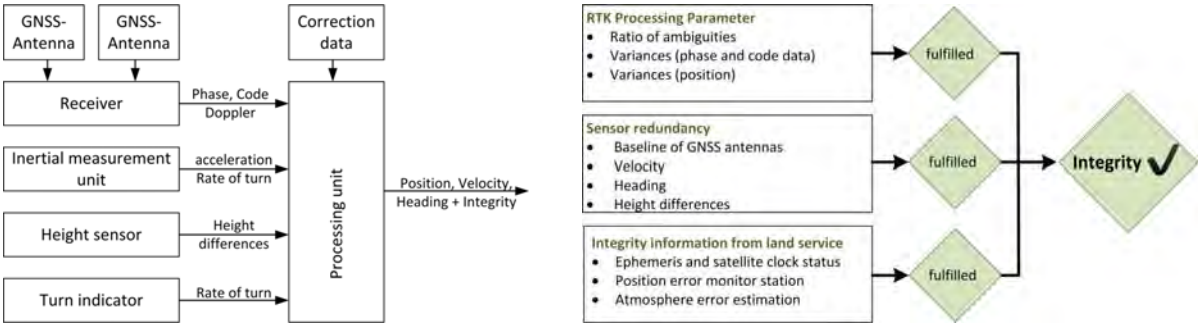

Figure 4: **On board processing with RTK algorithm and additional sensors (left), 3-stage integrity concept (right)**

5. PERFORMED TEST AND RESULTS

As described in the previous sections four main areas of development were conducted within the LAESSI project:

- New driver assistance functionalities,
- An on-board PNT unit which provides the required accuracy and integrity for 3D position and heading,
- Soft- and Hardware to provide integrity monitored GNSS corrections (RTK) and waterways information and
- a communication channel for transmitting high data rate GNSS corrections and waterway information via modified AIS base stations.

For testing and validation of the system concept two test areas were implemented. One test bed was installed in Koblenz along the Moselle River for first tests of system components and a second one at the Main River in the area of Würzburg for system integration and investigations over a longer part of the waterway, including several locks and bridges. Further tests were performed using a commercial 180 m long inland vessel (El Niño) which cruises between Rotterdam in the Netherlands and Linz in Austria. These tests should provide information how the system works on a regular trip and gain responds from the skipper about the daily use of the system.

5.1 Performed test

First tests regarding the performance of various sensors, data transmissions and communication were performed in the Koblenz test bed. The project team could validate that the several system components has shown the expected performance. In a second step full system integration were accomplished at the Main test bed using a larger measurement campaign on the MV Naab in October 2017. hese measurements have included performance tests of the new communication system based on modified AIS base stations. The results will be explained in the following sub sectors. During this test campaign a lot of other aspects were analyzed. They will be published in separate papers.

5.2 Test of communication equipment

Beside a lot of other measurements (e.g. analysis of the possibility to solve for high position accuracy and heading information) the test campaign enabled the test of the modified AIS transmissions on co-located frequency channels which will be usable with the currently developed VDES standard. As shown in Figure five AIS land stations were equipped with this additional functionality.

This configuration enabled availability tests of overlapping modified AIS base stations along a roughly 100 km river stretch. Fig. 6 shows a measurement of the signal propagation in the test area and indicates the good overlapping of the AIS and the “simulated VDES system”. Between Erlabrunn (Main River km 240) and Steinbach (Main River km 200) two AIS base stations were not installed. The coverage gap was accepted in order to test the switch over to a GSM communication as a backup and to identify the usage of this commercial communication system.

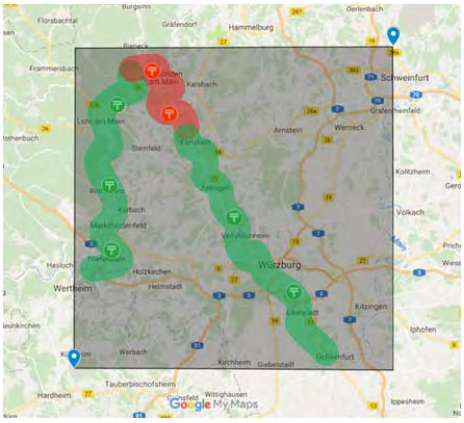

Figure 5: Test bed Main River with additional AIS land-based transmitting on new VDES frequency channels (green) and area for GSM connection (red); Dark grey, reginonal area for frequency channels 2025 and 2026

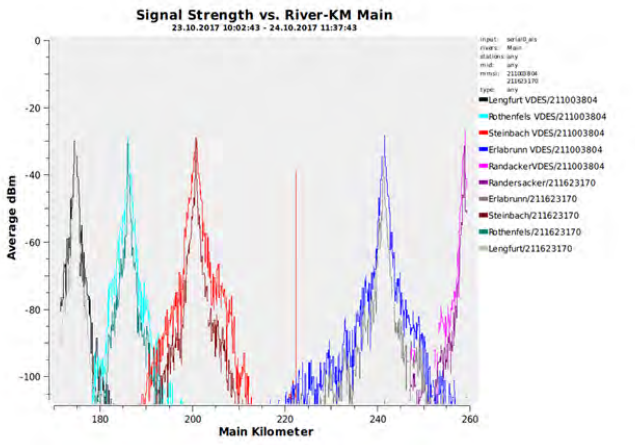

Figure 6: Coverage measurements for AIS and VDES frequencies along Main River, MV Naab 10/2017

A first analysis of the data received shows the difficulty to provide the data capacity, which is needed for a valid RTK fix. As shown in Fig. 7 a RTK fix solution was possible in most parts of the test bed (with exception of the north east part, which was not equipped with AIS). Nevertheless the data age was too high in many parts along the Main River test area. This is caused by the limited data capacity of the AIS channel. It should be noted that for the test period only transmissions on one of the two available AIS channels were used. With a combination of both channels a better result can be expected.

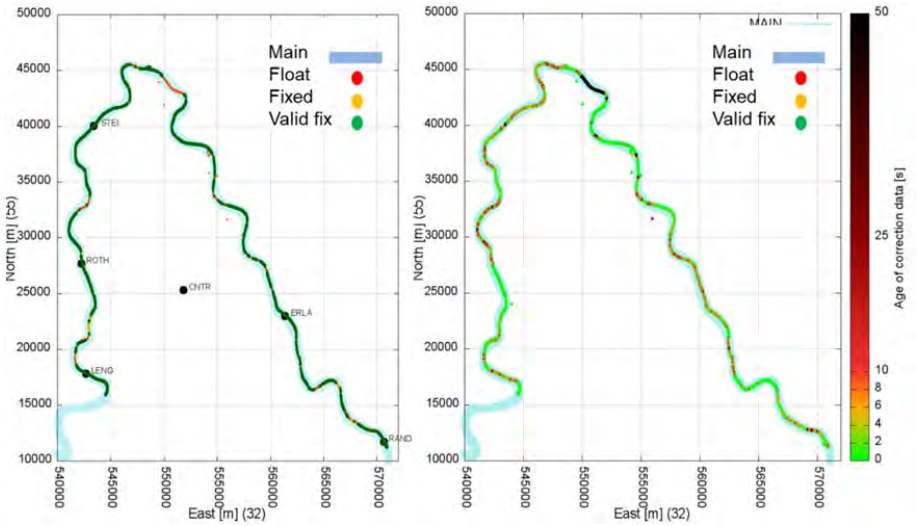

Figure 7: data analysis (fix solution and data age) for AIS and GSM at Main test bed, MV Naab 10/2017

		Valid KD	Float	Fixed	Fixed+ (4 s)	Fixed+ (2 s)
296 Day	Via GSM	92,5	14,1	83,8	79,7	79,3
	Via AIS	77,7	28,2	71,6	60,3	53,5
296 Night	Via GSM	100,0	3,7	96,3	95,9	95,9
	Via AIS	99,8	2.2	97,8	96,8	96,5
297 Night	Via GSM	100,0	0,1	99,9	99,8	99,8
	Via AIS	100,0	1,9	98,1	97,0	97,0
297 Day	Via GSM	92,9	10,8	86,5	82,3	81,9
	Via AIS	70,1	22,5	77,4	55,3	46,2

Figure 8: Availability analysis for various types of RTK fix for modified AIS and GSM, MV Naab, 10/2017

Fig. 8 provides a detailed overview about the availability of the tested communication options along the test area. As expected the availability of the modified AIS transmissions was only in a range of 80% due to transmissions only on one AIS channel with limited data capacity in contrast to GSM or the future VDES. However, the test indicates a need for more investigations in the methods how the data should be packed and coded before they will be transmitted. Both will be possible when real VDES technology with a much higher data rate becomes available.

5.3 Further achievements

As mentioned a lot of other activities, measurements, results and achievements were conducted within LAESSI. The following part will summarize some of the main results of the project. The main goal of the project was to develop and test first driver assistance functionalities for bridge warning, automatic track control, berthing and conning. All this functionalities could be successfully implemented and tested from innovative navigation GmbH. Fig. 9 provides examples with regard to the bridge warning and berthing assistant display. The distances indicated in the berthing display are calculated with regard to Inland ECDIS contours of quay walls etc. Fig. 10 shows track control and guidance information integrated in the radar display and the display concept with two monitors used for providing assistance information. As a basic element to provide reliable and integrity checked position, navigation and time data as input to the new applications, the German Space Agency (DLR) could implement and test a prototype PNT (Position, Navigation and Timing) data processer unit.

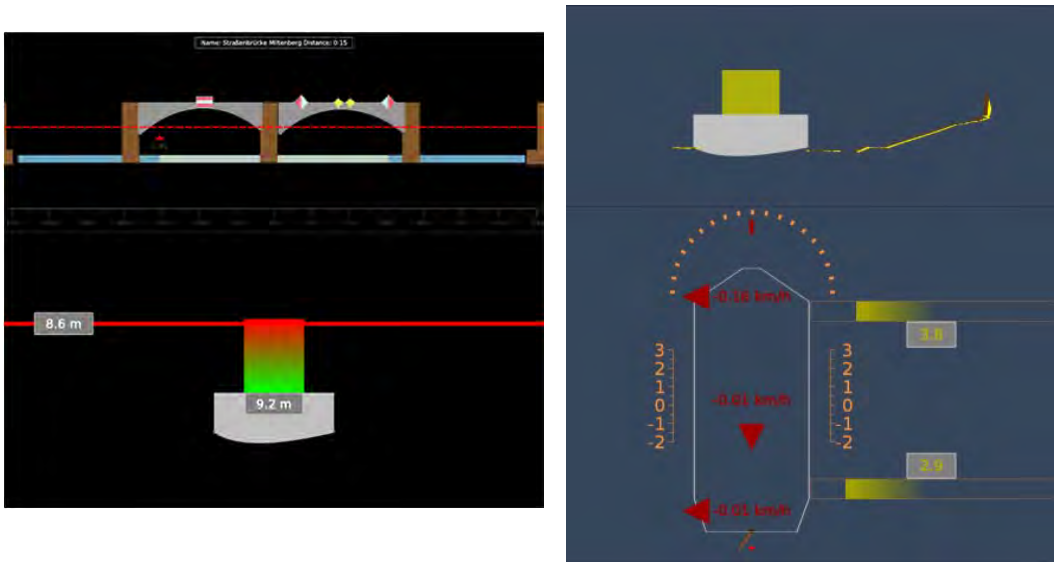

Figure 9: Examples of displays, left picture shows bridge height warning information, right picture shows berthing assitant with laser scanner results and distances to structures

Alberding GmbH has developed and tested new land-based services. Various software modules to provide the RTK corrections and the waterways information to the AIS land-based infrastructure were developed. The WSV was responsible for providing the communication channels for the test areas. Within the project a first VDES simulation could be performed and tested using AIS transmissions on new frequency channels. The results will support the ongoing standardisation process of VDES, e.g. AIS/VDES transmissions on co-located frequency channels.

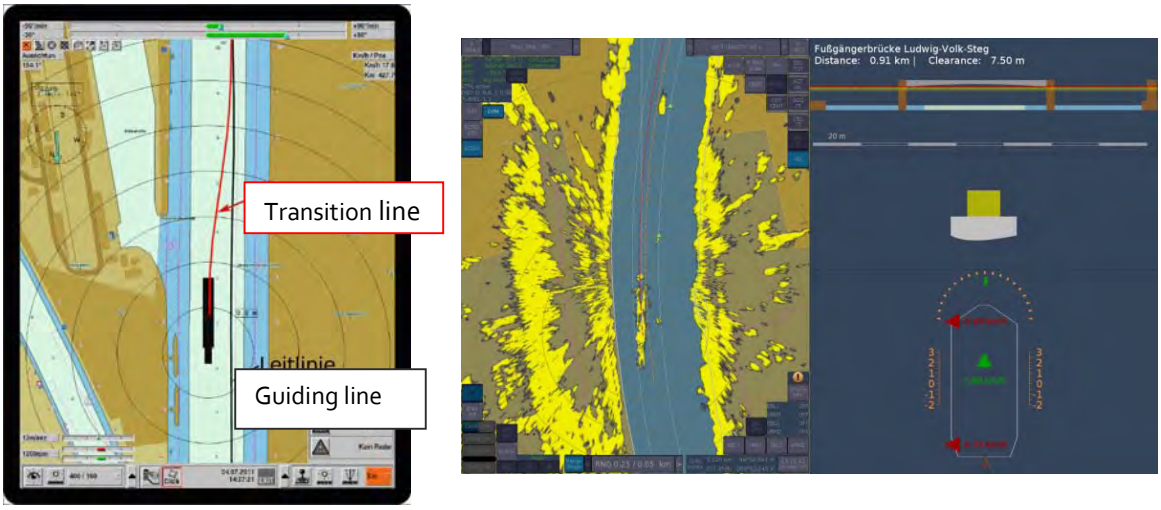

Figure 10: Automatic tracking and guidance system (reference: ISR, Stuttgart University), display concept

6. CONCLUSIONS AND OUTLOOK

The results gained in the LAESSI project are a first step into a driver assistance supported shipping of inland vessels. The tested functions, e.g. the bridge collision warning system can contribute to the safety of navigation on inland waterways. The first reactions by skippers according to functions and display of assistance data were very positive. The developments in LAESSI will provide basics for autonomous shipping in future. Relevant results could also be achieved which help to amend international standardization of river information services and systems, communication standards and data protocols.

The members of the LAESSI project team consider to further develop the system technology towards new on-board applications (e.g. enabling autonomous navigation of inland ships into a lock), to improve the provision of GNSS corrections (e.g. using new PPP methods), the performance of on-board PNT and the communication system (e.g. VDES). A follow-up research project is planned and may start in mid-2018.

References

Bober S (2015). AIS next generation – the development of the VHF Data Exchange System (VDES) for maritime and inland navigation, PIANC SMART Rivers 2015, Buenos Aires

Sandler M, Heßelbarth A, Ziebold R, Alberding J, Uhlemann M, Hoppe M, Bröschel M (2016). Setting up driver assistance functions for inland vessels based on high precision and integrity checked positioning information, MTE-ISIS Conference, Hamburg.

Sandler M, Heßelbarth A, Alberding J, Hoppe M (2018), LAESSI – final project presentation (has not yet been published), Würzburg

Strenge, R (2015). AIS land infrastructure on German Inland Waterways, PIANC SMART Rivers 2015, Buenos Aires

METHODS TO ASSESS BUBBLE SCREENS APPLIED TO MITIGATE SALT INTRUSION THROUGH LOCKS

by

Pepijn P.D. van der Ven[1,2], Tom S.D. O'Mahoney[1] and Otto M. Weiler[1]

ABSTRACT

Salt intrudes into the freshwater system via shipping locks located at the sea every time these open the lock gate. With increasing lock size and increasing shipping traffic intensity, this issue requires attention. The application of bubble screens along the lock's entrance is one of the available mitigating measures. The effect of such a screen is often expressed as a factor reducing the speed of the lock exchange process: the so-called salt transmission factor, which may reach 0.25, depending on the bubble screen design and operation. The effect on the salt intrusion during successive lockages may be enhanced further when the duration of the doors being open is minimized. This paper presents various methods to determine the effect of bubble screens on salt intrusion, a discussion on the assessment of its design with scale model tests or numerical computations as well as the effect of the salt intrusion on the inland water system.

1. INTRODUCTION

Salt intrusion and mitigating measures have been studied extensively in recent years. Shipping locks are a clear example of a location where salt intrusion via surface water would occur if not properly mitigated. The importance of mitigation is related to the required quality of the fresh water, for ecological reasons or due to its use for agriculture and/or drinking water.

Recent shipping traffic developments contribute negatively to salt intrusion unless proper mitigating measures are taken. Increasing shipping intensity demands more frequent lockages, with every lockage adding to the amount of salt intrusion through the lock. Furthermore, the enormous size of modern locks means they contain a large amount of salt water that potentially flows towards the inland water bodies. Sea level rise as a result of climate change also leads to higher water levels at sea locks and increasing salt intrusion. Similarly an increasing strain on freshwater resources requires that more attention is given to issues concerning water quality. This can also lead to less water being available for some mitigation measures, such as flushing of water through locks and sluices.

The research on salt intrusion through shipping locks has led to computational methods to model the exchange of water in the vicinity of the lock and the (ongoing) development of the coupling with regional models.

Furthermore, the studies have increased the knowledge of various salt intrusion mitigating measures – in particular the bubble screen, being the specific topic of this paper. Bubble screens are applied at shipping locks between salt and fresh water bodies, in order to decrease the rate of salt intrusion as a result of the locking process. Various measurements have been performed in the past decades to address the effectiveness of bubble screens in shipping locks. The potential of bubble screens is currently given a renewed assessment due to the developments mentioned above.

[1] Deltares, The Netherlands
[2] Corresponding author, pepijn.vanderven@deltares.nl

Other mitigating measures include the application of freshwater flushing discharge through the lock (Weiler et al., 2015) or selective withdrawal using a hydraulic structure (Boschetti et al., 2017). Changes in operation (e.g. keeping the lock gates closed as much as possible) may also reduce salt intrusion, as will be explained in this paper.

Compared to the application of a freshwater flushing, bubble screens are more expensive as the required air flow rate and pressure demand a significant compressor size. An important question therefore is to optimize the design or use of the bubble screen such that the required salt intrusion reduction is met at a minimum use of energy. The question how the bubble screen technology scales up towards the larger depths of modern locks should also be explored. Recent work, presented in this paper, has focused on the application of various research methods to contribute to these questions.

2. GENERAL CONSIDERATIONS OF THE LOCK EXCHANGE

2.1 Driving parameters of lock exchange

The salt intrusion through a lock during a day of lockages is determined by the number of lockages and the salt intrusion for each of these lockages. More shipping traffic leads, in general, to more lockages which leads to more salt intrusion. The number of lockages depends on the traffic passing the lock, which has a highly stochastic nature, and on how the lockkeeper handles this traffic. The lock operator decides, for example, how many ships are dealt with in one lockage.

The amount of salt intrusion per lockage depends on the salinity difference between the lock chamber and the approach harbour, as well as the water level and depth, the lock size and the duration of the gates being open.

Two types of processes contribute to salt intrusion through locks. The first one is the salt carried inland by the lockage prism, applicable in cases where the water level at the salt water side is higher than that at the freshwater side. The volume of the lockage prism is equal to the product of length and width of the lock chamber and the difference in water level. In delta areas, where salt and fresh water meet, the latter is usually relatively small.

The second contribution is related to the process of lock exchange: the exchange flow between the lock chamber and the approach harbour (at either side, one after the other) due to the difference in density of the salt and fresh water. Given sufficient time, this process will result in (almost) the entire volume of the lock chamber exchanging between both sides of the lock. Equal volumes of water will be exchanged in both directions, but due to the difference in salinity, a quantity of salt will move inland which is related to the volume of the lock, not the lockage prism. As the lock volume is usually much larger than the locking prism, lock exchange is often the dominant factor contributing to salt intrusion.

The evolution of a density current in a lock exchange in time (see Figure 1), for saltwater called the salt wedge, is well studied (Shin et al., 2004). The salt wedge initially extends over approximately half the depth H and has an initial velocity c_i which is related to the depth and the density difference as given in (1).

$$c_i = \frac{1}{2}\sqrt{g\frac{\Delta\rho}{\rho}H} \qquad (1)$$

In which

g gravitational constant, 9.81 [m/s^2]
ρ, $\Delta\rho$ density, density difference between lock chamber and approach harbour [kg/m^3]
H water depth [m]

It is clear from this formula that the amount of salt water which enters the inland waterway when the lock gate is opened increases when the density differences increases and when the water depth increases. Here an open, unhindered lock exchange is considered with unlimited water bodies on both sides.

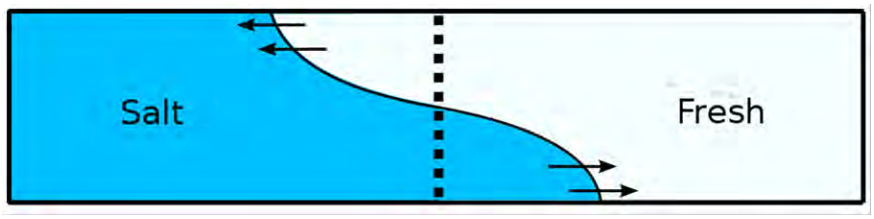

Figure 1: Schematic illustration of a lock exchange

When aiming to describe the process of lock exchange in practice, accounting for the finite volume of the lock and the operation of the lock gates, the formulation as proposed by Van den Burgh and De Vos (1962) and Vrijburcht et al. (2000) is most convenient. In this formula the relative lock exchange is given by (2).

$$U = \tanh\left(\frac{T_{\text{open}}}{T_{\text{LE}}}\right) \qquad (2)$$

In which

U	relative lock exchange, i.e. the exchanged volume as a ratio of the volume of the lock [-]
T_{open}	the duration of the doors being open [s]
T_{LE}	the 'theoretical' duration for a total lock exchange [s]

The theoretical duration for a total lock exchange, T_{LE} , is the time needed for the salt wedge (or the fresh wedge, depending on the lock head) to travel into the lock and back to the open door after reflecting at the closed end, assuming the initial velocity c_i as constant. This period is given by the following formula.

$$T_{\text{LE}} = \frac{2L}{c_i} = \frac{2L}{\frac{1}{2}\sqrt{g\frac{\Delta\rho}{\rho}H}} \qquad (3)$$

In which

L	length of lock chamber [m]
c_i	the initial velocity [m/s]

In many locks between salt and fresh water the value of T_{LE} is in the range of typical gate open times, leading to values of $T_{\text{open}}/T_{\text{LE}}$ in the range of 0.5 to 2.0.

2.2 Effect of bubble screens in the relative lock exchange

The effect of a bubble screen is that it hinders the process of lock exchange, reducing the mass flow rate of salt associated with it. The effect is quantified in the salt transmission ratio, η. The value of η that is achieved by a bubble screen is determined by the air flow rate, the depth of water in the lock head and the density difference between lock chamber and approach harbour. The factor has been determined for various mitigating measures in in-situ measurements (see Paragraph 4.1). Sometimes reference is made to a reduction factor but this is simply 1-η.

The theory behind this goes back to Abraham and Van den Burgh (1962). This salt transmission ratio reduces the exchange of water through the lock head and increases the time required for the (complete) exchange of the water in the lock, T_{LE}, with a factor 1/η.

Introducing this salt transmission ratio into (2) changes to the following equation.

$$U = \tanh\left(\frac{\eta\, T_{\text{open}}}{T_{\text{LE}}}\right) \qquad (4)$$

In which
η the salt transmission factor [-]

In this expression the meaning and value of T_{LE} remain unchanged; it does not include the effect of the bubble screen, but is based only on dimensions of the lock and the densities of water inside and outside of the lock.

The process in time related to this formulation is given in Figure 2, for two situations: one without a bubble screen, and one with a bubble screen with η = 0.4.

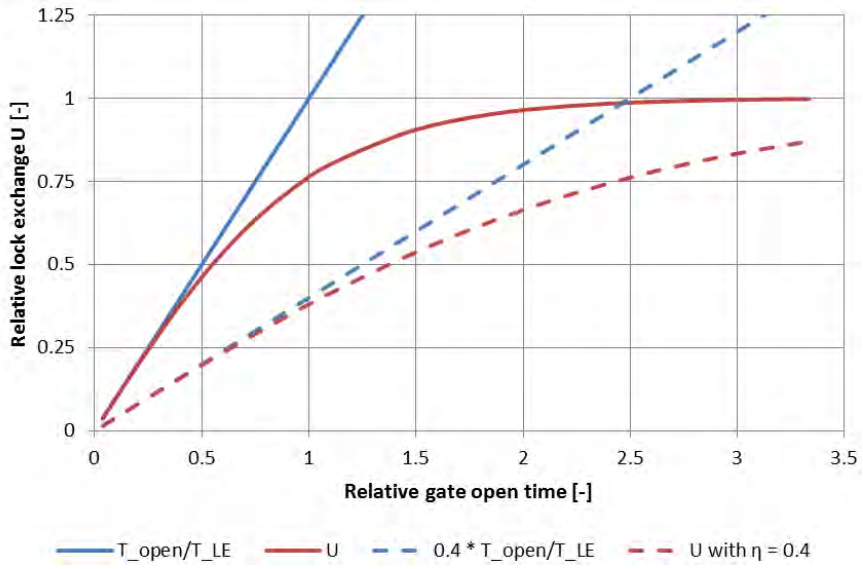

Figure 2: Relative lock exchange (*U*, red lines) as a function of the relative gate open time, showing an unprotected lock head (continuous lines) and a lock head with bubble screen (dotted lines)

Note that, in the case without bubble screen, when T_{open}/T_{LE} is 1, the lock exchange as described by (4) is about 76% complete. When applying a bubble screen with an η of 0.40 the lock has been exchanged at this time only 38%.

It is essential to understand, as is also shown in Figure 2, that the bubble screen reduces the speed of the lock exchange, but does not stop the process. This means that a bubble screen can only be effective when it goes hand-in-hand with restricting the time that the lock gates are open.

2.3 Application of bubble screens at both lock heads: effect on salt intrusion

The effect of a bubble screen becomes much stronger when it is applied at both lock heads. After a partial lock exchange with one of the approach harbours, the lock turns towards the other approach harbour, but due to the partial lock exchange over one lock head the density difference over the other lock head is smaller, reducing the speed of the lock exchange. Disregarding the effect of a difference in water level over the lock, the salinity and density in the lock chamber will vary around the mean of the values in both approach harbours after a number of cycles.

This variation of the salinity inside the lock chamber (i.e. maximum – minimum value of salinity) will be smaller than the difference in salinity at both sides of the lock and this ratio is a direct measure for the amount of salt transported through the lock per complete lock cycle (including both an upward and a downward lockage). This defines the parameter *Z*, the relative salt transport, being the ratio between the variation of salinity inside the lock and the difference in salinity at both sides outside the lock, see (5). It is an equilibrium value, reached after a (large) number of lock cycles with equal gate open times at both lock heads, in absence of a level difference over the lock.

$$Z = \frac{\Delta S_{\text{variation inside the lock}}}{\Delta S_{\text{conditions outside the lock}}} \qquad (5)$$

In which
ΔS difference in salinity (see text) [kg/m^3]

Knowing *Z* makes it easy to calculate the transport of salt through a lock, using (6).

$$\dot{M} = N \cdot Z \cdot \Delta S_{\text{conditions outside the lock}} \cdot V_{\text{lock}} \qquad (6)$$

In which
$\dot{M}$ the mass flux of salt per unit of time [kg/s]
N the number of complete lock cycles (up and down) per unit of time [1/s]
V_{lock} the volume of the lock chamber [m^3]

The value of *Z* has been calculated for a range of values and is shown below. Just like *U* (the relative lock exchange) the value of *Z* (the relative salt transport), is highly sensitive to the gate open times, which, together with a bubble screen, are essential to limit the lock exchange each time the gates are open at one of the lock heads.

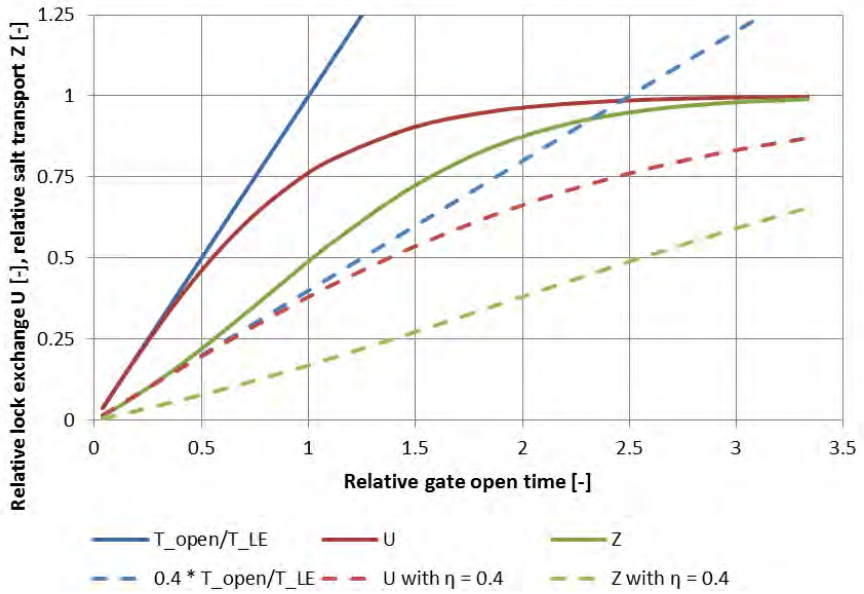

Figure 3: Relative lock exchange (*U*, red lines) and relative salt transport (*Z*, green lines) as a function of the relative gate open time, showing an unprotected lock head (continuous lines) and a lock head with bubble screen (dotted lines)

As shown in Figure 3, the application of bubble screens with a certain value of η in both lock heads reduces the salt intrusion when compared to the application in one lock head only (assuming complete lock exchange in the other, unprotected lock head). Note that this reduction is achieved by

a smaller variation of salinity in the lock chamber, which leads to smaller difference in density over each lock head, which in turn reduces the air flow needed to achieve the value of η. So a larger reduction of salt intrusion can be reached, with a smaller capacity of air compressors. This explains why, although these compressors have to run during a larger period of time (when either of the lock heads is open), it is generally favourable to apply bubble screens at both lock heads.

3. DETAILED SIMULATIONS OF LOCKING CYCLE AND SALT DISPERSION

3.1 Simulating the locking process

As the graphs and formulae in Section 2 show, the lock operation is a very important factor in the amount of salt intrusion and it implies that the lockkeeper is not only facilitating navigation, but is also controlling salt intrusion. Achieving a restriction in the time that the lock gates are open for ships can be difficult because the lock keeper has to balance these completely different interests. In some cases a large gate open time may be demanded for the safety of the operation, for instance when a large vessel approaches a sea lock, it may want to see the gate open in order to be sure that the manoeuvre does not have to be interrupted.

Furthermore, the lock utilization is highly variable, with variations in occupancy during the day or the night, with the tide at the sea-side, with variations over days of the week and over the seasons of the year. The vessel traffic may be asymmetrical, with one direction being dominant during part of the day or week, and the other direction at other times.

For the calculation of the salt intrusion in such varying conditions, and for varying applications of mitigating measures, the lockage process has been implemented in the computational program WANDA-Locks, which is embedded in WANDA, a one-dimensional program originally developed for complex systems of pipeline flow (see reference website), allowing a generic and explicit modelling method. The program has been validated using measurements at the Stevin Locks (De Groot, 2015) and the Krammer Locks (Weiler et al., 2015).

WANDA-Locks uses formulae for salt intrusion based on Uittenbogaard (2010) , including the impact of mitigating measures such as bubble and water screens by the salt transmission factor η that was introduced in Paragraph 2.2. The salt transport resulting from the levelling flow is taken into account by setting the hydraulic components (e.g. valves) according to locking procedures and having these being triggered by the actual water level in the lock. This ensures a realistic modelling of the locking process, going through the lockage cycle step by step.

The procedure explicitly incorporates the considerations of the lockkeeper and allows the inclusion of the stochastic nature of traffic demand. The model can be fed by either registrations of lock operation, or by a simulated operation, generated by vessel traffic models such as SIVAK (De Gans, 2010). Details of this schematization are given in Van der Ven et al. (2015).

3.2 Far-field modelling

The most critical salinity value is generally situated somewhere upstream, at the location of an intake of fresh water for agriculture, industry or drinking water. This is where salinity has to be kept below a certain criterion value. Between the navigation lock, ‘producing’ the salt, and the freshwater intake various processes play a role, leading to a different (lower) salinity at the intake than close to the lock. These processes can include density flows in the freshwater system, vertical mixing due to shipping traffic and the discharge of water from upstream towards the lock.

These ‘far field’ processes need to be considered using suitable hydrodynamic models in order to establish the difference between the salinity at the intake and at the lock and how this varies with several conditions, especially with the discharge. Examples of such models are Delft-3D or SOBEK

(both developed by Deltares). These models should include the salt intrusion through locks and sluices (as well as outflow through these points) as boundary conditions. It must be emphasized that the coupling is two-way, as described in Paragraph 2.3: the actual salinity at both sides of the lock determines the salt intrusion through the lock. Therefore, a so-called online coupling or an iterative computation procedure should be applied.

A suitable set of formulae to include salt intrusion through locks in far-field models in an online manner is not yet available. In view of computational time it preferably does not require a very detailed simulation of the locking process occurring at these locks. The formulae outlined in the previous section should form the basis for this coupling and these are planned to be implemented in the Deltares software.

4. DETERMINATION OF THE SALT TRANSMISSION RATIO η

The salt transmission factor η, which is used in the formulae and models discussed in Section 3, can be studied in scale model tests, with numerical computations or in situ. These methods will be discussed in the present section.

4.1 In situ measurements

In situ measurements can be used to determine the salt transmission factor η that applies to the lock exchange rate when a bubble screen is used. The salt transmission factor is defined as the ratio of salt intrusion with measures versus the salt intrusion for the lock without measures. The salt intrusion is the increase of the total mass of salt in the lock chamber during the exchange period. This period is assumed to be the same for the situation with and without measures.

Determining this transmission factor in situ comprises of measurements of the total mass of salt in the lock chamber before opening the door and after closing the door. To do so, conductivity measurement instruments are installed in the lock chamber, typically at 20-25 locations, measuring salinities along verticals distributed over the lock chamber. This grid of data points is used to calculate the total mass of salt. Abraham and Van den Burg (1962) present such measurements performed at the locks of Kornwerderzand and IJmuiden (both in The Netherlands), with depths ranging between 5 and 10 m.

Further in situ measurements can be found in Uittenbogaard et al. (2015a) and Keetels et al. (2011), who present the application an innovative combination of bubble and water screens at the Stevin Lock (The Netherlands). The dimensions of this shipping lock are 148 m length, 14 m width and 4.7 m depth. The tests consider an improved design of the bubble screen, using regulators to create a uniform distribution over the lock width and a specific placement of the bubble caps to create a dense bubble screen.

Conductivity meters were positioned in the approach harbours and at five verticals in the lock chamber, with five measurement points per vertical. The water levels, valve positions, opening and closure of the lock gates, the type of ship in the lock chamber and other parameters were recorded as well. The measurements were performed while the lock was in operation, i.e. with traffic through the lock.

Figure 4 presents a selection of the results of the tests, taken from Uittenbogaard et al. (2015b). Results from Abraham and Van den Burg (1973) have been included in the same figure (black dots). The salt transmission factor decreases with increasing air flow rate and varies with the design and the combination of mitigating measures. Previous tests show a typical transmission factor of 0.40, where the new design and operation of the bubble screen are shown to be able to reach values as low as 0.25±0.05 and even 0.15±0.05 when a fresh water screen is used additionally (see Keetels, 2011).

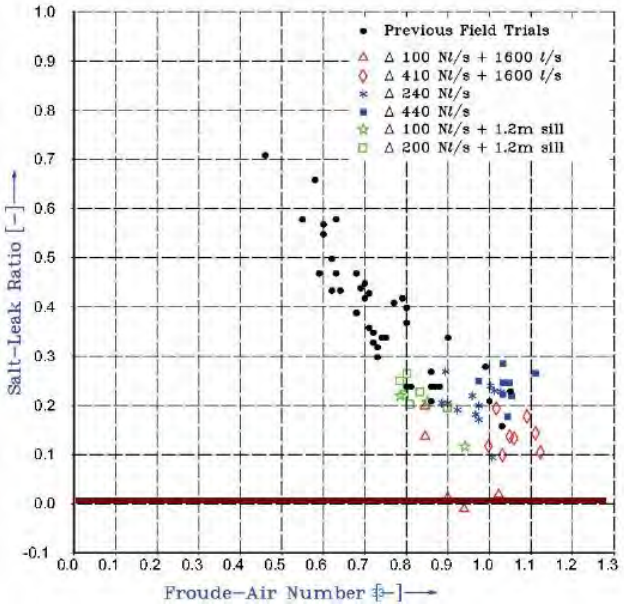

Figure 4: Results from in-situ measurements by Abraham and Van den Burgh (1973) and Uittenbogaard et al. (2015a) combined, showing the salt transmission factor η as a function of Froude air number (from Uittenbogaard, 2015b)

A similar design of bubble screen was tested subsequently at the Krammer recreational lock (The Netherlands) by Weiler et al. (2015), see Figure 5. The test set-up was similar to Uittenbogaard et al. (2015a), with an extensive grid of conductivity measurements in the lock and a detailed registration of lock operation. In contrast to the Stevin locks, the Krammer locks experience a tide of roughly 1.5 m amplitude (average condition). Furthermore, the Krammer makes use of a complex system of culverts to level the lock and to realize a flushing discharge, which were modelled using WANDA-Locks.

Tests included various bubble screen air flow rates and various combinations of mitigating measures: bubble screens, water screens and flushing discharge. The goal was not to find a single optimal setting of measures, but to assess the performance of several different settings. The availability of fresh water determines which setting to apply, e.g. using less flushing discharge in periods of a shortage of fresh water and compensating that with a higher bubble screen air flow rate. Lock operators were asked to perform measurements during night time, at strict 1 hour intervals, to facilitate the comparison of various settings of mitigating measures.

The measurements showed that the new system, using a bubble screen and flushing discharge, would sufficiently reduce salt intrusion. Furthermore, the measurement data was used to compare WANDA-Locks with and to identify required further developments of that model.

The pilot at the Krammer locks also evaluated the operational effects of a bubble screen: e.g. the ability for ships sailing into the lock to manoeuvre and to moor in the lock chamber. Furthermore, it focusses on the costs of conversion of the bigger commercial locks towards these innovative mitigation measures and the costs of operation of the bubble screens. These results have helped Rijkswaterstaat[3] in their decision to apply bubble screens at the commercial locks of the Krammer lock complex; this project is to be executed in the coming two years.

[3] Rijkswaterstaat is part of the Dutch Ministry of Infrastructure and the Environment and responsible for the design, construction, management and maintenance of the main infrastructure facilities in the Netherlands.

Figure 5: Bubble screen in the Krammer recreational lock (from Weiler et al., 2015)

The tests at the Krammer provided another determination of the bubble screen's salt transmission factor, i.e. the effect on the exchange rate during the lock exchange phase. Moreover, the tests provided a measurement of the effect of the application of bubble screens based on a standardized series of successive lockages.

4.2 Near-field scale model measurements

Paragraph 4.1 showed that a different design or operation of bubble screens can further reduce the transmission factors. This shows room for design and operation optimization: what would be the most efficient bubble screen? From the tests performed in the past it is assumed that an optimal bubble screen realizes (1) a uniform distribution of the air flow over the lock's width, (2) a uniform bubble size and thus uniform bubble rising velocity and (3) a dense bubble curtain without holes or openings. To determine design alternatives, it is obviously beneficial to be able to predict the performance of a bubble screen design before construction.

Scale model experiments provide a useful method for this assessment as, contrary to in-situ measurements, laboratory experiments allow good control of boundary conditions (e.g. water depth and salinity difference). Furthermore, scale model measurements can help to obtain a more detailed understanding of the physical processes of bubble screens as a salt intrusion mitigating measure, as laboratory tests generally allow more extensive measurements and visual inspections. These detailed observations are a required addition to theoretical studies, e.g. by Abraham et al. (1973), which provide excellent starting points.

Scale model research regarding bubble screens found in literature focus on several different topics, mostly on bubble screens in homogeneous water, e.g. to reduce wave penetration into port basins (e.g. Bulson, 1961). Scale model research on bubble screens to mitigate salt intrusion is rather scarce. This section presents a selection of such research.

Keetels et al (2011) have performed laboratory tests in preparation to the in-situ tests discussed in Paragraph 4.1. A flume approximately 0.30 m depth was used, consisting of a large compartment filled with salt water and a smaller compartment filled with fresh water. A gate in the flume separated the two compartments. The air injector, a perforated pipe of 1 cm diameter, was situated inside the saltwater reservoir near the gate. After the gate was opened, a gravity current started to enter the freshwater compartment while fresh water moved towards the saltwater compartment. Salinity was measured at two verticals, with 12 positions distributed per vertical. A lock-exchange experiment without any measures against salt intrusion was conducted for reference.

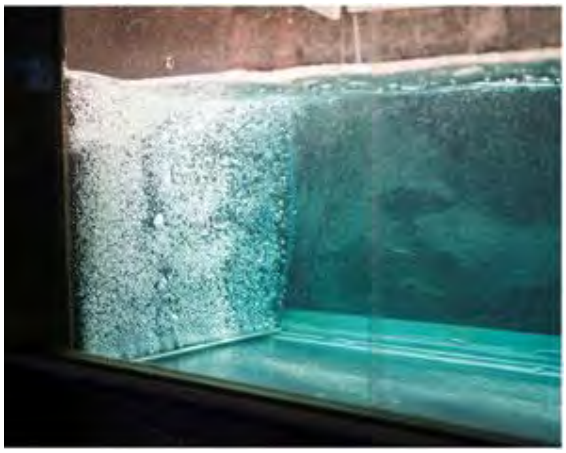

Figure 6: Closely packed air curtain in the laboratory (from Keetels et al., 2011)

Van der Ven and Wieleman (2017) present scale experiments of a bubble screen in a flume of 1 m depth and 1 m width. Their set-up is shown in Figure 7. The flow velocities were measured with electro-magnetic (EMS) instruments, which were installed to capture velocity components in the vertical as well as along the flume length. The instruments were moved in both the vertical and along the flume length to create a grid of measurement points. This measurement method could be used only since these experiments consider homogeneous water; the situation is assumed not to change in time. An important simplification is therefore that the performance of the bubble screen is evaluated only on the induced water motion.

Figure 7: Overview of scale model set-up by Van der Ven and Wieleman (2017): (a) bubble caps as built in the Krammer recreational lock; (b) caps used for the scale model of the bubble screen; (c) overview of the EMS instruments and bubble screen during a test condition

The results of Van der Ven and Wieleman (2017) show reasonable to good agreement with measurements done by Riess and Fanneløp (1998), who have considered a comparable small scale. Furthermore, the surface velocity shows good comparison to a full scale measurement performed by Bulson (1961). It is therefore concluded that the tests performed in this study are a reasonable representation of a real bubble screen. The accuracy of the measurements is a point of attention because of the limited accuracy of EMS instruments at the lowest flow velocities and the limited measurement duration per location. The measurements were performed in homogeneous water and

it is clear that, in order to assess the effect of a bubble screen as measure against salt intrusion, one should include the density difference in scale model tests.

Van der Ven and Oldenziel (2018) present recent scale model measurements that have been performed at Deltares. The goal of these experiments is to assess the difference in performance of varying bubble screen operation. As these differences may be subtle, measurements of high accuracy and at a high spatial resolution were required.

These tests too were at a small scale, having a flume of 2.40 m length, 0.50 m width and a water depth of 0.40 m. The set-up is shown in Figure 8. The flume was divided in two equal compartments by a metal sheet representing a lock door. One compartment was made saline and dyed blue, the other was kept fresh. As the door was lifted, a so-called lock exchange occurred, which was attenuated by the bubble screen. Air flow rate and bubble size were varied and tests were done with a density difference as well as in homogeneous fresh water.

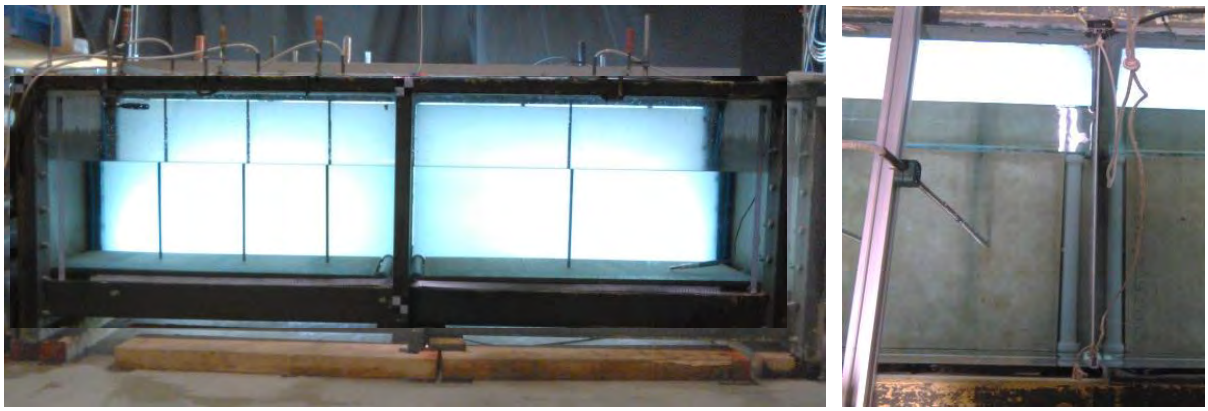

Figure 8: The setup used for the dye experiments; showing the tank of 2.40 m length, with four conductivity measurements rods clearly visible against the lit background (left) and the two bubble screen generators made from PVC-piles on either side of the separating sheet in the middle of the flume (right)

The experiments comprised two optical measurement techniques: (1) PIV measurements of the flow induced by the bubble screen (not shown here) and (2) the calibrated video-recording of the mixing induced by the screen and the exchange current by applying a dye to the salt water compartment.

The PIV measurements were performed in a separate tank with an identical geometry and for the homogeneous, fresh water cases only. The fields of view included the left hand side of the tank, including the bubble screen. An example of the velocity fields obtained in this way is given in Figure 9.

The dye recording was translated to a density map for every recorded time step. Three such maps are shown in Figure 10. The results provide insight in the several phenomena that occur: (a) the distribution of the entrained and mixed water over both compartments and (b) a density current on the flume floor due to a saline flow through the weaker lower part of the screen. Figure 11 shows the amount of dye within the left compartment, expressed as a percentage of the total mass of dye. This equals the salt fraction.

The two compartments can be interpreted as a lock chamber and an approach harbour. In Dutch reality, the approach harbour would not be confined, whereas the flume is obviously of limited dimension. This means that the sloshing seen in Figure 11 (black line) would not occur in reality and only the first approximately 20 seconds are representative. Note that the flume can however be seen to represent a sequence of locks chambers, e.g. the Panama locks.

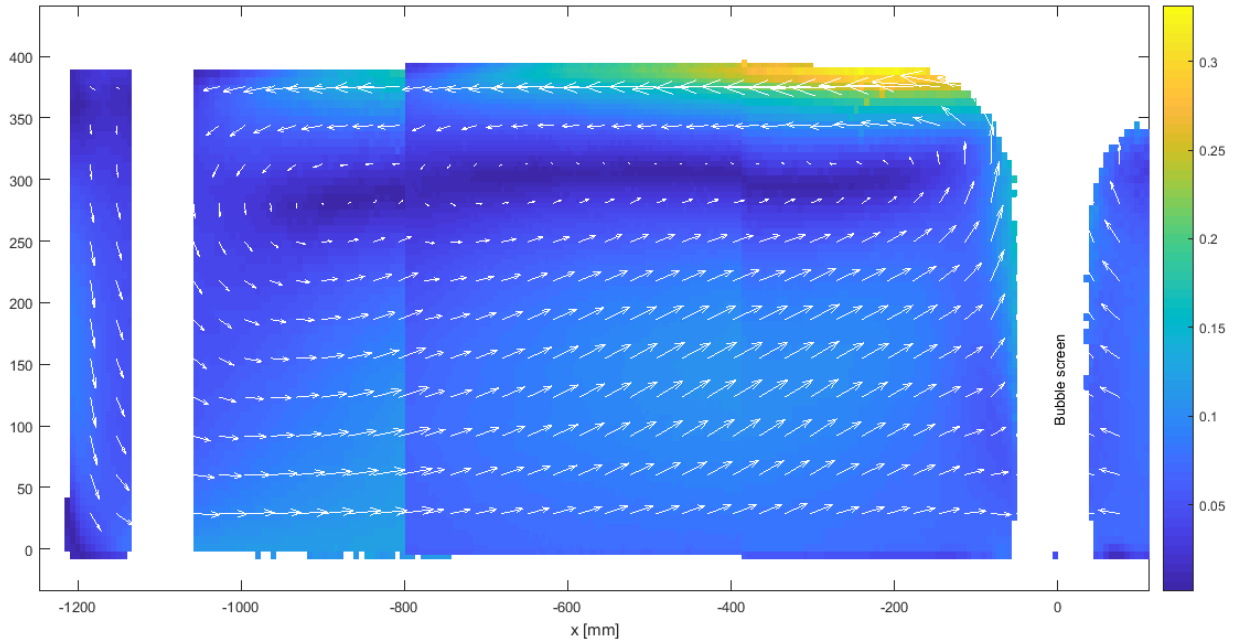

Figure 9: Induced flow velocities (colour shows magnitude) from a test in homogeneous water, on the left side of the bubble screen

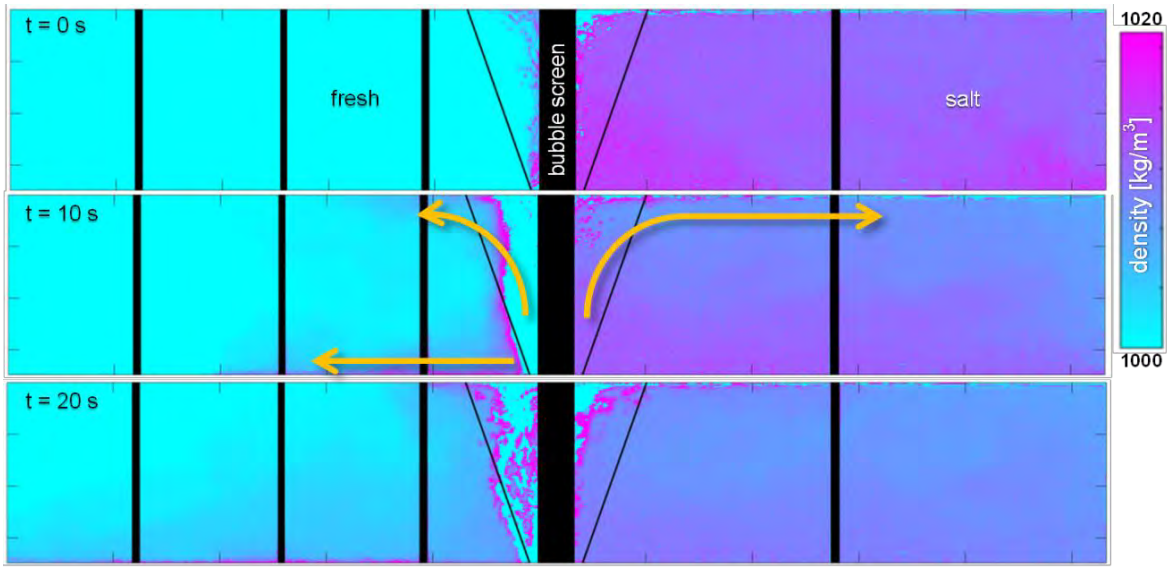

Figure 10: The exchange of fresh and saline water affected by the bubble screen, at various times after opening the lock door; from Van der Ven and Oldenziel (2018)

In Figure 11 the results of varying air flow rates (expressed in Froude air numbers, with $Fr_{air} \propto q_{air}^{1/3}$) are presented; multiple lines of the same colour denote repetitions of the same test. The situation without a bubble screen (black line) shows the sloshing of the unhindered internal wave. In the first 20 seconds, tests for Fr_{air} 0.80 and 0.95 show similar attenuation of the exchange flow. A higher air flow rate (Fr_{air} 1.1) increases mixing. This shows that increasing the air flow rate does not necessarily improve the performance of the bubble screen as mitigating measure.

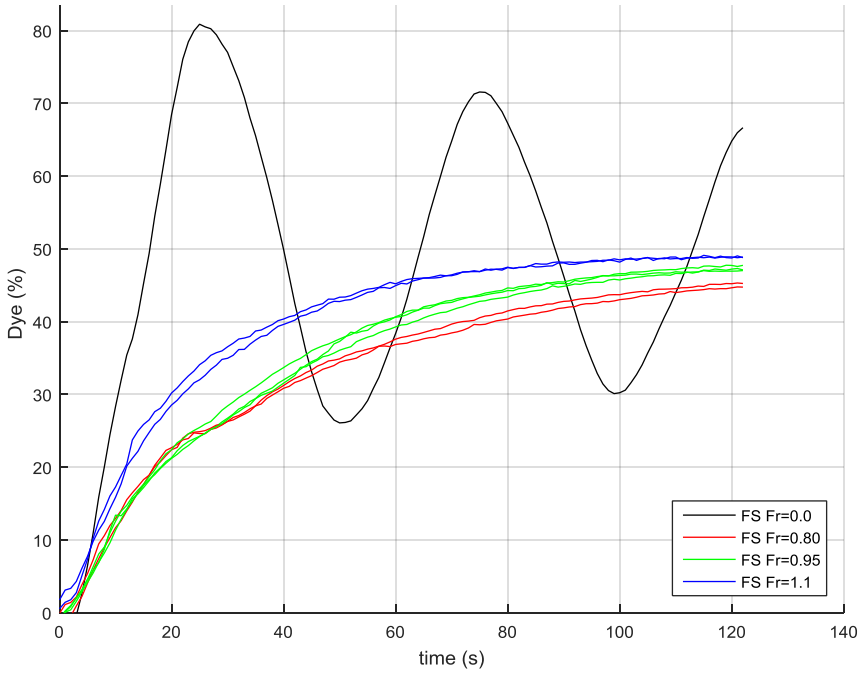

Figure 11: The salt mass in the left compartment of the tank, with varying air flow rate (Fr_{air} number), as a function of time (from Van der Ven and Oldenziel, 2018)

Van der Ven and Wieleman (2017) and Van der Ven and Oldenziel (2018) present scale experiments performed at a relatively small scale. To understand the scaling laws governing model tests on bubble screen performance, tests at larger scales may be necessary. Furthermore, future tests may comprise alternative bubble screen designs or further vary the applied air flow rate in order to show room for optimization.

4.3 Near-field numerical simulations

A third research method with great potential is the application of Computational Fluid Dynamics (CFD). An example is found in Meerkerk et al. (2015). In this research multiphase CFD models were applied to bubbly flows of different scales to judge their applicability. A successful validation was made for lab scale experiments of a bubble screen without density differences. The laboratory results were taken from literature, Wen and Torrest (1987). These experiments were made in a tank as illustrated in Figure 12, with dimensions L = 3.7 m, W = 1.2 m and D = 0.9 m. The bubble screen was made of a tube with holes, this was modelled in the CFD as a slit with D_{in} = 0.02 m. These dimensions are similar in order to the experiments performed at Deltares, described in the Paragraph 4.2.

The Computational Fluid Dynamics model uses a multiphase model in an Eulerian-Eulerian framework to describe the motion of both water and air (bubbles). In this framework the bubbles are not modelled explicitly but rather the domain is separated into control volumes (cells) in which the volume fraction of water and air in each cell is tracked. Momentum equations for both water and air are solved. These equations are coupled to each other with a multiphase interaction model. This includes the effects of buoyancy, entrainment, bubble lift and bubble drag. In this research the turbulence in the fluid is modelled using a Reynolds-Averaged Navier Stokes approach as this is the most applied and feasible for practical application. Other studies for bubble plumes have used an Eulerian-Lagrange framework (Fraga et al., 2016), where bubbles or parcels of bubbles are tracked as particles moving through (and coupled with) the water. Similarly turbulence has been modelled

with Large-Eddy Simulation (also Fraga et al., 2016). Both these approaches use far greater computational resources than those studied in Meerkerk et al. (2015) for bubble screens in locks.

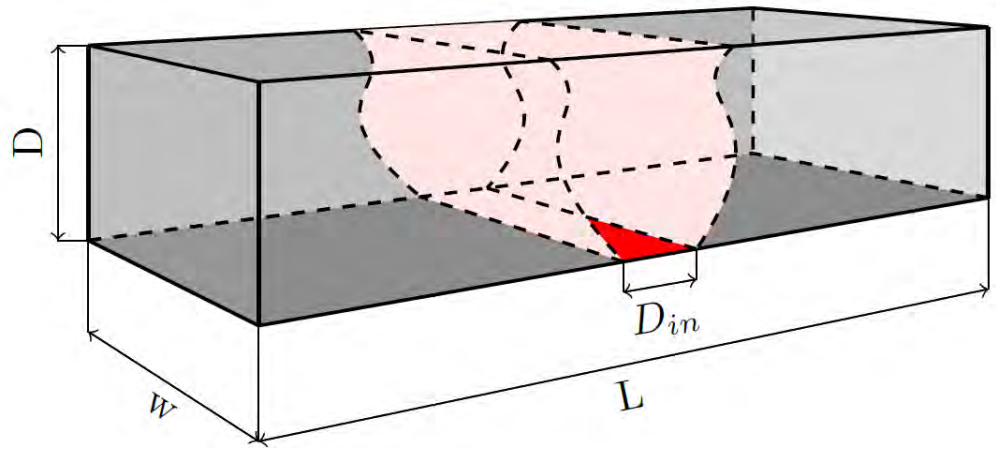

Figure 12: Illustration of the experimental tank used in Wen and Torrest (1987)

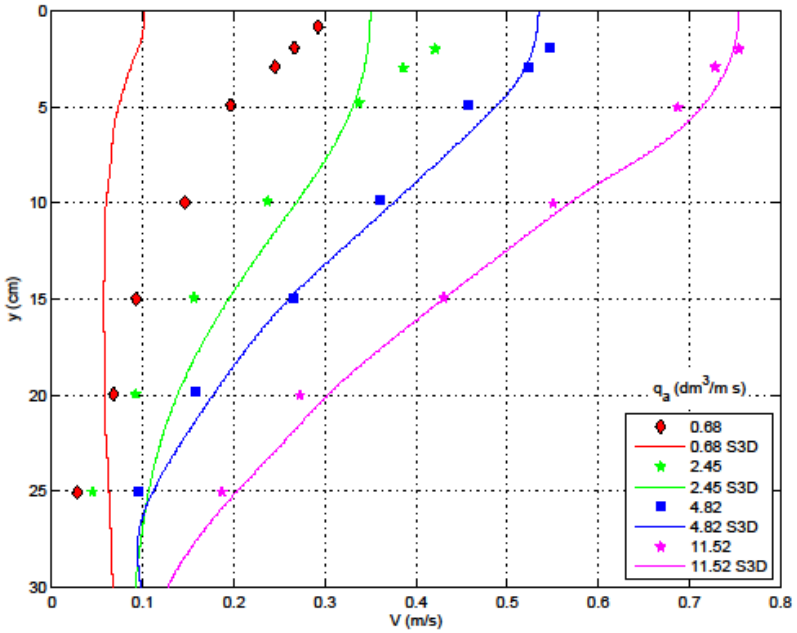

Figure 13: Results of the validation by Van Meerkerk et al. (2015)

The results of the validation in Meerkerk et al. (2015) are shown in Figure 13. For 4 different air flow rates the velocity profiles of the water in the top 30 cm of water (in a 90 cm water depth) are plotted at a distance 60 cm away from the axis of the bubble screen. These profiles are measured in the area away from the bubbles as the bubbles themselves often interfere with measuring equipment and the velocity profile at this offset location gives enough information about the water entrained in the bubble screen on its upward trajectory to assess the strength and effectiveness of the screen. CFD results can more easily give results at many locations in the domain but the validation has to be performed at the locations where measurements are available. The agreement in Figure 13 for the higher flow rates is good. For the lower flow rates the model performs badly.

Note that this model and validation is only for a bubble screen in freshwater and in steady state. The validation of a CFD model of a bubble screen as a barrier for salt intrusion has not as yet been attempted but the experiments at Deltares described in Paragraph 4.2 are the first data set with sufficient data to provide a validation set for CFD. Thus far only qualitative CFD simulations have been made where a bubble screen has been combined with a density flow from saltwater-freshwater interactions (see Figure 14).

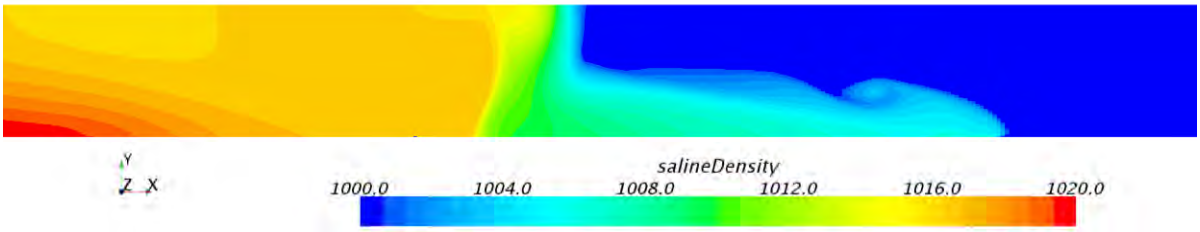

Figure 14: Result of a CFD computation of a bubble screen combined with a density flow

5. CONCLUSIONS

Salt intrusion through shipping locks is a concern at locations where restrictions on the salinity of inland waters apply due to ecological reasons or intake requirements for drinking water. This paper presents the main parameters affecting salt intrusion during the operation of sea locks, of which the number of lockages per day, the density difference over the lock and the dimensions of the lock are the most important. Based on this, it is easy to recognize the increasing relevance of research on salt intrusion given the global trends of increasing lock sizes and increasing traffic intensity.

Bubble screens are one of the possible measures to mitigate salt intrusion. This paper has focused on bubble screens but has also mentioned their performance when combined with a flushing discharge through the lock and/or water screens. Such combinations, and different bubble screen designs and operation have been tested in in-situ measurements that have been briefly presented here. These studies show that the salt transmission factor of bubble screens can reach as low as 0.25, which means that the lock exchange occurs four times as slow as it would in an unprotected lock. It is important to note that bubble screens reduce the speed of the process but cannot fully prevent lock exchange.

The performance of a bubble screen can be investigated a priori using scale model tests and/or numerical computations. This paper presents recent studies that evaluate and improve these methods, among which a scale model research that provides detailed data for the validation of numerical computations. These developments are currently ongoing.

When considering an intake point somewhere in a freshwater canal or lake, one should take into account not only the salt transmission factor η, but also the operation of the lock and the dispersion of the salt within the inland system. The effect of the bubble screen in terms of the reduction of salt intrusion resulting from successive lockages can be much greater than only a narrow consideration of the salt transmission ratio η. This paper presents a simplified method to compute the salt intrusion of successive lockages. The discussion given on the effect of door opening times is important as lock exchange will continue as long as the door is opened, albeit at a reduced rate when using bubble screens.

ACKNOWLEDGEMENTS

This paper presents studies commissioned by Rijkswaterstaat as well as research funded by the Dutch Ministry of Economic Affairs, through their TKI Deltatechnology program.

REFERENCES

Abraham, G. and Van den Burg, P. (1962), Reduction of salt water intrusion through locks by pneumatic barriers, Delft Hydraulics Laboratory, Publication no. 28

Abraham G, Van der Burgh P. and De Vos P. (1973), Pneumatic Barriers to Reduce Salt Intrusion through Locks, Rijkswaterstaat communications no. 17

Boer, L. de , (2017), In welke mate kan optimalisatie van de schutoperatie bijdragen aan het beperken van zoutindringing door schutsluizen?, BEng thesis, Hogeschool Rotterdam (in Dutch)

Boschetti, T., O'Mahoney, T.S.D., Bijlsma, A.C. (2017), CFD modelling of the mitigation of salt intrusion by selective withdrawal, 4th International Symposium on Shallow Flows (ISSF), 26-28 June 2017, Eindhoven, The Netherlands

Van der Burg, P. and De Vos, P. (1962), Luchtbellenschermen in schutsluizen, Rijkswaterstaat (in Dutch)

Bulson, P.S. (1961), Currents Produced by an Air Curtain in Deep Water – Report on Recent Experiments at Southampton, Dock and Harbour Authority, 1961, Vol. 42, Nr. 287, pp. 15-22

Fraga, B., Stoesser, T., Lai, C.C.K. and Socolofsky, S.A. (2016), A LES-based Eulerian Lagrangian approach to predict the dynamics of bubble plumes, Ocean Modelling, 97, pp. 27-36

Gans, O.B. de, (2010), SIVAK II Handleiding, Rijkswaterstaat (in Dutch)

Groot, I. de (2015). WANDA-Locks, het nieuwe zoutlekmodel, Deltares report 1209463-000-HYE-0002 (in Dutch)

Keetels G., Uittenbogaard R., Cornelisse J., Villars N., Pagee H. van (2011), Field study and supporting analysis of air curtains and other measures to reduce salinity transport through shipping locks, Irrigation and Drainage, 60 (Suppl. 1), 42–50

Meerkerk, M. van, O'Mahoney, T., Twerda, A. (2015), Development of a CFD Model of an Air Curtain for Saltwater Intrusion Prevention, 36th IAHR World Congress, 28 June-3 July 2015, The Hague, The Netherlands

Riess, I.R., and Fanneløp, T.K. (1998), Recirculating flow generated by line-source bubble plumes, Journal of Hydraulic Engineering, 1998.124:932-940

Shin, J.O., Dalziel, S.B. and Linden, P.F. (2004), Gravity currents produced by lock exchange, Journal of Fluid Mechanics, vol. 521, pp. 1-34

Uittenbogaard R.E. (2010), Voorstudie: ontwerpstudie en praktijkproef zoutlekbeperking Volkeraksluizen – Model voor zoutvracht-berekeningen. Deltares report 1201226-011-ZKS-0002 (in Dutch)

Uittenbogaard, R., Cornelisse, J. and O'Hara, K. (2015a), Water – Air Bubble Screens Reducing Salt Intrusion through Shipping Locks, 36th IAHR World Congress, 28 June-3 July 2015, The Hague, The Netherlands

Uittenbogaard, R., (2015b), Reduction of Salt Intrusion Through Shipping Locks, PAO Stroming en Golven rond Waterbouwkundige Werken, Lecture slides, 21 May 2015

Van der Ven, P.P.D., De Groot, I., Vreeken, D.J. and Weiler, O.M. (2015), Simulating Lock Operations in the Generic Salt Intrusion Model WANDA-Locks, 7th PIANC-SMART Rivers Conference, 7-11 September 2015, Buenos Aires, Argentina

Van der Ven, P.P.D. and Oldenziel, G. (2018), A Scale Model Study Assessing the Performance of a Bubble Screen Mitigating Salinity Driven Lock Exchange, 5th IAHR Europe Congress, 12-14 June 2018, Trento, Italy

Van der Ven, P.P.D. and Wieleman, V.A. (2017), The use of small scale experiments for a shipping lock's bubble screen, 4th International Symposium on Shallow Flows (ISSF), 26-28 June 2017, Eindhoven, The Netherlands

Vrijburcht, A. et al. (2000), Ontwerp van schutsluizen (Deel 2), Bouwdienst Rijkswaterstaat, ISBN 9036933056 (in Dutch)

WANDA, https://www.deltares.nl/en/software/wanda/

Weiler, O., Van de Kerk, A.J. and Meeuse, K.J. (2015), Preventing Salt Intrusion through Shipping Locks: Recent Innovations and Results from a Pilot Setup, 36th IAHR World Congress, 28 June-3 July 2015, The Hague, The Netherlands

Weiler, O.M., Zoutindringing door Kunstwerken – NKvdT 2017 – Schutsluizen, Deltares report 11200741-003 (in Dutch)

Wen, J. and Torrest, R.S. (1987). Aeration Induced Circulation From Line Sources. I: Channel Flows, J. Environ. Eng. Vol. 113, 82-98.

INNOVATIVE METHODS FOR WATERWAY INSPECTION: AN APPLICATION TO CANAL-TUNNELS

Emmanuel Moisan[1,2], Philippe Foucher[1], Christophe Heinkelé[1], Pierre Charbonnier[1], Pierre Grussenmeyer[2], Samuel Guillemin[2], Mathieu Koehl[2], Fabrice Daly[3], Stéphane Gastarriet[4], Catherine Larive[5].

ABSTRACT

In this contribution, we propose some innovative methods based on sonar, image and/or laser data acquisition to facilitate the inspection of navigable structures, focusing on canal tunnels. We address the problem of 3D reconstruction of fluvial infrastructures on the basis of three research studies conducted during a doctoral work. In the first study, we evaluated the capabilities of a sonar system by comparing the 3D reconstruction of a lock from sonar and laser data. The second research axis focused on the implementation of reconstruction algorithms of the whole canal tunnel, *i.e.* its above water and under water parts. We relied both on photogrammetric techniques for modelling the above water part of the tunnel and on sonar point clouds for reconstructing the underwater model. Sonar data and images were recorded dynamically and simultaneously from a prototype mounted on a boat. In the absence of GPS signal in the tunnel, photogrammetry is used for computing 3D model of the structure and to estimate he boat trajectory in order to register sonar profiles. The last study aimed at evaluating the experimental 3D model of the tunnel. A reference model of the tunnel has been previously built from static sonar and laser acquisitions. Advanced robust algorithms have been implemented to generate the static model. This evaluation results have shown that the 3D model can locate above water elements with a centimetric accuracy and underwater objects with decimetric accuracy. Finally, we also introduced classification algorithms to automatically detect some defects on tunnels linings. The proposed methods are basic building blocks for the construction of a new generation of inspection methods for waterway infrastructure.

1. INTRODUCTION

Inland navigation is a prime transportation vector, whether for freight or tourism, and represents a more environmentally friendly alternative to road transport. The maintenance of fluvial infrastructures is not only a matter of heritage preservation, but also a commercial necessity and a security issue. Their documentation and periodic inspection is challenging due to the variety and huge number of structures to be considered. For example, Voies Navigables de France (VNF, the French operator of waterways), manages more than 6700 km of waterways (including more than 4000 structures). Filling in the VNF structure database (called BDO) is, for the moment, performed through systematic and exhaustive technical surveys of the structures carried out on site by agents. It is a major effort, may hinder navigation and endanger operators (see Figure 1-left). For this reason, it is necessary to develop highly efficient methods that are minimally invasive to fluvial traffic and require as little human intervention as possible. In this presentation, we focus on a particular type of structures, namely canal tunnels, but the proposed methodologies could concern other waterway structures.

[1] Cerema, Project-team ENDSUM,Strasbourg, France
[2] ICube Laboratory UMR 7357, Photogrammetry and Geomatics Group INSA Strasbourg, France
[3] Cerema, Technical Division Water, Sea and Waterways, Margny-lès-Compiègne, France
[4] VNF, Division Infrastructure, Water and Environment, Béthune, France
[5] CETU, Materials, Structures and Tunnel Durability Department, Bron, France

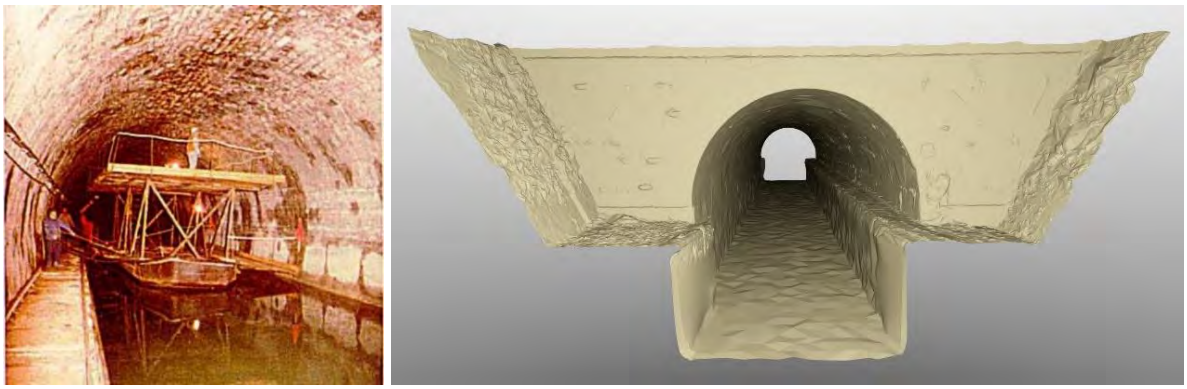

Figure 1: Inspection of the vault of a canal tunnel from a barge (right). The illustration comes from (Fagon Y. 2002). Example of a full 3D model of a canal tunnel (left)

Although there are only a small number of canal tunnels (e.g. in France, 33 tunnels are still in operation, for a total of 42 km of underground waterways), they are key to safe navigation. Located mostly on small gauge canals, they attract heavy touristic traffic. I this paper, we illustrate how up-to-date technologies (3D reconstruction by photogrammetry, high frequency bathymetry and pattern recognition techniques) may be used to design automatic tools for the detection of deterioration on structures and to produce accurate 3D models including both under- and above-water parts of the tunnels, even in the absence of GPS signal. We illustrate an example of such a model in Figure 1-right. In addition to this work on 3D reconstruction, we also explore the use of machine learning algorithms to detect defects automatically on the above-water parts of the tunnels.

With regard to 3D modelling, a doctoral work (Moisan E. 2017) funded by a Cerema scholarship from 2014 to 2017 allowed us to explore the whole-tube 3D imaging of canal tunnels by combining photogrammetry and high-frequency bathymetry sonar surveying. More specifically, three aspects, described in the next sections, were studied:

- evaluation of a recent technology in 3D sonar recording in a lock (Sect. 2)
- development of a 3D reconstruction pipeline based on image and sonar data acquired dynamically from a boat (Sect. 3)
- quantitative evaluation of the 3D model against a reference model of the tunnel, obtained from static laser and sonar acquisitions (Sect.4)

Section 5 is dedicated to pattern recognition algorithms that have been implemented for automatically detecting defects in the infrastructure. Section 6 concludes the paper.

2. 3D SONAR ASSESSMENT IN A LOCK

The objective of this section is to experimentally evaluate the capabilities of a recent multibeam echosounder technology by comparing sonar and laser 3D models built from static acquisitions.

2.1. Experimental setup

The experimental site is lock N°50 of Marne-Rhine canal (Souffleweyersheim, France) whose chamber obeys the Freycinet gauge (Duvergier J. 1879). In December 2015, we took advantage of a complete emptying of the lock for maintenance work to carry out terrestrial laser scanning (TLS) surveys using a *Faro Focus 3D X330* device (Figure 2-left). Once the lock was refilled (see Figure 2-right), static acquisitions were made with the mechanical scanning sonar (MSS) *Blueview BV5000* that consists of the MB1350 multibeam echosounder (MBES) mounted on a rotating mechanism.

Figure 2: View of the empty lock during the TLS surveying (left) and the lock after refilling during the MSS surveying (right)

It may be noticed that for the TLS survey, six scanner acquisitions were made from the bottom of the empty lock (Figure 3-a) and eight stations from the top of the lock. Spherical targets were placed around the lock chamber in order to facilitate the registration of scans. For the sonar, two acquisition configurations took place: three acquisitions were made with the sensor on a tripod at the bottom of the lock (Figure 3-b). In the other configuration, the device was immersed, upside down from the surface (Figure 3-c). To do this, the device was attached to a metal mast, which was fixed to a ladder placed transversely on the lock. In this configuration, a tacheometric prism was attached to the device mast. The sonar positions can thus be carefully surveyed with a total station. With this suspended configuration, the acquisitions were made every 5 meters, providing 9 point clouds. For each station, the sonar head performed three 360° rotations around its vertical axis, with a *15*°, *-15*° and *-45*° tilt angle, successively.

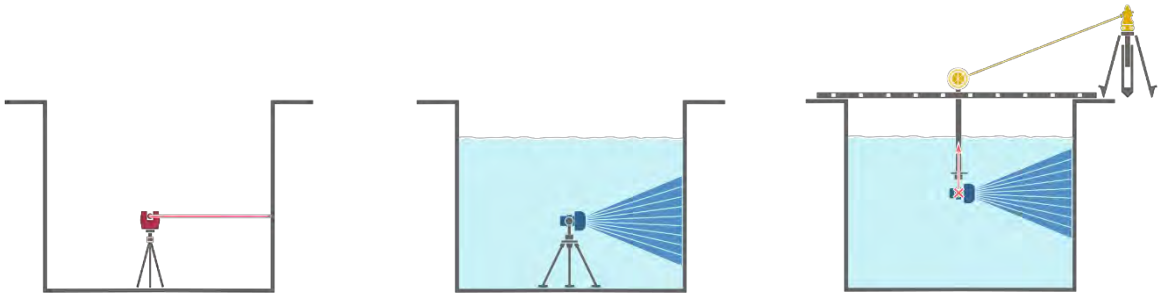

Figure 3: Terrestrial laser scanning (the device is in red) in the empty lock (left). Surveys of sonar point clouds in the filled lock. The device (in blue) is placed on a tripod at the bottom of water (middle) or suspended on a ladder and immersed upside down (right). The tacheometric prism (attached to the mast) and the total station (on the dock) are shown in yellow

The alignment of TLS point clouds was performed using *FaroScene* software with a sub-centimetric accuracy. The resulting model is illustrated on Figure 4-top. For the reconstruction of the 3D sonar model, there are no spherical targets in the water and the horizontal orientations of the scans are unknown. An original method must therefore be implemented to consolidate the model. This process includes a first step of translation and levelling through conventional topographic methods thanks to the prism positions and a second step in which point clouds are oriented horizontally using an *ad-hoc*

methodology. The entire registration process is described in (Moisan E. 2016). The resulting subaquatic model is shown in Figure 4-bottom.

Figure 4: Complete model of the lock from terrestrial laser scanning (top) and mechanical sonar scanning (bottom). Colours represent the scans of the 9 sonar static acquisitions

2.2. Results

The analysis of the sonar model focuses on three aspects. First, this experiment made it possible to assess the imperfections observed on the sonar point clouds. The second analysis is a quantitative evaluation of the 3D sonar model compared to the model obtained from the laser point cloud, considered as a reference. The final analysis aims at qualitatively assessing the possibilities of visualization and identification of details.

- **Artefacts**

Figure 5 shows the grainy aspect of the sonar model compared to the TLS one. In particular, we observe that the granularity of the MMS data increases with the distance from the acquisition station. Noise, inherent in the sonar measurements, explains some of these inaccuracies. It should be noted that the size of the sonar footprint increases with the distance from the sensor and the angle of incidence of the beam. Hence, we observe that the MSS model appears more granular in these unfavourable situations, i.e. long distance and at grazing incidence angles. This phenomenon is all the stronger in narrow environments such as tunnels or locks. This experiment also highlighted various artefacts in the sonar data. The first disturbance is due to the reflection of the signal on the water surface, as shown in Figure 6-left. This artefact can be easily filtered out if the water level is known. In our experiments, this level was measured with a tacheometer. We also observe acoustic anomalies that produce ghost objects. Artefacts related to backscattering of the sonar signal on a surface can occur and lead to the appearance of systematic shapes (Figure 6-left). For these two types of disturbances, manual filtering of outliers was performed before cloud consolidation. Finally, material dysfunctions can generate acquisition artefacts or the lack of acquisitions, as illustrated in Figure 6-right.

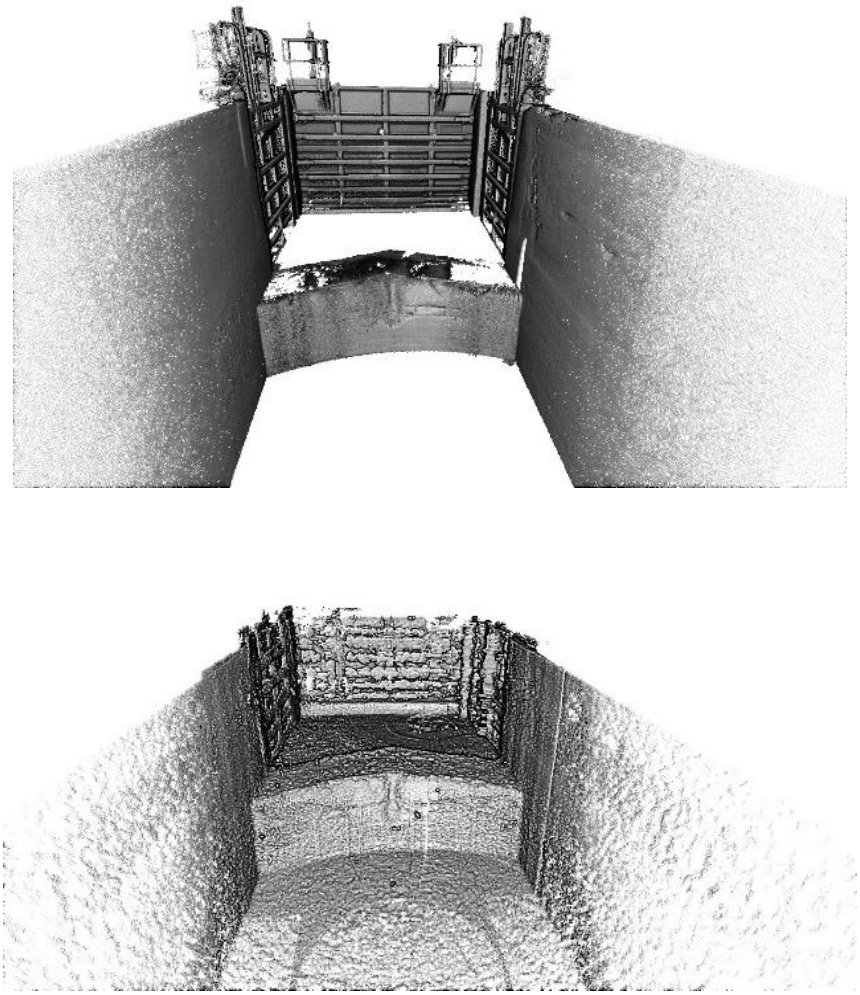

Figure 5: Laser (top) and sonar (bottom) models of the upstream lock gate

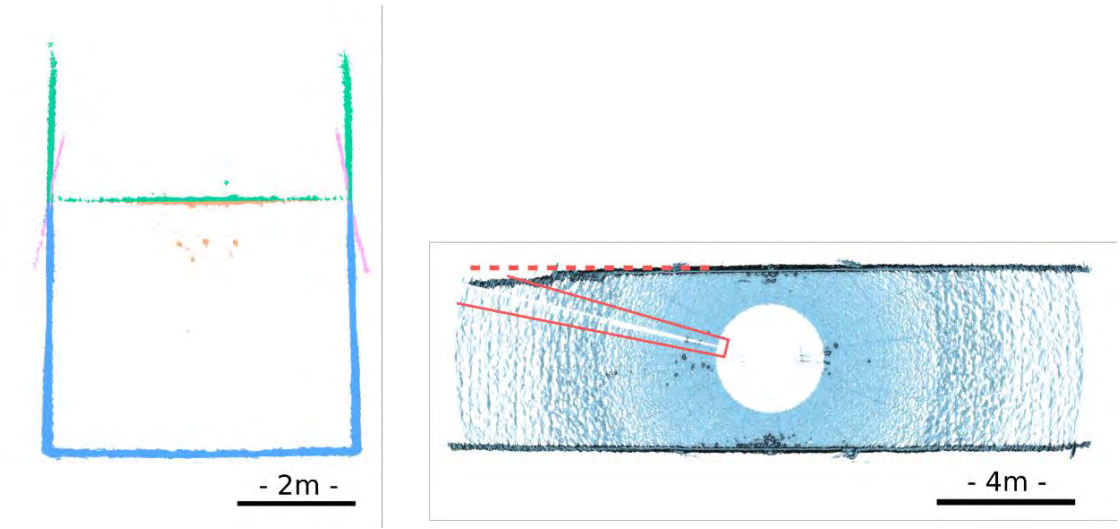

Figure 6: Examples of disturbances in sonar data: artefacts due to surface reflections (in green, left image), acoustic anomalies in the water column (in orange, left image), acoustic phenomena due to signal backscattering (in purple, left image). Acquisition anomaly (dashed line, right image) and lack of sonar measurements (red box, right image)

- **Quantitative assessment**

By working in the same coordinate system, we were able to compare the 2 models (MSS and TLS) by calculating the distances between both reconstructions. Note that the sonar model is a point cloud and the laser model is a mesh. It may also be noticed that we have restricted this quantitative analysis to the lock walls, considered separately. Results are gathered in the table 1.

Table 1: Distance analysis between the laser mesh cloud and the SONAR point cloud. By convention, distances are positive when the sonar points are inside the laser model

	Left wall	Right wall	Total
Mean	2.0 cm	1.8 cm	0.1 cm
Standard deviation	2.3 cm	2.4 cm	3.1 cm
Max	10.7 cm	10.3 cm	10.7 cm
Min	-6.5 cm	-9.8 cm	-9.8 cm

The differences between the sonar and laser models are in the range (-9.8, 10.7) cm. The mean (considering both walls simultaneously) of the distances is 0.1cm and the standard deviation is 3.1cm. However, by analyzing the means of the deviations for each wall, we observe a bias of about 2 cm. This bias represents a slight translation between the sonar and laser models transversely to the lock axis.

- **Visualization of details**

In this study, we analyse the sonar capabilities to distinguish details of the lock structure. We focus on two areas of the lock. In the first one, a rubble stone (approximate dimensions: 60x20x10 cm) was missing (Figure 7-a) and masonry joints are damaged (these cracks are about 4 cm wide and 4 cm deep). In the second area, we observe a cavity (approximate size: 50x100x15 cm) due to a spall (Figure 7-c). In the Figure 7-b,d, we can see that defects larger than 5 cm, such as stone defects or cavities, can be observed on the sonar model. Smaller details, such as damaged masonry joints are harder to detect. This experimental analysis highlighted the minimum size of defects that can be seen on a sonar model.

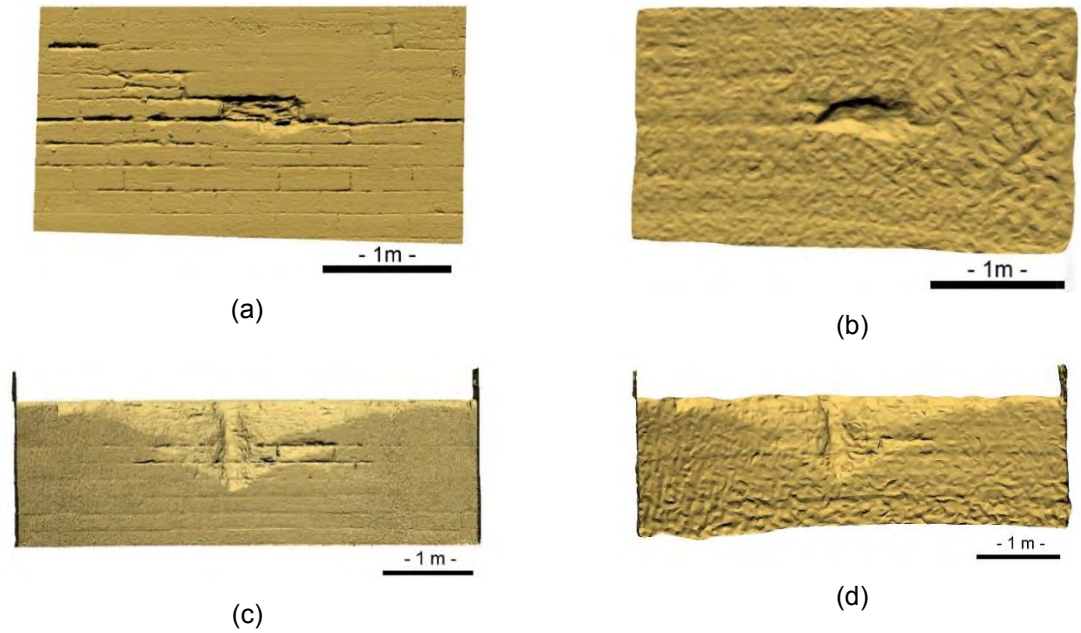

Figure 7: Details on the walls of the lock. Views of a lack of rubble stone on laser (a) and sonar (b) models. Views of cavities on laser (c) and sonar (d) models

3. FULL 3D MODEL OF A CANAL TUNNEL

The full 3D model of the canal-tunnel was built from images for the out-of-water part and bathymetric data for the underwater part. Images and sonar data were recorded simultaneously, in a dynamic fashion, from an acquisition prototype. The above-water part of the tunnel was reconstructed using photogrammetric techniques. However, given the high number of images, it was necessary to organize data to reduce computation times. For the underwater part, we used the trajectory of the boat for registering 3D sonar profiles. In traditional bathymetry, this trajectory is generally determined thanks to GPS tracking, possibly coupled to an inertial unit. In the case of tunnels, GPS signals are unavailable, and an inertial unit, used alone, may drift rather quickly. We therefore proposed to take advantage of photogrammetric methods to estimate the camera pose at each acquisition and thus, to retrieve the trajectory of the boat. Thanks to a preliminary determination of the system geometry, i.e. the relative positions of the sensors (cameras and sonar), we could consolidate the sonar profiles and compute the underwater model. The method is summarized in Figure 8.

3.1. Acquisition system

Since 2009, a French partnership composed of VNF, The Centre d'Études des Tunnels (CETU) and the CETE de l'Est (now the Cerema) in collaboration with the Photogrammetry and Geomatics Group of INSA has developed a visual inspection system dedicated to canal tunnels from acquisitions of image sequences. A modular prototype with lightings and cameras, mounted on a barge, has been devised for recording images of the vaults and sidewalls of the canal tunnel (see Figure 9). It may be noticed that the cameras can be oriented at several angles in order to visualize different areas of the vault. The imaging system consists of six 1920 x 1080-pixel resolution cameras. The image acquisition was triggered at a frequency of 5 Hz and synchronously for all cameras. It may be noticed that among these 6 cameras, there were two pairs of stereovision cameras: one pair to visualize the sidewall and the other for the vault. This second pair can be oriented at different angles to acquire images of all areas of the vault. The two remaining cameras have oblique sights to facilitate photogrammetric reconstruction.

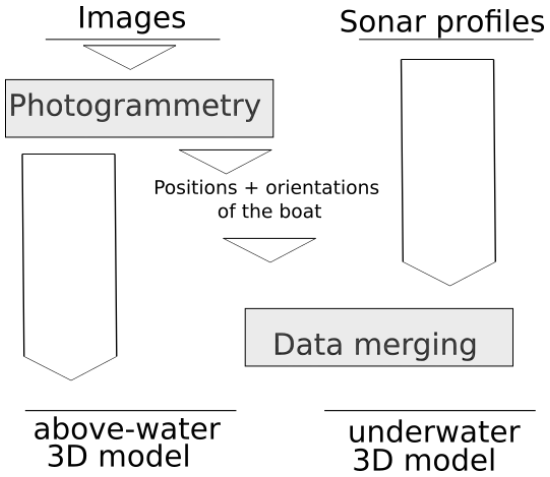

Figure 8: Methodogy for 3D reconstruction of a canal tunnel

The sonar device (MB1350) was attached to the front of the boat thanks to a removable pole. The sonar is oriented perpendicular to the canal axis. The device could be fixed to the pole with different acquisition angles. The aperture angle of the swath was 45° and sonar profiles were recorded at a frequency of 40Hz.

As the boat speed was about 1 $m.s^{-1}$, the inter-distance between two successive images was about 20 cm and, between two sonar profiles, about 2.5 cm. Moreover, a set of points and targets, previously implemented inside and outside the tunnel, has been surveyed for georeferencing the model (see Figure 10).

Figure 9: Our acquisition prototype mounted on a barge at the entrance of the tunnel (left) and inside the tunnel (right)

The tunnel where the experiments took place is located in Niderviller, on the Marne-Rhine canal in France. It is straight, 475 m long, covered in masonry and equipped with a pedestrian path on the ledge. We refer the reader to (Charbonnier P. 2014) for further details on this tunnel. For the experiment, three back and forth passages inside the tunnel were necessary to record data for the whole vault and the sub-aquatic part of the tunnel. Thus, a total of 3 sonar angles (11,25°, 45°, 90°) and 2 orientations of a stereovision pair had been planned to collect data for the entire tunnel (see Figure 11). Finally, for all passages, 90,000 images and 120,000 sonar profiles were collected.

Figure 10: Examples of targets viewed in the images. Catadioptric plate (left) and lasergrammetric target (right)

3.2. System calibration

Prior to the acquisitions, the system must be calibrated to allow the trajectory of the sonar to be deduced from that of the rigid block formed by the cameras. First, the focal length, the optical centre coordinates

and the coefficients for distortion correction of the cameras were determined (intrinsic calibration) (Zhang Z. 1999). Stereovision rigs were also calibrated in order to measure in 3D (Tsai R.Y. 1987).

The geometric calibration, second step of the process, consists in determining the physical offsets between sensors (or lever-arm). To compute these distances, the whole system was scanned using TLS device, as shown on Figure 12. To carefully determine the positions of the device acquisition centers in the laser model, the CAD (*Computer-Aided-Design*) models of the sensors, given by the manufacturer, were matched with the point cloud. Note that the sonar system was surveyed onshore. the model of the system (in red in Figure 12) and that of the sonar (in blue in Figure 12) were aligned from the geometry of the emerged part of the attachment pole. The offsets were then directly computed on the TLS model. Based on these relative positions, the sonar trajectory could then be estimated from the camera poses.

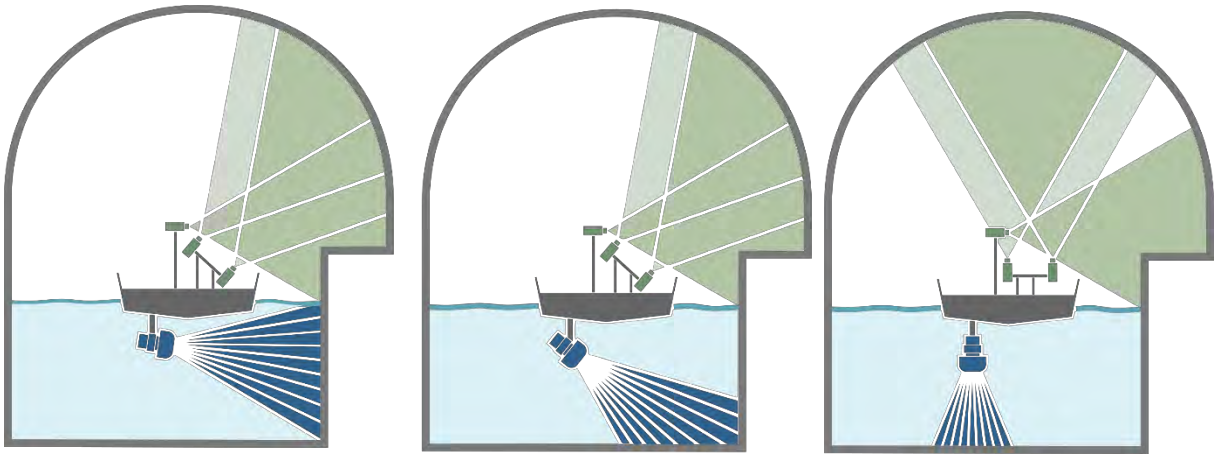

Figure 11: Sensor configurations with 3 sonar angles and 2 stereo rig angles

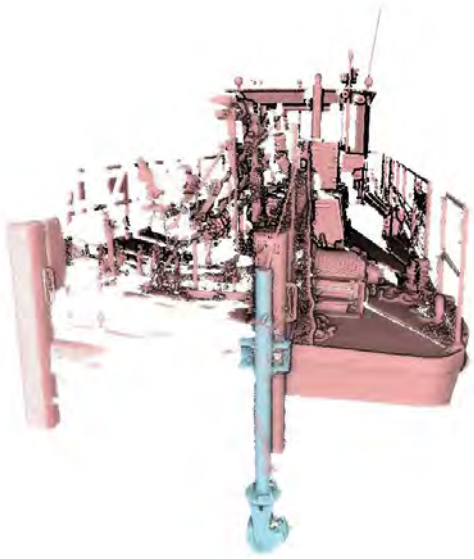

Figure 12: Whole system scanning for estimating the geometric calibration (lever-arm). The sonar device and its pole (in blue) are actually scanned onshore

3.3. 3D reconstruction

Considering the large amounts of data resulting from acquisitions, photogrammetry cannot be used directly for modelling the tunnel vault. It is necessary to implement a suitable methodology, which can be defined in two stages. First, we exploit the depth-disparity relationship of a calibrated stereovision system (Szeliski R. 2010) for pre-locating images. The difference, in pixels, between the position in the image of two points in two views of the same scene (disparity) is inversely proportional to the depth of the point in the scene. The proportionality coefficient depends on the difference, in meters, of the position between the two shots (stereo base). More specifically, applied to the stereo rig facing the sidewall, we can use this relationship to estimate the relative motion between two successive image acquisition positions, as detailed in (Albert J.L. 2013). Note that, as with any other relative location methods, positioning tends to drift due to error accumulations. We tackled this difficulty by using georeferenced points to readjust positions (Figure 10).

The second step consists in reconstructing the model itself. For computation reasons, it is impossible to process all the images at once to generate the tunnel model in a single piece. Therefore, we cut the tunnel into small sections (see Figure 13) that we call tiles. These tiles are modelled one by one and then aligned with each other. Typically, the length of a tile is 2m. Thanks to the pre-localization tool presented above, selecting and ordering the images of a tile is simplified.

Figure 13: Tile registration using Photoscan® software

Two softwares, MicMac (Rupnik E. 2017) and Photoscan[6], were tested for the photogrammetric computation of tunnel section models. Both computer tools provided similar results. A 2 m-sub-model is shown in Figure 13.

[6] http://www.agisoft.com/

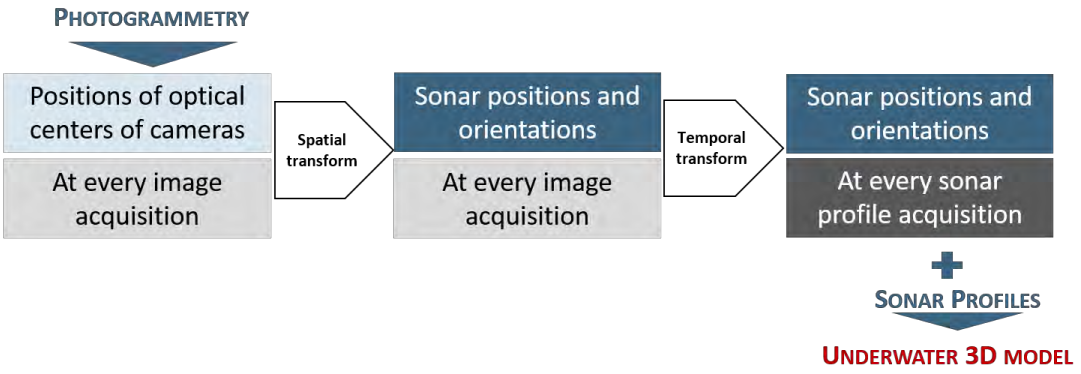

Figure 14: Sonar profiles referencement

Modelling the underwater part amounts to aligning the point profiles recorded by the multibeam echosounder. As shown in Figure 14, the reconstruction method of underwater model needs a spatial and a temporal transformation. First, the spatial transform aims at computing the absolute position and orientation of the sonar at each image acquisition. We aligned camera positions in the relative calibration system to their absolute locations, given by photogrammetry. We used the Procrustres method (Golub G.H. 2012) to compute both translation and rotation matrices. In the temporal-transform step, we synchronized sonar and images acquisitions by interpolations. Linear interpolations were applied to determine the sonar positions and spline interpolations were used to compute sonar orientations at every sonar profile acquisition. A “full-tube” 3D model of the first 30 meters of the tunnel was obtained in this way. The result illustrated in Figure 15, has been generated using Photoscan software.

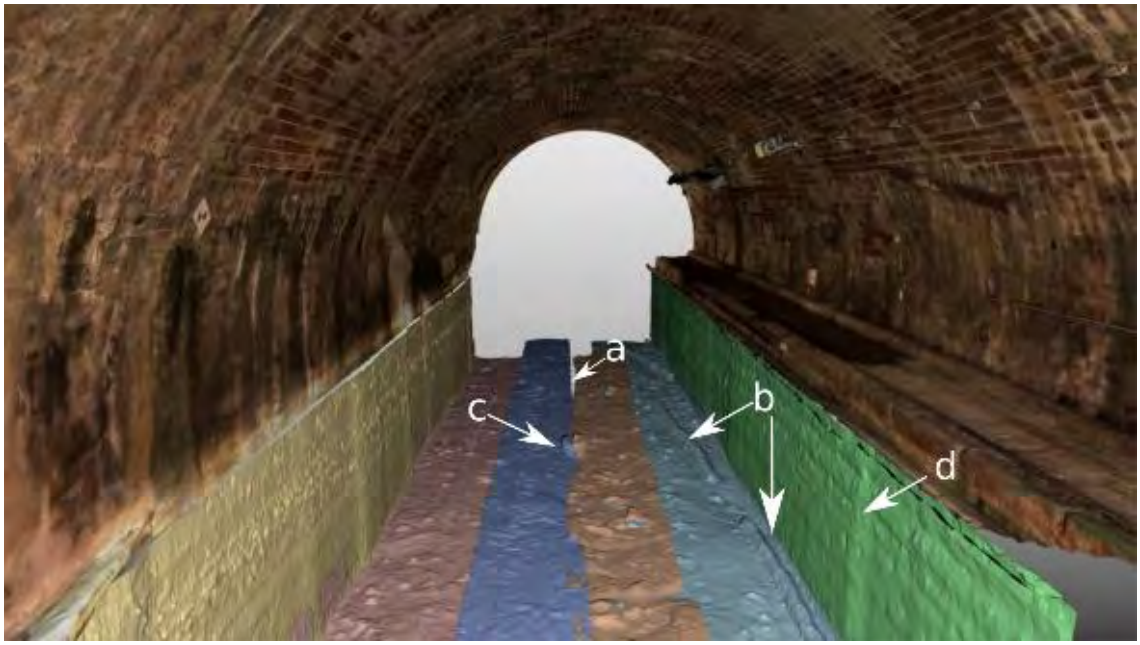

Figure 15: 3D model of the entrance of Niderviller tunnel. Colours represent the 6 different passes in the tunnel

Qualitative analysis of the resulting model shows that the juxtaposition of the photogrammetric and sonar models appears to be fairly consistent overall. The acquisitions from the different sonar passages also complement each other correctly. However, some gaps can be seen between passages due to the absence of measurements (see Figure 15, indication *a*). Some objects can also be seen on the bottom of the water, such as slide-rails (made of tropical wood, denser than water) that fell off the wall (see

Figure 15, indication *b*) and a cylindrical object, possibly a vehicle tyre (see Figure 15, indication *c*). Finally, we notice that the walls do not appear completely straight, when in fact they are. These discontinuities, illustrated by the indication *d* in Figure 15, are perhaps linked to the way the tiles are agglomerated. This discontinuity issue can be reduced by taking better account of the continuity of the trajectories between the tiles. An in-depth qualitative analysis is described in (Moisan E. 2017).

4. QUANTITATIVE EVALUATION OF 3D MODEL

4.1. Reference model

To quantitatively assess the accuracy of the 3D model, a reference model was built from static acquisitions. In practice, the entrances of the canal tunnel were surveyed by combining laser and sonar technologies (Figure 16-left).

A terrestrial laser scanner *(Faro Focus 3D X330* device) was used to scan the above-water part of the tunnel entrances from two stations (per entrance), located on either side of the canal. Spherical targets, visible on Figure 16-right, were placed around the environment to register TLS point clouds. The coordinates of the centres of the spheres were surveyed by conventional topography. Moreover, a set of reference points implemented on site is used to georeference model in the French reference coordinate system. The mechanical scanning sonar (BV500) recorded underwater data simultaneously with TLS acquisitions. At each entrance, two separate 10 m MSS static acquisitions were performed, one inside the tunnel and the other outside. MSS, mounted on a tripod, was immersed from a boat and stabilized at the bottom of the canal. Two wooden ladders, with known geometry, were partially immersed in the canal (Figure 16-right). They were scanned by both TLS and MSS devices.

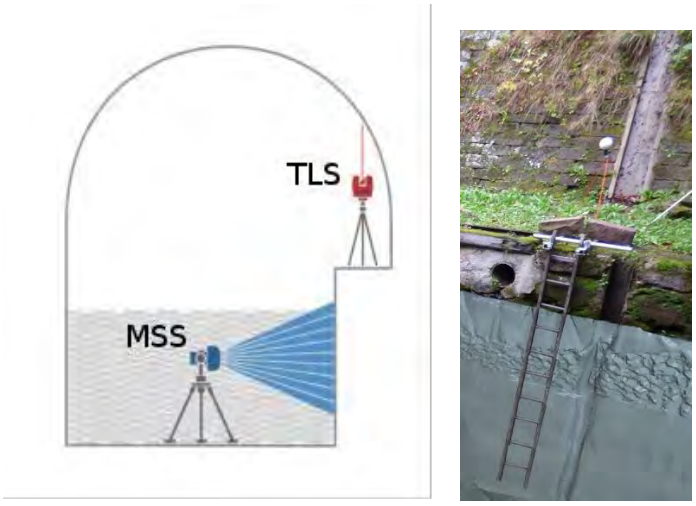

Figure 16: Experimental setup for laser and sonar scanning. Schematic representation of TLS and MSS stations (left). Ladder (synthetic representation for the underwater part) and sphere (in the background) positioning (right)

To generate the complete tunnel model, a possible approach consists in aligning sonar and laser models. However, this method would require an overlap between the two point clouds, which is not the case due to the different natures of the laser and sonar acquisitions. Hence, a methodology had to be implemented to reconstruct the model. In summary, the proposed method is based on geometric elements of the infrastructure (orientation of wall planes or ridges), known objects (ladders) and features extracted from the silhouette of waterline. This information has been extracted, using advanced robust algorithms and measured in underwater and above-water models in order to align them. We refer the reader to (Moisan E. 2015) for detailed explanations about the 3D reconstruction method of the

reference model. Figure 17 shows a meshed view of the resulting georeferenced model of the tunnel entrance.

Figure 17: Reference model of the west entrance of the canal tunnel. The dark disk in the middle of the canal indicates the location of the MSS station

4.2. Comparison between dynamic and reference models

We focalised the evaluation of the 3D model on the west entrance of the tunnel. The distances of the dynamic model (point cloud) to the reference model (mesh) are computed using Cloudcompare[7] software. The quantitative results show a significant difference between accuracies of photogrammetric and sonar models. The photogrammetric model (with Photoscan software) has an accuracy of 1.1 cm with a standard deviation of 1.1 cm. The approach that we have implemented to reconstruct the vault and the sidewalls of the tunnel seems relevant. Figure 18 highlights that the distance distribution to the reference model is not homogeneous. We observe stripes with large distances, transversely to the tunnel axis. It may be explained by an error in the alignment of some sub-models. Small deviations are often located in areas close to reference points.

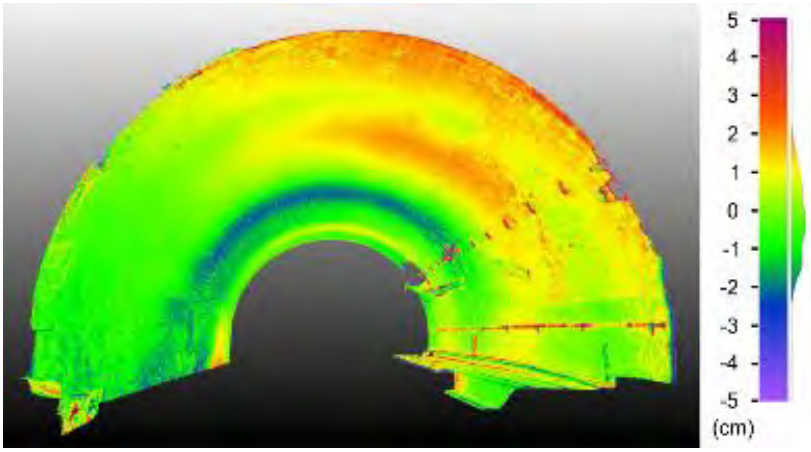

Figure 18: Visualization of the distances between the photogrammetric model and the reference model

[7] http://cloudcompare.org/

The evaluation of subaquatic models (the 6 passages are considered separately) reveals an accuracy in the range (5.7, 14.7) cm and a standard deviation in the range (1.9, 7.8) cm. These differences in accuracy with photogrammetric evaluation have several explanations: errors in the photogrammetric model, errors in the estimation of the system calibration or inaccuracies of MSS point clouds.

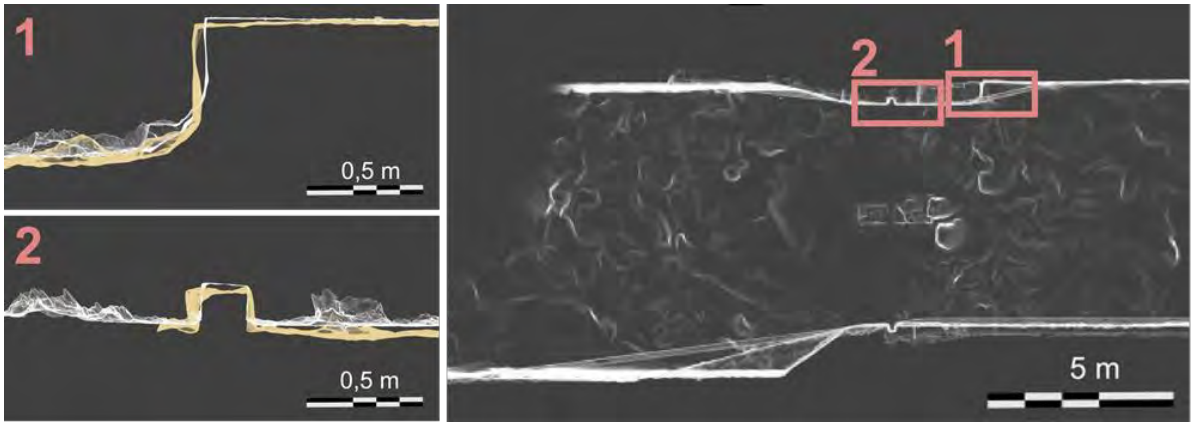

Figure 19: Overlay (with transparency) views of sonar (in orange) and laser (in white) models (left). Top views of the model (right) with the two areas of interest

Note that, by chance, a part of the sidewall was above water for static acquisitions (recorded by TLS) and under water for dynamic experimentation (scanned by sonar). We took advantage of this difference (10 cm) of water height in the canal to visualize some deviations (Figure 19). It may be seen that the details appear in the model at a position close to the reference points (Figure 10). The differences are about a few centimetres, which is consistent with our quantitative evaluation.

5. DEFECT DETECTION

Beyond 3D modelling infrastructures, an important point for tunnel inspection is the automatic detection in tunnel images. It is a challenging issue, due to the variability of situations in terms of tunnels and defects. Here too, advanced technologies and more specifically, machine learning *techniques*, are capable of providing high-performance tools. In this section, we explore a classification algorithm to detect and localise cracks, water leaks, exposed concrete reinforcements and damaged masonry joints in tunnel linings.

5.1. Classification method

The method we want to devise aims at detecting defects that are located in small parts of the images of the tunnel (Figure 20). It relies on a classification algorithm (or, in short, a *classifier*) whose role is to assign each image sample into a previously defined category, e.g. “defective” or “healthy” to characterize a surface state, “concrete”, “masonry” or “rock” to categorize a lining. In practice, images are not considered directly. Actually, different representations of them, called features, are used at the classifier input. The choice of the features depends on the observation of representative samples of the classes and on the knowledge of the problem to solve. In our work, we used features that relate to pixel values and their local relationships (Dalal N. 2005), contours (Xiao Y. 2014), or texture (Haralick R. 1973) gathered into feature vectors of about 3800 numbers.

In a first phase (supervised learning), a number of samples of each category are extracted from images. The corresponding feature vectors are presented to the classifier. Each vector having previously been labelled, the algorithm optimizes its internal representation to ensure the best possible correspondence

between its outputs and the expected labels. In the second phase (classification), the analyzed image is scanned using a sliding window. Each extract is transformed into a vector of characteristics, which is presented to the classifier who then assigns it a label. Of course, different images are used for training and for classification.

In this preliminary work, we relied on the Random Forest algorithm (Breiman L. 2001) to perform the classification task. More details about our implementation of the method may be found in (Foucher P. 2016).

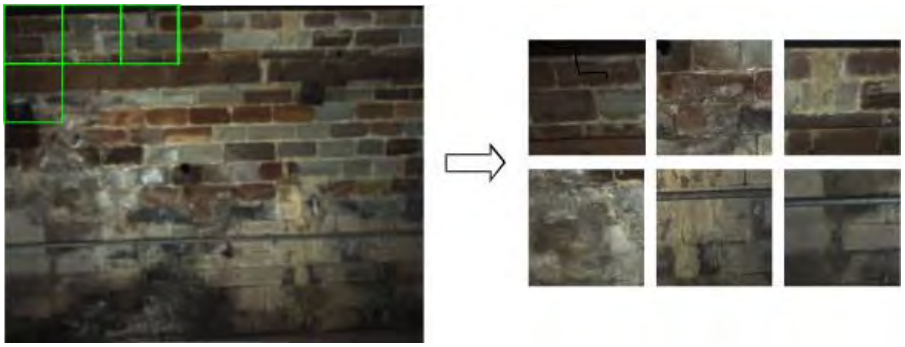

Figure 20: Extraction of samples (green rectangles) over the whole tunnel image. Every sample is classified into a category.

5.2. Results

We evaluated the classification method through two experiments. For each experiment, we selected a set of images to perform the learning process and evaluation. Approximately 500 samples per class were extracted from the images. The images that were not selected for the learning, were used to visualize and evaluate the performances of the algorithm on full-size images along the tunnel.

In the first experiment, we are interested in detecting moisture or more generally water leaks on images of a masonry tunnel. Each sample can be classified into category “water leaks” or “normal lining”. The sample evaluation provides a true positive rate (TPR) of 94% and a true negative rate (TNR) of 91.5% (TNR) corresponding respectively to the percentage of correctly classified samples in the “water leaks” and “normal lining” categories, respectively. Applied to a full-size image, the detection highlights the presence of water leaks, as shown in Figure 21.

Figure 21: Water leak detection (in blue) in images of a masonry tunnel

The second experiment aims at classifying the samples as “healthy” or “with defects”. These include surface defects typical of concrete tunnels: exposed reinforcement, pebble nests and wide cracks. The analysis of the results on a set of samples showed a TPR of 97.1% and a TNR of 95.9%. When we

applied this algorithm to the entire image, the detection of exposed reinforcements and pebble nests was visually correct. However, the algorithm seemed to have more difficulties to extract cracks (see Figure 22-left). Note that it was indeed possible to detect finer cracks, by using a specific training, but this is at the expense of a higher number of false alarms (Figure 22-right).

Figure 22: Defect detection (light areas) in concrete tunnel images. Example of a non-detected crack (blue box, left image). The same crack is detected using a more specific training (green box, right image) at the expense of a high rate of false alarms.

This exploratory work shows the relevance of supervised learning classification methods for automatically detecting defects in tunnels, despite the wide variability in the appearance of the linings and defects considered. The first results obtained on image samples give performances higher than 90% in terms of TPR and TNR. Quantifying performance on full-size image sequences, by comparison with a manually annotated base, should allow a finer analysis of the results. In perspective, we wish to explore other learning methods, such as deep learning, to increase detection performance. The use of convolutional neural networks (Goodfellow I. 2016) would also have the advantage of automatically learning the relevant descriptors.

6. CONCLUSION

In this paper, we have explored methods for reconstructing a whole tunnel. First, we reported on a first experiment in a lock, which highlighted the potentialities of a sonar for modelling a structure, and, in particular, its capacity to identify details. This experiment has shown that elements larger than 5 cm can be seen in the sonar model. In a second contribution, we have implemented and evaluated a 3D reconstruction pipeline of a canal tunnel from dynamic image and sonar acquisitions. Photogrammetry was used both to build the vault model and to compute the boat trajectory, which is necessary for georeferencing sonar data. An original approach has been proposed to build a reference model, based on laser and sonar static surveying. By computing distances between the dynamic model and the reference model, we provided quantitative results that showed a centimetric accuracy for photogrammetric reconstruction and a decimetric accuracy for underwater reconstruction.

Even if steps still need to be taken before a complete automation of the process can be achieved, this research has shown the feasibility of documenting engineering structures such as canal tunnels in 3D. The proposed techniques could also be generalized to areas where the GPS signal is inoperative. They are complementary to more classical bathymetry methods. Moreover, we have shown the feasibility of automatically detecting defects in the structure via pattern recognition methods, which may be generalized to other structures and to underwater elements.

In line with this collaborative research, and as part of its evolution towards digital technology, the so-called *VAF waterways* project, VNF is launching a first innovation partnership for high-throughput

collection of images of the linear components of its network (mainly embankments and dikes), from the waterway. The aim is to automatically pre-inform (using shape recognition technologies) the condition field in the VNF structure database. Moreover, the images will be made available through a geolocalized interface (similar to Google Riverview).

REFERENCES

Albert J.L., Charbonnier P., ChavantP. Foucher P., Muzet V., Prybyla D., Perrin T., Grussenmeyer P., Guillemin S., & Koehl, M. «Devising a visual inspection system for canal tunnels: preliminary studies.» *24th CIPA Symposium .* Strasbourg, France: ISPRS, 2013. 13-18.

Breiman L. «Random forests.» *Machine learning* (Springer) 45, n° 1 (2001): 5-32.

Charbonnier P., Foucher P., Chavant P., Muzet V., Prybyla D., Perrin T., Albert J.L., Grussenmeyer P., Guillemin S. & Koehl M. «An image-based inspection systme for canal-tunnel heritage.» *International Journal of Heritage in the Digital Era* 3, n° 1 (2014): 197-214.

Dalal N., & Triggs B. «Histograms of oriented gradients for human detection.» *Proceedings of International Conference on Computer Vsion and Pattern Recognition .* San diego, USA, 2005. 886-893.

Duvergier J. *5-6 août 1879, Loi relative au classement et à l'amélioration des voies navigables.* Vol. Tome soixante-dix-Neuvième, chez *Collection complète des lois, décrets, ordonnances, réglements et avis du conseil d'état*, de Noblet Ch., Larose L., 338-339. Bibliothèqe Nationale de France, Paris, 1879.

Fagon Y., Flaquet-Lacoux V., Brioist J.J., Dubois D. & Choquet C. «Tunnels canaux - fascicule 1 : surveillance, entretien, réparation.» Guide technique (in french), CETMEF, Compiègne, 2002.

Foucher P., Bah M.D., Charbonnier P. Boulogne C. & Larive C. «Classification automatique de défauts sur des images de tunnels par forêts d'arbres aléatoires.» *Congrès national sur la reconnaissnce de Formes et l'Intelligence Artificielle -(in french).* Clermont-Ferrand, France, 2016.

Golub G.H., Van Loan C.F. *Matrix computations.* 4th ed. John Hopkins, 2012.

Goodfellow I., Bengio Y. & Courville A. *Deep Learning.* MIT Press, 2016.

Haralick R., Shanmugam K. & Disntein I. «Textural features for image classification.» 3, n° 6 (nov 1973): 610-621.

Moisan E. «Imagerie 3D du "tube entier" des tunnels navigables.» Thèse de doctorat (in french), Université de Strasbourg, 2017.

Moisan E., Charbonnier P., Foucher P., Grussenmeyer P., Guillemin S. & Koehl M. «adjustment of sonar and laser acquisition for building the 3D refrence model of a canal tunnel.» *Sensors* 15, n° 2 (2015): 31180-21204.

Moisan E., Charbonnier P., Foucher P., Grussenmeyer P., Guillemin S., Samat O. & Pagès C. «Assessment of a static multibeam sonar scanner for 3D surveying in confined subaquatic Environments.» *International Archives of the photogrammetry remote sensing and spatial Information Sciences.* Prague, czech republic, 2016. 541-548.

Moisan E., Heinkele C., Charbonnier P., Foucher P., Grussenmeyer P., Guillemin S. & Koehl M. «Dynamic 3D modeling of a canal-tunnel using photogrammetric and bathymetric data.» *ISPRS Workshop "3D Arch".* Nafplio, Grèce, 2017. 495-501.

Rupnik E., Daakir M. & Pierrot Deseilligny M. «MicMac - a free open-source solution for photogrammetry.» *Open geospatial data, software and standards*, 2017.

Szeliski R. *Computer vision: algorithms and applications.* New York, USA: Springer-Verlag, 2010.

Tsai R.Y. «A versatile camera calibration technique for high-accuracy 3D machine-vision metrology using off-the-shelf TV cameras and lenses.» *IEEE Journal on Robotics and automation* 3, n° 4 (1987): 323-344.

Xiao Y., Wu J., & Yuan Y. «mCentrist: A multi-channel Feature Generation Mechanism for Scene Categorization.» *IEEE transactions on Image processing* 23, n° 2 (2014): 823-836.

Zhang Z. «flexible camera calibration by viewing a plane from unknown orientations.» *Proceedings of the seventh IEEE International conference on computer vision (ICCV).* Kerkyra, Corfou, Grèce: IEEE, 1999. 666-673.

Latest in Technologies for Navigational Locks

by

Timo Kiiso[1], Parveen Gupta[2]

ABSTRACT

The Panama ship lock extension has been a huge project not for only the civil engineering but also for hydraulic installations. The total installation of 6 locks together with water saving system has made it one of the biggest civil works in the field of navigational locks.

The water saving system of the locks of the Panama Canal extension makes it possible to save up to 60% of the water used during lockage of vessels. The water saving system consists of three basins built for every lock. In a normal lock system the water flow is always downstream with the lockage of a vessel. New Panama water saving system saves 60% of the water in the lock by using the water saving basins in three phases. The water saving process is an important improvement of the Panama Canal because the central Gatun lake gets most of its water from the rain fall and is also an important source for the water service in the Panama City.

The water flow to fill and empty the lock chambers, the water saving basins as well as the lock area between the rolling gates is realized through valves operated by hydraulic drive systems. The operating environments and the high demands on the reliability for the water saving system has setup high standards for the hydraulic system.

The hydraulic drive system of the 6 new locks consists of 152 special designed cylinders, each operated by a dedicated hydraulic power unit. Each hydraulic power unit can be operated locally. All lockage processes are operated by the machinery-control system (LMCS) and the lockage process can be operated automatically, semi-automatically as well as in manual mode with the LMCS. The hydraulic power units are equipped with a local control panels, which enables the manual operation at the power units.

The pipe work of the whole Panama expansion project consists of a length of about 22 km made of stainless steel. The oil used in the hydraulic system is an environmental friendly fluid to eliminate the impact to the environment during the overhaul of the hydraulic system.

Moreover, the challenge for the environmental aspects were taken into account during the design of the projects. Two main elements to ensure a long maintenance period and leak free operation of the cylinders were the quality of the piston rod surface and the sealing system of the hydraulic cylinder. The traditional way of making piston rod coating has been the chrome plating. Quite often the hard environment has set up a demand to have a stainless steel base material.

As an alternative there are new technologies in the market to avoid the expensive use of base material combined with the tight and crack free structure of the coating. The High Velocity Oxygen Fuel (HVOF) technology is used to produce coating on the piston rods especially on the large dimensions. By using the HVOF technology there is no need for the corrosion resistant base material and therefore the total cost for the appropriate corrosion resistance can be lowered. In addition, by using the HVOF technology it's possible to adjust the needed corrosion resistance according the operating environment by the different parameters of the HVOF process.

The other factor on the trouble free operation of the cylinder is the correct function of the tribological system at the piston rod. The piston rod is impacted on the abrasive materials as well as oxidation layer on the piston rod. To prevent the abrasive particles to enter in to the oil through piston rod and keep the oil inside the cylinder, the effective seal system is needed. The most common seal type used in the navigational locks is the chevron seal. However, the multiple amount of seals in the chevron package creates friction and is therefore uneconomic. The resent development in the field of seal material and construction makes it

[1] Center of Competence in Civil Engineering, Bosch Rexroth AG, Germany
[2] Bosch Rexroth Co., US

possible to introduce low friction solutions also for chevron seal. In addition, with the patented structure, the chevron seal design can be changed at the overhaul on the site without disassembly the cylinder.

There has been taken efforts also on the other type of actuators for the navigational locks. In the development work the hydraulic and also electro mechanical solutions have been realized. The latest development of the gate operating technologies let us introduce new features also on the field of information technology. It gives us an option to let the machinery communicate with the upper level control system i.e in case of maintenance needs.

The long hydraulic pipe works increase a risk of leakage in the navigational locks. Normally the risk has been minimized by setting high standards on the pipe work design and realizations. To avoid the field piping totally the self-contained actuators are needed. Self-contained actuators need only electrical energy and control signal. The movement is created in the actuator. There two types of self-contained actuator available for the ship locks.

The electro-mechanical actuators are presented for applications, where the need of force is adequate. The advantage of the electro-mechanical actuator is the easy installation, since no room for hydraulic power unit and no field piping are need. Unlike easily understood, the environmental protection has to be taken in to the consideration during the design of system also with electro-mechanical actuator. The lubrication system of the spindle consists of grease and it needs to be naturally leak free. Therefore, the sealing construction of also the electro-mechanical actuator has be taken well into the consideration. In addition, the electro-mechanical actuator is incapable to take impacts since the main operating element is a spindle. Therefore, the electro-mechanical solutions are used in the small roller gate systems.

Another type of self-contained actuator is an electro-hydraulic actuator. Like in electro-mechanical actuator it needs only electric power supply and the control signal. The electrical energy is transferred to movement by compact hydraulic unit located in the actuator. The electro-hydraulic actuator is suitable for high forces and applications, where impacts are expected from the moving elements like mitre-gates. The oil system of an electro-mechanical actuator is closed and the structure of the cylinder has normally three chambers, which enables the pendeling volume circulate inside the cylinder.

For the heavy sliding gate design there are normally a mechanical drive equipped with a gearbox. The redundancy is realized by a several electro-motors and gear box combinations. By using a closed loop hydraulic system with a direct drive concept, the operation and the redundancy can be realized easily and with a savings in the needed room and the weight of the total system. The direct drive can be also taking in to the consideration on the modernization projects, where an old mechanical drive need to be updated on the latest technological level.

The latest development in the information and sensor technology have made it possible to introduce new tools for the monitoring of the condition of the operating machinery in the ship locks. In the modern hydraulic system there are sensors detecting the characteristics of the system. The characteristics like temperature, vibrations, pressure level and pressure pulsations are detected and analyzed during the use of the system. The analysis provides a hydraulic health index for the new system and by monitoring this hydraulic health index, the need for the predictive maintenance operations can be planned in advance. By equipping the system with a remote access, the main operating characteristics can be easily checked without visiting the machinery.

Panama Canal Extension was the newest state of the art in 2009. The development in the technologies in the field of navigational lock has been progressed a lot since that time, especially in algorithms of sensing the hydraulic systems but also on the mechanical engineering of the components used in navigational locks. The further development of collecting and analyzing the data taken from the operating systems will make possible to design and build locks even more reliable by getting more online data from the sub systems operating parameter.

EROSION CONTROL PROGRAM AT THE PANAMA CANAL

by

Antonio A. Abrego Maloff[1], Maximiliano De Puy[2], Yared Cruz[3], Yesenia Cerrud[4]

ABSTRACT

The Panama Canal is one of the most significant engineering works in the world, located in an area with a unique diversity within the Republic of Panama. It stands as a magnificent excavation project, which exposes its greater complexity: a huge variety of geological formations, with different weathering and drainage patterns, areas of heavy rainfall, and large extensions of coastlines, which are subjected to surge waves produced by dozens of vessels transiting the Canal every day.

From the very beginning, when the Canal initiated its operations, many studies and projects have been carried out to reduce the erosion of the banks along the waterway. With the Canal Expansion project, this issue became more relevant, mainly because huge retaining structures and new slopes were to be built to safely accommodate the transit of much bigger vessels. Because of this, the control of the bank erosion and sedimentation in the channel are key points of the geotechnical and environmental monitoring of the area. The Erosion Control Program was developed to meet this need and is managed by the Geotechnical Engineering Section of the Panama Canal Authority (ACP). The main goal of this program is to reduce the erosion action on the bank slopes produced by the surge waves and also on the cut slopes due to rainwater runoff. Special efforts have been committed to develop designs for erosion control, based on two premises: experience from previous methods used; and new technology which helps to find a balance between investment, performance, and bioengineering.

This paper describes the methods used for the erosion control in some areas along the shoreline of the waterway, which were required not only to protect the slopes but also to protect very important structures located near the banks. The projects hereby presented demonstrate the impact that a proper and effective design can have on such a particular area as the Panama Canal.

1. INTRODUCTION

The construction of the Panama Canal required the excavation of large amounts of soil and rock from a vast extension of land named Gaillard Cut. This excavation, along with the construction of the Gatun Lake and the access channels for the locks, resulted in the creation of hundreds of mile of coastlines exposed to a heavy rainfall and subjected to surge waves produced by the vessels transiting the Canal every day.

In addition, the excavation of new slopes along the banks of the waterway poses new concerns to the Panama Canal Authority, since the lack of vegetation after the excavation leaves the soil vulnerable to erosion. The Panama Canal has an average rain precipitation of approximately 2,700 mm per year, making it necessary to develop a remedial plan against severe erosion before it occurred.

For many years, the Panama Canal Authority has been implementing remedial measurements not only to reduce the erosion of the banks along the waterway, but also to reduce erosion of newly excavated slopes along the Gaillard Cut due to the rainwater runoff. The Erosion Control Program was developed specifically to deal with these issues and also has been modified through the years to include other works such as protection of waterfront structures and marine facilities located along the waterway.

[1] Panama Canal Authority, Panama, AAbrego@pancanal.com
[2] Geotechnical Consultant, Panama, Maxdepuy@gmail.com
[3] Panama Canal Authority, Panama, YCruz@pancanal.com
[4] Panama Canal Authority, Panama, YCerrud@pancanal.com

This paper summarizes the design criteria and execution of three of those projects. The methodologies used for the design of these projects varies depending on several factors such as severity and extension of the damage; previous works performed in the area; soil conditions; infrastructure distribution in the area; operational conditions; etc.

The first project corresponds to a rockfill constructed in the Mamei Curve to protect the Panama Railroad Company tracks from surge waves produced by tugs and transiting vessels. The second project summarizes the construction procedure used 100 years ago to build the Cristobal breakwater, and describes the maintenance program implemented to keep the structure operational. The third project also describes the repairing works carried out to protect several slopes from surge waves in an area where the main offices of the ACP's Dredging Division are located.

2. EROSION CONTROL PROGRAM

The Panama Canal Erosion Control Program has been established to accomplish the following objectives:

- To monitor Canal banks and adjacent areas to identify sites representing a potential hazard to navigation and/or waterfront structures due to slides and erosion problems;
- To determine the main causes of the erosion and slide problems;
- To restore these sites to their original condition and ensure that the works performs efficiently for long periods;
- To use available and reasonably priced technology for the repairs.

The program includes not only bank erosion or other landslide problems outside the Gaillard Cut, but it also deals with the maintenance of all Canal breakwaters, the most important being the Cristobal Breakwater, which has an extension of more than 4.0 km and protects the City of Colon and the Atlantic entrance of the Canal.

The Erosion Control Program has been in place in Canal operations since 1914. However, it was only in FY 2006 that an independent cost structure was created and the program was separated from the Landslide Control Program.

The elements used to protect waterfront structures, marine facilities, and shoreline protection include anchored sheet piling walls, reinforced earth retaining walls, gabions, riprap and rock anchors, and slope excavation. Another type of slope protection implemented in the last decade along the cut slopes of the Gaillard Cut is the so-called surface erosion control, which is intended to protect newly constructed or excavated stable slopes from surface erosion using vegetation; in other words, ACP is "greening" its slopes.

The decision of the final design required for a specific erosion control work depends on several factors such as:

- Severity and extension of the damage;
- Previous works performed in the area;
- Soil conditions;
- Infrastructure distribution in the area;
- Operational conditions;
- Construction costs;
- Availability of construction materials;
- Loading condition (including tidal waves);
- Future use of the area;
- Past experience;

All the designs performed by the Engineering Division are based on common design practice of retaining structures applied to local conditions and based on past experience. There are several references used in the design of such specific solutions, being most of them obtained from PIANC, USACE manuals, textbooks, etc. Factors being considered are: environmental conditions, loading conditions, geotechnical considerations, type of structures, and operational conditions.

3. MAMEI CURVE PROJECT

The erosion in the shoreline due the wave action induced by the passage of vessels and tugboats has become a problem on the Panama Canal banks. Mamei Curve is located on the east bank of Mamei Reach, Juan Grande Reach, and Gamboa Reach (see figure 1). Along Mamei curve there is an embankment built for the existing railroad track of the Panama Railroad Company and the electrical span towers that carry the electricity supply to the Colon area; through that embankment also run the transatlantic fiber optic ducts. This area has presented erosion problem since 1955, caused by the wave action of ships as they pass through Mamei Curve. Erosion at the site is severe and is impacting the existing railroad track next to the bank of the Canal, the electrical span towers and a service road used by ACP.

The Mamei curve erosion control project aims to prevent the erosion and hazards to the railroad tracks. This project consists in the construction of a 2.4 km of riprap slope protection system, through Mamei Curve. It also includes the development of a double seal asphalt road.

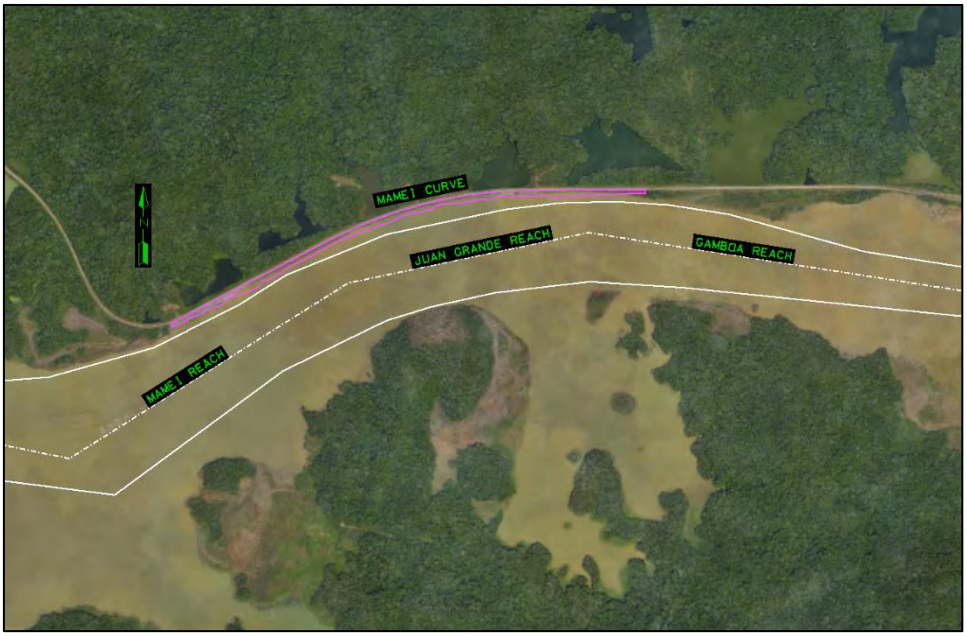

Figure 1: Location of Mamei Curve

3.1 Background

The construction of the Panama Canal finished in 1914, the railroad tracks were completed in 1912 and the drawings of the electrical span towers date back to 1937. The early erosion problems at Mamei curve started approximately in 1955. From 1955 to 1970 many control works along the bank were performed, without proper design. Since 1971 there are formal drawings and designs of the revetments installed in the area. The erosion control works consisted mostly of the placement of rockfill, two layers of quarry rock above a layer of crusher run and the use of filter fabric. The maximum depth of the riprap was 7-9 feet. Since 1993 many repairs were attempted including placement of rockfill and grouted rockfill.

In 2011 the erosion problem at Mamei curve was reported again. A new design for all the area was developed soon after that by the Engineering Division, and the repairing works began in 2014. The first phase of the project ended in 2015 and it is expected that the final stage of the repairing works will be executed in 2019.

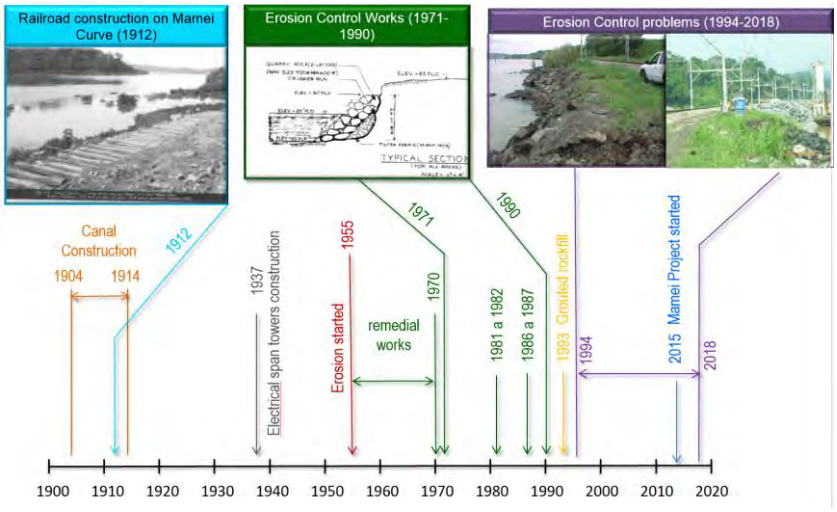

Figure 2: Timeline showing Mamei curve works

3.2 Geology

At the site, the geotechnical investigation shows that there are three layers of fill with a total thickness of about 30 m, underlined by natural ground that consists of the Bohio formation. Figure 3 shows the geological section of the area. The Bohio formation is found in the central part of the Canal area, its thickness is about 1000 feet and consists of a series of sandstones and conglomerates, which are medium to hard, massively jointed, and massively but crudely bedded. The conglomerates consist of angular to rounded pebbles, cobbles and occasional boulders up to six feet in diameter, embedded in a dark-gray, coarse-grained, angular sandstone matrix. There are some Tuff beds at scattered localities. Basalt intrusions ranging from a few feet to over 200 feet in width are frequent in the Bohio formation (Woodring, 1957).

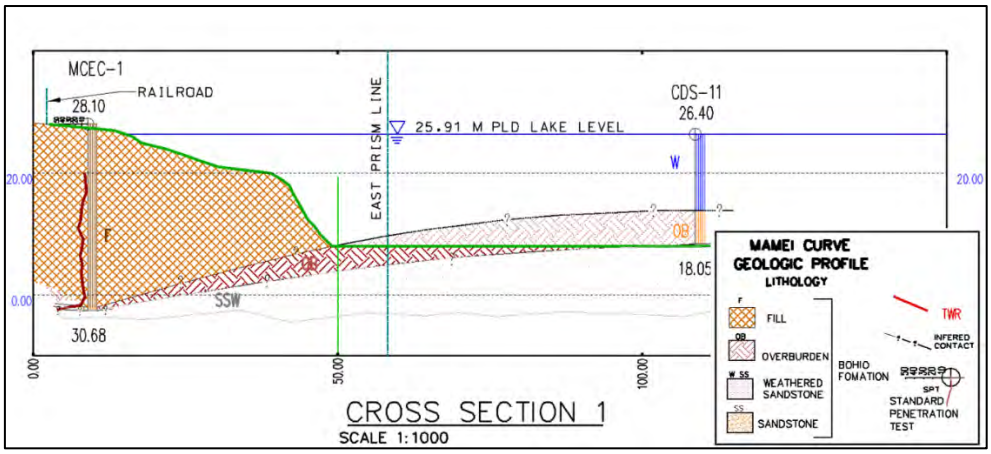

Figure 3. Geological section

3.3 Design

The selection of the required grading width and average mass requirements for the rockfill and the filter was designed using references of Hudson (Hudson, 1953 and 1969), Pilarczyk (Pilarzcyk, 1989 and 1995), the Rock Manual (CIRIA/CUR, 2007) and the US Department of Transportation (1989)

The rock size was designed for a generated wave height (Hs) of 1.80 meters and considering a rock armor unit weight (ρr) of 2.65 t/m3. The bank slope inclination was 34 degrees. The final median nominal rock diameter o equivalent cube size (D_{50}) was 0.95m. Figure 4 shows the riprap grading used for Mamei Control Erosion Project.

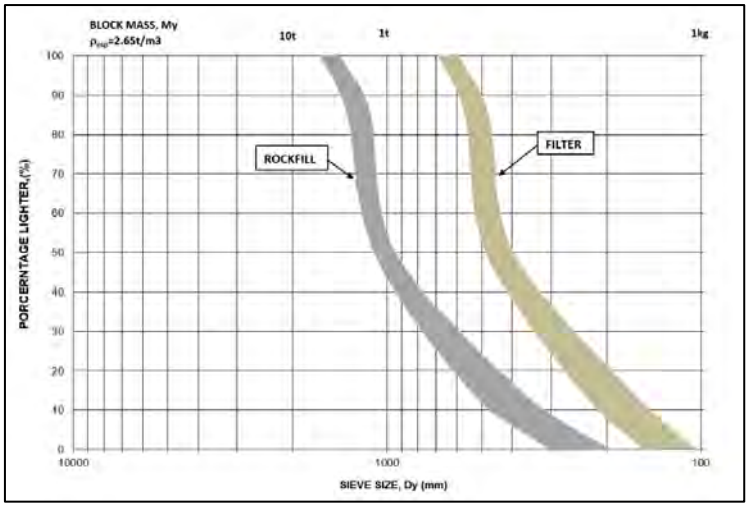

Figure 4: Riprap grading

Repair measures consist of placement of two rockfills, one underwater at the base of the slope (placed directly on top of the Bohio formation), and one at the top (sitting on the fill of the embankment). A filter is placed behind the top rockfill to prevent erosion of the existing ground. The underwater rockfill is necessary to increase the factor of safety of the slope to a value of 1.3-1.4, while the top rockfill is required to resist the wave action. Figures 5 and 6 show the typical sections of the revetment protection.

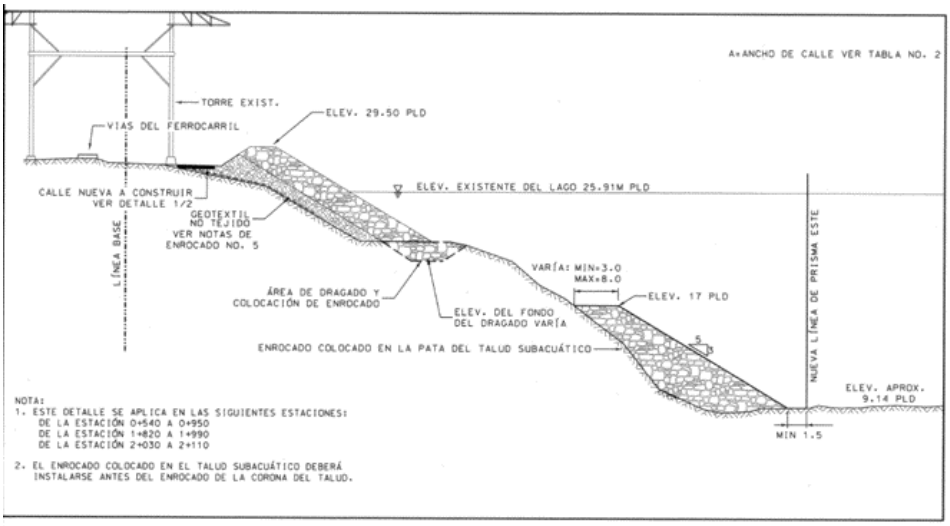

Figure 5: Typical revetment section

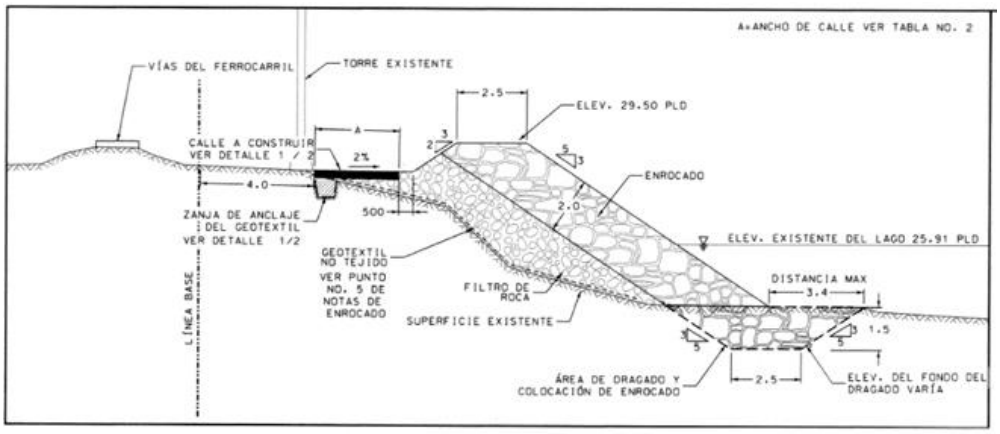

Figure 6: Typical revetment section

3.4 Construction

In the year 2015 part of the works were carried out. The contractor proceeded with the placement of the underwater rockfill and the top rockfill in some of the most critical sections of Mamei curve.

Due to the remote location of the project, all the material required for the project had to be transported using barges. From the stockpile area at the north of the Pacific access channel, all the armor stone was transported through the Gaillard Cut on flat-top barges to Mamei Curve. At the site, hydraulic excavators delivered the rock material with bucket and grapple. Table 1 shows the quantity of material used in the project.

Type of Material	Quantity
Underwater rockfill	41,000 m3
Top rockfill	82,000 m3
Filter rock	51,250 m3
Length of double seal asphaltic road	2,450 m

TABLE 1: Rock quantities

Figure 7: Transportation of the armor stone

Figure 8: Placement of armor stone in site

Figure 9: North view of the project

Figure 10: Plan view showing the project finished

4. CRISTOBAL BREAKWATER

4.1 Project description

The Cristobal breakwater was built almost 100 years ago to protect the north entrance of the Panama Canal against the swell of the Atlantic Ocean. It consists of two sections called East and West breakwater.

The West section begins in the west, at a place known as Toro Point in Fort Sherman, and travels approximately 3.5 km until it reaches the Canal navigation channel, as shown in Figure 11. The East section was not considered originally because the builder were not worried about the action of the trade winds that came from the North-East. However, the General Assembly of the Navy of the United States realizes that these winds were indeed a problem for the ships anchored in the bay so it decided to authorize the construction of the East section with a length of 2.0 km, which would not reach the land side on the east.

Finally, in the 1940´s, the last section of the breakwater, connecting the easternmost section of the East breakwater and Isla Margarita on the east, was constructed (Department of the Navy, 1949). The length of this section is approximately 1.0 km and was originally built to provide shelter to hydroplanes taking off from a US military base located in this area.

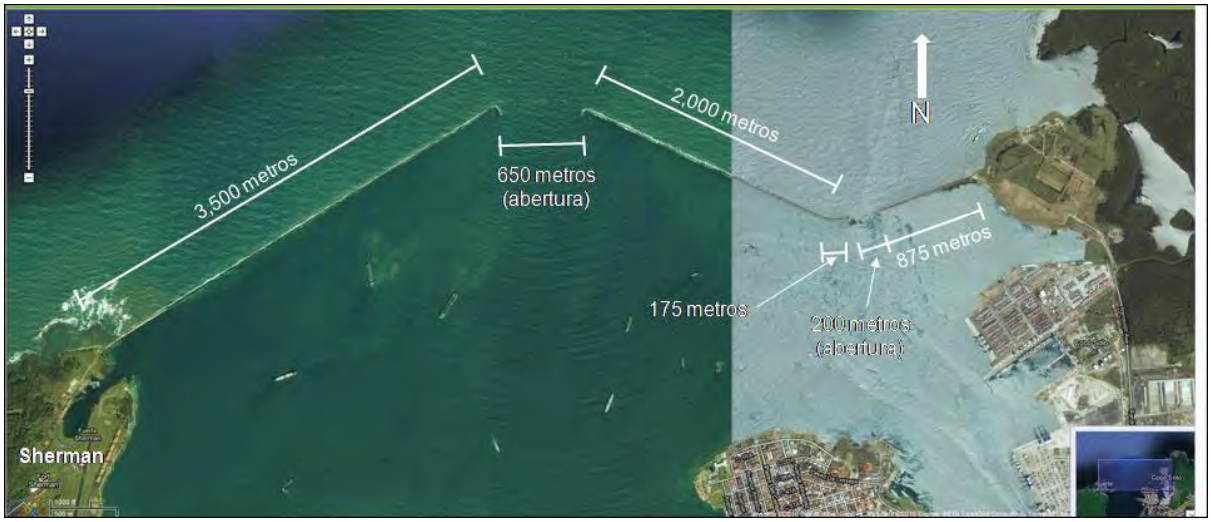

Figure 11: Plan view of the Cristobal breakwater

4.2 Construction Sequence

In 1909, the authorities in charge of the construction of the Canal established a plan for the construction of the Cristobal breakwater. At the beginning of 1910 the construction of the breakwater began.

4.2.1 West Section

For the construction of Cristobal's breakwater, a system similar to that used in the levees built in Lake Gatún and in the breakwater at the Pacific entrance was developed. The system consisted of driving piles on which a wooden structure (trestle) would be built. The trestle served as support for the rails used by the train carrying lateral unloading wagons in which the filling material for the breakwater slopes was transported (see figure 12). The core of the breakwater was constructed using this system, and later a protective shell would was placed on top (see figure 13 and 14).

Originally it was estimated that the total volume for the construction of the West side would be about 3,290,000 cubic yards of material. For the core of the rockfill, limestone was used, which was found near the area of Toro Point. However, given the fragility and low resistance to degradation by friction of the rock, it was not considered appropriate for the shell.

Figure 12: Pile driving and trestle assembling

Figure 13: Material for the core being dumped from the train

For the shell, it was planned to use a much harder and more resistant rock. Originally it was considered the basalt coming mostly from Culebra Cut. However, this rock had many joints and fault planes so it would not be possible to break into blocks large enough to resist the abrasion produced by the waves. Instead, it was proposed to use an andesite, which came from a deposit located near the town of Portobelo. This rock had characteristics of greater resistance to degradation by friction than basalt; this also allowed to extract the blocks with enough size so that they had an approximate weight of 15 tons.

Unlike the material for the core, which was loaded directly to the trains at Toro Point from the quarry located there, the Portobelo rock was transported to the site on barges. Originally the barges unloaded the blocks on railroad wagons, which were transported through the rails and threw at the specified points. Subsequently, this system was modified to allow the placement of the rock blocks directly from the barge to its final position in the breakwater using cranes mounted on the barge (see figure 14).

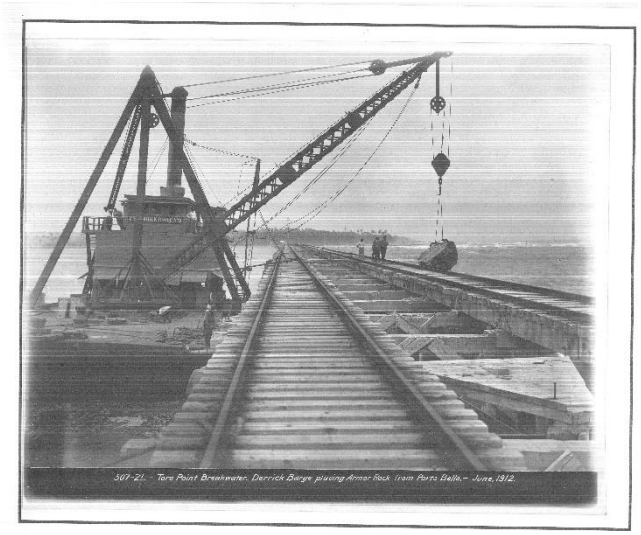

Figure 14: Rock blocks for the shell placed by a crane

4.2.2 East Section

As for the East breakwater, its construction was authorized in 1913 and started in October of that same year with the specific objective of protecting the channel of sedimentation produced by the action of the trade winds on the east coast of the bay. Unlike the West section, the material for the core and armor of the East section was brought by rail from Sosa Hill in the Balboa area. For this, the breakwater builders developed a system of rails that connected the Coco Solo area with the existing railroad used initially to haul material to the Atlantic sector from and to Panama.

The construction of this section of the breakwater used the same system as the West section, which consisted of a wooden trestle built on stilts, and on top of it were placed two rail lines to transport the material. However, unlike its western counterpart, due to topographical and economic considerations, the eastern breakwater was originally designed as a structure separated from the coast by almost 1.8 km, and with a length of approximately 2.2 km. Later this length was reduced to 1.65 km; but in 1916, despite all the damages suffered in the support trestle and railway lines, it was decided to increase the length of the breakwater to 2.0 km since the cost of it still was within the originally budget.

In addition to the rock extracted from Sosa Hill that would be used as east breakwater reinforcement, the decision was made to add concrete blocks as protection for the structure. For this reason, in 1915, a contract was awarded to a private company for the construction of 10,000 concrete blocks with an approximate weight of 15 to 25 tons each (figure 15).

Figure 15: Concrete blocks dumped for the shell of the East breakwater

4.3 Maintenance Program

As mentioned before, the main objective of the Cristobal breakwater is to protect the northern entrance of the Canal from the strong waves produced by the north winds. However, this same condition has greatly impacted the integrity of the structure throughout the years. Due to the strong waves in the area, part of the rocks initially placed in the breakwater have gradually disintegrated or have been displaced; for this reason, the structure has been losing its original form and decreasing its protection capacity.

Since its construction, the breakwater has suffered the ravages of the weather and storms in the area. Detailed reports from the construction period indicate that strong waves, produced by major storms in the Caribbean, damaged the structure several times, so the breakwater had to be repaired before it was even finished. During the last 40 decades, efforts have been dedicated to restore the breakwater to its height and original section. For this purpose, concrete blocks of different geometric shapes and sizes were initially used, but in the last 30 years, a different protection system was tested, consisting mainly of reinforced concrete lining units called dolosse (see figure 16).

The methodology for the design of this structures can be found in the literature (USACE, 2002), but basically this elements work by dissipating the energy of the waves instead of blocking it. In its design it is considered to divert aside most of the energy of the wave, which makes it more difficult to displace them, unlike objects of equal weight but with flat surfaces. As the waves hit them, the elements tend to interlock and form a more compact and porous wall at the same time.

Figure 16: 8 tons dolosse used repair the Cristobal breakwater

For the maintenance of the breakwater, ACP has developed a repairing schedule consisting in the construction of 500 reinforced concrete dolosse during one fiscal year and installing them the next fiscal year. This means that the breakwater is restored every two years.

For the construction of the dolosse, the contractors use an area next to Toro Point (west side of the breakwater) specifically designated for this task. From this area, the elements are then lifted by cranes and placed on barges, which transport them to the previously identified areas to be repaired. Figures 17 and 18 show these process as carried out by a contractor.

4.4 Breakwater zoning

Originally, the works of construction and installation of dolosse in the breakwater were programmed based on specific damages in the structure; however, this practice has been modified in recent years to allow the maintenance process to be carried out continuously. In order to determine where the damages to the structure have occurred is through a periodic inspection of the breakwater.

This visual inspection is done mainly by boat, although sometimes helicopter flights are also used; with this method it is possible to determine the exact points where the waves have moved or damaged the rocks, concrete blocks or dolosse. Once these points are identified, their exact location is determined through specialized equipment (GPS), and then plotted in a contract drawing.

ACP keeps record of all the areas repaired in the breakwater since 1982, when the dolosse were used for the first time. At that time, however, the current GPS technology was not available, so the actual location of the repairs is only approximate. Based on the plans drawn up at that time, which only indicated the approximate stationing of the damaged area, it was possible to establish, using a correlation of stationing vs. coordinates, the location where the dolosse were installed back in 1982.

Figure 17: Placement of dolosse on the barge

Figure 18: Installation of dolosse in the West breakwater

From 2001 onwards, there is a precise record of the location of the repairs done, so it is possible to establish a repair statistic for zones on the breakwater (Abrego, 2012).

The zoning that has been established in both sections of the breakwater begins from the premise that each section (East and West) have independent stationing. Therefore, station 0K+000 has been established on land for both sections: on the east side, this point is located at the beginning of extension of the 1940 breakwater, located on Isla Margarita; while for the west side, the point is located near the Toro Point lighthouse.

Given the extension of the two breakwaters, they have been divided into segments of 250 linear meters, so on the East side there are 13 zones, while on the west side there are 14 zones.

By plotting the distribution of the dolosse installed in the breakwater, it is easy to identify that most of the damage occurs in the areas near the main entrance of the Canal. In this point the structure is much more exposed to the action of the waves and the north winds. It is true that in other areas ACP have also installed dolosse for protection and repairing, however, the most critical area showing constant damage is that mentioned before (see figures 19 and 20).

Figure 19: Aerial view of the West section of the breakwater where most damages are reported

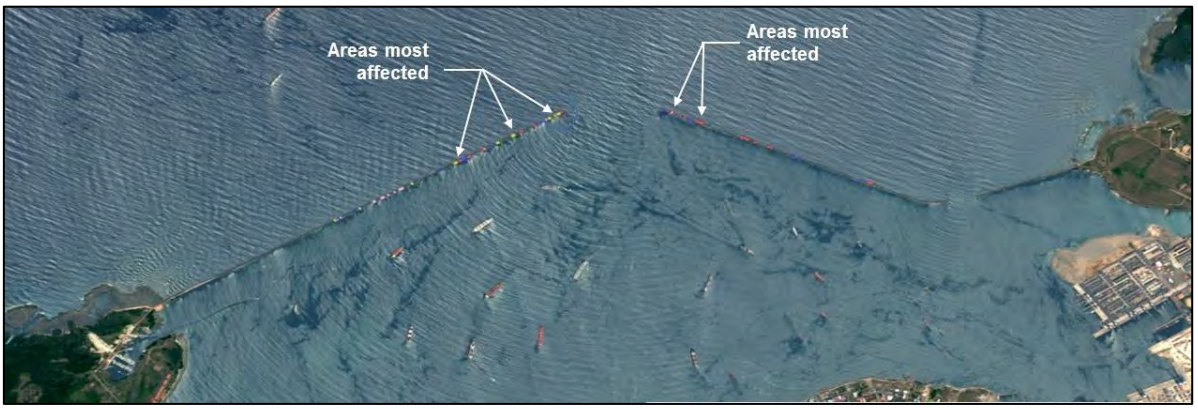

Figure 20: Plan view of the breakwater showing most affected areas

5. EROSION CONTROL FOR BUILDING 33 AND 37 IN GAMBOA

5.1 Project Description

The objective of this project was to restore the slopes around several facilities of the Dredging Division in Gamboa. In this area the buildings are located very close to the shoreline and the navigation prism line is only 20.00 m away from it. The town of Gamboa is located at the north side of the Gaillard Cut and is the base for all the dredging operations along the Panama Canal (see figure 21).

For the protection of the slope, it was decided to built-in a riprap with an extension of 300.00 linear meters, and for that it was necessary to install 8,000 m3 of rock blocks to control the erosion. The erosion in this area is produced mainly to the surge wave acting against the shoreline. In this point, all the vessel transiting northbound are exiting the narrowest section of the Panama Canal, the Gaillard Cut, therefore, once they reach Gamboa, there is an increase in their velocity which contributes to enhance the surge waves acting on the slopes.

Figure 21: Location of the affected area in Gamboa

5.2 Design Criteria

Once the problem was reported, several meeting took place with the owner of the facilities at risk in order to develop the scope of the repairs and verify their needs in terms of operational requirements.

In general, the design was develop to meet the following criteria:

- The structure must be permeable;
- Crest Elevation at 28.20m (considering the maximum elevation of Gatun Lake);
- The slope must be stable at each construction phase;
- The armor rock size must be big enough to control wave heights of 1.0 m above the maximum elevation of Gatun Lake (27.13m PLD)
- The navigation prism line is located 20.00m away from the shoreline (not the base of the slope);
- Distribution of ships: Neopanamax and tugboats
- The rock protection only covers the portion of the slope above the lake level and extends 1.00m below the minimum level of the lake (23.9m PLD)

5.3 Design

The typical developed section consists of a two-layer armor stone, with a geocomposite at the base, a splash apron of 3.0 m and a minimum subaquatic bench of 3.0 m, as shown in figure 22.

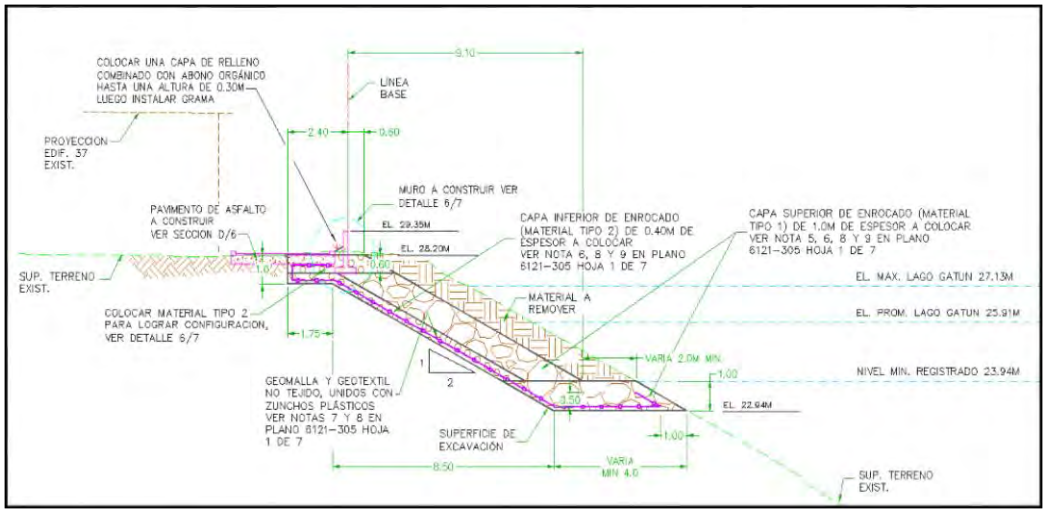

Figure 22: Typical design section

The grading of the rockfill used in the protection of the slopes was calculated according to the Hydraulic Engineering Circular (1989) and PIANC (1997). Table 2 shows the values for the rocfill:

Top Layer (Material Type 1)	
Rock size (m)	% passing
1 a 0.9	100
0.80 a 0.70	85
0.60 a 0.50	50
0.30 a 0.20	15
Underlayer (Material Type 2)	
Rock size (m)	% passing
0.30	100
0.20	50
0.10	15

TABLE 2: Rockfill grading

5.4 Construction

An important aspect of this project was the variety and quantity of restrictions imposed by the owner for the construction stage. Some of those restrictions were:

- The riprap would only be located on the upper part of the lake bank slope, where the toe of such slope is the navigation prism. Therefore, the rocks had to be placed with a small backhoe to avoid falling rocks to go beyond the prism line of navigation;

- The project is located in an area adjacent to Gatun Lake and near several facilities (offices, dock and green areas); the contractor had to restrict its construction area to small sections that were defined between 5 to 10m, with two work fronts (north and south). This was done to guarantee that the contractor completed each section before moving to the next one, thus ensuring the stability of the slopes;

- The contractor proposed to build the rockfill from the landside (avoiding the use of barges). For this, it was necessary to build a bench at the minimum level Gatun Lake would allow; thus ensuring the excavation of the underwater bench (base of the rockfill). In addition, the contractor had to use equipment with a minimum arm range of 8.00m;

- The existing soil in the slopes is a fill composed of residual material, which required the use of a geocomposite (geotextile and geogrid) to separate it from the rockfill. The geogrid was intended to protect the geotextile and distribute the load of the rockfill on the surface;

- The drains had to be extended and built through the rock.

Figure 23: Panoramic view showing the condition of the slope in 2012

Figure 24: Anchor trench for the geocomposite

Figure 25: View of the rockfill from the north

Figure 26: Aerial view of the finished project in 2017

References

Abrego, A., (2012), “Reporte de instalación de dolos en el rompeolas de Cristóbal”, Panamá Canal Authority, Internal Report.

CIRIA/CUR, (2007), “The Rock Manual. (2nd edition),”CIRIA C683, London, 2007.

Department of the Navy – Naval History and Heritage Command (1946), “Building the Navy’s Bases in World War II, Volume II, Part III - The Advance bases”, The Navy Department Library, Chapter XVIIII, Bases in South America and the Caribbean Area, Including Bermuda.

Federal Highway Administration. Hydraulic Engineering Circular No.11, (1989) “Design of Riprap Revetment”.

Hudson, R.Y., (1953), “Wave forces on breakwaters,” Trans Am Soc Civ Engrs, Vol 118.

Hudson, R.Y., (1959), “Laboratory Investigations of Rubble-Mound Breakwaters,” Proceedings of the Waterways and Harbors Division, American Society of Civil Engineers, Vol 85, No. WW3.

PIANC (1997), “Guidelines for the Design of Armoured slopes under Open Piled Quay Walls,”Report of Working Group No. 22 of the Permanent Technical Committee II, Brussels.

Pilarczyk, K. W. et al., (1989), “Dikes and revetments: Design, maintenance, and safety assessment. AA Balkema, Rotterdam.

Pilarczyk, K. W., et al., (1995), Coastal and Shoreline Protection: Erosion Control Using Riprap and Armourstone,” John Wiley & Sons, Chichester

USACE (2002), “Fundamentals of Design,” Chapter 5, Coastal Engineering Manual – Part VI, EM 1110-2-1100, April 2002

US Department of Transportation (1989), “Design of Riprap Revetment,” Hydraulic Engineering Circular No. 11, Publication No. FHWA-IP-89-016, Virginia, March 1989.

W. P. Woodring, (1957), “Geology and Paleontology of Canal Zone and Adjoining Parts of Panama,” Geological Survey Professional Paper 306-A, United States Department of The Interior, Washington.

PANAMA CANAL´S BANK LIGHTING

by

Rossana Peralta[1] and Maria Mora[2]

Abstract—Operating a recently expanded 24/7 waterway, while maintaining safety standards and addressing new traffic challenges requires the use of reliable aids to navigation systems. These aids to navigation systems include maritime buoyage system, sector lights with oscillating boundaries, ranges, and a bank lighting system. The bank lights installation is similar to lights on an airport runway, these are present on the east and west sides of the banks at the narrowest parts of the navigation channel, at Culebra Cut and at the approaches to the locks. The associated distribution power lines were scaled in order to meet the needs of the Panama Canal expansion and the construction of nearly 9 kilometers of access channels to the new locks on both the Atlantic and Pacific sides.

The first Bank Lighting system on the Panama Canal was installed between 1959 and 1961, and consisted of cool white light fluorescent fixtures. Over the years, the fluorescent fixtures were replaced with amber light low pressure sodium fixtures (LPS). For the Panama Canal expansion the new Bank Lighting project considered a technology migration to LED fixtures, keeping the performance in color and light output of the existing with a higher life expectancy, and lower maintenance costs. Over 10 km of overhead power distribution lines and 6km of underground power distribution lines were built in order to illuminate the east and west banks of the new access channels.

This paper presents the planning, design and construction of the electrical infrastructures and lighting system needed for the new Panama Canal´s bank lighting.

1. INTRODUCTION

One of the components of the expansion program of the third set of locks of the Panama Canal considered the adjustments required to provide navigation assistance systems for the new channels. These adjustments included new maritime buoyage system, sector lights with oscillating boundaries, ranges, and a bank lighting system. The bank lights were installed on the north approach to the Agua Clara locks and the north and south approaches of Cocoli locks. These lights are installed in the narrowest parts of the navigation channel and help to ensure the safety of ships in night transit demarcating the limit between water and land on the banks of the canal.

For the Agua Clara Locks access, over 65 luminaires on the west bank and more than 70 luminaires on the east bank, were installed, as shown schematically in Figure 1.

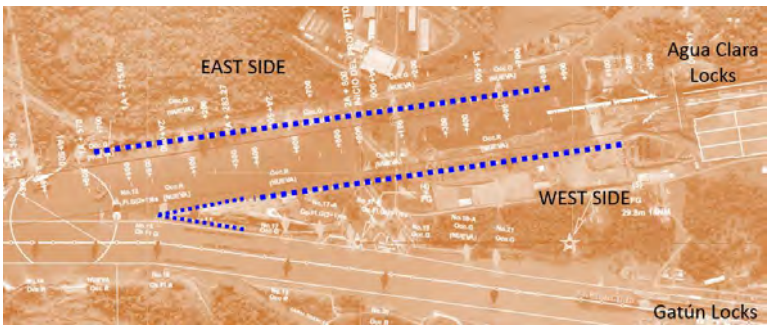

Figure 1: Atlantic Entrance Fixtures Layout

[1] Electromechanical Engineer, Panama Canal Authority, rperalta@pancanal.com.
[2] Electromechanical Engineer, Panama Canal Authority, mmora@pancanal.com.

At the north access of the Pacific Locks, over 170 luminaries were installed on the west bank and more than 165 luminaries on the east bank, spaced at 30 meters. In the bifurcation between the access to Pedro Miguel Locks and the new locks, 5 luminaries spaced every 20 meters were installed.

At the southern access to the Pacific Locks, more than 30 luminaires on the west bank and over 25 luminaires were installed at the bifurcation between the access channel to the Pacific Locks and Miraflores Locks.

2. **PLANNING**

The manufacture of the luminaire supports and their installation had always been executed through internal labor. However, due to the extent of the works for the expanded channel and considering the interaction with the Contractors of the new Locks and of the Approach Channel to the Pacific Locks, it was necessary to elaborate schemes for the supply of luminaires, manufacture of luminaire supports, extension of primary and secondary power lines in access channel to Atlantic Locks and extension of primary and secondary power lines in access channel to Pacific Locks. The luminaires at the southern access of the Pacific Locks were installed by internal force.

3. **DESIGN**

The required designs and specifications included studies for the replacement of Low Pressure Sodium luminaire to LED luminaire technology, designs and specifications for the fabrication of support arms, design and specification for the Atlantic works, design and specification for the North Pacific works and design for the South Pacific east and west banks works.

3.1 FIXTURES

For the development of the procurement specifications of the new luminaires, market studies, software simulations, field tests with measurements and validation by the Panama Canal pilots were carried out. These ensure the availability of heavy industrial proven solutions, with light color similar to the existing technology installed in the Culebra Cut, which would not cause glare to ship pilots, and friendly to the existing wildlife and environment of the area. Figure 2 shows a view of the software model simulation.

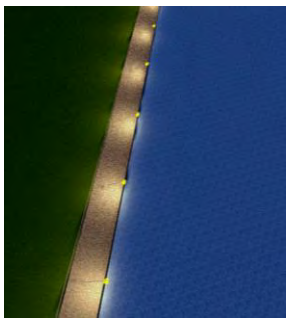

Figure 2: Software model of fixture arrangement

3.2 SUPPORT ARMS

The aluminum arms that support the luminaires have an extension of 6 meters in length and a pivot mechanism that facilitates the maintenance of the luminaires from the ground. To ensure the proper supply and operation of the arms, careful mechanical design drawings were developed, including detailed instructions for their manufacture, painting, delivery and storage.

3.3 ATLANTIC ENTRANCE WORKS

The design process for the works required in the Atlantic area begins with field inspections, surveying existing infrastructures, study of new channel design drawings and new locks. The conceptual design considered for the east bank the extension of about 2.8 kilometers of electrical circuit in medium voltage-12kV from a new electric substation, "Agua Clara", built to ensure reliable power supply to the Atlantic Locks. Due to the restriction in safety distances between the navigation channel, existing street, high-voltage aerial line and railroad tracks, this circuit was extended underground.

For the west bank, restrictions for vegetation and existing water lines required the construction of a section of 650mts of electric line with insulation for 12kV in protected cable. To the north the lines go near a heliport area that imposed restrictions on the use of air space. It was necessary to extend 550mts of the underground line.

Once the primary lines are built, low voltage distribution transformers provide the required voltage for the luminaires. From each distribution center, two secondary circuits, north and south, are derived, for a more reliable arrangement, each luminaire has an individual protection to prevent the failure of one affecting the rest of the circuit.

3.4 NORTH PACIFIC ENTRANCE WORKS

The design process for the works required in the north Pacific sector included field inspections, surveys of existing infrastructures, study of design drawings for the new access channel, dams and new locks. Figure 3 shows the wok area considered.

On the west bank, the extension of two 12kV circuits of 3.5 kilometers each in aerial configuration were built. For reliability, these circuits one north and one south have mooring capacity in a central point.

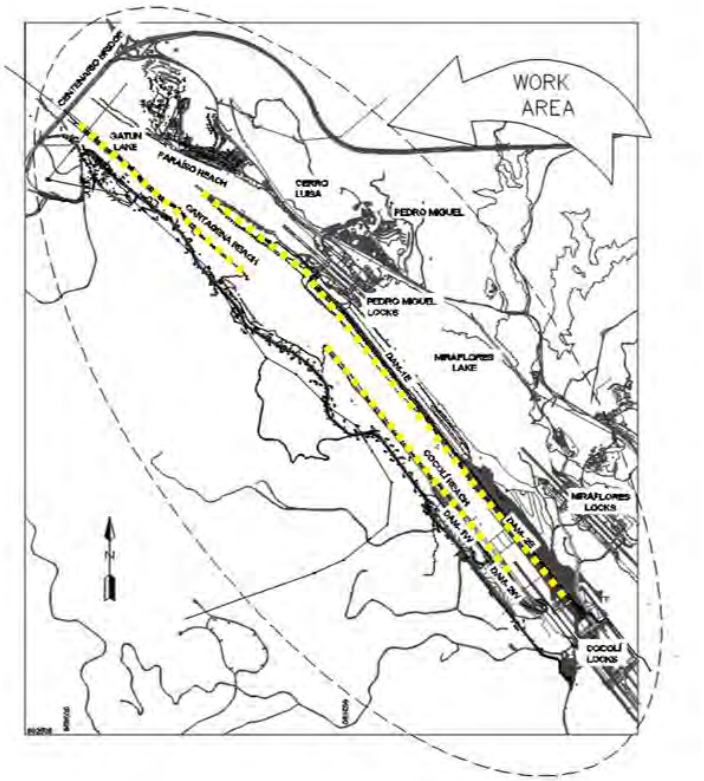

Figure 3: North Pacific Entrance

The east bank of the new north access canal to the Cocoli Locks is on the new island and is defined in most of its extension by the dam that divides Lake Gatun from Lake Miraflores. For this area the construction of an underground electric line of approximately 5 kilometers was considered as the most reliable solution for the electrical supply of the system.

3.5 SOUTH PACIFIC ENTRANCE WORKS

All the works in the South Pacific access to the new locks was executed with internal workforce. On the west bank, approximately 2 kilometers of medium voltage electric lines were extended. This branch that feeds navigation aid systems on the west bank, is provided with a normal power circuit and an alternate backup circuit.

In the eastern area, the bifurcation between the original canal and the new locks was illuminated, extending a secondary underground circuit from the electrical system of the locks. The lock´s electrical systems is highly reliable, with backup systems and redundant systems.

4. CONSTRUCTION

The process to the fixtures procurement was developed along with the Engineering Division of the Panama Canal and the Maritime Signaling Workshop of the Dredging Division, with the of Canal Port Captain and Contracts Division. The Maritime Signaling Workshop was also in charge of the fixtures final wiring and installation of all work areas.

The support arms procurement task was developed by specialists in Machine Design, Maintenance and Specifications. These items were manufactured in Panama with local contractor.

At the Atlantic Entrance the works were executed both with local contractors and internal workforces. The North Pacific Entrance works were executed by local contractor. At the South Pacific Entrance the works were executed by internal workforce alone, these works included tasks executed by floating crane Goliath in water.

The works were executed within the budgeted and without affecting the execution and delivery of the construction of the new locks and main dams. Figure 4 shows the South west Pacific entrance to Cocolí Locks banks lights in service.

Figure 4: South Pacific Entrance: West Victoria Reach bank lights-Photo by Edward Ortiz

Landslide Control Program at the Panama Canal

by

Carlos A. Reyes D.[1], Yesenia Cerrud [2], Laurentino Cortizo [3], Maximiliano De Puy [4]

ABSTRACT

Since the beginning of its construction, the safety and reliability of the Panama Canal excavations and dam structures have been a challenge**,** due to the heterogeneous and complex geological setup, added to a highly variable rainfall regime comprising average daily precipitations of 140 mm. At the Panama Canal a program has been adopted for the detection of landslide activity in its early stages to mitigate the related consequences and maintain the Canal operation. This program has been named as the Landslide Control Program and was implemented in 1968.

The execution of improvement projects to the navigation channel, including the construction of containment dams, excavations for widening, straightening, and deepening the navigation channel, especially the recent Canal Expansion, represented new challenges in the surveillance process. To overcome the new challenges, the Panama Canal Authority has undertaken an improvement process to incorporate state-of-the-art robotic and real-time monitoring technology. This paper presents the importance of the Landslide Control Program, and describes the methodology used to identify instabilities using data from the different types of instruments installed along the waterway, and the Protocol set forth for their stabilization.

1. INTRODUCTION

Landslides were a prevailing aspect since the construction of the Panama Canal. They resulted in 40 million cubic meters of additional excavation. Indeed, the most difficult problem related to the building of the Panama Canal was the control of landslides in Gaillard Cut, the narrowest segment of the waterway, 12.6 km in length, where the Canal crosses the Continental Divide (see Figure 1). The slopes in Gaillard Cut were shaped from the deep excavation required to build the Canal and the occurrence of landslides during this construction period was mainly due to the unstable geometry of the over-steepened slopes.

The slopes of Gaillard Cut have evolved continuously throughout the history of the Canal, as a result of the excavation of the original construction, the Canal widening, the straightening and deepening, the removal of landslides debris, and more recently, of the Canal Expansion. All these events have imposed new challenges in the surveillance process and demanded the use of new techniques for data acquisition and detection of landslides, improving the process through the years, to become a more efficient tool for detecting and evaluating landslide-prone terrains.

In 1968, Dr. Arthur Casagrande, acting as a consultant for the Panama Canal Company (PCC), recommended an empirical observational method to detect incipient landslides in Gaillard Cut. The complex geological environment in Gaillard Cut precludes the use of analytical methods as a tool for reliable predictions of slope movements. This observational method has undergone several improvements in the subsequent years, becoming progressively more reliable. It evolved to what is known today as the Landslide Control Program that has helped to detect and stabilize numerous potential landslides.

[1] Panama Canal Authority, Balboa, Panama, CAReyes@pancanal.com
[2] Panama Canal Authority, Balboa, Panama, YCerrud@pancanal.com
[3] Panama Canal Authority, Balboa, Panama, LCortizo@pancanal.com
[4] Geotechnical Consultant, Panama, MaxDePuy@gmail.com

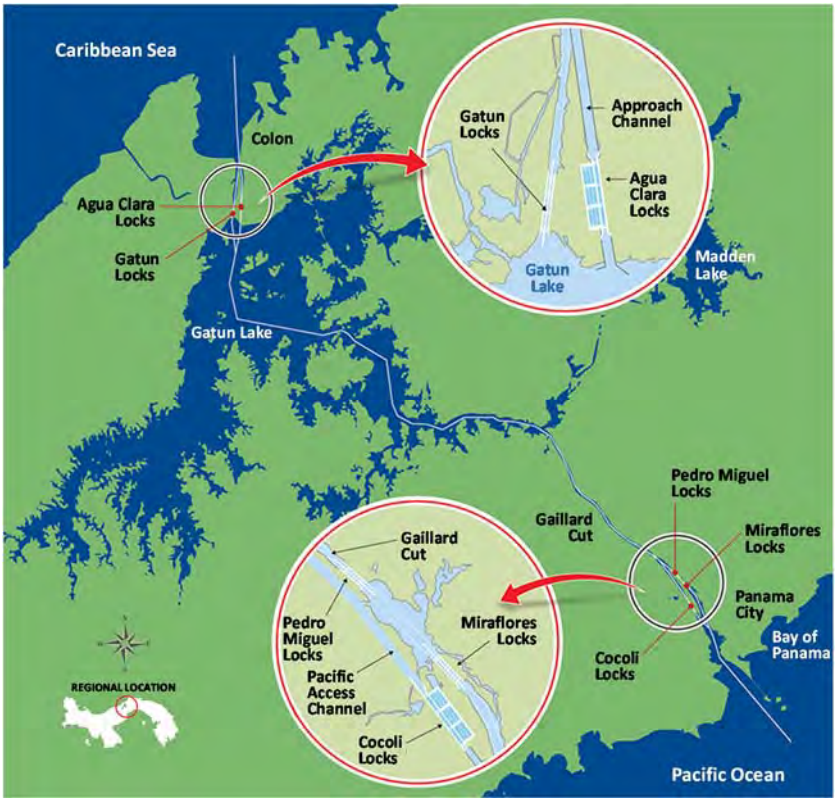

Figure 1: Gaillard Cut in the Panama Canal

Presently, the Landslide Control Program involves the surveillance of surface control points distributed along the banks, not only of the Gaillard Cut but also at the Pacific Access Channel (PAC). The observational method has demonstrated to be effective, particularly in areas with difficult geological conditions, as those present in Gaillard Cut. Also, the Landslide Control Program includes subsurface monitoring instrumentation installed in the excavated slopes and containment dams. It makes use of Casagrande and Multipoint Piezometers; traveler pipes for locating slip surfaces; open wells for ground water readings; among other instruments.

The Pacific Access Channel is a 6.2 km waterway, 218 m wide, derived from the south end of Gaillard Cut toward the new Cocoli Locks in the Pacific side (see Figure 1), that allows the transit of Post-Panamax vessels, at Gatun lake level of 25.91 m PLD (Precise Level Datum for the Panama Canal) and is separated from the Miraflores Lake (elevation 16.45 m PLD) by the East Borinquen Dams. This new access channel has cut slopes that have the potential to block the navigation channel in the event of a massive landslide.

In order to be more efficient and effective in detecting the potential risks of channel encroachment due to landslides in Gaillard Cut and the Pacific Access Channel, the Panama Canal Authority (ACP) allocates significant resources in state-of-the-art monitoring and data acquisition equipment to monitor different types of instruments installed along the banks of Gaillard Cut and the banks and containment dams along the Pacific Access Channel.

2. BRIEF HISTORY OF THE LANDSLIDE CONTROL PROGRAM

In May 1968, at the beginning of the rainy season, the Canal was threatened by a major incipient landslide. Hodges Hill, a Canal slope in Gaillard Cut, developed cracks about 2 meters across, just north of the Continental Divide and was in imminent danger of completely blocking Canal traffic for a month or more. A board of prominent consultants, among which was Arthur Casagrande, was convened to recommend a solution to the crisis. They recommended a stabilization plan consisting of nineteen horizontal drains drilled into the hill from the bank of the Canal, together with extensive drainage

systems installed on the upper slopes to divert runoff from the ground cracks. This action was implemented at a cost of $400,000, much lower than the $10 million considered necessary initially for a massive remedial excavation.

Under the leadership of Dr. Arthur Casagrande (see Figure 2), the board also recommended that the Canal initiated a "systematic surveillance of the banks of Gaillard Cut… to cover all critical slopes on both sides", an empirical observational method to detect incipient landslides. This recommendation was given due to the complex geological conditions in Gaillard Cut, which invalidate the use of analytical methods as a tool for early detection and improved control of landslide activity. The Landslide Control Program was created in response to this recommendation the following year. The program was referred to as the "Bank Stability Surveillance Program" or BSSP, which is now referred to as the Landslide Control Program.

Figure 2: Inspection at Hodges Hill Landslide - Beginning of Modern Landslide Control Program (1968)

3. GEOLOGY

The Geology of Gaillard Cut and the Pacific Access Channel is complex. It is composed of a series of weathered tuffs and sedimentary deposits interspersed with strong igneous hills. This geological environment in combination with the average rainfall regime of the area, of about 2,000 mm per year, pose a high and continuous risk of landslides along the banks of these navigation channels. In fact, the evidence shows that rainfall is the single most important cause of landslides in Gaillard Cut.

Don C. Banks et al, from the U.S. Corps of Engineers (1975), observed that "Rock formations exposed at shallow depth in the banks of the Panama Canal through Gaillard Cut are believed to range in age from Eocene to Miocene. All the rocks have been derived through volcanic and/or sedimentary processes from volcanic sources. These processes, alone or together, can result in a multitude of rock types. Accordingly, the banks revealed coarse, thick breccia formed with the involvement of sedimentary processes; thick massive volcanic conglomerates formed by rapid accumulation in water-filled basins; air-fallen tuff and tuff breccia; tuffaceous varieties of sandstone, siltstone and shale; and a few intrusive igneous rocks" (see Figure 3).

The sedimentary rocks, derived from marine and terrestrial deposits of both alluvial and volcanic origin, are highly variable, and many of the recurring beds are extremely weak, sometimes slickensided, and often expansive. These rocks are the vehicle for most landslide activity in the Cut, and the Cucaracha formation was a prime factor in the development of the massive slides of the later construction years.

The much stronger volcanic rocks, mainly agglomerates and basalts, also play an important part in Gaillard Cut landslide activity. The unusual sequence of geologic events, caused these igneous rocks

to form the peaks of many hills bordering the Canal, while the weaker sedimentary rocks support them, also forming the flatter lower slopes and the valleys between. The Canal was excavated through such valleys, resulting in basically unstable slopes. The intensive faulting in the Cut aggravates the problem by providing weakness planes to form the sides and "backscarps" of potential slides.

In addition, the bedding of the sedimentary formations generally dips downward from the east bank to the west in the Gaillard Cut, which has a mixed effect on landslide activity. Under this condition, east bank slopes tend to fail by traslatory motion along the inclined beds dipping toward the Canal, whereas on the west bank, where the bedding dips into the slope, slides are more likely to develop along circular failure surfaces.

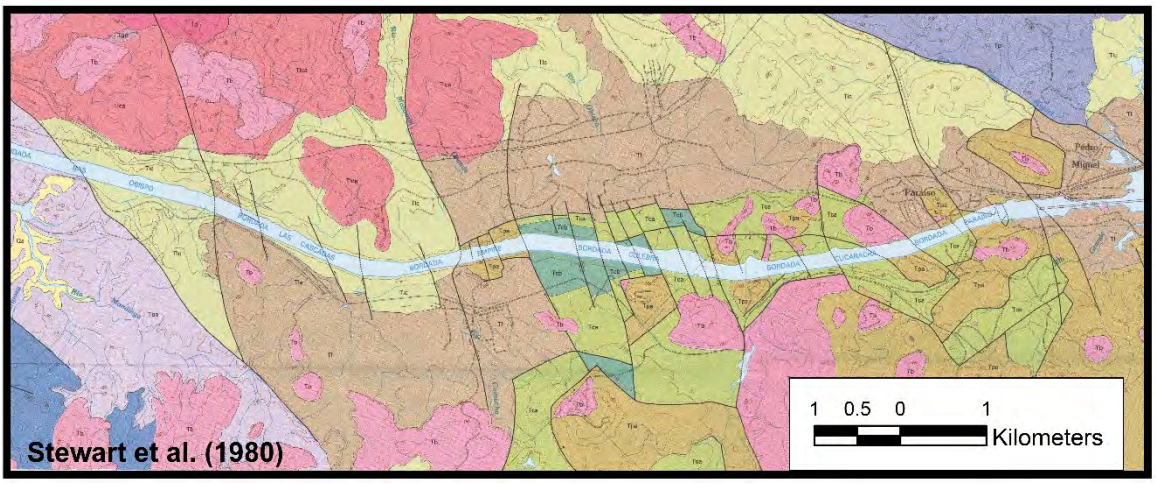

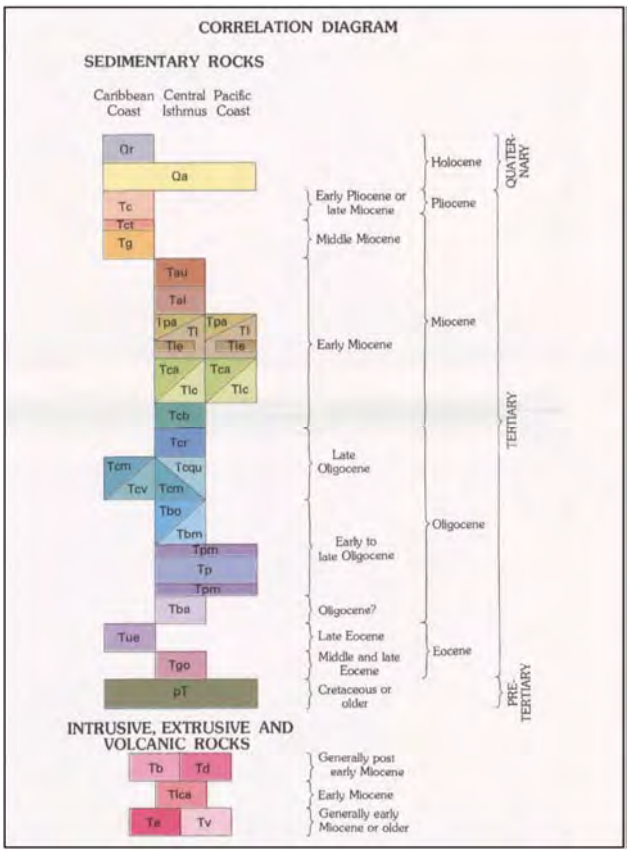

Figure 3: Geological Map of the Gaillard Cut

4. RAINFALL REGIME

Panama has a tropical rainy climate, hot all year round, with a dry season that usually commences at January and lasts until April, and a rainy season from May to December. The average annual rainfall in the Panama Canal is approximately 2000 mm and 2030 mm in Gaillard Cut. There are eleven meteorological stations located along Gaillard Cut and the Pacific Access Channel (see Figure 4): Gamboa, Cascadas, Sardinilla, Empire, Culebra, Gold Hill, Pedro Miguel, Miraflores, Cerro Cocoli, Victor Valdez and Cocoli 326. The data obtained from the meteorological stations is correlated with the pore pressure and surface deformations of the slopes, to analyze the soil behavior for managing and controlling landslides.

Figure 4: Location of meteorological stations along the Gaillard Cut and the Pacific Access Channel

When the sloped areas become entirely saturated, and the infiltration recharges the water table on the slopes, most of the time, landslides can occur. Heavy prolonged rainstorms, in the absence of some other external factor, trigger the majority of landslides in Gaillard Cut.

5. NATURE AND HISTORY OF LANDSLIDE ACTIVITY IN GAILLARD CUT

Since the construction of the Panama Canal until the Canal Expansion, about 545 million cubic meters of soil and rock were excavated. During the initial construction period, several major landslides occurred as the excavation of the waterway across the Continental Divide progressed to form what today is known as the Gaillard Cut. The constructors selected an arbitrary slope of 3V:2H for the excavated slopes along the whole length of the cut, either side, despite the type of materials found or required depth of the cut. The materials being excavated were too weak to sustain the excavated slopes. In addition to the weak strength of the rock, the rainfall water infiltration, the heavy blasting used to fracture the material to be removed, and the surcharge of the slopes with spoil were contributing factors to the development of such landslides.

Furthermore, the mechanics of landslides were not completely understood at the time and it was considered more economical and faster to allow for the landslides to develop and just remove from the toe of the slopes the mass that had moved until a stable slope was attained. The fact that such slopes had to be much flatter than required for stability before initial failure, due to the progressive weakening of the constituting materials, was not realized until much later.

Once the canal started operations in 1914, many slides reactivated, moving gradually or intermittently, and new slides developed in over-steepened slopes that had not yet failed, closing the waterway in several occasions. Most of the slide reactivations, or extension landslides, in Gaillard Cut are generated by the strain softening effects in weak rocks, and by prolonged periods of high precipitation that causes pore water pressure build-up. Other important factors in the development of landslides is the swelling of the underlying sedimentary material due to the unloading caused by excavations and the presence of sedimentary strata dipping towards the canal and discontinuities.

Most of these slides have been active more than once. Also, some failures occurred as a consequence of the improvement and maintenance of the navigation channel. Since year 1915 until 2017, there have

been a total of 175 landslides in Gaillard Cut. Figure 5 presents a chart indicating the number of landslides that have occurred per year.

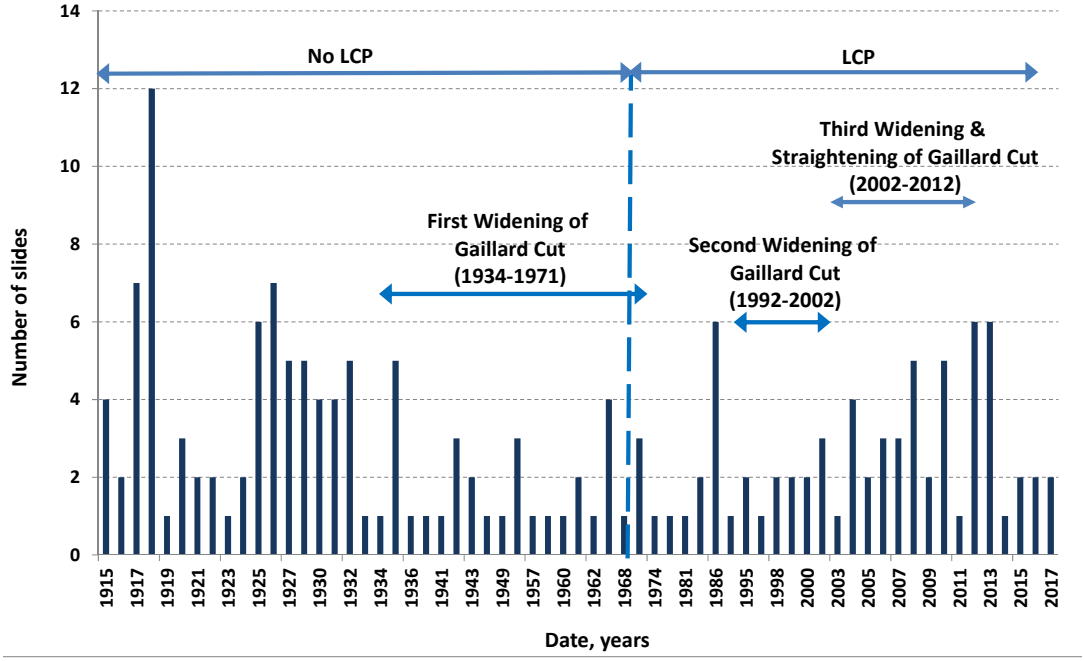

Figure 5: History of Landslide Activity (1915-2017)

6. CHANNEL IMPROVEMENTS

In addition to the internal factors already mentioned, the Gaillard Cut, being the narrowest section of the Canal, has undergone several improvement programs for its widening, deepening, and straightening:

- The Gaillard Cut Widening from 91.4 m to 152.4 m (300 feet to 500 feet), which was carried out completely on the west bank of the canal;
- The Second Gaillard Cut Widening from 152.4 m to 192 m (500 feet to 630 feet) at the straight segments and to 222 m (730 feet) at the curves, which affected both sides of the canal avoiding the most sensitive areas, such as the Cucaracha sector;
- The Third Widening & Straightening Program, from 192 m to 218 m (630 feet to 715 feet) at the straight segments;
- And the Canal Expansion Program, that included:
    - Further widening and straightening of the Gaillard Cut,
    - The construction of a new third set of locks, both at the Atlantic and Pacific sides of the Canal,
    - The excavation of a new access channel, with a length of 6 km, constructed to connect the Gaillard Cut with the Pacific Third Set of Locks, which required about 50 million cubic meters of unclassified excavation and the construction of four new earth fill dams, normally referred to as Borinquen Dams.
    - The widening and deepening of the canal entrances at the Pacific Ocean and the Caribbean Sea, and
    - The deepening and widening of the navigational channel through Gatun Lake.

A consequence of these improvement projects is the removal of all existing instrumentation in the areas affected by excavations. This is also true for any earthwork project that is performed for the remedial of instabilities. New instruments are installed following project completion. The amount, type, and location of the instruments is defined depending on final cut slope geometry, properties of constituent

materials, known geologic structures, past landslide activity, and remaining failure planes: The greater the landslide hazard is, the more instruments are installed.

7. IMPLEMENTATION OF THE LANDSLIDE CONTROL PROGRAM

The objective of the Landslide Control Program is to identify and remediate potential instabilities along the banks of the Panama Canal. The main benefit of the program is to reduce the risk of blockage or serious encroachment in the navigation channel.

7.1. Management

The Geotechnical Branch of ACP's Engineering Division is in charge of the management of this program; carries out all engineering work under this program, interprets and analyzes all data, performs all instrument installations, and develops any stabilization plans needed.

Also, the Geotechnical Branch issues an annual report which comprises: the history of landslide activities in Gaillard Cut from 1915 to the present; a description of the stabilization projects and other remedial works executed on the reporting year; projects to be executed the following year; the new surface and subsurface instrumentation to be installed; the location of all existing instrumentation, per type and sector; and the rainfall data and location of meteorological stations.

Other ACP branches support the program, such as Surveys Branch, which is responsible of the instrumentation readings; Maintenance Division, which performs the construction and maintenance of all access roads and drainage works, and the Dredging Division, in charge of removing any material that falls into the navigational channel.

7.2. Zonation Scheme of Gaillard Cut

A zonation scheme was developed for Gaillard Cut, resulting in 22 sectors that contain segments of the Cut characterized by similar topographic and geologic conditions Likewise, the Pacific Access Channel was divided into 4 sectors for monitoring purposes (see Figure 6). All sectors with existing or potential landslide activity in Gaillard Cut and the Pacific Access Channel are periodically monitored.

Figure 6: Surveyed Sectors in Gaillard Cut and Pacific Access Channel

7.3. Drainage Networks

Due to the significant effect rainfall has on the stability of the slopes, a series of drainage networks have been constructed along the banks to intercept the rainwater runoff and conduct it before it infiltrates the soil. The program also contemplates the regular maintenance of these networks.

7.4. Landslide Remedial Costs

The mitigation of landslides in the Canal represents savings in that the earthworks performed are far more economical than the losses resulting from the blockage of the navigation channel caused by a landslide and the subsequent removal of debris by dredging operations.

Figure 7 shows the number of landslides that have occurred in Gaillard Cut and the costs of the corresponding maintenance or remedial works, per year, from 1968 to 2014. It is a collection of historical failures due to rainfall.

The information was taken from the Panama Canal Company annual reports (1952-1980), the Panama Canal Commission annual reports (1980-2000), the LCP annual reports, the Risk of Landslides in Gaillard Cut Report (1988), and from the estimation of landslide shapes shown on published maps. Costs were not available for all of the events. Therefore, costs were estimated multiplying the excavation and dredging volumes by the corresponding unit costs in US dollars for the year 2014. For those remedial projects having cost information, costs were brought to their value in year 2014 by applying an annual increment of 2.5%.

In Figure 7, the year 1986 stands out from the rest with a total cost of 41.7 million dollars due mostly to the historical reactivation of East Cucaracha Slide on October 13th. The total volume of the stabilization works was about 3.5 million cubic meters. Of this volume, approximately 400,000 cubic meters fell into the navigation channel and were dredged (see Figure 8).

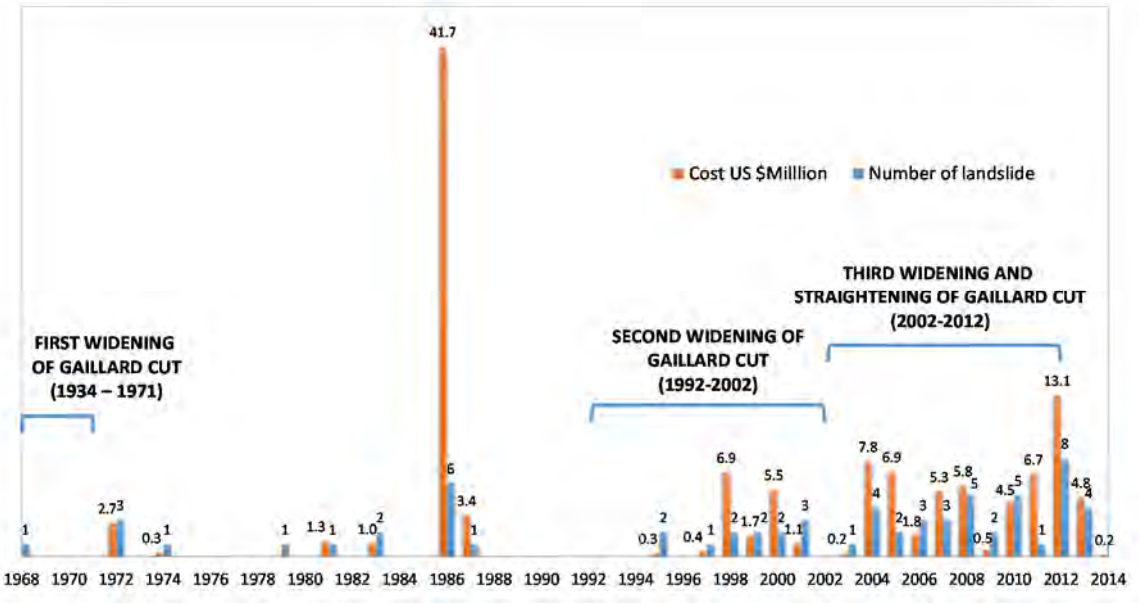

Figure 7: Landslides & Costs of Remedial Works (1968-2014)

Figure 8: East Cucaracha Slide Reactivation of October 13, 1986

8. INSTRUMENTATION

Due to the existence of many slide-prone areas along the Gaillard Cut and the threat they represent to the continued traffic of vessels along the canal, continued surveillance of slopes is performed by means of superficial and subsurface instruments. The instrumentation installed along Gaillard Cut is the main component of the monitoring program to obtain a picture of the slope behavior. The primary purposes of the instruments are to locate the slide surfaces, and to monitor the rate of movement and the variation of water pore pressures which could affect slopes stability. These measurements are used for detecting and forecasting landslide events and for issuing alerts. The different types and quantities of instruments installed in Gaillard Cut and the Pacific Access Channel are listed in Table 1.

Table 1. Landslide Control Program instruments

Instrument	Description	Quantity
Casagrande piezometers	Measurement of pore pressure at specific depth.	40
Multipoint piezometers	Measurement of pore pressure at different elevations in the same borehole.	33
Observation Wells	Measurement of the water table.	41
Traveler pipes	Measurement of depth of slide surfaces.	35
Real-time vibration wire piezometers	Real-time measurement of pore pressure at different elevations in the same borehole.	37
Real-time settlement cells	Real-time measurement of settlement and heave in soils.	2
Inclinometers	Measurement of subsurface movements and deformation.	4
Post-processing Superficial Monuments	Measurement of surface movements.	725
Real-time Superficial Monuments	Real-time measurement of surface movements.	165

8.1. Superficial Instrumentation

Superficial monitoring of movement is carried out on a continued basis for the early detection of slide activity and the timely execution of the corresponding remedial works. For this purpose, a series of

control points or monuments comprised of a steel pipe 955 mm tall, embedded in concrete and extending down 600 mm into the ground, with a pedestal at the top end to fix a reflecting device, are placed within the limits of each area to be monitored. In the Gaillard Cut, there are currently more than 700 active monuments being monitored. The position of each monument is periodically surveyed, normally on a monthly basis.

Although the monthly collection of data have proven sufficient for the confident detection of incipient movement, the frequency of surveys is increased for sectors where movement patterns are detected, especially when field works are conducted at such areas, to secure the safety of the personnel.

Surveying of monument positions is performed using Total Stations. A Total Station integrates an Electronic Distance Measurement (EDM) device with an electronic theodolite, and is capable of determining the distance and angles from the instrument to a particular point. The measurement is accomplished by the emission of a modulated infrared carrier signal which is redirected to its origin by a prism reflector at the target location. The signal is modulated at multiple frequencies, and the distance is obtained from the count of the integer number of wavelengths for each frequency.

The Total Station is placed on a fixed location with known coordinates at the bank of the Canal opposite to that where the monument to be surveyed is found. The monument position is recorded, along with the date of the reading, as displacements in the northing, easting, and elevation axes. With these data, the position coordinates of each surveyed monument are obtained and recorded.

Such data is transferred using ASCII text files to a software extension for ESRI ArcGIS developed by ACP personnel. The software extension reads the input files and thoroughly validates each position reading against a set of rules:

- Monument ID not found - new Monument ID
- More recent reading than current one found in database
- Displacement distance larger than threshold
- Displacement distance of zero
- Monument Location outside defined sectors
- Duplicate Monument ID & Date combination found in input
- Reading Date more recent than System Date
- Reading with coordinate values that are Null, Zero, or Outside valid ranges
- Duplicate coordinates & different Monument IDs found in input
- Existing Monument ID having no previous Readings
- Duplicate Monument ID & Date combination found in database
- Duplicate coordinates & different Monument IDs found in database

The software extension then computes increments along the three dimension axes, velocity, and acceleration; also, effective distance, direction, and inclination with reference to the original position. The calculated values are compared to certain established criteria to issue Movement Warnings when required. The criteria relate to displacement increment length and acceleration, and also to effective displacement length and consistency. For each monument, a warning is issued when any of the following is true:

- Successive position readings show displacement consistency with the total effective displacement. This is quantified as the result of dividing Effective Displacement by the sum of Displacement Increments. If the value obtained is equal or greater than 80%, the monument is considered to be moving in a given direction and sense.
- The monthly displacement increment is larger than 30 mm.
- The total effective displacement is larger than 100 mm.
- More than three successive movement acceleration increments are observed.

After this process, the software extension generates three geometric object datasets that represent the location of monuments, their displacement paths, and the effective displacement vectors. It also creates one raster image dataset, which is the outcome of an Inverse Distance Weighted Interpolation of the effective displacement distance of the superficial monuments considering only the positions surveyed during the time period of analysis which, by default, is the year (365 days period) ending the day the extension is executed. The resulting raster grid can be displayed using a color classification of the

displacement magnitude, obtaining an image that provides clear indications of potential landslides occurrence and extent of affected areas (see Figure 9), mostly when compared to grids generated for previous time periods.

New monitoring systems are available in the market that make use of the new technologies developed in recent years and the advancements in their application to surveying and data processing. The ACP has acquired such a monitoring solution comprised of robotic total stations that automatically scan for and locate the specified monument targets, communication equipment required for data transmission, and software for data processing and storage in a database, issuing warnings when displacements exceed threshold values established. This system is used to monitor more than 160 control points located on the new earth fill dams. Data is collected three times per day by fully automated equipment and processed in real time automatically be specialized software.

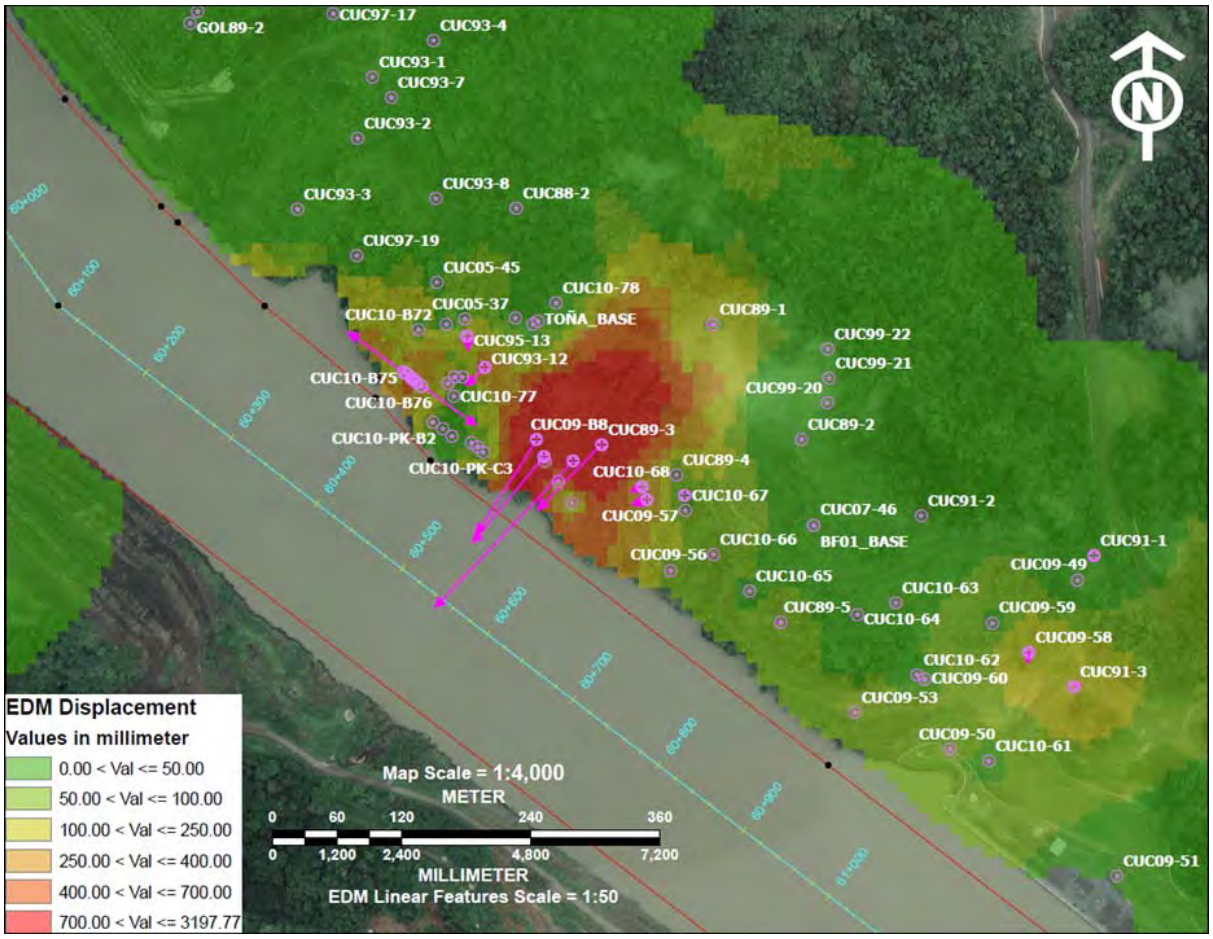

Figure 9: Superficial monuments location, displacement vectors, and color-classified representation of horizontal displacement

8.2. Subsurface Instrumentation

The instruments installed in the Gaillard Cut and the Pacific Access Channel include piezometers, observation wells, and traveler pipes, used to monitor pore water pressure and lateral deformations. The measurements are collected manually every month, and extraordinary readings are made when the daily accumulated rainfall is 90 mm or more.

In recent years, the amount of monitored monuments has increased significantly because of the increase in the extent of the areas disturbed as a result of the execution of the different improvement projects, especially those related to the Canal Expansion Program. The new earth fill dams are critical

to the operation of the canal and the preservation of water in the Gatun Lake, so constant monitoring is required to secure and preserve their safety

Because the Borinquen Dams are critical elements of the Panama Canal, a new Automated Data Acquisition System (ADAS) has been implemented to automatically read, store, and transmit the measurements from piezometers and settlement cells installed on the earth fill dams. The system uses a combination of dataloggers and vibrating wire interfaces integrated with multiplexers and radio communication devices which send the data via radio waves from the dam to Cerro Luisa, and then to the office in West Corozal. Additionally, there are some inclinometers installed at the dams, but they are read manually every 15 days, and additional readings are made when the daily accumulated rainfall is 90 mm or more.

9. ACTIVATION OF LANDSLIDE RESPONSE PROTOCOL

The Landslide Response Protocol implements procedures for identifying probable, imminent or current landslide emergencies which can affect the operation and safety of the Panama Canal Authority facilities and personnel. The early identification of existing or potential landslide is essential to opportunely initiate remedial measures with the objective of maintaining the waterway operational.

The protocol establishes three different risk conditions: Code blue, Code Yellow and Code Red (see Figure 10). Code Blue, or probable landslide threat warning, is activated when any signs of incipient movement are detected. Code Yellow, or imminent landslide threat warning, is applied when there is clear evidence of the occurrence of a landslide, such as cracks, but not foreseen as critical. Code Red, or existing landslide warning, corresponds to an Emergency condition, and is started when an existing landslide jeopardizes lives, the transit of vessels, or property.

Depending on the Code, different notifications are issued, and the support of different ACP Departments is requested immediately. The works comprise clearing tall grass and brush, surveying and mapping of the movements registered on-site and underwater, the use of construction equipment and personnel to initiate preventive or remediation measures, and dredging equipment to remove encroachment material if necessary.

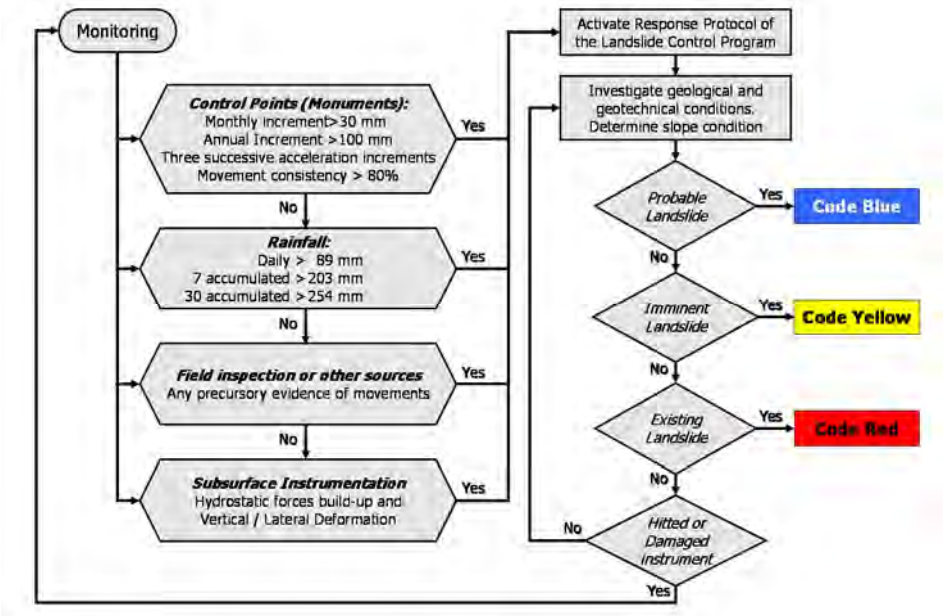

Figure 10: Landslide Response Protocol

9.1. Data Analyses

All collected data from the surveillance instruments are processed and analyzed to identify any sign of instability in the different areas. All instability features encountered are then evaluated in order to determine if there is a consistent displacement trend that might represent any threat to the general stability of the area. Also, rainfall data from the corresponding meteorological station is correlated with the instrument readings. The end result is the identification of the landslide risk condition. The analysis covers the following criteria:

- Control Points: The data of each monument issuing a warning is reviewed, first independently of the rest, and then, in the context of the surrounding area, as the degree of correspondence between the movements of all monuments within such area is evaluated. When a movement trend is identified in a given sector, further actions are performed as explained below.

- Rainfall: Given a potential instability is identified, rainfall records are reviewed. Also, rainfall intensity is constantly monitored by the Water Division, which is responsible for issuing notifications when the 24-hour rainfall average exceeds the 89 mm threshold for any of the meteorological stations.

- Field inspections: If either the rainfall intensity or the movement trend of a sector is above established criteria, a field inspection is conducted to the areas of concern, searching for other signs of movement, such as cracks, and tilting of trees and electric poles, and additional special data collection is performed for all existing instruments.

- Subsurface Instrumentation: The accumulated rainfall average is compared with the subsurface instrumentation data to detect if there is a direct correlation between rainfall intensity and variations of the phreatic level. Figure 11 shows the behavior of the pore pressure in a section of Dam 1E, the water elevation of Gatun Lake and the accumulated rainfall from the meteorological station of Cocoli. Data from groundwater measurements help to understand the flow regime present in the majority of potential slide areas in Gaillard Cut, many of the cut slopes are affected by water, because the shear resistance reduces as the pore pressure increases, causing instability.

The real-time data from the Automated Data Acquisition System is used to evaluate the performance of the dam relative to the expected performance or dam safety performance standards. The historical piezometric levels are used in the design of remedial excavation solutions.

Upon this evaluation, further actions may be necessary. Additional instruments may be installed to define the extent of the moving mass. Remedial measures are devised and implemented as required to stabilize the affected areas. In general, if the condition is critical, the stabilization works are executed either partially or entirely by internal forces, depending on the scope and magnitude of the works. Otherwise, the works are performed by contract.

This methodology has provided the means to recognize many instabilities in the early stages with sufficient anticipation to correct them before they would fail producing blockage or encroachment in the waterway. However, the behavior of slopes with similar initial patterns of movement may differ from one another depending on a variety of factors, such as geology, geomorphology, water table conditions, stress state of soil/rock materials, and failure mechanism of the area being monitored, among others. Therefore, the corrective measures to be adopted for instability remediation shall depend upon engineering judgment supported on site reconnaissance, supplementary geological investigations, history of slide activity and previous remedial works, and additional instrumentation when required.

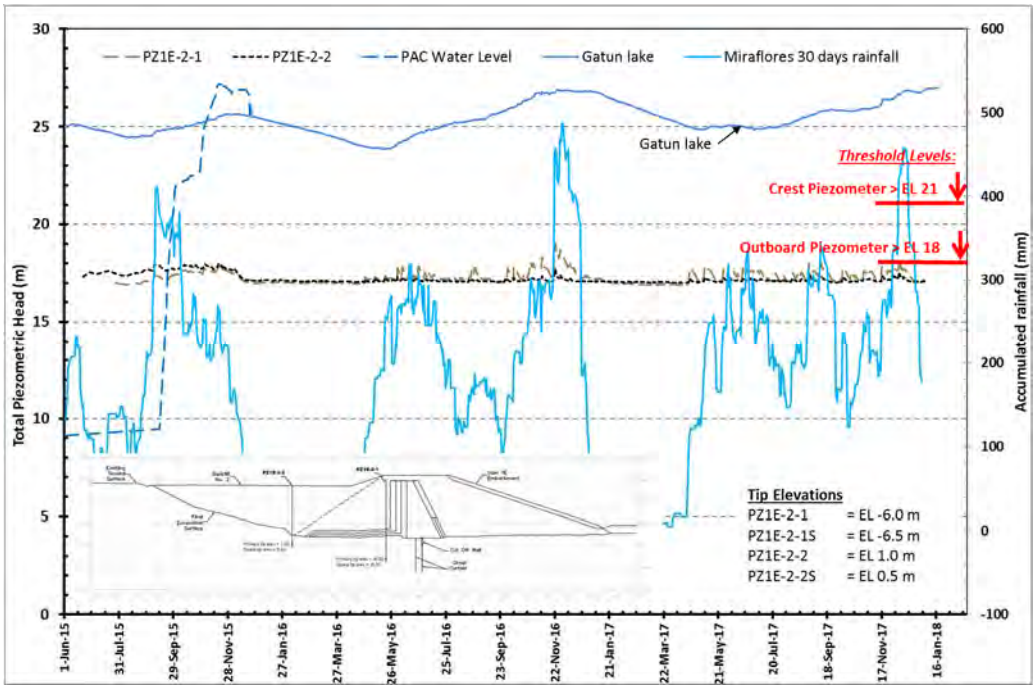

Figure 11: Vibrating wire piezometer Pacific Access Channel, Dam 1E

9.2. Geological and Geotechnical Investigation

After collection and review of all existing data on the slope, and a field reconnaissance of geologic and terrain conditions, further investigations are performed in areas of existing or potential landslide. The area is geologically explored by core drilling, using some of the drilled holes to install subsurface instrumentation. Along with the drilling, access roads are built, additional surface instrumentation is installed, drainage networks at the area are rehabilitated, improved, or built as required; and complete monitoring of the slopes is carried out.

9.3. Case Study: Monitoring and Remediation of Old Lirio Slide (2015)

The Old Lirio Slide area is located in Lirio Sector, at the central portion of the Gaillard Cut, on the west bank of Culebra Reach, from Canal station 58K+100 to station 58K+620. Elevation ranges between 27.5 meters and 60 meters PLD (Precise Level Datum used at the Panama Canal area).

In the past, several instabilities have occurred in this area, during and after the Canal construction. The most recent event before year 2015 occurred in June 17, 2013. Such event was located in the same area, between Canal stations 58K+250 and 58K+550.

The slide being studied occurred on December 7th, 2015. Several cracks were reported in the area (see Figure 12). Two days later, on December 9th, the Manager of the Geotechnical Branch activated the Landslide Response Protocol issuing an “imminent landslide” (Code Yellow) alert for this area.

The unstable mass was estimated to be 500 meter long and 200 meter wide, comprising approximately 2 million cubic meters. The potential encroachment was estimated to reach 50 meters into the west lane of the navigational channel.

In both, the June 2013 and the December 2015 events, the failure mechanisms were considered to be rotational, with a slip surface extending through layers of fill, clay shale, sandstone, conglomerate, and carbonaceous sandstone (see Figure 13).

Figure 12: Tension Cracks at Old Lirio Slide Area

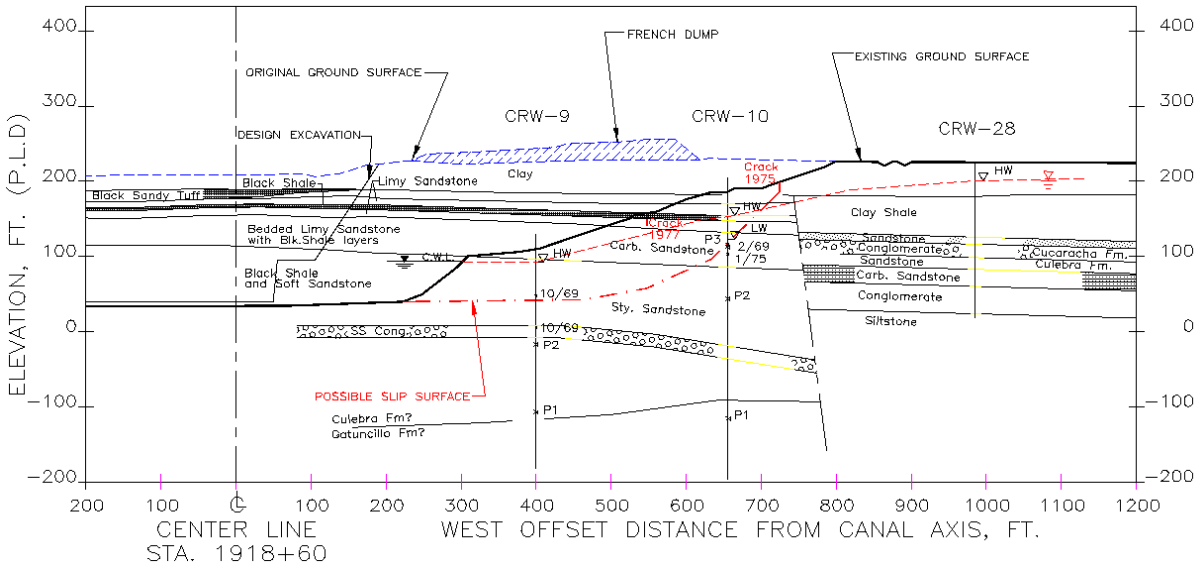

Figure 13: Geological Cross Section at Station 58K+479 m (1918+60 feet)

According to the Landslide Response Protocol guidelines, the instrument data was further analyzed. No additional geological or geotechnical investigations were required in this case. The remedial works were designed and implemented to stabilize the area. The works initiated on January 4, 2016. They were performed by ACP internal forces under the direction of the Geotechnical Branch and were completed by February 2017, after a 5-months interruption due to rainfall between July 2016 and January 2017. The works comprised the excavation of 204,000 cubic meters of unclassified material, the construction of a set of drainages with a total length of 170 meters, an inverted filter covering approximately 1825 square meters, and a french drain of about 168 meters long. No dredging works were required. Figure 14 shows the final excavation layout of the stabilized area in yellow, the excavation perimeter is shown in cyan, and the mapped cracks are shown in white.

Figure 14: Excavation Layout at Old Lirio Slide

Figure 15 presents a set of plan views showing color-classified raster images representing superficial displacements at the Old Lirio Slide area, and the corresponding vectors representing effective displacement in magenta. The first plan view shows data for the period beginning on January 1, 2010 and ending on June 30, 2013; some days after the June 2013 instability. The second plan view covers the period between July 1, 2013 and December 30, 2015, less than a month after the December 2015 landslide. The third raster shows the data indicating recorded displacements since January 1, 2016 up to March 15, 2018.

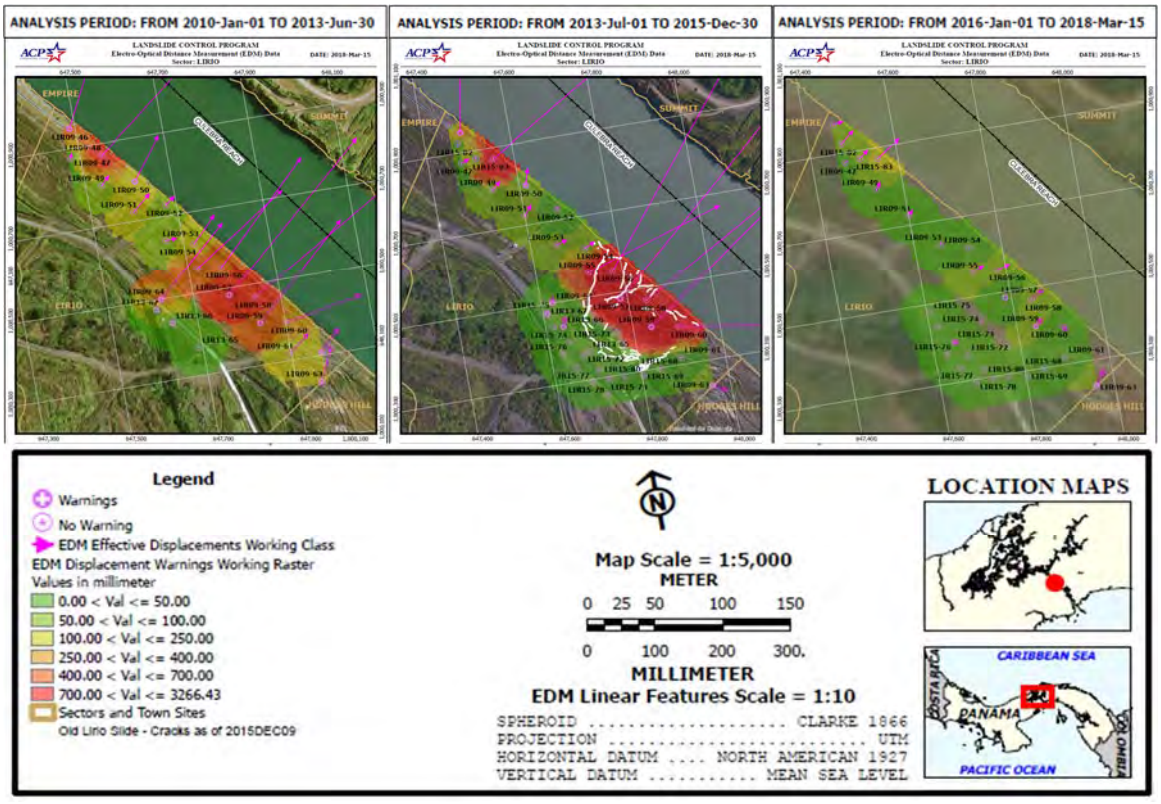

Figure 15: Displacement Vectors and Raster Images at Old Lirio Slide

Displacement vectors for the different monuments shown in the first plan view of Figure 15 indicate an average movement of about 1 meter that had accumulated for over three years before the June 2013 landslide occurred. Remedial works were performed for the next six months to stabilize the moving mass, including the removal of the material at the top of the moving mass and the construction and rehabilitation of drainages in the area. Even after the stabilization works were completed, movement towards the canal continued, and the new tension cracks developed by December 2015, shown on the second plan view in white, time at which the Landslide Response Protocol was reactivated and Code Yellow notifications were issued. New remedial works were executed as described previously, preventing any channel encroachment. The third plan view shows displacements smaller than 50 millimeters for most of the area, corroborating the landslide hazard has been mitigated.

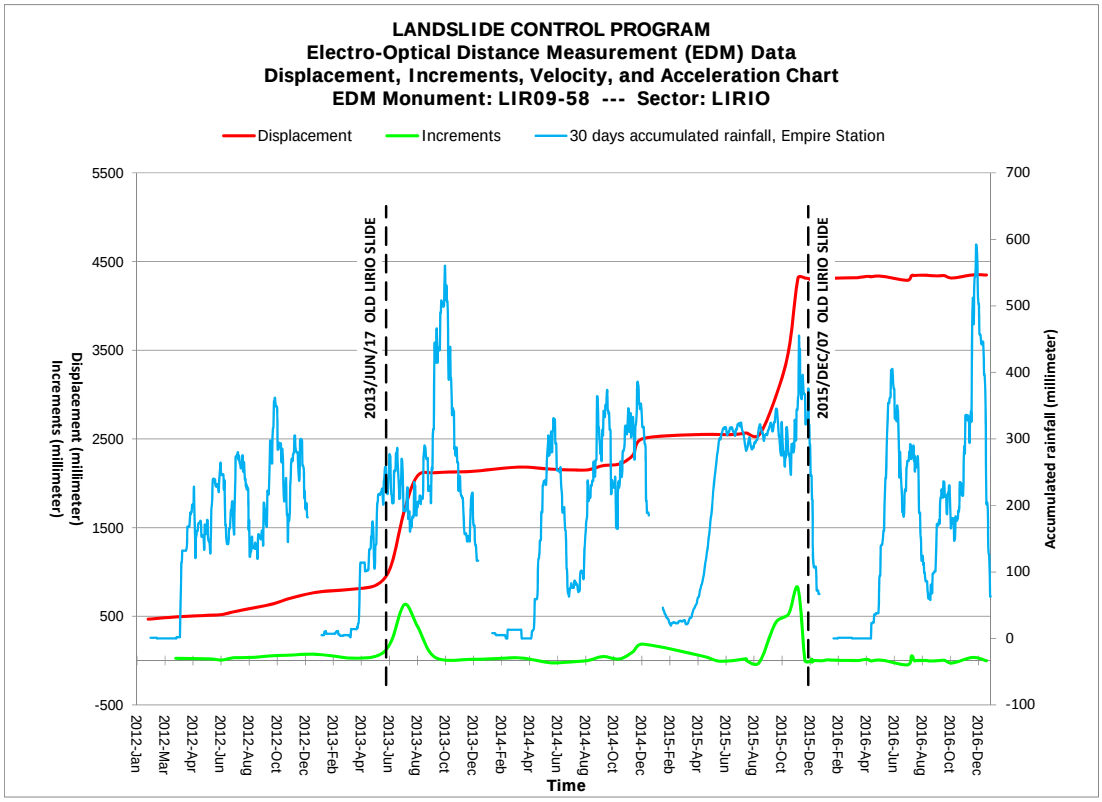

Figure 16: Effective and Incremental Displacement vs. 30-Day Accumulated Rainfall

Figure 16 shows a comparison between data for the effective and incremental displacements of Monument LIR09-58 and the 30-day accumulated rainfall, as recorded at the nearest meteorological station (Empire). The chart shows that the landslides mentioned above occurred during periods of heavy rainfall. Worth noting, the larger movements developed during the sustained periods of rain, which favor water infiltration and the consequent increase in water table and pore pressure, and not necessarily during the peaks of rain intensity, as shown.

10. CONCLUSIONS AND REMARKS

The occurrence of landslides in the Gaillard Cut is mostly due to the complex geological conditions combined with a high precipitation regime:

- Soft rock strata characterized by long-term loss of strength due to natural geological processes.
- Presence of discontinuities and weak planes, resulting from geological processes, that drive the geometry of failures.
- A direct relationship between the rainfall regime and the increase of hydrostatic forces and pore water pressure which largely affect the behavior of the soft rocks, such that rains are the main factor triggering Landslides in the Gaillard Cut.
- The progressive swelling/rebound of soft rocks due to the unloading caused by earthworks in the bank slopes.

The Landslide Control Program constitutes a risk reduction activity that supports the main business activity of the Panama Canal: The safe, efficient, and reliable transit of vessels through the Isthmus of Panama.

The Landslide Control Program does provide savings because:

- Any encroachment or blockage of the navigational channel that interrupts normal traffic through the canal represents a millionaire reduction of income.
- The removal of material from the navigational channel by dredging is far more costly than earthworks performed in the dry for the stabilization of a moving mass.

The Landslide Control Program has proceeded mostly as planned. To the present, the slopes of Gaillard Cut and the Pacific Access Channel are geologically explored and adequately instrumented, and are being effectively monitored for detection of incipient landslide activity.

References

Alfaro, Luis D. (1988). The Risk of Landslides in Gaillard Cut, Panama.

Alfaro, Luis, Beacher, Gregory, Guerra, Fernando and Patev, Robert (2015). Assessing and Managing Natural Risk at the Panama Canal. 12th International Conference of Applications of Statistics and Probability in Civil Engineering, Vancouver, Canada.

Banks, Don C et al (1975). Study of Clay Shale Slopes along the Panama Canal. Report 3. Engineering Analyses of Slides and Strength Properties of Clay Shales along the Gaillard Cut. Technical Report S-70-9. U.S. Army Engineer Waterways Experiment Station, Vicksburg, Mississippi.

Berman, George (1995). Landslides on the Panama Canal, Circum-Pacific Council for Energy and Mineral Resources, Earth Science Series, Vol. 16, Heidelberg,1995.

Berman, George (1985). Importance of Landslide Control in Excavation Design, Panama.

De Puy, M.A. (2016). Post-Constructions Landslides in the Panama Canal, Landslides and Engineer Slopes, Experience, Theory and Practice, Rome, Italy, ISBN 978-1-138-02988-0.

Mann, Anthony P. (1979). Landslide Control in the Panama Canal, Panama.

Reyes D., C.A. & Fernández P., L.C. (1996). Monitoring of Surface Movements in Excavated Slopes, Seventh International Symposium on Landslides, Volume 3, Trondheim, ISBN 90 54 10 81 85.

NO STANDARD LOCK GATES FOR THE NEW SEA LOCK IN IJMUIDEN, THE LARGEST LOCK IN THE WORLD

by

***Pieter van Lierop*[1]**

ABSTRACT

In the Dutch city of IJmuiden, a new sea lock is currently under construction. With a lock chamber of 500 m long and 70 m wide, it will be the largest lock in the world. The latest generation of seagoing vessels will be able to access the harbour of Amsterdam using this lock. At the same time, at an altitude of 8.85 meters above sea level, the Netherlands are protected from the rising sea water for the next two centuries. The lock must be constructed in between of the existing operational locks. Because of this lack of space, the water levelling system is incorporate in the rolling gates. The required performance of the gates as well as the drive mechanism, in terms of reliability, availability, maintainability, safety and robustness), was highly governing during the design process, and resulted in a final design that cannot be described as standard.

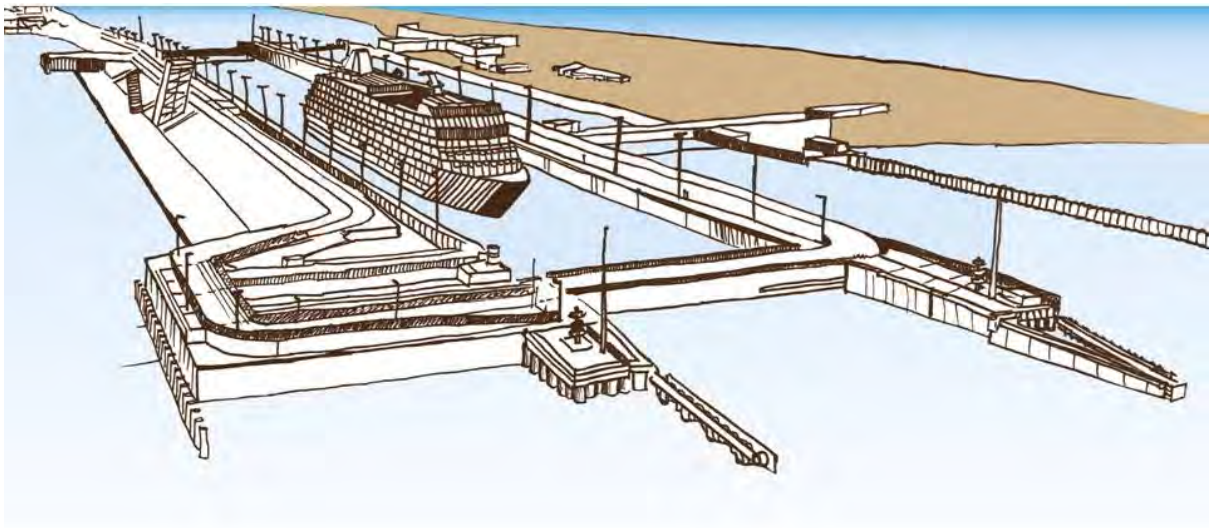

Key Words: inland navigation, locks, rolling gates, drive mechanism, levelling system

INTRODUCTION

After almost 100 years in operation, the existing Noordersluis (Northern Lock) in IJmuiden will be replaced with a new, larger lock system to improve the accessibility of the port of Amsterdam.

Because of the approaching end of the technical lifespan and the arrival of the end of the economic life of the Northern Lock, a new lock is needed. The new IJmond sea entrance is part of the clients (Rijkswaterstaat) lock renovation program. The scale of increase in vessel size makes it furthermore desirable to construct a new lock that is wider than the existing locks. This will simultaneously increase the capacity of the lock complex.

[1] Design leader Gates and Drive Mechanism at OpenIJ / Head of department of Steel and Movable Structures at Iv-Infra, p.j.c.vanlierop@iv-infra.nl

The most important work involved in the project includes:

- the design and construction of a new sea lock, including other modifications in the project area (waiting facilities and dredging works of the navigation channel) to enable safe and easy navigation through the new lock;
- the planning and execution of maintenance on the new lock for approximately 26 years;
- the uphold of the primary water-retaining structure in accordance with the Dutch Water Act is an important element of the work.

Rijkswaterstaat awarded the contract to the OpenIJ consortium which consists of BAM-PGGM, VolkerWessels, and DIF. The construction activities will be carried out by a BAM Infra and VolkerWessels joint venture. The work commenced in early 2016. The dredging activities will be carried out by subcontractors Van Oord and Boskalis.

This paper presents the design of the new lock gates and drive mechanisms.

LARGEST SEA LOCK IN THE WORLD

The new sea lock in IJmuiden will be in terms of length of the lock chamber (500 meters) and width (70 meters) the largest sea lock in the world (Figure 1). With these dimensions, it allows passage to the world's largest ships, which will be able to pass through the lock, regardless of the tide, and will strengthen the international competitiveness of the port of Amsterdam. At the same time the new sea lock is built 'future-proof'. At an altitude of 8.85 meters above sea level, the Netherlands are protected from the rising sea water levels for the next two centuries.

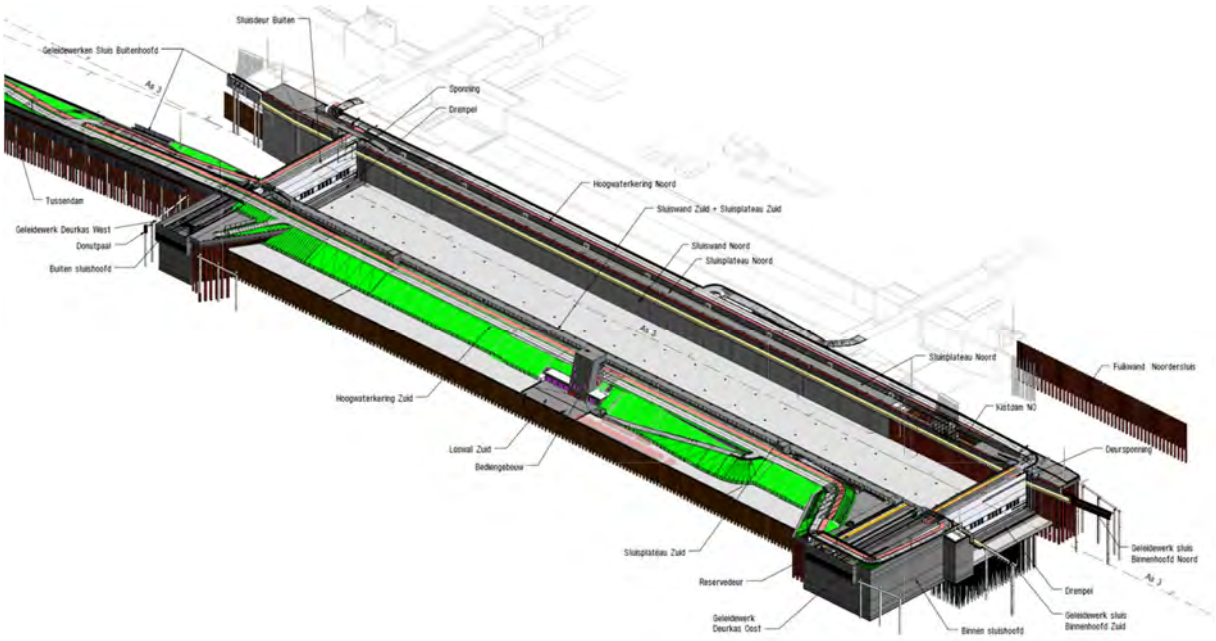

Figure 1: Overview of the new sea lock

REQUIRED PERFORMANCE

The functionality of a navigational lock is particularly determined by the lock gates and drive mechanism. Because the set of performance requirements, the environmental and spatial boundary conditions vary per lock, each lock requires a specific gate design and a standard solution is not available. This also applies to the new IJmuiden sea lock, where the design of the rolling gates (figure 2), measuring 72 meters in length, 11 meters in width and 25 meters in height, is governed by the required robustness and RAMS performance and the environmental conditions. A sufficiently reliable concept had to be developed, requiring minimal maintenance effort.

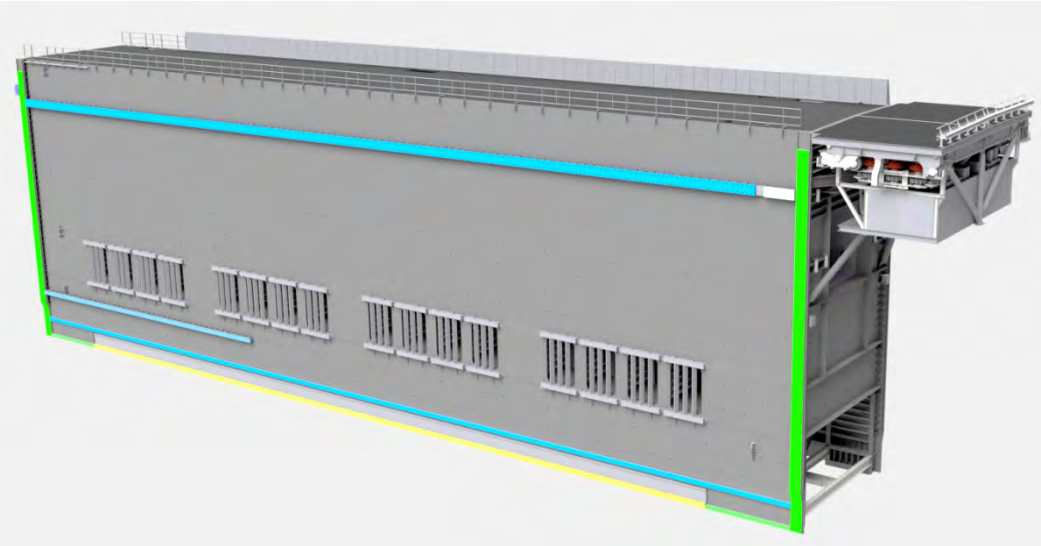

Figure 2: New rolling gate (72x25x11 meters)

Due to the small construction space, the limited width for the new lock heads and the rolling gates proved to be a difficult design challenge. The new sea lock is built between the existing locks, which will largely remain open to shipping and road traffic during construction (Figure 3). Because of the length of the gate recess, a common type of drive mechanism like a cable-winch gear, cannot be properly fitted.

Figure 3: Construction site in the middle of existing lock complex (February 2018)

Reliability

To meet the requirements of the reliability of the high water retaining function, the outer head as well as the inner head are being designed to such elevation, that they are both able to resist maximum sea water levels of up to 7,80 meters, while the water level of the inland channel will be at 0,40 meters below sea level. On top of both gates a motorway is provided to allow road traffic to cross the lock complex. To accommodate traffic, the height of the gate has been fixed at 6,25 meters above sea level, where an additional retaining wall serves as a high water barrier (Figure 4).

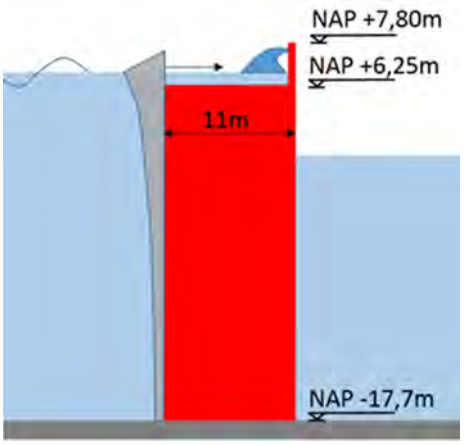

Figure 4: High water retaining function

Because of the design decision to construct the complete lock for maximum water retaining height, only three similar lock gates are being constructed, two operational gates and one spare gate, which is stored in a maintenance dock next to the inner head (Figure 5).

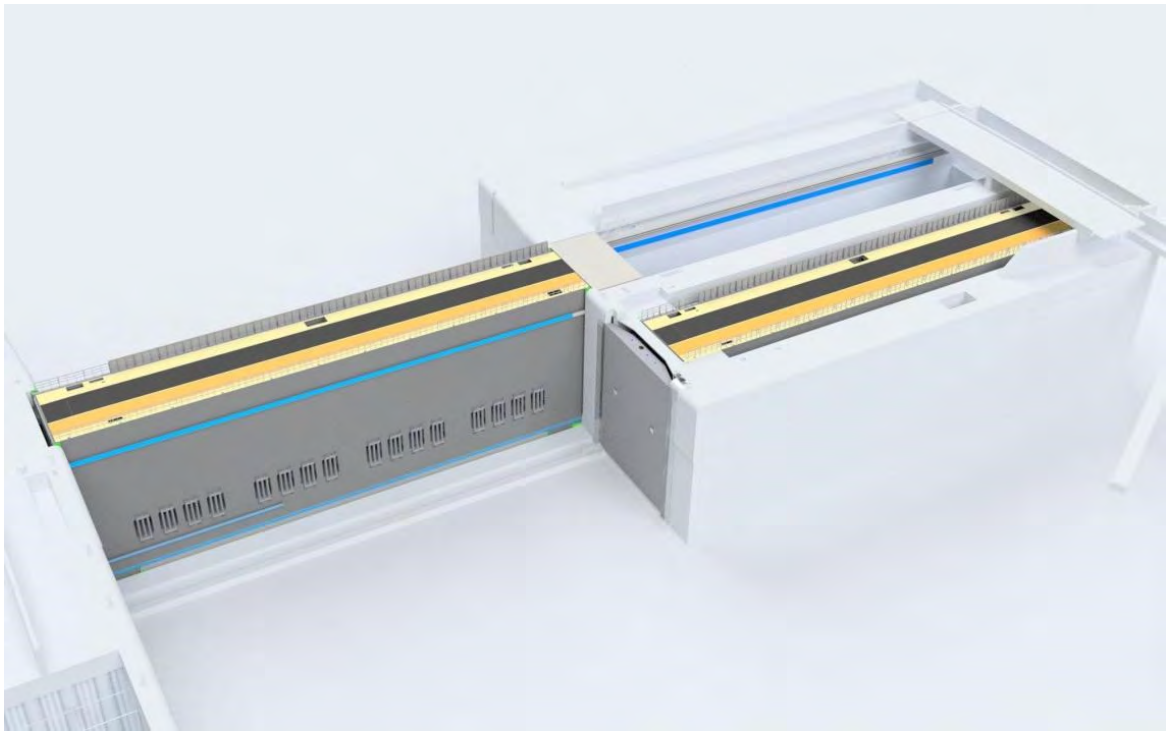

Figure 5: Inner lock head with maintenance dock

Availability and maintainability

Once the reliability of the lock as a flood defence is guaranteed, the most governing design challenge is to create a reliable functional lock facilitating a save and quick passage of vessels. An availability of 99% is required, which means that no more than 70 hours per year are available to carry out scheduled maintenance and that a maximum of 18 hours per year is available to solve unexpected malfunctions. In addition, a maximum delay of 24 hours is required to exchange one operational lock gate. To meet the availability requirements, the replacement frequency of the gates will be once in 15 years. The objective during the design process was. to reduce the amount of maintenance of difficult accessible parts. Therefore, the rolling gates are designed according to the 'wheelbarrow principle'. The gate rests on a lower roller carriage on the lock chamber side and on an upper roller carriage on the gate recess side (Figure 6). The upper roller carriage also serves as a road surface by means of

which onshore traffic can drive on and off, across the gate. In favour of maintainability, it is decided to minimize the amount of maintenance sensitive moving parts. During opening and closing, the gate will be guided horizontally by means of polyethylene guide strips fitted at different elevations on both long sides of the gate and in the rail beam structure at the sill level of the gate bay. Super-duplex stainless steel guidance blocks slide against the UHWMPE strips. In case of a critical failure of the rail track or the horizontal sliding pads, the rail beam structure can be rapidly lifted out of the water in one piece, after which a spare one can be put in place.

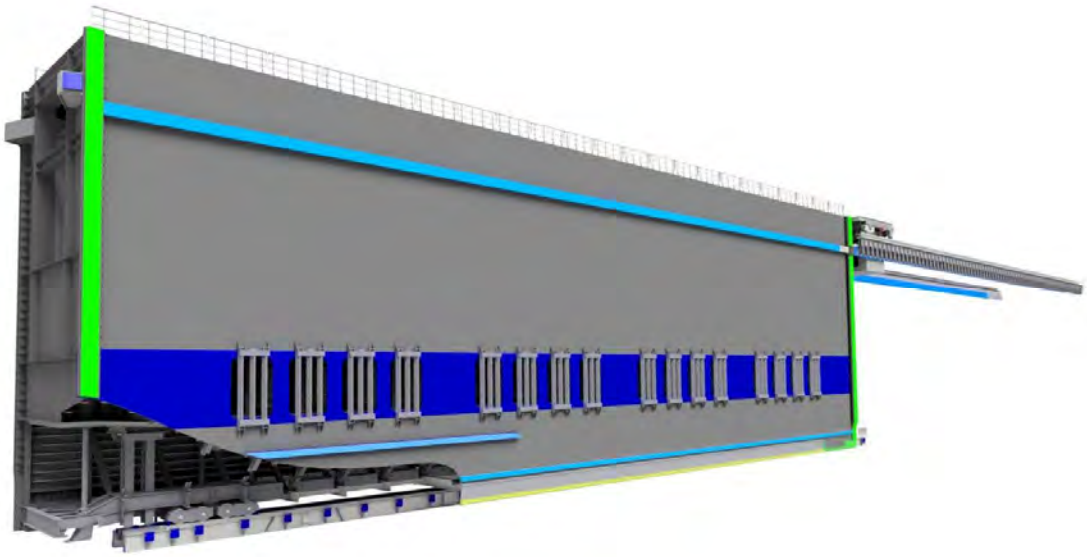

Figure 6: Wheelbarrow type rolling gate with horizontal sliding pads

GATE STRUCTURE

Steel structure

The lock gates resist high water levels on both sides and comprises two retaining shell sheets, with horizontal sheeting sections in between (i.e. the road deck, the bottom and top plate of the buoyancy chamber and the bottom plate of the levelling sluices), which requires minimal use of steel. In fact, the gate structure could be described as a girder resting on two supporting points and bending around the vertical axis (Figure 7). The gate will only start to bear down upon the concrete floor by the use of vertical columns and diagonal stays in the event of extremely high water levels or ship collisions. A flexible steel plate with UHWMPE blocks along the bottom side of the gate, works as a seal, and is also capable of distributing high bearing loads to the sill structure.

Figure 7: Gate steel structure (stripped outer sheeting) and cross section

The water retaining skin of the gate is constructed of plates that are stiffened by bulb profiles. This also applies to the horizontal plates of the buoyancy tanks. To prevent accumulation of sediment on top of the buoyancy chamber all stiffeners are located inside of the tanks.

The road deck is stiffened by trough profiles, commonly used in the Netherlands in steel bridge designs. The extra amount of buoyancy at water levels up to the top of the gate is taken into account.

In total, the steel structure (without hydraulic and electrical equipment and ballast water) weights about 2700 mTon.

Buoyancy and ballast system

To limit the deadweight on the roller carriages and rail structures, the gate will be equipped with a large rectangular buoyancy and ballast system with air chambers over the entire length and width of the gate. It is located on top of the levelling culverts, and reduces the self-weight of the gate from about 3000 mTon to an average service weight of 400 mTon. There are special ballast tanks to compensate for marine growth and sedimentation. All ballast tanks can be emptied in the event of a gate change, which causes the gate to float upwards and allowing transportation. Emptying of the buoyancy chambers will be carried out by the use of compressed air (Figure 8).

In case of extreme high water levels, the dry installation room in the upper level of the gate will become buoyant. To guarantee that the lock gate won't float, the service-weight will automatically increase by letting in water in overflow tanks.

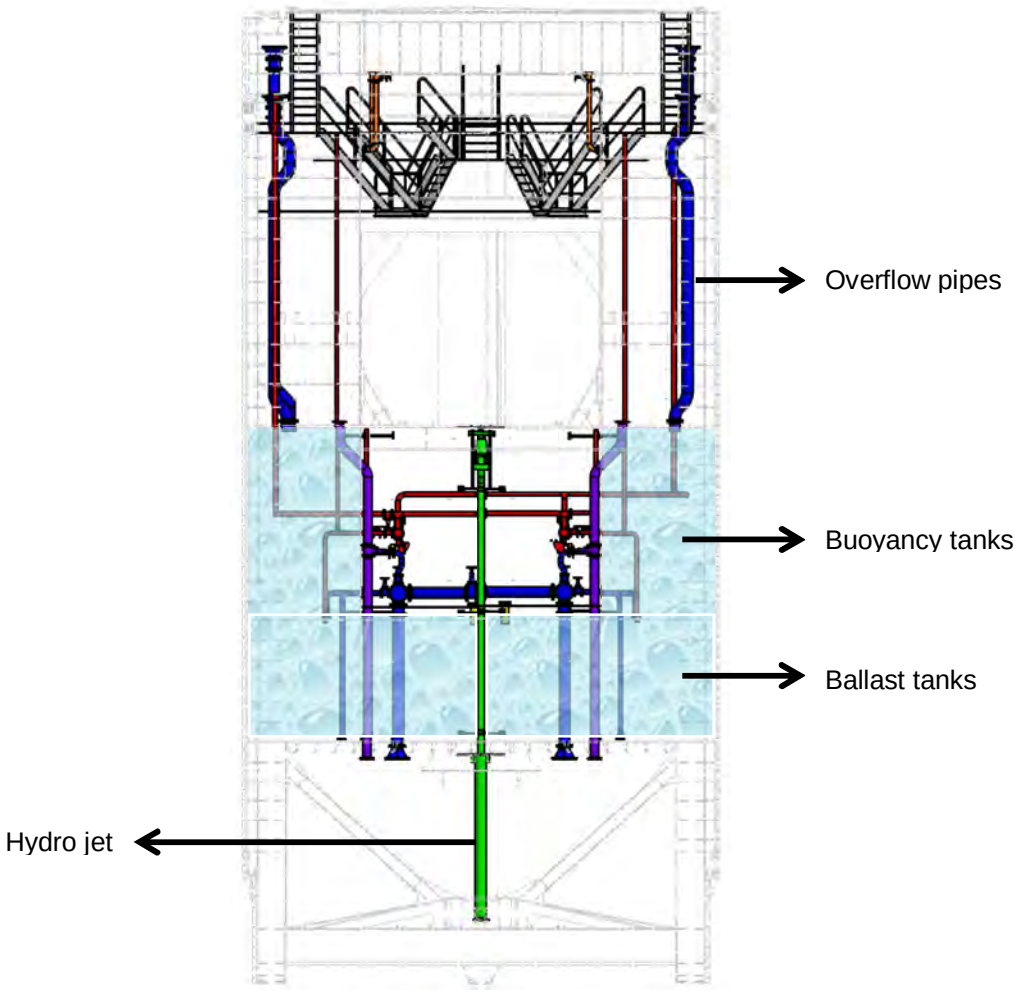

Figure 8: Filling and emptying system of the buoyancy tanks

Environmental conditions

The presence of floating debris, marine growth and sediment can lead to accelerated wear of the rail tracks, thus impairing the availability of the lock. To prevent this as much as possible, special facilities have been incorporated in the lock gate. At the front of the lower roller carriage a bull bar and dirt scraper have been fitted to the gate structure to push any obstacles encountered on the rail structure and on the guide beam into a collector well as the gate moves forwards. Additionally, a hydro jet pipe (Figure 8) will blow sand and sedimentation from the rail track.

In case the amount of sedimentation on the buoyancy tanks during operation seems to be much more than expected, external mixers or agitators can easily be installed.

To avoid that the lower roller carriage becomes overloaded due to accelerated marine growth or sedimentation as time passes, it is provided with a load sensor that will be continuously monitored. If there is an increase in the service-weight, it is possible to respond rapidly and compensate weight by pressing water out of these ballast tanks.

ROBUSTNESS

Ship collision

The steel gates were designed to be more collision-resistant than required by the client. The gate must retain its high water retaining function in case of a ship collision with a total impact energy of 34MJ. At the same time the gate should still be able to function properly after a collision up to a maximum impact energy of 12 MJ, without any lack of availability. In the event of these kind of ship collisions, the gate structures will undergo plastic deformation in a way that cracking does not occur in the shell sheeting. Computational dynamic FEM-analyses that simulated various collision scenarios demonstrate that the lock gate is sufficiently robust (Figure 9). Several scenarios have been established in consultation with the client Rijkswaterstaat, taken into account different variables like the water replacement (DWT) of the ship, its maximum speed, its bow shape and the water levels in front of the gate.

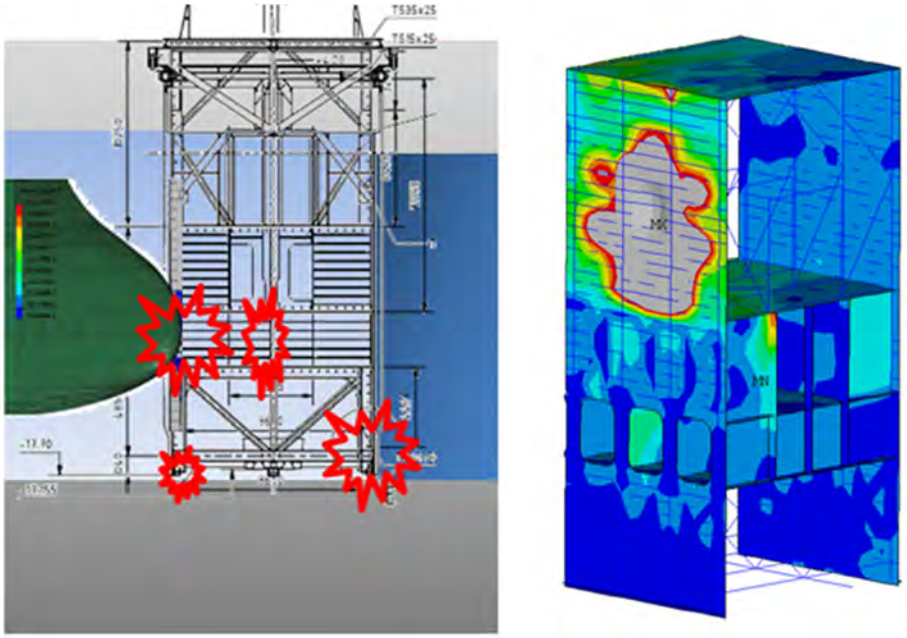

Figure 9: Impact scenarios and dynamic FEM-analyses

All hydraulic and electrical installations in the gates have been placed outside the collision-sensitive zone. For the same reason, the 16 levelling valves, each with their own hydraulic cylinder, have been placed at the center of the gates to prevent the slide guides from sustaining deformation in the event

of a collision. The air chambers have been compartmentalized to limit loss of buoyancy to a maximum of 10% in the event of a leak. In such a situation, the lock gate will still be able to fulfil its operational function and allow navigation through the lock.

Wave impact

To prevent overloading of the UHWMPE sliding pads and rail beam structure during opening and closing of the gate, the super-duplex guidance block in front of the gate is secured against overloading by a flexible suspension construction, mounted on rubber fenders (Figure 10). In case of high wave loads during opening or closing of the gate, the gate is pushed aside and then re-distributes the reaction forces to the sill structure. As a result of that, the gate drive mechanism will automatically reduce its speed.

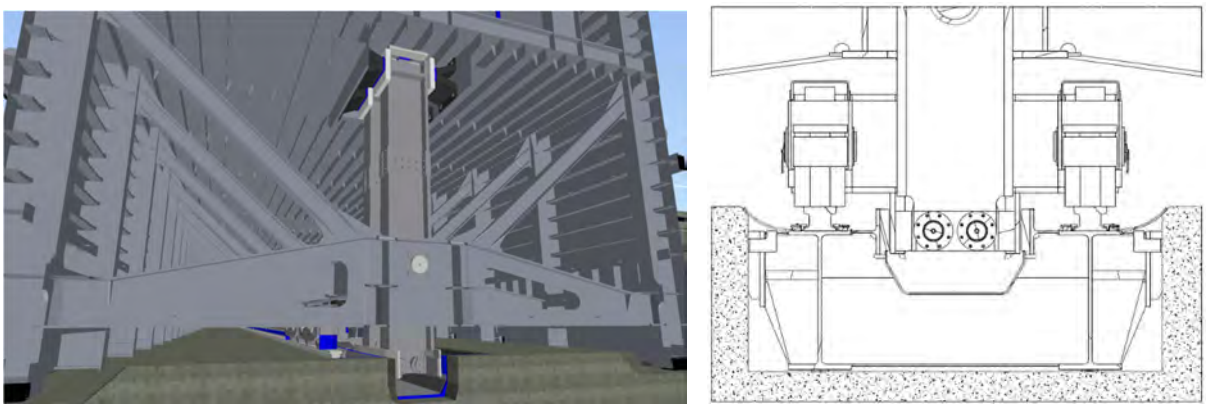

Figure 10: Cross section of horizontal guidance structure and rail beam structure

LEVELLING SYSTEM

General

The levelling system consists of sixteen levelling openings (2,2 meters wide and 3 meters high), positioned about 10 meters below the water level. They can be closed by means of hydraulically powered steel sluice gates (Figure 11), located in the middle of the gate structure. The decision to incorporate levelling through the gate instead of through short culverts in the concrete lock heads was once more the result of limited space in combination with the vulnerability of the foundations of the existing adjacent structure of the Northern Lock.

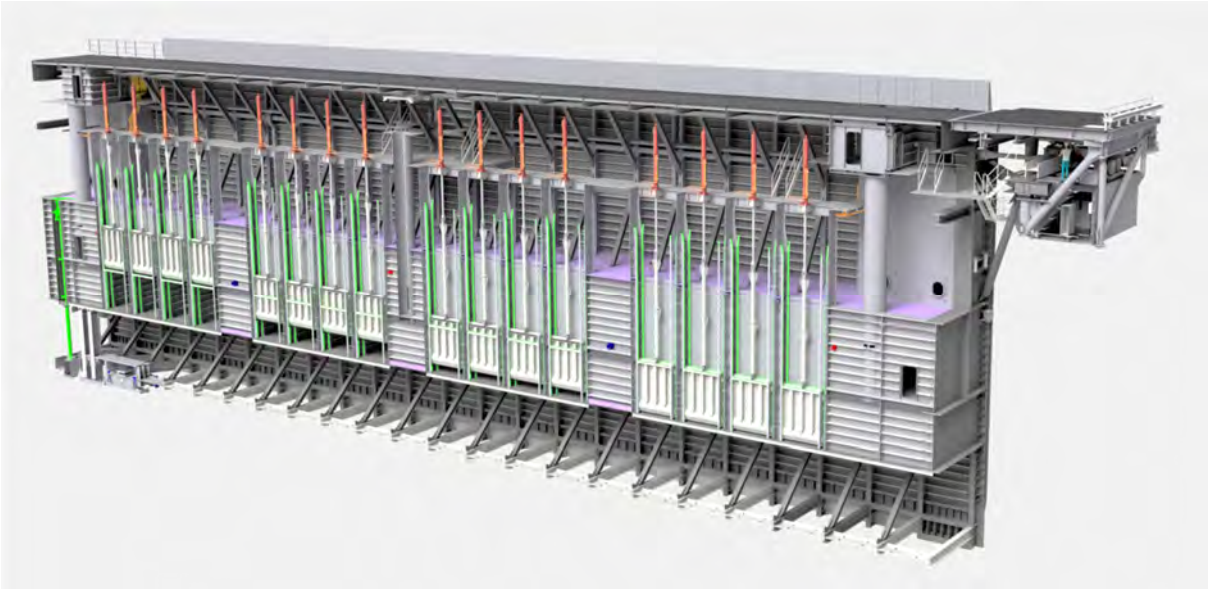

Figure 11: Isometric cross-section of the lock gate with 16 levelling sluices

Because the levelling system has to meet the high availability requirements, it is able to operate with only 14 sluices in most situations of differential head. That means in case one or two of the levelling sluices fail, time is available for maintenance or replacing the levelling gates.

Research and testing

The design of the levelling system (in particular determined by the dimensions and shape of the 11 meters long sluices, together with the triangular energy dissipation bars) must ensure that the required duration of the water levelling process in the lock chamber is met. At the same time hydraulic forces on the ship – and as a result of that the tensile forces in the mooring lines – should not exceed a critical value, due to the inlet of salt or fresh water. The maximum allowable force acting on the ship during filling or emptying the lock chamber is 0.20‰ in the longitudinal direction and 0.12‰ in the transversal direction expressed as a permillage of the displaced weight of a prescribed bulk carrier or container vessel. To verify the levelling system to be quick and save enough, a CFD-analysis has been carried out to determine the discharge coefficient at different sluice openings. Lockfill-calculations were made to determine the specific lifting programs at all possible differential heads over the active lock head and showed that the correct filling curves of the lock chamber have been achieved.

The Dutch research institute Deltares had been assigned to develop a scale model of the new sea lock. The design for the new lock, including the lock gates with detailed levelling sluices, gates and energy-dissipation bars, was built to a scale of 1:40. The total scale model, including the lock chamber and the entrances, was approximately 56 m long in total and 20 m wide (Figure 12).

The model tests make it possible to simulate the physical process during operation of the lock. The results of the scale-model were used to validate the numerical models (CFD and Lockfill). Besides aspects like the required levelling time and the measured hydraulic forces on the ships, the flow of fresh water and salt water when the doors are opened has been investigated.

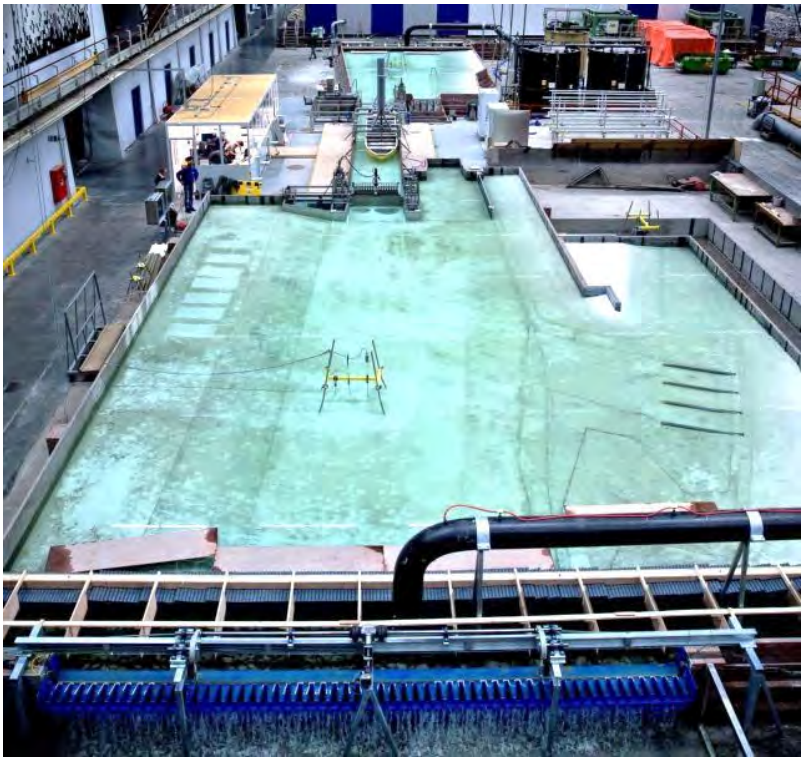

Figure 12: Scale (1:40) model test

Vortex induced vibrations

Dynamic calculations of the horizontal and vertical eigenfrequencies of the sliding sluice gates relative to the excitation frequencies of the water flow underneath the gates prove that the risk for unwanted vibrations is low. A specific design of the sluice gates (Figure 13), with a drop-shaped bottom girder and point-shaped rubber sealing, reduces the risk of vibrations due to vortex excitation of the water flow.

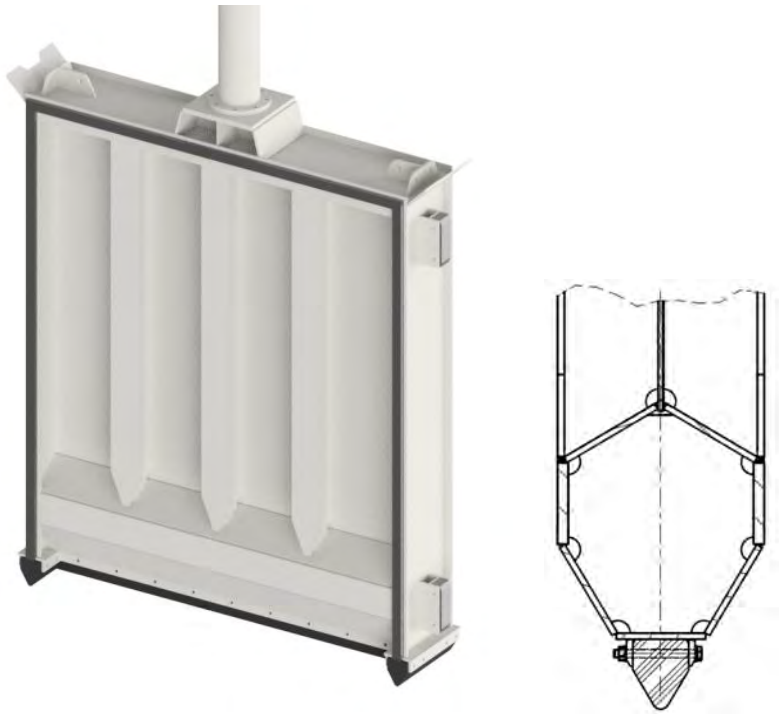

Figure 13: Sluice gate and cross section of bottom girder

LOWER AND UPPER CARRIAGE

General

At the location of both roller carriages, the gate will be supported centrically by one single elastomeric rubber bearing. These bearings allow the gate to move horizontally causing the gate to be pressed against its granite supports on the lock heads due to hydrostatic water pressure. In this way unwanted horizontal loads, which negatively affect the degree of wear, on the roller carriages wheels and rails are being prevented. This principle of load bearing of the supports of rolling gates is often being used in the Netherlands.

Lower carriage

For the design of lower wagon (Figure 14) this results in a relatively small carriage, compared to the size of the gate, with a total length of 4.5 meters and a wheelbase of 1.8 meters. It can be compared with the lower wagons of the new Panama Locks. Furthermore, the aim for the design of the lower wagon is to minimize the amount of maintain sensitive rotating parts. Because of this, the flexibility of the lower wagon is necessary to create a proper load distribution to each of the eight wheels (with a diameter of 800 mm.). To reduce the fatigue stresses on of the steel structure of the lower wagon, the construction tolerances of the concrete sill and the rail beam are very strict. The use of high strength steels (42CrMo5-04 for the wheels and 110CrV for the rails) and hardening up to 450-500 HB make that the wear is limited.

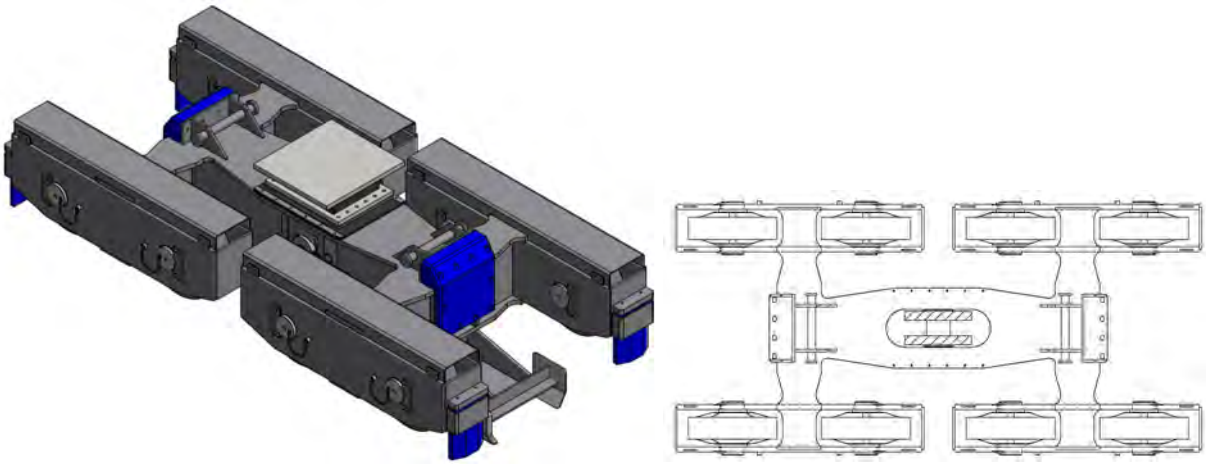

Figure 14: Isometric view and section of lower carriage

Upper carriage

The main objective of the upper carriage (Figures 15 and 16) is to transfer the vertical load of the lock gate to the concrete structure of the gate recess.

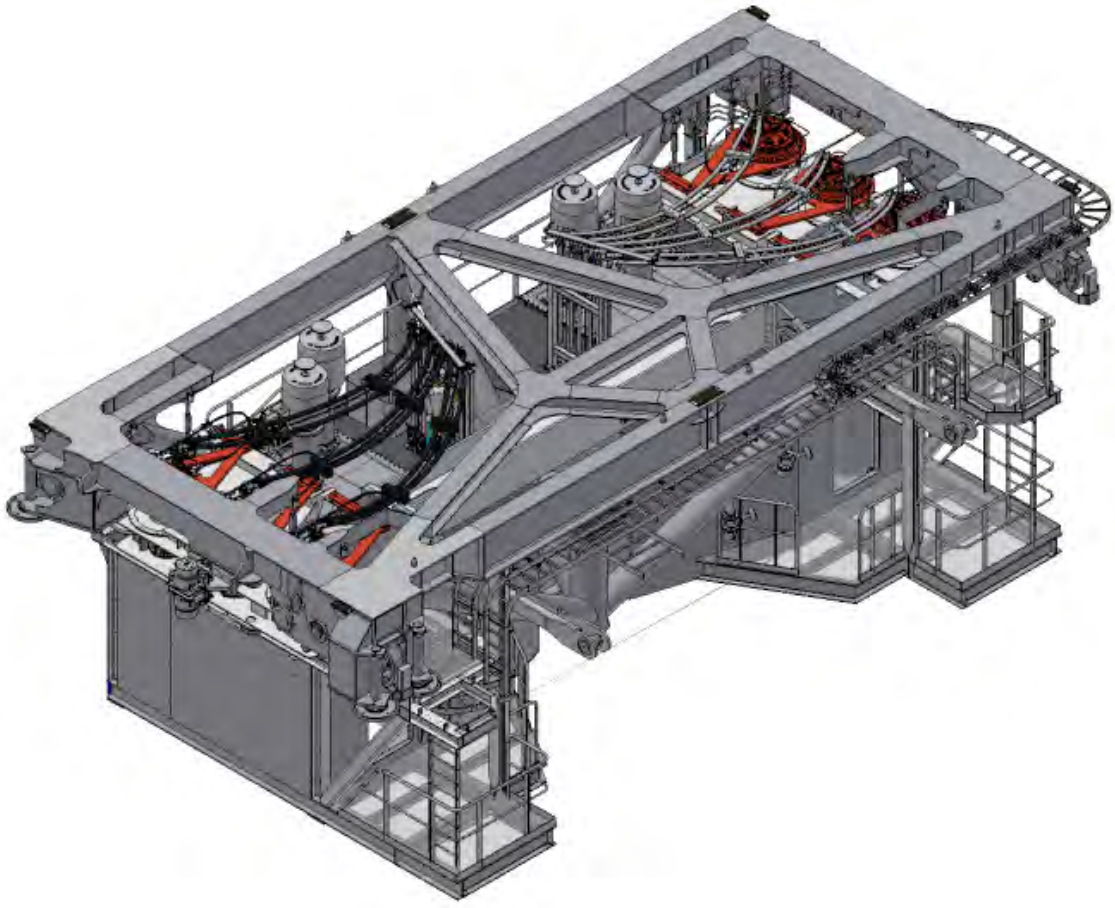

Figure 16: Isometric view of upper carriage without road deck

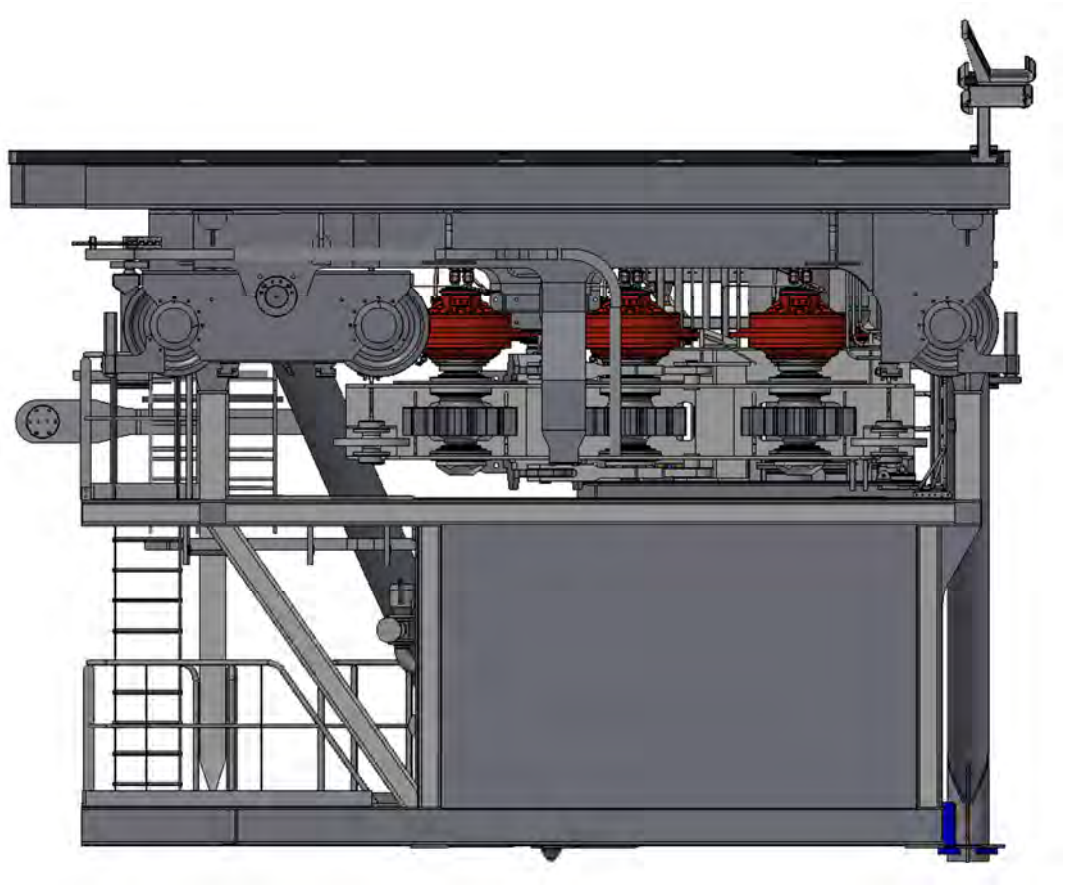

Figure 15: Side view of upper carriage

The gate transmits the vertical load to the upper wagon via a support frame. From the rubber bearing, the load is distributed over 6 wheels that run on 2 rails, one on each side of the gate recess. By using a bogie all vertical load is equally distributed (Figure 17). Besides the service-weight of the gate, the structure also carries the road deck used by traffic crossing the lock gate.

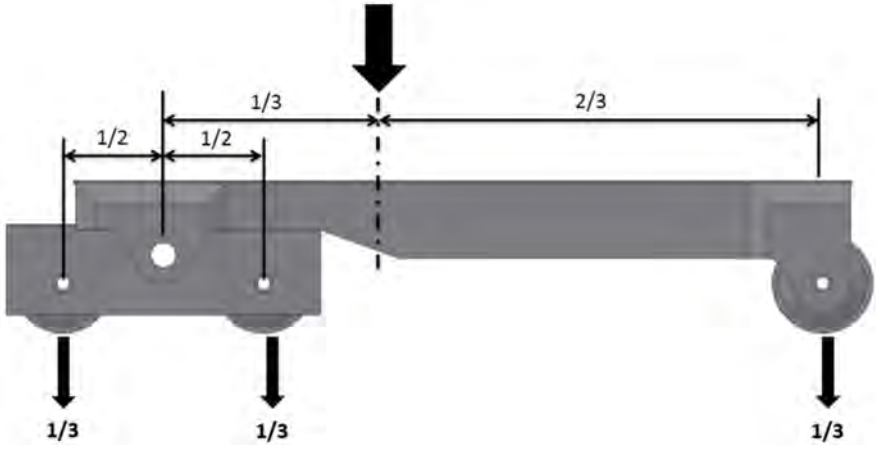

Figure 17: Load distribution upper carriage

In order to ensure the wheels run well on the rail during the entire movement distance of the gate, horizontal guided wheels are placed on one rail. Shifting of the upper carriage therefore is limited to a minimum, while the freedom of deformation of the concrete recess structure is not limited by fluctuating loads due to different water levels.

DRIVE MECHANISM

The upper carriage houses the machine room for the hydraulic driven transmission drive. The gate will be moved by six hydraulically powered pinions and two pin tracks on each side of the gate recess (Figure 18). Because of limited construction space, a conventional kind of drive mechanism like a cable-winch gear was not applicable. Finally, a life-cycle-cost analysis resulted in the design decision to move the gate by a pinion gear. Six 110kW electric motors give power to six hydraulic drive units which are connected directly to the pinions. A total traction force of 1500kN can be generated.

Due to the potentially large deformations of the concrete recess walls a penned track is preferred above a toothed track. In addition, a penned track results in a nearly longitudinal load transfer.

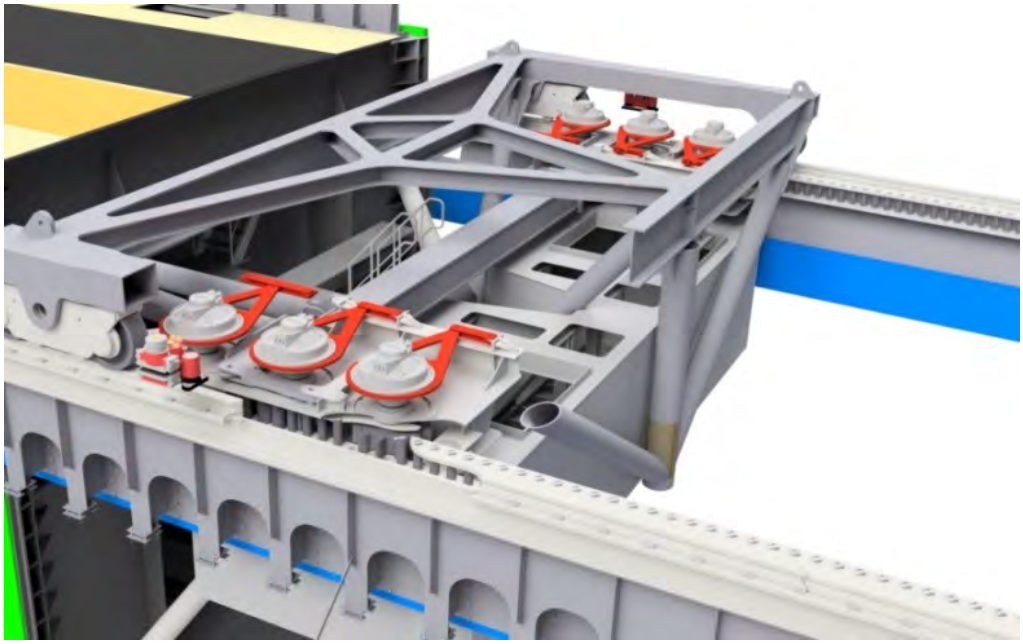

Figure 18: Pinion - pin track drive

The recess walls can undergo horizontal deformation by several centimetres. For this reason, the drive trains are pressed against the pin tracks by a central pressure bar with spring buffers (Figure 19). The drive trains are connected to the gate by two drive rods and suspended by pendulums to the main structure of the upper carriage.

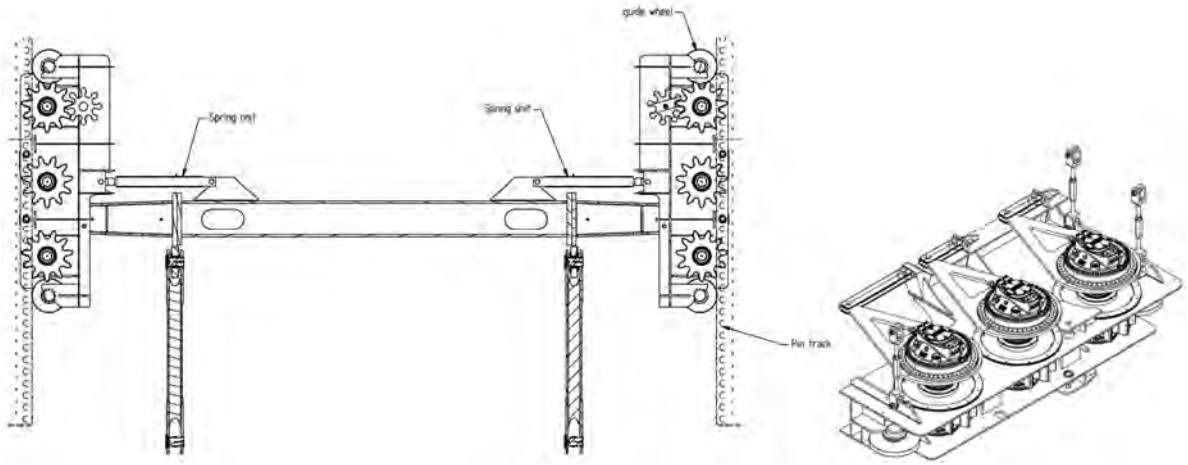

Figure 19: Suspension of drive trains

For the purpose of the required lock availability, redundancy of the drive mechanism is achieved through the installed overcapacity of the hydraulic gears. To meet the requirements of the speed of the gate movement during all possible environmental conditions (wave loading) only four of the six pinions are needed. If an electrical or hydraulic failure occurs in one of the gears, it will automatically isolate itself so that the movement of the gate will not stop. On the other hand, in favour of the lifespan (fatigue) of the mechanical components, all six engines will have to work.

CONSTRUCTION OF THE GATES

The fabrication of the steelwork is taking place in South-Korea (Figure 20). Since the lock is part of a flood defence and the gates are fatigue sensitive, the highest execution-class EXC4 according to Eurocode NEN-EN-1090 is required for the construction of the gates. In general, this results in an extra effort to the meet the required quality of the welds, the dimensional tolerances and the traceability of all steel plates.

To inform the steel manufacturer about these specific requirements clearly and correctly, it was decided to include the Korean manufacturer in the design process from the start of the preliminary design. Furthermore it was important to try to stay close to their practical experience of shipbuilding practice.

Figure 20: Steelwork fabrication of the lock gates in South Korea

The construction of the three gates takes about one and a half year. As soon as they arrive by a submersible vessel in the Netherlands, all electrical installations and hydraulics will be installed. After a testing period, they will be transported to the construction site and installed into the gate recesses.

Figure 21: Final situation

REFERENCES

Scale model of the new sea lock in IJmuiden, Deltares, 1230791-000-HYE-0006, final, February 2017

Joint development of hydropower and navigation on a major river: example of the Mekong River

Jean-Louis MATHURIN[1], Sébastien ROUX[2] and Benjamin GRAFF[3]

ABSTRACT

The study of the potential of the Mekong River for run-of-river hydroelectric development began almost 25 years ago, taking into account the joint development of navigation and other water usages, following the model of the multipurpose Rhône run of river cascade in France. Guidelines for locks design and operation were established by the Mekong River Commission (MRC) in 2009.

Today, a first hydropower project is under construction in Xayaburi (Laos), including a lock allowing crossing a lift of 39 m. Project reviews of high lift locks are still on course for several other developments under study in Laos.

CNR has contributed and is currently contributing to all these stages of joint development of hydroelectricity and navigation on the Mekong River, first on behalf of the MRC and nowadays on behalf of the Government of Laos.

The purpose of the paper is to highlight, along with the example of the Mekong at its various stages, the right principles and points of attention, to allow the harmonious development of navigation and hydroelectricity, on large rivers where modern navigation is emerging and where no major navigation structures exist.

Whatever the river considered, emphasizing the importance of global conception of the cascade, on contrast with a succession of disconnected development schemes, the paper deals notably with the search of a good compromise between the performance and safety for navigation, on the one hand, and the acceptable financial effort for the hydropower developer on the other hand, both at the guidelines adjustment phase and at the phase of guidelines enforcement for a new project review.

1 INTRODUCTION

Compagnie Nationale du Rhône (CNR), as concession holder for the Rhône River, is responsible for the production of hydroelectricity, navigation and agriculture since 1934 on a 550 km long river line, extending from the Alps (Swiss border) to the Mediterranean Sea in the south of France.

CNR Engineering, the integrated consulting office of CNR, brings to its external customers 85 years of experience and expertise in design, construction and operation of multipurpose run-of-river Hydroelectric Power Projects (HPP) along the Rhône River.

[1] CNR, Compagnie Nationale du Rhône
[2] CNR
[3] CNR

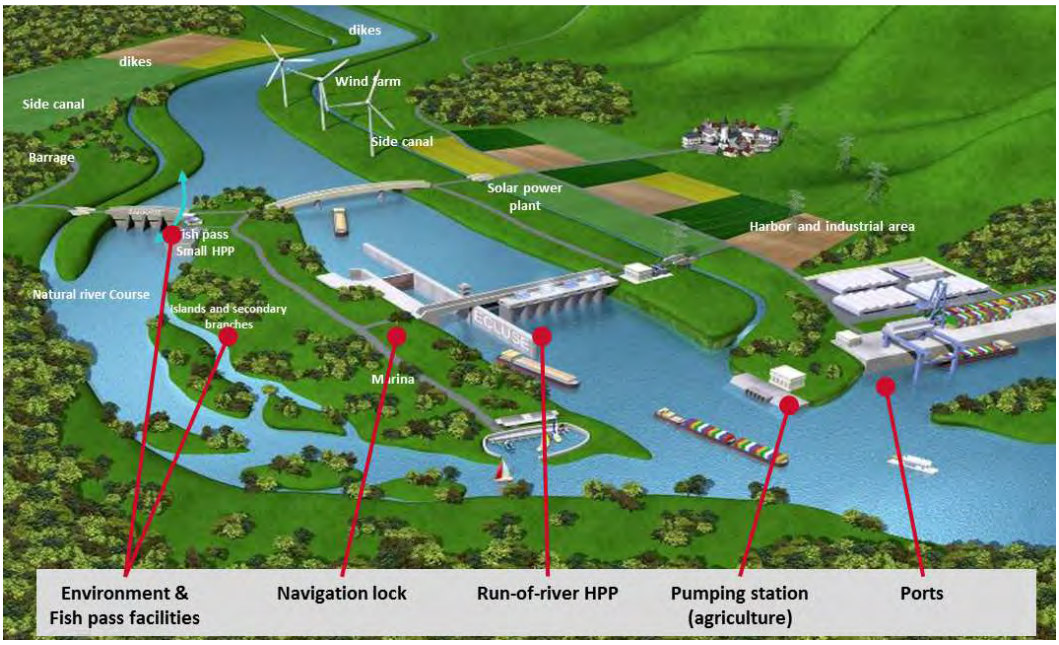

Fig. 1. CNR typical run-of-river multipurpose HPP

For nearly 25 years, CNR Engineering has been supporting the sustainable development of the Mekong River in close relationship with the Mekong River Commission (MRC) and its Member States (Laos, Thailand Cambodia and Viet Nam), particularly in the field of hydropower and navigation on the Mekong mainstream.

This paper aims at presenting this experience of joint development of hydropower and navigation on a major river. Thanks to its sound experience of integrated river development in both France and abroad, CNR is in a position to share its expertise regarding balance and efficient development of multipurpose HPPs along the same river including run-of-river hydropower generation and non-power interest such as inland navigation.

This paper engages CNR only and not its counterparts along the Mekong River.

2 CHRONOLOGY

CNR Engineering brings since nearly 25 years in Laos its know-how in terms of design and operation of hydroelectric run-of-river development.

In 1994, CNR Engineering did the master plan of the Mekong River for MRC. This Master Plan is still the reference study regarding Mekong River development.

Then in 2009, CNR Engineering carried out on behalf of the Government of Laos (GoL) the optimization study of the hydraulic and hydropower generation of five facilities planned on the Mekong mainstream upstream Vientiane in Laos. This study aimed at optimizing the cascade of 5 HPPs as a whole in the interest of GoL instead of an optimization project by project. This is still the reference study regarding the final design of the 5 corresponding projects.

Then, following a request of the Ministry of Energy and Mines (MEM) of the GoL, CNR Engineering assisted the developer of the Xayaburi project regarding hydrometeorology monitoring and forecasting, navigation and sediment management in order to optimize the design and to prepare operation phase. Xayaburi project consists of a power station totaling to an installed capacity of 1,285 MW and expected yearly energy production of more than 7,000 GWh. Furthermore, the project features a two-stage navigation lock, a spillway with 7 surface gates and 4 low level outlet gates, which have been designed specifically for the purpose of releasing sediments, and an intermediate

block. Extensive provisions for both upstream and downstream fish migration have been included (figure 2).

Fig. 2. General overview of progress of work as of January 2018 (photo: Marie Keller) From left to right: lock, spillway, low level outlet, intermediate block, power house and fish facilities

Xayaburi HPP is the first of the five HPP under development on the Mekong River upstream Vientiane. End of 2017, its construction was nearly 90% completed. The project and its final design are considered as a benchmark by the GoL and provide the minimum requirements every other mainstream project should feature. In particular, Xayaburi navigation lock has been the first lock to start operation on the Mekong River downstream China mid of 2015.

From 2015 onwards, CNR Engineering has also been entrusted by the MEM in several other missions:

- projects feasibility study (FS) reviews for 4 HPPs (Pak Beng, Pak Lay, Sanakham and Phou Ngoy) ensuring the consistency of the cascades design along the Mekong River and checking the quality of the design regarding hydrology, dam safety, sediment management and of course navigation;
- construction monitoring for Don Sahong HPP in the south of Laos as GoL Contract Engineer;
- FS of a Coordination and Monitoring Center dedicated to the coordination of operation and maintenance of all the multipurpose HPPs in Laos.

3 THE CASE OF MEKONG RIVER DEVELOPMENT

3.1 General outline of the cascade

The Lower Mekong River is a large potential source of energy. But, as in all lower courses of large rivers, development must respect other non-power water interests, notably navigation, and avoid, as much as possible, population resettlement.

Development of major rivers by realization of run-of-river cascades demonstrated its capacity to optimize services while limiting environmental and social impacts.

It is in this spirit and based on the model which has been proven on the Rhone River in France, that CNR conceived the overall hydropower development of the Lower Mekong, in 1994, on behalf of MRC.

The overall project concerned a 2300 km river course, from Chiang Khong (North of Thailand) to Phnom Penh (capital of Cambodia in the South), including the notable singularity of the Khone Phapheng waterfalls, 400 km north of Phnom Penh.

From Chiang Khong to Khone Phapheng waterfalls, corresponding to a river length of around 1600km, the total elevation gap is around 280 m. This gap has been split into 10 major steps.

The design of the Mekong cascades and of each site was done in order to:

- Minimize projects impacts on both downstream and upstream communities;
- Minimize the physical changes of the natural river regime;
- Comply with up to date standards of safety;
- Provide facilities which can be operated economically and safely, in harmony with other activities along the river;
- Provide lock facilities for passage of river boats and barges, taking into account future improvement and development of inland navigation;
- Provide appropriate facilities to support fish passage;
- Provide facilities for sediment routing, so that the natural sediment regime of the river can be maintained after projects commissioning;
- Provide practical and efficient facilities for electricity generation.

In this scheme, each step offered the opportunity of wide gauge navigation development on a great length of river (160 km on average), provided that a lock be built at each dam site, with an average drop of an acceptable order of magnitude (28 m).

In 2009, the Optimization Study of Mekong mainstream run-of-river hydropower, performed by CNR on behalf of the Lao Ministry of Energy and Mines, was dedicated to the formulation of an optimized scheme, from a hydraulic and power generation point of view, for the part of the cascade (5 sites) located in Lao PDR, upstream Vientiane. This study confirmed the spatial arrangement of the cascade, with some refinements regarding operating water levels to limit impacts on the riparian territories.

At present, on the course of the Mekong River in Laos, the construction of Xayaburi hydropower development is nearly 90% completed; Don Sahong HPP is under construction and shows progress of around 40%.

3.2 **Design of the navigation guidelines for the MRC**

In 2008, CNR Engineering was entrusted by MRC with a study dedicated to propose guidelines for planning, design, construction, and operation of navigation locks in relation with development of hydropower projects on the Lower Mekong Mainstream.

MRC wished to define good practices for the planning and design of the navigation locks within the Lower Mekong Basin context with the aim that, as far as possible, the development of hydropower projects on the Lower Mekong Mainstream would have a positive impact on the improvement of the navigation conditions.

The main challenge was how to set the size of the locks without traffic forecast, while preserving the potential development of navigation on the long run and not overburdening private hydropower developers. Indeed, hydropower development is an opportunity to develop navigation. Without hydropower development, there is no option for navigation improvement. But private developers have to bear all the costs related to navigation.

The first step of the study was devoted to benchmarking, especially with large rivers in Europe, which led to some key lessons:

- Hydropower developments on large rivers could finance wide gauge locks, sometimes with the support of public funding;
- Close coordination in the design, construction, maintenance and operation of locks and channels associated with “run-of-river” hydropower developments is essential;
- Hydropower developments provide an impetus for the construction of navigation facilities, but the increase in waterborne traffic may be gradual (20 to 30 year horizon);
- Impounded stretches and “natural” free-flowing channels may coexist along a river for a long period of time.

The second step consisted in taking into account navigation conditions, existing waterways or ongoing projects, upstream and downstream.

Upstream, consistency with the planned improvement of the Lancang / Upper Mekong in China was mandatory, with long term planned capacity of 4 x 500 DWT convoys.

Downstream, an important network of wide gauge waterways is operated in the delta of the Mekong River but the Khone Phapheng waterfalls at the border between Lao PDR and Cambodia currently present a physical obstacle to navigation. This is the reason why Don Sahong HPP located close to Khone Phapheng waterfalls in Sipandone does not feature any navigation lock.

Tentative proposals for lock dimensions and performance were made, taking into account long term vision (especially in this region of strong economic growth), sustainability, high reliability and consistency of projects along the Mekong Mainstream.

Considering waterway traffic capacity, and without any available global transport study, it was recommended that the envisaged hydropower developments include, at first stage, ship locks accommodating medium term traffic (i.e. 5 million tons per year as an order of magnitude) and allowing for future lock system expansion.

The design vessels envisaged was based on Chinese standards class IV (2 x 500 DWT) vessels, with a single line of barges (109 m x 10.8 m x 1.6 m). It was proposed to raise the draft up to 2.5 m, in the perspective of comprehensive development of the river with dams and complete impounding of the river.

Given current lock technology and taking into account reliability and life cycle costs (investment costs and maintenance costs), it was strongly recommended to limit the maximum hydraulic head of a single chamber to 30m, while the option of tandem locks (two-step locks) was considered to be a better alternative than ship lifts for crossing height differences greater than 30 m.

Emphasis was given to the coherence at river scale of transit time of each lock system, either with single chamber locks or two-step locks, leading to specifications for total lockage time (30 mn for a single chamber lock and 50 mn for a two-step lock) and for safe and smooth emptying/filling operations.

MRC issued the navigation part of its “Preliminary Design Guidance for proposed Mainstream dams in the Lower Mekong” in 2009 on these bases.

39 m high lock of Xayaburi hydropower project has been commissioned mid of 2015 according to these guidelines.

MRC guidelines are currently being revised but at the time this paper is written, the final version is not available.

3.3 **Xayaburi hydropower project**

In order to allow the vessel transiting the Xayaburi HPP, a two steps lock complex has been designed with a maximum head of 39.0 m for lF/E operations between the 2 lock chambers and 19.5 m for F/E operations between a lock chamber and upstream/downstream pond. Each lock chamber size is 120 m long by 12 m wide and has a minimum draft of 4 m.

CNR carried out an independent review of the lock design and released a set of recommendations in order to help the design to comply with MRC guidelines and to improve the navigation issues.

The main recommendations were dealing with the following items:

- Review of the number and dimensions of the filling & emptying system (F/E) components (culverts and ports) in order to improve the flow distribution,
- Review of the valves size and assessment of cavitation occurrence,
- Review of the water intake and outlets geometry in order to improve the flow distribution and reduce head losses,
- Assess the maintenance easiness of the filling & emptying system and bring modification in order to improve the limitation of the lane outage.

The review was performed on the basis of the MRC guidelines and was supported by implementing a 3D numerical model.

3.4 **The other hydropower projects**

Among the projects identified in the Mekong Master Plan in 1993-1994 and on behalf of GoL, CNR has been involved in the review of the following HPPs:

- Pak Beng HPP: this project is the northern most of the Low Mekong Basin dams. The project features a dam of 64 m height enabling a normal water level at 340 m asl, a 32.0 m navigation lock with a single lock chamber, spillway, fish passage and the powerhouse. The installed capacity is 912 MW.
- Pak Lay HPP: this project is located around 240 km upstream Vientiane. It is located downstream the Xayaburi HPP and upstream the planned Sanakham HPP. The project features a dam of 52 m height enabling a normal water level at 240 m asl, a 21.0 m navigation lock, spillway, fish passage and the powerhouse. The installed capacity is 770 MW;
- Sanakham HPP: this project is located on the mainstream of the Mekong River, 155 km upstream Vientiane. The project features a dam of 56 m height enabling a normal water level at 220 m asl, a 20.6 m navigation lock, spillway, fish passage and the powerhouse. The installed capacity is 660 MW;
- Phou Ngoy HPP: this project is located in the south of Lao PRD, 15 km downstream of Pakse city. It is the last project located upstream Khone Phapheng waterfalls. The project features a dam of 44 m height enabling a normal water level at 98 m asl, a 11.3 m navigation lock, spillway, fish passage and the powerhouse. The installed capacity is 728 MW.

For these 4 projects, CNR has been charged by GoL to review the FS regarding:

- Hydrology,
- Dam Safety,
- Sediment Transportation,
- Navigation.

CNR review takes place at the Lao level before submission of the project to MRC. The purpose of this internal review is to control the compliancy level of each project on the 4 above-mentioned topics in comparison with international standards, including but not limited to MRC guidelines. For the first three topics, international standards are based on ICOLD bulletins about safety of dams, World Bank operational policy on safety of dams, and international best practices regarding monitoring and modelling. For navigation, in addition to the MRC guidelines, CNR uses the European standards as well as the PIANC recommendations stemming from the available reports.

The main issues controlled and addressed by CNR regarding navigation during the reviews at Lao level are as follows:

- Lock design:
  - General design such as head, length, width that must fulfil specific requirements for navigation on the Mekong mainstream,
  - Design of the filling and emptying system,
  - Control of its hydraulic performances (lockage time, flow velocity in the culvert…),
  - Analysis of forces exerted on the vessel,
  - Risk of overfilling or over emptying of the lock if any;
- Lock approach and alignment:
  - Flow conditions both upstream and downstream for the range of discharge values corresponding to the operation of the lock,
  - Safety of access both upstream and downstream,
  - Length of guiding walls both upstream and downstream,
  - Sediment deposition in upstream and downstream approach channels and corresponding mitigation measures;
- Comparison between calculation on hydraulic modelling and measurements made on 2 physical models (scale 1/20 for the F/E system and scale 1/100 for the approach conditions);
- Maintenance, safety and operating policies taking into account both the coordination in the design and future operation

Usually, Developers are quite familiar with design and construction stages but the standards are not always fully appropriate or compliant with MRC guidelines for navigation.

Regarding operation of the project and, more precisely, operation of a navigation lock located in a cascade of dams, there is most of the time a lack of capacity and experience on the Developers side whereas it is important to keep in mind at design stage the future operation of each HPP, including their respective navigation locks.

By operation, we mean the follow-up of run-of-river concept, the definition of an appropriate operation pattern for the project and the management of the transparency of the project regarding flow, sediment and boats (considering only the 4 topics addressed by CNR) in order to ensure the safety of people, boats and dams whatever the inflow is.

The fact that the above mentioned HPPs are being developed by Independent Power Producers (IPP), has made the GoL aware of the need to set up a state agency dedicated to the coordination and the management of all the multipurpose hydropower plants implemented in Lao PDR. Regarding navigation in particular, the purpose is to make sure that navigation lock maintenance is coordinated at the level of the whole Mekong River in Lao PDR in order to limit the duration of navigation closure. CNR is currently working on a feasibility study for the implementation of Coordination and Monitoring Center (CMC), supported by its sound experience on the Rhone.

4 WHAT LESSONS FOR THE JOINT DEVELOPMENT OF HYDROPOWER AND NAVIGATION ?

4.1 Hydropower as an opportunity to develop navigation

The development of the waterway in shallow river courses can firstly be ensured by free flowing river training. This type of development, which aims at improving the conditions of navigation in low water by concentrating the flow of the river in a single channel, reaches quickly its limits (draft of the order of 1.5 m / 2m during low flow periods) that are incompatible with the transit of wide gauge boats, only able to compete economically with road and rail.

Finally, in shallow rivers courses, only water level control in low flow periods can ensure opportunities of year-round wide gauge navigation. From this point of view, the realization of run-of-river projects, by creating reservoirs -the lateral extension of which may be limited by dikes- allows the development of such navigation on long lengths of rivers with large draughts.

In lower courses of rivers, to take into account the full potential offered by the development of a river, there is no interest to implement high head dams. On the contrary, a cascade of run-of-river projects is particularly convenient. Navigation crossing is facilitated by acceptable lifts; transit of sediment can be permitted by suitable flushing device (implementation of Low Level Outlets) and good operation coordination.

By creating dams controlling water levels and financing all or part of lock structures, hydropower developments are major opportunities to improve navigation conditions on a river.

But, regarding power generation optimization, as well as impact minimization, operation coordination or navigation conditions coherence, the best method is to globally design the cascade of schemes at the river scale. That is all the more true with a different developer on each site. In that case, it is very suitable to implement a coordination and control body, as it is envisaged on the Mekong River, in Laos.

A second step of optimization has to be done at the scale of each individual site of dam and lock.

4.2 Choice of the lock dimensions

Lock dimensions must be based on a long term vision: length, width and depth can hardly be modified once they have been built and they have most of the time a very long service life (generally about 100 years). Lock chamber dimensions fix the design vessel for the connected waterways.

Another important point is the coherence at the regional level: existence of regional standards, or design with a view on further standards.

Technical- economical aspect should also be born in mind: total lock cost has to be compared with future transit projections to evaluate the general interest of the investment. Usually, considering only navigation transit issue is not enough profitable. Total additional cost of navigation works should be acceptable for the hydropower plant developer owner.

So, it is understandable that lock dimensions associated to hydropower is the result of a compromise between the performance and safety for navigation on one hand, and the acceptable financial effort for the hydropower developer on the other hand, especially on a river where industrial navigation is emerging.

4.3 Recommended design dispositions and guidelines

According to our experience, the guidelines with respect to navigation issue should be organized according to 9 major items detailed hereafter:

- General requirement

Give to the developer the definition of the different operating level and discharge that are required in upstream and downstream pond (as Lowest Navigable Level (LNL), Mean High Navigable Level (MNL), and Highest Navigable Level (HNL) in order to standardize these data for every project.

- Dimension and design vessel

Fix the lock dimension and layout and specify the design vessel for which the lock structure has to be studied and built.

- Lockage time and availability

Give the target filling and emptying time, specify the lock minimum availability and the maximum lock outage to be allowed. Give also the maximum allowable water slope and thus the acceptable level of forces exerted on the design vessel during a lockage. This second issue being in total opposition to the first one, indeed the faster the lock is filled/emptied, the greater will be the turbulence in the lock chamber and consequently the forces applied on the vessel.

These guidelines are very important since they permit determining the daily throughput and thus the transit capacity of the lock system. The main difficulty is obviously to set targets suitable to the navigation context, either for F/E time or for the water slope threshold value. Indeed too stringent requirement would lead to over design the lock F/E system and would severely increase the construction and operating costs.

- Location and alignment

Fix the required layout (such as the features of the guiding wall for instance) of upstream and downstream channels in order to ensure a safe approach from both sides for the design vessel. The designer has to study and take into account the natural flow fields and the man-made currents stemming from the HPP and/or the spillway operations. He has to check that the longitudinal currents, and cross-current do not exceed respectively 0.5 m/s and 0.3 m/s in lock approach channel (according to European standards). The sediments issues, especially the risk of major deposit in the lock approach channel and their management, are also addressed.

- Construction

Ask the designer to assess the navigation condition during the construction period (increase of the flow velocity due to the construction cofferdam for instance), to propose mitigation or alternative to keep the navigation and the goods transit going on during this period.

- Service life

Specify the functional life time of lock structure and lock equipment.

- Expansion

Specify the layout requirement for implementing a second lane of lock if needed in the future.

- Chamber equipment

Detail the minimum equipment to be implemented in the lock chamber such as bollards, ladders and gate protection device.

- Design, operation, safety and maintenance

Specify the requirement for issues such as lock access, control and command system, emergency accesses, redundancy in lock components, environmental impact. These items are generally not very well addressed by the developer in the design phase since they deal with issues that appear to be far away from the concern related to the design of the structure. They need anyway to be looked at with attention since they may lead to major modification of the design in its late stage.

Each lock being designed by a different developer, the introduction of such guidelines is of utmost importance in order to standardize the quality of every scheme. It also allows to check every design at the same level and to make consistent the lock structures along the full cascade on the river.

5 CONCLUSION

CNR has contributed and is currently still contributing to all these stages of joint development of hydroelectricity and navigation on the Mekong River, first on behalf of the MRC and nowadays on behalf of the Government of Laos.

This experience shows that run-of-river hydropower developments provide an impetus for the construction of navigation facilities over a great length of a major river, provided that the cascade of schemes is globally designed at the river scale, keeping in mind the coherence of operation conditions all along the future waterway.

In this aim, the implementation of common guidelines for navigation facilities are of utmost importance, especially for the design of locks which are major and costly structures which can hardly be modified once they have been built and, then, condition the maximum dimensions of the vessels. These guidelines allow standardizing the quality and performance of each lock system. This is all the more true when every scheme is designed by a different developer, which is the most frequent scenario.

When a new development is launched, in the framework of the overall cascade scheme, a second step of optimization has to be done at the detailed design level, taking into account the performance and safety for navigation, on the one hand, and the total cost of the project on the other hand.

NUMERICAL SIMULATIONS OF A LONGITUDINAL FILLING SYSTEM FOR THE NEW LOCK AT TERNEUZEN
by

T. O'Mahoney[1], A. Heinsbroek[1], A. de Loor[1], W. Kortlever[2] and K. Verelst[3]

ABSTRACT

The lock complex at Terneuzen in the Netherlands is the link between the Port of Ghent in Belgium and the Western Scheldt. The Flemish–Dutch Scheldt Commission (VNSC) is executing its plan to build a new large lock at this complex. As part of the research on the levelling system of the New Lock, Deltares has performed numerical calculations of a conceptual design, consisting of a longitudinal filling system, similar to the one present at the West lock in Terneuzen. For this conceptual design both detailed 3D CFD simulations of particular elements of the culvert system and 1D dynamic WANDA simulations of the entire system were carried out. The results of these simulations have been used to define contract requirements for the hydraulic design of the New Lock during the tender process.

1. INTRODUCTION

The canal from Ghent to Terneuzen forms the connection between the port of Ghent in Belgium and the Western Scheldt in The Netherlands. It is the only way for sea-going vessels to reach the port of Ghent. Since the water level in the Western Scheldt is dependent on the tide and the Ghent-Terneuzen canal has a fixed target level, a lock complex was built near Terneuzen.

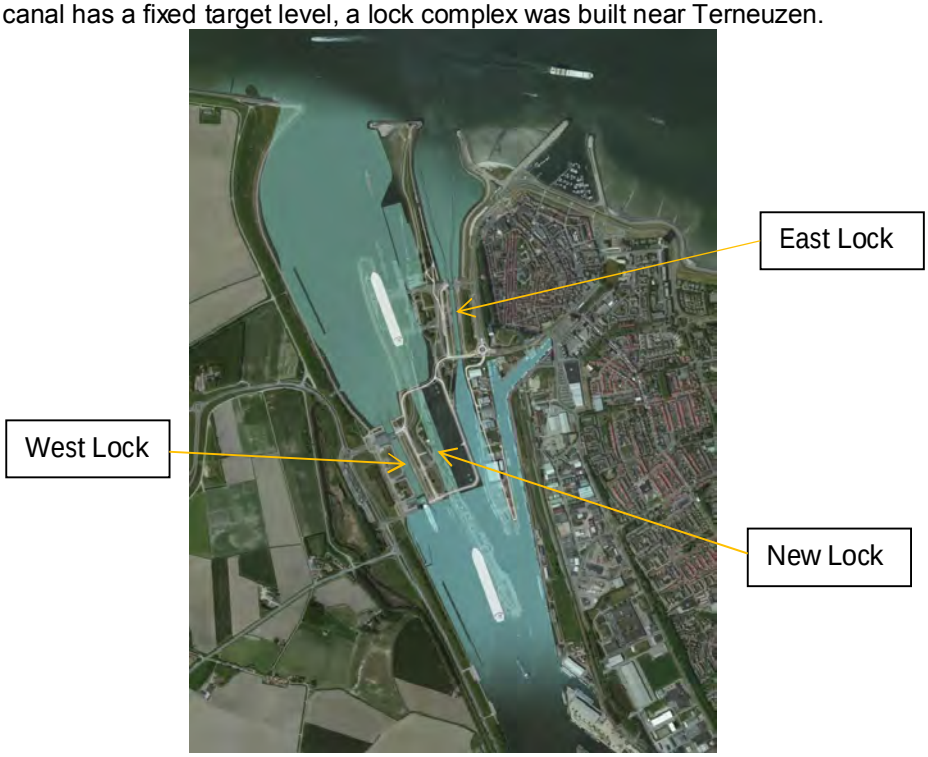

Figure 1: Layout of the new lock complex in Terneuzen (source: nieuwesluisterneuzen.eu)

[1] Deltares, Netherlands, tom.omahoney@deltares.nl
[2] Rijkswaterstaat, Netherlands
[2] Flanders Hydraulics Research, Belgium

The current lock complex consists of three locks: the Eastern Lock, the Middle lock and the West Lock. The West Lock is the largest and was constructed in the 1960s. It is sufficiently large to accommodate the Panamax class of sea-going vessels. The Flemish–Dutch Scheldt Commission (VNSC), a cooperation between the Dutch and the Belgian governments, is executing its plan to build a new larger lock at this complex, which will replace the Middle lock (Aerts et al. 2015). When completed, the New Lock will have two rolling gates at each head and a lock chamber with dimensions 55 m x 452 m between the outer doors at each head. This will rank it amongst the 10 largest locks in the world and will be sufficiently large to accommodate the Neo Panamax class of sea-going vessels. The water level of the canal is on average +2.13 mNAP (Amsterdam Ordnance Datum) and the lock operates between an extreme low tide of -2.69 mNAP (LAT) and a maximum lockage level of +4.60 mNAP on the Western Scheldt side. The largest head differences are therefore at low tide when the lock is filled from the canal or emptied to the Western Scheldt. The wish of the VNSC is that levelling can take place within 15 minutes for a head difference of 4 m, although the maximum allowed will be 20 minutes.

Recent hydraulic research at the scale model facility in Deltares, Delft, The Netherlands, on the levelling system of the New Lock of Terneuzen has shown that a system of openings in the rolling gate, as is being employed in the new sea lock of IJmuiden near Amsterdam (Kortlever et al. 2018), was not appropriate given the expected density differences across the New Lock and the desired levelling times. This conclusion is due to the large mooring forces caused by the density currents on the moored vessel during levelling (see Nogueira et al. (2018) and van der Hout (2018)). Consequently the choice was made for a longitudinal levelling system, similar to the one present at the West Lock in Terneuzen. The principle behind this choice is that density currents are generated at both bow and stern of the ship in the lock chamber and that the forces generated by these currents on the ship will partially cancel each other out leading to an overall reduction in the mooring forces. Decades of experience with the West Lock also give confidence that such a system will give acceptable levelling times even given the larger scale of the New Lock.

The final design of the lock is to be made by the contractor who will build the lock. Prior to the tender process of the New Lock, completed in the summer of 2017, additional hydraulic research was conducted at Deltares for VNSC to investigate the hydraulic dimensions of the longitudinal levelling system of the new lock. The preliminary scale model research with gate openings was completed only shortly before the start of the tender process. The additional research was conducted solely with numerical techniques in order to provide hydraulic information and requirements for the longitudinal levelling system in the tender process. A combination of 3D Computational Fluid Dynamics (CFD) of different components of the culvert system and dynamic 1D culvert simulations with WANDA (www.deltares.nl/en/software/wanda/) were used to simulate the levelling process. This approach cannot account for density flows in the lock chamber. The final design made by the contractor will partly be verified in a scale model where density differences can be accounted for.

The research regarded two alternatives for the longitudinal levelling system: One alternative where the lock is filled via bottom grids in the lock floor at ¼ and ¾ of the length of the lock chamber and one alternative where the lock is filled via openings in the wall at both sides of the lock and at both heads. The first system is similar to the levelling system of the current West Lock, the second system does not have direct antecedents, except a scale model investigation of the filling and emptying system of the Baalhoek Lock (WL Delft 1975), which was never constructed.

For both alternative filling systems detailed flow patterns and hydraulic resistances of the various elements were calculated with 3D CFD simulations. Emptying and filling situations were considered owing to the asymmetry of the system. Consideration was also given to the flow patterns in the approach harbour for the design of the intake openings. Subsequently, the calculated hydraulic resistances were used in the 1D dynamic model to simulate the levelling process in the lock chamber. The water level slope in the lock chamber could be calculated during the simulation to provide a first estimate of mooring forces and achievable levelling times. This model was also used to assess the inertia effects of the large culvert system, such as overtravel and to assess the time-

dependent asymmetry of the system. Due to overtravel, the water level in the lock chamber can overshoot the water level in the approach harbour and consequently influence the force on the gates during opening at the end of the levelling process. Unequal discharges through different branches of the culvert system can lead to large forces on the moored vessel in the lock chamber. The numerical simulations showed that both types of longitudinal filling systems were feasible for achieving the desired levelling times whilst maintaining a safe levelling process.

This paper only discusses the results of the numerical modelling for the system with bottom grids because the consortium which won the tender to build the New Lock (Sassevaart[1]) has chosen this type of system. The final design of the lock, including the design of the levelling system, is carried out by Sassevaart, who will follow a similar approach for the verification of the levelling system. Because this approach does not take into account density currents, the final verification of the levelling system of the New Lock, will be made in a physical scale model at the Deltares facility after the final design has been completed.

2. DESCRIPTION OF THE SYSTEM

The variant of a longitudinal filling system with culverts on one side of the lock chamber is based on the principle of the West Lock in Terneuzen (Philpott 1961), consisting of filling the lock chamber using two bottom grids (see Figure 2). These bottom grids are located at positions of ¼ and ¾ of the length of the lock chamber (here the length is considered between the two inner gates of the lock heads). This configuration allows for the filling of the lock chamber at two longitudinal locations whereby for the normative vessel a density current at both the bow and stern will develop.

The variant for this research shows some differences with the design for the West Lock, mostly owing to restrictions on space in the already existing lock complex. A first difference is that the culvert system is positioned along the lock chamber wall opposite the gate recesses whereas for the West lock the culverts are positioned around the gates recesses. Also the inlet ports of the culverts in the approach harbour are at the same level as the culverts along the lock chamber whereas for the West lock these ports exit at the bed level of the canal on both sides of the lock. Similarly, owing to considerations about the cost of the construction all elements of the culverts are to be located within 25 m of the lock chamber wall. Additionally, the West Lock has extra valves at the T-junctions to control the flow to each bottom grid. Owing to space restraints it is not possible to add such valves to the New Lock system.

[1] Sassevaart is a consortium consisting of BAM, DEME and Algemene Aannemingen Van Laere (Source: https://nieuwesluisterneuzen.eu/partners/sassevaart)

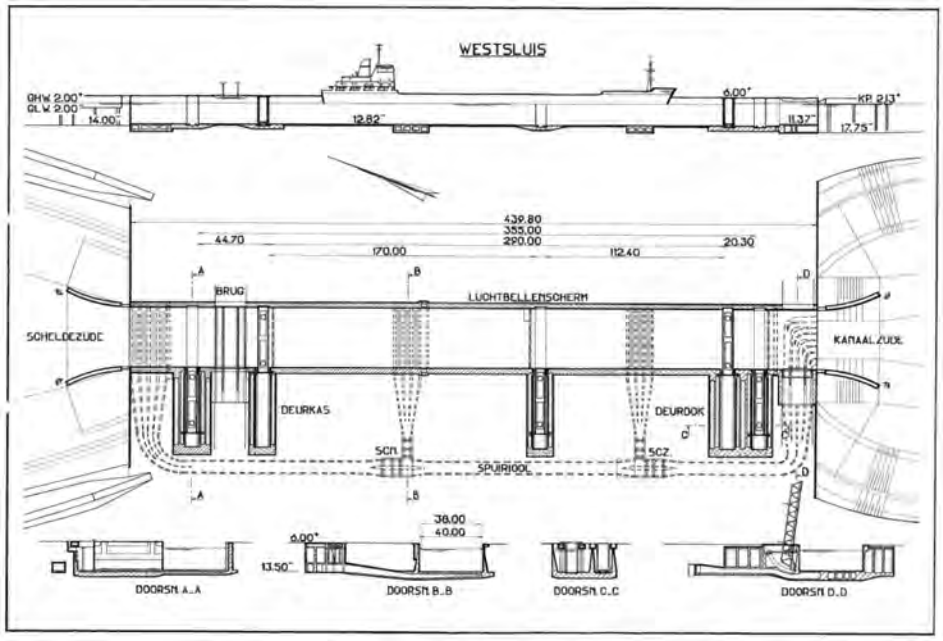

Figure 2: Summary view of the design of the West Lock

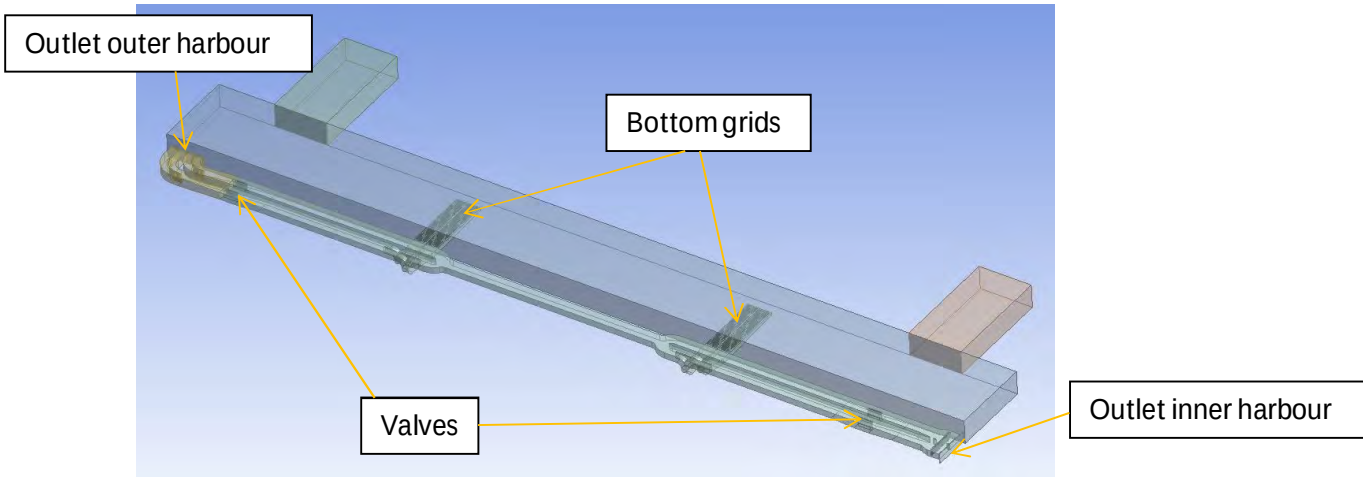

Figure 3: 3D CAD rendering of the culvert system studied for the New Lock.

The main dimensions of the conceptual design for the system of the New Lock (see Figure 3) are as follows:

- The culvert system consists of two culverts, each 4 m x 8 m. Between the two bottom grids the culverts converge. The total throughflow area in the culvert to each bottom grid is therefore 32 m^2,
- Each bottom grid is 45 m by 16.5 m. The throughflow area of each grid is 60 m^2 made up of 16x54 holes of 30 cm diameter each,
- The space beneath each bottom grid is split in two, separated by a central wall,

- Each culvert has a T-junction directed downwards which connects to a bottom grid. However, because the culverts converge between the bottom grids it is also possible for the flow to reverse itself at this convergence point and flow backwards towards the nearer bottom grid instead of onwards towards the farther bottom grid,

- The culvert valves are located at the location of the gates at each lock head and consist at each location of 4 separate valves of 5 m by 3 m, providing two valves per culvert. The smallest throughflow area in the system is located here, 30 m^2 per culvert,

- The outlet in the inner approach harbour, at the canal side, has dimensions 4 m by 22 m. The outflow direction follows the longitudinal axis of the culvert,

- The outlet in the outer approach harbor, at the Western Scheldt side, has dimensions 6 m by 22 m, being larger because of larger discharges for levelling in this direction. The outflow direction is perpendicular to the longitudinal axis of the culvert. This choice was made to generate a more favourable flow in the approach harbour for vessels entering the West Lock, whereby the flow from the new lock is directed away from the West Lock.

3. CFD MODEL OF CULVERT ELEMENTS

The culvert system was modelled using the commercial CFD software package Star-CCM+ (https://mdx.plm.automation.siemens.com/star-ccm-plus). The culvert system is divided into smaller elements and CFD models were made of each element to determine the flow patterns and resistance coefficients under steady boundary conditions. Both filling and emptying flow directions were considered. These CFD calculations cannot account for dynamic effects such as the inertia of the water, leading to overtravel in the lock chamber, or even the varying discharge in the culvert and water levels in the lock chamber. They are meant to provide the input of resistance coefficients to the 1D dynamic WANDA simulations. The resistance coefficients, ξ, were determined by the following formula:

$$\xi = 2A_{ref}^2 \Delta p/\rho Q^2 \qquad (1)$$

where A_{ref} is the reference flow area of the culverts [m^2] is, Δp is pressure drop across the element measured from the total pressure [Pa] (static pressure plus dynamic pressure), ρ is the density [kg/m^3] and Q is discharge [m^3/s]. A uniform density of 1000 kg/m^3 was used for these coefficients throughout this work.

The results of the CFD simulations are also judged based on flow uniformity through the bottom grids. Each bottom grid is split into sections as presented in Figure 4 and the proportion of the discharge through each section is analysed. The design is considered to be good on this aspect if the ratio of flow through each section of the bottom grid is close to 50/50 as this is expected to give lower forces on the vessels moored in the lock.

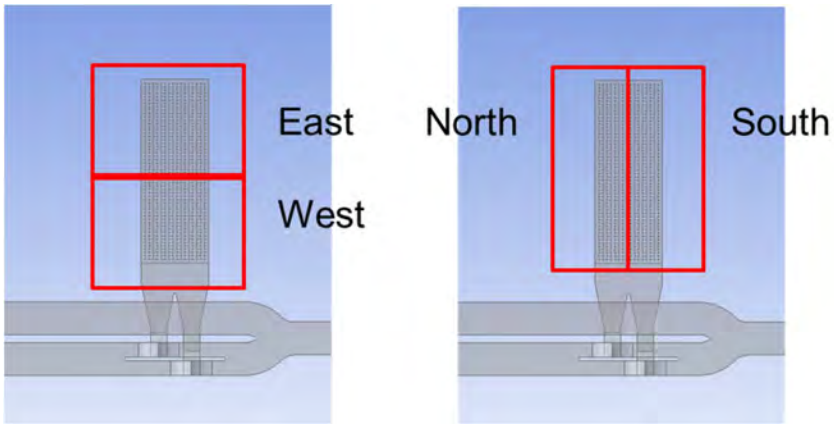

Figure 4: Plan view of the bottom grid showing the regions of interest for assessing flow uniformity

3.1 Geometry

Separate CFD models have been made for the outlet at the inner harbour, the outlet at the outer harbour and for the system of bends and T-junctions to the bottom grids including the outflow into the lock chamber. The model of the system of bends and T-junctions is for the analysis only split into sections (see Figure 5) to identify the areas of significant losses. The names of these sections are given in Table 1.

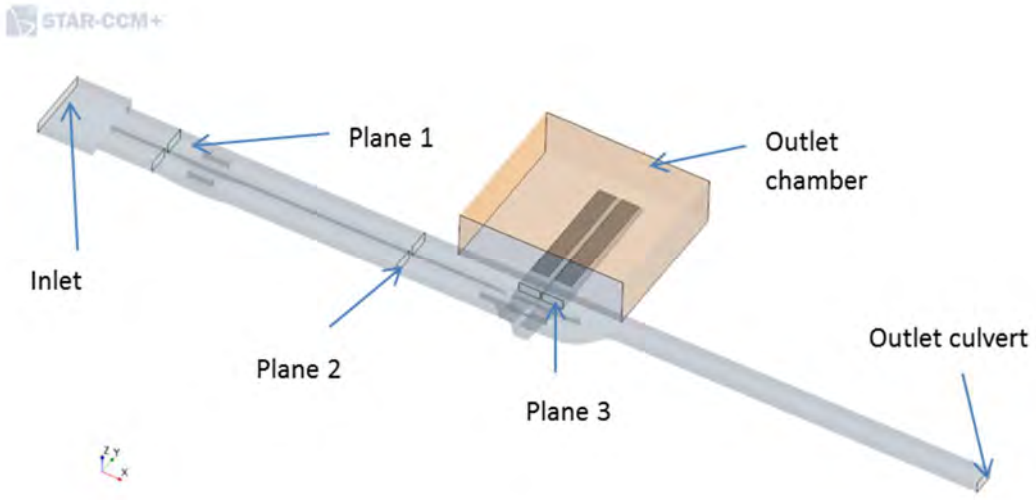

Figure 5: Isometric view of the CFD model of the culvert bends and bottom grid with locations of the planes between which the different elements are defined.

Element	Inlet plane	Outlet plane
Valves - chamber	Plane 1	Outlet chamber
Bend	Plane 2	Plane 3
Bottom grid	Plane 3	Outlet chamber
Valves – second culvert	Plane 1	Outlet culvert
T-junction	Plane 2	Outlet culvert

Table 1: Definitions of the elements in the CFD model

The intermediate planes 1, 2 and 3 are cross-sections of the culverts where the flow variables are calculated as averages over both culverts. The outlet chamber is an outlet volume, the width of the lock chamber and with approximately the lock depth. The outlet plane is a combination of the ends of the outlet chamber and the top, not including the walls of the lock chamber.

3.2 Mesh

The meshes for the simulations are made with the Star-CCM+ Trimmer mesh which uses hexahedral cells of mostly cube form. One exception is the mesh around the bottom grid which uses polyhedral cells. The grid for each of the final simulations is refined locally such that there is sufficient mesh refinement at the areas of the smallest cross-section, giving at least 20 cells between the dividing beams of the outflow port and at least 10 cells in each opening of the bottom grid. A prism layer is added at the walls of the culvert system to allow the boundary layer to be modelled with wall functions. The y^+ value is generally between the required $30 < y^+ < 300$ value for the validity of the wall functions and is no greater than 500 in the entire domain. The total number of cells for each geometry is then in the order of 13 million cells. Figure 6 gives an impression of the level of refinement in the models.

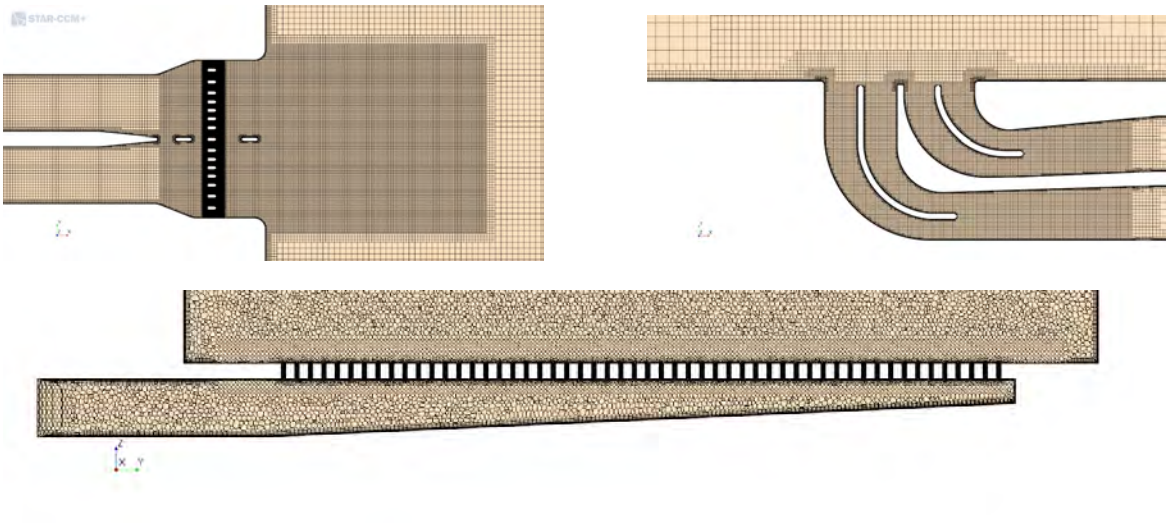

Figure 6: Detailed views of the areas of local mesh refinement for the models of the outlet at the inner harbor (top left),the outlet at the outer harbor (top right), and, the chamber below the bottom grid and the bottom grid (below)

3.3 Numerical settings

The numerical settings of the simulations can be summarised as follows

- Steady boundary conditions with an unsteady solver,
- First order implicit scheme for temporal discretisation,
- Second order scheme for spatial gradients,
- Segregated solver for pressure and fluxes,
- 10 internal iterations per time step,

- The time step used in the simulations varies between 0.5 s and 1.0 s,
- The realizable k-ε turbulence model is used, except for the simulations of outlet in the outer harbour where the k-ω SST model is used because it is known to be more effective for the prediction of separation points in curved bends,
- Constant discharge inlet boundary conditions are used of 100 m^3/s. For the simulations of the system of bends and T-junctions to the bottom grids a distribution between outlet chamber and outlet culvert of 50/50 is specified through a boundary condition of -50 m3/s volume flux at the outlet culvert boundary,
- A roughness of 2 mm is used for all concrete walls in the domain,
- No water surface is modelled. The outlet planes in the harbours and lock chamber are modelled as pressure boundaries. The focus of the work here is on the flow in the culverts so this is considered to be a reasonable approximation.

3.3 CFD results

The CFD simulations were run to investigate design differences for certain elements. The outlets to the approach harbours were assessed based on uniformity of the flow with low velocity, predominantly for the emptying direction, and on a loss coefficient which was not too high. The low velocity in the harbour is to minimize the hindrance to vessels moored or sailing in the harbour. The low loss coefficient allows the total discharge capacity of the entire levelling system to be high enough to achieve the required levelling times. To assess whether the losses were acceptable the complete levelling system was modelled in the one-dimensional WANDA model (see section 4 of this paper). After some iterations of the design for the inner approach harbour an outlet has been selected in which the flow is distributed over a wider area by a row of columns, perpendicular to the flow. The total outflow area was chosen such that the average velocity for the largest expected discharge during levelling was less than 2 m/s. The rack of beams was then designed to distribute the flow over this total outflow area. In Figure 7 the final result can be seen. The flow velocities between the beams are of course higher than 2 m/s but the flow is well distributed downstream of the beams and at the outlet t.

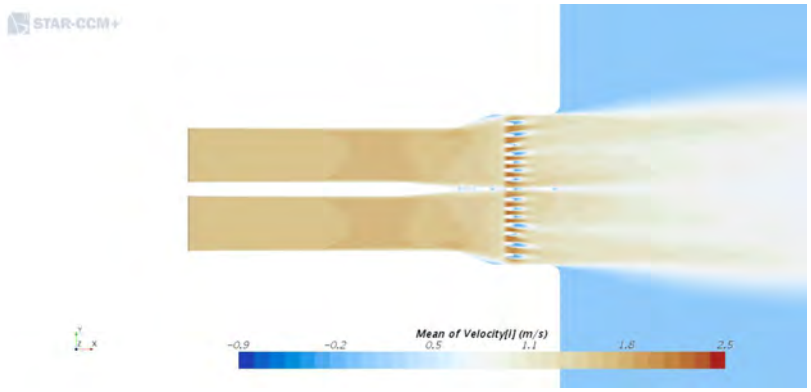

Figure 7: Top view of mean velocity field for the outflow at the inner harbor when emptying the lock

For the outer approach harbour a different solution has been chosen, namely an outlet which directs the flow away from the entrance of the adjacent lock (the West Lock). This, it is expected, will prevent unwanted high currents from emptying of the New Lock reaching the fairway of the entrance to the

older West Lock and should enable the operation of both locks to continue relatively independently of each other. At the outer head the emptying discharges are higher than at the inner head because the head difference at low tide (emptying into the outer harbour) is higher than the head difference at high tide (emptying into the inner harbour). Furthermore emptying into the outer harbour will cause a surface current due to density differences between lock and approach harbour.

Figure 8 shows the final solution for this outlet with 90 degree bend. Guide vanes are added into the culvert at the bend to steer the flow and a nearly perpendicular flow is achieved in this simplified outlet. The flow manages to take the bend without high concentration of flow in the outer bend.

Figure 8: Top view of velocity field for the outflow at the outer harbor when emptying the lock

For the bottom grids, similarly, the criterion of flow homogeneity was used to judge different designs. The sections of the bottom grid as shown in Figure 4 were used to define discharge ratios which should not deviate too much from 50/50. This criterion is to provide a uniform filling of the lock and to prevent asymmetric flow patterns in the lock during levelling, which can lead to high forces on the moored vessels.

A bottom grid with a throughflow area two times the area of the culverts is used in the conceptual design. Handbooks for internal flows (Miller 1978) claim that in order to have a uniform flow manifolds such as this bottom grid should not have a throughflow area larger than the throughflow area of the incoming duct or culvert. However, the West Lock has a ratio of throughflow area between bottom grid and culvert of 2 and a sloped floor underneath the grid which distributes the flow more evenly. This sloped floor has also been adopted in the conceptual design of the New Lock (see Figure 6 where this is visible in cross section). CFD simulations with a smaller throughflow area of the bottom grid were also conducted but these resulted in a large loss coefficient. Figure 9 shows another example of a design iteration which was conducted with the CFD. The two simulations shown are both with the larger bottom grid throughflow area. In the first simulation, the chamber underneath the grid is combined in one single chamber. Owing to the sharp turn that the flow makes from the culvert into this chamber a circulating pattern is formed which leads to a non-uniform flow out of the grid. This is improved by dividing the chamber into two separate parts, each fed from one branch of the culvert. The resulting flow out of the grid is not perfectly uniform but the ratio of flow through the different sections stays between the ratios 45/55 and 55/45 (see Table 2).

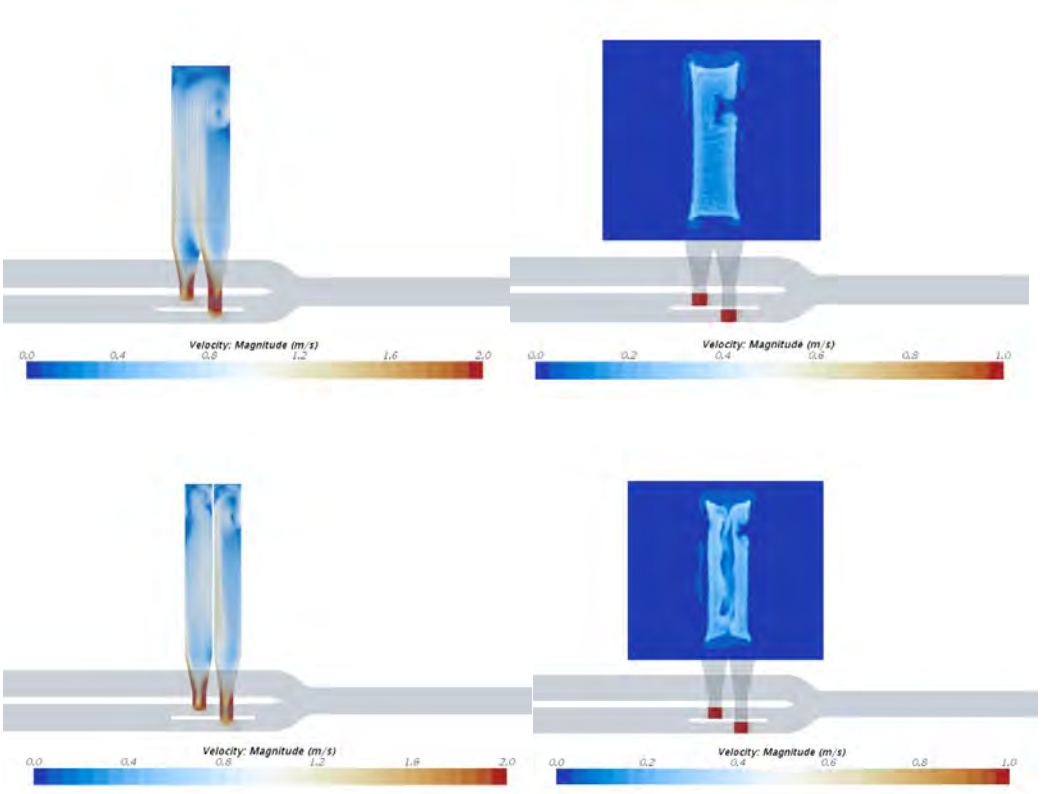

Figure 9: Top view of velocity field for the bottom grids, left in the chamber below the grids and right in the lock chamber above the grids. The top two figures are for a bottom grid with a single spacechamber and the bottom figures are for a bottom grid with two separate spaces under the gridlower chambers.

Figure 10 shows the velocity field above the bottom grid for an emptying scenario. The flow is almost symmetrical between the North and South sectors (see Figure 4 for definitions) but far from symmetrical between the East and West sectors. It is considered that for emptying this lack of symmetry is less important as the forces on the vessels in the lock tend to be more favourable for emptying scenarios. The distribution of flow within the bottom grid for the final simulations is given in Table 2.

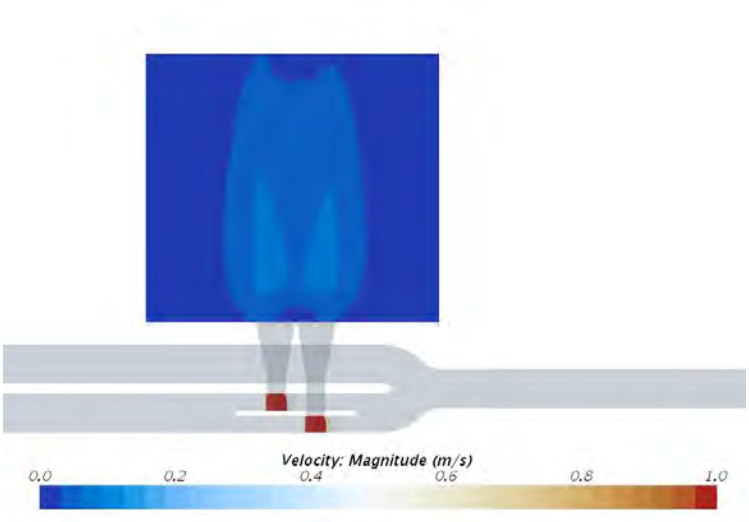

Figure 10: Top view of velocity field above the bottom grid by emptying

Simulation	East/West [%/%]	North/South [%,%]
Filling	54/46	52/48
Emptying	39/61	51/49

Table 2: Results of the flow distribution within the bottom grid

In Table 3 the summary of all loss coefficients for the different elements based on the final simulations is given as well as the totals for the trajectory to the northern grid (R1) and the southern grid (R2) for each scenario. The totals are deduced from the sum of the appropriate elements and are not the result of a single calculation in each case. The final total loss coefficients are then converted to a net throughflow area of the system by means of the discharge coefficient $\mu = 1/\sqrt{\xi}$. The reference throughflow area A is the throughflow area of the culverts at the valves (30 m^2) in all cases.

The system which was chosen to act as a reference system and which is simulated in the WANDA model of the next section therefore has at least a net throughflow area of 34.5 m^2 for filling and 33.0 m^2 for emptying.

Element	ξ [-]			
	Filling from Scheldt	Emptying to Scheldt	Filling from Canal	Emptying to Canal
Valves – chamber	1.95	1.72	1.95	1.72
Valves – outlet culvert	0.94	1.50	0.94	1.50
Bend	0.95	0.82	0.95	0.82
Bottom grid	0.71	0.57	0.71	0.57
Outflow	0.67	0.96	0.35	0.92
T-junction	0.34	0.21	0.34	0.21
Total (R1/R2)	2.62/3.61	2.69/4.06	2.30/3.28	2.64/4.02
μA [m^2]	34.5	33.0	36.5	33.5

Table 3: Values of the loss coefficients and net throughflow areas

3.3 Conclusions CFD

The conclusions of the CFD can be summarized as follows:

- A variant of the longitudinal levelling system with bottom grids is designed such that the discharge capacity of the system has at least 33 m^2 of net throughflow area for emptying and a net throughflow area of 34.5 m^2 for filling, assuming an equal discharge through both bottom grids,

- A bottom grid with 60 m^2 of throughflow area and well distributed holes, together with a chamber below with an appropriately sloping floor can achieve a good distribution of the flow into the lock chamber such that the proportion of discharge through each half of the each bottom grid stays within percentages 45/55 and 55/45 for filling. For emptying this distribution is not achievable but also not necessary,

- The outlets in inner and outer harbour as simulated provide an acceptably uniform flow into the approach harbour, which should minimize the hindrance to the vessels entering the West Lock, given the spatial constraints on the location and size of these outlet constructions.

4. WANDA MODEL OF LEVELLING SYSTEM

4.1 Model setup WANDA

WANDA is a 1D dynamic flow solver for pipeline systems which can be used for free-surface flows in locks with valve and culvert components. The following aspects are accounted for:

- Wall friction of culverts using the Darcy-Weisbach formulation,

- Inertia of the water in the culverts, using Newton's second law,

- Local loss coefficients,

- Discharge dependent loss coefficients for T- and Y-junctions,

- Lifting programme of culvert valves,

- Valve position dependent loss coefficients,

- Surge waves (translatory waves) in the lock chamber and water level slopes in the lock chamber, including the reduced cross sectional effects due to the presence of the ship cross section,

- Solution of Saint-Venant equations for computation of the water level variation in the lock chamber.

The effects of density differences cannot be taken into account

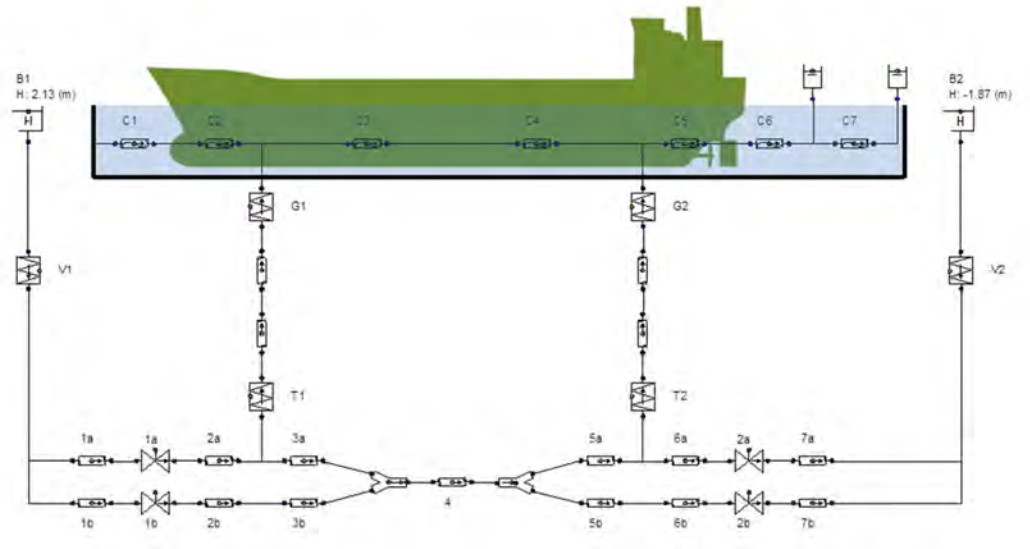

Figure 11: Schematic view of the WANDA model

A schematisation of the WANDA model for the levelling system is given in Figure 11. Elements 1a, 1b, 2a, 2b are valves representing the lifting valves in the culverts. The water level in the approach harbours is defined by elements B1 and B2, the water level in the lock chamber is represented by the C elements. All other elements represent resistance and pipe elements of the culvert system. The vessel is accounted for in the lock by means of a reduced throughflow area of the lock chamber elements C2-C5. This gives a more accurate estimate of the water level slopes in the lock chamber and consequently the levelling forces on the vessel in the lock chamber can be assessed. Table 4 summarizes the conditions of the selected simulations. The water levels considered are the normative water levels. The simulations were conducted for a lock chamber of 427 m length which corresponds to the situation where at one head an outer gate is used and at the other head an inner gate. The volume of the gate recesses which are in connection with the lock chamber are also accounted for.

Sim.	Condition	Lockhead	Scenario	Waterlevel harbor [NAP +m]	Waterlevel lock [NAP + m]	Head [m]	Lifting time valve a [s]	Lifting time valve b [s]
1	Filling	Inner	Scheldt low	2.13	-1.87	4.00	780	780
2	Filling	Outer	Scheldt high	4.60	2.13	2.47	780	780
3	Emptying	Outer	Scheldt low	-1.87	2.13	-4.00	320	320
4	Emptying	Inner	Scheldt high	2.13	4.60	-2.47	320	320
5	Filling	Inner	Scheldt low	2.13	-1.87	4.00	730	880
6	Emptying	Outer	Scheldt low	-1.87	2.13	-4.00	400	270

Table 4: Summary of the conducted simulations

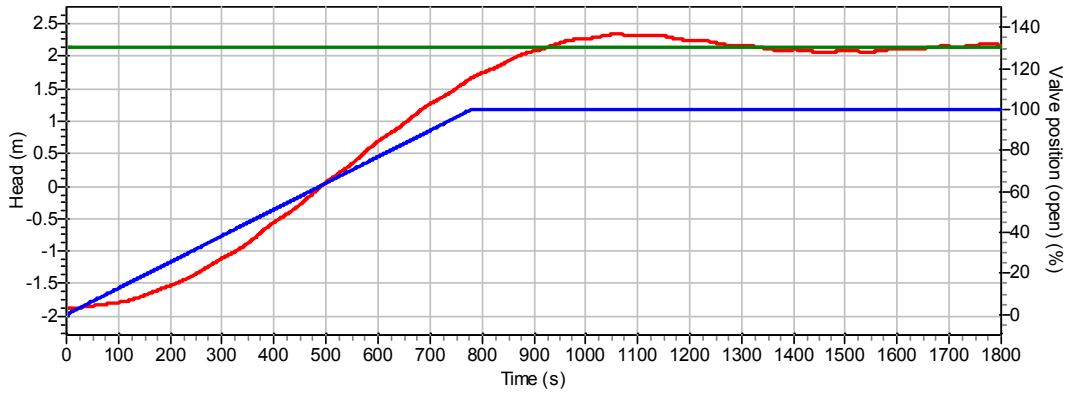

Figure 12: Water levels (red and green lines, left axis) and valve position (blue line, right axis) for Sim 1

Figure 12 shows the water levels of the harbour (green line) and lock chamber (red line) during levelling as well as the valve position (blue line) for a single simulation (Sim 1). It shows that equal water level is reached for the first time at 900 s, the required levelling time of 15 minutes. The overtravel is also visible as the water level in the lock chamber rises above the harbour water level, reaching a peak at approximately 1050 s. A summary of these results can be found in Table 5.

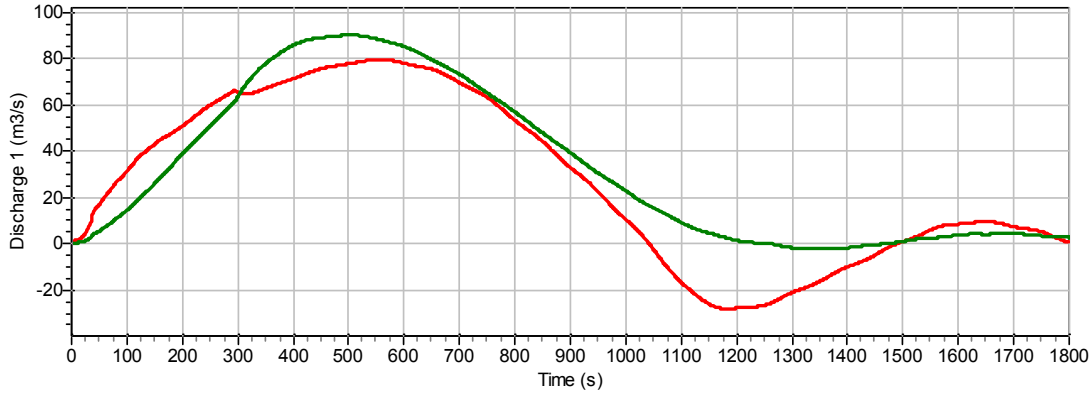

Figure 13: Discharge through the two grids during levelling for Sim 1

Figure 13 shows the discharge through the two bottom grids with the red line grid 1, closest to the active head and the green line grid 2, farthest away. The flow through the nearest grid rises quicker than through the other but the maximum discharge is higher in the farther grid. This behaviour is very dependent on what occurs at the Y-junction. Figure 14 shows the behaviour of discharge distribution in time around the Y-junction. In Figure 14 the red line shows the flow along the branch between grid 1 and the Y-junction (3a in Figure 11). A negative value indicates that the flow is from the Y-junction to grid 1. This occurs at the beginning of levelling as some of the flow from the outer culvert (3b in Figure 11) takes the shorter route to the lock chamber via grid 1. Later in the levelling process the direction of the flow in the branch 3a is reversed as some of the flow from the inner culvert (2a in Figure 11) bypasses the first grid and travels to the second grid. The complexity of this element makes it difficult to determine the expected behaviour with accuracy and it is therefore a source of uncertainty in the numerical model approach described in this paper.

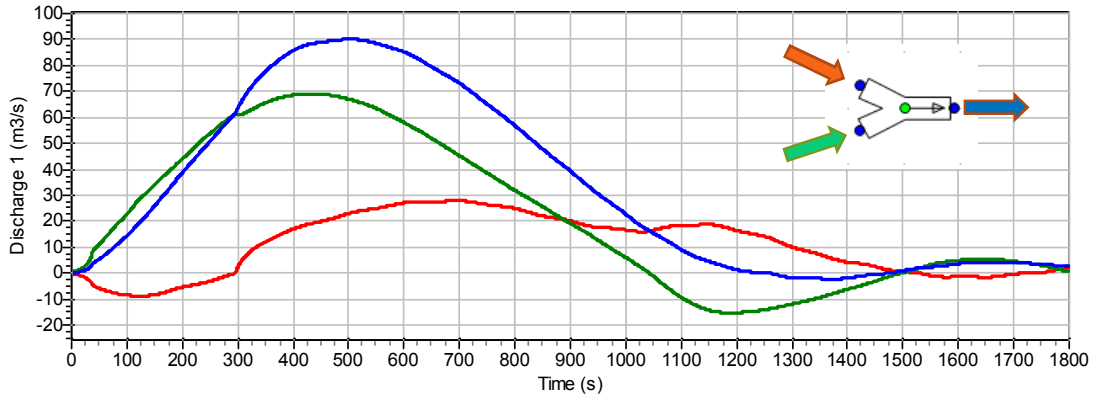

Figure 14: Discharge through different culvert elements adjacent to the Y-junction during levelling for Sim 1. The definitions of the positive sense of discharges (the red, green and blue lines) is depicted with the corresponding coloured arrows around the Y-junction in the graph

The results of the simulations with the levelling system are assessed based on the variation in time of the ratio of the discharges through each bottom grid. Clearly the ratio cannot be close to 50/50 throughout the entirety of the levelling process as there are occasions when the flow through one grid is very small whilst there is still flow through the other. Of importance to a safe levelling process is that this discharge is evenly distributed between the two grids when the discharges are high (near the moment of maximum discharge). This will reduce the water level slope along the ship in the lock chamber and also, although this cannot be modelled here, ensure that a density current of almost equal strength is initiated at both bow and stern of the ship. Figure 15 shows the time evolution of the ratio of the discharges through the bottom grids to the total discharge for Sim 1. The vertical solid black line in the middle of the Figure is the moment of maximum total discharge. The shaded area is the period ±25 % of the total levelling time around the moment of maximum discharge. The Figure shows that the ratio of discharges stays between 45/55 and 55/45 within the shaded area.

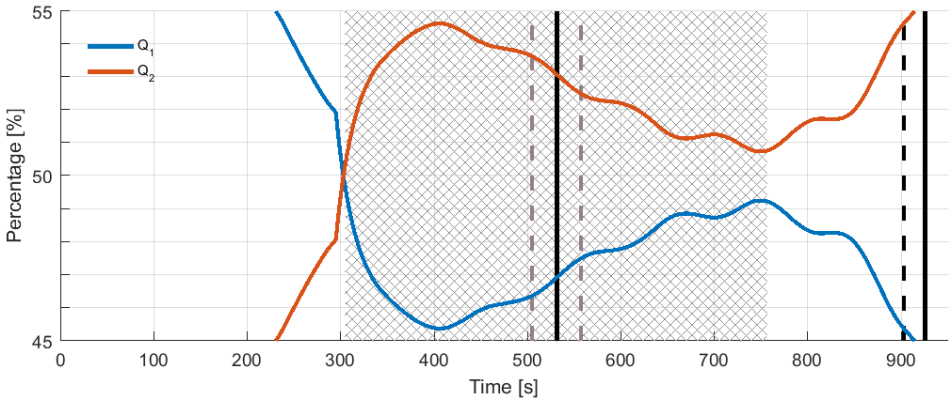

Figure 15: Discharge through different bottom grids during levelling for Sim 1 as a percentage of the total discharge. The vertical solid black line is the moment of maximum total discharge. The shaded area is the period ±25 % of the total levelling time around the moment of maximum discharge

Figure 16 shows the same scenario as Sim 1 but with an adjusted valve lifting programme (Sim 5 in Table 4). This lifting programme uses different lifting speeds for the valves in the two culverts. The Figure shows that by using the valves an improvement in the ratio of discharges between the bottom grids can be achieved.

For emptying the distribution is worse. Figure 17 shows an emptying scenario, Sim 6. In this Figure, even though the valve programme has been improved the discharge ratio does not stay within 45/55 and 55/45 within the shaded area. Instead the discharge ratio stays within 45/55 en 55/45 for a period of ±10% or ±15% of the levelling time around the moment of maximum discharge.

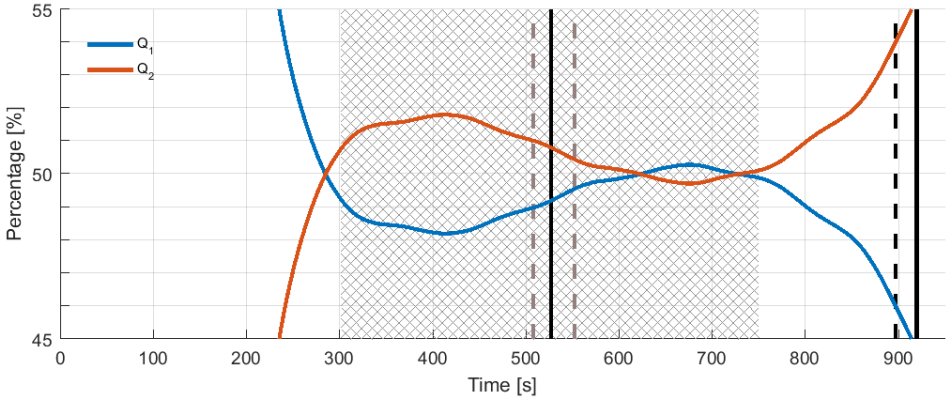

Figure 16: Discharge through different bottom grids during levelling for Sim 5 as a percentage. The vertical solid black line is the moment of maximum total discharge. The shaded area is the period ±25 % of the total levelling time around the moment of maximum discharge

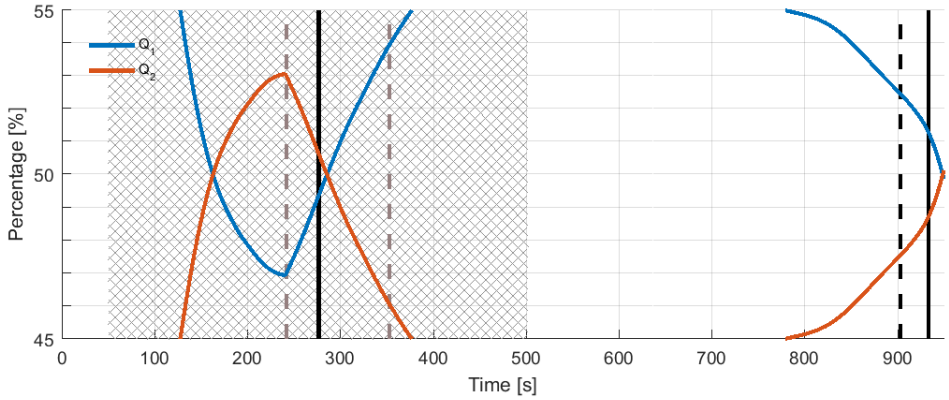

Figure 17: Discharge through different bottom grids during levelling for Sim 6 as a percentage of the total discharge. The vertical solid black line is the moment of maximum total discharge. The shaded area is the period ±25 % of the total levelling time around the moment of maximum discharge

Table 5 shows the summary of the levelling time, calculated force on the ship, maximum discharge for both bottom grids, discharge ratio and maximum value of overtravel for the six simulations of Table 4. The levelling times are always sufficiently fast to be acceptable (approximately 15 minutes or faster). The maximum force shown in the table accounts only for the modelled water level slope in the lock chamber and not for any additional forces owing to density currents and therefore no comparison is made here between this value and the allowable mooring forces. In addition, the force is only in the longitudinal direction and does not account for transverse forces. Finally it can be concluded that the overtravel in the lock will be no more than 21 cm. The design of the lock gate should take this into account although again density differences are not accounted for in these simulations.

Sim.	Levelling time [s /min]	Max. force [‰]	Max. discharge R1 [m^3/s]	Max. discharge R2 [m^3/s]	Discharge ratio at max. discharge [% / %]	Max. overtravel [cm]
1	902 / 15.0	0.104	79.6	90.1	46.9 / 53.1	20.6
2	821 / 13.7	0.053	51.6	60.4	46.1 / 53.9	14.8
3	896 / 14.9	0.109	-102.4	-81.2	55.8 / 44.2	-11.6
4	684 / 11.4	0.034	-77.3	-61.8	55.6 / 44.4	-11.5
5	897 / 15.0	0.078	84.5	87.2	49.2 / 50.8	20.0
6	902 / 15.0	0.104	-91.7	-92.3	49.8 / 50.2	-11.2

Table 5: Results of the WANDA simulations for the variant with bottom grids

3.3 Conclusions WANDA

The conclusions of the WANDA simulations can be summarized as follows:

- The designed variant of the longitudinal filling system with bottom grids shows computed levelling times of 15 minutes
- Where needed, by adjusting the valves, the discharges through the two bottom grids can only be made to be within the ratio 45/55 and 55/45 during a time period concentrated around the middle of the levelling process owing to inertial effects. This period is defined here as the moment of maximum discharge ±25% of the total levelling time for filling. For emptying this period should be reduced to the moment of maximum discharge ±15% of the total levelling time,
- The maximum computed overtravel of the system is about 20 cm,
- The largest uncertainty in the results comes from the modelling of the Y-junctions as the resistances of these elements will be dependent on the discharge ratios through each branch and in this research only one ratio per element has been calculated. It is recommended to study these elements in more detail for similar systems.

5. CONCLUSIONS

As a conceptual design, a longitudinal levelling system with two bottom grids is designed for the New Lock of Terneuzen. This levelling system achieves levelling times of 15 minutes or less for a 4 m head without large forces on the moored vessel if the following hydraulic conditions are met:

- a discharge capacity of the system with at least 33 m^2 of net throughflow area for emptying and a net throughflow area of 34.5 m^2 for filling,
- When performing a stationary CFD simulation of the flow in the system, the flow into the lock chamber through each half of the each bottom grid stays within percentages 45/55 and 55/45 for filling,
- The discharges through the two bottom grids are within percentages 45/55 and 55/45 during a time period concentrated around the moment of maximum discharge ±25% of the total levelling time for filling. For emptying this period should be reduced to the moment of maximum discharge ±15% of the total levelling time.

The final design of the lock, including the design of the levelling system, will be carried out the contractor selected for building the lock. This final design will follow a similar approach as described in this paper for the verification of the levelling system. Because this approach does not take into

account density currents the final design of the levelling system is to be verified in a scale model because the effects of density currents will be dominant for the forces on the moored vessel and as of yet no numerical tools are available to study this with sufficient accuracy.

6. REFERENCES

Aerts, F., De Winne, K., (2015) Challenges in the design of the New Lock Terneuzen, Smart Rivers 2015, Buenos Aires Argentina, PIANC, Paper 126.

Van der Hout, A. , (2018) Scale model research and field measurements for the two new sea locks in the Netherlands, World Congress 2018, Panama, PIANC, Paper 188

Kortlever, W., Van der Hout, A., O'Mahoney, T., de Loor, A., Levelling the New Sea Locks in the Netherlands; Including the Density Difference, World Congress 2018, Panama, PIANC, Paper 103

Miller, D.S., (1978) Internal flow systems, BHRA.

Nogueira, H., van der Ven, P., O'Mahoney, T., de Loor, A., van der Hout, A., Kortlever, Wim., (2018) Navigation Locks: Effect of density differences on the forces acting on a moored vessel, Journal of Hydraulic Engineering, 144(6)

Philpott, K.L., (1961) Progress Report on the Terneuzen Lock Investigation, Waterloopkundig Laboratorium: Delft.

Waterloopkundig Laboratorium Delft (1975) Zeesluis Baalhoek, Verslag Modelonderzoek (in Dutch), Technische Rapport M1210

An application-oriented model for lock filling processes

by

Fabian Belzner[1], Franz Simons[1] and Carsten Thorenz[1]

1. INTRODUCTION

The German federal inland waterway network is the biggest waterway network in Western Europe with a length of 7,300 km. In 2016 about 221 million tons of cargo were transported on these waterways which equals 8 % of the whole transportation volume in Germany. Part of the waterway network are about 400 lock chambers which are key elements of the waterway infrastructure as they enable ships to overcome water level differences: These are located at impounded rivers, between sections of canals or at connection points. The safe and efficient operation of these locks is essential for the transport of goods on the waterways. One of the main tasks of the German Federal Waterway Engineering and Research Institute (German abbreviation: BAW) is to support the government in the design process of these locks in case of new construction or reconstruction. Ideally the costs for construction and operation of the locks can be minimized while still guaranteeing a short cycle time and a safe passage.

During the early planning period of a lock the hydraulic system has to be designed regarding several demands concerning structure, operation and safety. From a hydraulic point of view, a filling system has to be found that triggers minimal forces acting on the vessel and guarantees a short filling time. Every change on the filling system or the valve opening velocity can have a high influence on the forces acting on the ship and can result in breaking hawsers. An overview of the hydraulic and constructional needs of ship locks is given by Partenscky (1986) or in PIANC (2015).

Today, the determination of the forces acting on a vessel can be carried out by on-site measurements, physical or numerical models. On-site measurements are very complicated because a lock prototype and a real ship are needed. Measurement techniques must resist high forces, high pressures, flow velocities and in some cases very low temperatures and the measuring procedures must be safe for the ship and for the staff. The measuring period can be limited by factors like the amount of traffic or the weather conditions. Often only a few experiments are possible and the measurement techniques have to be planned carefully because there is no chance to change methodology during the experiments. Bousmar et al. (2017) describe these on-site measurements as essential for the diagnostic of existing locks but also mention the struggles of measuring under difficult circumstances.

During the design process of a new lock on-site measurements are impossible because often no prototype exists. The classical way to investigate and optimize planned locks is to conduct physical experiments at a scale model. Such experiments are e. g. described by Thorenz and Anke (2013) or Van der Ven et al. (2015). Scale models have the advantage that they can be constructed in a dry and heated laboratory and a large number of experiments can be conducted within a short time. However, the construction time of these models is at least several months, for complicated locks it can be even more than one year. The results can be influenced by scale effects or unwanted interaction between the model physics and the measurement technique and it is not possible to reproduce all relevant effects in a scale model. For example the strain behavior of the mooring lines is typically not reproduced in physical models, because the handling of the lines in reality is often unknown and difficult to predict. Nevertheless, physical scale modeling of locks is the most common method to determine forces acting on a vessel due to the high level of reliability and the large amount of experience available.

In line with the increasing computational power in the last years, a large progress in the development of multidimensional numerical methods happened (Thorenz 2009). Today it is possible to perform high resolution three dimensional simulations of transient hydromechanical phenomena like the filling of a lock. A number of methods to simulate the swimming vessel exist. However, these methods require high skill

[1] Federal Waterways Engineering and Research Institute, Germany, fabian.belzner@baw.de

levels and substantial computer power. The simulation time for a lock filling process with swimming vessel, moving valves etc. uses several days of computing time even on a cluster computer system and is therefore not yet suitable for the everyday-simulation of a large number of cases. The numerical elevation of the filling and emptying system of the new Panama Canal locks is given by Thorenz (2010), an overview on the numerical methods to simulate the lock filling process with OpenFOAM® is given by Thorenz et al. (2017),

For the early planning stage, but also for the assessment of small constructional changes in the final planning, both methods are not suitable. Carrying out physical or numerical model tests, takes often too much time. Therefore, simplified models are desirable, which consider the main hydraulic phenomena and allow a rough estimation and short-time prediction of the expected forces on the ship together with the filling times. For the most basic phenomena analytic equations are available. For a better approximation, more complex tools are necessary. An example is LOCKFILL which allows analyzing the filling and emptying of a lock chamber through the lock head (De Loor 2016). Lockfill is based on the super-positioning of the solutions for different equations which describe the flow field in the lock chamber which were derived from analytic considerations.

Experience has shown that the consideration of the wave propagation in the lock chamber is essential for the ship forces. Here, a tool is presented which is based on the 1D Saint-Venant equations and allows the simulation of a lock filling process to determine the forces acting on the vessel due to different hydraulic conditions. In this paper, we first describe the most important aspects of the hydrodynamics of the lock filling process. Following this, the numerical scheme of the new 1D lock model is described. Afterwards, we show results from a calibration using data from physical model tests, and we point out limitations of the model. The paper will end with a summary and conclusions on the presented topic. All symbols used in this paper are listed and explained in Section 7.

2. HYDRODYNAMICS OF THE LOCK FILLING PROCESS

During the filling process of a lock chamber with a through-the-gate system different phenomena can be observed which can interact with each other. The main phenomena causing longitudinal forces acting on a vessel are:

- An initial surge wave triggered by the valve opening,
- the propagation of a filling jet,
- a water level slope due to the zero velocity boundary at the downstream end of the chamber,
- dynamic effects like wave propagation in the chamber and
- energy losses due to wall friction or contraction-expansion losses.

All the impacts of these phenomena have to be regarded to estimate the forces acting on the vessel during the lock filling process. The longitudinal forces acting on the vessel result from two predominant mechanisms: one is the downhill force resulting from a water surface slope; the other one is the force resulting from a filling jet hitting the vessel. The latter should be avoided in general. A further description can be found e.g. in Vrijburcht (1991).

The inflow in the lock chamber Q [m³/s] at any time can be expressed as a function of the pressure difference Δh [m], the valve opening area A_{valve} [m²] and a dimensionless discharge coefficient μ [-] which takes into account the geometry of the control section. The discharge coefficient can be estimated from literature, physical or numerical models. For the sluice gate type of valve it is usually between 0.6 and 1.0. Note: Δh is the maximum available pressure difference, i. e. for submerged filling systems it is the difference between the water levels in the upstream outer harbor and the lock chamber and for free flow it is the maximum pressure height over the control section. The inflow into the lock chamber can be calculated from:

$$Q = \mu \cdot A_{\mathrm{valve}} \cdot \sqrt{2g \cdot \Delta h} \tag{1}$$

For a known gross area of the lock chamber A_{chamber} [m²], the water level development can be computed from:

$$\frac{dh}{dt} = \frac{Q}{A_{\text{chamber}}} \tag{2}$$

At the beginning of the lock filling process a first surge wave, triggered by the inflow gradient, results in a slope in downward direction. The slope resulting from this first flush I_{flush} [-] is proportional to the gradient of the inflow:

$$I_{\text{flush}} = -\frac{\mathrm{d}Q}{\mathrm{d}t \cdot (W_{\text{chamber}} \cdot h - A_{\text{vessel}})} \tag{3}$$

where W_{chamber} [m] is the chamber width and A_{vessel} [m²] is the cross sectional area of the vessel. According to equation (1) the inflow in the lock chamber scales almost linear with the valve opening velocity. Therefore, the water level slope due to the first flush scales also linearly with the valve opening velocity. For locks with large lift heights and potent energy dissipation at the lock head, the force resulting from this surge wave may become dominant. This initial force can be minimized by reducing the initial valve opening velocity for a certain time at the beginning of the filling process. As the discharge in this early period is small anyway, the reduction of the initial valve opening velocity will hardly increase the filling time. Figure 1 (a) shows this slope and the resulting force in downstream direction. After this first flush a velocity distribution from the upstream to the downstream edge of the lock chamber is developing.

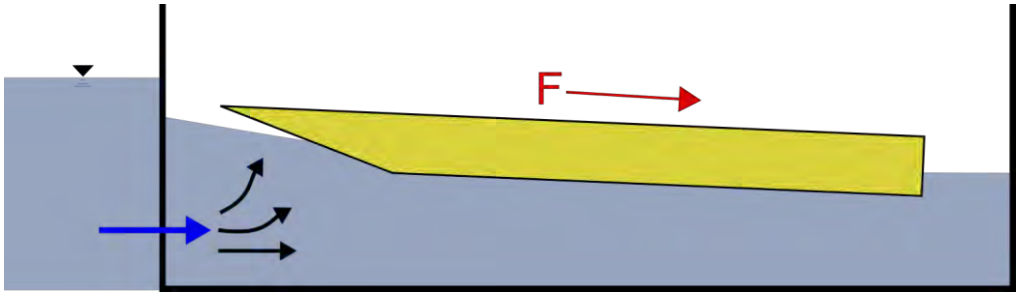

(a) Water level slope in downstream direction due to first flush

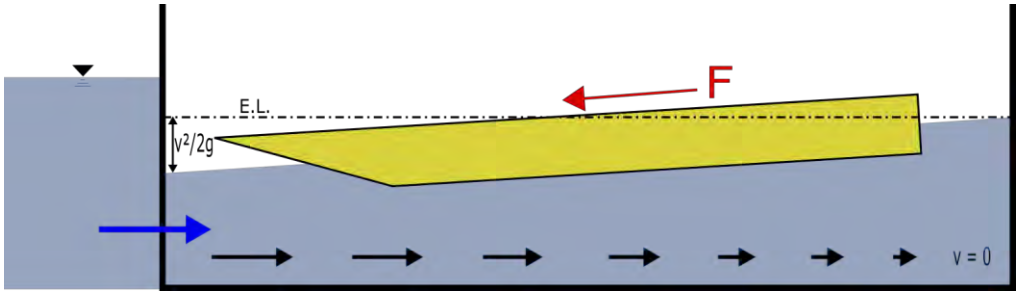

(b) Water level slope in upstream direction due to decreasing velocity

Figure 1: Temporal progression of ship forces during lock filling process

With an “ideal” energy dissipation at the lock head, the mean velocity u_{mean} [m/s] behind the upstream inlet corresponds to the inflow divided by the available cross sectional area of the lock chamber:

$$u_{\text{mean}} = \frac{Q}{W_{\text{chamber}} \cdot h - A_{\text{vessel}}} \tag{4}$$

The downstream gate of the lock chamber is closed during the filling process. Thus, the velocity at the end of the chamber is zero. Assuming a constant total head in the lock chamber and a linear decreasing velocity head from the upstream to the downstream edge like it is shown in Figure 1 (b), a stationary sloped water surface I_{stat} [-] in upstream direction is developing to compensate the decreasing velocity head. Consequently, this slope depends on the inlet velocity u_{mean} and the length of the lock chamber L_{chamber} [m] and can be calculated by (5).

$$I_{\mathrm{stat}} = \frac{u_{\mathrm{mean}}^{\ 2}}{2 \cdot \mathrm{g} \cdot L_{\mathrm{chamber}}} \tag{5}$$

Considering the longitudinal forces as downhill forces and neglecting the jet near the vessel and other dynamic phenomena, the forces acting on the ship can be roughly estimated from the water level slope around the vessel by summing up the slopes and multiplying by the mass of the vessel $\mathrm{m}_{\mathrm{vessel}}$ [kg]:

$$F = (I_{\mathrm{flush}}^{n} + I_{\mathrm{stat}}^{n}) \cdot \mathrm{m}_{\mathrm{vessel}} \tag{6}$$

The surge waves are propagating in the chamber and are reflected at the upstream and downstream ends. As a result sloshing occurs. The cycle time T [s] can be calculated by the shallow water wave celerity equation and the geometry of the chamber and the vessel:

$$T = 2 \cdot \left(\frac{L_{\mathrm{chamber}} - L_{\mathrm{vessel}}}{\sqrt{g \cdot h}} + \frac{L_{\mathrm{vessel}}}{\sqrt{g \cdot \left(h - \frac{A_{\mathrm{vessel}}}{W_{\mathrm{chamber}}}\right)}} \right) \tag{7}$$

A first approximation of the forces acting on the vessel during the lock filling process can be done without great effort using equation (6). Substantial dynamic effects like wave propagation, the influence of the filling jet, friction losses or the development of the forces over the time are neglected in this simplified approach. Nevertheless this approach allows a rough approximation of the forces acting on a vessel using a pocket calculator within a few minutes. But it must be pointed out that dynamic effects can have a huge and dominant influence on the results and these are neglected here. Thus, a more sophisticated approach should be used.

3. 1D LOCK MODEL

3.1. Introduction

Due to the deficiencies of the simplified analytic approaches it was decided, to implement a 1D model for the lock filling process. It was assumed, that this is more straight-forward than the adaptation of the analytical approximations to more complex situations and the super-positioning of effects. Furthermore, the 1D approach offers the possibility for future enhancements, e.g. the coupling to 1D pipe network models in order to simulate more complex filling systems.

3.2. Basic equations

The flow in a lock chamber in case of filling from the head has a strong domination in longitudinal chamber direction. The water surface is assumed to be horizontal, a hydrostatic pressure distribution is predominant and the energy slope is small. Neglecting phenomena which might cause lateral water level slopes and forces, the flow in the lock chamber can be described by the one dimensional (1D) Saint-Venant equations which allow the calculation of the water depth and a mean flow velocity in discrete cross sections in the chamber. The 1D Saint-Venant equations are a set of two partial differential equations describing the conservation of mass and momentum in channel flow. The derivation and several numerical approaches for a solution of these equations are described by Cunge et al. (1980). Using the two main variables Q [m³/s] and A [m²], the 1D Saint-Venant equations are given in a conservative formulation as (Jirka, Lang 2009):

$$\frac{\partial A}{\partial t} + \frac{\partial Q}{\partial x} = q \tag{8}$$

$$\frac{\partial Q}{\partial t} + \beta \cdot \frac{\partial}{\partial x} \cdot \left(\frac{Q^2}{A}\right) + g \cdot A \cdot \frac{\partial h}{\partial x} = g \cdot A \cdot (I_{\mathrm{o}} - I_{\mathrm{e}} - I_{\mathrm{R}}) \tag{9}$$

I_0, I_e and I_R in equation (9) are the slopes due to a sloped bed, local contraction-expansion losses and friction. The longitudinal forces acting on the ship can be derived from the water level gradient.

3.3. Consideration of the filling jet

One requirement for using the 1D Saint-Venant equations is the assumption of a uniform flow distribution within every cross section. In reality a filling jet can develop from the upstream gate leading to a strongly non-uniform velocity distribution because of the high velocity inside of the jet and small velocities in the surrounding (cf. Figure 9). Due to the proportionality of the local momentum flux to the square of the local velocity, the mean flow velocity cannot be used anymore to calculate the convective acceleration in equation (9). To correct this, the Boussinesq coefficient β [-] is commonly used which regards the ratio of the mean flow velocity $\bar{u}$ [m/s] and the sum of local flow velocities in the jet. Here we are regarding a discretized version, where A [m²] is the overall cross sectional area which can be divided in K areas A_k [m²] with the velocities u_k [m/s]:

$$\beta = \frac{\sum_0^K u_k^2 \cdot A_k}{\bar{u}^2 \cdot A} \tag{10}$$

Assuming only two cross sectional areas A (the whole cross sectional area) and A_{jet} [m²] (the subarea of A with the jet in it), equation (10) can be simplified to:

$$\beta = \frac{A}{A_{\text{jet}}} \tag{11}$$

Due to the balance of the convective acceleration and the gradient of h in equation (9) for constant discharges, a lowering of the water level is the consequence of high β values resulting from a distinct jet. This must be reproduced in order to model the influence of a filling jet on a vessel. The effect can also be observed in physical experiments for locks with little energy dissipation at the upstream head.

3.4. Consideration of the vessel

The modeling of a swimming vessel with a 1D hydrodynamic approach is difficult and leads to a complicated solution. Thus, here a simplified approach was chosen. The ship is approximated by reducing the cross sectional area in the region of the vessel by the cross sectional area of the ship A_{vessel} [m²]. This is done initially for every cross section of the model by computing the wetted cross sectional area of the lock from:

$$\mathrm{A} = \mathrm{h} \cdot W_{\text{chamber}} - A_{\text{vessel}} \tag{12}$$

During the simulation gradients of the water surface are computed from the wetted cross sections. As the cross sectional area of the lock chamber decreases at the bow and increases at the stern without causing a gradient in the water level, the computation of the spatial gradient of h according to equation (9) must be adjusted by the vessel area:

$$\frac{\partial h}{\partial x} = \frac{\partial (A + A_{\text{vessel}})}{\partial x \cdot W_{\text{chamber}}} \tag{13}$$

3.5. Discretization

Due to the absence of an analytical solution for the 1D Saint-Venant equations a finite difference approach for the discretisation in space and time was chosen. Hereinafter the index i is denoting the current point in space, $i-1$ and $i+1$ are the grid points in front of and behind the point i (Figure 2). The index n denotes the current time step, $n+1$ the next time step and $n-1$ the previous time step. Δt is the size of one time step and Δx is the distance between two cross sections. For discretisation in space a staggered grid was chosen. The cross sectional area $A_{i+1/2}$ is calculated between the two cross sections i and $i+1$, where the discharges Q_i and Q_{i+1} are calculated. This strategy has stability advantages and is comparable to the finite volume approach, where the flux is calculated at the faces of each cell.

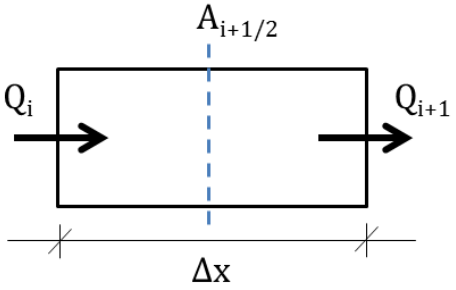

Figure 2: Points of calculation of A and Q

For the discretization in time the Crank-Nicolson method was used in order to obtain second order accuracy in time. The gradients between two cross sections can be calculated at half a time step or can be shifted by the Crank-Nicolson factor θ [-] like it is shown in equation (14) for the cross sectional area and in equation (15) for the discharge:

$$A^{n+\theta} = (1-\theta) \cdot A^{n+1} - \theta \cdot A^{n} \tag{14}$$

$$Q^{n+\theta} = (1-\theta) \cdot Q^{n+1} - \theta \cdot Q^{n} \tag{15}$$

For $\theta = 0$ the gradients are taken explicitely from the known time step, for $\theta = 1$ the gradients are taken implicitely from the future time step and for $\theta = 0.5$ a second order accuracy in time is obtained. A detailed description of the method can is given by Crank et al. (1947).

The derivations from the continuity equation (8) were discretisized in the following manner:

$$\frac{\partial A}{\partial t} = \frac{A_{i+1/2}^{n+1} - A_{i+1/2}^{n}}{\Delta t} \tag{16}$$

$$\frac{\partial Q}{\partial x} = \frac{Q_{i+1}^{n+\theta} - Q_{i}^{n+\theta}}{\Delta x} \tag{17}$$

Discretising equation (8) with equations (16) and (17) and solving it for the wanted variable $A_{i+1/2}^{n+1}$ for the future time step $n+1$ leads to (18):

$$A_{i+1/2}^{n+1} = A_{i+1/2}^{n} - \frac{\Delta t}{\Delta x} \cdot (Q_{i+1}^{n+\theta} - Q_{i}^{n+\theta}) + \Delta t \cdot q_i \tag{18}$$

The discretisation of the parts of the momentum equation (9) is more complicated due to the non-linear terms:

$$\frac{\partial Q}{\partial t} = \frac{Q_{i}^{n+1} - Q_{i}^{n}}{\Delta t} \tag{19}$$

$$\beta \cdot \frac{\partial}{\partial x} \cdot \left(\frac{Q^2}{A}\right) = \left(\beta_i \cdot \frac{Q_{i+1/2}^{n+\theta} \cdot Q_{i+1/2}^{n+\theta}}{A_{i+1/2}^{n+\theta}} - \beta_{i-1} \cdot \frac{Q_{i-1/2}^{n+\theta} \cdot Q_{i-1/2}^{n+\theta}}{A_{i-1/2}^{n+\theta}}\right) \cdot \frac{1}{\Delta x} \tag{20}$$

$$g \cdot A \cdot \frac{\partial h}{\partial x} = g \cdot \frac{1}{2} \cdot \left(A_{i+1/2}^{n+\theta} - A_{i-1/2}^{n+\theta}\right) \cdot \frac{(A + A_{\text{vessel}})_{i+1/2}^{n+1} - (A + A_{\text{vessel}})_{i-1/2}^{n+1}}{\Delta x \cdot W_{\text{chamber}}} \tag{21}$$

$$g \cdot A \cdot (I_{\text{o}} - I_{\text{e}} - I_{\text{R}}) = g \cdot \frac{1}{2} \cdot \left(A_{i+1/2}^{n+\theta} - A_{i-1/2}^{n+\theta}\right) \cdot (I_{\text{o}} - I_{\text{e}} - I_{\text{R}}) \tag{22}$$

Discretising equation (9) with equations (19), (20), (21) and (22) and solving it for the wanted variable Q_i^{n+1} for the future time step $n+1$ leads to equation (23):

$$Q_i^{n+1} = Q_i^n - \frac{\Delta t}{\Delta x} \cdot \beta_i \cdot \frac{Q_{i+1/2}^{n+\theta} \cdot Q_{i+1/2}^{n+\theta}}{A_{i+1/2}^{n+\theta}} + \frac{\Delta t}{\Delta x} \cdot \beta_{i-1} \cdot \frac{Q_{i-1/2}^{n+\theta} \cdot Q_{i-1/2}^{n+\theta}}{A_{i-1/2}^{n+\theta}} - \Delta t \cdot g \cdot \frac{1}{2} \cdot \left(A_{i+1/2}^{n+\theta} - A_{i-1/2}^{n+\theta}\right) \cdot \frac{(A + A_{\text{vessel}})_{i+1/2}^{n+1} - (A + A_{\text{vessel}})_{i-1/2}^{n+1}}{\Delta x \cdot W_{\text{chamber}}} + \Delta t \cdot g \cdot \frac{1}{2} \cdot \left(A_{i+1/2}^{n+\theta} - A_{i-1/2}^{n+\theta}\right) \cdot (I_{\text{e}} + I_{\text{R}}) \quad (23)$$

3.6. Boundary conditions

As boundary conditions a zero flux condition is applied for the downstream end of the lock chamber. The solver core allows adding fluxes and also the specification of the momentum transported with the flux at any point of the lock chamber. The fluxes are added as sources to the continuity equation and the momentum equation. In the following, we are regarding the simplified case of a through-the-head system. In this case, the fluxes are added to the first node of the mesh. The inflow is calculated by equation (1) depending on the water level difference Δh between the lock chamber and the upstream harbor, the effective valve opening area A_{valve} and a discharge coefficient μ. The water level difference can be determined from the known upstream water level and the chamber water level of the previous time step. The valve opening area A_{valve} is a prescribed function of time and also known. The discharge coefficient μ describes the performance of the valve as a function of the valve opening. It can be determined a-priori with physical models or numerical simulations or, though with lower reliability, values from prior projects with similar geometry can be used. If prototype measurements or a physical model of a lock with the same valve geometry exist, the discharge coefficients can be determined by a comparison of the water levels over the time.

3.7. Solution procedure

The equations (18) and (23) allow the calculation of the cross sectional area A and the discharge Q for every cross section for the time step $n+1$. But this requires the values of A and Q at the Crank-Nicolson time step $n+\theta$, which would lead to an implicit solution algorithm. To avoid the solution of a non-linear equation system, a predictor-corrector method was used. At the beginning of the first predictor-corrector loop the values for the future time step $n+1/2$ are predicted by the explicit Adam-Bashforth multistep method like shown in equations (24) and (25):

$$Q^{n+\frac{1}{2}} = Q^n + \frac{Q^n - Q^{n-1}}{\Delta t} \cdot \frac{1}{2} \cdot \Delta t = 1.5 \cdot Q^n - 0.5 \cdot Q^{n-1} \quad (24)$$

$$A^{n+\frac{1}{2}} = A^n + \frac{A^n - A^{n-1}}{\Delta t} \cdot \frac{1}{2} \cdot \Delta t = 1.5 \cdot A^n - 0.5 \cdot A^{n-1} \quad (25)$$

Assuming a constant gradient, the Adam-Bashforth method predicts the value of a future time step from the known time step and the gradient between the current and the previous time steps (Zhao, Zhang 2011). As a result of the extrapolation to $n+1/2$ a Crank Nicolson factor of $\theta = 0.5$ is used for the first prediction. With $\mathrm{Q}^{\mathrm{n+1/2}}$ from equation (24) the discretized continuity equation (18) is solved for the first time. The result A^{n+1} is weighted with the Crank Nicolson equation (14). The results $A^{n+\theta}$ from equation (14) and $\mathrm{Q}^{\mathrm{n+1/2}}$ from equation (24) are used to solve the momentum equation (23) for Q^{n+1} which is weighted with equation (15). After the first predictor loop is finished, $A^{n+\theta}$ and $Q^{n+\theta}$ exist and the equations (18) and (23) are solved again to correct A^{n+1} and Q^{n+1} in a first correction loop. From the results a better value for $A^{n+\theta}$ and $Q^{n+\theta}$ can be calculated by equations (14) and (15) leading to better results for A^{n+1} and Q^{n+1} in additional correction loops. Equations (18) and (23) are solved fully explicit for $\theta = 0$, implicitly for $\theta = 1$ and for $\theta = 0.5$ the scheme has second order accuracy in time. With this implicit scheme a solution can be obtained after some iterations without having to solve a linear equation system. A graphical representation of the algorithm can be seen in Figure 3.

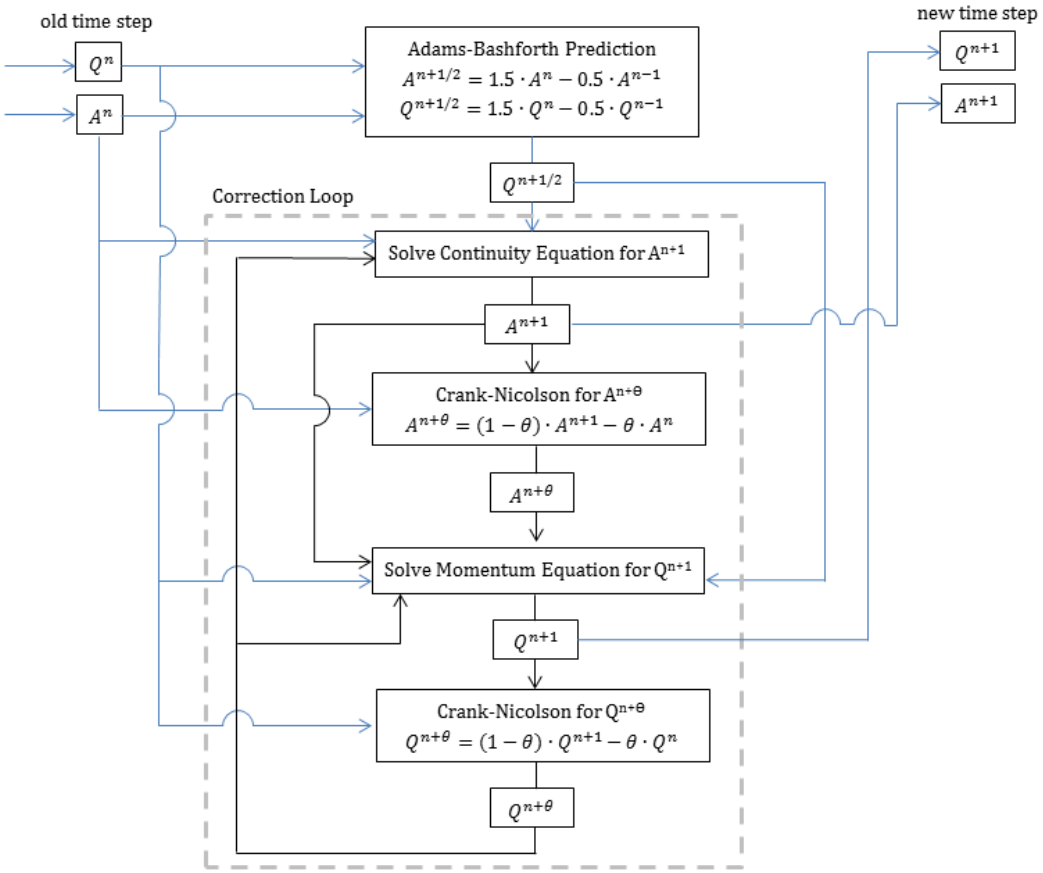

Figure 3: Predictor-Corrector solution scheme

3.8. Software implementation

Based on the presented numerical algorithms the tool LoMo (short form of “BAW Lock Model”) was implemented, which simplifies the usage and provides a graphical representation of the results. LoMo is developed in the object-oriented programming language Java. Due to the platform independency of Java byte code, the releases can be executed on all major operating systems.

The computational core of LoMo is strictly separated from the graphical user interface using the model-view-controller design pattern (Gamma 2011). The graphical user interface (Figure 4) is based on the JavaFX library and can be easily internationalized using the Java ResourceBundle concept (Oracle 2018a). Currently, English and German internationalizations are available. Case setups can be stored to and read from XML files using the Java XML binding (JAXB) library (Oracle 2018b). The software design intends to simplify the extension by new chamber filling methods.

The BAW actively supports the Open Access policy of the German federal government. We signed the “Berlin Declaration on Open Access to Knowledge in the Sciences and Humanities” (Max-Planck-Gesellschaft 2003) in 2016 and declared an own open access guideline. In the spirit of this guideline the software is freely available and open source, licensed under the GNU General Public License 3 (Free Software Foundation 2007). Source code and releases can be found at GitHub (https://github.com/baw-de/lomo). You are welcome to test the software, to participate in the development and to give us feedback on GitHub. There is, however, no warranty for the accuracy and meaningfulness of the results.

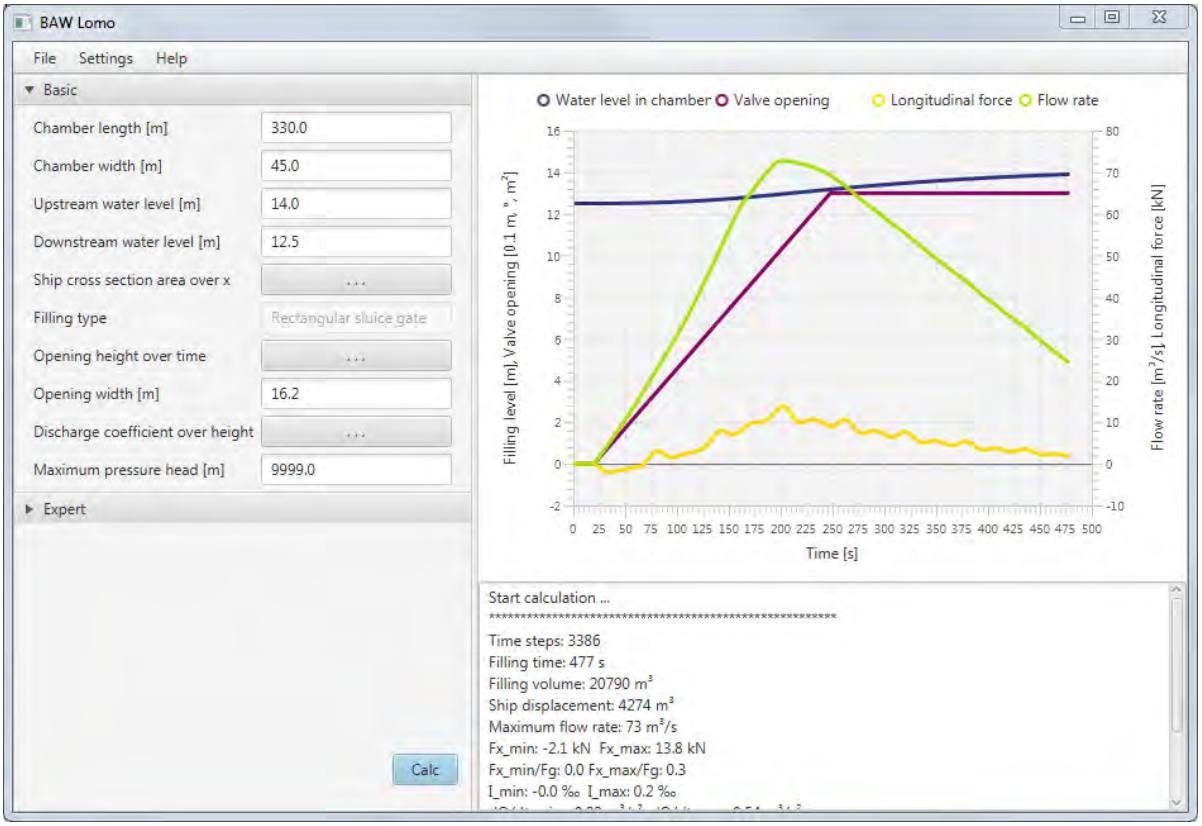

Figure 4: Graphical User Interface

3.9. Setup and Calibration parameters

The model is setup with the physical dimensions of the lock chamber and of the vessel in the lock chamber. Furthermore, the valve and filling system characteristics must be chosen and a valve opening curve must be defined. The calibration of the model can be carried out by comparing the results with laboratory results, results from three-dimensional numerical models or on-site measurements. There are two most important calibration parameter groups:

- The hydraulic performance of the filling system influencing the filling time and triggering waves. This is calibrated by the discharge coefficient as a function of the valve opening.
- The propagation of the jet which leads to a water level decrease and a slope in upstream direction.

Both parameters strongly influence the longitudinal forces acting on the vessel and have to be calibrated by known results.

4. COMPARISON WITH PHYSICAL MODEL RESULTS

4.1. Introduction

For calibration and validation purposes, several physical model results of the BAW were used. Here we present a model that was originally constructed for the validation of 3D numerical methods. Due to the objective of the physical model it was constructed as a very simple lock with one sluice gate valve and a continuous bottom between upstream outer harbor and the lock chamber. The vessel had the geometry of a push barge with a length of 3.01 m and a width of 0.46 m. The lock chamber had a hydraulic length of

6.32 m and a width of 0.48 m. The drop height was 0.08 m. Further dimensions are shown in Figure 6. The water level in the upstream outer harbor was kept constant by a labyrinth weir (Belzner et al. 2017). Several experiments with different valve opening velocities and ship positions in the chamber were performed to validate and calibrate the 1D model. The forces acting on the vessel during the lock filling process were determined by measuring the displacement of a spring bar. Additionally the water levels were determined by floating water level gauges. The inlet flow was determined from the temporal variation of the water level in the lock chamber. Figure 5 shows a detailed view of the upper part of the lock chamber with the gate (left), the vessel and the floating water level gauges. A further description of the evaluation of forces acting on a vessel with physical models is given by Thorenz, Anke (2013).

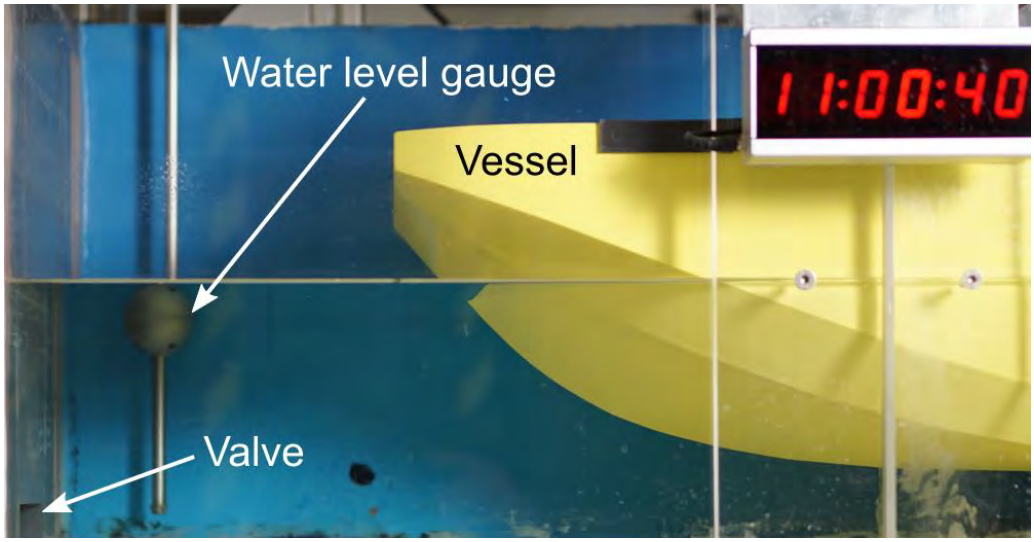

Figure 5: Photo of the inlet section of the physical model

4.2. Calibration of the hydraulic parameters of the filling system

After the known geometric properties were incorporated into the model, the unknown hydraulic parameters have to be calibrated. These are mainly the discharge coefficient as a function of the valve opening and the jet coefficients. Figure 7 shows the discharge coefficient depending on the valve opening for a typical sluice gate valve. The discharge coefficient was determined by a comparison of the inflow calculated from the results of a physical model with the inflow calculated by the 1D model with same geometrical boundary conditions and the same valve geometry and opening velocity.

Figure 8 shows a case which was used for the calibration of the discharge coefficient by comparison of the results determined with the physical model and calculated by the 1D model. The purple line shows the valve opening. The valve is opened in 390 s. The red and dark blue lines show the water levels measured in the laboratory model and calculated with the 1D model, respectively. For calibration the light blue and green lines which show the inflow in the laboratory and 1D models were regarded. The discharge coefficient depending on the valve opening position was adjusted until a good match between the light blue and the green lines was reached for the rising branch of the inflow.

It must be noted that discontinuities in the discharge coefficient or the valve opening velocity trigger waves running through the chamber and thus must be avoided. The forces acting on the vessel are downhill forces which react on waves. Thus, discontinuities in the discharge coefficient directly affect the longitudinal forces acting on the vessel.

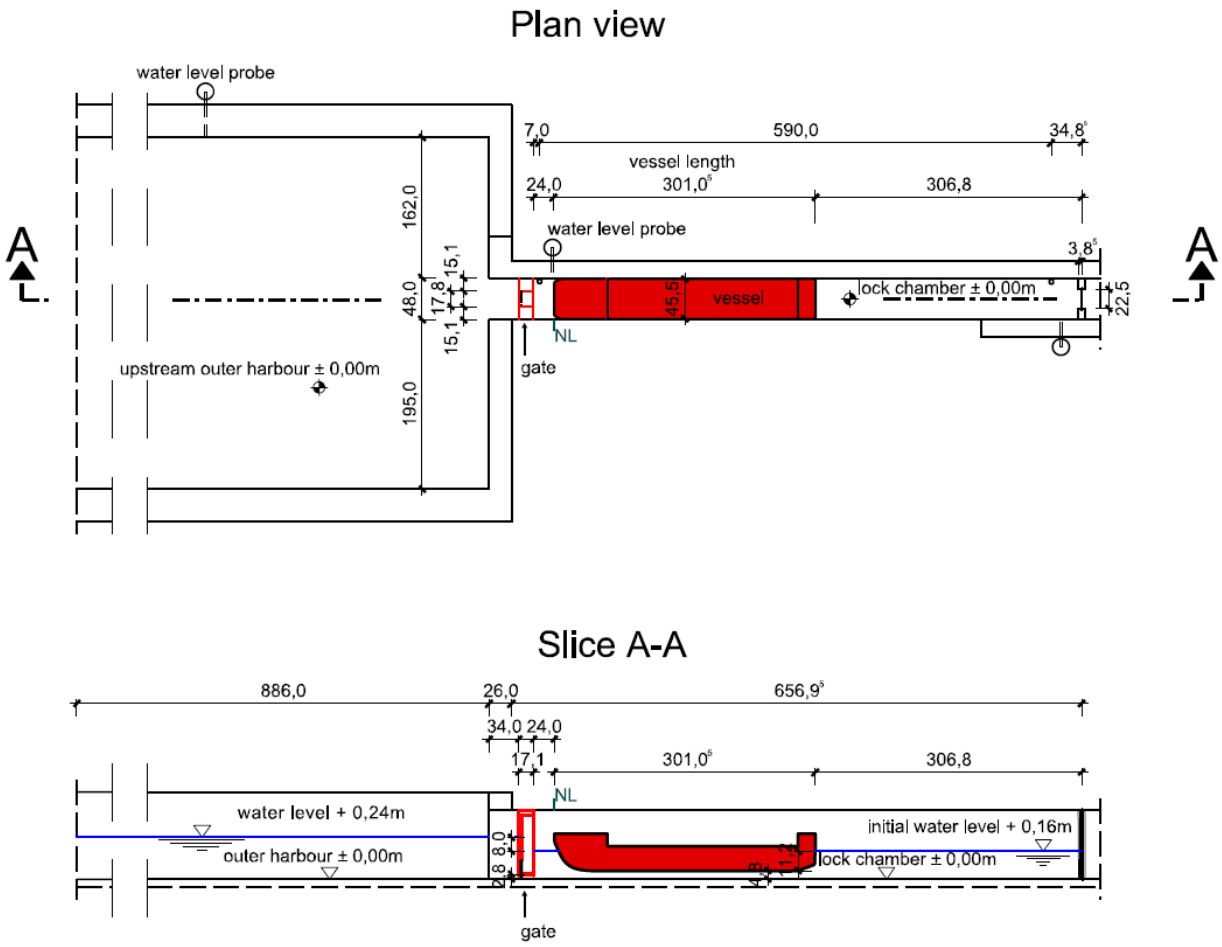

Figure 6: Construction plan of the physical model

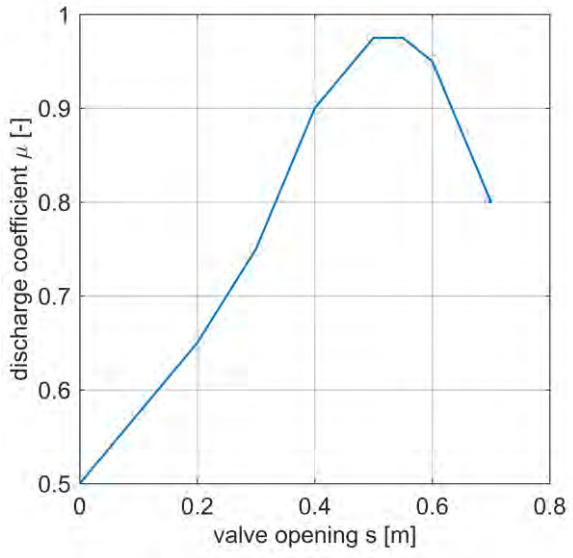

Figure 7: Discharge coefficient depending on valve opening

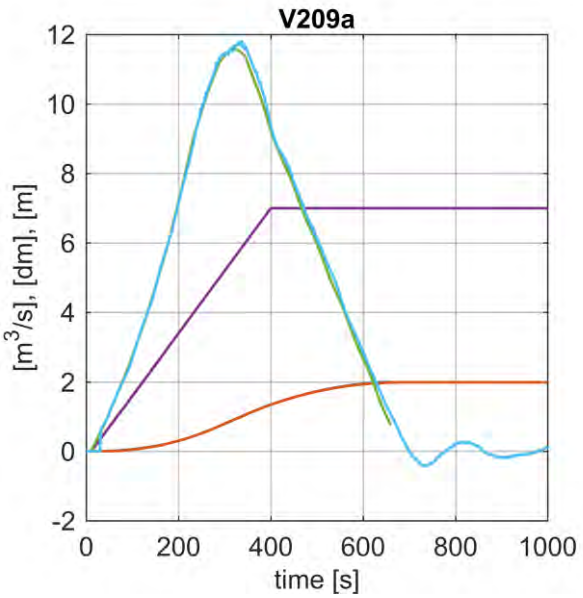

Figure 8: Calibration case for valve discharge coefficient with 1.8 mm/s valve opening velocity

4.3. Propagation of the jet

According to equation (11) the value β is reciprocal proportional to the jet area in every cross section which requires a description of the jet propagation in time and space. Figure 9 shows the upstream gate of a lock with a through-the-head filling system and a possible propagation of a filling jet inside the lock chamber. This jet results from a small valve opening area compared to the cross sectional area of the lock chamber. The cross sectional area of the jet is at least equal to the valve opening area, grows with increasing distance from the upstream head and cannot exceed the cross sectional area of the lock chamber. In-between these limits the shape of the jet has to be described by a function of time and space. The valve opening area and thus the initial jet cross section changes over time because the valve opening is a prescribed function of time. The jet cross section in the lock chamber is the sum of the initial jet cross section and the growing depending on the distance to the gate. This growth can be parameterized with a linear coefficient and an exponent.

The expansion rate of the jet is described with a linear coefficient c_2 and an exponent c_3 in equation (26) assuming that the initial jet cross section at the upstream head is a function of the current valve opening area A_{valve} [m²] and the coefficients c_0 and c_1.

$$A_{\text{jet}} = c_0 + c_1 \cdot A_{\text{valve}}(t) + c_2 \cdot x^{c_3} \tag{26}$$

For a linear spreading of the jet area the coefficient c_3 is equal to one, for a quadratic spreading c_3 is equal to two. For a flat, wide jet close to the ground a linear increase of the jet cross section over the length can be assumed. For a free circular jet a quadratic growth can be assumed. The description of the jet is complex and might change during the further development of the BAW lock model.

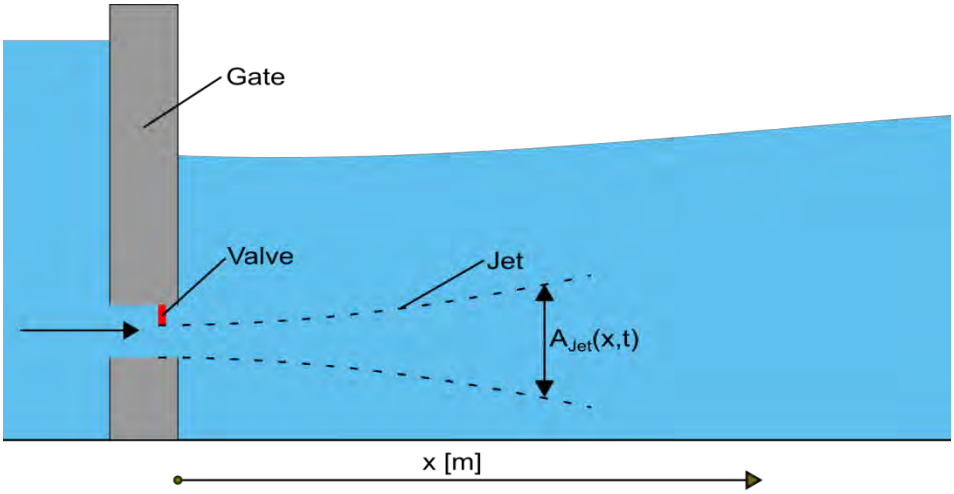

Figure 9: Propagation of the filling jet, definition sketch

Due to a strong dependency of the forces acting on the vessel from the ratio of jet cross section to chamber cross section a good parameterization of the jet propagation is significant for proper results. The parameterization can only be conducted by a comparison of the forces observed at the prototype or in physical experiments with the forces calculated by the 1D model. The thinner the jet, the more distinct is the water level slope to the upstream head and thus the forces acting in upstream direction. The initial jet cross section is described by the coefficients c_0 and c_1. For an initial jet cross section which equals the valve opening area c_0 can be set to $c_0 = 0$ and c_1 to $c_1 = 1$. The coefficients c_2 and c_3 must be parameterized to describe the jet propagation over the whole distance. Thus, at least two experiments must be carried out for calibration, one with the vessel close to the upstream head and one with the vessel more apart from the head. The forces calculated with the 1D model must fit both experiments as good as possible. Figure 10 shows a comparison of the calculated forces with the forces determined in physical experiments. The left subfigure shows the comparison with an experiment where the vessel position was close to the upstream head, the right subfigure shows the comparison with an experiment where the vessel position was in the middle of the lock chamber.

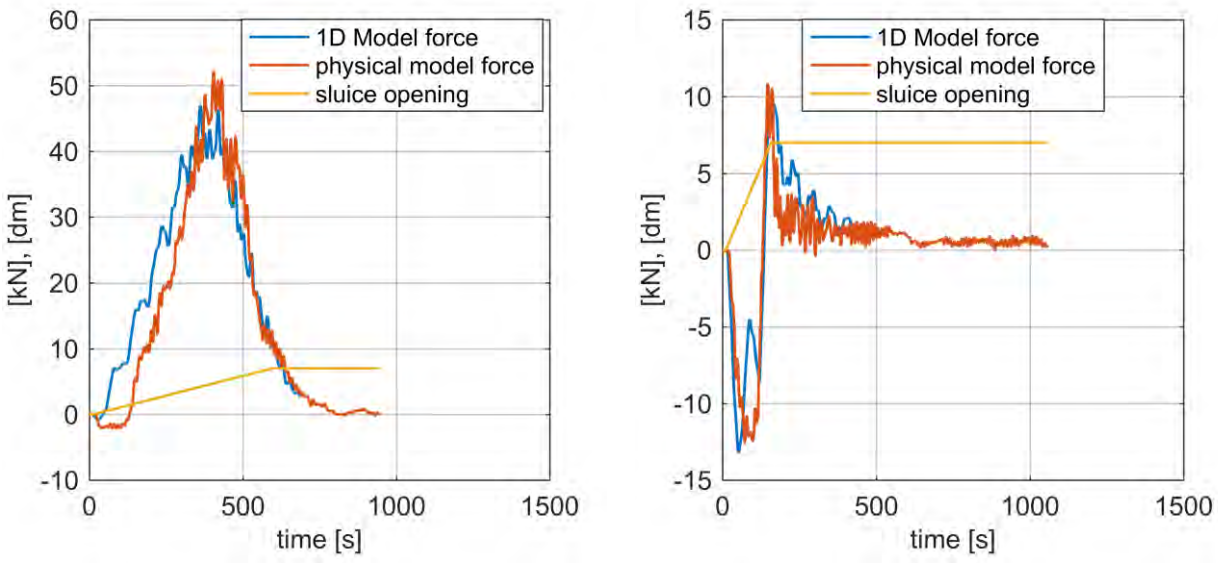

Figure 10: Calibration Case: Comparison of measured and simulated forces acting on a vessel for different vessel positions and valve opening velocities. left: vessel position near the upstream head, right: vessel in position in the middle of the lock chamber

4.4. Validation with physical model results

After the hydraulic parameters for the discharge and the jet propagation were calibrated, additional runs of the physical model were used for the validation of the model behavior. For the validation procedure the experiment was repeated with the previously determined values for the discharge coefficient but a smaller valve opening velocity. Here, the valve was opened in more than 800 s. The results are shown in Figure 11. Regarding the discharges, a very good agreement for both the rising side and the falling side of the discharge curve can be found.

For the further validation, the forces acting on the vessel were evaluated. The results of the validation experiments are shown in Figure 12. The calculated forces show a good agreement with the forces determined in the physical model. The left subfigure shows the comparison with an experiment where the vessel position was close to the upstream head, the right subfigure shows the comparison with an experiment where the vessel position was in the middle of the lock chamber.

In Figure 12 (right) an oscillation of the forces determined in the numerical model can be seen, which does not exist in the physically determined forces. This could be due to the absence of damping effects in the numerical model. Furthermore a gap of a few seconds in the rising branch of the forces in Figure 12 (left) can be noticed which can also be seen in Figure 10 (left) where the numerically calculated forces occur earlier than the forces determined in the physical experiments leading to comparable maximum values. The reason for this gap could not be clarified yet. It might result from a not exact initial valve opening in the physical model. However, the forces calculated with the 1D model shown in Figure 12 show a good agreement with the physical experiments, especially regarding the extrema of the forces which are the major criteria for the design process.

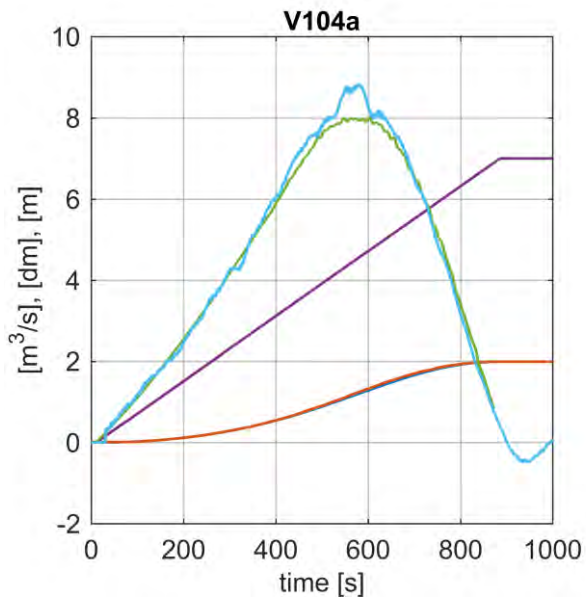

Figure 11: Validation case for valve discharge coefficient with 0. 8 mm/s valve opening velocity

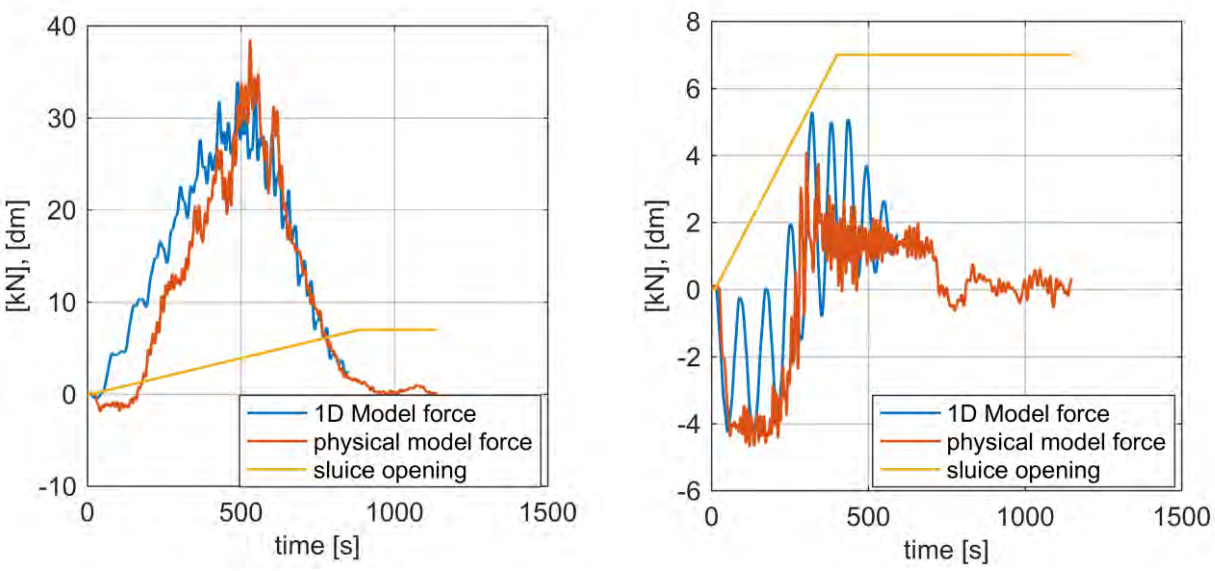

Figure 12: Validation case: Comparison of measured and simulated forces acting on a vessel for different vessel positions and valve opening velocities. left: vessel position near the upstream head, right: vessel in position in the middle of the lock chamber

4.5. Prediction of forces based only on experience

For validation the developed model was used to predict the forces acting on a ship for another lock with a different filling system, different dimensions and another vessel. Based on the experience from previous usage the calibration parameters were guessed as good as possible without regarding the results from physical investigations of this lock. Later, the predicted discharge over time and the forces acting on the vessel were compared to the results from physical experiments.

To test the accuracy of the prediction, the lock Bolzum was used. It is filled through the upstream head. To control the inflow, a segment gate instead of a sluice gate valve is used. The lock has a width of 12.5 m and a hydraulic length of 164 m. The vessel has a length of 105 m and a draught of 2.80 m. The upstream head of the lock is equipped with an energy-dissipator-grid, so that the influence of the jet is negligible. The inflow was calculated by equation (1), but the performance of the segment gate is expressed by the term $A \cdot \mu$ [m²] depending on the segment opening angle (Figure 13, left). This is done because the opening area of the segment gate is difficult to calculate due to its radial shape. Instead of the lift height a segment opening angle is prescribed over the time.

The dimensions of the lock and the ship together with the water levels at the beginning of the filling process are known values. For the performance of the segment gate the correlation between opening angle and $A \cdot \mu$ from Figure 13 (left) was taken. It was determined with a three dimensional numerical model from another project with slightly different geometry of the segment gate. With the 1D model a simulation was performed opening the segment within 800 s from 0° to 20°. The calculated discharge and the forces acting in the ship compared to the results determined from a physical model are shown in Figure 13 (right). The calculated discharge shows a good agreement with the discharge from the physical model. The maximum discharge differs about 5 %. However, the gradient of the rising discharge is slightly steeper in the physical model suggesting an underestimation of the segment gate performance in the region of small gate opening angels. Comparing the forces both lines agree qualitatively. The first flush is more distinct in the physical model, which might result from a sudden opening of the segment sealing at small opening angels. In this region the physical model is not completely applicable. Nevertheless, a good agreement between the 1D calculation and the laboratory experiments could be shown.

But note: In this case the prediction was made to a comparable lock and vessel size. Attempts to predict the forces for a sea lock which is much bigger failed. Here a basis calibration with another sea lock with comparable dimensions should be performed.

5. LIMITATIONS OF THE DEVELOPED MODEL

The 1D lock model is based on the one dimensional Saint-Venant equations. One of the fundamental estimations for applicability of these equations is a mainly one dimensional flow. Flow in the perpendicular directions is neglected in the equations. Flow in lateral direction may trigger lateral forces acting on the vessel, which cannot be determined with the 1D model. The longitudinal forces determined with the model are depending on four influencing factors:

- geometry
- valve opening velocity
- valve discharge coefficient
- jet propagation

It can be assumed that the geometry of the lock and the vessel and the valve opening velocity are known quantities and that these quantities are correctly entered in the software. The valve discharge coefficient is not known a priori and has to be determined in experiments or taken from literature, which is an uncertainty using the model. It cannot be ensured that this efficiency can be transferred to prototype size due to small adjustments in the construction which may change the hydraulic behavior of the system. Another uncertainty using the model is the parameterization of the propagation of the filling jet, which has a large influence on the forces acting on the vessel. The propagation of the jet can be determined with physical or numerical models, but this requires additional effort. The jet propagation must be parameterized by determining the force acting on a vessel as a result of the jet propagation. Thus, a scale model or on-site measurements with different vessels or vessel positions should exist to guarantee a suitable parameterization. Due to the sensitivity of the jet propagation to the size, shape and position of valve, culvert shape and gate it is difficult to predict suitable jet parameters if no information from a similar lock exists.

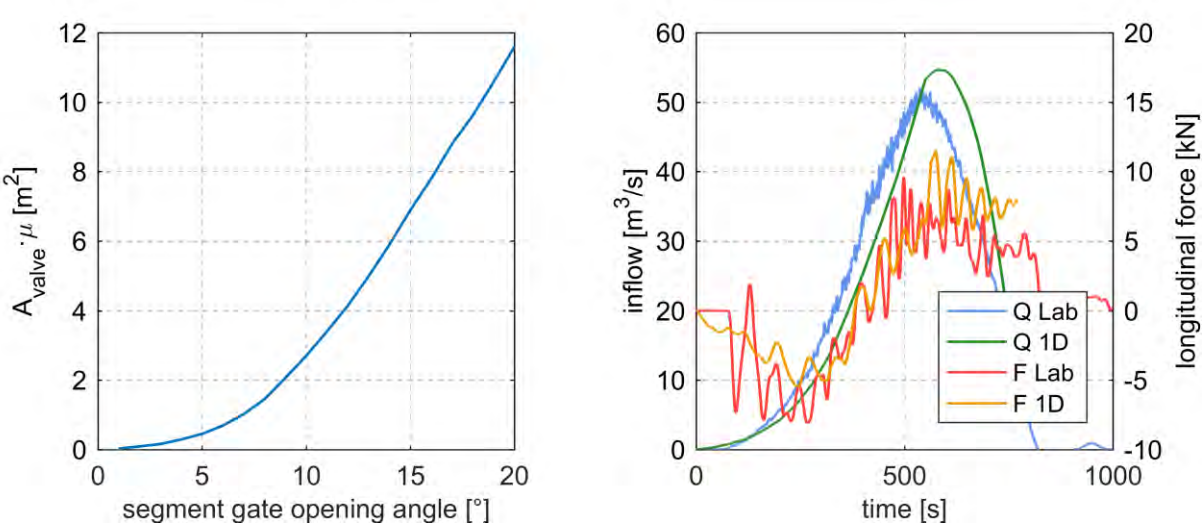

Figure 13: Left: Segment gate performance depending on the segment opening angle; right: Comparison of estimated inflow and forces from the 1D model with the inflow and forces determined in physical experiments

6. SUMMARY AND CONCLUSIONS

During the lock filling process forces are acting on the vessel in the lock chamber. For the design process of the filling system and to specify the valve opening velocity it is crucial to know these forces. The main hydraulic phenomena triggering forces are explained in this paper for lock filling through the head. Existing methods to determine the forces are discussed. A one dimensional model which allows the short-time prediction of the longitudinal forces is introduced and the calibration parameters and their impacts are mentioned. Due to the open data policy of the BAW, the developed software including the source code is available as open-source.

The model allows the user to calculate forces acting on a vessel during the lock filling process under different hydraulic boundary conditions in a very short time. If a physical model exists to perform a reasonable calibration a prediction of the forces occurring for different valve opening velocities or ship positions can be performed with a high certainty. This allows calculations based on data of a physical model even if the model itself does not exist anymore.

The extrapolation to locks with other geometries and filling systems is much more uncertain because the calibration parameters have to be estimated. Here the engineer has to be careful due to the effect of a bad calibration, which might underestimate the calculated forces. A working energy dissipation at the upstream head decreases the forces acting on the vessel due to a decreasing influence of the jet. Furthermore, the uncertainties due to a bad calibration of the jet propagation decrease, too.

7. NOTATION

Δh	[m]	water level difference between outer harbor and the lock chamber
μ	[-]	discharge coefficient
Q	[m³·s^{-1}]	flow rate
g	[m·s^{-2}]	gravitational constant (g=9.81 m·s^{-2})
h	[m]	water level
A_{chamber}	[m²]	gross area in the lock chamber
A_{vessel}	[m²]	cross sectional area of the vessel
W_{chamber}	[m]	width of the lock chamber
$\mathrm{m}_{\text{vessel}}$	[kg]	mass of the vessel
F	[N]	longitudinal force acting on the vessel
A	[m²]	overall cross sectional area
β	[-]	Boussinesq coefficient
q	[m^2·s^{-1}]	specific discharge
L_{vessel}	[m]	length of the vessel
T	[s]	wave cycle time
n	[-]	time step index
A_{valve}	[m²]	valve opening area
u	[m·s^{-1}]	velocity
L_{chamber}	[m]	length of the lock chamber
I	[-]	slope
A_{jet}	[m²]	cross sectional area of the filling jet
Δt	[s]	time step size
Δx	[m]	distance between two cross sections
θ	[-]	Crank Nicolson factor
B_{vessel}	[m]	width of vessel
i	[-]	grid index
c_0, c_1, c_2, c_3	[-]	parameter to describe jet expansion

8. REFERENCES

Belzner, F.; Merkel, J.; Gebhardt, M.; Thorenz, C. (2017): Piano Key and LabyrinthWeirs at German waterways: Recent and future research of the BAW. In Sébastien Erpicum, Frédéric Laugier, Michael Pfister, Michel Pirotton, Guy-Michel Cicero, Anton J. Schleiss (Eds.): Labyrinth and Piano Key Weirs III: CRC Press/Balkema, pp. 167–174.

Bousmar, Didier; Savary, Celine; Swartenbroekx, Catherine; Zorzon, Gil (2017): Feedback From 10 Years Of Field Measurement On Navigation Locks. In : Hydrolink Magazine, 1/2017, pp. 10–13.

Crank, J.; Nicolson, P.; Hartree, D. R. (1947): A practical method for numerical evaluation of solutions of partial differential equations of the heat-conduction type. In *Math. Proc. Camb. Phil. Soc.* 43 (01), p. 50. DOI: 10.1017/S0305004100023197.

Cunge, Jean A.; Holly, Forrest M.; Verwey, Adri (1980): Practical aspects of computational river hydraulics. Boston u.a.: Pitman (Monographs and surveys in water resources engineering, 3).

De Loor, Alexander (2016): LOCKFILL. User & Technical Manual. Deltares. Delft. Available online at http://oss.deltares.nl/documents/645319/645571/Lockfill+Manual, checked on 3/7/2018.

Free Software Foundation (2007): GNU General Public License 3. Available online at https://www.gnu.org/licenses/gpl-3.0, checked on 3/9/2018.

Gamma, Erich (2011): Design patterns. Elements of reusable object-oriented software. 39. printing. Boston: Addison-Wesley (Addison-Wesley professional computing series).

Jirka, Gerhard H.; Lang, Cornelia (2009): Einführung in die Gerinnehydraulik.

Max-Planck-Gesellschaft (2003): Berlin Declaration on Open Access to Knowledge in the Sciences and Humanities. With assistance of Prof. Dr. Martin Stratmann. Edited by Max-Planck-Gesellschaft. München. Available online at https://openaccess.mpg.de/67605/berlin_declaration_engl.pdf, updated on 2/15/2018.

Oracle (2018a): Class ResourceBundle. Edited by Oarcle. Available online at https://docs.oracle.com/javase/8/docs/api/java/util/ResourceBundle.html, checked on 3/7/2018.

Oracle (2018b): JAXB. Java Architecture for XML Binding. Edited by GitHub. Available online at https://javaee.github.io/jaxb-v2/, checked on 3/9/2018.

Partenscky, H.-W. (1986): Binnenverkehrswasserbau. Schleusenanlagen. Berlin Heidelberg NewYork Tokyo: Springer.

PIANC (2015): PIANC InCom WG 155. Ship Behaviour in Locks and Lock Approaches. With assistance of Carsten Thorenz, Jeremy R. Augustin, Didier Bousmar, Jean-Pierre Dubbelman, Arcelio Hartley, Peter Hunter et al. Edited by PIANC.

Thorenz, Carsten (2009): Computational Fluid Dynamics in lock design. State of the art. PIANC INTERNATIONAL WORKSHOP "Innovation in Navigation Lock Design". Brussels, Belgium, 2009.

Thorenz, Carsten (2010): Numerical evaluation of filling and emptying systems for the new Panama Canal locks. In : 32nd PIANC International Navigation Congress 2010. Liverpool, United Kingdom, 10 - 14 May 2010. Red Hook, NY: Curran.

Thorenz, Carsten; Anke, Jens (2013): Evaluation of ship forces for a through-the-gate filling system. Smart Rivers 2013. Liege (BE), Maastricht (NL), 2013.

Thorenz, Carsten; Belzner, Fabian; Hartung, Torsten; Schulze, Lydia (2017): Numerische Methoden zur Simulation von Schleusenfüllprozessen. In Bundesanstalt für Wasserbau (Ed.): BAW Mitteilungen 100. Kompetenz für die Wasserstraßen - Heute und in Zukunft. Forschungs- und Entwicklungsprojekte der BAW. Available online at http://henry.baw.de/bitstream/20.500.11970/102493/1/mb_100_07_Thorenz_Numerische.pdf.

Van der Ven, P.; Van Velznen, G.; O'Mahoney, T.; De Loor, A. (2015): Comparison of Scale Model Measurements and 3D CFD Simulations of Loss Coefficients and Flow Patterns for Lock Levelling Systems. In PIANC (Ed.): 7th International PIANC-SMART Rivers Conference. With assistance of Lucía Torija. Buenos Aires, Argentinia.

Vrijburcht, A. (1991): Forces on ships in a navigation lock induced by stratified flows, Stellingen.

Zhao, Bin; Zhang, Bo (2011): Comparison of different order Adams-Bashforth methods in an atmospheric general circulation model. In *Acta Meteorologica Sinica* 25 (6), pp. 754–764. DOI: 10.1007/s13351-011-0606-6.

Scale model research and field measurements for two new large sea locks in the Netherlands

by

A.J. van der Hout[1,2], H.I.S. Nogueira[1], W.C.D. Kortlever[3], A.D. Schotman[4]

ABSTRACT

In the Netherlands two new large sea locks are currently being built: the new lock of IJmuiden, providing access to the port of Amsterdam and the new lock of Terneuzen, providing access to the port of Ghent. Both navigation locks will be part of existing lock complexes that form a barrier between fresh and salt water. During levelling and when the gate is opened significant forces will develop on the vessels in the lock chamber due to density currents. This paper describes part of the physical scale model research and field measurements that have been carried out during the design process of these locks, focusing on the forces on moored vessels that develop during the lock-exchange. The results of these studies have been used to determine requirements for lock operations for the future largest locks in the Netherlands, at IJmuiden and Terneuzen.

1 INTRODUCTION

Both new locks of IJmuiden and Terneuzen will be much larger than the existing locks to be able to receive larger vessels in the future. As, together with the dimensions of the new lock chambers also the size of the vessels travelling though the new locks will increase, it is expected that hydrodynamic forces on the vessels will increase in the future. Since the strength of the mooring lines does not increase proportionally to the mass of a vessel with larger dimensions, the occurrence of hydrodynamic forces is more critical for these larger vessels. The mooring line loads and vessel motions resulting from hydrodynamic forces during levelling and the lock-exchange are therefore a decisive factor in the design and operation of the new locks.

To have a good understanding of the hydraulics of the new locks, extensive studies have been performed during the design process of the levelling system of these locks using both numerical and physical models. A general overview of the design process of these two new sea locks in the Netherlands is presented by Kortlever *et al.*, 2018 and the role of numerical models in the design of the levelling system of the new lock of Terneuzen is addressed by Mahoney *et al.*, 2018.

Since both the new lock of IJmuiden and Terneuzen are sea locks, a density difference over the lock is present and for both locks the density current leads to dominant forces on the moored vessel during levelling and the lock-exchange. For the lock of IJmuiden and Terneuzen two different types of levelling systems are used: openings in the lock gate for IJmuiden and a longitudinal filling system with bottom grids for Terneuzen. The development of hydraulic forces during levelling will therefore be different for both locks. However when the gate is opened, the processes will be similar for both locks. When the gate opens, water with different densities on both sides of the gate will exchange due to pressure differences, whereby the denser (saltier) water will flow underneath the less dense (fresher) water and the fresher water will flow over the saltier water. This process is called a lock-exchange and it is only to a limited extent influenced by the design of the levelling system of a lock. This process is described in detail by Vrijburcht, 1991 and is illustrated in Figure 1. An overview of the effects of density differences during levelling for the new lock of IJmuiden is provided by Nogueira *et al.,* 2018. The research described in this paper, shows that the forces on the vessels in the lock chamber, as a result of the density currents when opening of the gate, will often exceed the forces during levelling.

This paper focuses on the lock-exchange process in the new locks of IJmuiden and Terneuzen and the hydrodynamic forces related to this phenomenon on the vessels moored in the lock. Design options to influence the large-scale process of gravity driven currents are limited and the occurring

[1] Deltares, Boussineqweg 1, 2629 HV, Delft, Netherlands
[2] Delft University of Technology, Ports and Waterways, Building 23, Stevinweg 1, 2628 CN, Delft, Netherlands
[3] Rijkswaterstaat, Ministry of Infrastructure and the Environment, Griffioenlaan 2, 3526 LA, Utrecht, Netherlands
[4] Pilot Association Amsterdam-IJmond, Kanaaldijk 242, 1975 AJ IJmuiden, Netherlands

forces are therefore hard to influence. In practice the forces on the ships are therefore handled with operational measures, instead of by extensive design modifications to the lock itself. The objective of the research presented here was to provide engineers and pilots with information on the magnitudes an evolution of forces that can be expected in the new locks, so that they can better prepare on how the future operation of mooring and unmooring vessels and sailing out of the lock will change in these larger locks.

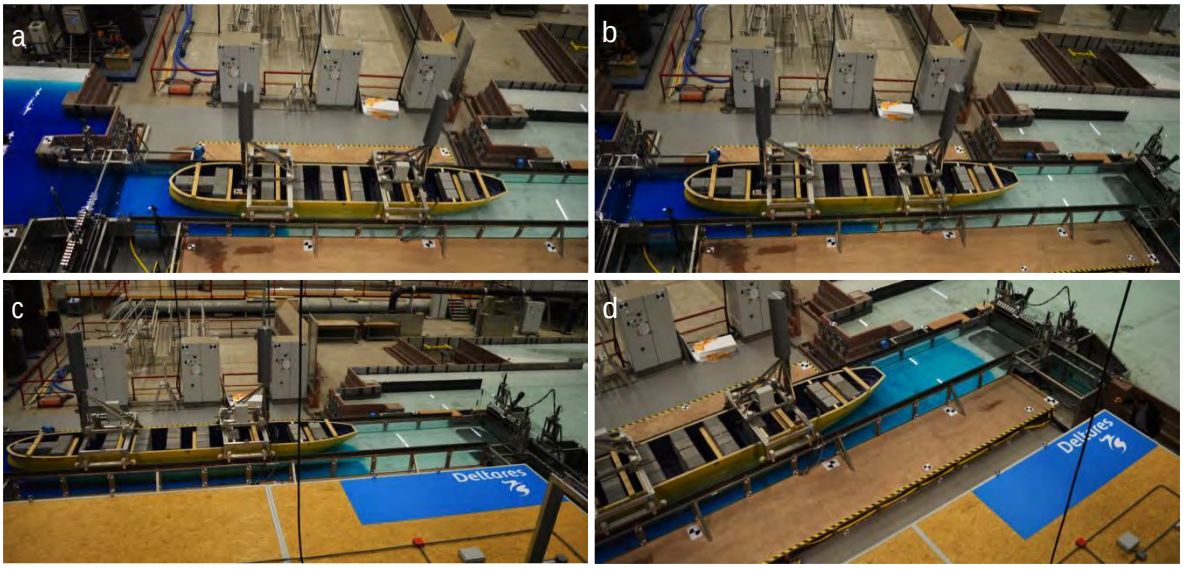

Figure 1: A lock exchange process, in which salt water (colored blue) enters a fresh lock chamber after the gate is opened. The pictures are taken sequentially in time from (a) to (d).

For the design of the levelling system of both locks, a design vessel was defined with maximum allowable dimensions for which the locks would still be able to achieve acceptable levelling times. For the study on lock-exchange effects however, described in the present paper, also smaller vessels have been considered. From an operational point of view these smaller vessels will be more relevant than the largest vessel that can pass the lock, since they will visit the new locks more frequently and these vessels will be the first vessels that the pilots will have to guide safely through the new locks.

The study described in this paper consists of three parts:

- Physical scale model study on the design vessel for both IJmuiden and Terneuzen
- Physical scale model study on a smaller vessel in the new lock of IJmuiden
- Field measurements in the North Lock of IJmuiden

By combining the results of the three abovementioned measurement series, a clear view was obtained on what operational requirements need to be met during the lock-exchange in the new locks of IJmuiden and Terneuzen.

2 MAIN PARTICULARS OF THE NEW LOCKS

2.1 New lock of IJmuiden

The new lock of IJmuiden will have a length of 545 m and a width of 70 m. The floor level of the lock chamber is located at NAP-17.75 m (NAP = Amsterdam Ordnance Datum) and for daily operation water depths typically vary around 18 m, with head differences typically around 1 to 1.5 m. The maximum operational water levels at the sea side can range from NAP-1.65 m to NAP+4.00 m, under extreme design conditions. The water level of the canal will remain relatively constant at a level of NAP-0.40 m. The new lock of IJmuiden is aimed to be in operation in 2020.

The new lock is significantly larger than the currently operational North Lock (Noordersluis in Dutch), which will be replaced by the new lock of IJmuiden. The North Lock is presently the largest lock of the IJmuiden lock complex with main dimensions of 400 m x 50 m x 15 m (length x width x depth). The North Lock is comparable in size to the new lock in Terneuzen and can therefore serve as a reference for that lock.

2.2 New Lock of Terneuzen

The new lock of Terneuzen is equipped with four gates and will have a minimum length of 402 m and a maximum length of 452 m, and a width of 55 m. The floor level of the lock chamber is located at NAP-16.80 m and operational water levels at the sea side range from NAP-2.69 m to NAP+4.60 m. In the current design of the lock, a sill is present at the inner head with its top at the level of NAP-14.12 m to reduce salt intrusion into the canal. In the future this sill may be heighted, if needed. The presence of a sill at the inner head will reduce forces that develop during the lock-exchange at that head. If the sill is heightened in the future, the lock-exchange forces may be reduced even further. What makes the situation in Terneuzen different from the new lock of IJmuiden is that the canal has a higher water level than in IJmuiden. The water level of the canal is located at a constant level of NAP+2.13 m. As a result of this, higher head differences, will occur on a more frequent basis than in IJmuiden, with daily head differences up to 4 m. The lock is aimed to be in operation in 2022.

3 FORCE CRITERIA

When designing the levelling system of a lock, criteria are determined for the maximum allowable forces on the vessels moored in the lock. These criteria are typically based on the maximum forces that can be handled by the minimum strength of the mooring lines required for that type of vessel, under the assumption that all hydrodynamic forces are absorbed by the mooring lines and that horizontal vessel motions need to be restricted. Usually a safety margin is included in these criteria; for example, the mooring line loads are not allowed to exceed 50% of the minimum breaking load (MBL) of the mooring lines. These maximum allowable force criteria are often expressed as a permillage of the weight (displacement) of a vessel. The larger the displacement of a vessel is, the smaller is the value of the maximum allowable force permillage, since the required strength of the mooring lines does not increase proportionally to the weight of the vessel.

Hydrodynamic forces during levelling have different origins and have typically a fast-varying character, e.g. as a result of translatory waves. Also when the gate opens such fast-varying translatory waves may develop as a result of a small residual water level difference over the gate at the end of levelling. During the subsequent lock-exchange process however, the character of the hydrodynamic force changes more gradually due to the relatively large scale and slow nature of density currents, and the force due to density currents is always directed to the side of the vessel where the water is saltier. In addition, also the way of handling the vessel after the gate has been opened is different from the way during levelling. During levelling all horizontal vessel motions need to be restricted and the vertical displacement of the vessel is compensated for by careful control of the winches. After the gate has been opened however, the vessel needs to be unmoored and to a certain extent controlled vessel motions can be allowed as the vessel prepares to sail out of the lock. In addition, once the gate is open and the mooring lines are disconnected it is also possible to use the main propeller and possibly tugboats to control the motions of the vessel. Due to the different character of the operations during levelling and the lock-exchange, the mooring criteria as defined for levelling do formally not apply to the lock-exchange.

The mooring criteria as defined for levelling will however be mentioned as a reference in this paper, although they are formally not applicable to the process studied here. However, by comparing the forces that develop during the lock-exchange to the force criteria for levelling, insight is provided whether the hydrodynamic forces can be absorbed theoretically by the mooring lines alone, or that additional measures might be required. The force criteria and occurring hydraulic loads will not only be expressed as a permillage of the vessels weight in this paper, but also as absolute values in metric tons. This makes it easier to compare different vessels (or the same vessel with different draughts) to each other and it allows for a straightforward comparison to typical mooring line strengths and tugboat capacities, which are typically expressed in metric tons.

The force criteria for levelling of the new locks at IJmuiden and Terneuzen are defined as a maximum longitudinal force and maximum transversal forces acting at the location of the fore and aft perpendicular of the vessel. The combination of the three forces (longitudinal, transversal fore pp., and transversal aft pp.) determines the maximum allowable surge force, sway force and yawing moment. The mooring criteria for the different vessels (see Section 4 for the main particulars of the vessels) considered in this study are given in Table 1.

Table 1: Force criteria for the different considered vessels in metric tons (and as permillage of the actual weight of the vessel). $F_{crit,\ long}$ = maximum allowable longitudinal force, $F_{crit,\ trans}$= maximum allowable transversal force at the fore and aft perpendicular.

Name	Type	Draught [m]	$F_{crit,\ long}$ [ton] ([‰])	$F_{crit,\ trans}$ [ton] ([‰])
Breesaap	Design vessel IJmuiden	14.05	38 (0.20 ‰)	23 (0.12 ‰)
The Flying Dutchman	Small vessel IJmuiden, loaded	14.00	24 (0.21 ‰)	16 (0.14 ‰)
The Flying Dutchman	Design vessel Terneuzen	12.50	24 (0.24 ‰)	16 (0.16 ‰)
The Flying Dutchman	Small vessel IJmuiden, ballast	9.00	24 (0.35 ‰)	16 (0.24 ‰)

4 PHYSICAL SCALE MODEL

To simulate the complete levelling cycle of both new locks at IJmuiden and Terneuzen a physical scale model facility has been built at Deltares at scale 1:40. The overall objective of the scale model research was to determine the levelling times that can be achieved for the considered levelling systems and to study the lock-exchange that occurs when the gate is opened. To that end, the physical scale model has been equipped with movable gates that open automatically after levelling.

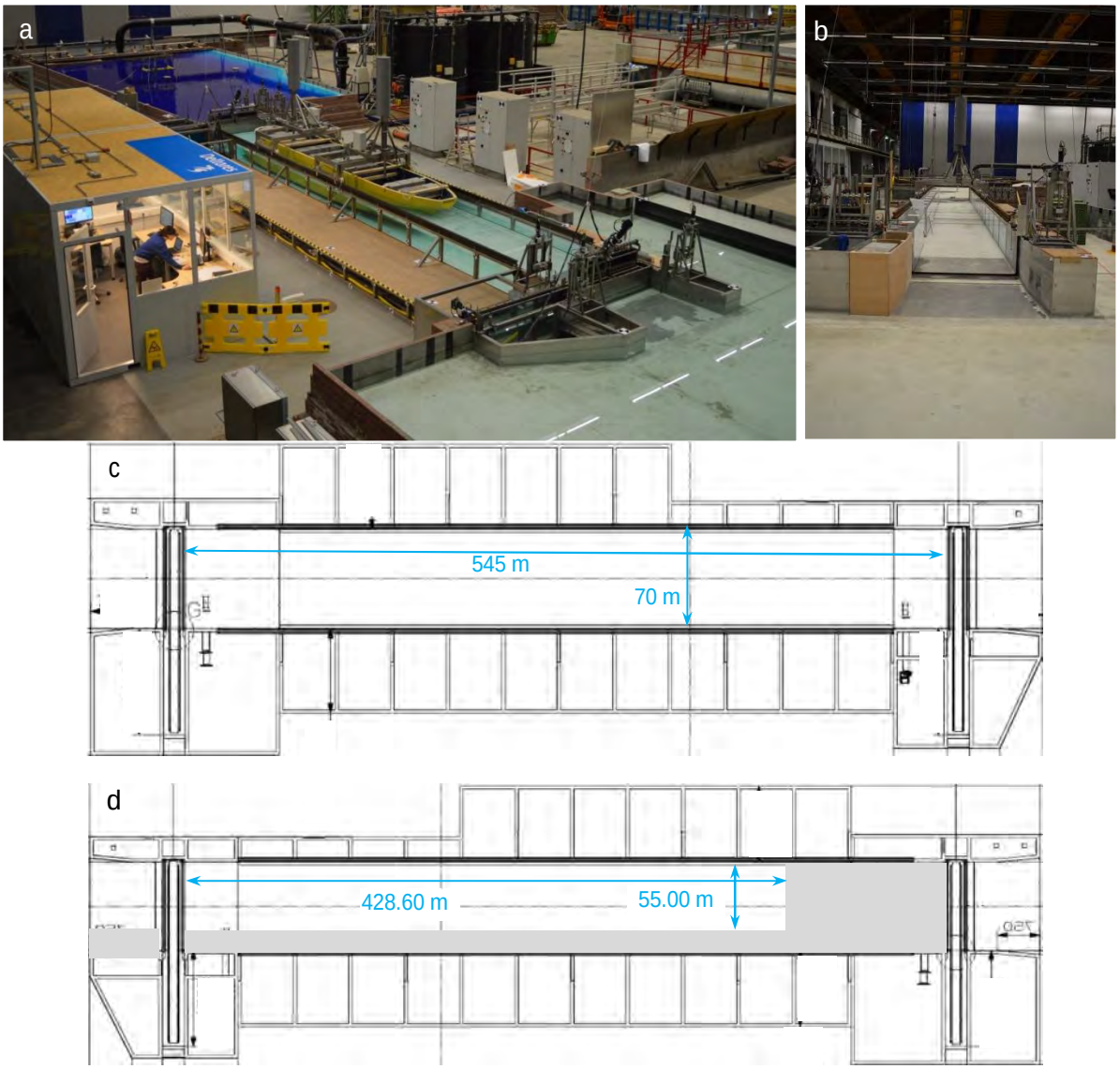

Figure 2: Overview of the scale model facility of IJmuiden (a) and modified lock chamber for the lock of Terneuzen (b). The main dimensions of the lock are given in (c) for the IJmuiden tests and in (d) for the Terneuzen tests.

In the scale model, the lock chamber, the lock heads, the levelling system and also parts of the approach harbours are represented. In Figure 2 an impression of the scale model facility is given. A

predetermined density difference over the lock is maintained by adjusting the water density of the approach harbours between tests. The approach harbours have been equipped with movable weirs to set the water levels in the approach harbours to the desired level. Vertical density profiles have been determined at several locations in the scale model by measuring conductivity and temperature. Furthermore, water levels, flow velocities, positions of valves and gates, and forces on the vessel have been measured. In total more than 200 measurement channels have been logged simultaneously.

Originally, the physical scale model has been built for the hydraulic study of the new lock of IJmuiden. To be able to also test realistic situations for the new lock of Terneuzen, the available scale model has been modified to match the dimensions of the new lock of Terneuzen, including the sill at the inner head.

4.1 Scale model measurements for IJmuiden

In the hydraulic scale model studies for the new lock of IJmuiden two vessels have been considered, the design vessel *Breesaap* and a smaller vessel *The Flying Dutchman*, at two draughts. Both vessels are bulk carriers and the main particulars are given in Table 2. Also a container vessel was studied in the design process of the new lock, but for conciseness this vessel will not be considered in this paper. The *Breesaap* represents the largest vessel that can pass the new lock under normal levelling conditions. The *Flying Dutchman* is representative for an Aframax class of vessels that now visits the port of Amsterdam on a regular basis and is one of the larger vessels that currently passes through the North Lock. Figure 3 shows both vessels in the physical scale model of the new lock of IJmuiden.

Table 2: Main particulars of the considered vessels for the new lock of IJmuiden

Name	*Breesaap*	*The Flying Dutchman*
Type	bulk carrier	bulk carrier
Length over all (Loa)	330 m	257 m
Length between perp. (Lpp)	320.75 m	252 m
Beam	52 m	40 m
Draught, loaded	14.05 m*	14 m
Draught, ballast	-	9 m
Displacement, loaded	$1.91 \cdot 10^8$ kg	$1.12*10^8$ kg
Displacement, ballast	-	$6.68*10^7$ kg

* This is maximum allowable draught in the lock. When coming from the seaside, the vessel will be lightered from its maximum draught of 18 m to this draught before entering the lock.

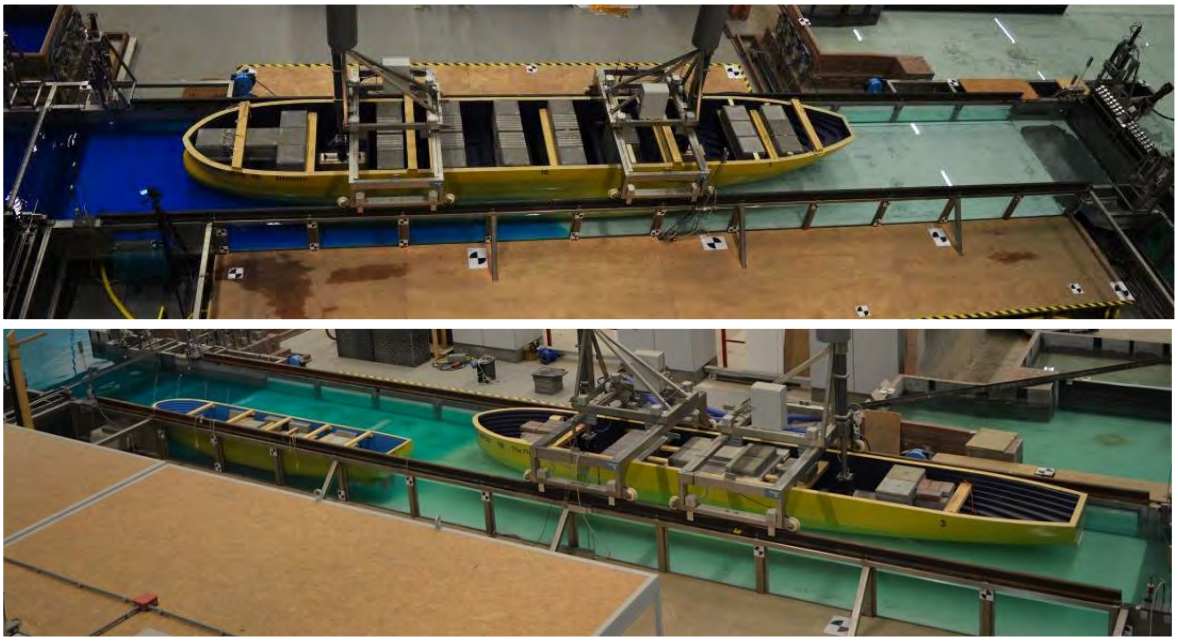

Figure 3: The vessels used in the scale model study of the new lock of IJmuiden during a lock-exchange, with Breesaap (above) and The Flying Dutchman (below, on the right). In the lower panel also a smaller vessel has been moored in the lock to investigate the effect of multiple vessels in the lock chamber at the same time.

The hydraulic studies that were performed for the design of the levelling system for the new lock of IJmuiden were extensive. In total more than 250 tests were performed in the physical scale model. In approximately one third of these tests the gate was opened after levelling and a lock-exchange occurred. The variations that were studied considering the hydrodynamic forces during lock-exchange included: opening the gate after filling and emptying conditions, for inner and outer lock head, with different initial water level differences, different positions of the vessel in the lock chamber, different initial density differences, variations of density distribution in the lock-chamber (homogeneous or stratified), variations in the gate program and the effect of multiple vessels in the lock chamber simultaneously. For conciseness not all variations which have been studied will be discussed in this paper. Only the main conclusions will be discussed, highlighting the most important characteristics of the lock-exchange process.

4.2 Scale model measurements for Terneuzen

The bulk carrier *The Flying Dutchman*, considered a smaller vessel for the new lock of IJmuiden, is defined as design vessel for the new lock of Terneuzen (see Table 3). The draught that was considered in the tests is 12.5 m, being the maximum draught at which the vessel may enter the lock independent of the tide.

Table 3: Main particulars of the considered vessel for the new lock of Terneuzen

Name	*The Flying Dutchman*
Type	bulk carrier
Length over all (Loa)	257 m
Length between perp. (Lpp)	252 m
Beam	40 m
Draught	12.50 m*
Displacement	$9.84*10^{7}$ kg

* This is the maximum draught in the lock considered in the tests. The vessel has a maximum draught of 16.3 m.

The hydraulic study for the new lock of Terneuzen consisted of more than 50 tests, including a wide range of hydraulic conditions. The performed test program included seven tests in which the gate was opened after levelling, also for different hydraulic conditions. The initial head difference at the beginning of levelling was varied, since for filling conditions the density difference over the gate at the end of levelling (when the gate is opened) is determined by the amount of water that is introduced into the lock chamber during levelling. For emptying conditions, the density difference over the gate is hardly influenced by the levelling process. In addition to the tests in which the gate was opened after levelling, several “pure” lock-exchange test haven been performed without levelling prior to opening of the gate. These tests can be considered as representative for emptying tests. In these pure lock-exchange tests several different gate programs have been tested, to investigate the influence of the gate opening program on the hydrodynamic forces on the moored vessel.

In the tests presented in this paper, mainly conditions at the inner head are considered. In an earlier performed measurement campaign also some preliminary results for the lock-exchange at the outer head were obtained. The setup of these tests will not be described in detail here, but in those tests a vessel that was slightly wider than the design vessel was considered then and not the full range of water levels could be studied. Although the results of these preliminary tests are not fully representative for the actual situation of the new lock of Terneuzen, the findings from this preliminary study will be incorporated in the discussion of the results, as they are thought to be illustrative for the dominant physical processes for the lock-exchange at the outer head.

5 FIELD MEASUREMENT CAMPAIGN

Following the physical scale model work, a field measurement campaign was conducted in which forces on vessels in the North Lock of IJmuiden were measured during the lock-exchange. This measurement campaign was conducted by the Pilot Association Amsterdam-IJmond (Schotman, 2017). The main reason for performing these measurements was to serve as a reference for the forces that were found in the scale model tests. This would help the pilots to determine a relation between the physical scale model results, under well-known controlled conditions, and the current day-to-day practice of the pilots, in which conditions are not always well defined.

The forces that occur in reality during a lock-exchange are usually not known. Pilots are aware of density forces due to the lock-exchange, but mooring line forces are not monitored. The crew on deck adjusts the tension in mooring lines based on experience and their perception, such as the peeps and squeaks of the winches. The pilot oversees the response of the vessel and will give appropriate orders to the crew members controlling the winches. Although, the process is normally well under control and ships are handled merely based on extensive experience, it is on beforehand not always known how large lock-exchange forces will be and incidents with relatively large vessel motions or breaking lines still happen occasionally.

Before the start of the measurements it was for example not clear, whether or not the forces that currently occur during the lock-exchange in the North Lock exceed the formal levelling force criteria regularly. Since for the new locks it was expected that this would be the case, the field measurements helped the pilots to assess whether this exceedance would lead to operational problems, or that under normal operations also forces higher than the force criteria for levelling could be handled safely. Another aspect was that knowing the magnitudes of forces that currently occur under normal conditions, would place the higher forces that will occur in more extreme conditions in the new, larger locks in perspective.

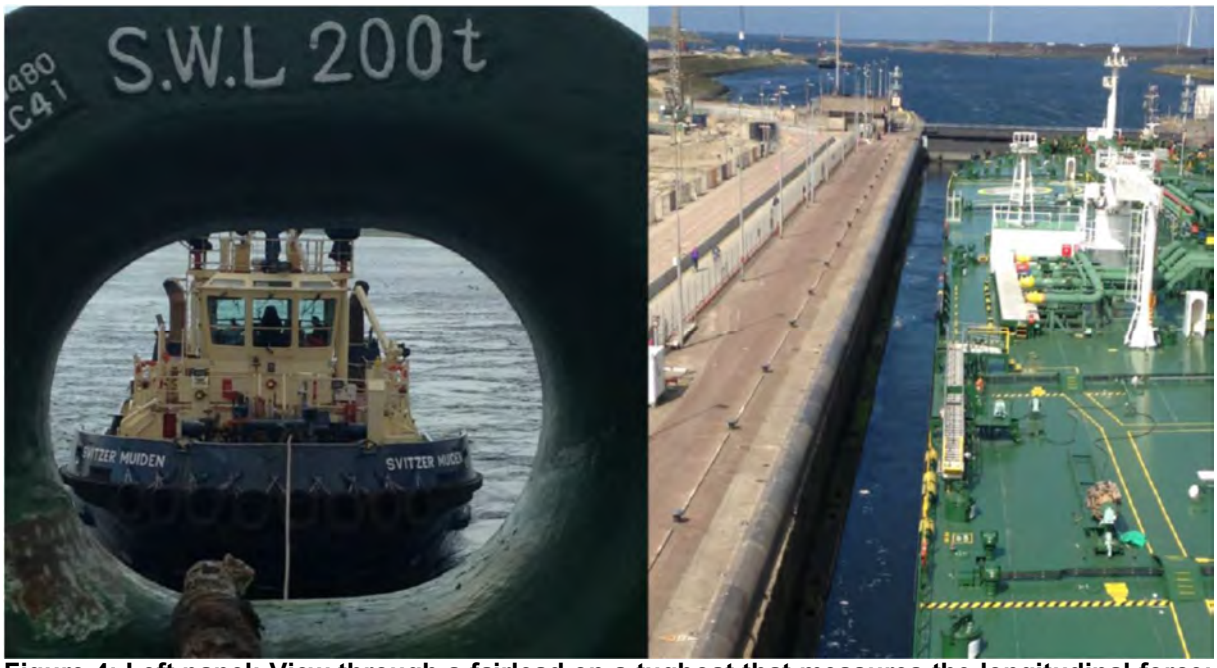

Figure 4: Left panel: View through a fairlead on a tugboat that measures the longitudinal force; right panel: Aframax tanker 'Densa Crocodile' in the North Lock during the measurement campaign.

The forces during the lock-exchange in the North Lock are measured using a tugboat. The vessel was connected to the tugboat by a line from the aft, via the center lead. Figure 4 gives an impression of a measurement. In all tests the vessel was positioned at approximately 80 m from the gate of the outer head. The tests started the first moment the gate started to move. All lines to the bollards on the chamber wall were disconnected as quickly as possible and in all tests this was the case before the gate was fully open. At the moment that the pilot observed that the vessel started to move forward as a result of the density current, using an accurate pilot positioning system, the tugboat was ordered to pull backwards to compensate the movement. The movement of the vessel was monitored carefully and by adjusting the power of the tugboat, the vessel was kept in position for a large part of the lock-exchange process. The forces in the mooring lines were monitored on the on-board equipment of the tugboat or derived from the tugboat capacity diagram. Although the measurement method is quite crude, it was a quick and accessible approach that provided reliable first order of magnitude results. Repetitions tests confirmed the reliability of this method, by giving similar forces under similar conditions with similar vessels.

In the measurement campaign only situations for the outer lock head were considered, meaning that the (outgoing) vessel sails from the canal towards the sea. For this situation, the longitudinal force is larger than the transversal forces and thought to be the most important from operational viewpoint.

Therefore only the longitudinal force is measured. Although transversal forces can be significant as well, measuring these would lead to a more complex measurement set-up which was unfortunately not possible within this project. Four types of vessels are considered in the tests, summarized in Table 4.

Table 4: Considered vessel types in the field measurements

Type	Dimensions *(approx.)* L x B [m]	Loading condition	Draught *(approx.)* T [m]
Aframax	250 x 44,0	Loaded	14
		Ballast	9
Panamax	225 x 32,2	Loaded	14
Handysize	183 x 32,2	Loaded	12
Handysize-wide	183 x 40,0	Loaded	10

The test campaign was conducted in the period of April – October of 2017 and a total of eight tests have been performed. All tests have been performed under similar conditions, with weather conditions that were as mild as possible to avoid external influences, such as wind effects. The water levels of the outer approach harbour were around mean lockage level during the tests, ranging between NAP-0.66 m and NAP+0.67 m.

One of the largest unknowns during the tests was the density distribution in the lock and in the approach harbour at the moment that the gate opens. The density difference over the gate, driving the lock-exchange, depends among others on the fresh water discharge from the neighboring flushing sluice, meteorological conditions, and previous lockages and may vary between tests. The tests have therefore been conducted during a relatively dry period of the spring and summer. In the wetter periods of that summer, in which more variation of the density on the canal side of the lock may be expected, no tests were carried out. Since no density measurements were available, a realistic estimate of the density difference had to be made to be able to interpret the results. Based on available historic measurements, it has been assumed that in all test a density difference of 12 kg/m^3 was present between the outer approach harbour and the lock chamber.

To verify the assumption that the density difference would not vary too much between the tests, a repetition tests was included in the test program and it confirmed indeed only a small variation in the measured longitudinal force. Furthermore, it was expected that due to possible strong easterly winds the density difference over the lock would increase, due to upwelling effects in the outer approach harbour. By also conducting an additional test immediately after a period with strong easterly winds, it was confirmed that for this condition the longitudinal force increased significantly, up to 45 %, during the lock-exchange (results of this verification test are not presented in this paper for conciseness).

6 MEASUREMENT RESULTS

6.1 IJmuiden (physical scale model)

For the new lock of IJmuiden two vessels have been considered: the design vessel (*Breesaap*) and a smaller Aframax class bulk carrier (*The Flying Dutchman*), see Table 2 for the vessel characteristics. The results will be discussed for these two vessels separately.

Design vessel (Breesaap):
Figure 5 shows and example of measured water levels and forces on the vessel in time. It illustrates how forces develop during a typical lock-exchange for the design vessel in the new lock of IJmuiden.

For conditions in which the lock is filled through the outer head, the forces during levelling exist mainly of a combination of translatory waves and a slower varying density force. When the gate is opened, a sharp increase in the longitudinal force is observed due to the density current that creates a water level gradient over the length of the ship. The longitudinal force is directed towards the outer approach harbour (always in the direction towards the saltier water), pushing the vessel out of the lock. The maximum longitudinal force is reached shortly after the gate has been fully opened and only decreases slowly over the next 45 minutes. Also the transversal forces are significant, pulling the vessel off the lock wall. It takes a little longer for the transversal forces than for the longitudinal force to reach their maximum value.

For the inner head, the development of the forces is different from the outer head. For the filling condition that is shown, quite large translatory waves can be observed in the longitudinal force during levelling. Also already a strong buildup of transversal force is present during levelling, due to the incoming fresh water through the lock head. When the gate opens, the transversal force on the bow increases especially, pulling the bow off the lock wall. The magnitude of the longitudinal force also increases, but remains smaller than the magnitude of the transversal forces. The longitudinal force is now directed into the lock chamber (towards the saltier water), pushing the vessel backwards towards the closed gate.

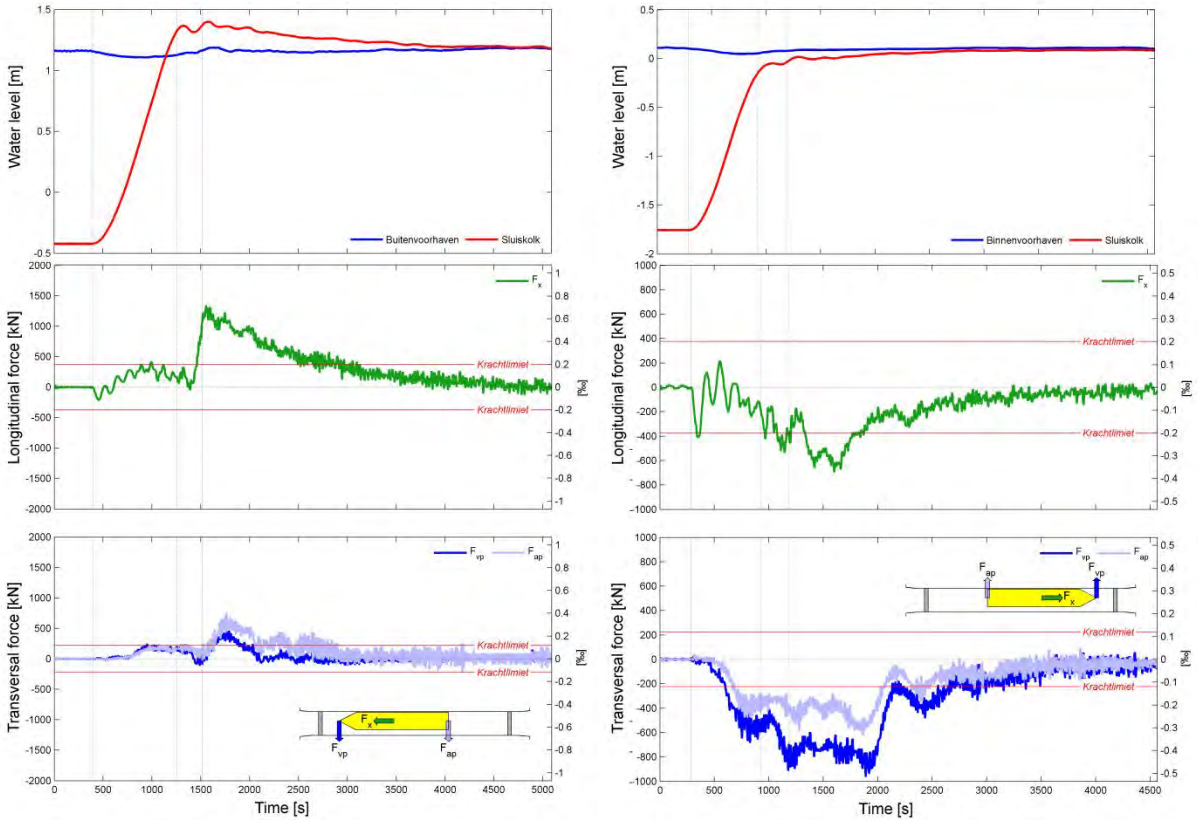

Figure 5: Typical results for the development of the hydrodynamic forces during levelling and the lock-exchange. Left panels: opening the gate after filling through the outer head, right panels: opening the gate after filling through the inner head. Top panels: water levels in the lock chamber (red) and approach harbour (blue). Middle panels: longitudinal force (green). Bottom panels: transversal force bow (dark blue) and transversal force aft (light blue). The gray vertical lines indicate in chronological order: Start of levelling, End of levelling (gate starts to move), and Gate is fully opened. The horizontal red lines indicate the force criteria for levelling (Note the difference in vertical scales for the left and right panels).

The results presented in Figure 5 illustrate the main challenges considering the lock exchange process. For outgoing ships at the outer head, the longitudinal force is the largest and the most relevant. Since this force is directed towards the open gate, the risk of a collision with the gate is small and the density driven current actually helps the vessel to leave the lock. The main challenge is to release all the mooring lines in time, before the vessel gains to much speed and cannot be stopped. When mooring lines cannot be released in time, there will be a chance on line breakage. Also, when two vessels are moored in the lock chamber simultaneously, the second vessel will have to wait until the first vessel has sailed out of the lock, before it can release its mooring lines. During that period, the mooring lines have to be able to withstand the hydrodynamic forces due to the lock-exchange.

For ingoing ships at the inner head, the transversal force on the bow has the largest magnitude and is the most relevant from operational point of view. Pilots need to take sufficient precautions that the bow is not pulled off the wall by the density forces, with the risk that the vessel will hit the opposite wall or another adjacent vessel (e.g. a tugboat). The longitudinal force is also significant, but not as large and might be easier to control, since it takes some time before it reaches its maximum value. At that moment in time the mooring lines may already be released and the main propeller can be used to compensate the longitudinal force. However, one should be aware that in case of engine failure this is

actually a critical situation, since the vessel will be pushed backwards, towards the closed gate, which has a water retaining function in this setting.

Considering the complete data set that has been obtained from all the conducted measurements, the range of maximum values of forces due to the lock-exchange for the design vessel of the new lock of IJmuiden is given in Table 5. These results mainly include tests which a relatively large density difference, to obtain maximum design values, but also a number of tests with a relatively low density difference (i.e. 10 kg/m^3). The highest values in Table 5 can therefore be interpreted as upper limits and the lower values as realistic common situations.

Table 5: Range of magnitudes of the maximum forces measured during lock-exchange for all tested conditions for the design vessel of the new lock of IJmuiden.

Outer head	
$F_{long,\ max}$	58 – 136 ton
$F_{trans,\ max,\ bow}$	32 – 79 ton
$F_{trans,\ max,\ aft}$	36 – 76 ton
Inner head	
$F_{long,\ max}$	34 – 75 ton
$F_{trans,\ max,\ bow}$	40 – 98 ton
$F_{trans,\ max,\ aft}$	24 – 64 ton

The main conclusion drawn from this overview is that forces as a result of the lock-exchange will be large. Also under relatively mild conditions forces will well exceed the formal levelling criteria (longitudinal: 38 ton and transversal: 23 ton). It was furthermore concluded that the largest forces during the lock-exchange do not always occur under extreme water level conditions. On the contrary, when water level heads are small, the density differences at the end of levelling are often the most extreme, since not much water is sluiced into the lock chamber during levelling. This means that the most severe lock-exchanges will occur at water levels that happen on a daily basis.

Furthermore, it is important to consider that the maximum force alone is not showing the complete picture. Also the moment in time at which this force occurs is important. It is therefore essential to also consider the development of the forces during lock exchange in relation to the operation in practice. The density current propagates relatively slowly and when the gate is opened the vessel will remain fully moored for only a short period.

Smaller vessel (The Flying Dutchman)

To investigate how the forces during the lock-exchange would change as a function of vessel size, also a smaller ship, *The Flying Dutchman* (see Table 2), was considered in the physical scale model. This type of vessel was of particular interest for the Pilots, since it is comparable to (relatively large) vessels that currently visit the IJmuiden North Lock.

For this vessel “pure” lock-exchange tests have been carried out, without prior levelling. Both lock-exchanges at the outer and the inner lock head have been tested. The water levels of the approach harbours corresponded to mean conditions, with NAP + 0 m for the outer approach harbour and NAP – 0.40 m for the inner approach harbour. The initial density difference over the active gate was around 16 kg/m^3. Two loading conditions of the vessel have been considered (loaded and in ballast), to investigate the influence of the draught of the vessel on the resulting forces. Table 6 shows the results of a selection of the performed tests.

When comparing the hydrodynamic forces that are measured on *The Flying Dutchman* and the *Breesaap* under similar hydrodynamic conditions, it was found that the forces on the smaller vessel are smaller than on the design vessel. The forces are still quite large however and exceed the formal criteria as defined for levelling (24 ton in longitudinal direction and 16 ton in transversal direction, see Section 3) also for this smaller vessel. Similar to the design vessel, the longitudinal forces are largest at the outer head and the transversal forces on the bow are largest at the inner head. For the outer head, it is shown that the forces due to the lock-exchange in loaded condition are larger than in ballast condition, which can be expected based on the larger blockage of the vessel, which is defined as the wet cross-sectional area of the vessel A_{vessel} divided by the wet cross-sectional area of the lock A_{lock}. For the lock-exchange at the inner head, this is not the case, since the maximum longitudinal force is largest in ballasted condition. The difference between transversal forces on the bow, which are the most relevant for this condition, is small for the two loading conditions.

Table 6: Maximum lock exchange forces on *the Flying Dutchman* in the new lock of IJmuiden

Test	Draught [m]	Initial density difference [kg/m^3]	Lock head	$Fl_{long,max}$ [ton] ([‰])	$F_{trans,\ max,\ bow}$ [ton] ([‰])	$F_{trans,\ max,\ aft}$ [ton] ([‰])
IJM1	14	16,5	Outer	69 (0.61)	28 (0.25)	49 (0.43)
IJM2	9	16,5		46 (0.68)	15 (0.23)	16 (0.24)
IJM3	14	16,2	Inner	29 (0.26)	49 (0.43)	36 (0.32)
IJM4	9	16,4		36 (0.54)	45 (0.68)	16 (0.24)

The results for both lock heads show that the lock-exchange behaves fundamentally different for both lock heads. This is related to the fact that after opening the gate the interface between fresh and salt water has a different vertical position. At the outer head, a salt water wedge enters the fresh lock-chamber over the bottom, while at the inner head a fresh water wedge enters the saltier lock chamber in the top of the water column. This is illustrated in Figure 6 and was already described by Vrijburcht, 1991.

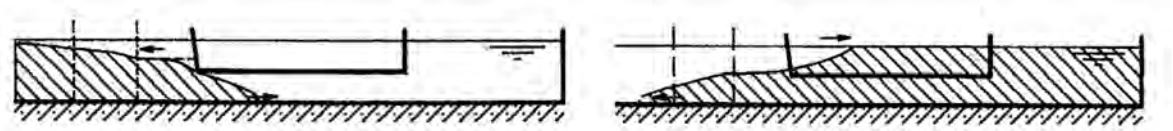

Figure 6: Schematised exchange process in a lock with initially fresh water (left) and initially salt water (right). Adapted from Vrijburcht (1991).

6.2 Terneuzen (physical scale model)

In the tests for the new lock of Terneuzen presented here, a different levelling system (openings in the lock gate) was considered than that will be actually built (longitudinal filling system with bottom grids). During the design process of the lock, design considerations changed as a result of the physical scale model study (see also Kortlever *et al*. 2018). The overall performance of the final levelling system will be verified in a new physical scale model study in the near future. The different levelling systems will lead to a different density distribution in the lock chamber at the end of levelling and this may thus lead to (small) differences during the lock-exchange. It is expected that the main conclusions presented here will still hold for the new levelling system that is now being designed. Note also that only lock-exchanges after filling the lock are affected by the changes in the design and not lock-exchanges after emptying.

For the new lock of Terneuzen mainly lock-exchanges at the inner head have been considered. Also some “pure” lock-exchange tests (without levelling) at the outer head have been performed, although this was a rather small dataset during a preliminary phase of the test campaign. The maximum forces during the lock-exchange are summarized in Table 7. The density difference in all tests was approximately 16 kg/m^3. Similar to the other datasets that are considered in this paper, the forces during the lock exchange are large and exceed the current criteria defined for levelling.

Table 7: Range of magnitudes of the maximum forces measured during lock-exchange for all tested conditions for the design vessel of the new lock of Terneuzen.

Outer head	
$F_{long,\ max}$	53 – 77 ton
$F_{trans,\ max,\ bow}$	28 – 32 ton
$F_{trans,\ max,\ aft}$	28 – 35 ton
Inner head	
$F_{long,\ max}$	28 – 49 ton
$F_{trans,\ max,\ bow}$	14 – 42 ton
$F_{trans,\ max,\ aft}$	6 – 27 ton

In the preliminary test campaign, during which the lock-exchange at the outer head has been studied, the maximum water level at the outer head could not be achieved due to height limitation of the model basin at that time. The maximum water level that then was considered was NAP + 1.23 m, while in the later test campaign, after adjustments to the test setup, water levels in the outer approach harbour up to NAP + 4.60 m have been considered. Since from all performed measurements it is concluded that lock-exchange forces generally increase with larger water depths, it is therefore expected that in reality forces at the outer head may even exceed the upper values mentioned Table 7.

6.3 IJmuiden North Lock (field measurements)

The results of the field measurement campaign can be used to relate the forces that are measured in the physical scale model for the new locks to the daily practice in the North Lock. The results of the field measurement campaign in the North Lock are presented in Table 8. The measured maximum longitudinal force $F_{long,max}$ ranges from 25 ton to 47 ton for lock-exchanges at the outer head. When the measured forces are expressed as a permillage of the displacement of the vessel, it ranges from 0.30 ‰ (Tectus) to 0.59 ‰ (Stena Premium). During the lock-exchange, the longitudinal forces exceed in the majority of the tests the typical force criteria for levelling, which are defined for the North Lock as 0.25 ‰ and 0.30 ‰ for 45,000 dwt and 90,000 dwt vessels respectively (Delft Hydraulics, 1983).

Table 8: Test conditions and results of the field measurement campaign in the North Lock.

Test no	Name vessel	Type	Loading condition	Wind direction and force	Length [m]	Beam [m]	Draught (aft) [m]	Draught (bow) [m]	Displacement [ton]	$F_{long,max}$ [ton]	$F_{long,max}$/Displ. [‰]
NO1	Stellata	Aframax	Loaded	NNW 2	238	42	13.9	13.9	117,573	43	0.37
NO2	Densa Crocodile	Aframax	Loaded	W 4/5	244	44	13.7	13.7	109,160	47	0.43
NO3	Dong-a-thetis	Aframax	Ballast	NNW 3	250	44	8.8	5.8	56,476	25	0.44
NO4	Tectus	Panamax	Loaded	WZW 3	228	32.2	14.1	14.1	84,300	25	0.30
NO5	Nave Atropos	Panamax	Loaded	NNW 1	225	32.2	12.8	12.8	77,083	30	0.39
NO6	Alpine Mary	Handysize	Loaded	ESE 2	183	32.2	11.7	11.7	51,212	25	0.49
NO7	Torm Carina	Handysize	Loaded	N 1	183	32.2	11.8	11.8	53,119	25	0.47
NO8	Stena premium	Handisize – wide	Loaded	W 2	183	40	10.4	10.4	58,965	35	0.59

Since the performed tests were not conducted under extreme conditions, it shows that in practice density induced forces during the lock-exchange will often be larger than during levelling. Furthermore it is shown that, since no large problems are encountered during daily operation, pilots are well capable of controlling the vessel under conditions in which current force criteria are exceeded. When the results for the different vessel types are considered, the following observations are made:

Aframax: The dimensions of the vessels in test NO1 and NO2 are similar and the measured value of $F_{long,\ max}$ is of the same order of magnitude for both tests, around 45 ton. This confirms reasonable repeatability given the large number of uncertainties related to the test setup. In test NO3 an Aframax tanker is considered in ballast condition and the longitudinal force decreases to 25 ton at this smaller draught.

Panamax: The Panamax size vessels are shorter and less wide than the Aframax size tankers. The measured forces for this vessel class are also significantly lower than for the Aframax class: 25 – 30 ton.

Handysize: Compared to the Panamax-type vessels, the length of the Handysize class vessel is much smaller, the draught is only slightly smaller and the beam is similar. The measured forces are similar to those found for the Panamax size vessels: 25 ton. Based on these results it is concluded that the length of a vessel is not a dominant factor for the longitudinal force during a lock-exchange.

Handysize-wide: The vessel that is considered in this class has same overall dimensions as in the Handysize class, but is significantly wider. The larger beam results in an increase of 10 ton for the maximum longitudinal force: 35 ton.

Based on comparisons of the measurement results for the different vessel classes, the most important factors related to the main dimensions of the vessels governing the magnitude of longitudinal forces during a lock-exchange can be identified: the draught of the vessel is important (Aframax loaded vs ballast conditions), the beam of the vessel is important (Handysize vs Handysize-wide) and length is of less importance (Panamax vs Handysize). These results confirm that the blockage of the wet cross-section is a dominant factor that determines the forces due to density driven currents. The relation between the measured forces and the blockage is illustrated in Figure 7, showing the results presented in Table 8 graphically.

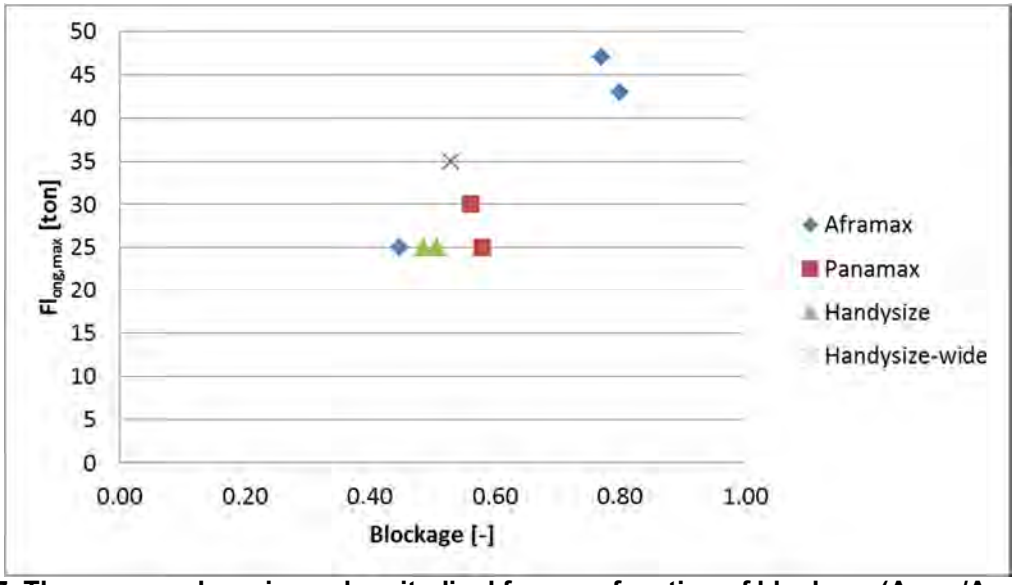

Figure 7: The measured maximum longitudinal force as function of blockage (A_{vessel}/A_{lock}).

Because in the scale model tests of the new locks of IJmuiden and Terneuzen a vessel (*The Flying Dutchman*) is considered that is comparable in size to an Aframax tanker, the results of tests NO1, NO2, and NO3 will be used to find a relation between the physical scale model measurements and the field measurements. This comparison provides insight in how much lock-exchange forces may change for these types of vessel in a larger lock.

7 COMPARISON OF DATASETS

When comparing the different datasets, the main challenge is that the tested conditions vary between the dataset. Not all tests have been conducted with the same density difference for example and often multiple parameters are varied at the same time, which makes inter- or extrapolation between the tests not straightforward. To allow for a fair comparison between the different locks, it is necessary to identify the dominant factors influencing the forces during a lock-exchange. This is possible using all measurement data, because the data sets are quite extensive and consider many hydraulic variations. Below the most important factors are identified that influence the water level slopes over the vessel during the lock-exchange.

- Density difference: a larger density difference over the gate at the moment that the gate opens will result in a stronger lock-exchange and higher forces on the vessel. The density difference will be influenced by the preceding levelling process, by meteorological circumstances, and to a certain extent also by previous lockages.
- Blockage: a larger blockage will generally result in a larger density difference over the length of the vessel, which leads to higher forces.
- Relative under keel clearance: the relative under keel clearance is defined as water depth divided by draught of the vessel. The more a vessel is positioned in the upper part of the water column, the larger the forces will be. Furthermore, a larger water depth will lead to a stronger lock-exchange and to larger forces.

- Transversal asymmetry: the magnitude of transversal forces will increase when the difference in density distribution on both sides of the vessel increases. This will be the case when transversal asymmetry, which is often related to the beam of the vessel, increases. When there is no asymmetry - e.g. a vessel is moored in the centerline of the lock- no transversal forces due to density differences will occur.

Most of these aspects are closely interrelated and they are sometimes counteracting each other. For example, a larger water depth will often go hand in hand with lower blockage ratios. As the one will generally lead to an increase and the other to a decrease of lock-exchange forces, it is often hard to predict on beforehand in what situation the largest forces will occur. By selecting individual tests from different datasets, in which only one parameter was varied these general trends could be identified. This is illustrated in Figure 8, in which tests are compared with the same density difference and blockage. The relative under keel clearance, dependent on water depth and draught, varied between the tests, showing larger forces for the tests in which the vessel was more located in the upper part of the water column (corresponding with a larger value of the relative under keel clearance). Note that the transversal asymmetry also varies between the tests (i.e. vessels with a different beam in the tests in North Lock and different lock widths for the tests with *The Flying Dutchman*), but this mainly influences the transversal forces and not the maximum longitudinal forces.

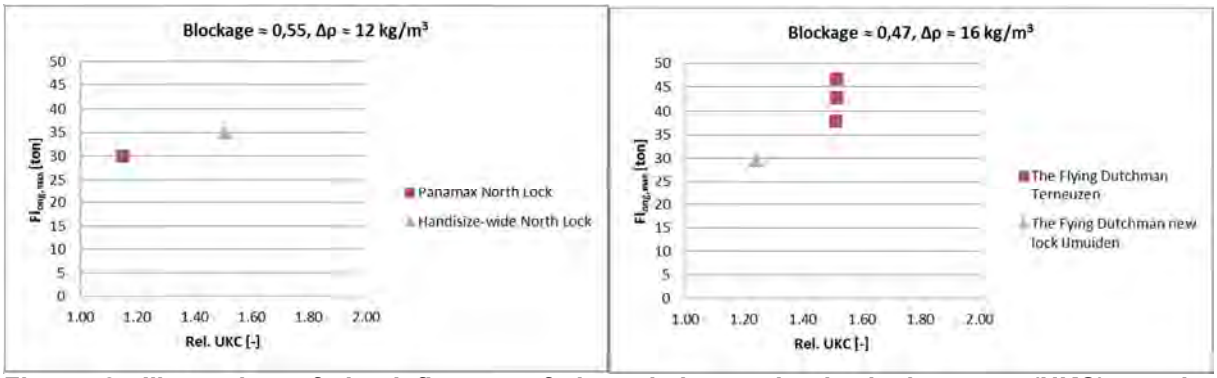

Figure 8: Illustration of the influence of the relative under keel clearance (UKC) on the maximum longitudinal force for test with similar density difference and blockage. Left panel: outer head tests in the North Lock of IJmuiden for two different vessels (field measurements). Right panel: inner head tests for two different locks with *The Flying Dutchman* (scale model measurements).

Taking into account the dependencies mentioned above, the datasets described above are compared and the main findings are summarized below:

In the North Lock, the measured longitudinal forces during the lock-exchange at the outer head exceed the formal force criteria for levelling for Aframax-size vessels by approximately a factor of two. For a similar size vessel in the new lock of IJmuiden the measured forces in the physical scale model were even higher. But it should be considered that in the physical scale measurements a homogeneous density difference of 16.5 kg/m^3 was present and the in the field measurements in the North Lock the density difference is estimated at 12 kg/m^3. When the results are corrected for this difference, it is likely that the longitudinal forces at the outer head will increase only lightly, by approximately 0 % - 20 %, in the new lock of IJmuiden under similar circumstances. The main reason for the relatively small force increase is that the blockage in the new lock is a factor 2 smaller than in the North Lock for the same ship, although the lock itself is much deeper. For the transversal forces at the outer head not enough information is available to make a good comparison between the North Lock and the new lock of IJmuiden.

When comparing the new lock of IJmuiden to the North Lock for inner head lock-exchanges, the two most important factors are also the larger water depth in the new lock and the smaller relative blockage due to the larger lock dimensions. From the results presented in Table 6 follows that, by comparing test IJM3 and IJM4 with different draughts, the influence of blockage is not as pronounced for the inner head as for the outer head. It is therefore assessed that the longitudinal forces in the new lock of IJmuiden will remain comparable to the North Lock for similar size vessels. The transversal forces will increase however, as a result of the increase in asymmetry due to the larger lock width.

For the design vessel of the new lock of IJmuiden, the lock-exchange forces will be larger than for the smaller Aframax-size vessels. The maximum forces will not increase exactly proportional to the displacement of the vessels (displacements differ by almost a factor 2), but the increase in forces will be a little smaller. It is expected that under similar conditions the lock-exchange forces on the design vessel will be one and a half times larger than on an Aframax-size vessel.

In the new lock of Terneuzen, larger longitudinal forces than in the new lock of IJmuiden can be expected for similar vessels. This is mainly due to the fact that the water depth in lock chamber is typically larger in Terneuzen than in IJmuiden, due to the higher level of the canal. As a result of the larger water depth, the lock exchange will be stronger. Transversal forces are comparable between the new lock of Terneuzen and IJmuiden, although the asymmetry will be larger in the new lock of IJmuiden.

The insights described above are summarized in Table 9. The situations for which it was not possible yet to give a good estimate of typical magnitudes of lock-exchange forces are indicated with a question mark.

Table 9: Relative comparison of the maximum forces during lock-exchange between the currently operational North Lock and the new locks of IJmuiden and Terneuzen.

Situation		Outer head		Inner Head	
		$F_{long,\ max}$	$F_{trans,\ max}$	$F_{long,\ max}$	$F_{trans,\ max}$
A	Aframax-size vessel in the North Lock	1	1	1	1
B	Aframax-size vessel in the new lock of IJmuiden	~1.1 x A	?	~A	> A
C	Design vessel in the new lock of IJmuiden	~1.5 x B	~1.5 x B	~1.5 x B	~1.5 x B
D	Design vessel in the new lock of Terneuzen	> B	~ B	> B	~ B

8 SUMMARY

The presented physical scale model studies and field measurements yielded new insights into the dominant factors that are important in lock-exchange processes of sea locks. The results of these studies have been used to determine requirements for lock operations for the future largest locks in the Netherlands, at IJmuiden and Terneuzen. The hydrodynamic forces that develop during a lock exchange process are influenced by many factors and it is therefore difficult to predict on beforehand in what situation the largest forces will occur.

It has been shown that hydrodynamic forces on a vessel during a lock-exchange will often exceed the forces during levelling. These larger forces can typically be coped with by operational measures, because the operation of unmooring and sailing out of the lock is different than line handling during the levelling process itself. However, in the design of new sea locks, one should be aware of the potentially large forces due to density currents when the gate opens and these lock-exchange effects should be studied as an integral part of the design of the lock.

After the results of the field measurement campaign and physical scale model results have been compared, it was concluded that in the future situation larger forces on vessels may be expected than currently experienced in the existing large sea locks. The results of the presented studies will help pilots to prepare on how to handle the larger vessels in the future largest locks in IJmuiden and in Terneuzen.

References

Delft Hydraulics, (1983). Noordersluis of IJmuiden, beknopt verslag onderzoek, R1759/M1859 (in Dutch).

W.C.D. Kortlever, A.J. van der Hout, T. O'Mahoney, A. de Loor, (2018). Engineering the Levelling Systems of the Sea Locks in The Netherlands; Taking into Account the Effects of the Density Difference, 34th PIANC world congress, Panama 2018, may 7-12.

T. O'Mahoney, A. Heinsbroek, A. de Loor, W.C.D. Kortlever (2018). Numerical simulations of two types of longitudinal filling system for the New Lock at Terneuzen, paper nr. 181, 34th PIANC world congress, Panama 2018, may 7-12.

H.I.S. Nogueira, P. van der Ven, T. O'Mahoney, A. de Loor, A.J. van der Hout and W.C.D. Kortlever (2018). Effect of Density Differences on the Forces Acting on a Moored Vessel While Operating Navigation Locks, Journal of Hydraulic Engineering, Volume 144, Issue 6 – June 2018, 10.1061/(ASCE)HY.1943-7900.0001445.

A.D. Schotman, (2017). Kolkuitwisseling in de Nieuwe Zeesluis: een gevaar of niet?, MSc. thesis Opleiding tot Registerloods (Master in Maritime Piloting), Stichting Opleiding en Deskundigheidsbevordering Registerloodsen (STODEL), 22 december 2017 (in Dutch).

A. Vrijburcht, (1991). Forces on ships in a navigation lock induced by stratified flows, Doctoral thesis Delft University of Technology, WL | Delft Hydraulics, publication nr. 448.

RENOVATION AND REDESIGN OF THE MALAMOCCO LOCK GATES IN THE VENETIAN LAGOON

by

dr. ir. Jeroen Hillewaere[1], dr. ir. Hendrik Blontrock[1], ir. Dieter Gevaert[1],
prof. Francesco Ossola[2], prof. Enrico Foti[3], Dario Berti[4] and Sara Lovisari[2]

ABSTRACT

As a part of the major storm surge barrier project to protect the Venetian lagoon from high tides, a large navigation lock was built at Malamocco, Italy. Only months after commissioning, the sea side lock gate was severely damaged during a storm in 2015. First, a thorough investigation of the damage phenomenon has been carried out to determine the physical phenomena causing damage to the lock gate. Afterwards design improvements regarding the layout of the lock gates have been developed. The efficiency of these design improvements was quantified by means of model scale testing. This paper focuses on the design improvements that can be made to avoid future damage to the lock gates. Finally, based on an extended risk and reliability analysis and in view of retaining the most cost-effective solution for the problem, the lock gates have been reviewed and if needed redesigned. A different approach for renovation and redesign is proposed for either gate of the Malamocco lock.

1 INTRODUCTION

To protect the Venetian lagoon as well as the iconic historic heritage of the city of Venice from flooding, the Italian government initiated the MOSE project (MOdulo Sperimentale Elettromeccanico; E: Experimental Electromechanical Module). Together with other measures, such as coastal reinforcement, raising of quaysides, etc., the MOSE project basically consists of storm surge barriers at the three large inlets to the Venetian lagoon: Lido (north and south), Malamocco and Chioggia, as shown in Figure 1a. Each barrier consists of an integrated system of rows of mobile flap gates as illustrated in Figure 1b. In case of forecasted *acqua alta* high tides, the mobile flap gates are raised to isolate the lagoon temporarily from the high storm surges on the Adriatic Sea.

To allow vessels to enter or leave the Venetian lagoon when the MOSE system is operational, navigation locks are constructed at each of the inlets. At Malamocco, the main access lock was constructed to guarantee the accessibility of the Port of Venice in Mestre for large ships during *acqua alta*, see Figure 1a. The ships intended to use the lock are tankers (up to approx. 70.000 DWT), bulk carriers (up to approx. 80.000 DWT), container ships (up to approx. 60.000 DWT) and RORO vessels (up to approx. 50.000 DWT). At present no passenger ships use the access channel to the port of Venice via the Malamocco inlet. At the Lido and Chioggia inlets, small locks are constructed inside service harbours to allow emergency vessels, fishing boats, etc. to shelter and transit.

The entire MOSE project was initiated by law (L.171/73) in 1981. The Consorzio Venezia Nuova (CVN) is responsible for the execution of the works and the subsequent maintenance and acts on behalf of the Italian Ministry of Infrastructure and Transport (Venice Water Authority). Construction, coordinated by CVN and

[1] SBE nv, Slachthuisstraat 71, BE-9100 Sint-Niklaas, Belgium, +32 3 777 95 19
www.sbe.be (jeroen.hillewaere@sbe.be; hendrik.blontrock@sbe.be; dieter.gevaert@sbe.be)
[2] Consorzio Venezia Nuova, Arsenale Nord, Castello 2737/f, 30122 Venezia, Italy, +39 041 5293511
[3] Università degli Studi di Catania, DICA, Via S. Sofia 64, 95123 Catania, Italy, +39 095 7382713
[4] COMAR, Costruzioni Mose Arsenale scarl, Sestiere Castello 2737/f, 30122 Venezia, Italy, + 39 041 2708434

executed by COMAR, began simultaneously in 2003 at all three lagoon inlets. At present, the construction works are still underway and the primary line of defense of the MOSE system is expected to be finished by the end of 2019.

The Malamocco lock was finished and operational in the course of 2014 as the lock was intended to be used as access channel to the lagoon during the installation works of the barrier flap gates at Malamocco. Only months after commissioning, however, the sea side lock gate was severely damaged during a storm. This paper focuses on the damage phenomenon and how the lock and the gates have been adapted to avoid future damage.

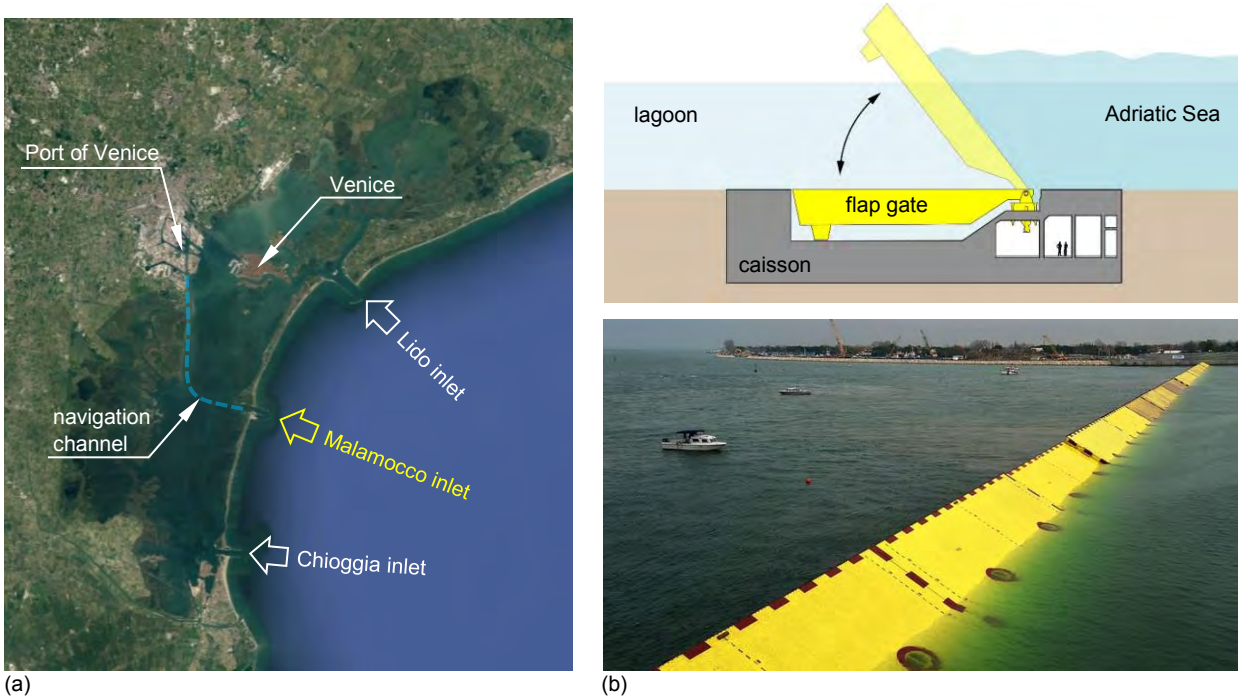

Figure 1: (a) Overview of the Venice lagoon and the MOSE system locations. (b) Design principle and picture of the mobile flap gates of the MOSE storm surge barrier.

2 THE MALAMOCCO LOCK AND THE DAMAGE

2.1 Original design of the lock

With a length of 380m, a width of 50.5m and a sill level at -14mIGM1942, the navigation lock at the Malamocco inlet is the largest lock in the MOSE system. As shown in Figure 2, the lock is equipped with two identical sliding gates, one at the lagoon side and one at the sea side. No redundant lock gates are foreseen.

The original lock gates were designed as sliding gates supported on two hydrofeet. As shown in Figure 3, a hydrofoot consists of a removable supporting tube in the lock gate with a horizontal bearing at the bottom. The hydrofeet are supported on a UHMWPE sliding track on the bottom of the lock. Whenever the lock gate is moving, pressurized water is pumped through small nozzles in the bearing plate of the hydrofoot, creating a thin water film beneath the hydrofoot and reducing the friction between the hydrofeet and the sliding track. A couple of pictures of the sliding track and the hydrofeet of the existing lock gate are shown in Figure 4.

The lock gates are 54.3m long and 16.5m high. The total weight of the lock gate with all technical equipment is around 1300 tonnes. The lock gate is designed with a ballast chamber that allows adjustment of the operational net weight of the lock gate and manipulation of the lock gate in floating position.

(a)

(b)

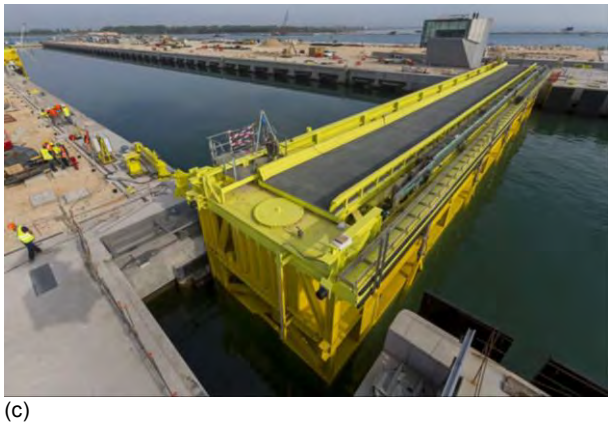

(c)

Figure 2: (a) Overview of the Malamocco inlet & lock. (b) Aerial photo of the Malamocco lock. (c) Overview of the existing sea side lock gate during installation.

The choice for the net operational weight of the existing lock gate is defined by the nominal bearing capacity of the hydrofoot system. The bearing capacity of one hydrofoot varies between a minimum of 100kN and a maximum of 1350kN in the existing design. The net operational weight of the lock gate varies between these limits with changing water levels because the technical rooms located at the top of the lock gate act as supplementary buoyancy chambers with varying water levels, as shown in Figure 3. As a result, the static reaction force of the ballasted lock gate on the hydrofeet may not exceed 1250kN per hydrofoot at the lowest water level (-1.0mIGM1942) and 180kN at the highest design water level (+2.7mIGM1942). Furthermore, as a result of variations in hydrofeet forces during motion of the lock gate, the maximum bearing capacity is reduced further. When the gate is moving, the traction force causes an increase of the vertical reaction on one hydrofoot and a decrease of the vertical reaction on the other hydrofoot.

In the existing lock gates, skin plating is only foreseen on one side of the lock gate. This is because the lock gates at Malamocco will only be operational at exceptional *acqua alta* high tides. Therefore, only skin plating is foreseen at the lagoon side of both lock gates, leaving the internal structure of the lock gates open on the sea side.

Filling and emptying of the lock chamber occurs through the lock gates, via 10 levelling tubes located at the bottom of the gate structure. The opening and closing of the horizontal levelling tubes is operated hydraulically with vertically operated sliding valves, located at the sea side of the lock gate. On top of the lock gate, a road platform is foreseen to allow traffic and pedestrians to cross the lock chamber. At both ends of the road platform, movable platforms are foreseen that are operated hydraulically as well.

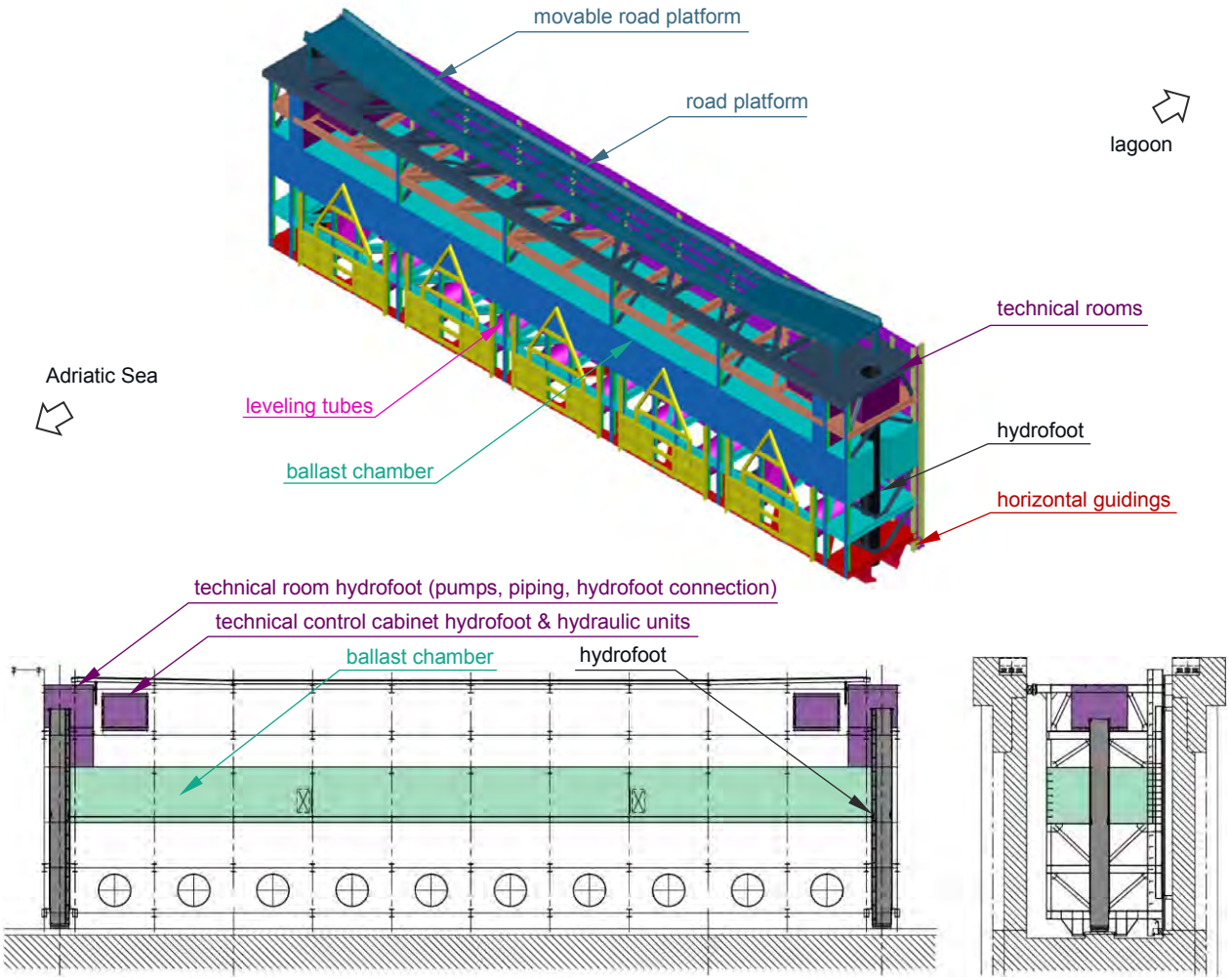

Figure 3: Schematical 3D model & cross sections of the existing lock gates.

(a) (b)

Figure 4: (a) Sliding track during construction. (b) Hydrofoot extracted from the existing lock gate.

2.2 Damage and problem description

The existing sea side gate suffered severe damage during a nocturnal storm on the Adriatic Sea on the 5-6th February 2015. This damage was caused by vertical uplift forces on the lock gate. Subsequent lifting and falling of the lock gate on the sliding track caused damage at several points. Damage was inflicted on the guiding structures of the lock gate but more importantly, the lifting and falling of the hydrofoot bearings on the sliding track led to failure of bolted connections between the inner and the fixed outer hydrofoot tubes. These bolted connections were located in the technical spaces at the top of the lock gate, see Figure 3, where the pumps, filters and control equipment of the hydrofoot system were located. The bolted connection is an integral part of the water tightness system of the hydrofeet, the failure of the bolted connections led to flooding of these technical spaces and put the lock gate out of service.

The cause of the damage being unknown at that time, precautionary measures were taken by CVN and COMAR to avoid any further damage to the lock gates. Both gates were pulled into the gate recesses to avoid direct attack of waves on the lock gates. Additionally, the gates were ballasted with water filled bags to increase the net weight of the lock gates.

3 INVESTIGATION OF THE DAMAGE PHENOMENON

After a full inventory of the suffered damage and some preliminary studies, a.o. Grasso et al. (2015) and Volpato et al. (2015), CVN appointed SBE to carry out a full investigation of the damage phenomenon and to propose design solutions for both the sea side and lagoon side lock gates. SBE is an engineering consultant situated in Belgium with more than 25 years of experience. It is internationally renowned for the engineering design of some of the largest locks in the world, a.o. in the Port of Antwerp in Belgium, in the Netherlands, in Panama, etc.

One of the primary tasks in this investigation was to determine the wave climate in front of the lock gate at the time of the incident, since no wave monitoring devices were present in the Adriatic approach harbour at that time. A numeric study was therefore carried out, cf. Reijmerink et al. (2016), to reverse engineer the incident wave conditions based on available offshore data. Additional goals of this study were to confirm the results of the original wave study on which the design of the existing lock gates was based and to study wave penetration in the lock chamber when the sea side gate is in the gate recess. Additionally, wave amplifications originating from reflections off the temporary island were studied in detail, because this temporary situation was not considered in the original wave study and hence not taken into account for the design of the existing lock gates.

Based on all available studies and based on the inspection of the damaged lock gate, several critical aspects were identified to be at the origin of the failure of the sea side lock gate at Malamocco. A full account of the investigation leading to this conclusion is not within the scope of this paper. Only the main conclusions with respect to the design of the lock gates are therefore summarized in the following.

The first critical cause is related to the specific properties of the incident waves attacking the lock gates. This issue is particularly acute for the Malamocco lock gate given the **long wave periods** found at this location. The wave study by Reijmerink et al. (2016) reconfirmed that the wave period may be as high as approx. 10 to 12s under normative storm conditions at the lock location. For wave periods of this magnitude, the wave length could be in the order of 100-150m. Given that this is much longer than the width of the entire gate, the gate will feel either a peak or a trough over its whole width. Furthermore, the dynamic wave pressures resulting from long wave periods penetrate deep enough to cause significant alternating uplift and downlift forces on the ballast tank of the lock gate. For shorter waves with a wave period of e.g. 4s and corresponding wave lengths of the order of meters, there will usually be a peak and a trough across the width of the gate, averaging to smaller net vertical forces. Additionally, the dynamic wave pressures decrease much faster with depth for shorter wave periods and the pressures may not penetrate deep enough to cause fluctuating vertical forces.

A second critical factor is the **ballast and open volumes** in the gate. The positioning of the technical rooms that house the hydrofoot technical equipment at the top of the lock gates, see Figure 3, and to a lesser extent the hollow box girder beam for lateral guiding of the gate are very unfortunate. These components are not below the water level at all times and therefore unintentionally act as supplementary buoyancy chambers for the lock gate. As a result, with changing water levels, e.g. under long wave impact, the net operational weight of the gate will fluctuate, even if the ballasting condition of the lock gate is kept fixed.

Third, it is unsure what the actual **ballasting condition of the lock gate** was at the time of the incident. It is not unlikely that the net weight of the lock gate was insufficient at the time of the incident. Because there is no weight monitoring system in the existing lock gates, it is impossible to tell at any specific time what the net operational weight of the lock gate is.

Finally, it should be mentioned that there was **no hydraulic head** acting on the lock gate during the storm. Since the MOSE system is not yet operational, the water levels in the Adriatic Sea and the lagoon were the same at the time of the incident. The lock gate was hence not pressed against its sealings and no resisting frictional forces were present.

4 DESIGN IMPROVEMENTS

It is believed that the combination of the aspects listed in the previous section have led to the failure of the sea side lock gate at Malamocco. Based on the understanding of these physical phenomena, structural adaptations and design improvements have been proposed to alleviate the effect of fluctuating vertical forces, as listed below. Some of these improvements are obvious and need no further confirmation while others require elaboration to quantify the efficiency of the proposed measures.

(I) Elimination of the technical spaces between the lowest and highest design water levels

It needs no further clarification that the net operational weight of the lock gate should at all times be under control and not subject to water level variations and by extension wave action. Therefore, in the new design, all ballast compartments and technical spaces should be moved below the lowest design water level, taking into account wave action.

(II) Perforation of the ballast tank

To minimize pressure differences above and below the ballast tank, perforation tubes may be foreseen in the ballast tank so that excess pressures may be alleviated by flow through these tubes. The size of these perforation tubes should be verified to quantify the efficiency of this design adaptation.

(III) Reduction of wave penetration into the lock gate (sea side skin plate, etc.)

Closing off the seaside of the lock gate should reduce the penetration of pressures into the gate structure. As the penetration is reduced, the pressure differences below and above the ballast tank as well as the resulting uplift forces should decrease as well. It should be noted however that even a small gap is sufficient to allow pressure penetration of pressure into the gate. The smaller the gaps however, the larger the pressure losses through these gaps, and the smaller the resulting uplift forces.

To quantify design improvements (II) and (III), both a numerical study (Pancham et al., 2016) and a physical model test campaign (Lena et al., 2016) have been performed in the framework of this study. In these studies multiple different configurations have been considered. In this report, the following configurations are reported, see also Figure 9:

(1) The basic lock gate configuration similar to the existing design but with lowered ballast compartment according to improvement (I);
(2) Similar to configuration 1, with added skin plate at the sea side;
(3) Similar to configuration 2, with perforation of the ballast tank;
(4) Similar to configuration 3, with smaller gap at the lock floor;

(5) Similar to configuration 4, with smaller gaps at the lateral sides of the lock gate. Since the gate recess is much wider than the lock gate itself, see also Figure 2c, the gap between the gate and the civil works is considerable and the effect of closing it off should be studied. This alternative is only relevant in a 3D testing environment.

4.1 Numeric sensitivity analysis

The numerical study consisted of 2D CFD simulations for configurations 1 to 4. Because of the 2D character of these simulations, configuration 5 could not be considered due to its inherent 3D character. In fact, configuration 5 could therefore be considered identical to configuration 4 in a 2D schematization. The numerical model used for the simulations was the open-source, general-purpose CFD-toolbox OpenFoam using the wave generation and absorption toolbox waves2Foam (Jacobsen et al., 2012).

For each configuration, the mean peak vertical forces were determined and compared for several sets of regular wave conditions, as discussed in detail in Pancham et al. (2016). The wave conditions considered were artificially determined in the framework of a sensitivity analysis. This way, the effect of wave conditions and the efficiency of the proposed design optimizations could be assessed.

From the simulations, the vertical net force on the lock gate is found to decrease from configuration 1 to 4, with additional design improvements being made. For normative wave conditions (wave period in the order of 10.0s), the peak vertical forces in configuration 4 are up to 70% lower than in configuration 1. The simulations also show that the vertical forces increase with increasing wave period, increasing wave height and decreasing water level. This is all the result of larger pressure variations at the gap between the bottom of the skin plate and the lock floor.

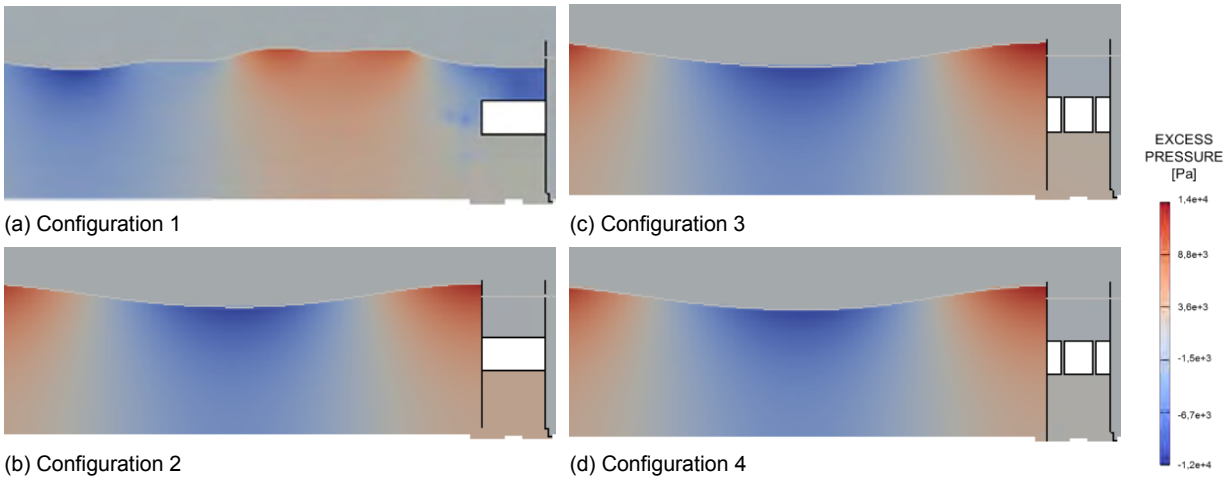

Figure 5: Excess pressure plots for configurations 1 to 4, determined by means of 2D CFD simulations (Pancham et al., 2016)

The simulations allow to assess and compare the pressure fields in the different configurations as well. In Figure 5, the excess pressure field is shown for configurations 1 to 4 at one time frame with resulting uplift forces for illustration. The excess pressure shown in these plots is defined as the pressure in excess of the hydrostatic pressure, i.e. the wave-induced pressure field. It can be observed for configuration 1 that large wave-induced pressure differences occur above and below the ballast tank as the wave impacts and penetrates the gate structure. This results in large alternating vertical forces on the lock gate. The addition of a skin plate in configuration 2 decouples the pressure on top of the buoyancy chamber from the wave-induced pressure. However, this is not sufficient to significantly reduce the vertical force acting on the gate due to wave action underneath the buoyancy chamber. The subsequent addition of vertical tubes in the buoyancy chamber in configuration 3 significantly reduces the vertical force on the gate. Finally, the vertical

forces are reduced even further by making the gap between the sea side skin plate and the lock floor smaller. The smaller the cross sectional area ratio (smaller height of the gap), the smaller the vertical force will be on the lock gate, because the pressure difference on the ballast tank and through the vertical tubes will decrease along with a decrease in the mass flux through the gap at the bottom, in and out of the gate.

In conclusion, the 2D CFD simulations confirm the physical phenomena taking place as presented in section 3 and qualitatively establish confidence in the proposed design optimizations. However, there are a couple of important limitations:

- No 3D effects are taken into account. This leads to simplifications on many points: the importance of the lateral gaps (cf. configuration 5) cannot be quantified; the perforation of the ballast tank is schematized as an equivalent 2D area ratio; the effect of the lock gate in opened position cannot be quantified, the net forces are based on extrapolations from values 'per running meter', etc.
- No irregular waves have been considered in the 2D CFD simulations.
- At the highest water levels, wave overtopping of the gate occurs. Because of the 2D character of the simulations, this leads to inaccurate results for configuration 2 and to a lesser extent configurations 3 and 4 as well, as the water that is captured in the gate structure above the ballast tank cannot drain towards the recesses, etc. Additionally, the overtopping waves may influence the pressure distribution as well.

4.2 Model scale tests

To study the effects that could not be studied in the 2D CFD simulations and to determine actual design loads, physical scale model tests have been performed in the shallow water basin of the MARIN research facilities in the Netherlands (Lena et al., 2016). The scale model tests were performed on a simplified wooden model of the lock gate at a geometrical scale of 1:20. Based on previous investigations, the model was simplified to the main components that influence the wave induced vertical forces, i.e. the ballast compartment, skin plating, filling/emptying tubes, etc. The complex inner structural supports and stiffeners in the lock gate were not modelled to scale and to six square frames above and below the ballast tank to give the requested rigidity to the model.

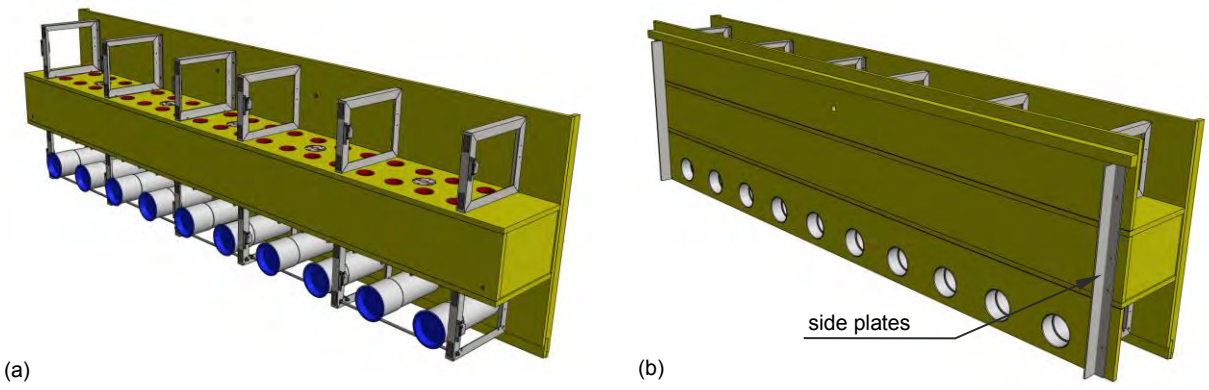

Figure 6: 3D rendering of the modular scale model in configuration 1 (a) and configuration 5 (b).

As illustrated in Figure 8, the scale model was rigidly connected to a six component frame in order to directly measure the wave induced forces and moments in six degrees of freedom. The recesses of the gate and the geometry of the lock floor were modelled as well, in order to properly reproduce the water flow around the gate.

Based on the 2D CFD study, it was concluded that the size of the gaps between the gate structure and the recesses has a major influence on the reduction of the vertical forces. However, in the model scale setup, special attention had to be paid to avoid any connection or accidental contact between the gate structure

and the recesses that could affect or invalidate the force measurements. The setup was designed so that a minimum distance of 5mm would be respected in all the gaps. This distance was considered safe in order to compensate for any deformations of the setup when subjected to the highest wave loads and to avoid any contacts. At the same time, this introduces some inaccuracies in the model set-up as well, since the gaps will be significantly smaller in reality. Based on the results of the 2D CFD simulations, this simplification is deemed conservative as forces are expected to decrease with smaller gaps.

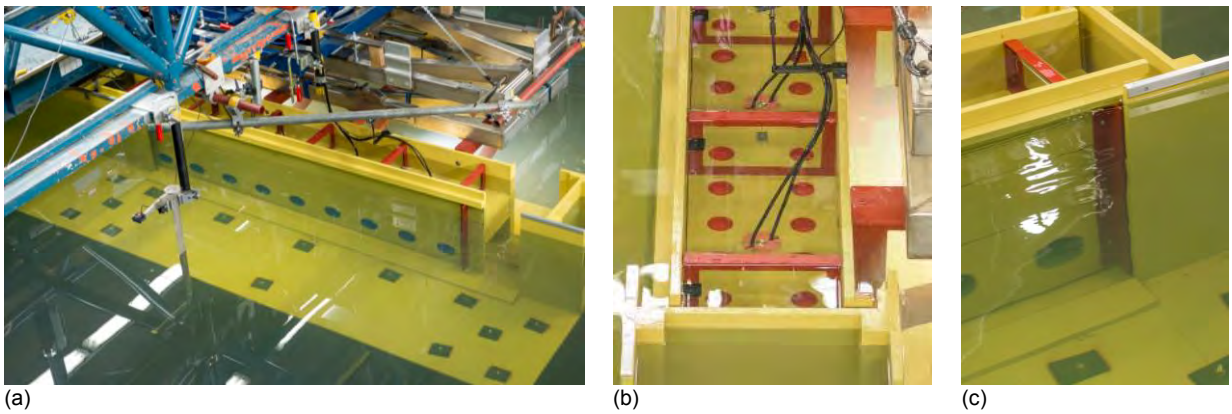

(a) (b) (c)

Figure 7: (a) Overal view of the test setup. (b) Side top view of the scale model in the basin; the plastic caps to close off the vertical tubes are visible; pressure sensors were installed on the top and botttom of the ballast tank as well to validate the force measurements. (c) Side plating to close of the gate recesses.

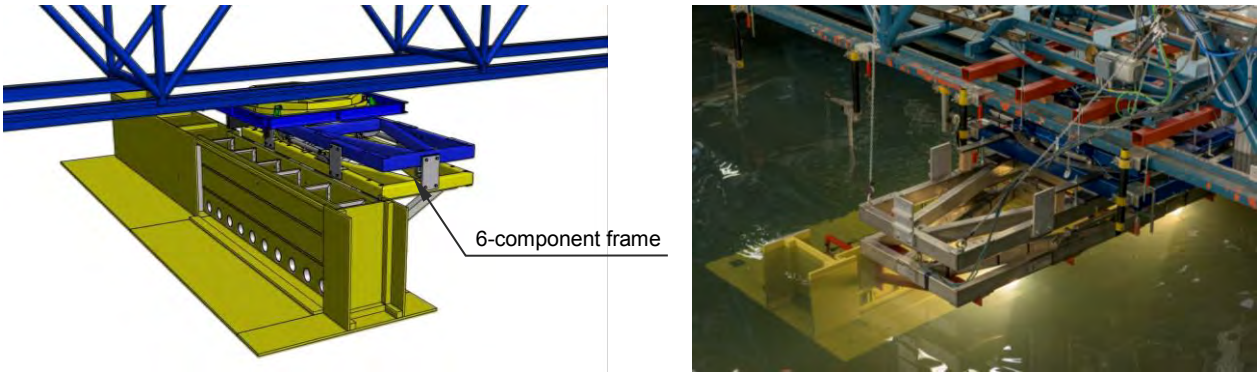

Figure 8: 3D rendering of the six component frame attached to the scale model & picture of the setup in the test basin.

In the scale model tests, only normative wave conditions have been considered. Based on the meteomarine wave studies, a.o. Reijmerink et al. (2016), the normative wave conditions are related to the two principal wind directions in the area: Bora conditions (60°N) with very intense winds but shorter fetch lengths and Scirocco conditions (140°N) with very long fetch lengths across the deep waters of the central Adriatic Sea and limited effects of shoaling. Both conditions result in reasonably large wave periods (in the order of 10–12s).

In the wave study of Reijmerink et al. (2016), it was concluded that the wave climate in front of the lock gate was very disperse as a result of reflections in the approach harbours and no preferential wave direction could be determined. Therefore, the most conservative situation with irregular waves approaching the lock gate perpendicularly have been tested in the scale model tests.

In Figure 9, the results of the scale model tests for four normative wave conditions (Bora/Scirocco at high/low water level) are shown and compared with the numerical results of the 2D CFD simulations (Pancham et al., 2016).

During the first series of tests at high water levels, it was observed that the uplift forces increased in configuration 2 before decreasing again in configurations 3 to 5. The reason that configuration 2 yields worse results than configuration 1 is attributed to 3D effects in the scale model tests. Also, the effect of wave overtopping may play a part in this behaviour. In any case, configuration 2 was omitted in the second series of tests at lower water level because it was clear that the perforation of the ballast tank has a major impact on the vertical forces on the lock gate.

For configuration 1 a large variability of the vertical forces is observed depending on the incident wave conditions. For the geometries where significant structural changes have been undertaken (e.g. configuration 5), the vertical forces are much less dependent on external factors and the vertical forces are in a much smaller range. The smaller the range, the more predictable the vertical forces become, independently of the applied wave conditions.

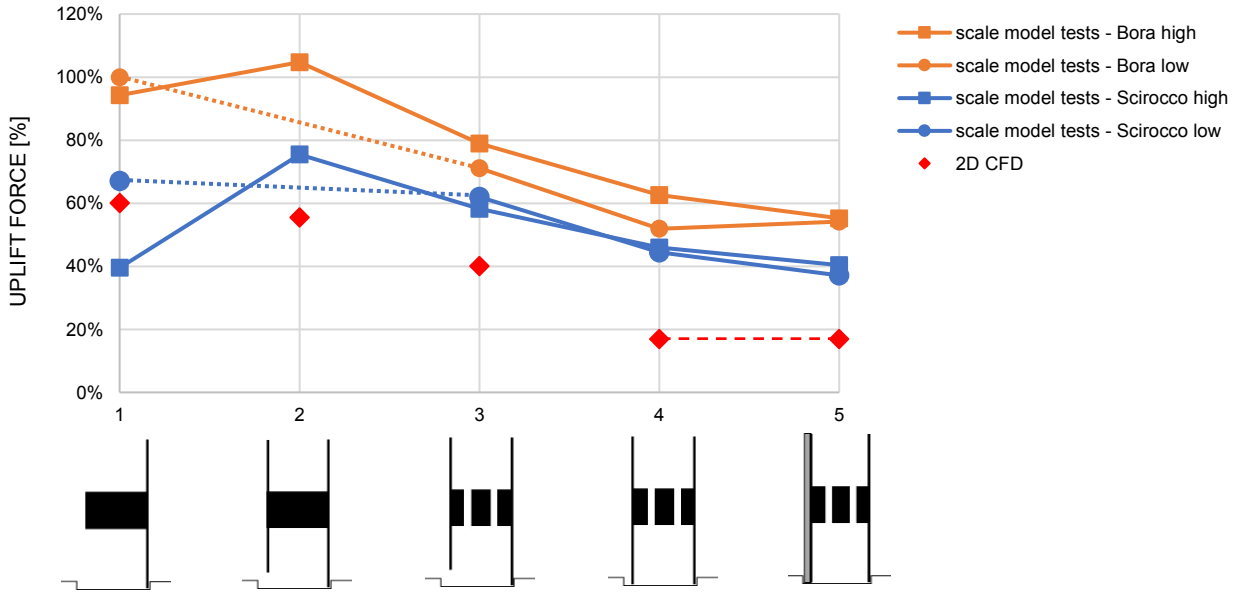

Figure 9: Comparison of peak uplift forces from scale model tests (Lena et al., 2016) and from 2D simulations (Pancham et al., 2016); values are scaled w.r.t. the largest force in configuration 1.

The comparison between the scale model tests and the results of the numerical sensitivity analysis should not be expected to yield identical results. The results cannot match for several reasons: different wave conditions were considered (wave height, wave period, regular vs. irregular), 2D vs. 3D effects are taken into account, etc. In general, the numerically predicted forces are much smaller than the forces determined through scale model testing and the efficiency of the design optimizations is also larger in the numerical simulations. The latter is most likely related to the fact that the gap between the lock gate and the lock chamber is much smaller in the numerical simulations (configuration 4) than in the scale model tests. As discussed this is one of the deficiencies of the scale model tests to avoid inaccurate results.

Nevertheless, it is interesting to observe that a similar trend can be observed for both the numerical and the scale model test approaches. The subsequent measures (skin plate, perforation, closing the gaps) result in a gradual optimization of the original design. The scale model tests also illustrate that closing off the lateral gaps towards the gate recesses (cf. Figure 7c) results in a further decrease of the vertical forces.

Concluding, it is clear that configuration 5 yields the best improvement of the layout of the gate in view of vertical force reduction. The vertical uplift forces are reduced by up to 40%. Also, the vertical force becomes more predictable in the sense that the variability of the peak vertical forces in different wave conditions is much smaller for configuration 5 when compared to configuration 1.

5 RENOVATION AND REDESIGN OF THE MALAMOCCO LOCK GATES

Aiming at a safe design for the Malamocco lock gates for the future, both the existing sea side gate and the lagoon side gate have to be adapted. However, a substantially different solution is considered for both gates based on different operational conditions of the gates as outlined in the following.

5.1 Renovation principles

Resulting from an extensive risk analysis and aiming at a safe design solutions for both lock gates, a substantially different solution has been selected for either gate. The current differentiated approach is aimed at providing reliable solutions for both gates in the most cost-effective way.

Since the **sea side lock gate** is part of the primary line of defense of the MOSE system, a safe and reliable solution is required under all conditions. In this light, the sea side lock gate had to be entirely redesigned from scratch. The redesign of the sea side lock gate consisted of a dual solution where the design optimizations discussed in section 4 are implemented on the one hand and the net operational weight of the lock gate is increased on the other hand. The redesign of the new sea side lock gate is described in detail in the next section 5.2.

From a reliability-safety point of view, the operational conditions of the **lagoon side lock gate** are very different from the sea side gate. Indeed, by imposing that the sea side lock gate must always be in the closed position during operation of the lagoon side gate, the direct influence of the wave climate from the Adriatic Sea on the lagoon side lock gate can be eliminated as illustrated in Figure 10. Wave actions on the lagoon side lock gate while moving are therefore only wind-driven and determined by a relatively short fetch length; in this case the length of the lock chamber. A smaller wave period (2.0 to 3.5 s) and a smaller wave height may be therefore be expected to act on the lagoon side gate during operation.

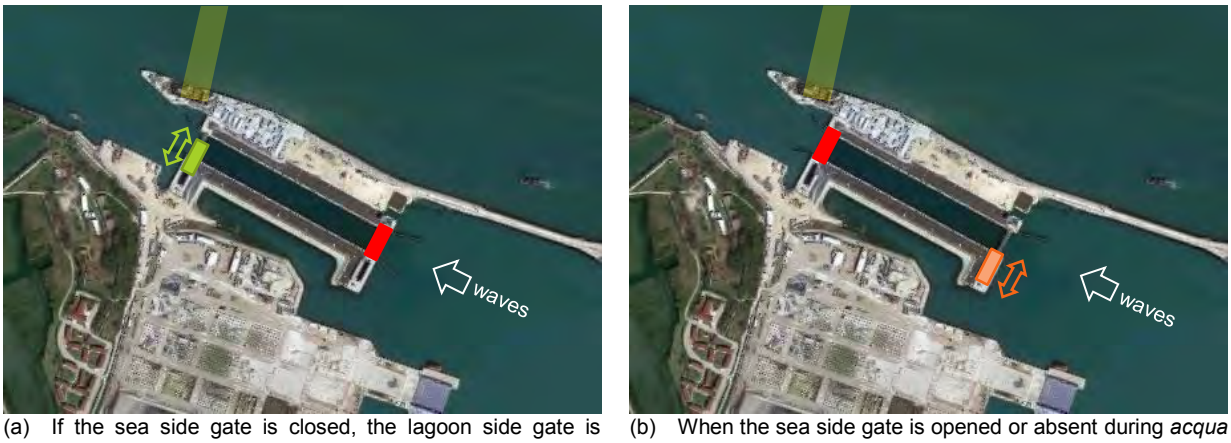

(a) If the sea side gate is closed, the lagoon side gate is protected and can be operated

(b) When the sea side gate is opened or absent during *acqua alta*, the lagoon side gate must be closed and anchored.

Figure 10: Operational principle for the lagoon side gate.

Because the lagoon side gate was not damaged during the storm and in view of cost-effectiveness, it was decided to retain the existing design of the lagoon side gate with some important design changes.

The first major design change comprises the addition of a mechanical anchorage system on the gate. This anchorage system should provide the necessary resistance against uplift forces from wave action in the

situations that waves originating from the Adriatic Sea can reach the lagoon side gate, i.e. when the sea side gate is in open position or away for maintenance. In these situations, the lagoon side gate must be closed and in anchored position. The restrictions on the operation of the lagoon side lock gate are incorporated in the newly designed control system of the entire lock complex.

In the light of reliability and safety, this approach is acceptable because the likelihood of an extreme event in combination with one of the above scenarios is much smaller and measures can be taken to avoid or limit the occurrence of such events. The sea side gate should e.g. not be taken out for maintenance in a season when high waters and storms are likely to occur. In the unlikely event that such a situation would nevertheless occur, additional safety measures are available, e.g. the complete filling of the ballast chambers of the lagoon side gate to increase the net weight of the gate as much as possible. This is an emergency measure that takes time and costs money and should therefore not be considered in a primary line of defense.

In the existing lock gate, however, there is no weight monitoring system available. This is the second design change that was made to the lagoon side gate. At the top of the hydrofoot tubes, several structural changes are made to install a direct force measurement load cell. By incorporating this weight monitoring system in the control system of the lock complex, a warning alert can be programmed whenever the net weight of the gate becomes too low for the predicted sea conditions. Addtionally, the connection of the inner and outer tubes of the hydrofoot system is relocated outside the technical rooms.

5.2 Redesign of the sea side lock gate

While the lagoon side gate is in the secondary line of defense and sufficient safety measures can be installed to allow small design modifications, this is not the case for the sea side lock gate. The sea side lock gate is part of the primary line of defense of the MOSE system and a safe and reliable solution is required, under all conditions, at all times. To achieve this, it was decided to design a completely new sea side lock gate, based on the design optimizations as discussed in the previous sections.

Besides the qualitative approach in the discussion of the paper until now, the design value of the uplift forces can be determined based on the scale model test results. The design value is found by applying a safety factor on the maximal peak value of the uplift forces from the tests. The safety factor was determined through a statistical safety analysis allowing for a 1% exceeding probability and accounts for all measuring uncertainties (repeatability of the measurements, corrections for static force measurements, etc.) and modeling uncertainties (wave condition variability, modeling simplifications, scaling deficiencies, etc.).

Although the design optimizations result in a significant reduction, the design value of the vertical uplift force was found to remain fairly high. In this light, a dual solution was developed for the design of the new lock gate. On the one hand, all design optimizations (I, II and III) as discussed in section 4 were implemented to reduce the vertical uplift forces due to wave action. An overview of the eventual design of the lock gate with these structural changes is shown in Figure 11. On the other hand, the resistance of the lock gate to vertical uplift forces had to be increased. The latter can only be achieved by increasing the net operational weight of the lock gate.

As discussed in section 2.1, however, the support system of the existing lock gates is based on two hydrofeet, sliding along a sliding track on the lock floor. Hydrofeet have a limited bearing capacity however, which would largely be exceeded by increasing the weight of the lock gate. Therefore doubled or tripled hydrofoot support would be required to allow motion of the lock gate but there are many practical and technical objections to such a proposal. Above all, the supporting technical equipment that should also be tripled in such a scenario must be relocated into the ballast chamber of the lock gate to comply with design improvement (I). Doing so, the net operational weight of the gate is decreased to the point that the weight becomes insufficient to resist the vertical uplift forces, which is unacceptable.

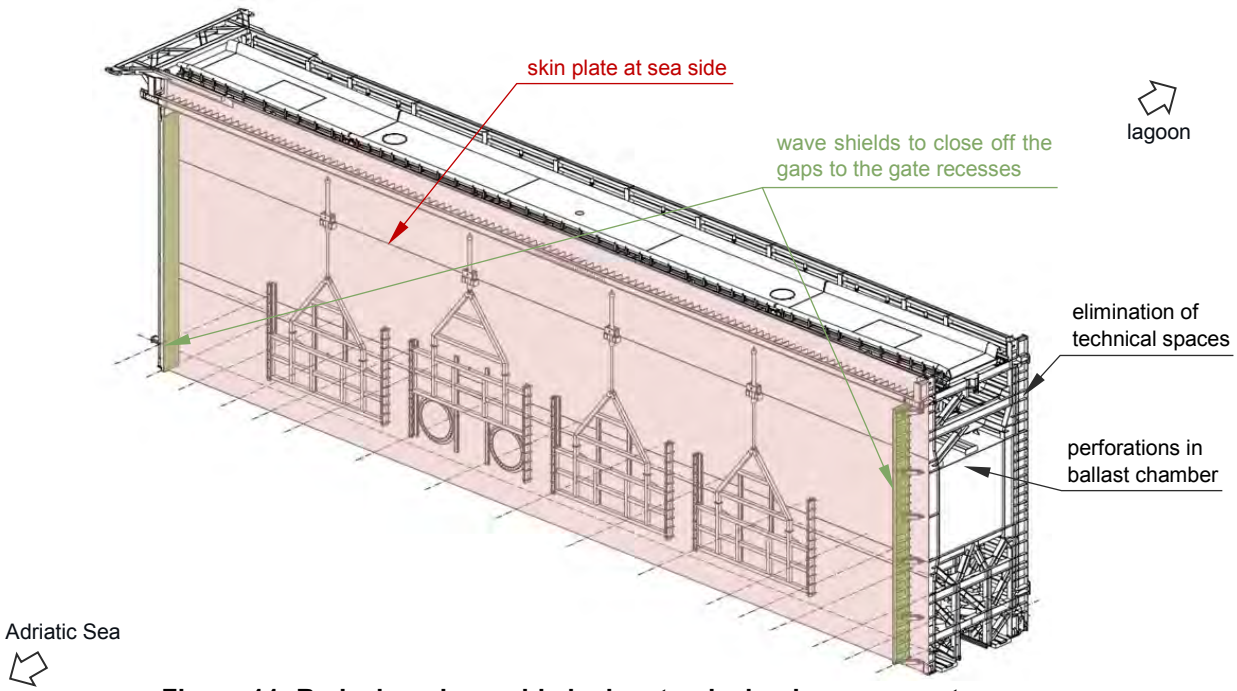

Figure 11: Redesigned sea side lock gate: design improvements.

Taking into account all technical and practical objections and given that a robust and reliable solution is required for the sea side lock gate, an alternative supporting system has been proposed: the redesigned lock gate will be supported on two lower rolling wagons instead of hydrofeet. The rolling wagons can be designed for much higher bearing capacities and by using two lower rolling wagons, it is possible to fit the new design within the existing civil structures. There are some important changes in the design of the lock gate itself as well as changes that have to be made to the existing civil works of the lock complex to achieve such a design.

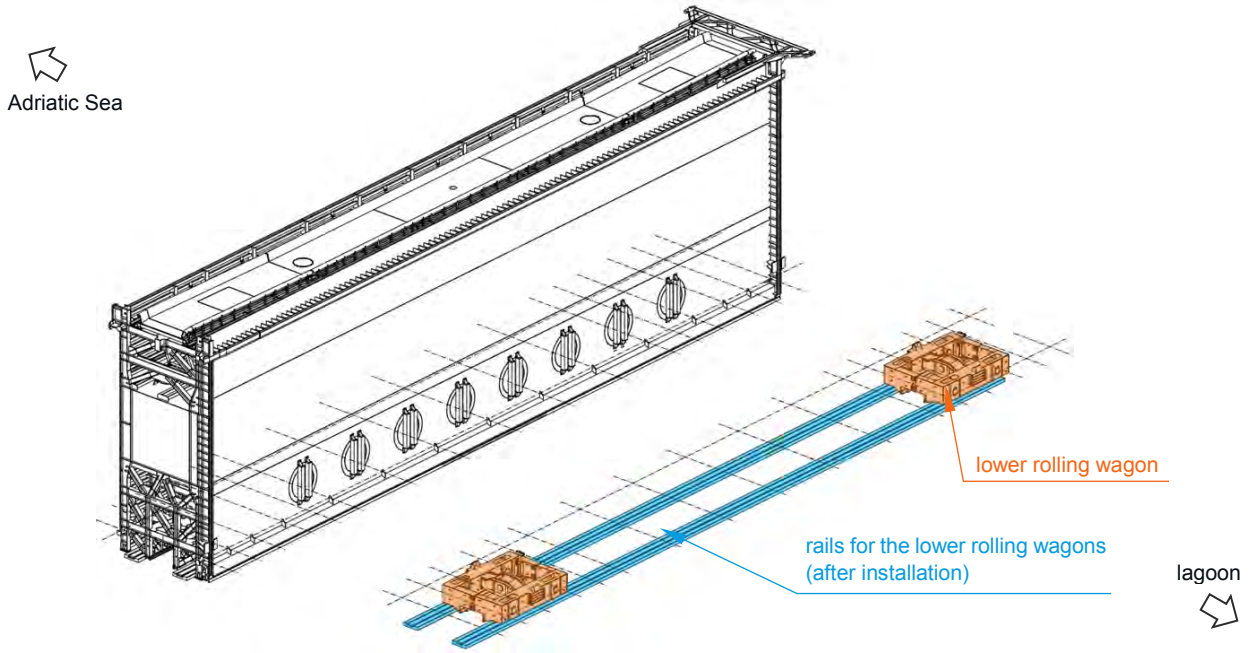

Figure 12: Redesigned sea side lock gate: lower rolling wagons & rail system.

First of all, a rail system needs to be installed at the bottom of the gate recess and the lock chamber. The overall geometry of the rails and the rolling wagons is shown in Figure 12. The presence of the sliding track (see Figure 4a) is both an added value as it is used as lateral guiding structure for the rolling wagons, as well as an important constraint for the design of the rolling wagons. The rails are constructed on either side of the sliding track. Since the lock chamber and gate recesses cannot be put in dry conditions for maintenance a habitat structure has been designed for the construction of the rail structures and the installation of the rails. The habitat structure is purposely designed for this application and allows to construct the rail structure in segments of 12m on either side of the sliding track in dry conditions. The habitat is equipped with a moving mechanism that allows it to move on the lock floor, without the need to be lifted and lowered again by cranes at the surface. An overview of the habitat structure is shown in Figure 13.

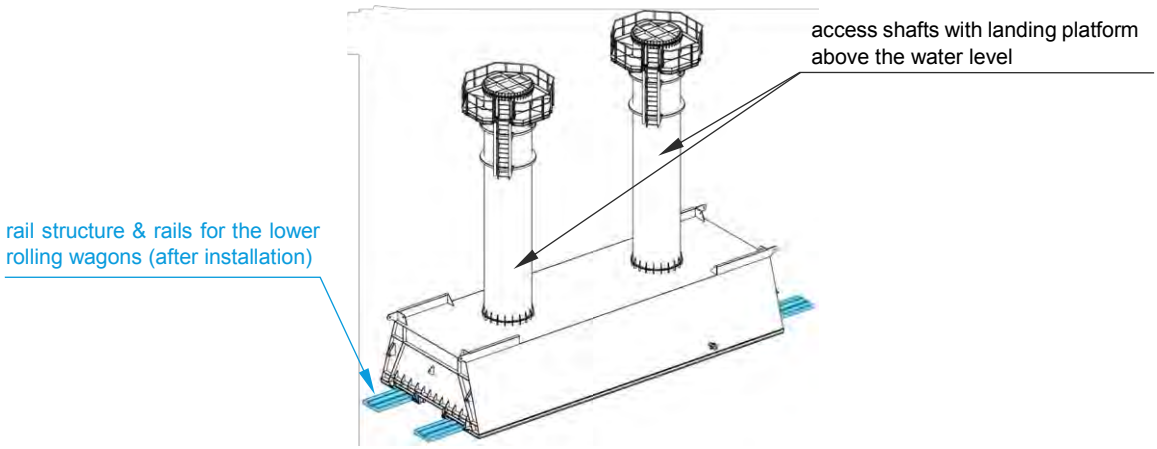

Figure 13: Habitat structure that will be used to install the rail system on the lock floor.

Similarly as for the lagoon side gate, a weight monitoring system is foreseen in the design of the new sea side lock gate. By monitoring the weight of the gate at all times, warning alerts can be incorporated in the control system of the lock complex if the net weight of the gate is too low for the predicted wave conditions so that precautionary measures (e.g. increasing the ballasting condition) can be taken. Not only the water level in the ballast compartments is monitored, but the reaction forces on the lower rolling wagons are also directly measured by means of load cells that are installed in the reaction tubes of the lock gate, as shown in the cross section of the new sea side lock gate in Figure 14.

It can be observed in the figures (e.g. Figure 14) that only 8 levelling tubes are present in the new sea side lock gate instead of 10 levelling tubes in the original design. This is due to the presence of the lower rolling wagons and the shifted location of the reaction tubes. To make sure that the levelling time is not decreased as a result of this adaptation, several remedial measures can be proposed. Either an increased diameter of the levelling tubes could be used or the lifting speed of the levelling valves may be increased, as long as the hydraulic forces on the ships in the lock remain acceptable during levelling. In the new design of the sea side lock gate, the original tube diameter was retained but a dual lifting speed was proposed for small and high head differences.

The increased weight of the gate requires an increase of the traction force for the driving mechanism of the lock gate to ensure that the lock gate can still be operated in a reasonable time frame. The new driving mechanism is designed in such a way that the original power requirements are retained and only minimal adaptations are required to the civil works. All equipment is installed in the purposely built technical room at the end of the gate recess.

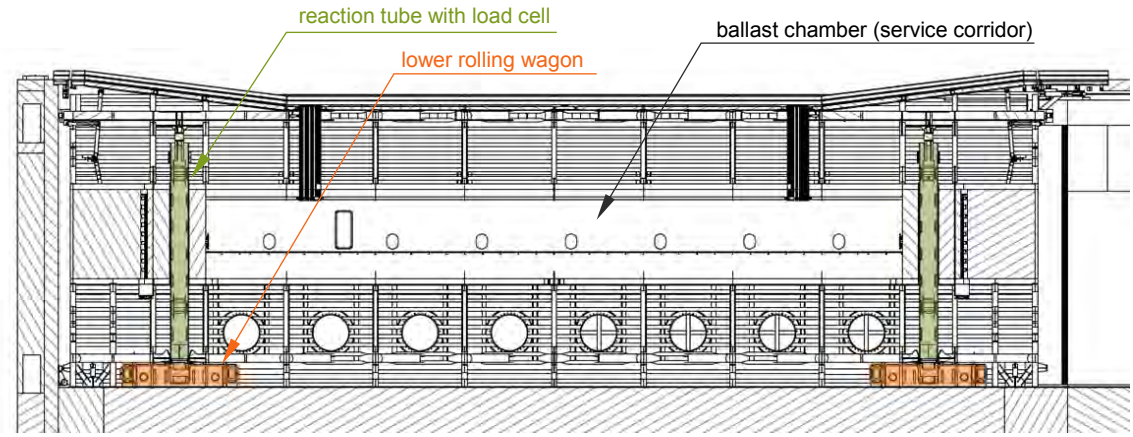

Figure 14: Redesigned sea side lock gate: cross section.

Given the urgency to finish the MOSE system, the design studies for the lock gates had to be performed in the shortest possible time frame. The exploratory and preliminary design phase, including the investigation of physical causes and design optimizations took SBE about six months to complete. This period included the hydraulic research and tests performed at MARIN. The final design of the lock gate and the preparation of tender specifications was finished in about one year. At present, the construction works for both the new sea side gate and the improvements of the lagoon side lock gate are underway and the primary line of defense of the MOSE system is expected to be finished by the end of 2019. The Malamocco lock is expected to be fully operational by March 2020.

6 CONCLUSIONS

After a thorough investigation of the damage phenomenon through terrain inspections and numerical simulations, the physical phenomenon causing the damage was discovered. The combination of the specific wave climate with long wave periods at this location and the open structure of the existing lock gate with technical rooms acting as buoyancy chambers above the lowest design water level has led to unacceptable vertical uplift forces.

Based on the understanding of the underlying physics, design improvements have subsequently been developed. The efficiency of these design improvements was quantified by means of scale model tests and the uplift forces were reduced by up to 40%.

Finally, based on an extended risk and reliability analysis and in view of retaining the most cost-effective solution for the problem, a different approach for renovation and redesign was proposed for both gates of the Malamocco lock. The engineering design was performed in approx. For the lagoon side lock gate, minor design adaptations were proposed in combination with an updated control system regulating the operation of the lagoon side lock gate under firm restrictions. For the sea side lock gate, an entirely new design was made. All proposed design optimizations were taken into account and a new support system had to be designed for the lock gate.

REFERENCES

Grasso, N., van den Boom, H., Della Valentina, E., Koning, J. (2015). Dynamic Wave Loading on Malamocco's Gate. MARIN, Report No. 26841-1-TM.

Jacobsen, N.G., Fuhrman, D.R., and Fredsøe, J. (2012). A Wave Generation Toolbox for the Open-Source CFD Library: OpenFoam. International Journal for Numerical Methods in Fluids, **70**(9), 1073-1088.

Lena, C., Los-Elsenbroek, R. (2016). Malamocco's Gate; Captive Tests. MARIN, Report No. 29291-1-BT.

Pancham, A., Jacobsen, N., O'Mahoney, T. (2016). 2D CFD modeling of wave loads on the Malamocco lock gate. DELTARES, Ref. 1230489-000-HYE-0009.

Reijmerink, B., Caires, S. (2016). Wave conditions reaching the sea side of the Malamocco lock gates. DELTARES, Ref. 1230489-002-HYE-0001.

Volpato, M., Adami, A. (2015). Rapporto Finale del Modello Fisico. PROTECNO, Report No. 436001RF-1MaV.

THE PORT OF OSTEND: CONSTRUCTION WORKS FOR THE WIDENING OF THE INNER APPROACH CHANNEL

Filip Mortelmans[1] and Hadewych Verhaeghe[2]

ABSTRACT

For the last phase of the masterplan for the port of Ostend, the inner approach channel needs to be widened. As the existing timber pier at the western side is protected by law as heritage, widening of the channel is only possible towards the eastern side. To allow this significant widening of the channel, extensive works will be needed at the site 'Halve Maan'. Since the project area is located within the active port, and partially in protected habitat area, a lot of site specific requirements had to be taken into account. All these constraints had a significant influence on the design which resulted in a multidisciplinary project, that can be split in 3 different sub-projects. A new seawall and a new retaining wall were designed, and an existing quay wall had to be stabilized.

1. INTRODUCTION

Ostend is situated in the middle of the Belgian coastline. Although for many centuries Ostend was considered one of the most important ports at the Southern North Sea, it has a relatively small harbour.
At this moment, the harbour traffic mainly consists of general cargo, but from time to time cruise ships also call at the port. And during 2018 a new ferry connection to Ramsgate (United Kingdom) will be established, which will increase vessel traffic in the port. During the last years, a changeover to 'Blue Growth' has been made by the port of Ostend. This resulted in an extensive growth of the employment related to the construction of new wind farms in the North Sea.

The harbour of Ostend has been changed a lot during the last ten years. In Figure 1 a view on the old harbour (before 2008) versus the harbour at this moment (2018) is shown.

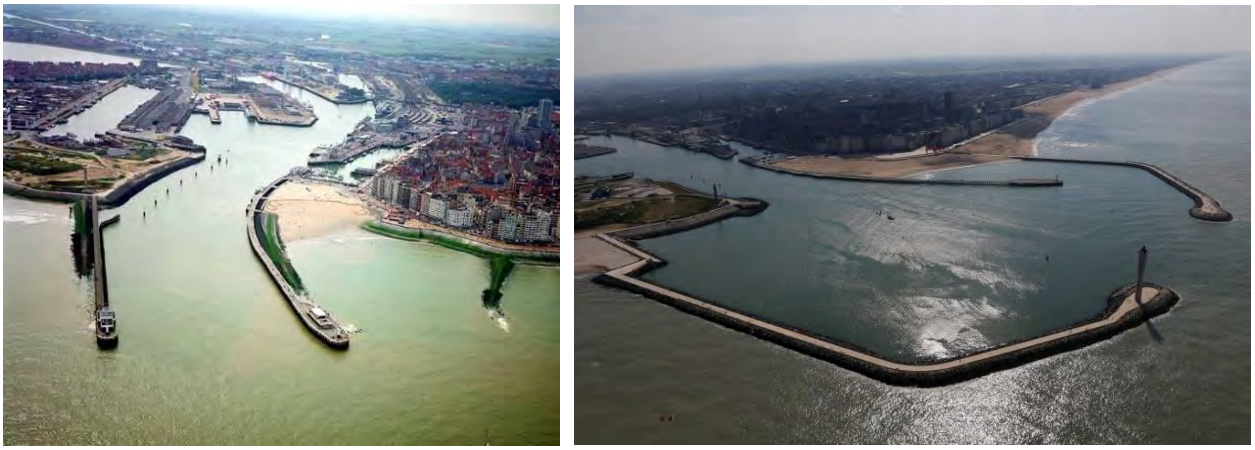

Figure 1: The harbour of Ostend before 2008 (left) and today (2018), the timber pier at the western side of the harbour is protected by law (monument) (picture © Department of Mobility and Public Works)

[1] ir. Filip Mortelmans, TRACTEBEL, Ports and Waterways division, Oostende, Belgium.
Filip.Mortelmans@tractebel.engie.com
[2] dr. ir. Hadewych Verhaeghe, Department of Mobility and Public Works, Flanders, Belgium.
Hadewych.Verhaeghe@mow.vlaanderen.be

The construction works at the harbour entrance in Ostend fit into the larger 'Integrated Coastal and Maritieme Plan for Ostend' which was set up by the Flemish Community. With the widening of the inner approach channel, this plan will be completed.

2. MASTERPLAN FOR THE PORT OF OSTEND

2.1. General description and previous works

The so-called 'Integrated Coastal and Maritime Plan for Ostend' was set up by the Flemish Community at the end of the previous century. The objectives of this plan were:

- to protect the city of Ostend against flooding: the maximum allowable overtopping discharge for a storm with return period R = 1000 year is restricted to 1 l/s/m;
- to make the harbour of Ostend accessible for larger ships: access for ships with lengths up to 200m is required;
- to approach the harbour expansion and coast protection in an integrated way.

In order to make the harbour accessible for ships with a length up to 200m, important modification works at the harbour access were necessary.
At the outer part of the harbour, the access channel was relocated so that an access more perpendicular to the coast line was created. The existing eastern pier had to be removed to make this possible. Further, two new breakwaters were constructed to realize a more sheltered area for ships when entering the harbour (see Figure 1).
The history and extensive studies for the masterplan of Ostend, and the design of the two breakwaters are described into detail in Verhaeghe et al. (2010).

More inwards the harbour, the approach channel also has to be adapted to allow these larger ships to enter the harbour safely. At present the approach channel at that location is enclosed by a timber pier at the western side, and a seawall with the harbour site 'Halve Maan' at the eastern side (see Figure 2). As the timber pier is protected by law as heritage, widening of the channel is only possible at the eastern side.

The widening of the harbour approach channel inside the port of Ostend concerns the last phase of the works in the framework of the 'Integrated Coastal and Maritime Plan for Ostend'. The design studies for these works are described in this paper.

2.2. Last phase of the masterplan – widening of the approach channel

In 2015 extra navigation simulations were performed with different vessels (cruise-ships, RoRo-ferries and cargo-ships) to optimize the design of the inner channel (Verwilligen et al., 2016). It was concluded that the inner channel should be widened from 80m to 125m at the most northern point of the site 'Halve Maan' to 145m at the most southern point of the site 'Halve Maan'. The proposed design for the new approach channel can be seen in Figure 2, together with an impression of the navigation simulation study. To allow this significant widening of the channel, extensive works will be needed at the site 'Halve Maan'.

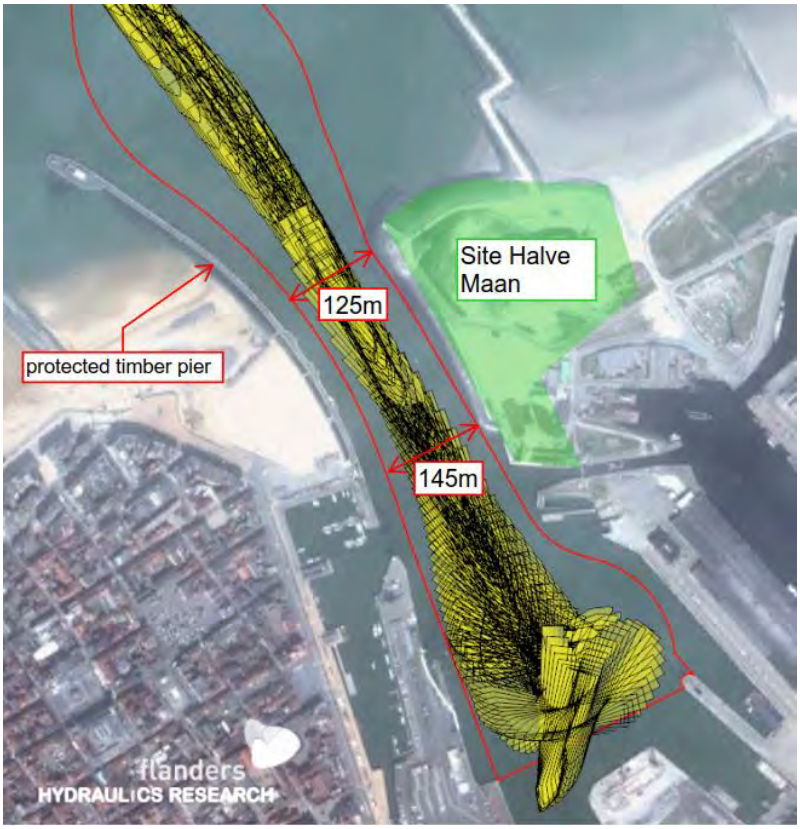

Figure 2: Navigation simulation and proposed design for the location of the widened entrance channel

3. SITE CONDITIONS

3.1. Historical evolution of the site and relevance for the works

The project area is situated at the eastern side of the entrance channel towards the port of Ostend, and has known a rich history, depending on the historical needs of the port. The earliest relevant development of the area can be situated approximately 150 years ago. Around 1860 a basin was constructed behind a moon crested dike, together with a new lock 'Leopoldsluis' (Figure 3). This basin had to collect the seawater at high tide and release it through the lock at low tide. The goal was to use the corresponding scour phenomenon as a natural way of maintaining the required drought in the entrance channel. After World War I the Leopold basin was filled up again (Figure 3), but the existing lock remained intact.

Figure 3: 'Halve Maan' site – 1860 with basin and lock, 1950 with filled basin

At the end of the 20th century the entrance channel was deepened and widened to allow larger vessels to call at the port of Ostend, leading to the current configuration of the site with a long revetment extending parallel to the entrance channel (Figure 4). During these works, the lock 'Leopoldsluis' was partially demolished and a lot of earthworks were performed to create a new stone revetment. The revetment was repeatedly damaged during heavy storms, and an additional rock berm was constructed in the northern zone. Finally, early 21st century, following the latest developments in the offshore wind industry, a heavy-duty quay wall and corresponding pavement area for the assembly of large windmill components was constructed at the south side of the site. This heavy-duty pavement area consists of pile mattress systems and concrete slabs on deep foundation piles, capable of resisting loads up to 10t/m².

Figure 4: 'Halve Maan' site as it is today, with existing dike and revetment parallel to entrance channel

It is clear that the site has undergone many changes during its existence, but the moon crested dike (='Halve Maan' in Dutch) has always remained in place and has given its name to this area situated at the east side of the entrance channel of the port of Ostend.

Due to the radical impact of the works which are foreseen, the historical development of the site is considered quite important. Indeed, as will be explained further in this paper, a lot of design constraints (geotechnical characterisation, retaining wall solutions, environmental requirements, …) can be explained by the rich history of the project area.

3.2. Geotechnical conditions

An extensive soil investigation at the site 'Halve Maan' was performed, principally consisting of in situ cone penetration testing (CPT). The CPT's were mainly realized on land, but several nearshore CPT's were also performed at the location of the existing revetment (using a jack-up platform). Additionally, multiple boreholes and corresponding laboratory testing was performed. During the works, it is also foreseen to dig some exploratory trenches during the works to detect the remainders of the old lock 'Leopoldsluis'.

In general, distinction can be made between two principal geotechnical zones (Figure 5), with the old lock as a distinct transition point. The northern area can be considered as having favorable soil conditions over the entire depth, mainly consisting of medium dense up to very dense sands. A second southern area has less favorable soil conditions, with soft deposits up to a large depth. These soft deposits can be characterized as soft clay, even with an organic content at some locations. Geotechnical properties of the soil below the soft deposit correspond well to the northern geotechnical area. In general, soil characteristics were determined using Eurocode 7 (CEN, 2014), combined with the results of the laboratory testing (where applicable).

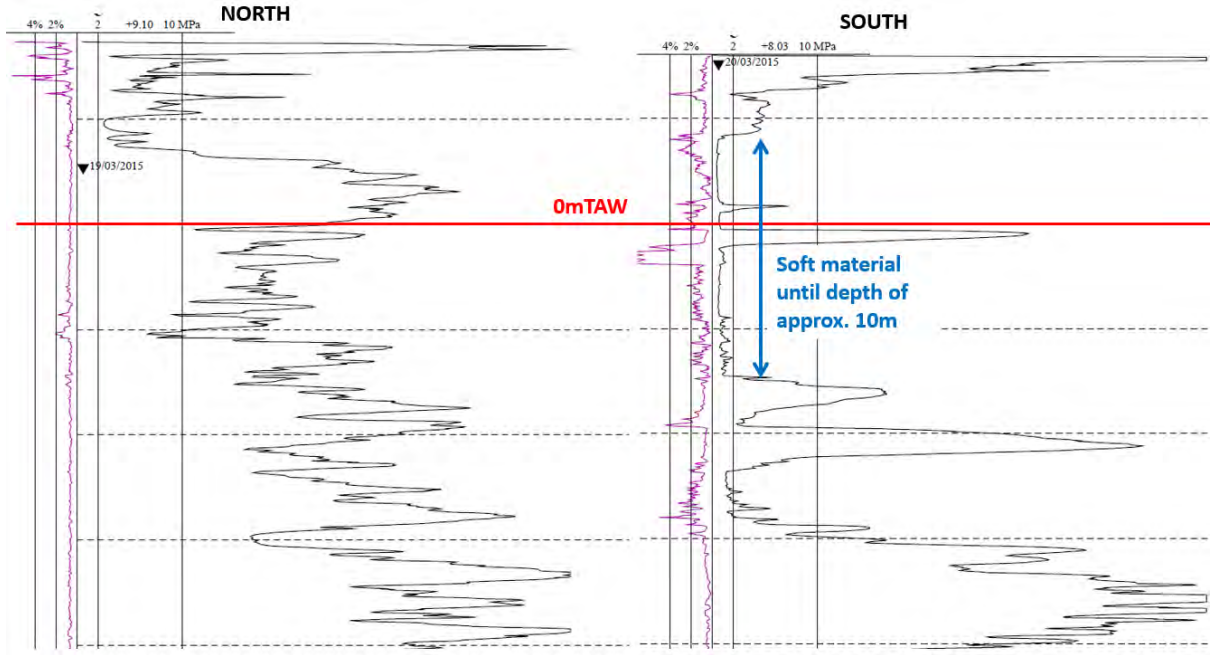

Figure 5: Typical geotechnical conditions at the 'Halve Maan' site

Knowing the history of the site, the sharp geotechnical transition between northern and southern area is not very surprising. Indeed, as mentioned in paragraph 3.1, the area south of the old lock used to be a basin and was backfilled shortly after World War 1. Most likely a backfill material of low quality was used, which explains the sudden change of sandy soils towards soft deposits when crossing the location of the old lock.

3.3. Metocean data

The design wave conditions at the location of the new construction were determined for a return period of 100 years. Numerical simulations were performed using Mike 21 BW with short-crested waves for different wave directions. In Figure 6 a contour plot is given, showing the calculated significant wave heights inside the harbour of Ostend for a storm with return period = 100 years with waves coming from north-west.

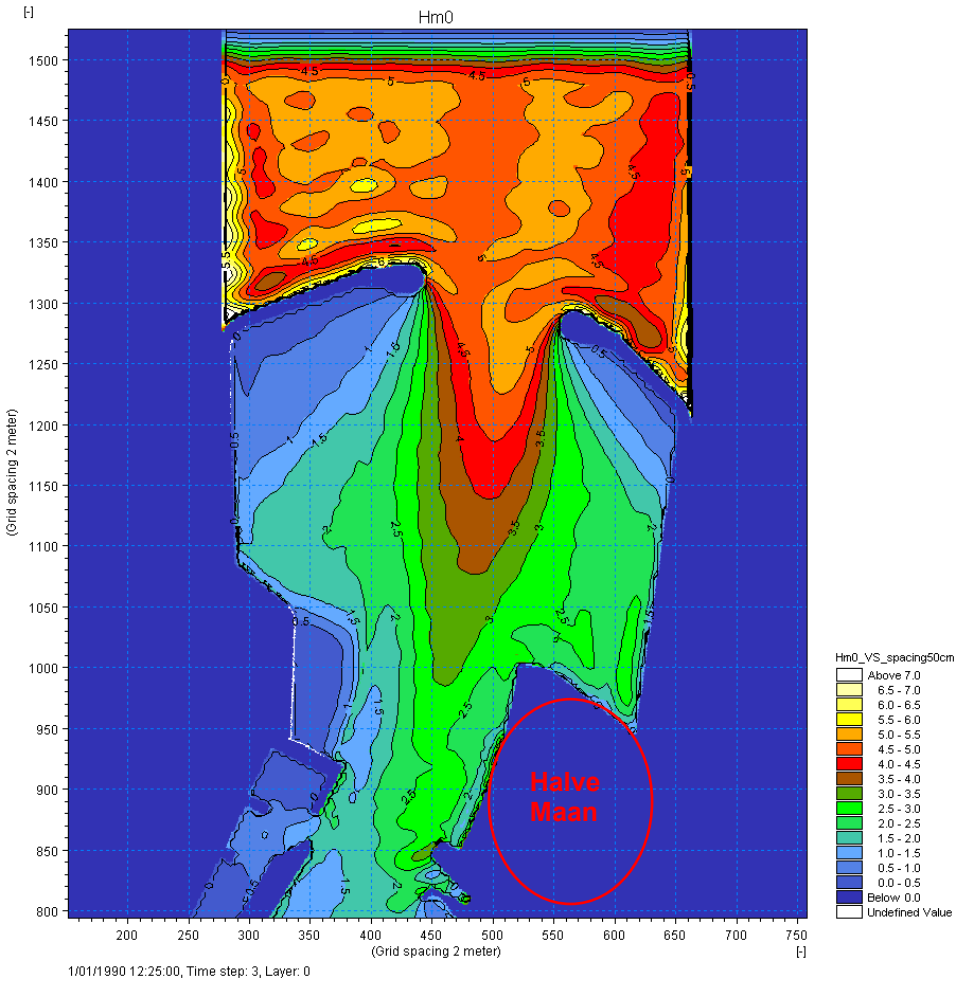

Figure 6: Contour plot of H_{m0}, return period = 100 years, waves from NW

The wave heights obtained at some distance before the 'Halve Maan' were used for the design of the new revetment. The corner of the 'Halve Maan' is exposed to the largest wave heights: design waves with wave height H_{m0} = 4m and peak period T_p = 10,85s are obtained. The corresponding 100-year water level is +6,7m TAW.

3.4. Archeological investigation

An archaeological study showed that the site has no particular historical value and up to today no special measures are foreseen. However, there is a small risk of unexploded ordnance (UXO) which still pose a risk of detonation. During construction, this will be a point of attention, certainly because of the many excavations that are foreseen for the works.

3.5. Environmental constraints

The site was assessed thoroughly from an environmental point of view and it was concluded that the environmental constraints were of utmost importance.

Study of the groundwater levels and the local topography (combined with the historical evolution of the site as described in paragraph 3.1) led to the definition of two potentially interesting areas for recovery of the original vegetation (Figure 7). First, a northern zone was identified which could be interesting for the development of brackish grassland. Secondly, contrary to the saline northern area, a southern zone with sweet water conditions was detected. This zone was evaluated to be interesting for the development of wet dune vegetation.

Based on these two observations, it was decided to perform two excavations to restore part of the project area into its original vegetation (total volume of earth to be excavated approx. 21.000m³). The development of the expected salt marsh vegetation requires a regular flooding (typically every spring tide), which is obviously not the intent of the works that will be performed. Therefore, an artificial siltation of the area will be required.

Figure 7: Zones with a potential for recovery of original vegetation (blue = brackish conditions, orange = sweet water conditions)

Moreover, a large part of the area is located in a so-called habitat area (dune area), which is protected by Belgian law. Due to the widening of the entrance channel, part of this habitat area will be excavated and cannot be recovered. This loss of habitat area was compensated by restoring another similar area in its original conditions. This compensating area was defined during the master planning phase and covers a surface of 0.95 hectares. This strict limitation on the seizure of protected habitat area imposed an important constraint for the design of the widening of the entrance channel.

3.6. Conclusion

It is clear that the works cover a range of challenges of building into an existing harbour with limited space and many boundary conditions. The interference with existing structures, the poor geotechnical conditions, the close presence of exploitation zones etc. all had a significant influence on the final design.

4. WIDENING OF THE APPROACH CHANNEL

4.1. Definition of project zones

To allow larger vessels to enter the port safely, the entrance channel should be widened from 80m to 125m at the most northern point of the site 'Halve Maan' to 145m at the most southern point of the site 'Halve Maan' (Figure 2), meaning that the entrance channel becomes wider when going deeper into the port. To allow for this widening, a new shoreline needs to be developed as well as a connection to the dike 'Halve Maan' in the north and the existing quay wall in the south.

Due to the interference between nature, infrastructure and existing exploitation zones, the works were split into three main project areas and a site-specific design was developed for each of these zones. Following project zones were defined (see Figure 8):

- Northern area: apart from the limitation on the seizure of habitat area, the edge of the approach channel could be shifted quite easily in this area. Due to the good soil conditions, a new revetment proved to be the preferable design solution. The existing dike is also reinforced to resist the high wave loads and reduce overtopping.
- Middle area south of the existing lock: this zone is characterized by unfavorable soil conditions, meaning that the construction of a new slope and revetment was not so obvious (a very gentle slope would be required, leading to very high volumes of soil to be excavated). Moreover, the existing pile foundations of the heavy-duty pavement for the offshore industry would interfere with this new slope. Therefore, it was decided to develop a retaining wall solution for this area, with the advantage that the existing heavy-duty pavement will still be functional after the works.
- Southern area: at the most southern point, the new entrance channel comes very close to the existing quay wall at the corner of the 'Halve Maan' site. This quay wall was originally designed for a water depth of 6.6m, while the new approach channel goes up to a depth almost 9m. Due to the close distance of the new entrance channel to the quay wall, measures had to be taken to stabilize this existing quay wall and allow for this increase in water depth.

Figure 8: Definition of project zones and indication of old/new approach channel

4.2. Northern area – construction of new revetment (?)

4.2.1. Geotechnical design

As explained earlier, for the northern zone there is a strict geometrical constraint related to the present habitat directive area. Therefore, instead of simply shifting landwards the existing seawall, a structure with a steeper slope was designed. Due to the favourable soil conditions, the geotechnical design of the slope was quite straightforward and a rather steep slope of 10H/4V covered with a revetment was designed, followed by a protected berm and a more gentle unprotected slope (see typical cross section in Figure 9).

The unprotected slope is somewhat steeper than what normally would be designed for an exposed slope in active water. However, experience of the port authorities in the neighbouring port of Zeebrugge indicates that no major erosion issues are expected, since a stone covered willow mattress is foreseen on the berm, extending to a level including the active zone during wave action (1.5 times the wave height below the sea level). Nevertheless, an inspection programme has been developed to monitor the actual state of the slope during the lifetime of the structure. If necessary, an additional gravel layer can be provided to stabilize the unprotected slope in case of unacceptable scour.

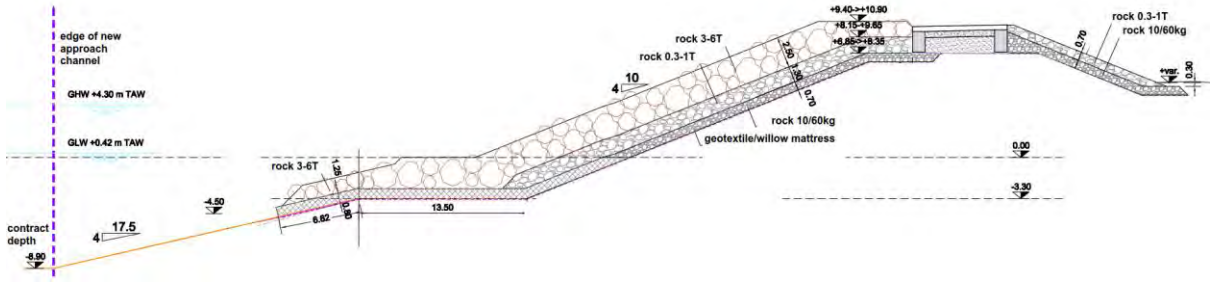

Figure 9: Typical revetment cross section (rock armour layer)

4.2.2. Hydraulic design – armour stability

For the hydraulic design, distinction can be made between the seaward directed zone and the roundhead exposed to perpendicular wave attack with high waves, and the zone parallel to the entrance channel where wave heights are slightly smaller and wave attack is almost parallel to the revetment. This lead to two different designs for the armour layer, as shown in Figure 10.

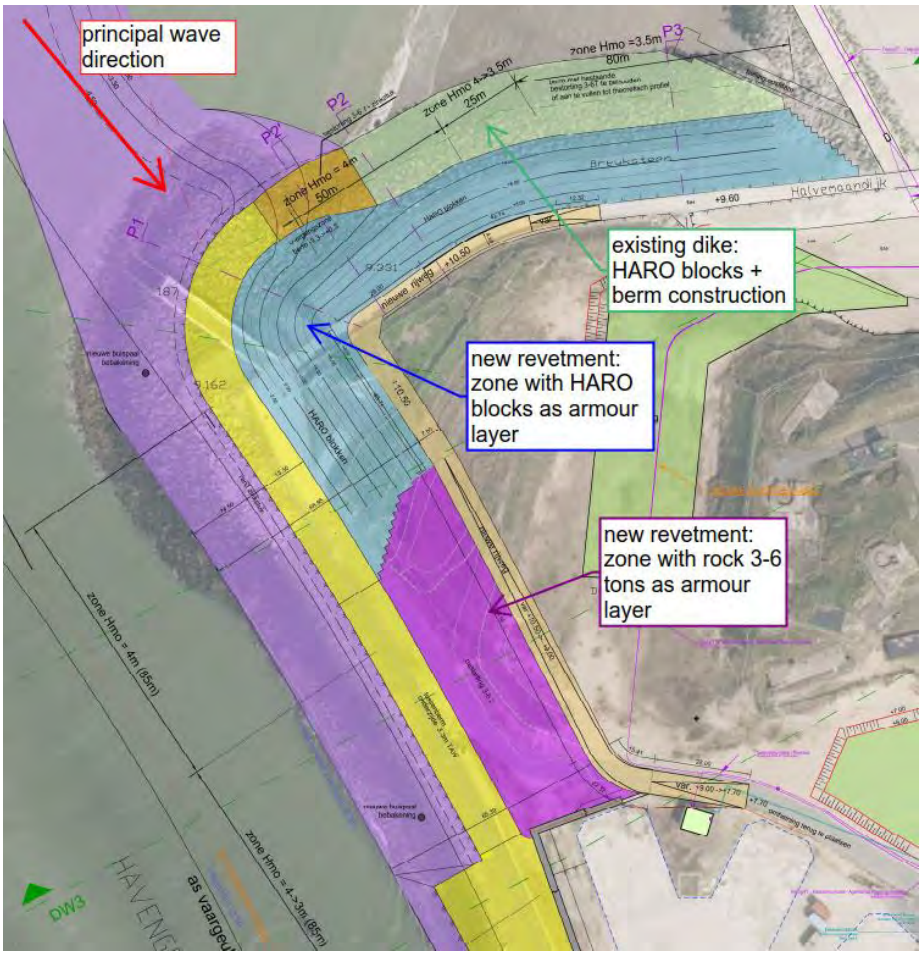

Figure 10: Design for northern project area (revetments and protection of existing dike)

The northern zone is oriented towards the harbour entrance and hence exposed to significant hydraulic loading. Due to the orientation of the two breakwaters protecting the port entrance, a quasi-perpendicular wave attack can be expected. In this area, a protection using one layer of concrete HARO blocks (weight 15 tons) was designed to resist significant wave heights up to 4m (typical cross section is shown in Figure 11). For hydraulic stability the common rules in the rock manual (CIRIA, 2007) were used. As a conservative approach a stability coefficient equal to K_D = 4 was defined for the design of one layer of HARO blocks.

For the underlying second armour layer, the normal filter criteria would require a layer with 1-3 tons grading (W/10, with W the weight of the HARO blocks). However, practice has shown that these large stones can lead to issues when positioning the prefabricated HARO blocks. Therefore, as an innovative approach, it was decided to apply a smaller grading to allow for an easier construction process. Research at Gent University (D'Hont and De Kimpe, 2013) demonstrated that for a single layer of HARO blocks an underlayer with an average weight of W/20 (with W the weight of the HARO blocks) can be applied, leading to a practical grading of 0.3-1 tons armour stone.

The HARO blocks are placed on the to be excavated slope where the entrance channel is widened, and on the roundhead that will be built to make the transition towards the existing dike 'Halve Maan'. To reinforce this existing dike (consisting of smooth granite blocks), it is also foreseen to add a cover of HARO blocks (see plan view in Figure 10).

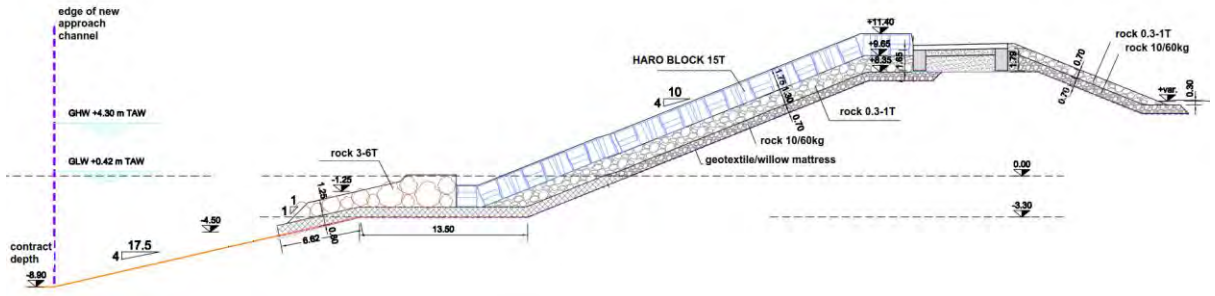

Figure 11: Typical revetment cross section (HARO armour layer)

The zone parallel to the entrance channel is experiencing somewhat smaller wave heights when going into the port. But from hydraulic perspective, the major difference compared to the northern area is the fact that the obliqueness of the waves differs significantly. Wave direction is almost parallel to the revetment (approach angle is 80° measured perpendicularly on the revetment), meaning that hydraulic loading of the revetment is considerably reduced. Because of this reduction a double armour layer consisting of 3-6 tons proved to be sufficient (cross section shown previously in Figure 9).

4.2.3. Hydraulic design – overtopping

The height of the seawall is limited to achieve an economically (less earthworks) and environmentally (minimize use of habitat area) acceptable design. Obviously, this results in significant overtopping in extreme conditions and as a practical design criterium, it was decided to limit the overtopping discharges to 50l/m/s for 100-year metocean conditions. This high value was considered acceptable since no buildings or occupied space are located in this zone (only habitat area) and the majority of the discharge naturally returns to the approach channel. Overtopping was calculated according to the latest EurOtop manual (Van der Meer et al., 2016), which lead to the definition of sea wall height (in general, the existing terrain level needs to be increased with 1m).

Due to the considerable overtopping, the rear side of the seawall is also exposed to significant hydraulic loading. This has to be verified, since a progressive erosion at the backside of the seawall would lead to overall failure of the seawall. Based on the calculated flow velocity, the required stone size to be hydraulically stable in the overflowing water was determined, which resulted in an additional armour layer 0.3-1 ton at the backside of the seawall.

At the existing dike 'Halve Maan' it was not possible to simply increase the height of this existing seawall to limit the overtopping values. Luckily, current sea bed level in front of the dike is limited and a berm consisting of 3-6 tons armour stone is already in place, which has a beneficial effect on the overtopping discharge. Moreover, the HARO blocks that will be placed on the dike lead to an additional reduction in overtopping. Calculation showed that the combination of berm and HARO revetment is sufficient to limit the overtopping to the acceptable values, and it is only foreseen to reinforce the berm to a minimum level and width (corresponding to the geometry that was considered in the design).

4.3. Middle area – construction of new quay wall

The middle project area is located near an existing exploitation zone used by the offshore industry. Intended as a handling area for heavy windmill components, pavement of a large part of this exploitation zone was designed for a uniform load of 10t/m² using deep foundation techniques. Two foundation systems were applied to allow for this high surcharge load: reinforced concrete slabs on deep foundation piles, and flexible pile mattress systems on short concrete piles. Moreover, geotechnical conditions for this area are quite challenging with soft soils (clay, peat) up to depths of 15m. Based on the above, shifting the existing seawall landwards was considered not expedient and as an alternative a quay wall was designed. The quay wall consists of a combi-wall (tubular piles as primary unit and intermediate double AZ sheet piling) with inclined ground anchors (pre-stressed grouted anchors) and a concrete capping beam, the typical cross section can be seen in Figure 12.

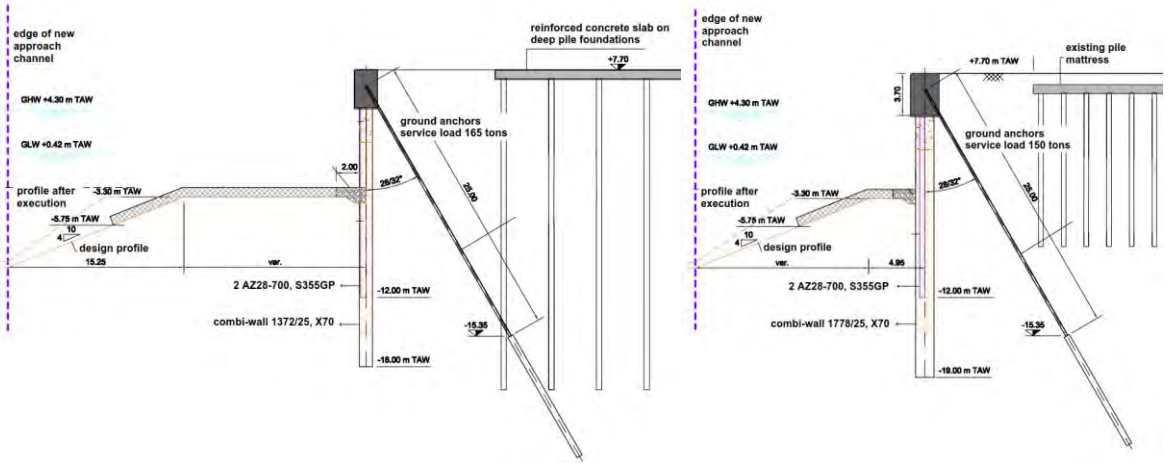

Figure 12: Typical retaining wall cross sections

To limit the retaining height of the wall, if was foreseen to maintain a berm in front of the wall since there is no requirement for mooring of vessels in this area. Although this reduced the retaining height significantly, overall load on the wall was still significant due to the considerable water pressure (tidal variation) and the poor soil conditions behind the wall (leading to high active soil pressures). Therefore, a heavy combi-wall proved to be necessary. Since the entrance channel becomes wider when going south, the available berm becomes narrower, and in the most southern zone becomes the critical section for the combi-wall design (see plan view in Figure 13). In this critical section, the combi-wall consists of large tubular piles diameter 1778mm (cross section shown in Figure 12).

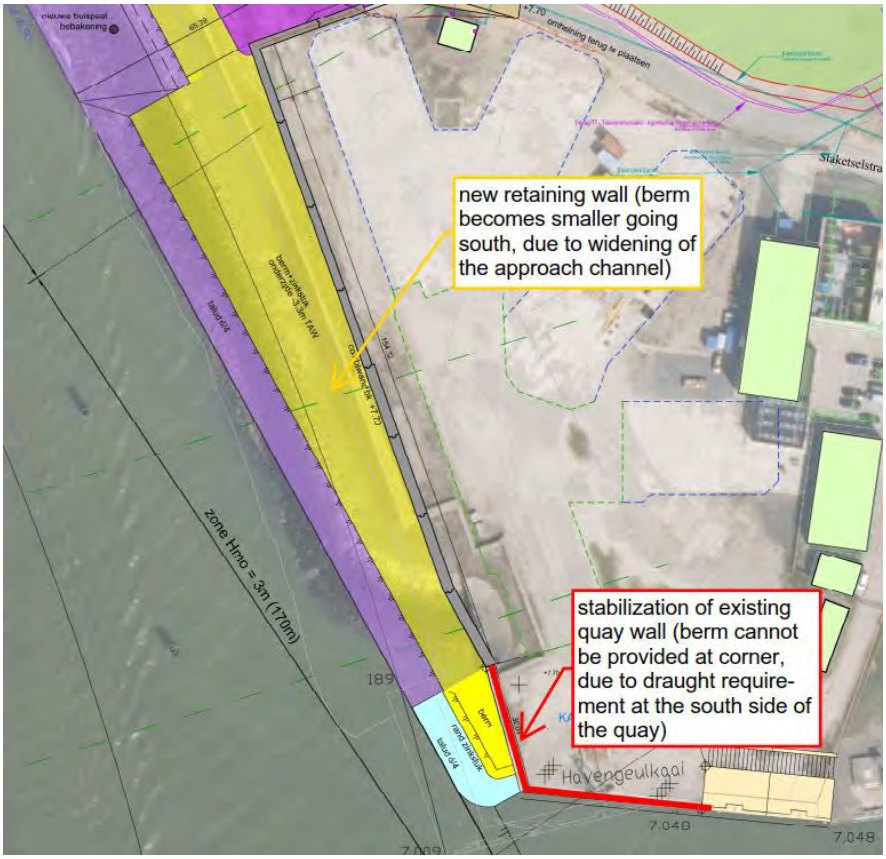

Figure 13: Design for middle and southern project area (retaining wall and quay wall stabilization)

Since the berm is located at a shallow depth to have a maximum effect on the quay wall (approx. 3m below MLW), it is potentially subjected to wave action in extreme conditions. Because the berm is of key importance for quay wall stability, it was designed to be hydraulically stable under the extreme wave action. This resulted in a scour protection consisting of a willow mattress covered with stones up to 300kg. This scour protection is applied on the horizontal part of the berm as well as on a part of the slope. A design profile allowing for some scour was taken into account in the calculations, and a monitoring programme has been developed to assess the scour progression during the lifetime of the quay wall.

A particular point of interest is the anchoring of the quay wall. Due to the presence of the existing pile foundations that have to be preserved, top fixation of the quay wall was not particularly straightforward. Interference with the existing pile foundations is unavoidable but has to be limited to the absolute minimum to avoid issues during construction. Therefore, the following methodology was developed:

- It is foreseen to make an exploratory trench prior to the works to have a clear idea about the position of the existing pile foundations.
- Based on this topographic campaign, the anchor positioning will be confirmed. The design philosophy of the anchors is as follows (see Figure 12 for a comparison between the two design situations):
    - For the zone with deep pile foundations (spaced approx. 4.13m) in the north, it cannot be avoided to cross the piles with the anchors. However, with a pile spacing of 4.13m, it is considered feasible to provide two anchors between each pile row (meaning that anchor spacing automatically is 2.065). But since only the first pile row can be detected with the exploratory trench, angle of the anchors is minimized to avoid potential interference with second pile rows, leading to an inclination angle of 60° (with the horizontal).
    - For the zone with more shallow pile foundations in the south, spacing of these piles is only 2m in all directions, which was considered too small to allow for anchors to be drilled in

between the existing pile foundations (only the first pile row can be detected with certainty). Therefore, anchors are designed to be drilled underneath these piles, leading to an inclination angle of 60° (with the horizontal. On the other hand, this meant that spacing of the anchors could be selected without restriction, and an intermediate distance of 1.48m was selected for these anchors.

Based on the above, it is clear that the anchors have to be positioned quite vertically to avoid interference with the existing deep foundations of the pavement area. Due to this inclination, combined with the poor geotechnical conditions, design anchor loads were quite high with service loads up to 165 tons. Fortunately, the grout body can be positioned in a very dense sand layer with average cone resistances $q_{c,av}$ up to 25MPa and more. Geotechnical capacity was theoretically demonstrated using the common rules in CFMS (1995). Additionally, capacity was verified according to latest Belgian practice (Huybrechts et al., 2008). Both methods lead to acceptable results with respect to anchor capacity. Since anchor service load is high and inclination is quite vertical, an extensive full-scale testing programme is foreseen to validate the design loads for these ground anchors. This full-scale testing programme foresees in several tests for each anchor type. For each anchor type, a separate reaction beam on pile foundations shall be constructed and additional CPT testing at each test location is foreseen to validate the theoretical calculation of the anchors. Goal of the testing programme is to validate the anticipated service loads (absolute value) and assess if creep under this maintained load remains within the acceptable limits.

4.4. Southern area – stabilisation of existing quay wall

In the southern project area, the existing seawall ends in a quay wall. This quay wall of the Danish type has to be preserved, as it is the loading area for the offshore exploitation zone mentioned in the previous paragraph. Since the widened channel comes quite close to this existing quay wall, a solution had to be found to reinforce the quay wall and allow for an increase in depth. Modifications to the existing quay wall were considered too complex, and preference was given to less invasive solutions. Since the main issue was an increase in depth at a certain distance from the quay wall, but within the passive wedge, it was decided to build a gravel berm in front of the quay wall (Figure 14). Using this berm made it possible to avoid a significant increase in bending moment in the retaining wall and allowed for sufficient earth resistance (passive earth pressure in front of the wall). It is noted that this berm solution is only acceptable because there is no requirement to allow berthing of vessels along the quay side parallel to the approach channel. The berm is hydraulically protected using the same system as for the retaining wall in the middle project area (willow mattress covered with stones).

However, for the corner section of the quay wall the widened channel comes so close to the quay that a simple berm proved to be insufficient to provide the required degree of safety with relation to ground failure. Moreover, vessels need to be able to berth at the part of the quay wall perpendicular to the approach channel (required draught approx. 6m below MLW), meaning that at the corner point of the quay wall a berm solution is not possible. The design was developed further to take the 3-dimensional spatial distribution of soil pressures into account in the corner section of the quay wall. An analytical solution for the problem was derived, leading to a slight reduction in the active soil pressures acting on the sheet piles in the corner section. This was also verified with a simplified 3D numerical model, which confirmed the analytical results. Calculation showed that using this approach, bending moments in the quay wall remain within the acceptable values w.r.t. resistance of the sheet piles themselves. Nevertheless, an additional reinforcement was necessary since a sufficient earth resistance (passive earth pressure in front of the wall) could not be guaranteed. Therefore, it was decided to increase the passive resistance by construction of vertical gravel columns in front of the retaining wall as shown in Figure 14. The gravel columns have a diameter of 70cm and are placed in a triangular grid, with inter-distance of 1.80m. Due to the gravel the average shear characteristics of the soil inside the passive wedge are improved, to the level that is required to guarantee the necessary factor of safety on the passive resistance in front of the wall.

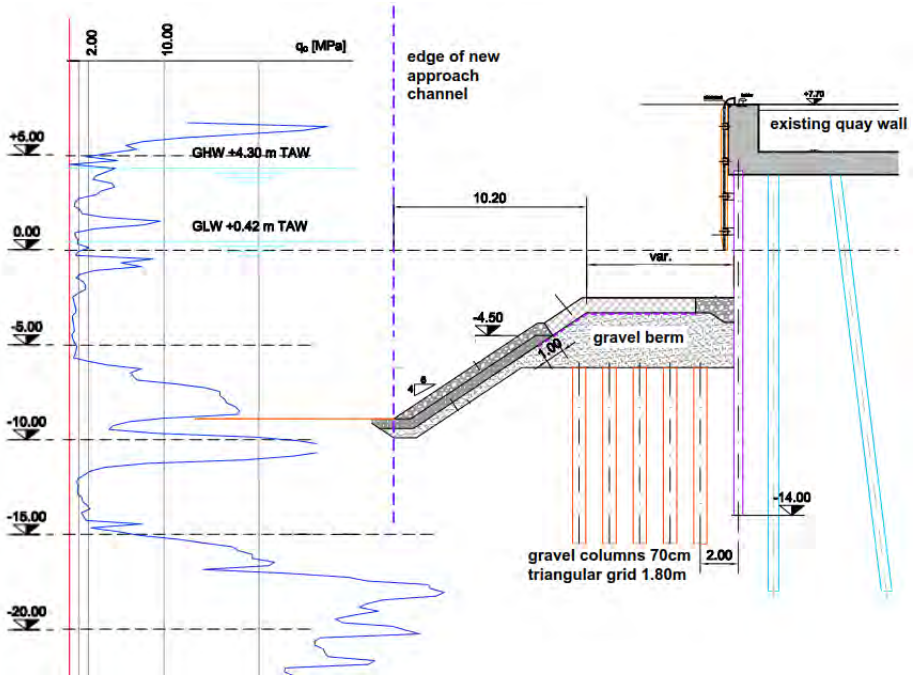

Figure 14: Typical cross section stabilization of quay wall with stone columns and gravel berm

4.5. Execution of the project

The project will be launched for tender in spring 2018, construction works should start towards the end of 2018 and should be finished in the course of 2020. When the envisaged works are finished, the last phase of the masterplan for the port of Ostend will be completed.

5. CONCLUSION

For the last phase of the masterplan for the port of Ostend, the entrance channel needs to be widened to make the harbour of Ostend accessible for ships with lengths up to 200m. To make this expansion possible, the existing site 'Halve Maan' needs to be modified thoroughly. An extensive research was performed to determine all site-specific conditions which lead to an exhaustive list of requirements that had to be taken into account: interference with existing structures, the poor geotechnical conditions, the close presence of exploitation zones, the strict environmental constraints etc.

All these constraints had a significant influence on the design which resulted in a multidisciplinary project, that can be split in 3 different sub-projects. In the northern area, a new revetment was designed using the latest design guidelines, completed with practical experience for this field of application. For the middle area, a new combi-wall was designed using heavy ground anchors with service loads up to 165 tons. Finally, in the southern corner section, the existing quay wall was reinforced using a gravel berm and gravel columns in front of the quay wall.

As the works cover a range of challenges related to building into an existing harbour with limited space and many boundary conditions, the project is a typical example of modern day port expansion works. It is demonstrated that it is possible to realize this type of project successfully, but a significant design effort is necessary to fulfill all stakeholder needs in agreement with all site-specific requirements

6. REFERENCES

CFMS (1995), Recommandations T.A.95 - Tirants d'ancrage - Recommandations concernant la conception, le calcul, l'exécution et le contrôle.

CIRIA, CUR, CETMEF, (2007), The Rock Manual. The use of rock in hydraulic engineering (2nd edition), C683, CIRIA, London.

D'Hont C. en De Kimpe F. (2013), "Technische en economische evaluatie van éénlagige deklaagelementen bij storsteengolfbrekers", Universiteit Gent.

CEN (2014), EN1997-1: Eurocode 7: Geotechnical design – Part 1: General rules, and Belgian application document.

Huybrechts N, De Vos M., Tomboy O., Maertens J. (2008), Integrated Analysis of the Load Test Results & Suggestions for a Harmonised Anchor Design and Test Methodology in Belgium in the Eurocode 7 Framework, Proceedings of the International Symposium "Ground Anchors - Limelette Test Field Results": 14 Mai 2008, Brussels, Belgium, Volume 1.

Van der Meer, J.W., Allsop, N.W.H., Bruce, T., De Rouck, J., Kortenhaus, A., Pullen, T., Schüttrumpf, H., Troch, P. and Zanuttigh, B. (2016), EurOtop. Manual on wave overtopping of sea defences and related structures. An overtopping manual largely based on European research, but for worldwide application. www.overtopping-manual.com.

Verhaeghe, H., Van Damme, L., Goemaere, J., De Rouck, J. and Van Alboom, W. (2010). Construction of two new breakwaters at Ostend leading to an improved harbour access. Proc., 32nd Int. Conf. on Coastal Engineering, ASCE, Reston, VA.

Verwilligen, J.; Eloot, K.; Peeters, P.; Mostaert, F. (2016). Nautische optimalisatie ontwerp Halve Maandijk te Oostende: Deelrapport 2 – Realtime manoeuvreersimulaties. Versie 4.0. WL Rapporten, 15_067. Waterbouwkundig Laboratorium: Antwerpen, België.

STUDY ON GOOD NAVIGATION STATUS - GOOD NAVIGATION STATUS IN ACCORDANCE WITH THE TENT-T GUIDELINES

by

Sim Turf[1]

Keywords: Good Navigation Status, Good Navigation Status guidelines, TEN-T network, exemption criteria, waterway infrastructure

ABSTRACT

On behalf of the European Commission a pan-European consortium[2] conducted a study to substantiate the concept of GNS referred to in article 15(3)b of the TEN-T guidelines[3]. This article stipulates that "rivers, canals and lakes are maintained so as to preserve Good Navigation Status (GNS) while respecting the applicable environmental law". The following definition was developed during the study: "*Good navigation status means the state of the inland navigation transport network, which enables efficient, reliable and safe navigation for users by ensuring minimum waterway parameters values and levels of service*". Moreover, GNS is to be achieved considering the wider socio economic sustainability of waterway management transport characteristics. The key focus of GNS is on physical waterway infrastructure.

The main outcomes of the study are:

- a concept for good navigation status,
- a network assessment (identify the existing bottlenecks)
- roadmaps for critical sections of the TEN-T network
- good practise guidelines for implementation of the GNS concept (a manual that shall serve as guidance for waterway administrations on how to achieve and maintain a Good Navigation Status on the European waterway network by 2030)
- exemptions criteria (criteria for justification of exemption of the minimum requirements on draught (2.5 m) and heights under bridges (5.25 m), in accordance with article 15 of the TEN-T guidelines)

The paper will focus on the guidelines towards achieving a Good Navigation Status and on exemptions criteria for not reaching the TEN-T minimum requirements (related to draught and height under bridges).

INTRODUCTION

One of the objectives of the Trans-European Transport Network (TEN-T network[4]) is to ensure that European waterways are well integrated in the European transport system, promoting as much as possible inland navigation as a sustainable transport mode. The TEN-T guidelines stipulate that, by 2030, navigable waterways of European interest have to achieve "good navigation status". This means that these waterways have to help in reaching the full potential of inland navigation in Europe. However, the TEN-T guidelines do not provide a definition for GNS. On behalf of the European Commission a pan-European consortium conducted a study (*Good Navigation Status – Good Navigation Status in accordance with Article 15(3)b of the TEN-T guidelines*) in order to define the GNS concept together with the Member States, river commissions and users.

The objective of the study is to substantiate the concept of GNS referred to in article 15(3)b of the TEN-T guidelines. This article stipulates that "rivers, canals and lakes are maintained so as to preserve Good Navigation Status while respecting the applicable environmental law". More specific, the study specifies, in close cooperation with relevant experts, a broadly accepted concept of GNS

[1] Flemish Ministry of Mobility and Public Works (Belgium), sim.turf@mow.vlaanderen.be

[2] Viadonau, Planco, Inland Navigation Europe, STC-NESTRA and the Flemish Ministry of Mobility and Public Works

[3] Regulation (EU) No 1315/2013 of the European Parliament and of the Council of 11 December 2013 on Union guidelines for the development of the trans-European transport network.

[4] https://ec.europa.eu/transport/themes/infrastructure/about-ten-t_en

and a common methodology that allows a sufficient level of differentiation to the various corridors and specific demand requirements and transport characteristics.

The main outcomes of the study are:

- a concept for good navigation status,
- a network assessment (identify the existing bottlenecks)
- roadmaps for critical sections of the TEN-T network
- good practise guidelines for implementation of the GNS concept (a manual that shall serve as guidance for waterway administrations on how to achieve and maintain a Good Navigation Status on the European waterway network by 2030)
- exemptions criteria (criteria for justification of exemption of the minimum requirements on draught (2.5 m) and heights under bridges (5.25 m), in accordance with article 15 of the TEN-T guidelines)

This paper will focus on the guidelines towards achieving a Good Navigation Status and on exemptions criteria for not reaching the TEN-T minimum requirements (related to draught and height under bridges).

I represented the Flemish Ministry of Mobility and Publics Works in the pan-European consortium that conducted the study between January 2016 and December 2017.

DEFINITION OF GOOD NAVIGATION STATUS AND IMPLICATIONS

Good Navigation Status definition

The following definition was developed during the study based on the desk research and consultation of the experts and stakeholders:

“Good Navigation Status means the state of the inland navigation transport network, which enables efficient, reliable and safe navigation for users by ensuring minimum waterway parameter values and levels of service”

Moreover, GNS is to be achieved considering the wider socio-economic sustainability of waterway management

Good Navigation Status for inland waterways part of the TEN-T Network

The waterways of international importance included in the TEN-T Network are intended to be part of a sustainable transport system serving the needs of the EU Internal Market. This concerns the waterways of the core and comprehensive TEN-T Network, while for inland waterways the core network equals the comprehensive network.

The GNS shall address the TEN-T Network from the legal point of view. Good Navigation Status has to be achieved (and thereafter preserved) by 31 December 2030 according to the article 38 of the TEN-T guidelines.

The legal text from the TEN-T guidelines is Article 15.3:

Transport infrastructure requirements

1. Member States shall ensure that inland ports are connected with the road or rail infrastructure.

2. Inland ports shall offer at least one freight terminal open to all operators in a non-discriminatory way and shall apply transparent charges.

3. Member States shall ensure that:

(a) rivers, canals and lakes comply with the minimum requirements for class IV waterways as laid down in the new classification of inland waterways established by the European Conference of Ministers of Transport (ECMT) and that there is continuous bridge clearance, without prejudice to Articles 35 and 36 of this Regulation.

At the request of a Member State, in duly justified cases, exemptions shall be granted by the Commission from the minimum requirements on draught (less than 2,50 m) and on minimum height under bridges (less than 5,25 m);

(b) ***rivers, canals and lakes are maintained so as to preserve good navigation status, while respecting the applicable environmental law;***

(c) rivers, canals and lakes are equipped with RIS[5]*.*

The GNS concept aims to fully respect the competences of national authorities in line with the subsidiarity principle and to ensure a common approach for administrations sharing the responsibility for inland waterways of international importance.

Geographic coverage of Good Navigation Status

The following map presents the waterways which belong to the TEN-T Network.

Figure 1 : Map of TEN-T Inland waterways

It is clear that GNS is not limited only to the "Core Network Corridors[6]", it has a wider scope. It does cover all waterways according to article 38 of the TEN-T guidelines including for example the (isolated) inland waterways in Sweden, Finland, Lithuania, Italy, Portugal and Spain. Moreover, although not part of the TEN-T Network, also smaller waterways (e.g. CEMT II and III class waterways) and waterways in non-EU Member States may benefit from application of the GNS concept and related good practices in waterway planning and maintenance.

The GNS concept is based on best practices and state of technology in the EU and is valid as well for inland waterways of international importance in EU neighboring countries. Through the presentations and discussions about GNS at the 60th and 61st Working Party meetings on Inland Waterway

[5] River Information Services

[6] http://ec.europa.eu/transport/infrastructure/tentec/tentec-portal/site/maps_upload/SchematicA0_EUcorridor_map.pdf

Transport at United Nations Economic Commission for Europe (UNECE) in Geneva (Switzerland), it became clear that representatives from countries such as Ukraine and Moldova are also very interested in the GNS concept and application. This will help to facilitate efficient international trade and transport with the EU and to develop inland waterway transport in these countries.

Good Navigation Status Components

The following scheme presents the components of GNS with the distinctions between hard and soft components:

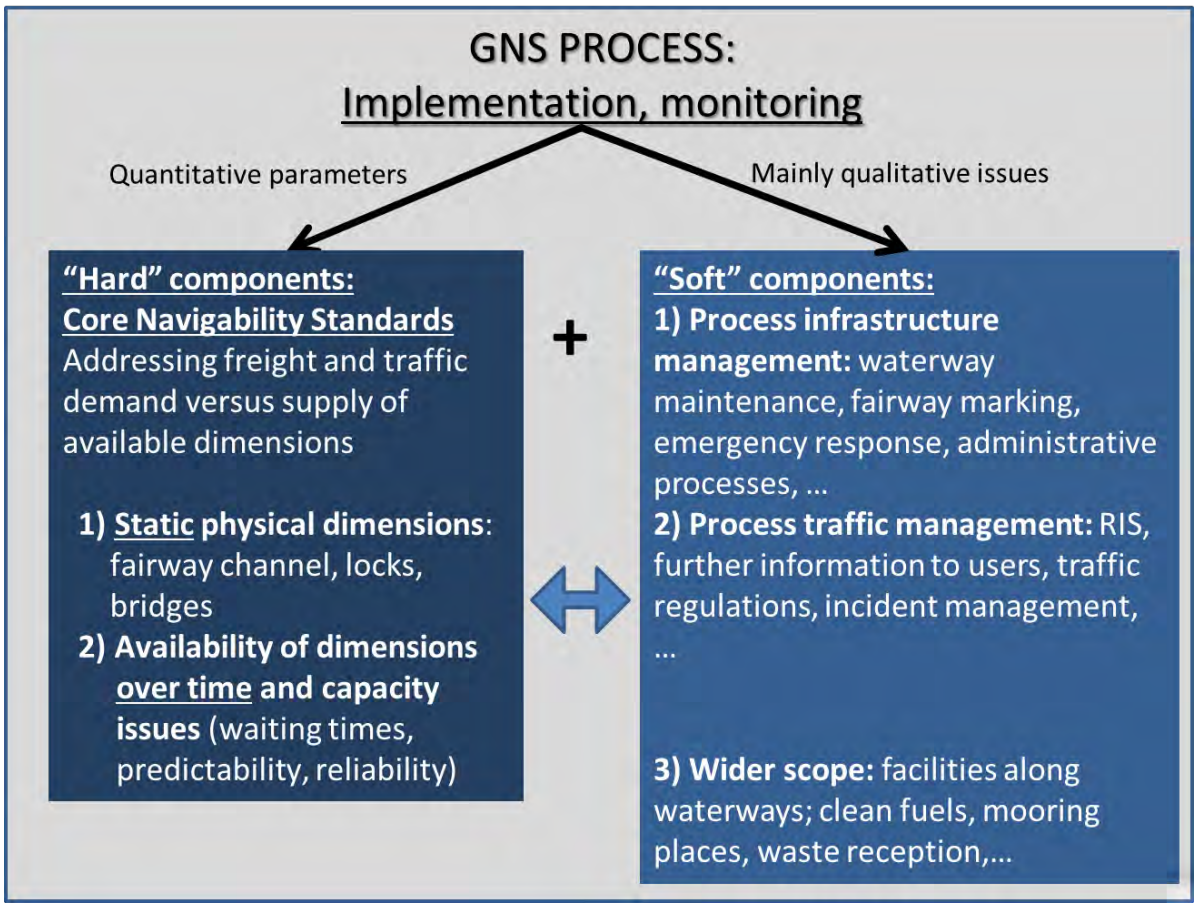

Figure 2: Schematic view on the GNS Concept

It shall be noted that external developments shall be taken into account in the GNS process. This may be the development of transport demand (e.g. shifting freight flows origin-destinations, growing/decreasing commodities, etc.), impact of climate change (changing water levels) as well as innovations which may lead to new possibilities to improve navigation on waterways and the waterway management (e.g. more advanced surveying and monitoring approaches).

Specification GNS "hard" components

- The "hard" components shall have the following characteristics:
  - focus on physical waterway infrastructure as direct output of waterway management activities and measures;
  - coherent set of measurable quantitative indicators (presenting the parameter value) applicable to the entire TEN-T waterway network identified according to a common methodology making GNS measurable and comparable on sections of the TEN-T waterway network;
  - they are directly targeted by TEN-T guidelines and/or (trans)national agreements and regulations such as the European Agreement on Main Inland Waterways of International Importance (AGN).

- The indicators for GNS “hard” components relate to the physical waterway infrastructure and its use. They will:
  - describe the dimensions of the navigation channel in rivers, canals and lakes (e.g. depth, width, height standards) and of locks, ship lifts and bridges, which are determining the vessel dimensions and will allow a comparison with the target parameter value (e.g. current draught versus target draught);
  - describe the availability of the navigation channel (e.g. closures, available draught during the year) and the availability and capacity of locks, ship lifts and moveable bridges.

- For GNS ”hard” components, at the request of Member States, exemptions may be granted by the European Commission from the TEN-T minimum requirements: in case the target value on the draught (2.5 m) and height under bridges (5.25 m) cannot be reached because of justifiable reasons.

Concerning the “hard” components, it is important to create common understanding where the TEN-T minimum requirement, related to draught and height under bridges, apply. The TEN-T requirements apply specifically to the navigable channel: the part of the waterway in which a targeted depth, width and vertical clearance (navigable cross-section) is maintained to enable continuous navigation.

In relation to the targeted depth, the TEN-T requirements explicitly mention the target value on the draught of the vessels, which is the vertical distance between the waterline and the lowest edge of the keel of a vessel. As regards “draught” for the minimum requirement in the TEN-T guidelines (2.5 m as mentioned above), this is seen as a value of least 2.5 m of possible draught of the vessel while still being able to safely navigate on the section of the TEN-T Network. Local targets shall apply for the respective depth of the navigation channel, taking into account the appropriate safety margins between the bottom of the river, lake or canal and the keel of the vessel. For rocky bottoms, this will be a higher safety margin compared to soils that consist of clay or sand. For the Rhine for example an ‘under keel clearance’ is typically applied between 0 and 50 cm. Moreover, for developing realistic and attainable (local) targets and compliance to the TEN-T requirements for vertical dimensions, waterway administrations have to consider occurrences of variation in water levels and longitudinal and cross currents, in both rivers and canals. Water level fluctuations in waterways occur as a result of differences in discharge, tides, seasonal variations, wind setup, translation waves etc. These fluctuations affect the dimensions of free-flowing rivers and impounded (regulated) waterways, but also causes variations in canals with fairly fixed canal water level.

Regarding free-flowing river sections, target values should be related to reference water levels in these sections, in order to reflect the natural and statistical variations in water discharge. The reference high and lower water levels are of particular importance for the design of the waterway, which refer to the water levels at which the full functionality of the waterway is available to for inland navigation. Higher or lower water levels, relative to the determined reference water levels, may result into restrictions to height under bridges and waterway profile (even obstruction). When determining the reference water levels for a waterway, the probability, severity and duration of the restrictions must be taken into consideration, in case the water level exceed the range of reference water levels. The reference water levels, both high and low, are set by the water management authority and laid down in its management plan.

Specification GNS “soft” components

The ”soft” components include both process-related management aspects of infrastructure (e.g. maintenance, marking) or of traffic (e.g. information to users), which contribute to an improved score on the indicator linked to the ”hard” components. Moreover, the soft components are a compilation of processes and utilities that determine and affect the level of service on and along waterways. For example, improved maintenance processes shall provide a better value for the actual depth (available draught) of the navigation channel of the section. Another example is the more accurate information and predictions about the water levels which allows ship-owners to increase the payload (transport efficiency).

Furthermore, soft components may optionally address a wider[7] scope of inland navigation infrastructure which is not directly related to navigation itself (e.g. facilities along waterways such as

[7] beyond navigation channel, locks, ship lifts and bridges

for clean fuel bunkering, waste disposal, resting places, car-lifts, shore-power, internet connections). For some of these elements also a legal reference is found in the TEN-T guidelines.

Furthermore, it shall be remarked that port, terminal and handling facilities are of key importance to achieve a competitive inland waterway transport operation. However, in Article 15.3b of the TEN-T guidelines GNS is addressing rivers, lakes and canals defined under (Article 14.1 a),b) and c)). Article 15.3b does not explicitly mention the status of related infrastructure, inland ports, associated equipment, telematic applications (RIS) or connections of the inland ports to the other modes in the TEN-T Network. It can therefore be concluded that from a legal viewpoint the focus shall be the quality of the fairway channel.

GNS ”soft” components have the following characteristics:

- Infrastructure and traffic management process components are important for GNS as they influence the level of ambition and achievement of the targets for the GNS ”hard” components (e.g. actual available draught and waiting times).
- The impact of introducing GNS ”soft” components might vary from region to region, depending for example on whether infrastructure management processes are already in place or have to be newly introduced
- Specific EU regulations apply for these components:
    - Implementation of standards set out in the RIS Directive on the comprehensive network (Article 15.3 c)
    - Implementation of the standards set out in the Clean Fuels Directive on the core network (Article 39.2 b)

”Soft” components are not always measurable in a quantitative manner on the TEN-T Network at the level of specific sections. Some can be monitored by means of qualitative descriptions about processes covering multiple sections of the TEN-T Network or even entire corridors. An example may be the description of the information systems in place to provide forecasts about the expected water level situation on the section of the waterway network. (pan-European consortium (2017))

MINIMUM STANDARDS OF A PROCES ON GOOD NAVIGATION STATUS DEVELOMENT

The GNS concept shall include minimum standards for both the process and methodology for achieving GNS in a systematic way for the sections of the TEN-T Network. Member States shall incorporate the GNS process in their waterway management plan. Some countries with a long standing history of inland waterway transport and a large inland waterway transport market will already have these processes into large extent and it makes no sense to repeat or replace what is already there. Consequently, no specific GNS development plan is needed for such situations in order to avoid administrative burden. However, other countries may develop GNS development plans in order to ensure that GNS is being implemented. Furthermore, such plans including GNS processes may be a pre-requisite to apply for co-funding from the European Union for rehabilitation and upgrading works.

Scope of the GNS process: towards GNS in waterway management plan

The GNS process primarily focuses on the “hard” components, or the physical dimensions that make up the core navigability standards (navigation channel – width/depth, lock availability and bridge clearance) on the river, lake or canal.

Furthermore, in order to avoid unnecessary and unacceptable administrative burden for Member States and waterway managers, it is clear that it does not make sense to run again a full-fledged GNS process on stable and well performing waterway sections that already fulfil core navigation standards over a longer period of time. The GNS process and GNS development plan shall focus on the most relevant, critical and volatile issues. Especially sections that have a combination of the following situations shall be in the focus of a GNS development plan:

- Free-flowing waterways: variable width, depth or height dimensions usually occur on free-flowing river sections. These limitations (or rather their unpredictable variations) have a negative impact on the reliability and economic efficiency of inland waterway operations. In the absence of frequent maintenance or rehabilitation works, the set targets for the reference low water level will be compromised, causing insufficient depth on too many days to be able to use

the possible draught of the vessel. As a consequence, inland waterway operators (and their customers) are faced with deteriorated load factors and fluctuating and high freight rates. In many cases fluctuation is due to unavoidable natural circumstances (lack of precipitation), but it may be aggravated due to lack of maintenance or rehabilitation. Severe fluctuations of the available navigable channel depth reduce the attractiveness and competitiveness of inland waterway transport. If there is poor anticipative management, specific attention shall be given to remedial measures and rehabilitation that improve performance of the sections.

- Sections with limited lock availability: limitations in lock availability and capacity will in general lead to unpredictable delays and waiting times. This has a direct negative impact on economic efficiency and reliability of inland waterway operations. Consequently, the share or non-productive operational hours is raised and the on-time reliability of inland waterway transport – usually one of the strongest competitive factors of inland waterway transport – is impaired. GNS measures may aim at increasing the capacity or improving the performance.
- Sections with too limited width, depth or height dimensions: curve radii, width of canals and height of bridges (with generally stable dimensions) can be bottlenecks in certain corridors. The GNS process should be aimed at identifying such limiting infrastructure bottlenecks and produce solutions for their remediation.

A focus on these “hard” or physical components of the waterway infrastructure is legitimate, as these components are direct outcomes of any waterway management measures on the one hand and have the largest economic impacts on inland waterway transport operations on the other. User consultation is a key mechanism to identify bottlenecks in the infrastructure and to discuss the possible solutions.

Key characteristics of a Good Navigation Status process

The proposed process to develop GNS is viewed as a continuous improvement cycle. The proposed process should fulfil the main attributes of integrated waterway management:

- Targeted: Every waterway maintenance, management or rehabilitation activity should be performed within the framework of defined targets, e.g. target values, levels of service, etc.
- Strategic: For a coordinated, effective and efficient achievement of targets, a specific waterway management strategy should be applied, aiming for achieving and maintaining GNS at least by the time-horizon 2030 and maintaining the status from 2030 onwards.
- Multi-disciplinary: Waterways are not only traffic routes but are characterized by a variety of other uses with sometimes conflicting priorities.
- Participatory: Due to the multi-disciplinary character of waterways, participatory management is advisable in order to understand and respect the other uses of waterways. All relevant stakeholders should therefore be engaged in the planning process to achieve and maintain GNS.

in addition, discussions with stakeholders and waterway managers revealed that the GNS process should fulfil following additional requirements:

- Fact-driven: the process should create transparency for all involved parties, that is, (non)compliance with target values should be easily monitored by means of selected performance indicators.
- Minimum administrative burden: the process and reporting efforts should be minimised by means of using available data and digital sources to the maximum extent possible, possibly supported by the EC providing funds to develop the data and interface with TENtec and the legislative backbone (e.g. RIS Directive). Furthermore, it should be pursued to harmonize available databases (e.g. UNECE Blue Book, TENtec and national waterway databases) and mitigate multiple requests and delivery of similar data.
- GNS process as a means to an end: data collection and reporting is not a goal in itself: the GNS process should ultimately result in a well-functioning European waterway system in line with the provisions of the TEN-T guidelines, which is verifiable by monitoring the GNS KPIs on the TEN-T Network and through feedback from transport users, properly taking into account specific conditions such as reference water levels.

It is not the intention of the proposed GNS process to identify or re-define target dimensions for waterway sections at the start of each process cycle. The existing national and supra-national regulations and regimes provide in general a good starting basis for improvement cycles aimed at reaching already agreed targets values. Through the study it became clear that on many waterways meeting the current targets is already challenging (e.g. having sufficient draught on waterways such as the Danube, Elbe and Oder).

On the other hand, the proposed GNS process could provide guidance to waterway managers on how to determine adequate targets for navigation channel dimensions (also for waterways not meeting CEMT[8] IV requirements). This shall be part of a long-term vision or a plan to implement a cyclical process for reaching and maintaining GNS, also based on stakeholder consultations. In this way, the GNS process contributes to improving and monitoring navigability conditions on a permanent basis, supported by waterway administrations experienced in long-term planning and working in cyclical processes.

The proposed GNS process contains six main steps, which are described in the following sections.

The six steps in the proposed minimum GNS process

Based on various good practice examples the main elements of a minimum GNS process have been formulated and structured in six process steps.

Some of the proposed process steps are already part of the normal procedures in various countries. They therefore reflect usual practice in some countries and would be easily accepted by stakeholders in these countries, notably the waterway managers. A GNS Plan shall refer to these good practices and available documents and waterway management plans. The main added value of this process description is based on the fact that for the first time all process steps are consolidated into one cyclical process, inspired by the good practices and the best process elements encountered throughout Europe during the study.

The proposed GNS process uses the best of both (or rather more) worlds. The resulting GNS process shall normally be carried out in yearly cycles. As it is a cyclic process, the GNS process can basically start in any of the process steps (i.e. should not necessarily start in the monitoring phase). In any case, a description and evaluation of the status-quo is needed as an initial starting point. This may lead to a review of targets and specification (see grey circle).

Achieving GNS by 2030 will require deployment of a process which is characterised by the following six steps:

[8] Classification of an inland waterway according to the European Conference of Ministers of Transport.

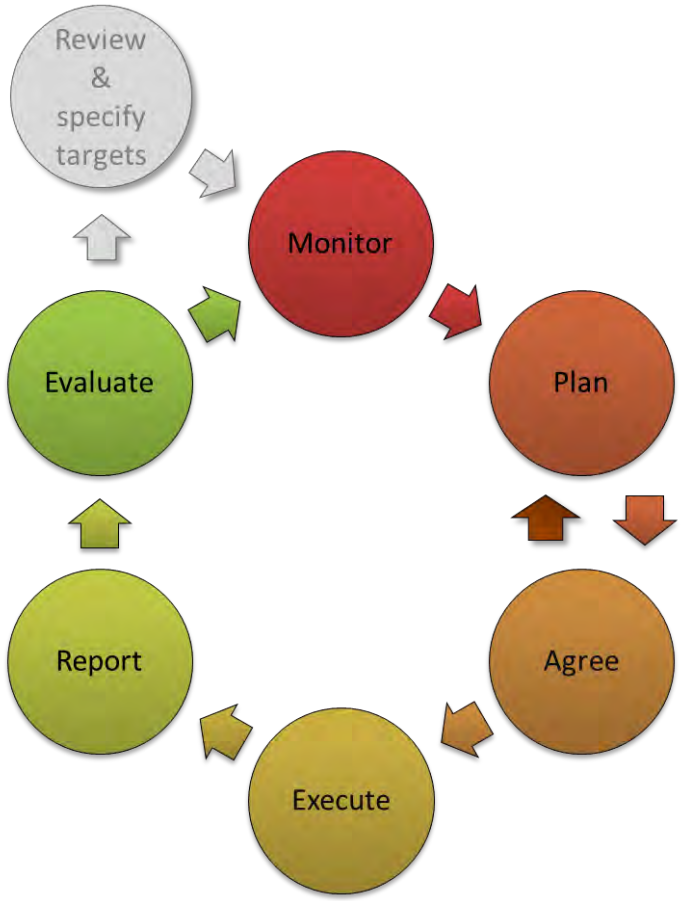

Figure 4 : Schematic view on the six process step to achieving GNS

Step 0: Review & specify targets

It is not the key objective of the proposed GNS process to identify or define new target dimensions for waterway sections at the start of each cycle. Target review and specification is therefore not included as a default, but as an optional, initial process step (if needed). Strategic in-house guidelines and targets, which pertain to fairway maintenance, are normally already in place. Only if overall waterway management targets are apparently lacking with a view to reaching GNS by 2030 (e.g. compared to TEN-T minimum standards on draught and bridge clearance) or if evaluation activities (Step 6) lead to the conclusion that waterway management targets need to be revised or refined, a consultation of stakeholders shall be initiated. This as input for the process to (re)define target values and to agree on a long-term vision to reach the (re)defined target values to achieve and maintain GNS.

Step 1: Monitor and analyse status of the waterway

Topical data on the “hard” components, i.e. the physical status of the waterway are collected in the first step for the TEN-T inland waterways, and optionally/voluntarily this may be extended to smaller waterways and non-EU waterways. Closures for navigation of waterways and the current state of the navigation channel (depth/width) shall be monitored on the basis of hydrographic riverbed surveys. Furthermore lock closures and waiting times at locks and lock availability shall be monitored, for instance through data from electronic lock dispatching tools. Based on the analyses of collected data the most critical waterway sections in the particular year shall be identified.

Step 2: Plan measures

At the end of Step 1 a list of bottlenecks or critical sections in the waterway network is identified by the waterway managers and transport users in view of reaching GNS by 2030 latest. It shall take into account existing plans to improve the navigation conditions. Based on these monitoring results and analyses, the remedial and/or preventative actions and measures need to be defined, planned and presented in waterway management or GNS Plans prepared by Member States. The remedial and/or preventative measures need to be specified and planned, so they can be presented and discussed with stakeholders (Step 3) and later be executed (Step 4). The stakeholders to be officially involved (and to be granted the status of a party to the approval procedure) in the planning phase shall depend

on national provisions and the scope of the project (e.g. navigation authorities, land-owners, national park authorities). A clear and important example in this respect is the close interaction that shall be organised with the environmental requirements and interests stemming from the EU Water Framework Directive (WFD) and the objective to reach Good Ecological Status on European waters.

Step 3: Agree on measures

Stakeholder engagement and acceptance is key to the success of the GNS process. Administrations in charge of maintaining and improving the performance of waterways for navigation need to include stakeholders at various levels and from multiple fields of expertise. Especially critical waterway sections on which the different uses (e.g. ecology, flood protection, recreation) are conflicting or where the achievement of GNS is most heavily disputed will require a process in which all different stakeholders and interest groups are integrated, in order to come to commonly accepted solutions. The basic aim should be the integration of all relevant interests (shipping industry objectives, environmental objectives, fishery, etc.) into the design of measures, thus preventing later barriers and significantly reducing the amount of potential compensation measures. Successful good practices on stakeholder engagement are characterised by regular, recurring and fact-based communication.

Step 4: Execute measures

In most European countries works related to maintenance and improvement activities are carried out by private contractors on the basis of framework agreements covering a time span of several years. Before actual start of the works a briefing meeting shall be carried out. A meeting is scheduled with the contractor in which the details for the measures are finalised. During the maintenance works, work safety supervision as well as ecological and local/technical site supervision should be carried out. If legal or ecological issues occur during the maintenance measures, they have to be clarified in cooperation with involved experts.

Step 5: Report outcomes

The outcomes of fairway management measures have to be properly documented and reported. First of all, the work of possible contractors has to be monitored and controlled. The reports drafted by the (ecological and local) site supervision as well as the final hydrography survey of both the dredging and the dumping sites are analysed for this reason. In addition, information necessary for monitoring of performance indicators is collected. Data are not only processed nationally, but key performance data should also be transmitted to the TENtec database, in order to maintain a topical overview of the navigation status of the various European waterways.

Provision of continuous and target group-specific information on the state of the fairway to the users of the waterway and other stakeholders is key to the GNS process. For example, good practices from the Danube corridor have shown that regular and continuous ex post information on fairway management activities (e.g. dredging activities, fairway channel relocation, hydrographic surveying, lock revision activities) as well as their outcomes (e.g. number of days per month with fairway channel depth of more than 2,50 m, average waiting times at locks) contributes to enduring and committed stakeholder involvement in the GNS process.

Step 6: Evaluate measures

The term "evaluation" is understood as the assessment of the effects that measures have to maintain or upgrade the status waterway with view to reaching GNS targets. This concerns for example the effects of fairway maintenance and rehabilitation measures (i.e. maintenance dredging works or repositioning the course of the navigation channel) on the availability of targeted navigation channel indicators. When it comes to evaluation of width/depth dimensions, it is based on monitoring the hydro-morphological changes in the riverbed and the monitoring of ecological effects of measures. Regarding measures addressing lock availability and bridge clearance, mostly automated data sources (e.g. RIS/NtS[9]) can be used to analyse and evaluate impacts of measures over the past period.
In order to increase customer satisfaction, waterway administrations shall make use of consultative instruments. Anonymous user surveys help to evaluate their performance in connection with regular maintenance activities, or the provision of information, etc.

[9] Notices to Skippers

Organisational approach for the GNS process

This section comments on the possible organisational setting in order to implement the GNS process in practice, while ensuring adequate coordination at the EU level, for the purposes of the functioning of the TEN-T waterways network.

It shall be noted that GNS is a new requirement introduced by the TEN-T guidelines. Administrations and stakeholders affected by the new requirement have to act and address the requirements consequently. The adaptation should not result in additional work load without added value, but rather on a possible change of working practices, on the basis of strengthened cooperation at river basin and European levels, where needed. It shall be noted that many waterway managers already have such GNS processes and cross-border coordination processes established. Additional processes and organisational structures may therefore not always be needed.

In a preliminary manner, the organisational requirements for implementing in practice the GNS process can be summarised in the following points, distinguishing the national level (level 1), the connected international waterways (level 2), the European level (level 3) and pan-European level (level 4):

National Level (level 1)

- A national body will be assigned in charge of the GNS process in each concerned Member State. Typically, this will be the national Ministry of Transport or administrations in charge of national inland waterways.
- The body contributes to the identification / implementation of infrastructure improvements, maintenance works, process traffic management, etc. ("hard" and "soft" GNS components).
- The body identifies sections where targets for the "hard" GNS components cannot be reached for physical or operational reasons and prepares the corresponding requests for exemptions to the minimum TEN-T infrastructure requirements.
- The national body establishes the waterway management plans or similar documents, incorporating the GNS processes. If needed a national GNS development plan is prepared, e.g. in case of processes not yet existing in national waterway management plans, in case of exemptions to be requested or in case of requests to the EU for co-funding of rehabilitation or upgrading projects. The body ensures proper involvement and consultation of stakeholders about service quality levels in the different sections of the inland waterway network and provides information.

Connected international waterways (level 2)

- A body in charge of international coordination of the GNS processes (normally the International River Commissions and/or coordination bodies of macro-regional strategies existing in the EU).
- The international body can act as platform for monitoring the effective achievement of GNS, coordinated cross-border actions and may propose measures adapted to international waterway in question.
- The international body provides technical advice to national authorities, may conduct GNS related studies for the river basin, etc.

European level (level 3)

- European Commission provides a database with up-to-date information on the GNS status of each inland waterway transport section in the TEN-T Network (TENtec system, see figure 5 below), which can be used as a basis for monitoring and network assessments for GNS.
- European Commission provides for a cooperation framework with national bodies, inland waterway transport industry sector representatives, international River Commissions (for example, by means of a formal "Expert Group"), supported by monitoring studies and network assessments (e.g. using TENtec data).
- Cooperation at EU level serves to update and further elaborate GNS guidelines and evaluate, in due time, the progress achieved.
- In the cooperation framework, European Commission consults with the group proposals for granting exemptions.

- Inland waterway transport infrastructure works needed for achieving / preserving GNS are identified and noted in the TEN-T Corridors Work Plans. EU Funding / Financing measures are envisaged for those works in the context of CEF / Regional Funds actions.

Pan-European level (level 4)

- UNECE may consider to support the GNS process by means of alignment between GNS development plans and TENtec with AGN and the Blue Book, thus avoiding double work.
- In particular, the coordination and alignment of the navigability standards between EU member States and neighboring countries may be a topic to address at the UNECE platform. Seamless transport across the whole of Europe will also require coordination with non-EU Member States. (Quispel M., Armbrecht H., Turf S. et al (2017))

TENtec

TENtec is the European Commission's information system to coordinate and support the Trans-European Transport Network (TEN-T) policy. TENtec has two main functions:
1.The collation of technical, geographical and financial data to be used to inform policy-making and political decision-making processes related to TEN-T and its associated funding programme, the Connecting Europe Facility (CEF). The core TENtec modules deployed for these purposes are OMC (Open Method of Coordination) and iReport, both of which are accessible through the TENtec Private Portal;
2.Provision of technical support to the Innovation and Networks Executive Agency (INEA) and its grant management functions. This incorporates supporting the necessary workflows for issuing grant agreements after completion of the selection cycle for new projects, including proposal submission and reception, and the required web interfaces. The core TENtec modules deployed to meet these requirements are eSubmission services, Action Status Report, Project Follow-Up, Evaluation and Grant Agreement.
In addition to its primary dual function, TENtec also enables the European Commission to easily compile information and create timely reports and maps. This benefits all parties involved in TEN-T project implementation processes, providing greater transparency, data quality and a systematic up-to-date overview of the budget execution and technical implementation for each TEN-T/CEF project.
Another important function of TENtec is its capacity to act as a bridge to the ministries of Member States and other key stakeholders (DG REGIO, DG ENV, EIB and neighbouring countries), including support for transport modelling of future policy and budgetary scenarios, briefings, the mapping of TEN-T/CEF co-funded projects and other layers such as alternative fuels and secure and safe parking.
TENtec also played an integral role in the Core Network Corridor studies, providing vital data collection services and compliance maps built upon selected technical indicators, based on the TEN-T Regulation.
As regards inland waterway infrastructure, detailed data is being collected for the years 2014 and 2015 as regards the waterways, locks, bridge as well as ports and alternative fuel infrastructure. Included are 35 parameters for the inland waterway links, 8 parameters for locks, 9 parameters for lock chambers and 6 parameters for bridges. A number of parameters does address hard components of GNS. This concerns information on the CEMT classification, data on the dimensions of the allowed vessels, data on the maintenance targets for the navigation channel, reference water levels, waiting times at locks, the reliability of the dimensions (e.g. draught), the height under bridges and into what extent the local targets and minimum TEN-T requirements have been reached.
In order to minimise the administrative burden, as much as possible available sources are used to fill TENtec with the values for the parameters. This included also usage of (aggregated) data extracted from Notices to Skippers, Fairway Information Services and ECDIS and RIS Index, which have a legal backbone through the RIS Directive. Moreover, many data are rather static and do not change on a year-by-year basis.
More information about TENtec: **https://ec.europa.eu/transport/themes/infrastructure-ten-t-connecting-europe/tentec-information-system_en**

Figure 5: Explanation TENtec

EXEMPTIONS

This concerns exemptions for not reaching 2.5 m draught or 5.25 m height under bridges according to the article 15(a) in the TEN-T guidelines.

At the request of a Member State, in duly justified cases, exemptions shall be granted by the Commission from the minimum requirements on draught (less than 2,50 m) and on minimum height under bridges (less than 5,25 m).

The TEN-T guidelines require that river, canals and lakes that are part of the TEN-T Network comply with the minimum requirements for class IV waterways according to the CEMT, which prescribes the horizontal dimensions (width and length of the allowed vessel). In addition, the TEN-T guidelines state that as regards the vertical dimensions at least 2,50 m draught for the vessel and 5,25 m passage height under bridges shall be available.

The rationale for the minimum requirements is that inland waterway transport on the TEN-T Network can only fulfil its transportation role when there is sufficient capacity for European cross-border traffic. Local waterway sections on the TEN-T Network which do not have sufficient draught and height under bridges may prevent inland navigation from providing efficient, reliable and punctual services. Such bottlenecks may hamper the functioning of the TEN-T Network and result in negative external costs undermining the full potential of inland waterway transport and its benefits for the EU Internal market.

Some sections of the inland waterways that have been included in Annex I of the TEN-T Guidelines do not meet the specified minimum vertical dimensions. According to the TEN-T Guidelines, infrastructure improvements would be needed to ensure that those sections meet minimum draught and height under bridges by 2030 (all TEN-T waterways are part of the TEN-T Core Network).

Nevertheless, the TEN-T Guidelines foresee the possibility of exemptions for the minimum draught of a vessel of 2.5 m and 5.25 m minimum passage height under bridges. That means that the sections in question can continue to be part of the TEN-T Network even if they involve a limitation on transportation capacity.

The TEN-T guidelines impose three procedural conditions to acquire an exemption for not reaching the minimum dimensions as regards draught and height under bridges:

- The request for exemption has to be formulated and submitted to the European Commission by the concerned Member States.
- The concerned Member State has to "duly justify" the request
- The European Commission has to approve the request.

The specific procedure and details as regards exemptions need to be formulated and decided upon by the European Commission. However, the following description can be provided as an example how the exemptions could be seen and applied. This description is based on the stakeholder consultations and meetings with experts which took place during the study on GNS.

Nature of the exemptions

In principle, it is conceivable to distinguish between "temporary", "permanent" and operational" exemptions. Such exemptions may be granted based on “ex ante” requests (e.g. permanent exemptions). However, exemptions may also be relevant on the basis of ex post assessments, for example, due to unforeseen circumstances, such as incidents which may block a link or bridge for a long time or due to long low water periods causing limited draught. The thresholds would need to be defined as regards when an exemption is needed, taking into account the added value of the exemption procedure in relation to the involved administrative burden.

Of course a "Temporary" exemptions shall be limited in time. For example, a Member State responsible for the inland waterway section affected by limitations for navigation in draught and/or height under bridges may require time beyond 2030 to execute infrastructure maintenance or works needed in order to meet minimum requirements as regards draught or height under bridges. The European Commission may grant a temporary exemption to bridge such a period.

In exchange, "permanent" exemptions would apply to sections where there is an overwhelming physical impossibility, risk of serious and irreversible environmental damage or otherwise overriding public interest reasons that prevent achieving the minimum requirements as regards draught and height under bridges for navigation.

In addition, it is conceivable to consider "operational" exemptions, for example regarding certain periods of the year where minimum draught cannot be achieved because of meteorological and hydrological conditions while taking into account the statistical method for the reference high/low water levels (e.g. extreme high water, extreme low water periods, ice).
Furthermore, incidents or infrastructure works may cause closures of inland waterways. These cases for “operational” exemptions can be identified and substantiated by means of the reference water levels applicable to the specific waterway stretch as well as thresholds for the duration of closures in relation to the cause or reason for the closure. Moreover, monitoring the dynamic draught levels and height under bridges as well the availability of the network (closures) can be an input for ex post assessments to judge whether an exemption is needed. Possibly this ex post assessment can be done with TENtec data stemming from Notices to Skippers and Fairway Information Services.

Impact of the exemptions

The impact of the draught and height under bridges limitations shall be considered. In principle, the impact can be seen as:

- Small: limitations do not seriously affect the basic functioning of IWT operations;
- Medium: there are traffic restrictions, but IWT operations can still be performed
- High: limitations are a serious TEN-T bottleneck.

Criteria can be defined for the classification, for example by means of calculation of the costs of the limitation for the transport industry. Furthermore, feedback and input from transport user organisations (e.g. EBU, ESO,) may be used to classify the impact. Such classification can also be related to priority setting, e.g. in relation to co-funding by the European Commission for rehabilitation works to improve the performance of the network and making the network compliant with the minimum standards as regards the draught and height under bridges.

Administrative matters to be considered

In connection with the procedure foreseen in the TEN-T guidelines, the following matters would require attention:

<u>Identification of sections requiring exemptions</u>

In advance of the final date for completion of the TEN-T Core Network (2030), waterways sections requiring exemptions for the draught and height under bridges should be identified based on the GNS network assessment and monitoring of depth of navigation channels and height under bridges. Limitations shall be identified and the impact on inland waterway transport operations shall be estimated (small, medium, high). Subsequently, the identification should clarify the nature of the required exemption (temporary, permanent, operational).

<u>Deadline for requesting exemptions</u>

The concerned Member States should request the exemptions to the European Commission well in advance of the 2030 final date. This concerns ex ante assessments, notably as regards the permanent and temporary exemption types. All concerned parties that use the waterways sections in question (operators in cross-European trade, shipping companies, countries/regions linked to the waterways in question, etc.) should be adequately involved. Concerned parties may also provide input or validate the classification as regards the impact on inland waterway transport operations (small, medium, high).

<u>Elements supporting the request for the exemptions</u>

Each waterway section is unique and the reasons for the exemptions would have to be examined on a case-by-case basis taking into account the local conditions.

Exemptions, depending on their nature (temporary, permanent, operational) would require, in principle, solid supporting justification on the basis of:

- Technical / engineering / hydro-morphological / hydrological explanations
- An assessment of the impacts for the environment

- Economic / funding / social arguments

Examination and justification of the exemptions by the European Commission

The responsibility of granting an exemption falls under the responsibility of the European Commission. Each waterway section is unique and, probably, the exemptions and their impacts would have to be reviewed on a case-by-case basis by the European Commission. The European Commission would have to consider possible conditions (e.g. time extensions, compensatory measures, alternative parameter targets to be achieved as regards draught and height under bridges).

Information to third parties

Third parties affected by exemptions to minimum requirements in a particular section of the TEN-T Network should be adequately consulted at the different stages of the process (examination of the request and final decision). (pan – European consortium (2017))

CONCLUSION

The GNS study was an important first step as input for discussion and exchange of knowledge and good practices to be continued on European, regional and national level. Important is to further specify the local targets for GNS, since this requires local knowledge on the market conditions and the hydrology and hydro morphology. Examples are the targets for the depth of the navigation channel and targets for the reliability of navigation.

Another element for further development is the issue of exemptions for not reaching 2.5 m draught and 5.25 m height under bridges. Discussions between the European Commission and Member States are recommended to further elaborate the procedures and approach. It is likely that this will be taken into account in the evaluation of the TEN-T Guidelines in 2023.

REFRENCES

Quispel M., Armbrecht H., Muilerman G.J., De Schepper K., Van Liere R., Turf S. (2017). Final report of the study on Good Navigation Status – Good Navigation Status in accordance with Article 15(3)b of the TEN-T Guidelines

Quispel M., Armbrecht H., Muilerman G.J., De Schepper K., Van Liere R., Turf S. (2017). Task 7 Report (Guidelines towards achieving a Good Navigation Status) of the study on Good Navigation Status – Good Navigation Status in accordance with Article 15(3)b of the TEN-T Guidelines

SYSTEMATIC TECHNIQUES FOR FAIRWAY EVALUATION BASED ON SHIP MANOEUVRING SIMULATIONS

Evert Lataire[1], Marc Vantorre[2], Maxim Candries[3], Katrien Eloot[4], Jeroen Verwilligen[5], Guillaume Delefortrie[6], Changyuan Chen[7] and Marc Mansuy[8]

SUMMARY

Ship Manoeuvring simulators are commonly used for training purposes. For research purposes the simulations can be human controlled on a full mission bridge simulator but the human interaction can be bypassed and the mathematical model of the simulator can be fed with different types of input. These different simulations types, *fast-time position captive*, *fast-time track captive, fast-time track predefined controls* and *fast-time track controller*, as well as *real-time simulation* are explained and the merits of each type are illustrated with an example of a deep-drafted and wide vessel on the Canal Ghent Terneuzen.

1 INTRODUCTION

Over the last decades ship sizes have increased dramatically for different types of vessels (including container ships and LNG-carriers). Fairways often have not increased at the same rate. As a result, larger ships may now sail in areas that were originally designed for smaller vessels. In some cases new infrastructures, especially locks, make it possible for larger ships to get access to an existing canal which might lead to problems when the bathymetry of the canal is kept status-quo. The Knowledge Centre Manoeuvring in Shallow and Confined Water (www.shallowwater.be), which is a collaboration between Flanders Hydraulics Research (FHR) and the Maritime Technology Division of Ghent University, wishes to share their experience in evaluating and investigating possible bottlenecks in such situations. This paper presents some methodologies that are used to evaluate manoeuvres in shallow or confined water based upon simulation techniques.

Systematic investigation of ship manoeuvring in shallow and confined water is performed by Flanders Hydraulics Research (FHR) and Ghent University (UGent) through five different simulation techniques. Each of these techniques essentially relies on the same mathematical manoeuvring models which are nowadays available for a large range of sea-going and inland vessels at different loading conditions and under keel clearances (or water depth to draft ratio). Most ships in the simulator fleet have in-house developed modular mathematical models of the tabular type (Delefortrie *et al.*, 2016). New developments, updates, improvements and extensions are based upon research carried out in the Towing Tank for Manoeuvres in Confined Water (co-operation Flanders Hydraulics Research and Ghent University) or other test facilities available at FHR (lock access model, flumes, full-scale measurements).

In principle, the core of a mathematical model is a set of differential equations, i.e. the equations of motion of the ship, which express the equilibrium between inertial forces and moments on one hand and all internally and externally generated forces and moments acting on the ship on the other. The latter can be subdivided in hydrodynamic reaction forces and moments on the hull due to the ship's accelerations and velocity components through the water, the forces and moments induced by the ship's propulsion system and controllers (rudders, thrusters, …), hydrodynamic forces induced by the vicinity

[1] Post-doctoral assistant, Ghent University, Evert.Lataire@ugent.be

[2] Professor, Ghent University, Marc.Vantorre@ugent.be

[3] Post-doctoral researcher, Ghent University, Maxim.Candries@ugent.be

[4] Professor, Ghent University, Senior Researcher, Flanders Hydraulics Research Katrien.Eloot@mow.vlaanderen.be

[5] Senior Researcher, Flanders Hydraulics Research Jeroen.Verwilligen@mow.vlaanderen.be

[6] Senior Researcher, Flanders Hydraulics Research Guillaume.Delefortrie@mow.vlaanderen.be

[7] PhD student, Ghent University, Changyuan.Chen@ugent.be

[8] Researcher, Ghent University, Marc.Mansuy@ugent.be

of the lateral boundaries of the navigation area (bank effects) and due to the interaction with other ships (ship-ship interaction), forces and moments caused by waves, forces exerted by tugs, anchors, mooring lines, winches, contact with fenders and structures, and finally aerodynamic forces due to wind. It should be emphasized that all forces and moments of hydrodynamic origin are, moreover, significantly dependent on the water depth. This list is not exhaustive.

The number of differential equations of a mathematical manoeuvring model, i.e. the number of degrees of freedom (DOF), is minimum three (the horizontal degrees of freedom: surge, sway, yaw), often four (including roll) and maximum six (including the vertical motions: heave and pitch). The mathematical models used at FHR cover all six degrees of freedom, the models discussed in this paper will be mainly restricted to the three horizontal degrees of freedom. In case a 3 DOF or 4 DOF approach is used, the vertical degrees of freedom may be covered by a separate mathematical model which calculates the vertical motions, which are dominated by squat (sinkage and trim) in absence of waves.

Essentially, the following input is required to calculate the forces and moments formulated in the mathematical model:

- the ship's position (absolute, and relative to the horizontal and vertical boundaries of the navigation area), in all considered degrees of freedom;
- the ship's velocity components (over ground and through water);
- the ship's acceleration components (over ground and through water);
- the propulsion settings (e.g. propeller rate of revolution, pitch setting, …);
- the control settings (e.g. rudder angle, rate of revolution of bow/stern thrusters, …);
- the wave climate;
- the wind field;
- parameters w.r.t. other external forces (tugs, lines, …).

It should be mentioned that throughout this paper the term "position" is used for determining both the coordinates of the origin of a ship-bound coordinate system with respect to an earth-bound coordinate system, and the angular rotations between both systems. Therefore, the heading angle of a ship is included in the term "position". Similarly, "velocity components" and "acceleration components" refer to both linear and rotative components; e.g. a ship's rate of turn is also considered to be a velocity component. For a 3 DOF mathematical model, the position is given by (x_0, y_0, ψ), velocity by (u, v, r) and accelerations by ($\dot{u}, \dot{v}, \dot{r}$).

Among the different simulation techniques which will be discussed, a first distinction can be made between real-time and fast-time techniques. The authors are aware of the fact that these terms might have another meaning in a different domain of engineering sciences. In ship manoeuvring simulation, the term "real-time" means that the duration of a virtual, simulated event is equal to the duration the event would take in the real world, so that the real and simulated time scales are equal. This is typically a requirement if the input of the controls of the ship (rudder deflection, propeller rate, tug assistance, bow or stern thrusters) is given by a human (captain, wheelman, pilot, skipper), based on visual observations.

If there is no need for the simulation to take as long as it would take in reality, the simulation can be speeded up. The time needed for such a simulation is determined by the computing time required to run the calculations. Since the duration of the calculation/simulation is usually (much) shorter than real-time, these types of simulation are referred to as "fast-time" simulations (or, alternatively, simulations without human interaction). Four types of fast-time simulation will be discussed, each type having its own merits and disadvantages, whilst only one type of real-time simulation is considered. All five types will be described and discussed in Section 2, and applied to a bulk carrier sailing southbound on the Canal Ghent-Terneuzen, connecting the port of Ghent (Belgium) with the lock system in Terneuzen (the Netherlands) which gives access to the Western Scheldt and to the North Sea.

2 SIMULATION TYPES

In this section, four types of fast-time (FT) simulations will be considered: *fast-time position captive*, *fast-time track captive, fast-time track predefined controls* and *fast-time track controller*, as well as *real-time simulation*, involving human control. The distinction between the different types depends on the following characteristics:

- Real-time or fast-time;
- Predefined or free trajectory (captive or free-running);
- Predefined control settings; automated track control or human interference;
- Time dependent or independent output (steady or non-steady);
- Force output or trajectory output.

2.1 Fast-time Position Captive

The FT Position Captive type of simulation is the simplest of the four types of fast-time simulation. The mathematical model is used in a steady mode, which means accelerations are zero so their effect is not accounted for. The mathematical model calculates the forces and moments based on constant input values for the position (x_0, y_0, ψ), velocity components (u, v, r), propulsion settings, control settings, environmental (wind, waves, current) and external parameters. Due to the steady character, there is no time dependency (Table 1).

Due to the forced character of the simulation run, there is in general no equilibrium between the forces and moments acting on the ship and the external forces (Figure 1); therefore, the sum of forces and moments is expected to be non-zero. These forces and moments are available for further analysis as a function of the input parameters. Besides horizontal forces and moments, a similar approach can be followed for calculating vertical motions due to squat in case a separate mathematical model for vertical motions is available.

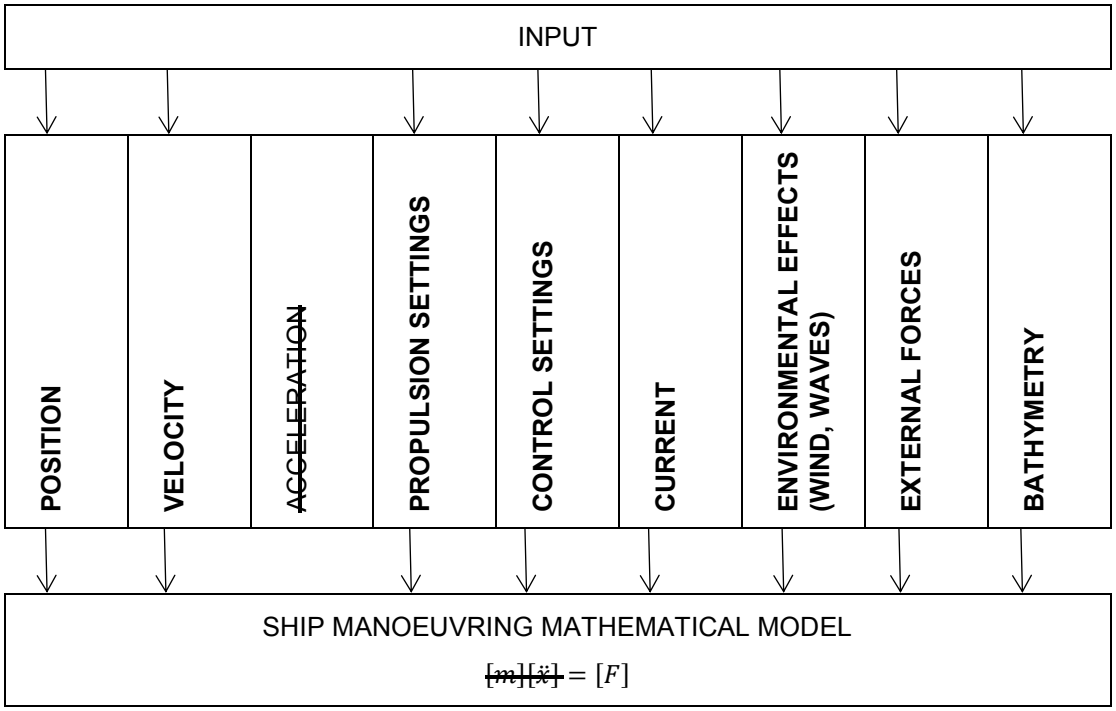

Figure 1 Calculation scheme of Fast-time Position Captive

This type of simulation can be used for investigating the effect of systematic parameter variations. As a first (simple) example, this type can be used to calculate the residing forces acting on a ship for a range of combinations of forward speed and propeller rates, which leads to a self-propulsion curve (u, n) of a ship at different water depths, at different lateral positions in a canal, etc. Similarly, the sensitivity of operational variables to parameter variations can be assessed.

Another application of this fast-time simulation is published in (Eloot, Verwilligen and Vantorre, 2007). A systematic study was carried out to determine the feasibility of a meeting manoeuvre between two Panamax vessels in the Culebra/Gaillard Cut, which is the narrowest section of the Panama Canal. It must be emphasized that the investigated situation is not up to date anymore, because in the meantime the Cut has been widened, deepened and straightened. The distance to the bank (or buoy line), the forward speed and three propeller rates were systematically calculated. The mathematical model provided a net yaw moment for each combination of forward speed, distance to the bank and propeller action. This yaw moment needs to be compensated by the rudder capacity, which can be obtained by re-running the simulations with maximum rudder deviation. As such the safety margin for the manoeuvre can be derived as plotted in Figure 2.

This technique can also be applied to assess which effort is required to keep a ship on a predefined steady track, and whether this effort can be realised by own controls or by means of tugs.

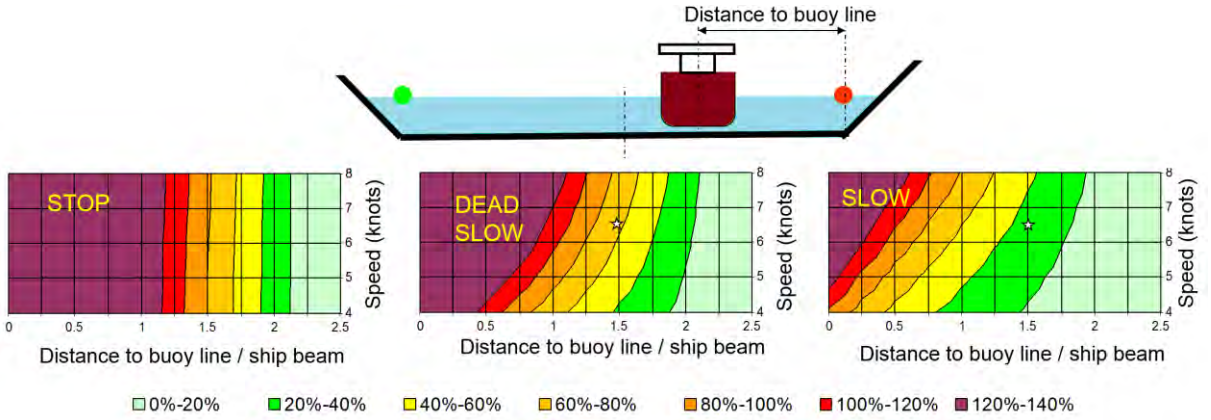

Figure 2 Required rudder capacity at different propeller rates and lateral positions from the buoy line

2.2 Fast-time Track Captive

The second type of fast-time simulation is very similar to the *FT Position Captive* but differs in the way it copes with accelerations. During the *FT Track Captive* simulations the vessel performs a predefined trajectory as a function of time by imposing the values for the horizontal acceleration components. At the starting time, the first calculation run uses the initial position and initial velocities from the input. The position of the next time step is only based upon the predefined accelerations. If the accelerations are all set to zero then the ship simply continues at the same speed in all directions (i.e. a rectilinear or circular trajectory, depending on the initial value for the rate of turn). As for *FT Track Captive* simulations, the trajectory of the vessel is prescribed, and local restrictions such as banks or other shipping traffic can be added to the simulation environment. The output of *FT Track Captive* simulations concerns time series of the net forces and moments that are computed by the mathematical model. Unlike *FT Position Captive* simulations, the forces originating from the ship's accelerations are taken into account during the calculations (Figure 3, Table 1).

One of the applications of this type of fast-time simulation is the comparison with full-scale measurements. During a full-scale measurement extra equipment is taken on board to measure the position of the ship with high accuracy (both in the horizontal as well as vertical directions) and to register the use of propeller and rudder. With these measurements the sailed track can be analysed and the accelerations (along all axes) derived from these accurate positions. This matrix with the accelerations $\dot{u}, \dot{v}, \dot{r}$, propulsion settings and control settings at every time step can be used as input for the *FT Track Captive* simulation. In this way, the full-scale measurement is replayed in the simulation. Since the position of the ship is directly linked to the input accelerations and not based on the forces and moments on the vessel, again there is no force (nor moment) equilibrium; as a result the output of the simulation run are time series of net forces and moments. The latter are of high interest for the validation of the mathematical model. In (Verwilligen *et al.*, 2015) a comparison is made between full-scale measurements on the inland vessel *MT Elise* and a *FT Track Captive* simulation.

Deviations between the original track and the simulated track may occur due to the accuracy of the integration of accelerations to positions.

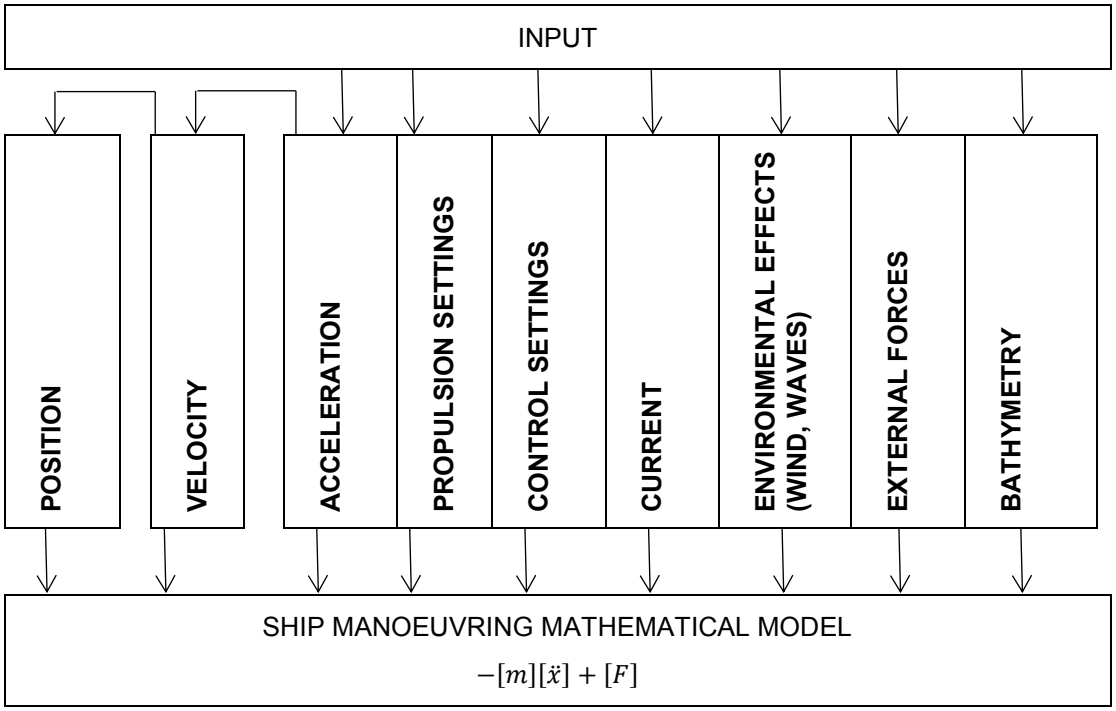

Figure 3 Calculation scheme of Fast-time Track Captive

2.3 Fast-time Track Predefined Controls

When applying the previously discussed simulation types, the equations of motions formulated in the mathematical model are not solved. This will be different for the simulation types described hereafter, where the mathematical model continuously solves a set of differential equations defining the manoeuvring behaviour of the ship. At every time step, typically 0.025 s, the forces and moments which act on the ship, are calculated; and superposed, and are transformed via Newton's second law into linear and rotative accelerations, which by integration lead to refreshed (linear and rotative) velocities and, finally, positions and directions.

The *FT Track Predefined Controls* method is therefore the first method with a total force equilibrium at every time step of the calculation (Table 1). In this type of simulation the net forces and moments are zero. As a consequence, the exact trajectory of the ship is only known after the simulation. The input for the simulation is, except for the initial time step t_0, the list of propeller rate, rudder deflection and tug assistance for every other time step. At every time step the mathematical model calculates all forces and moments, and with the superposition of all these forces and moments an acceleration (in all directions) is derived. Integration of these accelerations results in the velocity and position of next time step, so this is the first simulation type with a closed loop. In this type of simulation the simulated vessel sails freely in the environment. The simulation environment should not be laterally restricted, as one cannot predict the trajectory of the simulator vessel. Again, the force balance is respected at every time step throughout the simulation (Figure 4).

The most well-known example of *FT Track Predefined Controls* is the simulation of full-scale trials with a predefined procedure such as turning circle tests or crash stop tests.

In (Verwilligen *et al.*, 2015) the results of the full-scale measurement with the *MT Elise* are also used as input for this type of simulation. Instead of the derived accelerations, the full-scale measured rudder angle and propeller rate are used as input for the simulation. The output of the simulation is the followed trajectory (which deviates from the trajectory of the *MT Elise* because of differences between reality and simulation), speed and rate of turn. These outputs can be compared with the full-scale measurements and, when found satisfactory, details of the full-scale measurements can be investigated. For example the augmented resistance because of the high blockage as calculated in the mathematical model can

be further investigated and conclusions can be drawn on the real trip based upon the *FT Track Predefined Controls* simulation.

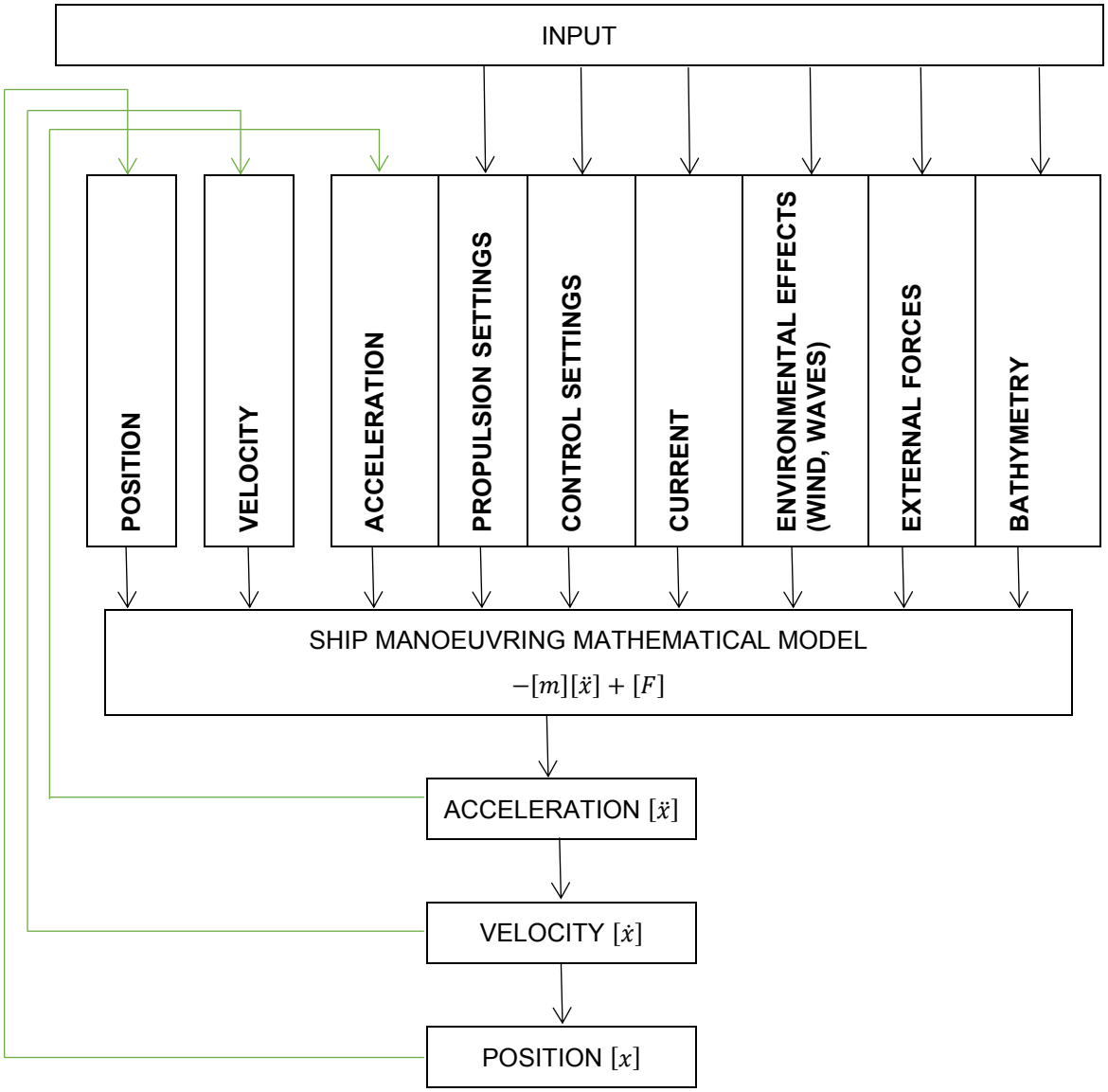

Figure 4 Calculation scheme of Fast-time Track Predefined Controls (closed loop in green)

The *FT Track Predefined Controls* results in a trajectory and manoeuvring behaviour which is more realistic because of the respected force balance but it is hard to duplicate an exact trajectory because the path of the vessel is unknown beforehand. Small deviations from the desired path on a narrow canal, for example, may result in excessive bank effects which then result in an unsuccessful simulation.

2.4 Fast-time Track Controller

This is the most advanced type of fast-time simulation. The simulation takes full use of the mathematical model and the controls of the ship (rudder and propeller) are changed in time through the Track Controller (Figure 5). This Track Controller is a type of simulated autopilot which steers the ship so it aims to follow a predefined path at a predefined speed. It uses a cost function with weight factors for different positions on the ship (e.g. at the bow, amidships and at the aft) so that the subsequent position (this is the feedback) of the ship which deviates least from the desired position is associated with the lowest cost. The number of positions that are considered in the calculations is also a setting. The input of this type of simulation is the desired trajectory and the settings of the Track Controller (Eloot, Verwilligen and Vantorre, 2009).

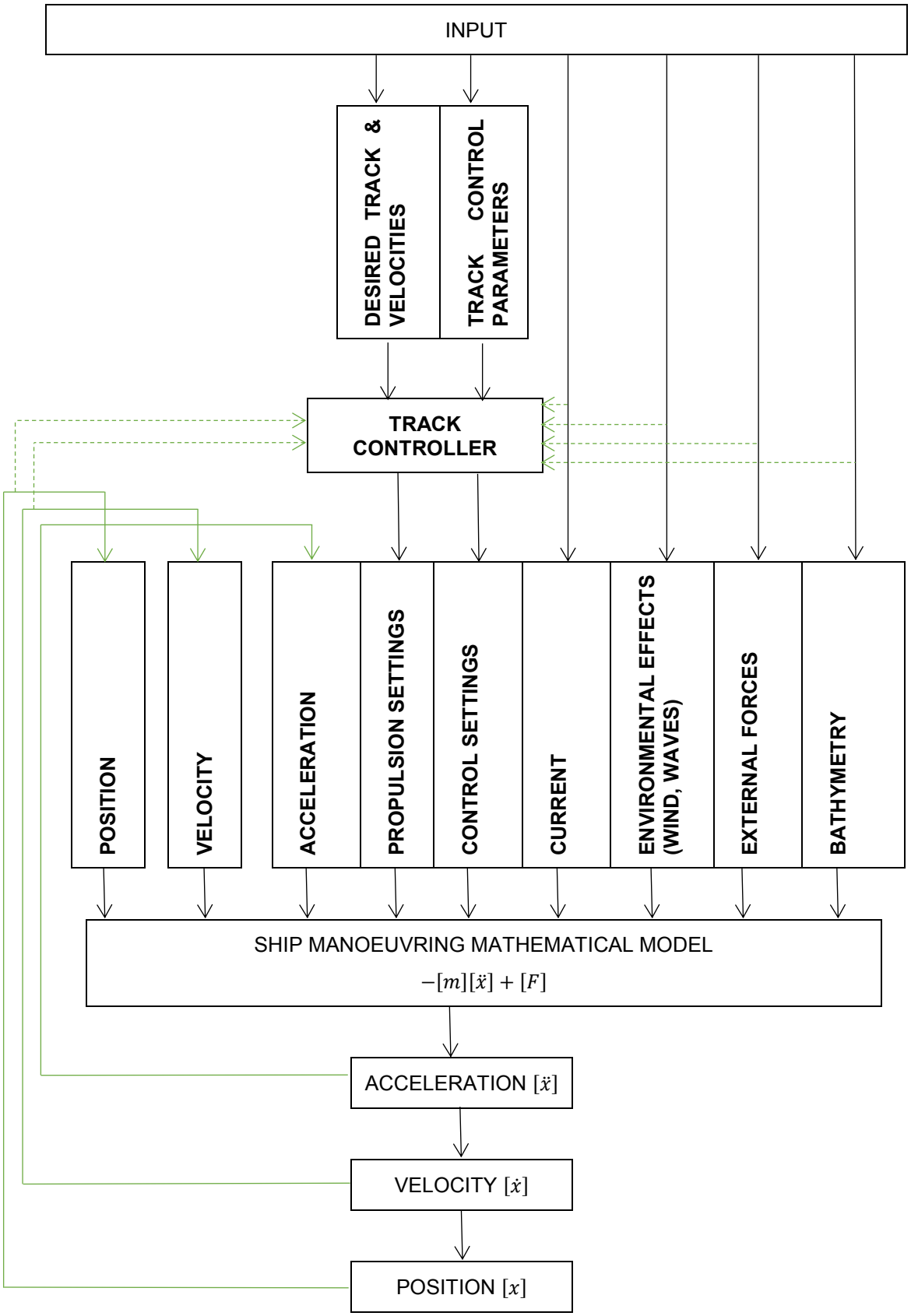

Figure 5 Calculation scheme of Fast-time Track Controller

3 REAL-TIME SIMULATION

In real-time simulations, the steering devices, like the engine's telegraph, rudder angles and thrusters, are controlled by a human person who also commands, if required, tug assistance (Figure 6). In other words, the actions of the person in charge of the simulations provide the only input for the mathematical model.

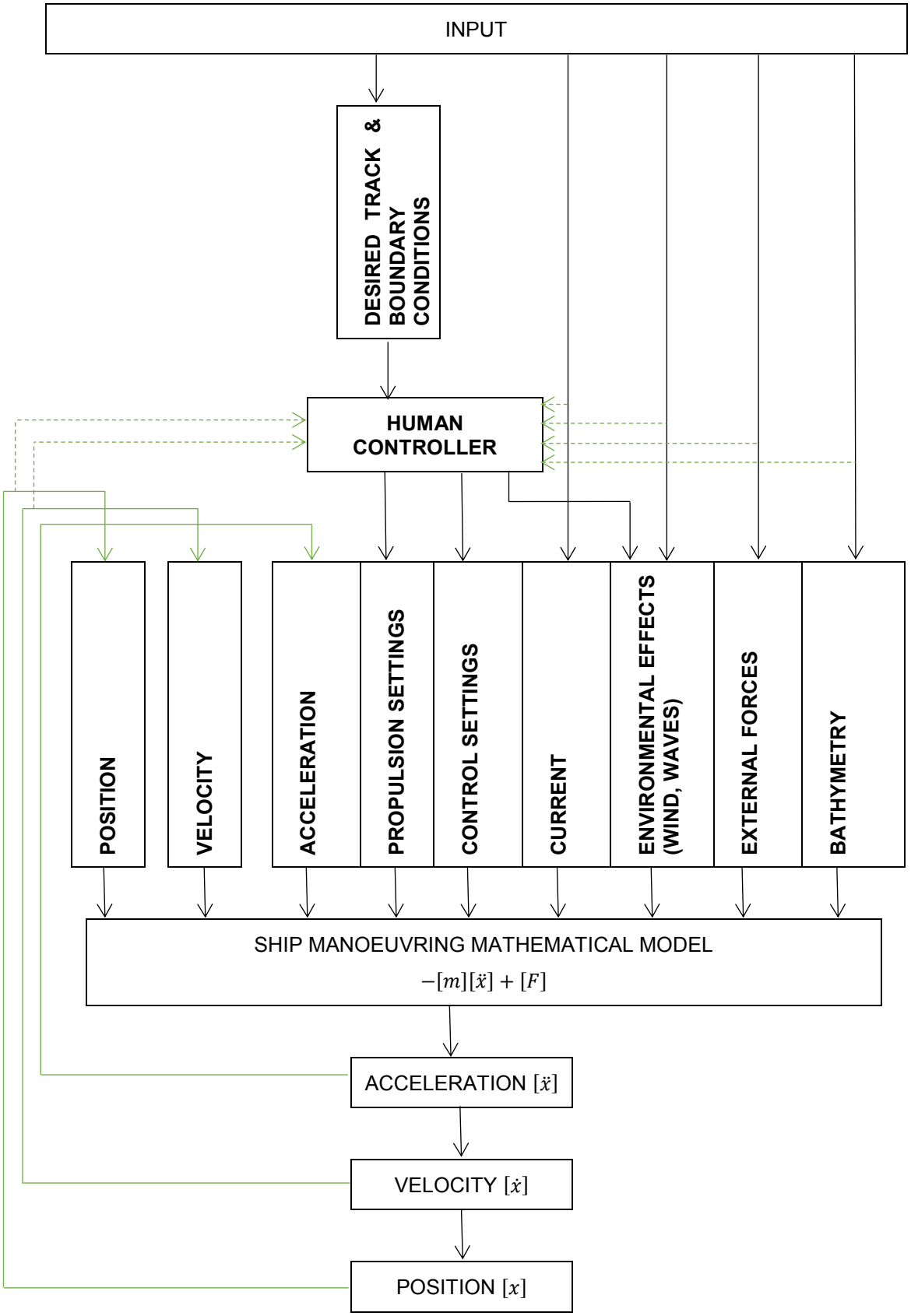

The advantage of real-time simulations is the completeness of the simulation technique by introducing the person (expert) in the loop. Obvious disadvantages of this tool are the relatively time consuming process for systematic investigation and the variability of the simulations, better known as the human factor during the simulations. Exact repeatability is not possible and the number of different set ups that can be tested for evaluation purposes is rather low, since only about 10 to 20 different simulation runs can be carried out per working day. The impact of the experience, skills and personal style of the seaman can have a significant impact on the results of the simulations.

Figure 6 Full mission bridge simulators 225 and 360+ at FHR

Real-time simulations can be used for the validation of the mathematical model. If a new manoeuvring model of ship is derived from model tests carried out in the towing tank then this manoeuvring model is tested by an experienced person familiar with the ship in real life. The same experienced person can also contribute to studies in which a new navigational situation is created. A limited amount of simulation setups is chosen and systematically carried out, often by different commanders and at a variation of environmental conditions like wind force and direction, tidal currents or water depths.

4 CASE STUDY: CANAL GHENT-TERNEUZEN

Different types of simulation will be explained and applied to a bulk carrier sailing southbound on the Canal Ghent-Terneuzen (CGT). This canal was originally dug in 1823 to connect the city of Ghent (Belgium) via the river Scheldt with the North Sea. In Terneuzen (The Netherlands), where the canal connects with the Western Scheldt, different locks in varying sizes were built. Nowadays, three locks are available. The West Lock is the largest with a length of 290 m and a width of 40 m, allowing a maximum fresh water draft of 12.5 m. In 2012 it was decided to build a new and larger lock in Terneuzen with a length of 427 m and width of 55 m. The lock is expected to be operational in 2022 (Sassevaart and Vlaams-Nederlandse Scheldecommissie, 2018).

The distance between the Port of Ghent (since 2017 *North Sea Port,* together with Flushing and Terneuzen in the Netherlands) and the locks in Terneuzen is about 10 nautical miles (18 km) and the narrowest (theoretical) section on the canal is a trapezoid which is 62 m wide at the full canal depth of 13.5 m and 155 m wide at the free surface (Figure 7).

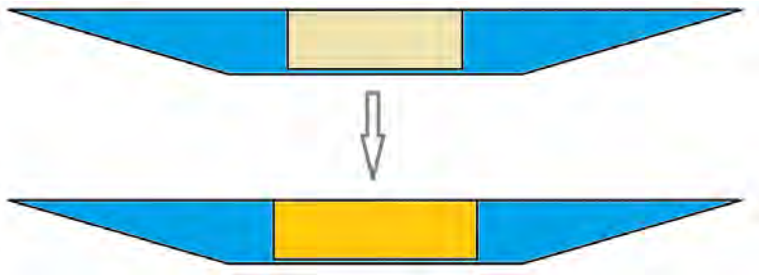

Figure 7 Smallest theoretic cross section of the Canal Ghent Terneuzen with midship sections of a ship BxT 37x12.5m² and 43x12.5m²

Nowadays, the draft of the vessels on the Canal is restricted to 12.50 m, which leaves a gross under keel clearance of 1 m or 8%. The largest vessels are bulk carriers, which are either of Panamax type (breadth 32.2 m, length over all up to 265 m) or Kamsarmax type (length over all 230 m, breadth 37 m). The maximum allowed speed for vessels with a draft of more than 10 m is 9 km/h, 12 km/h for vessels with a draft in between 4 and 10 m and 16 km/h for vessels with a draft of less than 4 m. The bottom section of the Canal is too narrow to allow meetings between large ships. The main challenges for captains and pilots on the canal are: the narrow cross-section (with a blockage of 32 % for the ships with BxT 37x12.5 m²), the bends, the passage of bridges which restrict the available width, and the bank effects. With respect to the latter, it can be stated that the effects of the port and starboard side banks more or less compensate each other in case of a centric course, but on different locations the symmetry is disturbed due to the presence of side docks. This will lead to transient bank phenomena which are much more difficult to handle than steady effects.

4.1 Example 1: FT Track Captive at CGT

On March 14th 2017 a full-scale measurement campaign was carried out on a bulk carrier (LxBxT 229.5x36.9x12.5 m³) sailing southbound on the Canal Ghent-Terneuzen. The results of this accurate position measurement was then used for the input of *FT Track Captive* simulations. Based upon the positions first all accelerations (in the horizontal plane) are defined. Then these accelerations are listed to be used as input for the simulation.

Figure 8 Trajectory from the full-scale measurements and FT Track Captive simulations on the CGT

In Figure 8 the position of the bulk carrier from the full-scale measurement is plotted together with the positions in the *FT Track Captive* simulation. Special attention should be drawn to the accuracy and definition of the inputted accelerations. Small deviations in the accelerations may result in too large drifting of the absolute positions.

Having a simulation of a full-scale measurement gives the opportunity to investigate the forces and moments the ship undergoes into more detail. The squat of the ship at full-scale can be compared with the squat of the same ship, but also forces like bank effects which cannot be measured at full-scale can be investigated in more detail.

4.2 Example 2: FT Track Predefined Controls at CGT

If the trajectory of the full-scale measurement would be plotted together with the trajectory from the *FTT Predefined Controls* based upon the rudder and propeller settings of the full-scale measurements. The deviations between both increase the longer the simulation takes because there is no feedback in the control system between the desired position (from the full-scale measurement) and the position in the simulation. The settings of propeller rate and rudder angle are set before the start of the simulation and

the simulation simply picks the predefined propeller rate and rudder angle for each time step. Because of the force equilibrium another position in the small Canal will result in (very) different bank effects which results in a different position which results in different bank effects and so on and so forth.

4.3 Example 3: FT Track Controller at CGT

Figure 9 FT Track Controller trajectory of a 43m wide bulk carrier leaving the lock at Terneuzen sailing southbound on the Canal Gent-Terneuzen

When the new lock in Terneuzen is finished, larger ships are expected on the CGT. To investigate the nautical impact and to find the bottlenecks on the Canal for such a new type of vessel, *FT Track Controller* simulations can systematically investigate and point out the expected issues on the canal. Figure 9 shows the trajectory of a 43 m wide bulk carrier (which does not fit at present into the existing lock of Terneuzen) sailing on the Canal Gent Terneuzen. One of the findings of the simulation was that the longitudinal resistance force on the ship increased significantly compared to sailing in open water. This increase of resistance is related to the increased blockage (ratio between midship area and canal cross section area), as can be seen in Figure 7 as well as the small under keel clearance (water depth,13.5 m to draft 12.5 m ratio). This under keel clearance will even decrease more because of the squat of the ship when sailing at a forward speed through the canal.

4.4 Example 4: Real-time simulation at CGT

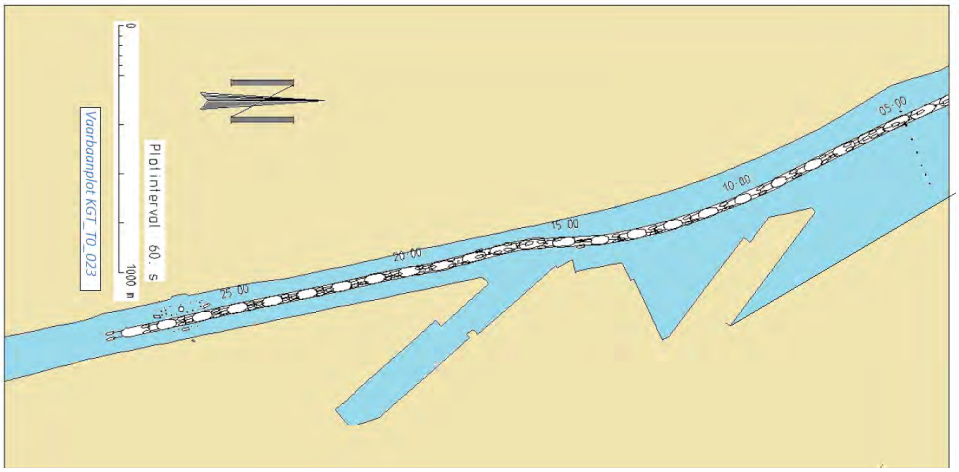

Figure 10 Trajectory of a Real-time simulation with a bulk carrier sailing from the lock at Terneuzen up to the crossing of the bridge at Sluiskil

In Figure 10, the last section of a 27 minute long trajectory is plotted of a real-time simulation with a bulk carrier sailing southbound on the Canal Gent Terneuzen from close to the locks in Terneuzen until the crossing of the bridge at Sluiskil. A distance of about 3000 m is sailed in this simulation. In the research for investigating the impact of wider vessels on the Canal some parts on the Canal are selected for real-time simulations while the entire Canal was taken into account for the fast-time simulations. The combination of both (real-time and fast-time simulations) is a typical technique to have a wide systematic series of results for the entire scope of the research without spending too much time and resources during the (relatively) expensive real-time simulations.

5 CONCLUSIONS

The calculation core of a simulation is the so called mathematical model. In a real-time simulation a human controls the ship similar as in real life (tiller, telegraph, tug commands etc.), this control is the input of the mathematical model which updates at a high frequency to be able to generate a smooth projected image. When the same mathematical model is no longer fed with human commands then the simulations is a fast-time simulation. Four different types of fast-time simulations can be carried out and each has its own advantages and disadvantages. These four type of fast-time simulations together with the real-time simulations can provide a profound indication of the feasibility of the manoeuvrability a specific ship in a, for example, confined fairway.

6 REFERENCES

Delefortrie, G., Eloot, K., Lataire, E., Van Hoydonck, W. and Vantorre, M. (2016) '*CAPTIVE MODEL TESTS BASED 6 DOF SHALLOW WATER MANOEUVRING MODEL'*, in Proceedings of 4th MASHCON. Hamburg, Germany: Bundesanstalt für Wasserbau (BAW), Karlsruhe, Germany, pp. 273–286. doi: 10.18451/978-3-939230-38-0.

Eloot, K., Verwilligen, J. and Vantorre, M. (2007) '*A methodology for evaluating the controllability of a ship navigating in a restricted channel'*, in Archives of civil and mechanical engineering: quarterly. Oficyna Wydawnicza Politechniki Wroclawskiej, pp. 91–104. doi: 10.1016/S1644-9665(12)60016-8.

Eloot, K., Verwilligen, J. and Vantorre, M. (2009) '*Safety assessment of head on encounters and overtaking manoeuvres with container carriers in confined channels through simulation tools'*, in MARSIM '09 Conference, Proceedings. Panama City, Panama: Panama Canal Authority ; International Marine Simulator Forum, p. C-20-1/12.

Sassevaart and Vlaams-Nederlandse Scheldecommissie (2018) https://nieuwesluisterneuzen.eu/.

Verwilligen, J., Delefortrie, G., Vos, S., Vantorre, M. and Eloot, K. (2015) '*Validation of mathematical manoeuvring models by full scale measurements*', in Marsim 2015. Newcastle, UK, pp. 1–16.

Simulation type	**Fast-time Position Captive**	**Fast-time Track Captive**	**Fast-time Track Predefined Controls**	**Fast-time Track Controller**	**Real-time human controlled simulation**
Human interaction	no				yes
captive/free running	captive		free running		
time step t(n-1) influences t(n)	no		yes		
accelerations	no	yes			
Force equilibrium	no, net forces present		yes		
time calc = time sim	no				yes
exact path is known before calculation	yes		no		
track	predefined (theory or derived from full-scale),	depends on accelerations	depends on mathematical model	depends on Track Controller	depends of human
controls	no, predefined	predefined accelerations	no, predefined rudder and propeller rate	through Track Controller and desired track	human (pilot, captain, skipper)
simulations/24h	+100	+100	<100	<50	10 to 20
advantages	fast, relatively low computing power	fast	fast	more realistic path than other fast-times	completeness
disadvantages	sensitive to realism of input track no force equilibrium	no forces equilibrium	sensitive to rudder and propeller rate settings	sensitive to Track Controller settings time-consuming	time consuming exact repeat not possible low number of tests/day rather expensive

Table 1 Overview of five types of simulations used at FHR

Improving traffic flow analysis: the integration of trajectory analysis in capacity modelling. A case study applied to the Nord-Pas-de-Calais ECMT-Va-canals

by

Adams R., Zimmerman N., Doorme S., Vandenbroucke T., Noël Chr., De Decker K., Pannemans B., Page S.[1], Thorel X., Laborie Cl.[2]

ABSTRACT

In order to investigate the need and to define priorities of investments in the improvement of the traffic flow in Northern France a trajectory study and a traffic flow study are being executed for the ECMT Class Va network of Nord-Pas-the-Calais. The named Canal à Grand Gabarit links the Port of Dunkerque with the Scheldt River and its connections with the navigable waterways of Wallonia (Belgium) in a west east direction. In a south-north direction it will link the future Canal Seine Nord Europe with the Deûle-Lys river connection, and will as such provide a high performing inland waterway connection between the Seine basin (France) and the ports of the Western Scheldt and further on Rotterdam (Belgium-Netherlands). To accommodate the expected increase in traffic, potential bottlenecks will have to be identified, and improvements investigated and proposed.

The trajectory analysis allows to study the geometrical constraints to navigation, and their impact on safety, ease and fluency of the traffic on a case by case evaluation, in which the interaction between ships, or between ships and the waterway infrastructure is investigated. The required space between ships, and between ships and infrastructure can be defined for different ease, safety or fluency categories of the waterway. Such analysis will however not allow to define the viability of the waterway network to accommodate the traffic. For this purpose a traffic model is used, the latter will however be fed with the nautical intelligence of the trajectory analysis.

A desk top analysis is used to test the existing and design canals, and their ease and safety level. Sections with the lowest ease levels can as such be identified, as well as critical sections for overtaking and encountering other ships. These are the prime objectives for real time navigation simulations that are used to define the functional constraints of the different waterway sections. Viability and conditions of ship-ship and ship-infrastructure encounters can be defined through these simulation: speed, required space (length and width), possible ship (class) combination, for different equipment, flow conditions, … This information is used to both propose and investigate measures for improvement of the infrastructures or canal, or to either accept a lower functionality and impose restrictions to the navigation (e.g. reduced speed, alternating traffic …). To understand the effect of traffic fluency of such a decision, however, a traffic model is used.

A traffic model allows to build up an image of the traffic flow for a given traffic density in a given network with its given geometric characteristics. With increasing density the flow will at first increase linearly, but will reach a maximum for a specific density, after which flow decreases again, and finally comes to a standstill.

The traffic model will be used as an instrument to identify bottlenecks for the traffic flow for expected traffic after the construction of the Canal Seine Nord Europe, and to support well balanced decisions for both structural and soft measures to accommodate the expected traffic flow. It is worth to investigate whether investments in enlargement of the waterway are useful, if lock capacity remains unchanged, and whether the effort should be put in the upgrading of the lock complexes or in the bottle necks of the canal proper.

[1] International Marine and Dredging Consultants (IMDC), Van Immerseelstraat 66, BE2018 Antwerp, Belgium
[2] Voies navigables de France (VNF), Direction territoriale Nord-Pas-de-Calais

The existing traffic model IMDC Waterways (Adams et al., 2014), has been improved to include berthing times at intermediate destinations such as quays, and to take into account temporary constrictions of the fairway due to ships being (un)loaded. Speed or alternating traffic is either imposed (regulations) or calculated on the basis of ship characteristics.

The model is a so called hybrid traffic model combining theory from both microscopic as macroscopic traffic models, to allow a reduction of calculation time compared to pure microscopic models. The handling of ships is on an individual level (microscopic), checking the ship by ship. It is macroscopic in the sense that stretches with similar geometric characteristic are defined as single links characterized by the most constraining cross section. Links are defined to handle the traffic in a realistic way, without compromising calculation time. Traffic is generated based on an Erlang distribution law, which may vary in function of the traffic density at any given time (variation during the day, during the week – largely due to operating times of the locks). After a warming up period an image of the traffic is built. Allowing to evaluate the traffic capacity of the waterway network including locks, quays, ports and waterway sections. Calibration is based on known traffic flows.

Knowledge from the real time simulations of the trajectory analysis is used in the traffic model: to limit ship speed in critical sections during encounters or overtaking maneuvers, to define required space for the manoeuvers by specific ship classes, and to check whether the manoeuvers are possible or whether traffic must alternate. The insights from the traffic model flow back to the definition of measures to be investigated by the real time simulations.

The study will focus on the traffic modeling, and the interaction between the trajectory study and the traffic study.

1. INTRODUCTION

An increase in traffic is expected on the navigation network of Nord-Pas-de-Calais with the construction of the Canal Seine-Nord-Europe by 2023. Moreover ship size will increase, and though the network is classified as ECMT Class Va, calibration works are required to accommodate the larger vessels. Indeed the network is constructed not taking into account recent waterway design guidelines. As a consequence several bottlenecks exist for even ECMT Class Va.

A geometrical analysis was conducted to identify the bottlenecks. As the removal of the bottlenecks is costly, Voies Navigables de France (VNF) first aims at prioritizing the bottlenecks. To this end they launched two studies to analyze the consequence of the bottlenecks on safety of navigation and on the travel time.

The identification of bottlenecks is based on the geometric testing of the design against the design principles, which assume a certain ease level for navigation. In reality navigation is possible also in more constrained situations, but in which safety is still guaranteed. Moreover, encounters of other ships not always occur at these bottlenecks, implying that waiting time for encounters at bottlenecks may still be very low, and resolving the bottleneck not economically justifiable in terms of gains in ease of navigation and travel time.

Real time navigation simulations will be used to study the safety level of navigation, a traffic flow study is used to calculate travel time and to evaluate effect of bottlenecks on the travel time, secondly to evaluate whether measures are required.

2. THE NETWORK

2.1 General

The ECMT Class Va network of Nord-Pas-de-Calais, encompasses the Canal à Grand Gabarit, linking the Port of Dunkerque to the Scheldt, and the connections with the Belgian network, through the Deûle (Class Va till Lille), and then connected to the Belgian Lys through the Lys Mitoyenne, both planned

for upgrading, on the one hand, and the Scheldt (Class Va till Tournai, but also being upgraded in Belgium).

This network can be considered as Class Va, corresponding to units of 110m x 11.4m and a loading capacity of 1500 to 3000 ton. Measures to bring the network to 3000 ton have been largely achieved between 1951 and 1972 with the construction of locks of 144.60m x 12m. In practice, major bottlenecks remain, because of the reduced width of the canal and the limited space in bends.

Moreover, the network is isolated from the rest of the European ECMT Class Va network as the connections with the North are either limited to ECMT Class IV, or are only partially functional as a Class Va waterway (limitations in draught, although upgrading is underway), to the south the gabarit is even more limited, only up to 800 ton (Canal du Nord), and even 650 ton (Canal de Saint-Quentin).

Therefore currently the Class Va traffic is largely limited to internal traffic on the network of Nord-Pas-de-Calais.

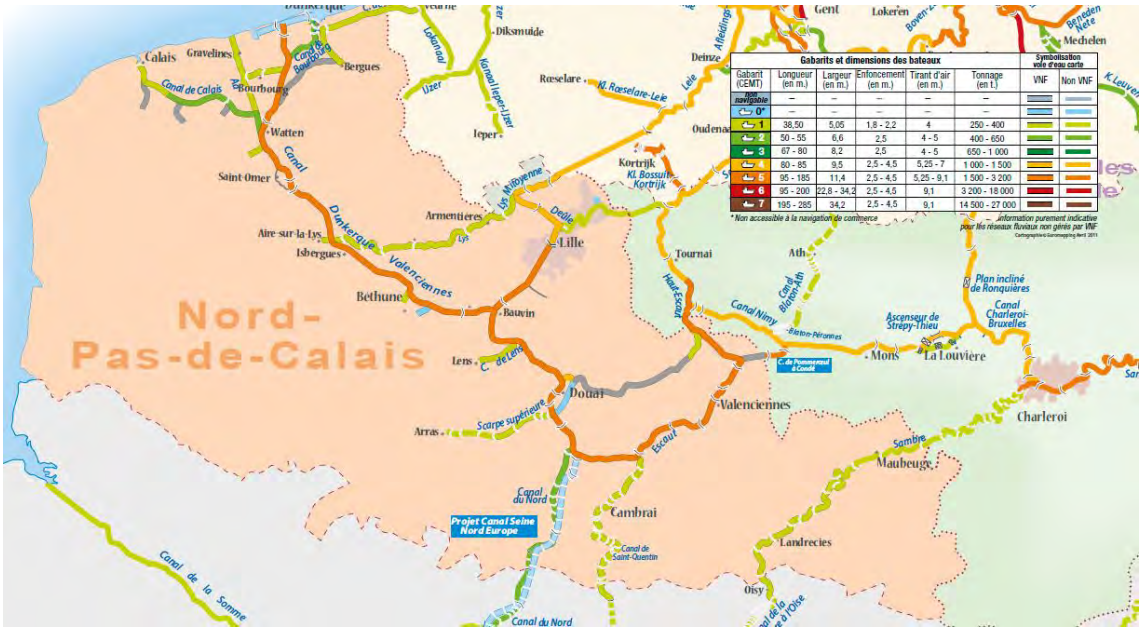

Figure 1: situation of the ECMT Class Va network of Nord-Pas-de-Calais, and connections to the north, east and south (source: VNF)

The Class Va network of Nord-Pas-de-Calais is situated at the heart of the Seine-Scheldt liaison, defined as a priority axis of the Trans European Network. Currently several projects are conducted in France and Belgium to bring the waterways in line for establishing a network at Class Va level. To the south the Canal Seine-Nord Europe will be constructed to navigate to the Seine with push barges of 185m long. Towards the North the Deûle, Lys, and Scheldt are being calibrated to also allow push barges to the Ports of Ghent, Antwerp and further on the Netherlands. To the East the Canal Condé-Pommeroeul and the recalibration of the Scheldt-Sambre liaison will allow navigation of 110m long units to the Sambre, further on the Meuse, and finally the Rhine, Main, Danube liaison (Figure 1, Figure 2).

After implementation of these projects the Class Va network of Nord-Pas-de-Calais will be at the center of a strategic transport network linking major river and maritime ports of Western Europe with its hinterland and the continental fluvial network. The development will significantly contribute to the competitiveness of fluvial transport in the region. This will, particularly in the network of Nord-Pas the Calais, lead to following major effects: on the one hand the increase in transport volume, on the other hand the scaling towards larger vessels, at cost of the smaller, less competitive units. Whereas today's transit and transport to the area is limited to small units, the Class V units (large Rhine ships 110m,

Va, extended large Rhine ships 135m, Va+, and push barge convoys with two barges, 185m, Vb) will become more abundant in the future. The latter however need to be decoupled, as the useful length of the actual locks is limited to 144m.

Figure 2: Flemish interpretation of the inland navigation network (binnevaart.be)

2.2 Characteristics

The current study concerns the entire class Va network of Nord-Pas-de-Calais, including the branches Dunkerque-Bauvin, Bauvin-Comines, Bauvin-Mortagne du Nord and du canal Condé-Pommeroeul. The entire network is accessible to ECMT Class Va, the Lys mitoyenne even to Vb in alternating traffic. In reality however it's a false gabarit. The canals are old and width is limited to 30 to 34m, while 34m would be required according the guiding design principles (Circulaire 76-38). Local narrowing occurs at bridges, and no appropriate over width has been considered in bends (Figure 3). The actual accessibility was assessed in a theoretic analysis.

The network contains 16 lock complexes, the most consisting of one chamber, three consist of 2 chambers (the locks of Douai, Couchelettes, Goeulzin, of which the second chamber is sized to ECMT Class IV). The main locks are of 144.60m x 12m. The locks on the Lys Mitoyenne on the other hand are at ECMT Class Vb.

The lock of Fontinettes has an exceptionally high jump of 13m, which results in difficulties in the management of the water level and largely determines the water use.

There are 79 public quays along the network, of which half are interfering with the design waterway (distance of less than 1.6m between design waterway and a moored Class Va ship. Moreover there are 172 bridges, of which half with a narrow section, requiring speed reduction for two way traffic, and another quarter even a speed reduction for alternating traffic.

Traffic includes local transport and transit, leading to an estimated yearly throughput of about 5000000 ton in the most visited sections in 2016 (Figure 4).

Figure 3: example of bend with the lack of an adaquate width addition according standard design rules

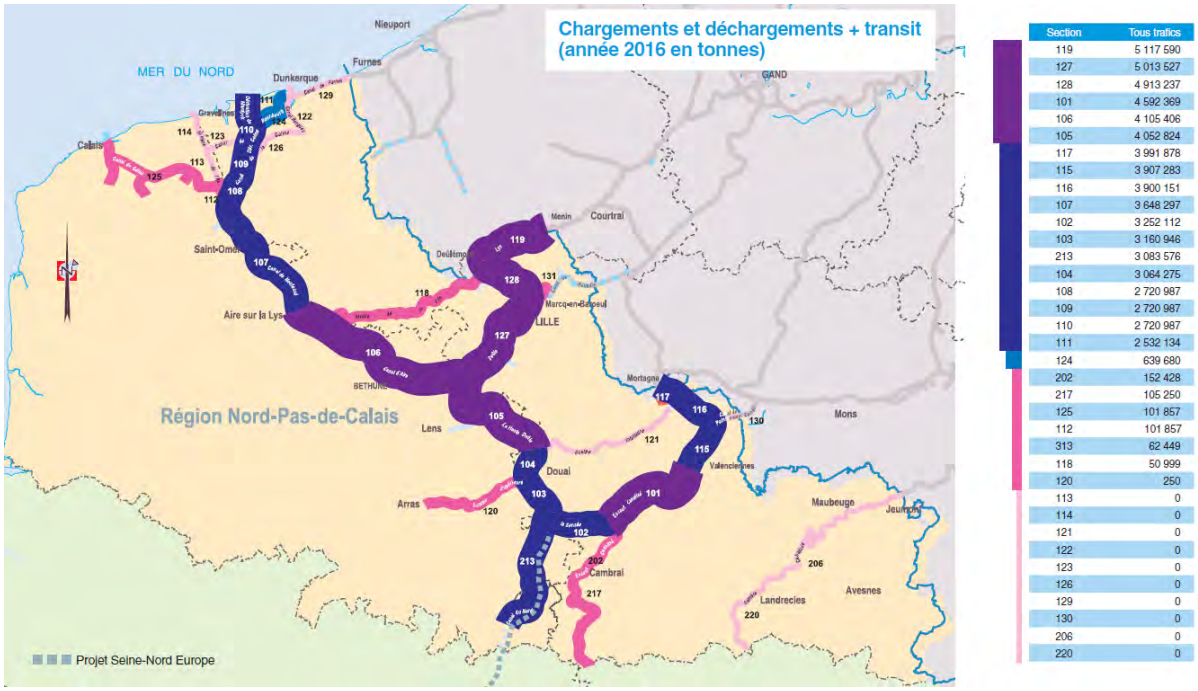

Figure 4: distribution of traffic flow on the inland navigation network of Nord-Pas-de-Calais (source: VNF)

Fleet structure for future is expected to change, as a consequence of the scaling after the construction of the Canal Seine-Nord Europe (Table 1, number of ships at the Cuinchy lock, Stratec 2012).

Table 1: Fleet structure for current and future traffic situations

Unit	ECMT Class	Actual (~5 Mt/y)	Traffic 10 Mt/y	Traffic 15 Mt/y
Freycinet	I	27%	23%	11%

Campinois Dortmund-Ems Kanal (DEK)	II III	27%	31%	25%
Rhein-Herne-Kanal (RHK)	IV	31%	25%	25%
Grand rhénan	Va	15%	18%	24%
Grand rhénan allongé	Va+	0%	3%	15%

Vessel speed is limited to 12 km/h for empty ships, and 10 km/h for loaded ships, and is further reduced to 6 km/h in the port area of Lille and Douai. Locally alternating sections have been defined.

Trajectory studies are based on the principle that a waterway design according to the guidelines in force, in this case Circulaire 76-38, has a certain ease level (navigation speed and fuel consumption), and moreover a certain level of safety. However, beyond this level navigation may still be safe, given a reduction of speed. Although there may be some an economic loss, but navigation may still be competitive. The safety level can be defined as a condition beyond which navigation is not possible at safe conditions anymore.

2.3 Network evaluation

In complement of the geometric study an evaluation was carried out to check whether the network fits not only to the ease level, but also corresponds to the safety level. Beyond that level calibration measures are required. In between, navigation may still be possible in a competitive mode, if traffic allows, but should be checked with real time navigation simulations.

The safety level contains largely three reductions in regard of the ease level:

- under keel clearance(UKC)
- the over width
- the navigation rectangle (blockage factor)

In the current study, rather than identifying the section in which the design waterway does not fit the actual one, as such identifying the bottlenecks, the analysis aims at defining the level of accessibility. The evaluation is done on the basis of cross sections, bend curvature, the wet section, for three accessibility levels: two way, selective alternating traffic for unit IV, strictly alternating traffic, for both ease and safety levels, defining situations qualifying for further investigation by real time, or requiring measures (below safety level) (Table 2).

Table 2: Accesssibility level of the Grand Gabarit network of Nord-Pas-de-Calais, as identified in the desktop study

Accessibility level	**Va [%]**	**Va [km]**	**Va+ [%]**	**Va+ [km]**	**Va++ [%]**	**Va++ [km]**	**Vb [%]**	**Vb [km]**
Two way ease	76%	181	70%	168	69%	167	25%	59
Two way safe	17%	42	16%	39	16%	38	54%	130
Selective alternating ease	1%	2	3%	7	3%	8	2%	5
Selective alternating safe	3%	8	5%	12	5%	13	7%	16
Strictly alternating ease	2%	5	5%	11	5%	12	10%	23
Strictly alternating safety	0%	1	0%	1	0%	1	2%	4
Navigation impossible (incl. lock entrance)	1%	1	1%	1	1%	1	1%	2
Total	**100 %**	**240**	**100 %**	**240**	**100 %**	**240**	**100 %**	**240**

Table 2 shows that the entire network is accessible to class Va, Va+ and Va++. The actual navigability in two ways is present on 181 km of the network, 42 other km do strictly spoken not conform to navigation in two ways, but it can be allowed if proven feasible by real time simulations.

For bend curvature, investigations are proposed for bends when the bend radius is classified as (Table 3): minimum reduced < R < minimum normal. For situations with R between minimum normal and R>10 x L, investigations are only required for higher current velocities, which do not occur in this project. If R is lower than minimum reduced measures are required.

Table 3: bend characterisation of the network

km / % of network Bend radius	Va	Va+	Va++	Vb
R < reduced	0km / 0%	4km / 2%	4km / 2%	17km / 7%
reduced ≤ R < normal	25km / 10%	22km / 9%	22km / 9%	13km / 5%
normal ≤ R < 10*L	87km / 36%	114km / 48%	115km / 48%	134km / 56%
R ≥ 10 x L	128km / 53%	100km / 42%	99km / 41%	76km / 32%
Total	**240km**	**240km**	**240km**	**240km**

For the bends, simulations are only required for Va+ and Va++ (and Vb).

The blockage factor (1/n) is investigated distinguishing between n=10 allowing high velocities with low fuel consumption, n=6 with some resistance and higher fuel consumption, but for which navigation is still a very competitive transport mode, n<3, with lower speed and high fuel consumption, which only is locally acceptable. Analysis shows n to be between 5 and 6, only locally (lock entrance, values lower than 3 are encountered. No simulations are required for this criterion.

3. TRAFFIC

Traffic is determined combining the lock registers to the list of voyages. The former does not contain information on the ship class, but includes the ship registration number. The voyages contain the registration number and transported load in tons. For each registered vessel the ship class was derived by attributing it to a class on the basis of the full charge (respectively 400, 650, 1000, 1500 and 3000 ton as a limit for ECMT Class I, II, III, IV and Va respectively. The resulting fleet structure corresponds well to the passages of locks as determined by Stratec (2012). A next step is the temporal distribution, hourly during the day, daily during the week, monthly during the year, of ship passages at the locks, on the basis of the lock register, showing a peak in the morning and a decline to the end of the opening hours. (Vessels outside service time pass at payment.) During the week traffic is lower on Saturday and Monday, reflecting the weekend. Throughout a month, there are no specific patterns, while throughout the year influence may be seen from peaks in coal transport (winter), grains (summer).

Distribution of loading rate is determined by dividing the load by the deadweight tonnage. Histograms show that load is generally between 60 and 100% for all units. However a relevant portion is unloaded for the larger classes. This can partially be attributed to the contribution of container traffic which does not conform to a distribution in weight categories. The amount of empty and fully loaded vessels is estimated on the basis of the lock registers, containing an estimate of the transported tonnage. In absence of a specified load the vessel can be assumed empty. The share of empty and fully loaded ships based on the lock register, can be compared to the estimated tonnage on the basis of the Origin Destination (OD) Matrices. The total transported tonnage estimated based on the lock register is systematically lower than the tonnage estimated by the Observatoire du Transport Fluvial. The latter provides the sum of both full and partial passage or entry of a section, also if they not pass the lock, while the lock register only records ships passing the locks, excluding loads that that are discharged or charged before the lock, hence the lower tonnage of the latter.

The spatial distribution shows the predominance of ECMT Class IV and Va on the Dunkerque-Bauvin Branch, and the smaller classes on the Bauvin-Mortagne Branch, which is related to the contribution of ECMT Class I by the (actual) Canal du Nord (Figure 5).

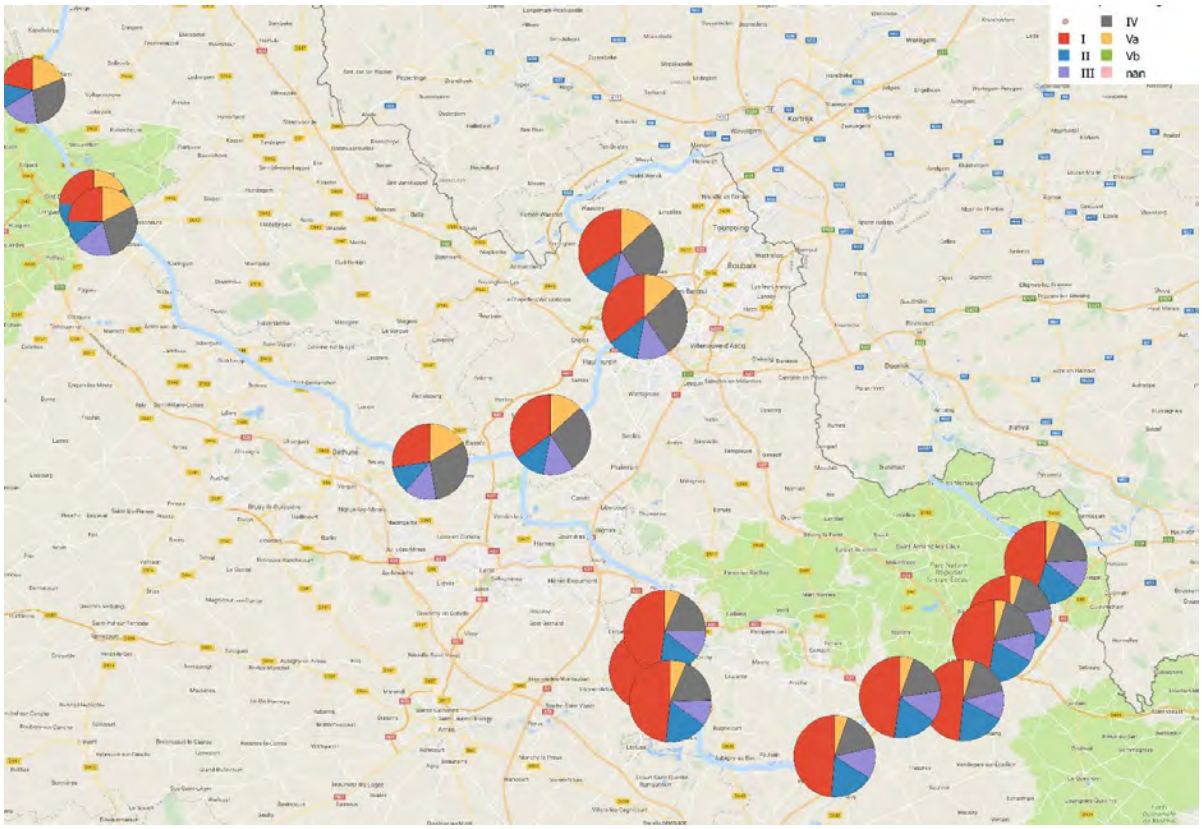

Figure 5: distribution of fleet structure in different sections of the network, showing the predominance of the smaller ship sizes in the Eastern part as a consequence of the limited gabarit of the Canal du Nord

4. THE TRAFFIC FLOW MODEL

The used model is IMDC Waterway, which is a traffic flow model for inland waterways, which was presented at PIANC World Congress in 2014 (Adams et al., 2014). It is an event driven model capable of simulating branched networks. It has been further developed to also allow simulation of maritime traffic in estuarine access channels and complex ports setting such as the Western Scheldt (Delecluyse et al., 2018).

In this study it is applied to the ECMT Class Va network of Nord-Pas-de-Calais. Currently the model has been set up and calibrated for the Dunkerque-Arleux Branch, and will be expanded with the Comines-Arleux Branch (connection to the Lys), and the Mortagne-du-Nord-Arleux Branch (connection with Scheldt and Canal du Nord), to include the entire Grand Gabarit network (240km). A module for converting the model results to a web based result viewer has been created allowing the VNF to follow up progress of calibration, and to consult intermediate simulation results.

The model consists of elements of 500 to 5000m, long defining the accessibility levels as defined in the trajectory study. All lock complexes are included with defined operating times from 06h30 to 20h30 for the current situation, and 24h/24 for future traffic scenarios.

The traffic generator has been expanded to include Erlang distributions of any shape and rate (number of occurrences and duration), and is used to generate traffic at all present quays (79) and entry points of the network (4 on the extremities of the Class Va network, 6 on the branches of smaller gabarit waterways connected to the network).

Traffic is generated for current and future situations. In contrast to the current heterogeneous fleet structure (Figure 5), the future fleet structure of the macroeconomic study (Stratec 2012) is expected to be more homogeneous, as smaller ships classes will gradually disappear, and larger ships will also be able to navigate the Canal Seine Nord Europe.

The model was used to calculate current (5 Mt/y) and future traffic scenarios (10 and 15Mt/y). Although the model calculates speed using Schijf's law, effectively taking the water displacement into account, speed is truncated using the legal speed limits.

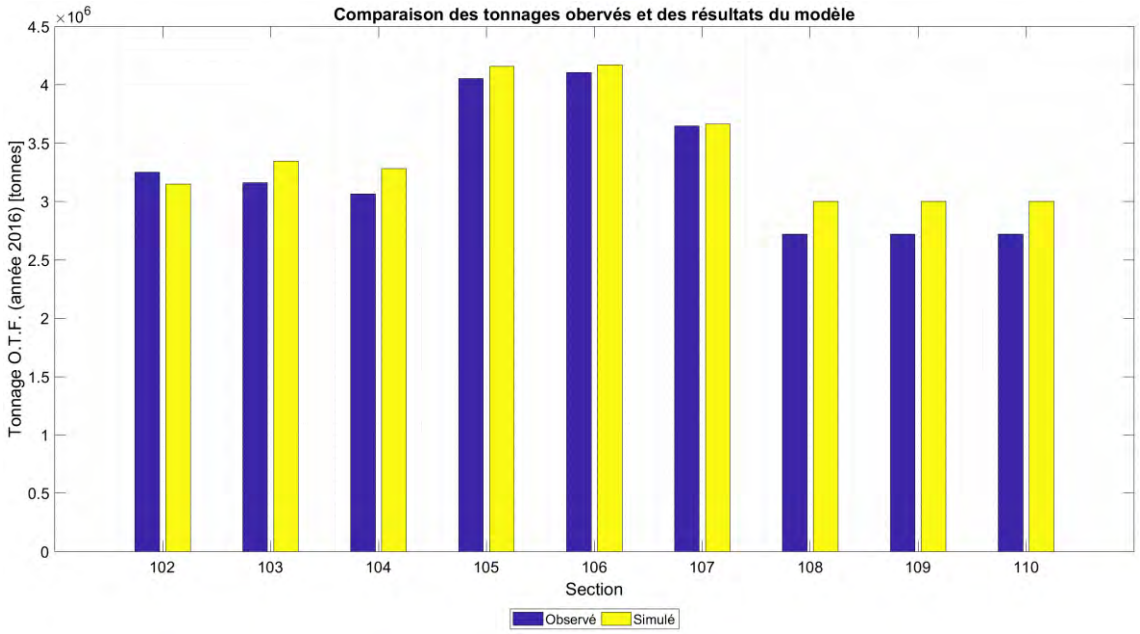

Figure 6: calibration of the traffic flow

For the current situation different fleet characteristics have been imposed at the level of the different OD relationships of all quays and entry points. Despite lacking information to unambiguously correlate ships with charge load, results show a good correspondence between observed (assumed) and simulated tonnage, indicating both the overall good approximation of the correlation of lock register with load statistics on the one hand (error of less than 10%), but also the simulation of the traffic distribution by the model (Figure 6). Also observed and simulated fleet composition, and temporal distribution (hourly during the day, daily during the week) correspond well, despite the obvious imperfections of the data.

Therefore, it can be concluded that both assumptions on the data and on the traffic generation can be considered reliable. Today, no accurate data are available on travel time, but the model reproduces presumed travel time (17 to 18h), indicating that the model is fit to simulate the traffic flow. The model has been used to calculate the travel time, ship encounters, study the lock operation, waiting times, number of waiting ships, lock occupancy, water consumption of the locking operation, … for both current and future situations.

A weakness in the statistics of VNF is the translation of container traffic to tonnage. Two parameters which are difficult to combine. This will become more critical for future situations as container traffic is expected to increase after commissioning the Canal Seine-Nord Europe.

First results for the Dunkerque-Arleux Branch indicate that today locks account for most of the time loss (Figure 7). Using the comfort definition for lock capacity (a maximum of 10% of the ships have waiting times of a full lock cycle), this has been reached already today at the Cuinchy and Fontinettes locks. Time loss at the multiple lock complexes is low.

After multiplying the traffic on this branch, also the Pont-Malin and Flandres locks seem to become critical. Total travel time increases with about an hour (average), but with up to 2 hours for about 10% of the ships when traffic is doubled, and even up to 10 hours for 10% of the ships when traffic increases to 300% (about 5 hours for 50% of the ships).

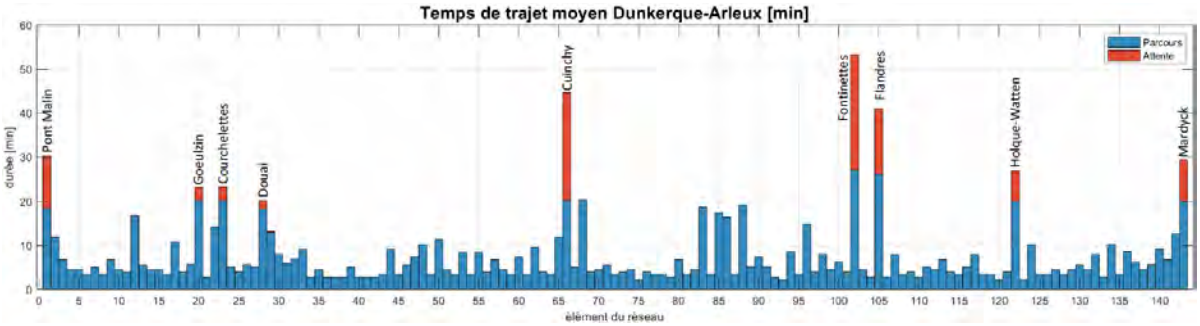

Figure 7: calculated travel (blue) and waiting time (red) in the different model nodes

Time loss on this branch seems to be negligible compared to the time lost at the locks. Some time loss is registered at the bend of the Marlettes bridge and the bend at the Ocre bridge. Both are reported bottlenecks in the trajectory study. They appear also here as a consequence of the combined incidence of traffic and the presence of these bottlenecks. They are also the only notable bottlenecks in future traffic situations (2 and 3x the current traffic).

Another result is the number of ships waiting at the locks. This result will be used by VNF for the dimensioning of the waiting areas, which is yet another study VNF is executing in the frame of preparing the Grand Gabarit network. The first results indicate that on the Dunkerque-Arleux Branch currently even at the most saturated lock the number of more than two waiting ships at a time is less than 10% of the time, but this increases to more than 20% of the time in Cuinchy with 2x traffic.

It is expected that water consumption increases to about 200 and 230% at Fontinettes when traffic is multiplied with 2 and 3 respectively. Today, this lock has an average consumption of about 3 m³/s. An increase of consumption is critical to the residual discharge to the Lys River, which is a main source of fresh water to the Scheldt estuary, where there is a problem of water shortage in periods of drought already today.

A protocol has been defined to study the bottle necks identified by the desktop study with real time simulations. The results of which will be used to refine the input and network definition of the traffic flow model. This will allow to redefine ship speed, particularly during encounters, and in narrow sections such as bridges and quays, to impose different rules for ships passage. The input of real ship behavior on travel time will be valuable in improving the traffic flow model.

Finally, the model will be used to study if the network is adapted to handle the expected traffic after the commissioning of the Canal Seine-Nord Europe, where it needs to be improved, and to define priorities in investments. From the first tests it appears that the locks determine the traffic flow, and will be critical to the functioning of the canal. The solution of bottlenecks may however result in transferring the bottlenecks to other locations. The traffic flow model will allow to investigate this. The hydraulic consequences also deserve a closer look: availability of water resources and the management of water levels in the canal reaches.

5. CONCLUSIONS

A traffic flow model has been constructed for the Dunkerque-Arleux Branch of the ECMT Class Va network of the Nord-Pas-de-Calais Region in France, and will be expanded with the other branches connecting it with the Deûle-Lys, Scheldt and Sambre-Meuse basin, and the future Canal Seine-Nord

Europe, to represent the 240 km long northern French branch and ECMT Class Va connection between the Seine and Northern and Eastern European inland navigation networks.

The model has been calibrated based on traffic data from lock registers and load statistics, to produce realistic fleet structure, load statistics and travel times. The intelligence of a trajectory study of the same network is used to define the rules for ship encounters of different classes at different locations in the network. The model will be further improved using the return from real time navigation simulations, to verify calculated speed and impose speed of encounters based on tests.

The model will allow to identify bottlenecks for the traffic flow, and to confirm whether it is worth to effectively tackle nautical bottlenecks, and whether solving the bottlenecks leads to other problems with the traffic flow. The first results indicate that the locks present the major limiting factor to the traffic. Time loss in the canal, despite not being constructed using the standard design guidelines, appears to be small compared to time loss at locks, particularly when traffic is increased to the expected level after construction of the Canal Seine-Nord-Europe. The question is whether it is worth to invest in solving these bottlenecks, or possible to improve network performance in allowing higher sailing speeds. It may finally be more interesting to impose speed reductions in order to reduce damage to embankments. These situations still need to be investigated.

The expected increase in traffic clearly also puts additional stress on the availability of water resources. Pumping stations may be considered not only to reduce water consumption put also to control water levels as a result of the locking operations.

6. REFERENCES

Adams R., Bayart P. & Doorme S. (2014). IMDC WATERWAYS, A design tool tailored to the need of integrated design of waterway infrastructure. 33rd PIANC World Congres, San Fransisco.

Egis (2014), pour VNF Nord Pas de Calais (SMO). Etude géométrique du réseau fluvial à grand gabarit du Nord-Pas-de-Calais - Rapport de phase 1: Note de synthèse. DGAB-010-0.

INNOVATIVE HIGHLIGHTS – RENEWAL OF SÖDERTÄLJE LOCK

by

J.R. Augustijn, M.Sc.[1]*; W.P.J. Langedijk, M.Sc.*[2]

Keywords: locks; lock gates; innovations in locks; inland navigation; structural design; mechanical design; duplex steel; segment gates; tainter gates

1. INTRODUCTION

The lock in the Södertälje Canal is situated between Lake Mälaren and the Baltic Sea. It was built in 1924 and with a chamber length of 135 metres and a width of 20 metres; it is the largest lock in Scandinavia. The average differential head is 60 cm.

The construction of a new lock is necessary to meet the growing volume and size of marine traffic. Over the years, not only the amount of shipping has increased but also the size of the seagoing vessels. The new lock will have a width of 25.3 metres and a length of about 170 metres. The renewal of the lock is part of the large-scale Mälaren Project.

The renewal project consists of the extension and widening of the lock chambers, the construction of two new lock heads and lock gates plus a new bascule bridge. The client is the Swedish Maritime Administration and the project is performed by Züblin Scandinavia AB partnering with the client. Design and engineering of the lock heads, including the sluice gates, are performed by joint venture S3P, consisting of the two Dutch engineering firms MH Poly and Iv-Infra.

As requested by the client, a special type of lock gate will be used: a segment (or: tainter-) gate made of duplex steel (a type of stainless steel). This type of gate is rarely used for locks in The Netherlands. Duplex steel is more expensive than regular carbon steel, but it has the benefit that maintenance during the structure life is minimised. The gates are partly circular, rotate around a horizontal axis and are also used for the levelling of the chamber. In addition, the gates can hold water in both directions and can be rotated up and above water level for inspection and maintenance.

Another unique feature of this project is that the lock heads will be built at the side of the existing canal, after which they will be moved to their final position as complete structures. As a result, the canal can, for as long as possible, remain available for shipping during the construction phase.

[1] S3P (Iv-Infra b.v. & MH poly Consultants & Engineers b.v.), The Netherlands;
J.R.Augustijn@Iv-Infra.nl
[2] S3P (Iv-Infra b.v. & MH poly Consultants & Engineers b.v.), The Netherlands;
W.P.J.Langedijk@Iv-Infra.nl

Figure 1: Visualisation of the future Södertälje lock
(Source: Swedish Maritime Administration through Sweco Architects)

2. Structural and Mechanical Design

2.1. Tainter Gates

2.1.1 Layout

A tainter gate consists of a leaf gate with arms connecting it to the horizontal axles. The leaf gate has a skin plate formed as a cylinder segment. The 2x2 radial arms connect the leaf gate to the two main axles situated in machine buildings on either side of the lock. At the back of the skin plate, two buoyancy chambers are integrated into the structure. Moreover, the structure is built up with main and secondary girders and stiffeners. The buoyancy chambers ensure that the gate will tend to close automatically, although, for safety reasons, it will be locked in position when opened or closed. The circular shape of the skin has the advantage that the line of action of hydrostatic pressures remains close to the main axles and that the arms can transfer the forces to them by the normal force. End stops integrated in the threshold secure the position of the gate in closed position. To avoid ships damaging the gate arms, a modular fender structure is mounted on the lock head and between the gate arms and the canal.

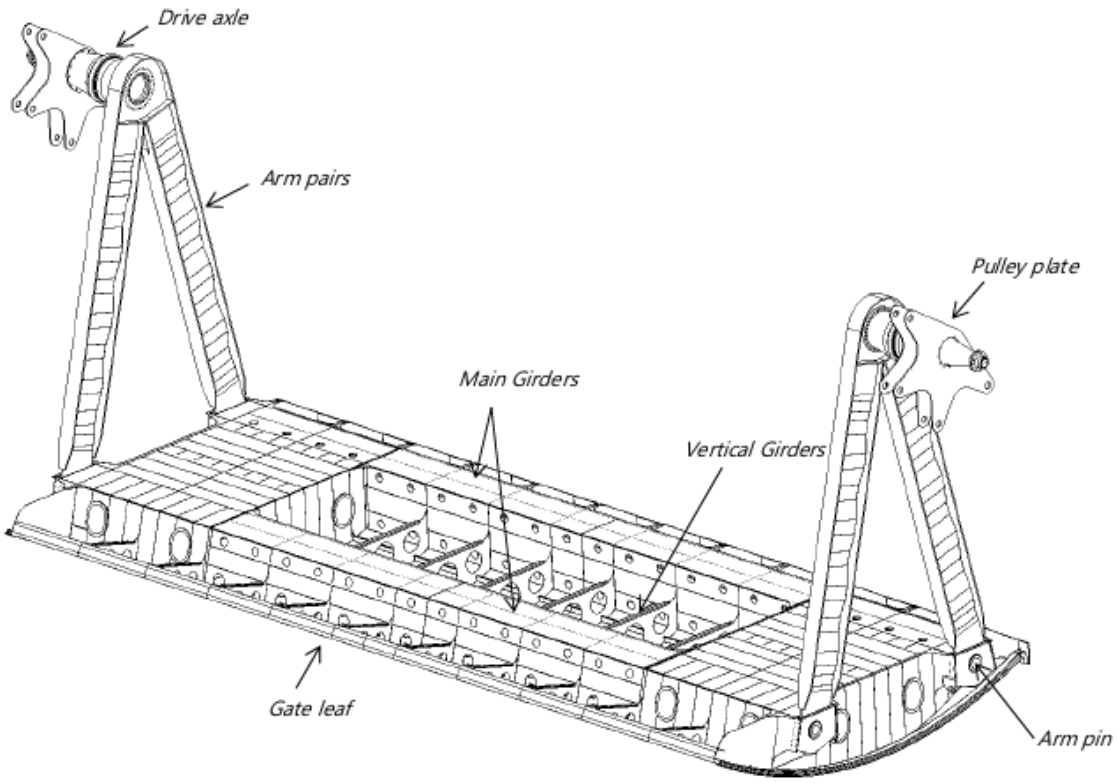

Figure 2: Structural design tainter gate

2.1.2 Buoyancy Tanks

The buoyancy tanks are fatigue sensitive due to the alternating position of the tanks relative to the water surface. This results in severe hydrostatic pressure differences between open and closed positions. Since a direct connection of skin-stiffeners against the tank skins leads to high stresses, they need to be disconnected from the tank plates or placed in line with the internal tank stiffeners. To reduce peak stresses on this type of connection, gusset plates are used.

With regards to fatigue, the internal buoyancy tank stiffeners are critical. The tank skin plates need to be properly supported so that bending stresses near internal bulkheads are kept to a minimum. Standard skin stiffeners like L-profiles or bulb flats have insufficient stiffness and result in poor fatigue life. Hence, continuous stiffener rings are used to support the tank skin plates. On the plates where continuous rings cannot be placed, stiffener plates with soft-toes are applied to minimise stress concentrations.

Manholes of 600x800mm are placed at the side of each tank. This allows for direct access to each tank.

2.1.3 Gate Arm Detailing

A common design approach for tainter gates is a rigid arm connection with the gate leaf and a flexible connection with the drive axles. During the design process, two major issues were found regarding the arm pairs and the connections to the gate leaf and drive axles:

- Due to global deflection of the gate leaf, bending is introduced through the rigid flange connection to the arm pairs. These bending stresses occur every cycle, resulting in fatigue near the flange connection.

- The flexible asymmetric connection of the axles to the arm pairs reduces the drive torque capacity of the arm pairs. The failure mode is a loss of stability. The design of this connection (regarding plate thickness and brackets to aid stability) will be governed by the emergency load cases “single sided drive” and “blockage”. To increase stability and enhance the torque capacity of the connection, the plate thickness of the flexible plate needs to be increased and brackets need to be added. However, this eliminates the benefits of a flexible connection.

It can be concluded that the arm-drive axle connection is too flexible, and the arm-gate leaf connection is too rigid for an optimal design. To solve the issues described above, the arm pairs were redesigned. This redesign used a rigid arm-drive axle connection and a flexible arm-gate leaf connection. This alternative design adapts better to global deflections and reduces bending of the arms, improving fatigue life of the bolted connections and arm pair details. The flexible connection between the arm pairs and the gate leaf consists of a pinned connection, which is also helpful from the point of view of installation and maintenance.

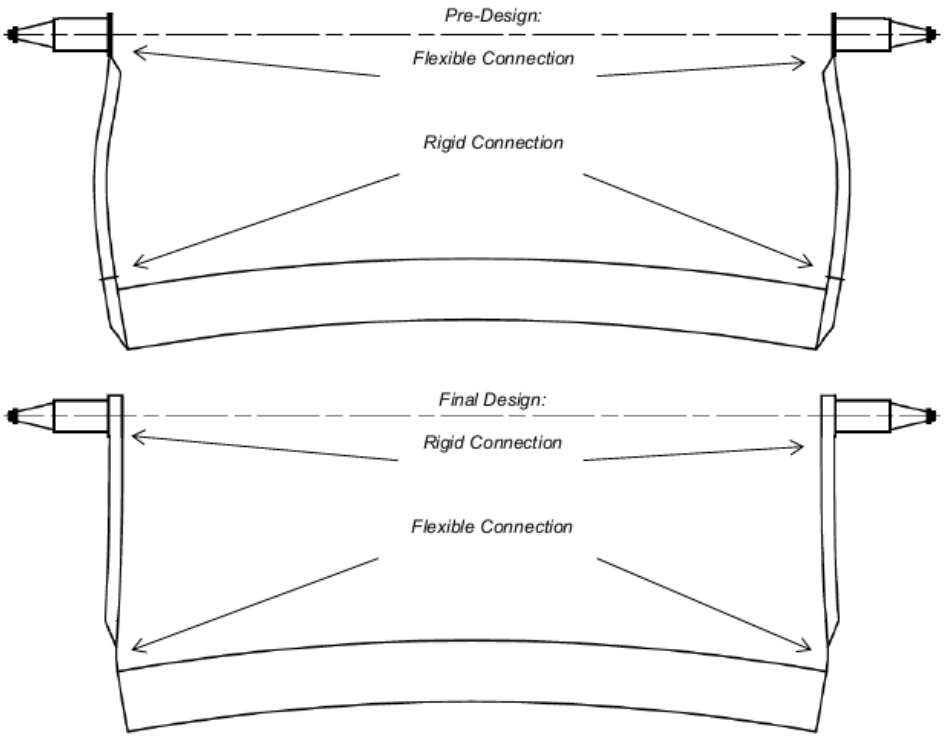

Figure 3: Arm detailing principles

2.1.4 Ship Collision

The sluice gate is checked for a 250t vessel collision at a speed of 1 m/s. The location of the impact, as well as the bow shape of the vessel, have major effects. Reaction forces are high, but local deformations are minimal.

The sluice gate, drive axles, bearing skids and concrete are designed to withstand these reaction forces. If a larger vessel impacts the gate, the weakest link is the pinned connection between the gate leaf and the arms, although the breaking load of the pins is uncertain due to a range in material properties.

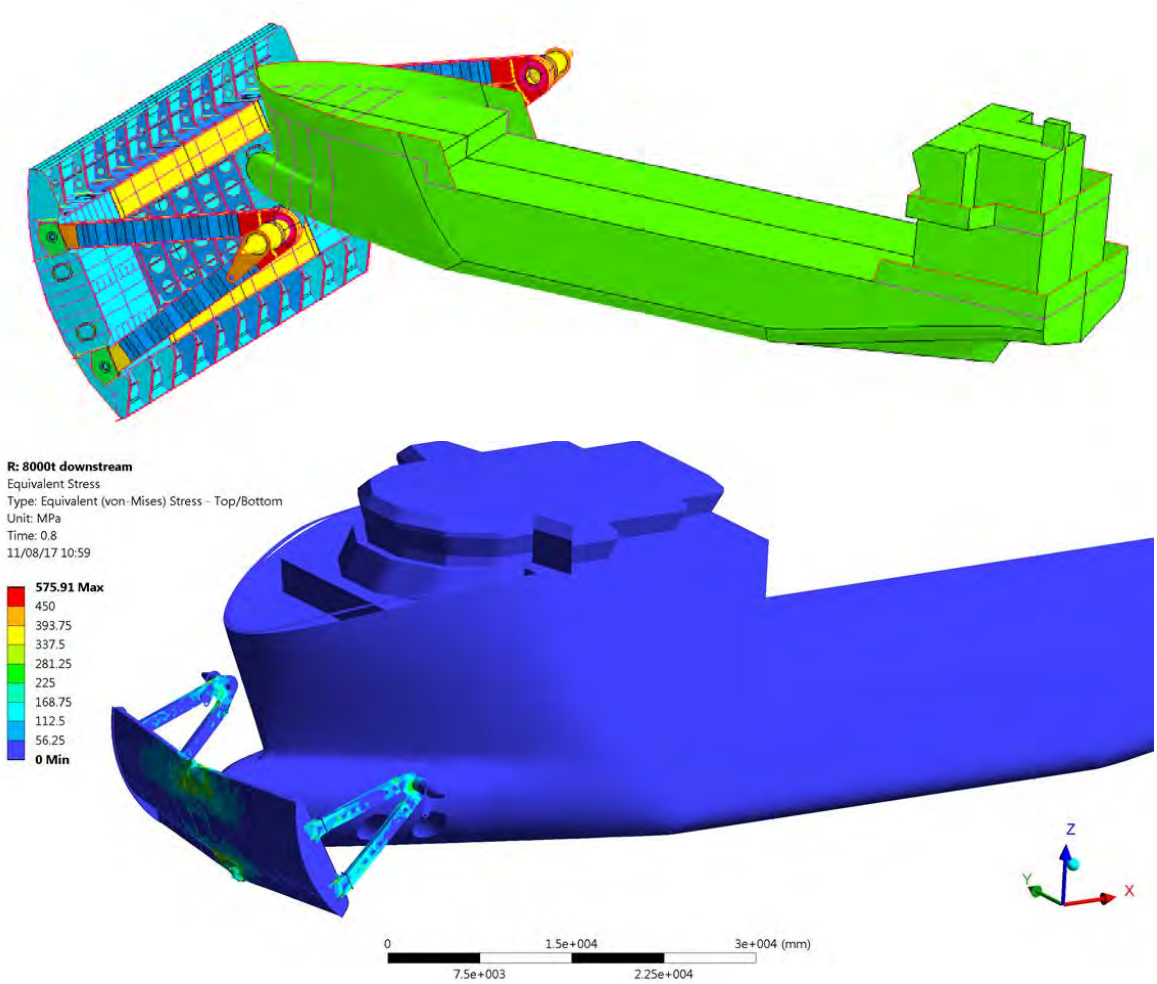

Figure 4: Ship collision analysis

2.1.5 Main Interfaces and Sealing Design

The interface between the gate seals and their opposite surfaces in the lock head requires specific attention. This is because of the circular shape at the sides and the fact that it needs to be both watertight and durable. While opening, due to the innovative arrangement, the side seals will move away from their contact surfaces instead of sliding along them, limiting friction and wear of the seals. While opening, the gate will temporarily be stopped at 5°, where an indented part of the skin forms a maximum opening to allow the water in the lock chamber to level with the water on the other side of the gate.

The sealing is arranged with rubber profiles on both sides and on the bottom of the closed gate. For the side seals, two mirrored self-activating seals are applied with a nominal (theoretical) compression of 10 mm when the gate is fully closed. The construction tolerances (based on DIN 19704-2) and structural deformations determine the sealing design. For the bottom seal, this leads to a total

compression capacity of 37 mm, with a nominal compression of 20 mm. Because of a relatively large deformation of the slender gate leaf, the contact area of the embedded plate in the threshold is perpendicular to the deformation direction.

Another important aspect is the compression stiffness of the bottom seal. In a closed position, the gate must make contact with the end stops and the bottom seal should be compressed. Both the buoyancy and the drive system are responsible for the forces that compress the bottom seal. For this reason, a double self-activating seal will be applied.

2.3 Drive System

2.3.1 Layout

Each gate is moved by two hydraulic cylinders located at each main axle. The main bearing positioned near the gates arms and a secondary bearing inside the machine building support each axle. Each axle assembly, the pulley plates, the main and secondary bearing, and the drive cylinder are integrated on one skid, which can be positioned and aligned in the desired position and direction, both at the start of the project and if necessary, adjusted in a later stage. This ensures that any eventual settlements over time will not lead to unnecessary high stresses, friction and wear in the main bearings.

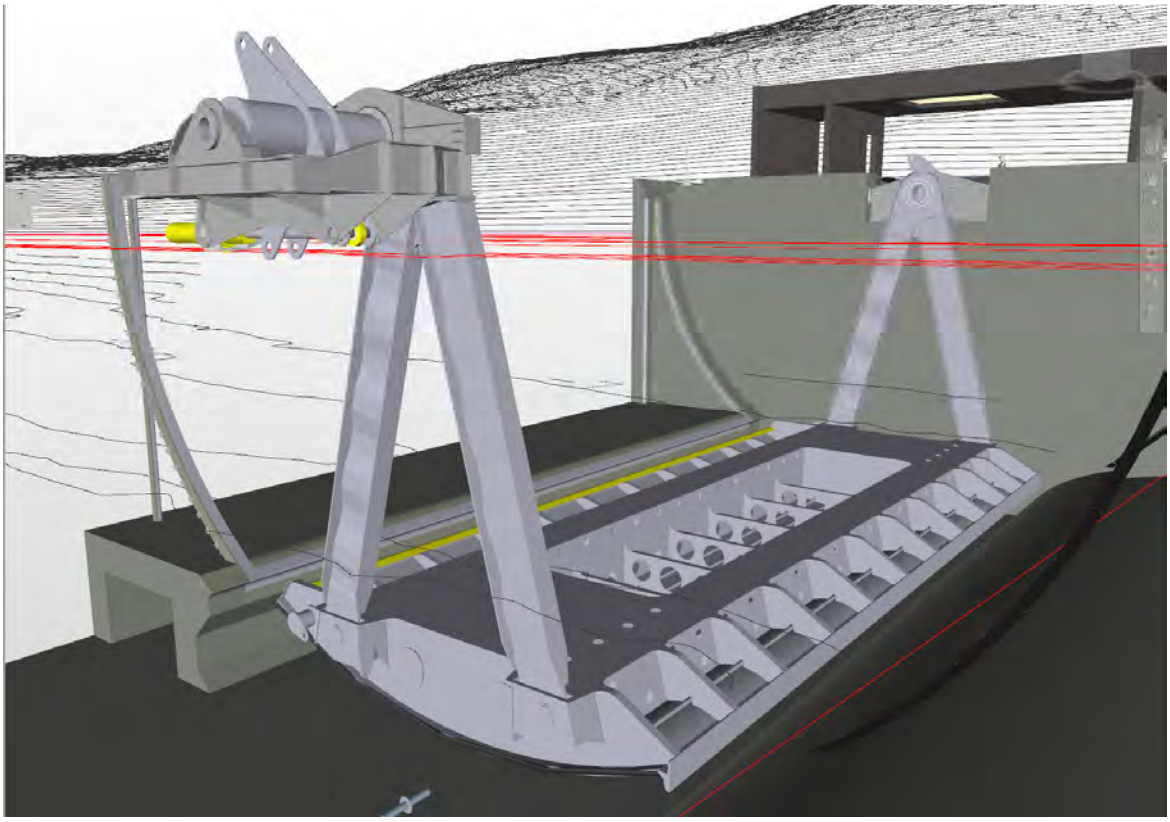

Figure 5: Gate and gate arms relative to drive system

2.3.2 Gate Positions

On each side of the sluice head, the tainter gate is equipped with a hydraulic cylinder to move the gate. These cylinders are connected to pulley plates and are welded to the gate axle. In the closed

position, the gate has an angle of 60 degrees to a vertical axis. In the opened position, this angle is 0 degrees. The position of the lock is regulated by the cylinders. A locking pin in an oblong hole in the pulley plates secures the position of the gate in both positions.

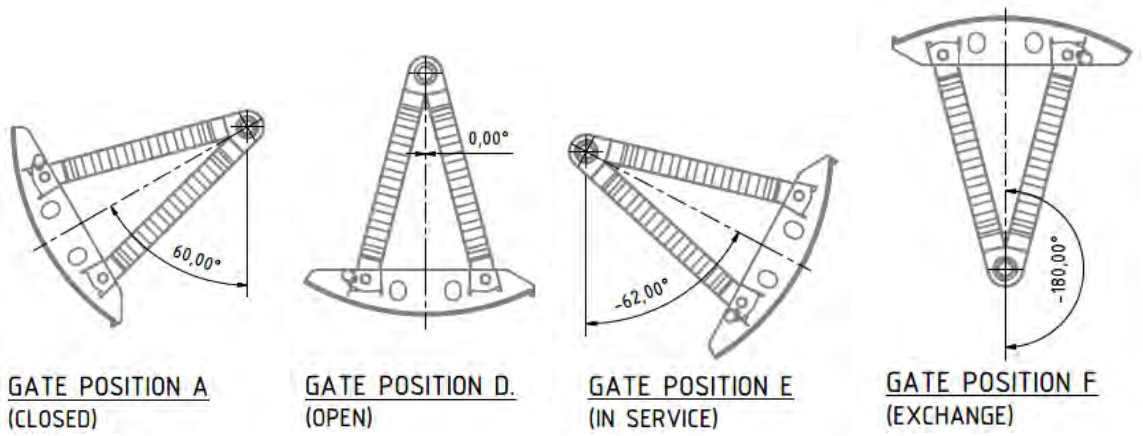

Figure 6: Gate positions (excl. position -120^0, in service)

For maintenance, the design allows for two gate positions. At an angle of -62 degrees the bottom seal is maintainable. By replacing the cylinder to another hole in the pulley plates, this position can be reached and locked with the locking pin. To put the gate with buoyancy tanks back into open position, the cylinder drive will be needed. For a complete inspection of the gate leaf and arms, a gate angle of -120 degrees is foreseen. Because of the weight of the structure without buoyancy, a mobile crane is needed to lift the structure. An additional support frame in both gate recesses can be rotated to support the structure vertically.

In vertical position (-180 degrees) the gate arms and gate leaf can be mounted and replaced if necessary. An extra gate leaf and a pair of gate arms will be fabricated and stored on site to increase availability in the case of major damage to the structure. The design also provides a second locking pin for this gate position.

2.3.3 Integrated Drive Skid

In the machine room, several mechanical components for the driving of the gate are foreseen, such as the bearings, hydraulic cylinder and two locking pins.

For the following reasons, a steel structure with all mechanical components included (drive skid) is designed to improve manageability of several interfaces.

- Avoids strict tolerances for all separate connections to the concrete structure.
- Provides optimal adjustability of the gate axles. The skid is supported is such a way that by customising the shim plate thickness, the axles can easily be aligned. This is important to be able to allow for any future movements of the sluice head due to settlements.
- Optimises transfer of loads. The forces generated by the drive cylinder must be in balance with reaction forces on the bearings. Embedded structures and local

reinforcement in the concrete structure are optimised when forces are internally transferred through the skid.

- The drive system can be tested anywhere with several advantages.

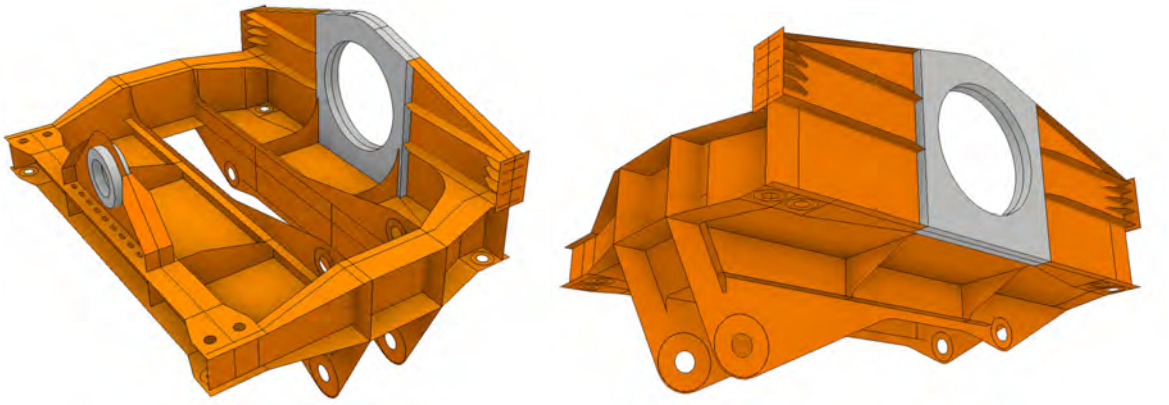

Figure 7: Drive skid

2.3.4 Material Choices Drive System

Rather than a bronze bushing, a composite bushing has been chosen for the bearings. The lower stiffness of the composite material results in better stress distribution. The bearings will be placed in two parts meaning that both parts can be rotated should there be an occurrence of wear. Maintenance and replacement of the main bearings can be carried out in the machine room thanks to a separate watertight shield on the outside of the sluice head wall. In the design, a possible replacement of the gate axle from inside the machine room has also been taken into account.

Both the drive skid and the watertight shield will not be executed in stainless steel. The drive skid will never be in contact with water due to the presence of the watertight shield. The watertight shield is removable by use of a temporary shield which is situated between both structures.

The gate arms are connected to the main axles with a bolted connection. The main axle is supported by two bearings: the main bearing and a secondary bearing. To limit fatigue, loading a proper alignment of the bearings is required. This is crucial for the durability of the steel structures.

2.3.5 Fatigue analysis

The gate arms and axles are loaded by cyclic loading thus fatigue is a potential risk. The fatigue analysis needs to consider gate movements, drive forces and hydraulic loading. For each opening cycle, the buoyancy of the gate leaf results in bending moments in the gate arms and local bending in the buoyancy tanks.

For each opening cycle, a water level difference must be taken into account, including the dynamic forces due to levelling. In addition, the possible misalignment of the gate axles is considered in this analysis. Fatigue analysis is performed with a misalignment of 10mm for each support. The actual alignment of the gate axles will be measured during the inspection, mainly during the period when settlements of the sluice head are expected. The skid (including the gate axles) will be adjusted if necessary.

3. DUPLEX STEEL GATES

3.1 Material Selection

Contrary to common practice worldwide, the client, Sjöfartsverket, proposed a type of lean duplex rather than carbon steel as a base material for the lock gates and bridge. Although this material is more expensive than carbon steel, it has the advantage that an additional corrosion protection system would not be needed, which has a positive effect on maintenance costs and time. Various grades of stainless steel materials are available, each with different corrosion resistance.

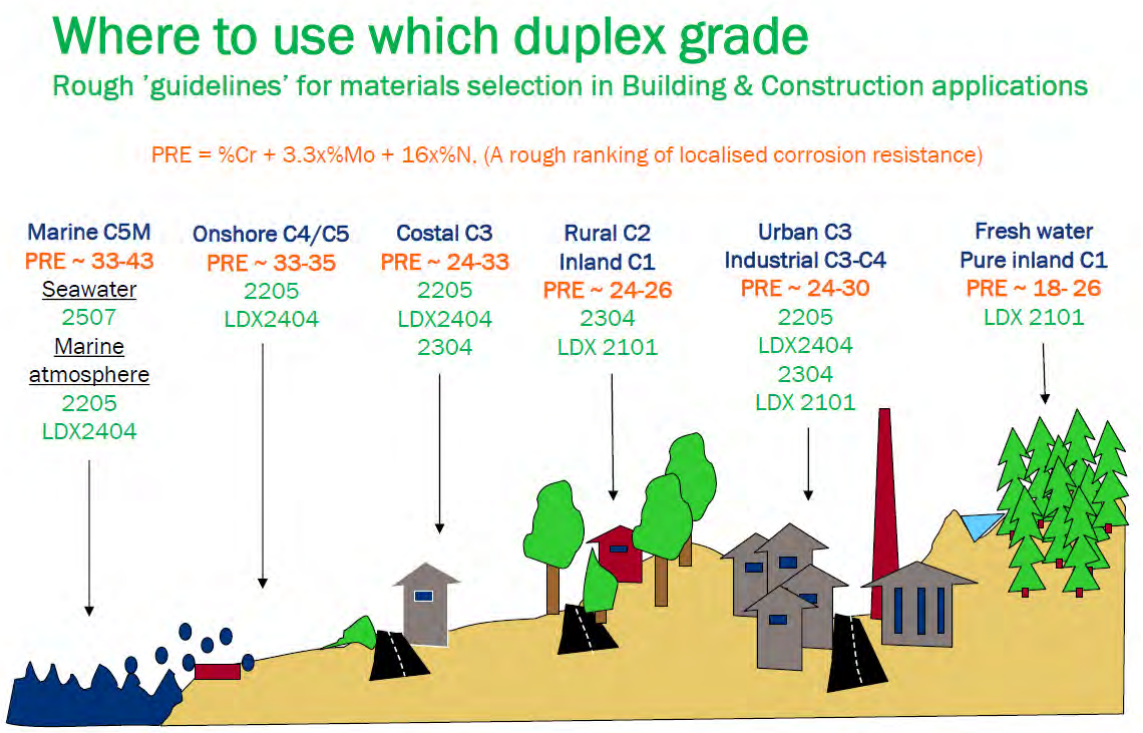

Figure 8: Where to use which duplex grade

Corrosion resistance of stainless steel materials (Austenitic and/or Duplex Stainless Steels) is influenced by the following factors:

- Pitting resistance of selected material grade (PREN)
- Environmental conditions (presence of water, chlorine and other contamination, temperature)
- The effect of fabrication methods (welding and cold forming, flame straightening) on the stability of the microstructure
- Applied improvements of the fabricated finish

In the case of the Södertälje lock gates, the main driving factors influencing the choice of material are the submersion in brackish water and the risk of deposits and/or accumulation of contamination containing salts and bacteria in the open areas. Available materials vary with respect to the provided PREN (pitting resistance equivalent number) and CPT (critical pitting temperature), which both need to be considered. Eventually, Grade UNS S32205 / EN 1.4462 was selected for the lock gates. For optimal corrosion protection, aluminium anodes will also be applied to the gate.

3.2 Effects of Material Choice on Fabrication Methods

Welding affects the corrosion resistance of the applied material. As corrosion resistance is generally reached through a proper range for the austenite-ferrite ratio (phase) of the material, incorrect welding parameters and improper cooling rates can have a negative or even detrimental influence. A proper base material has a 50%/50% phase balance (A/F). To be able to properly weld, or apply other heat treatments (e.g. plasma cutting, preheating, flame straightening), specific attention needs to be payed to the heat input in relation to the thickness to avoid slow cooling rates and formation of detrimental phases such as Sigma phase. The welding parameters and welding conditions should be optimised to ensure a 40%/60% (A/F) phase balance in the heat affected zone. While in principle, all known welding processes can be used and appropriate welding consumables are available, specific welding qualification samples must be made for each specific grade and range of thickness and welders must be trained and qualified to reproduce these. All heat affected surfaces will require a good surface finishing followed by pickling and passivation.

In addition to heat treatments, cold deformation potentially also has a negative influence on the corrosion resistance. This is due to the phenomenon that an austenitic phase causes martensite at high deformation grades. In the design, specific attention is given to the extent of cold forming, the locations where it is applied and the presence of welds in these regions.

Fumes of (dry) plasma-cutting and welding of Stainless Steels is dangerous for the health of operators, welders and environment because of Cr6. Therefore, extraction of fumes and fresh air helmets for welders are required.

3.3 Fabrication Requirements for Use of Duplex Steel

There are specific requirements when building according to Eurocode and when using specific materials for construction. For this, a project specific fabrication specification had to be drawn up. This specification describes the specific coded requirements that need to be met when building with the prescribed materials for the structure. This Specification summarises the additional requirements for fabrication and assembly of the bridges, lock gate structures including related components and lists additional requirements based on SS-EN 1090-2, the National Annex (BFS 2015-6) as well as the contractor’s requirements.

Several highlights of this specification are (the list is not complete).

- The fabricator, or his authorised representative established within the European Economic Area, is responsible for the affixing of the CE marking.
- Maximum carbon content and carbon equivalent (CEV) for weldability of carbon steels.
- Weldability properties, to be demonstrated by representative tests, which are to be executed on the maximum supplied thickness and for the lowest and highest anticipated heat input used during fabrication welding.
- Material testing requirements for through-thickness testing, ultrasonic examination, notch toughness, tensile, hardness and bend testing, Charpy V-notch testing,

examination of the micro-structure shall over the full thickness for detrimental phases and intermetallic phases near the centreline, the presence of pitting and weight loss, intergranular corrosion tests.

- Demonstration of weldability properties by representative fabrication welding conditions for both minimum and maximum product thickness and for each delivery source.
- Requirements with respect to the chemical composition of materials.
- Thickness tolerances and surface conditions.
- Requirements with respect to identification and traceability of essential fabrication history.
- Avoidance of contamination; requirements for lifting equipment and other tools.
- Requirements and test methods with respect to the applied heat straightening procedures and for cold deformation.
- Qualification of welding procedures and welding personnel.
- Processes to perform welding procedure qualification tests and ferric chloride corrosion tests.
- Requirements with respect to precautions for pre-heating, welding, cooling down after heat treatment, cleaning, blasting, pickling and Non-Destructive Testing (NDT).

4. INTEGRATED 3D MODELLING, STRESS ANALYSIS and BIM

For the structural analysis of the leaf gates, a direct link between 3D modelling software Inventor (used to generate drawings) and FEM analysis software, established Ansys Workbench. The FEM model was generated from the 3D design ('surface') model and any required changes and optimisations found in the structural analysis were fed back into the 3D model. This way the drawings are automatically consistent with the structural analysis, optimising time and quality.

To be able to do this, however, the model created in Inventor does not include the thickness of the materials, which is why it is called a 'surface model'. The final thicknesses as determined in the FEM analysis must be modelled in the 3D design, turning it into a 'solid model'. From this solid model, 2D drawings can be generated. The solid model can also be used as input to the Building Information Model (BIM) in which all the available building information can be integrated and all interfaces are made visible.

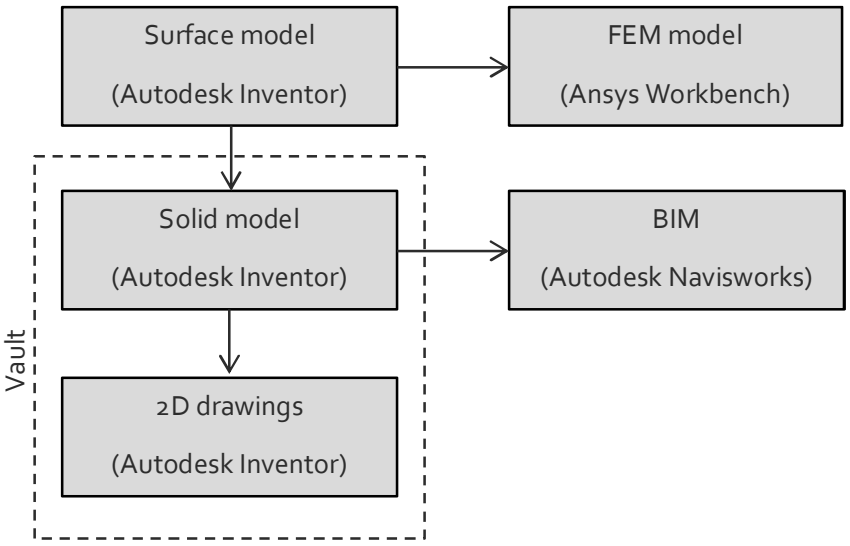

Figure 9: Modelling process

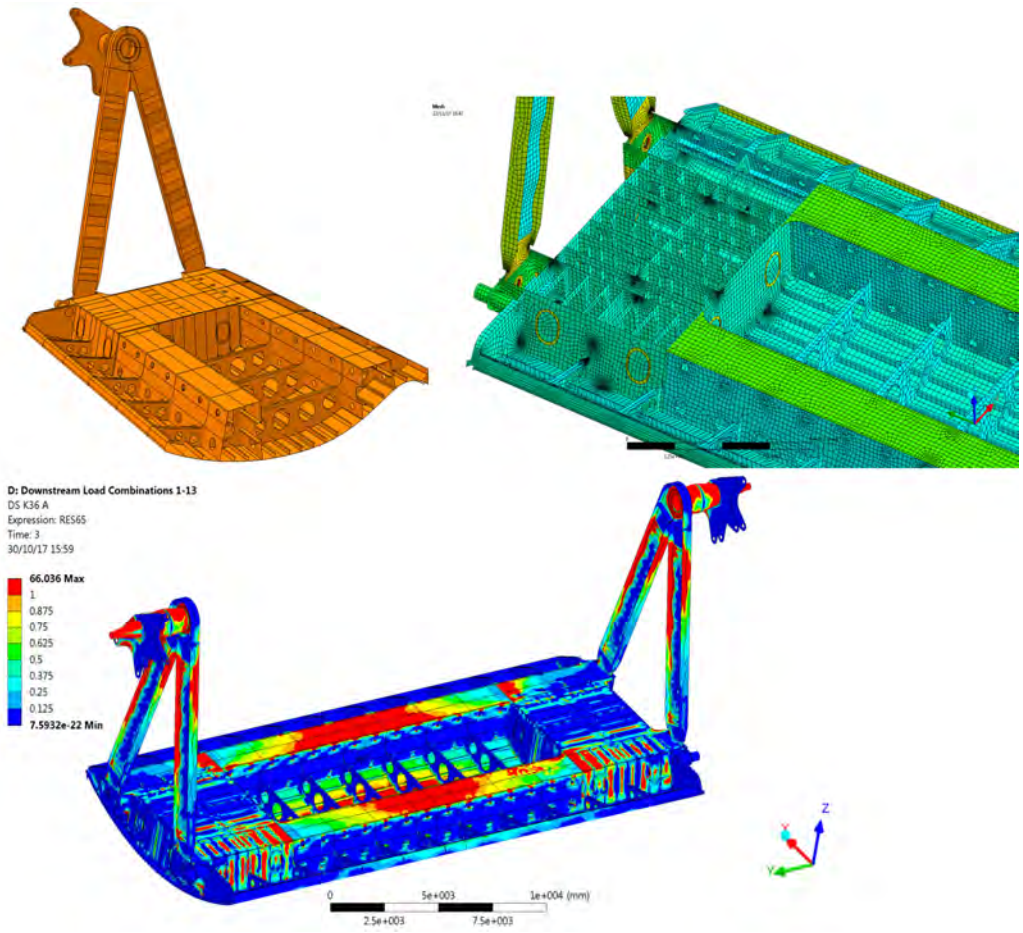

Figure 10: 3D model in inventor and FEM, mesh generated from it in Ansys Workbench and stress plot after FEM analysis

For the FEM analysis of details, such as the analysis of critical weld details, it is required to 'zoom in' and thus apply a finer element mesh. In Ansys Workbench it is possible to break a FEM model into sub-models or the reverse; combine separate detailed models generated by Inventor. These blocks are then analysed separately, each with their own model, but linked to each other by the overall geometrical environment. Since they are all linked, the data generated in separate blocks is automatically used by the other blocks.

In addition to the linking of models and sub-models, separate analysis types, such as linear, dynamic and elasto-plastic (collision) analyses can also be linked. Thanks to this structure, the overall design process is parametric and has a high level of integration. This allows for flexibility while designing and optimisation of the design.

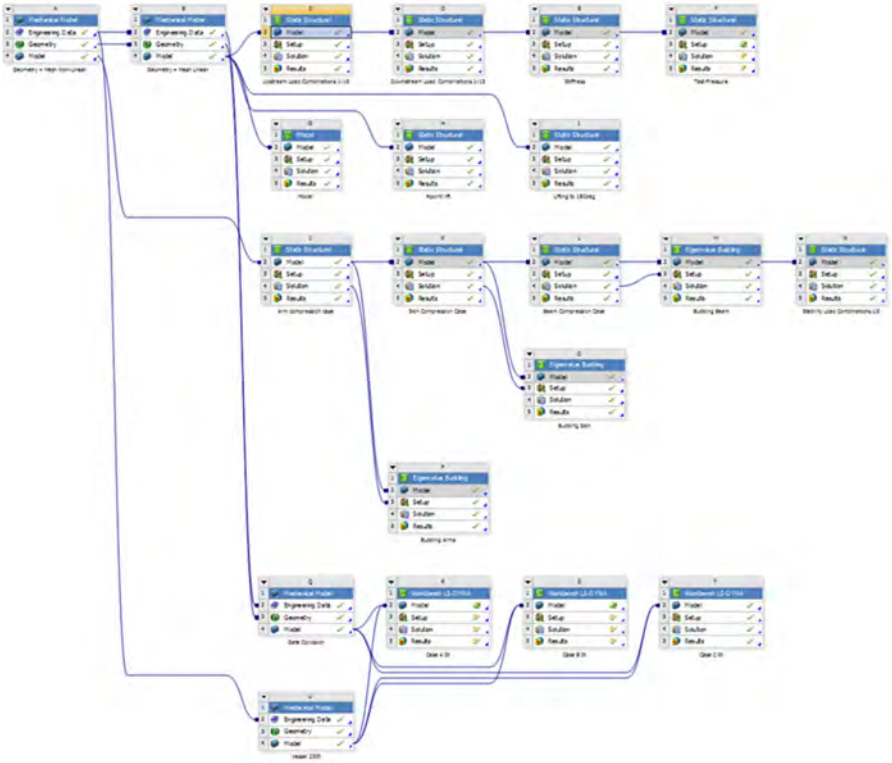

Figure 11: Process of FEM model integration

5. Construction Method

To allow ship traffic to continue during most of the construction phase, the lock heads are constructed in building pits at the side of the canal. Construction of the lock heads is thus carried out in dry conditions. The interface areas for the gate seals consist of embedded duplex steel and are prepared in a 2nd stage concrete cast so that they can meet the stringent geometrical tolerances required for such areas. Mock-up tests with the drive system and with dummy structures for the seals will be also carried out in these dry conditions.

The original plan was to move the lock head from the construction pit to its final position by skidding, but after an evaluation of schedule, risks and costs, the alternative, based on floating was chosen. When the lock head is in place, it will be temporarily supported by four jacks at the corners. Hereafter, the gap between the bottom of the canal and the lock head will be filled up with concrete. Moving and sealing the lock heads in their final position is to be carried out within a maximum of one week for each.

Building on top of the footprint of an already present lock and dealing with surrounding existing buildings and infrastructure means that the surrounding buildings, temporary structures and new structures which add to the lock function itself, like the bascule bridge, the moveable walkway and the machine buildings, all require specific attention to interfaces. There are many situations where interference can be critical, which requires the various design teams to work together seamlessly.

6. RISK MANAGEMENT

7.1 General

During the design process optimisations and possible risks were investigated. Maximal availability leads to a support system of the openable walkway (double rolling bridge at the upstream sluice head) without a support on top of the closed gate.

Natural frequencies are calculated by means of modal analysis using different amounts of added mass in various directions. Cylinder stiffness is included in this analysis and has a large contribution to the result. The rotational natural frequency range is between 0.25Hz and 0.55Hz. From the quasi-static CFD analysis, frequencies within this range are found. Due to the damping of the surrounding water and the non-linear spring characteristic of the cylinder, it is expected that resonance will not occur. For this reason, the design of the drive system is based on a larger hydraulic cylinder, with good damping properties and a higher capacity than minimally required cylinder diameter.

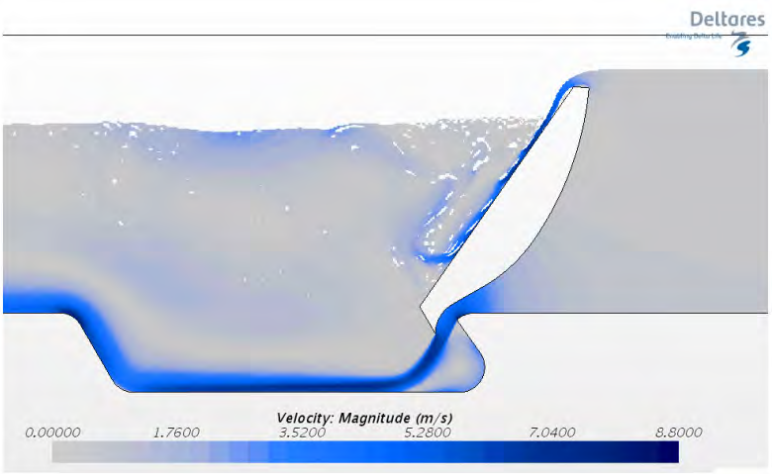

Figure 12: CFD-study

7. CONCLUSION

For the renewal of the lock in the Södertälje Canal, several innovative and state of the art design strategies, as well as construction methods, have been used.

During the design process, the integration of 3D surface models and FEM models allows for a high level of flexibility. Integration of the main axles and the drive cylinders on integrated skids, allows for a quick construction and adjustability when the positioning of the lock head changes over time due to settlements.

The choice for a duplex steel as a material for the gates and main axles is a relatively new approach to allow for lower maintenance costs and higher availability of the lock during its life. To be able to do so, however, specific precautions are to be taken in the manufacturing process.

Constructing the lock heads at the side of the existing canal and moving them to their final position as complete structures allows for a high level of availability of the lock during this large-scale renewal project.

In 2021 the new sluice will be opened. The design of the stainless steel tainter gate will be an interesting example for future sluice designs.

HISTORICAL QUAY WALL RENOVATION IN ANTWERP, BELGIUM

by

Gerrit Feremans[1], Reinhilde Vanhooydonck[2] and Koen Segher[3]

Abstract: The historical quay walls of the river Scheldt are a major landmark of Antwerp. After almost 150 years of continuing instabilities, the right bank quays are stabilized along their entire length. This durable renovation project, being challenging in its own right from a geotechnical point of view, is further complicated by the requirement to preserve the historical bluestone facing as well as the historical position ('quay line') of the quays. Innovative techniques are devised to restore the Scheldt quays to their old glory in a cost efficient way. The works are currently ongoing in several zones, two of which are discussed as case studies in this paper.

Key words: waterway infrastructure, quay walls, renovation, stabilization, historic masonry

1 INTRODUCTION

Among the most characteristic features of the city of Antwerp (Belgium) are its historical Scheldt quays. Stretching about 5.5km along the western edge of the city centre, the quays were constructed at the end of the 19th century. Severe indications of instabilities have been observed as early as during the construction itself. Despite the multitude of efforts to alleviate these instabilities over the last century, they continue until today.

In 2005, the council of the city of Antwerp and DVW (i.e. De Vlaamse Waterweg nv, the independent agency of the Flemish Government in charge of the management of the Scheldt river banks including the protection against storm surges) have agreed to carry out the most significant renovation works in over a century. Three main goals were set for this long term plan:

- The stabilization of the historical quay walls with a quay level of +7mTAW. (TAW i.e. 'Tweede Algemene Waterpassing' is a topographic reference level in Belgium corresponding to the low water tide in Ostend: 0mTAW);
- The protection of the city against increasing storm surges as a result of climate change. This goal is part of the integrated Sigma Plan (the plan to protect the whole of the tidal Sea Scheldt bassin against storm surges) and requires a new storm surge barrier (+9,25mTAW) to be built on the existing quays.
- A facelift to restore the city's link with the river by incorporating urban development and mobility, creating new public domains and preserving historical monuments. The quay walls are a significant part of the latter.

In this paper, the focus is on the stabilization of the historical quay walls. First, the history and the construction of the quays are treated, along with a description of the stabilization measures taken since their construction. Then, the master plan for the stabilization of the quay walls is explained before focusing on two case studies of stabilization works in the final section of the paper.

2 A BRIEF HISTORY OF THE QUAY WALLS

2.1 A brief history

Over the last centuries, the river banks of the city of Antwerp have been reorganized several times. After a first wave of harbour expansion works initiated by French Emperor Napoleon at the end of the 18th century, the city experienced an industry boom when the toll charges on the Scheldt were lifted by the

[1] gerrit.feremans@sbe.be, SBE nv, Belgium
[2] reinhilde.vanhooydonck@vlaamsewaterweg.be, De Vlaamse Waterweg nv, Belgium
[3] koen.segher@vlaamsewaterweg.be, De Vlaamse Waterweg nv, Belgium

Dutch in 1863. By the end of the 19th century, the course of the river Scheldt was straightened to make the harbour more accessible, more spacious and more efficient. As a result, all right bank quays had to be renewed. The works were carried out in the northern stretch of approx. 3.5km (1877-1884) and the southern stretch of approx. 2km (1897-1903).

Significantly altering the natural course of the river, hundreds of medieval houses, the old ship yards and the Spanish fortress near the city centre had to be demolished to build the new quays. As a result, the quay walls were only partially constructed on the existing banks and mostly in wet conditions in the original river bed, as shown in Figure 1. These circumstances have had an important influence on the design and the construction method of the quay walls.

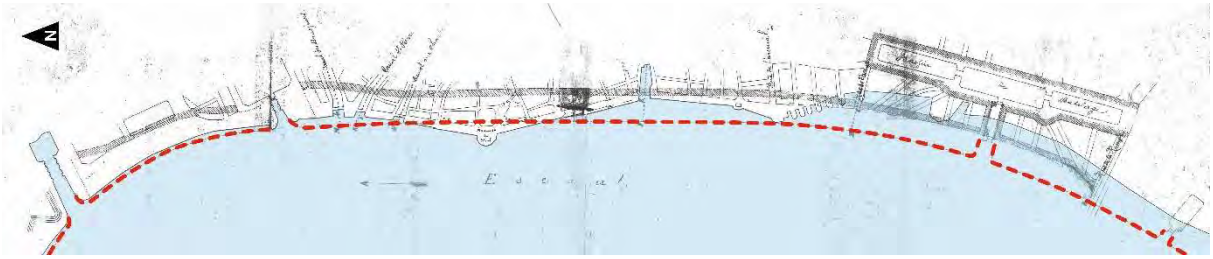

Figure 1: Location of the new quay walls (red line) w.r.t. the original river banks at the end of the 19th century (based on the original construction plans).

2.2 Construction method

The quay walls were designed as massive gravity retaining walls, as shown in Figure 2. The foundations of these gravity walls were conceived as massive concrete bodies, constructed within a pneumatic caisson. The steel caissons are about 25m long, 9m wide and 2,5m to 5m high. The bottom level of the caissons is located between -10mTAW and -15mTAW.

On top of the foundation caisson, temporary steel walls were mounted to allow for the construction of the actual masonry gravity walls in dry conditions. The tidal river Scheldt has mean water levels varying between approx. 0mTAW and +5,5mTAW at resp. low and high tide. Once the low tide line of the river Scheldt was reached, the foundation caissons were filled with concrete. Above the low water line, the quay walls were cladded with quarried Belgian bluestone on the riverside to enhance the durability of the walls. Once the quay wall had reached its final height at approx. +7mTAW, a sand fill was carried out behind the quays to level the surface. In some areas fascine mattresses were used to stabilize the significant underwater filling operations.

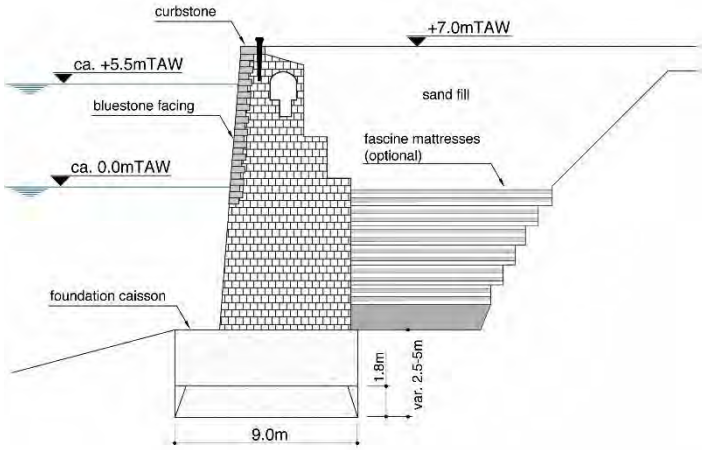

Figure 2: Standard section of the masonry quay walls on top of the foundation caissons, filled with concrete

2.3 Stability issues

As early as during the construction works, the new quay walls started to show signs of instabilities. The resistance against translation proved insufficient and in some areas the quay walls gradually shifted in the direction of the river.

The main cause is attributed to several crucial mistakes in the original design. Not only were the geotechnical soil characteristics underestimated, also and even more importantly, the influence of the ground water levels was disregarded in the design. The foundation levels should thus have been set deeper. Furthermore, it was observed upon completion that the drains behind the quays were mostly malfunctioning.

Although measures were taken instantly during the building phase, at several occasions over the last century severe instabilities have been reported. These instabilities are mostly attributed to high groundwater levels behind the quay walls. The most severe stability issues were encountered in the south, where the new quays had to be constructed in the original river bed (cfr. Figure 1) and where the presence of the tertiary Boom clay layer influences the stability. This significant tertiary clay package is found at shallower subsurface depths in the south than in the north.

As a result, a patchwork of temporary and permanent remedial measures can today be found along the Scheldt quays, some of which are illustrated in Figure 3:

- To increase the sliding resistance, additional counterfort caissons have been placed in front of the quay walls in large stretches of the quays. Sometimes, clay or blast furnace slag embankments were placed in front of the quay walls as a permanent measure as well.
- To alleviate the risk of tilting, additional drains and stress relieving vaults were installed behind the upper parts of the gravity walls. In several areas, the soil behind the quay walls was removed and replaced by lighter materials such as ashes. Exceptionally, the soil behind the quays was permanently excavated, making the quay in this zone useless for any activity.

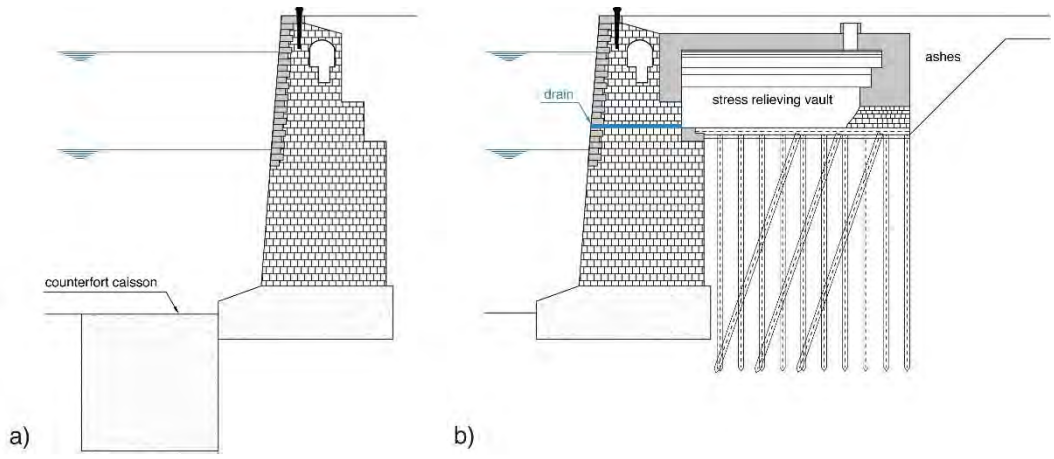

Figure 3: Remedial measures to limit horizontal movements with (a) counterfort caissons in front of the quay wall or (b) stress relieving vaults behind the quay walls

3 A MASTERPLAN FOR THE STABILIZATION OF THE QUAYS

Knowing this history of instabilities, a masterplan for the renovation of the quays was commissioned by DVW. The overall condition and stability of the quays was surveyed and studied along the entire 5,5km length.

First of all, all recorded historical instabilities and stabilization measures were inventoried for each zone. This was accompanied by thorough field inspections, a borehole campaign and diving inspections. A multitude of damage phenomena were found. Some of the most frequent observations are listed in Figure 4.

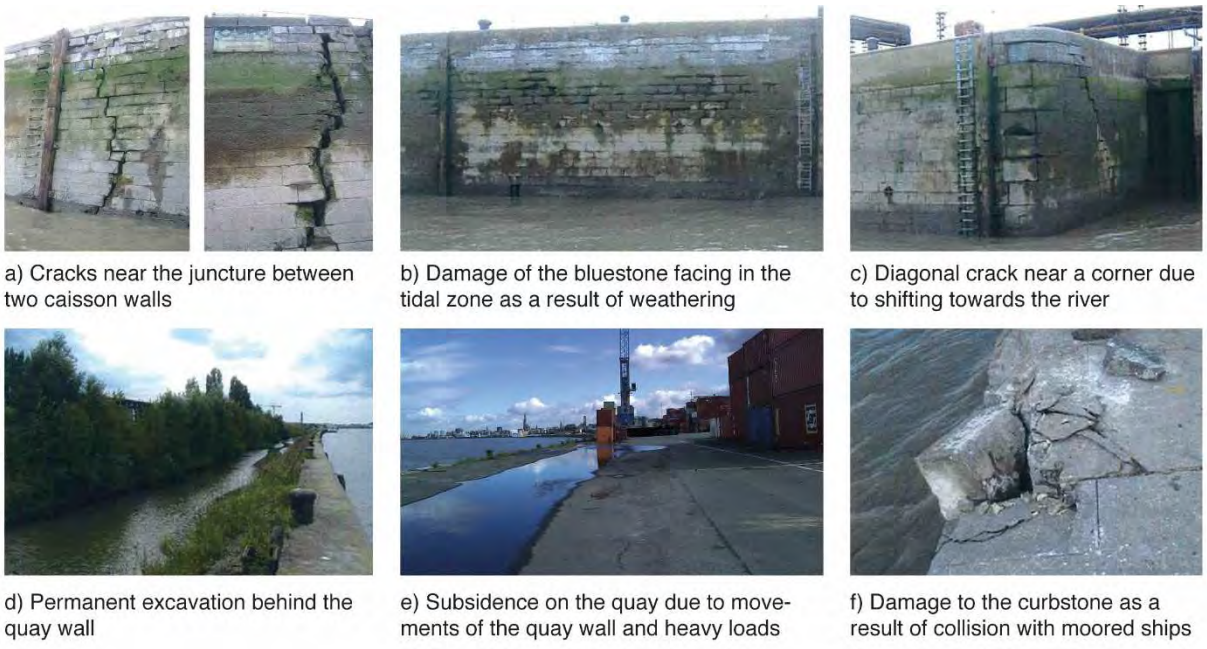

a) Cracks near the juncture between two caisson walls

b) Damage of the bluestone facing in the tidal zone as a result of weathering

c) Diagonal crack near a corner due to shifting towards the river

d) Permanent excavation behind the quay wall

e) Subsidence on the quay due to movements of the quay wall and heavy loads

f) Damage to the curbstone as a result of collision with moored ships

Figure 4: Inspection of damage phenomena on the Scheldt quay walls

It is clear that not all the recorded damage was due to the instability of the gravity walls, e.g. cases (b) and (f) in Figure 4. Nevertheless, the renovation of the quays is seized as an opportunity to tackle all observed damage phenomena for the future.

Then, calculations were performed to assess the stability of the quays in the current situation, taking into account all remedial measures carried out over time (additional counterfort caissons, relieving vaults, etc.). An extensive geotechnical survey determined the soil characteristics according to present day practice. Subsequently, the stability checks for bearing capacity, shifting & tilting resistance, global sliding etc. were performed in line with the current design codes.

The results of these geotechnical calculations showed that the required safety for the different failure criteria was met in nearly none of the sections. Even after grading the requirements down to a unity check and after calibration of the parameters assuming that a section that had never encountered damage or instabilities in the past should be the reference for equilibrium, the bearing capacity and the resistance to translation proved insufficient in nearly all the sections of the quays.

Based on all data and calculation results collected, a risk chart was developed to indicate the zones with the highest instability risks and hence the highest priority for renovation. In addition, remedial measures were proposed ranging from expensive to cost-effective or, in other words, drastic reconstruction to minor restauration according to the state of the quay walls in each zone.

With the conclusion of the study phase in 2010, the long term masterplan was developed. This masterplan splits the renovation works into subareas with higher/lower risks and priorities. It includes several requirements for future use of the quays. Harbour activities are abandoned as a future use for the main part of the historic quay zone, but mooring of ships at the historic quays is still desired and is taken into account in the calculations as summarized in the following.

- It should be possible to use the quays for mooring of ships, e.g. the design vessels used in the design of d'Herbouvillekaai as specified in Table 1. Therefore, the original bollards installed every 20m along the quays are incorporated in the new design. The required characteristic bollard pull is 1000kN.
- The overload on the quay areas redeveloped as public domain should be at least 20 kN/m².
- In areas where the new storm surge barrier is located close to the quay wall these loads are incorporated in the quay wall renovation design.

		MARITIME NAVIGATION		INLAND NAVIGATION
		passengers	freight	freight (cat. VIb)
LAO	(overall length)	260m	224 m	140m
LPP	(length between perps)	220m	220m	-
B	(beam)	33.1m	32.3m	15m
D	(draught)	7.6m	8m *	3.9m
DWT	(deadweight tonnage)	37 600tons	approx. 30 000tons *	-

* maximum allowable draught restricted from 13.3m to 8m for mooring along the Scheldt quays

Table 1: Design vessels for mooring along the renovated quay wall at d'Herbouvillekaai

4 CASE STUDIES

The stabilization of the quays officially started in 2012. Several subprojects are currently being executed or prepared. In the following, two cases explain the design of the stabilization and several practical issues of execution.

4.1 Case 1: d'Herbouvillekaai

4.1.1 Monitoring & emergency measures

Based on the first conclusions of the stability study discussed in the previous section, the displacements of the quay walls were carefully monitored as none of the quays met all present day safety standards. The dedicated expert panel indicated that several precautionary measures had to be taken in the subarea with the highest risk of instabilities. In this zone along D'Herbouvillekaai in the southern part of the quays, horizontal movements of the quay walls could still be observed, despite all measures that had been taken in the past (counterfort caissons, relieving platforms, etc.). Additionally, this area was at the time still being used for intensive transshipment activities.

As a precautionary measure, the allowable load in the zone of influence of the quay wall was restricted since additional permanent displacements up to 7mm had been measured after the quay had temporarily been used for storage of steel beams. Additionally, an elaborate monitoring campaign was set up. Inclinometers and monitoring wells were installed to follow the evolution of the shifting and tilting movements of the quay walls.

The results of this monitoring campaign were alarming. Despite the restrictions on the allowable loads, the measurements indicated that the shifting movement had worsened. The results also show that the measured displacements are only the result of the moving gravity walls as the soil below the foundation caissons remains stationary.

In 2011, the restrictions were intensified but by September 2012 progressively worsening displacements could still be observed. In one measurement even a tilting of the walls was diagnosed, as shown in Figure 5. As a result, all industrial activities on the quays were prohibited with immediate effect in this area.

Other remedial measures included the installation of a clay berm in front of the gravity walls and eventually even the excavation of soil behind the quays to alleviate the active soil pressures, as shown in Figure 6. Despite these drastic measures the shifting and tilting continued, albeit at a slower rate as shown in the inclinometer results in Figure 5.

4.1.2 Stabilization design

The deteriorating state of the already damaged quay walls numbered down the options for renovation drastically. Any solution considering the reuse of the existing quay walls in the future had to be disregarded for several reasons. First of all, there was no room for experimentation with new techniques in the area. The mere fact that an implicitly uncertain technique would have to be carried out in close vicinity of the already unstable quays was inadvisable. Furthermore, the overall stability in any of the scenarios with reuse would always somehow depend on the structural integrity of gravity walls in their

current state. Finally, any solution with a permanent berm in front of the quays for stabilization, similar to the temporary solution in Figure 6, was also not an option as this compromises the requirement for the mooring of ships along the entire length of the quays.

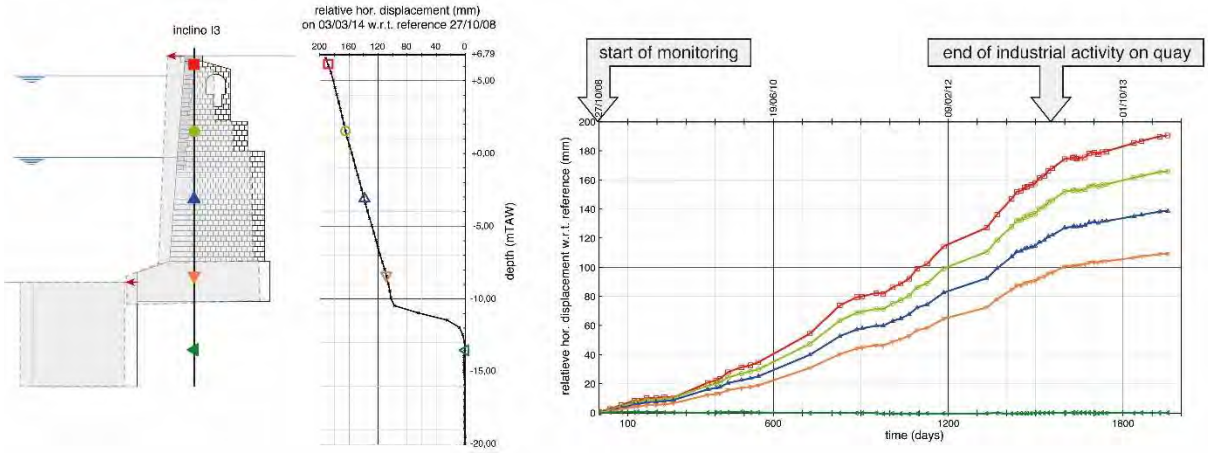

Figure 5: Relative horizontal displacements as a function of depth and time from inclinometer measurements inside the quay wall at D'Herbouvillekaai

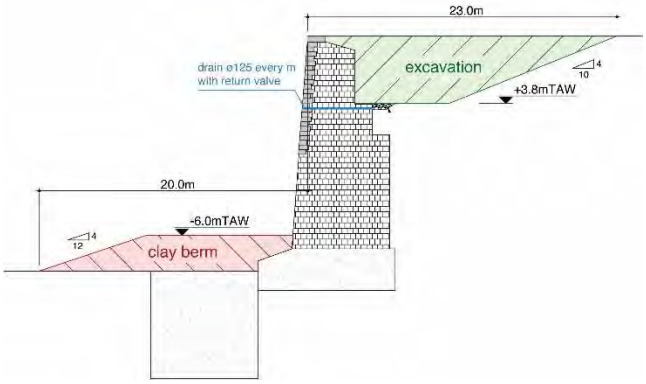

Figure 6: Drastic remedial measures along D'Herbouvillekaai in 2012: clay berm and drained excavation

Another important influence factor is the risk of encountering problems or instabilities during construction. Solutions where the entire present quay wall is retained and encapsulated inside a new retaining structure could involve execution problems, e.g. when counterfort caissons are damaged. Furthermore, an encapsulated wall would damage the historical 'line' of the quays.

In the end, the only viable and durable solution was the radical reconstruction of the quay walls, at the exact historical position, as shown in Figure 7. The existing gravity walls are entirely demolished (including the pneumatic foundation caissons) and replaced by a tube combined retaining wall with 37.5m long steel tubes. Two rows of anchors are attached to an anchor wall located 38m inland. This sheet piling wall is used as retaining wall during the construction phase. The river bed near the toe of the combined wall is protected with a rocky debris fill. Any original counterfort caissons present in the river bed are left at their current location. Removing them would influence the stability of the new retaining walls in a negative way.

4.1.3 Preservation of the historical bluestone facing

The original look of the historical Belgian bluestone facing and curbstones will be preserved by integrating the original bluestone in 7.5m high capping beams on top of the combined wall. To achieve this, the bluestone is carefully removed during the demolition of the gravity walls.

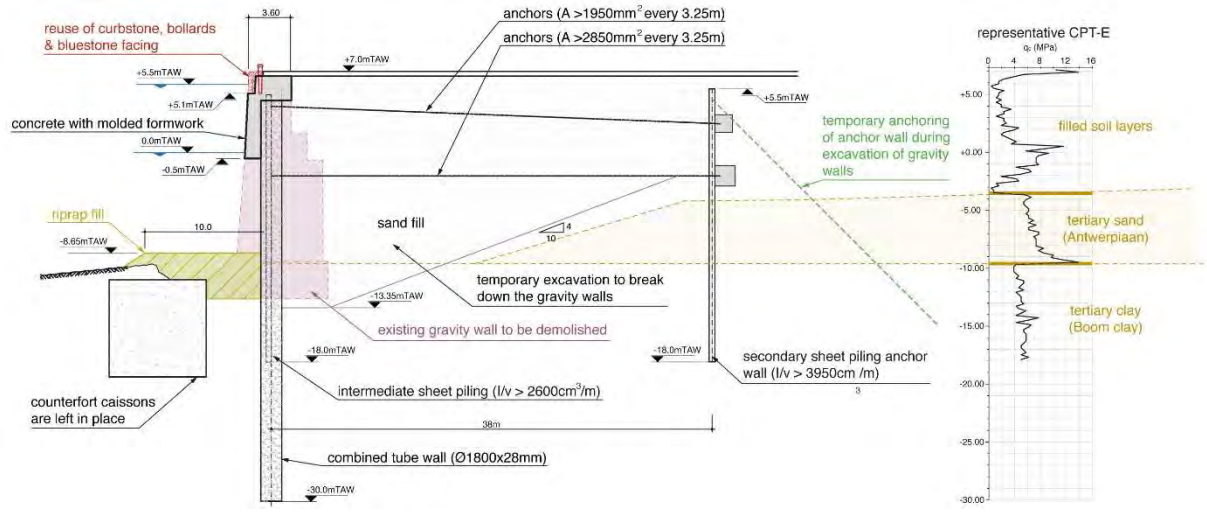

Figure 7: Stabilization design along D'Herbouvillekaai

A detailed photogrammetry showed that it is unfeasible to reuse all bluestone blocks since many stones in the tidal area have weathered and broken over the last century (cfr. Figure 4b). Moreover, a lot of blocks, visually in a good state when still at place, decomposed during or shortly after removing them out of the historical masonry. Because too many stones had become too brittle to reuse, the following innovative solution was introduced to maintain the look of the historical quay walls.

Under the high water line, concrete walls are installed of which the outer formwork is a mold of the original bluestone masonry, see Figure 8. This mold is made on site to preserve the original look of the quays. This approach was approved by cultural heritage given the fact that most of the concrete surface will be covered with mossy and muddy deposition in the tidal zone over time, eventually resembling the current state of the quays. There are several additional advantages:

- In contrast to the bluestone masonry, the concrete is not susceptible to large scale cracking and loss of joint material in the masonry as a result of weathering.
- Only the historical bluestones with the best quality are reused above the high water line.
- The execution is much easier, faster and thus cheaper.

Figure 8: Original bluestone facing (left) and new concrete molded formwork with on top three rows of reused blue stone blocks (right)

4.1.4 Construction phasing and lessons learned

First, the anchor wall and two transverse walls are installed to create a temporary retaining structure behind the original gravity walls. Once the temporary ground anchors in these retaining walls are installed, the construction pit is excavated. Note that the works are carried out in phases in 5 adjacent zones, starting in the middle and moving outwards. The transverse walls can hence be reused in the

construction pit of the adjacent zone with temporary ground anchors being installed in the opposite direction. It is important to note that the design is meticulously followed up during execution to avoid interference of the permanent anchors and the temporary transverse ground anchors. Permanent anchors in the vicinity of future temporary ground anchors are protected with steel casings.

In the next phase, the blue stone facing is removed carefully and then the gravity walls are demolished using explosives. Because of the presence of sensitive buildings nearby the construction site, a trial blast campaign is first performed. During these trial blasts, vibrations are measured on nearby buildings. These measurements are used to optimize the blasting program. Thereby, each demolition phase is monitored closely, resulting in a subsequent optimization of the blasting program in the next zone.

The foundation caissons are loaded with a higher dose of dynamite than the upper masonry wall. The dynamite bars are inserted from the top of the wall in semi-vertical boreholes. Before blasting at the boundaries of the demolition zone, vertical joints are drilled in the wall in order to prevent damage of the neighbouring quay wall. The explosives are detonated during a high tide to prevent flyrock.

After the explosions, the masonry is reasonably well fragmented. However, the steel foundation caissons are tougher than expected. Especially in the first zone, the caissons are not very well fragmented after blasting. Additional demolition works are carried out using a pontoon based hydraulic crusher. For the next two zones, a higher dose of dynamite is used and this improved the fragmentation.

Afterwards, the debris is dredged and the steel, concrete and masonry parts are separated. The steel parts are transported to a recycle plant and the concrete and masonry are transported by ship to a crushing plant for reuse outside this project. An aerial view of the project site after demolition of the first zone is shown in Figure 9.

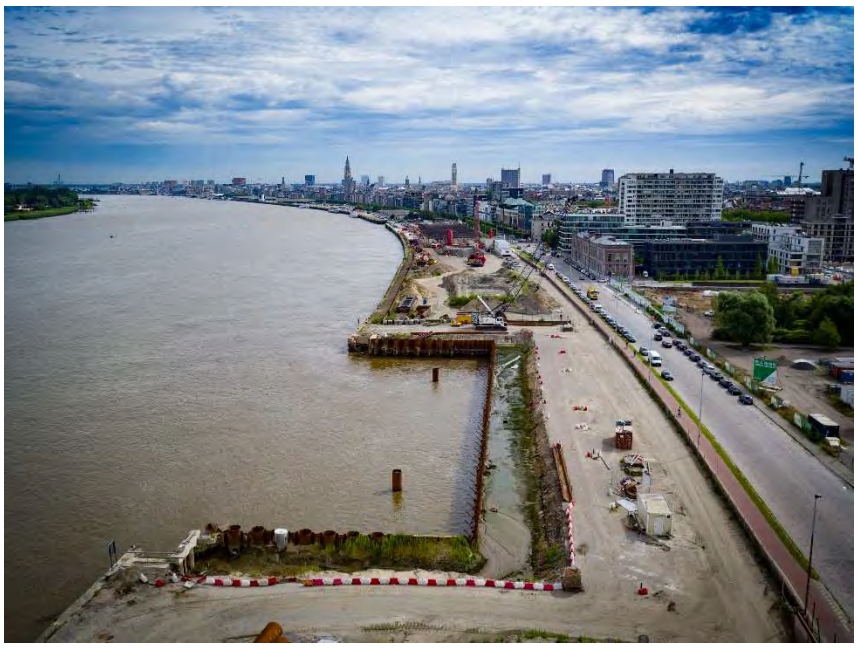

Figure 9: Aerial view of project zone after demolition of quay wall in the first zone (source: Braincube commissioned by DVW)

Then, the new front wall is installed using floating equipment. This combined wall is composed of steel tubes (1800/28) with a length of 37.5 meter and intermediate steel sheet piles (AZ36-700N) with a length of 25.5 meter. The elements are installed by vibration driving and further impact driving with characteristics as shown in Table 2. No other measures are needed to achieve the final depth without generating unacceptable damage or nuisance in the surrounding.

Two double sheet piles of the combined wall are partially omitted to achieve the same water level in the tidal river and in the construction pit at all times. Note that the free standing front wall is not capable of withstanding a large water level difference.

	Vibration driving	Impact driving
Steel tubes: weight of 46.3 tons for 1 tube (front wall)	PVE 300M - total weight including clamps: 45 tons - max. centrifugal force: 6 150 kN - max. frequency: 23 Hz	S-280 (hydraulic hammer) - total weight: 30.5 tons - max. blow energy: 280 kNm - blow rate: 45 bl/min
Sheet piles: weight of 5.1 tons for a double sheet pile (anchor wall and intermediate sheet piles of front wall)	ICE 1412 - total weight including clamps: 13 tons - max. centrifugal force: 2 300 kN - max. frequency: 23 Hz	S-70 (hydraulic hammer) - total weight: 8.3 tons - max. blow energy: 70 kNm - blow rate: 50 bl/min

Table 2: Driving characteristics of sheetpiles and tubes

Subsequently, the rocky debris fill is installed at the toe of the front wall and a sand backfill is placed under water in the construction pit up to a level of -2mTAW. This fill is compacted by vibroflotation. Cone penetration tests are carried out in order to verify the compaction of the fill. When compaction is sufficient the two remaining sheet piles are installed to close the construction pit. Then, the pit is dewatered. On places where no fill is placed after installation of the front wall, as a result of the high silt transport rates of the river Scheldt, a significant siltation is reported. The bottom of the pit is cleaned and profiled.

On the landside of the anchor wall a second construction pit is excavated and dewatered as shown in Figure 10. This pit is used for the construction of the concrete waling beams and for the tensioning of the permanent anchors. These anchors are strand anchors with a double corrosion protection according to NBN EN 1537. First, the lower anchors are installed and tensioned slightly with 40 tons. The construction pit between the anchor wall and the front wall is partially filled. Then, the lower anchors are tensioned to a final lock off load of 200 tons. In the next phase, the upper anchors are installed and tensioned to a lock off load of 140 tons. Afterwards both construction pits are completely filled.

Figure 10: View of the first (left) and second (right) construction pit (source: Braincube commissioned by DVW)

Finally, the large capping beam is constructed at the top of the front wall by means of prefabricated concrete elements with a weight of 90 tons each and a height of 6 meter as shown in Figure 11. These elements are mounted on the combined wall and the joints between the element and the steel wall are sealed. In the transverse walls of each element, interconnection holes are foreseen every 1.0 meter in vertical direction. These holes are supplied with a fine metallic grid which is water permeable and which holds fresh concrete. An interconnection between the river and the chamber formed by the element and the steel wall is essential to secure the stability of a mounted element in the tidal environment. This will prevent the element from displacing and floating. Reinforcement is placed in the chamber and

consequently concrete is poured in steps of 1.0 meter. Before each pouring phase previous concrete surfaces and rebar are cleaned. The bollards are integrated in the concrete capping beam.

Figure 11: Prefabricated concrete facing elements of the front wall with interconnection holes, ready for placement (left) and elements mounted on the combined wall (right)

Finally, the historical bluestone masonry and curbstone are placed above the high water line. The bluestone blocks are recycled from the old gravity wall. Experience shows that only 30 to 40 percent of the original stones is fit for reuse after dismantling the old wall. Due to the historical port activities on the project site, the original curbstones have disappeared or are heavily damaged, which makes reuse impossible. New Belgian bluestone curbstones are applied here.

A temporary surface finishing is foreseen on the quay areas until the final works on the new storm surge barrier (+9,25mTAW) commence.

4.2 Case 2: De Gerlachekaai

4.2.1 Test phase

The quay walls at De Gerlachekaai are in a better condition than the quay walls at D'Herbouvillekaai. Hence, measures with a minor impact on the original quay walls were at first considered for stabilization.

In a first design effort, a stabilization technique with transverse grout walls below the current gravity walls was considered as shown in Figure 12. Five parallel and equidistant shear panels were foreseen per foundation caisson to extend the foundation depth. Each shear panel consisted of multiple cylindrical VHP jet-grout columns with a large diameter. The jet-grout columns were constructed after drilling through the existing masonry walls and foundation caissons from the quay platform. They were armoured with rebar steel upon completion. Before the jet-grouting started, all voids and cracks intersecting with the drill holes were gravitationally injected with a cement grout. Additionally, ground anchors had to be installed to limit the horizontal movements of the quay walls. An integrated concrete capping beam with bluestone façade was constructed at the top of the gravity wall. The joints between adjacent caissons under the low water line were repaired.

While this remedial technique is much less invasive, it is also more risky. The jet-grouting had to be performed at very large depth, in a very stiff clay layer, underneath the historical structure. As a result, the quality of the grouting operation was difficult to control. It was therefore decided to perform the stabilization in a test section first to assess the efficiency of the proposed design.

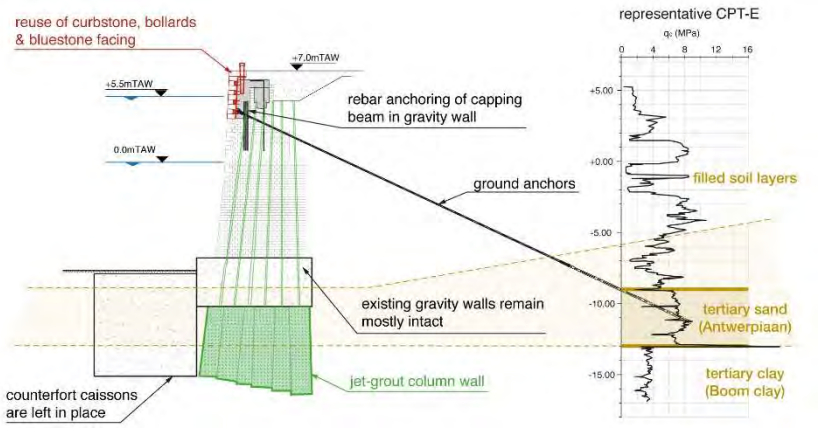

Figure 12: Stabilization design with jet-grouting in test phase

Already during the first jet-grouting operations, problems were encountered. The spoil return flow at the top of the drill hole was not continuous. The quality of the large diameter grout columns was investigated with core drill holes. Many clay inclusions were found along the entire depth of the grout columns, as shown in Figure 13. The formation of these inclusions was attributed to the properties of the tertiary Boom clay. Due to the high stiffness and plasticity of this pre- and overconsolidated clay layer, it seemed impossible with large diameter jet-grouting to cut loose clay particles that are small enough to travel through the ring gap in the drill hole. As a result, clay chunks block the ring gap in the drill hole and pressure is built up, within seconds, in the subsoil. The spoil is then directed to alternative low resistance paths, e.g. via the bottom of the caissons, and the quality of the grout columns is drastically reduced. In addition, during jet-grouting operations, the movement of the quay wall was monitored continuously. Even after successfully executing the first series of grout walls, unacceptable movement of the historical quay wall was monitored during jet-grouting operations.

Figure 13: Core drill holes of the jet-grout columns at De Gerlachekaai with clearly visible clay inclusions

About 20 different sets of jet-grouting parameters were tested, but none of them gave satisfying results. In the end, it was decided that the performance of the grouting technique was too uncertain in the Boom clay and this stabilization technique was completely abandoned.

4.2.2 Stabilization design

A more expensive but more controllable design was developed for this area of the quays. In the optimized design, which also preserves a big part of the historical wall, a diaphragm wall is installed behind the quay walls, as shown in Figure 14. The diaphragm wall is embedded in the Boom clay at a depth of -23mTAW. The horizontal stability of the diaphragm wall is ensured with 2 rows of ground anchors every 1.8m. An additional ground anchor is installed every 20m at the location of a bollard.

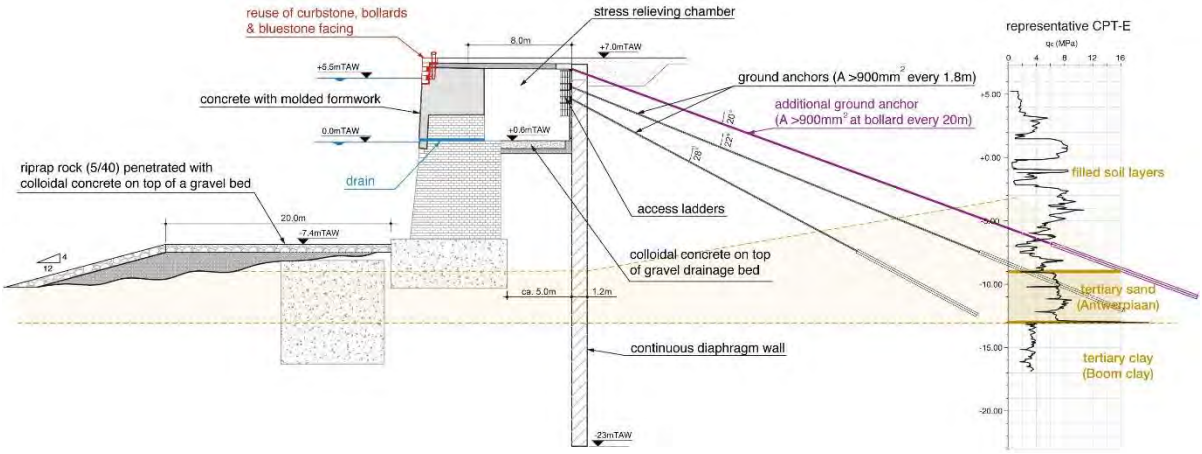

Figure 14: Stabilization design for De Gerlachekaai

Between the original gravity wall and the diaphragm wall, stress relieving chambers are additionally installed to reduce the loads on the original gravity wall. Four drainage tubes per caisson are drilled through the original masonry wall to allow the stress relieving chambers to follow the tide in the river Scheldt.

Similarly as in the design of D'Herbouvillekaai, the upper part of the masonry quay walls is replaced by a concrete structure to enhance the durability of the quays in the tidal zone for the future. Again, the outer formwork is a mold of the original bluestone masonry. Above the high water line, the original bluestones as well as the bollards are reused together with new Belgian bluestone curbstones.

At the river side, a small elevation of the original river bed and a new bed protection, which should avoid erosion, are foreseen. Inside the stress relieving chamber, the floor is conceived as a 0.6m thick layer of colloidal concrete on top of a gravel drainage bed.

4.2.3 Execution phasing and lessons learned

Because the changes to the original gravity walls are less drastic in this area, the phasing of the works is less complicated in comparison with D'Herbouvillekaai. In the first phase, the new bed protection is installed. A rip rap layer with a variable thickness and a width of 30 meters is placed at the toe of and parallel to the quay wall. Then this layer is covered with immersed asphalt mattresses to obtain a durable bed protection as shown in Figure 15.

Figure 15: Immersion of the asphalt mattresses in front of the quay wall

Afterwards, the new diaphragm wall is constructed behind the quay wall. After partial excavation behind the existing quay wall, the ground anchors are installed. The excavation continues until the bottom level of the relieving chamber and the chamber floor is constructed. In the next phase, the chamber front wall and the chamber roof plate are constructed as shown in Figure 16. At the locations of the bollards, additional ground anchors are placed.

Figure 16: View of the chamber front wall placed on the existing quay wall (left) and view inside the stress relieving chamber (right)

Now, holes can be drilled at the bottom of the relieving chamber, connecting the river Scheldt. At the rhythm of the tides, twice a day, the chamber fills with water from the river, relieving the old historical wall from water pressure. The first chamber went operational in 2015. Because of the high silt transportation rate in the river, monitoring of the sedimentation load in the chamber is necessary. Through the two years of measurement, we notice a sedimentation of silt against the diaphragm wall diminishing in a funnel shape to the drilled holes at riverside. After 2 years, the sedimentation seems to find an equilibrium. However, further monitoring is required for the next years to implement a maintenance program if necessary.

Finally, the top of the original quay wall is demolished and the new concrete capping beam is installed. The original bluestone masonry and the bollards are installed as well. The old curbstone is in very bad shape which makes it impossible to reuse. Therefore, a newly mined Belgian blue curbstone is placed, marking this very special place in the city of Antwerp.

5 CONCLUSIONS

Almost 150 years ago, the new quay walls required cutting edge technology to be constructed. After several attempts over the last century to alleviate the instabilities resulting from serious design defects at the time of building, the present renovation project intends to preserve the iconic Scheldt quays for the generations to come. To reach this goal in a cost effective way, innovative and site-specific techniques are required once more.

Originally estimated as works for the next 15 years, the conclusion of the entire renovation project of the Scheldt quays, including all works for the storm surge barrier and the urban facelift of the quay area, might take (much) longer. By tackling the most unstable zones first, our understanding of the Scheldt quay wall structures has greatly improved. This gives ground for optimism for the future renovation works.